Lehrstuhl für Computergestützte Modellierung und Simulation | Prof. Dr.-Ing. André Borrmann
Lehrstuhl für Architekturinformatik | Prof. Dr.-Ing. Frank Petzold

Proceedings of

33. Forum*Bauinformatik*

07. – 09. September 2022

Herausgeber:
Martin Slepicka, Lothar Kolbeck,
Sebastian Esser, Kasimir Forth,
Florian Noichl, Jonas Schlenger

Technische Universität München

Herausgeber
Sebastian Esser, Kasimir Forth
Florian Noichl, Jonas Schlenger
Martin Slepicka, Lothar Kolbeck

Layout & Satz
Martin Slepicka
Lothar Kolbeck

Rein digitale Veröffentlichung über das mediaTUM-Portal der Technischen Universität München

DOI: 10.14459/2022md1686600
URL: https://mediatum.ub.tum.de/1686600

Logo: Forum Bauinformatik | www.forum-bauinformatik.de
Umschlagfoto: Astrid Eckert | Technische Universität München | Leonhard Obermeyer Centrum

Vorwort

Das Forum Bauinformatik dient seit 1989 regelmäßig dem Austausch des wissenschaftlichen Fachbereichs der Bauinformatik. Die mittlerweile 33. Ausgabe findet 2022 nach 1993, 2001 und 2013 zum vierten Mal in München statt. Das Fachgebiet der Bauinformatik erfreut sich in den letzten 3 Jahrzehnten einer stetig zunehmenden Aufmerksamkeit. In verschiedensten Teilbereichen treffen vielfältige Entwicklungen von Methoden und Technologien auf immerwährend an Relevanz und Komplexität gewinnende Herausforderungen. Im Rahmen des Forum Bauinformatik erhalten Wissenschaftler und Wissenschaftlerinnen von Studierenden über Promovierende bis hin zu Promovierten aus dem DACH-Raum die Möglichkeit, Themen und Erkenntnisse unter Gleichgesinnten vorzustellen, zu diskutieren und abgeschlossene Projekte zu präsentieren. Da sich die Arbeit der Mitglieder unseres Netzwerks nicht auf den deutschsprachigen Raum beschränkt, sondern vielfältig auch mit Partnern und Kollegen aus der internationalen Forschungsgemeinschaft erfolgt, freuen wir uns besonders, sowohl deutsch- als auch englischsprachigen Beiträgen eine Plattform bieten zu können. In diesem Konferenzband sammeln wir die insgesamt 52 Beiträge von mehr als 20 verschiedenen Institutionen. Besonders freuen wir uns, zum ersten Mal den Prof. Heinrich Werner Preis (1931-2022) für das beste Paper verleihen zu können, mit dem wir an die für die Bauinformatik wegweisende Arbeit von Prof. Heinrich Werner erinnern wollen. Wir wollen uns herzlich bei allen AutorInnen und BetreuerInnen bedanken, die sich in Form von Beiträgen und im Review in diese Konferenz einbringen, und wünschen allen Teilnehmenden eine spannende Konferenz voller anregender Diskussionen und Anstößen für die weitere Arbeit.

F. Noichl, M. Slepicka, L. Kolbeck, S. Esser, K. Forth, J. Schlenger

München, September 2022

Preface

Since 1989, the Forum Bauinformatik has regularly served as a platform for exchanging scientific works and views in the field of construction informatics. The 33rd edition will take place in Munich in 2022, for the fourth time after 1993, 2001, and 2013. Since then, the field of construction informatics has steadily enjoyed increasing attention. In a wide variety of sub-areas, diverse developments in methods and technologies meet challenges that constantly increase in relevance and complexity. Within the Forum Bauinformatik, scientists from students to doctoral candidates to professors from the DACH region are given the opportunity to present and discuss topics and findings among like-minded people and present completed projects. Since the work of the members of our network is not limited to the German-speaking region but also takes place in many ways with partners and colleagues from the international research community, we are particularly pleased to offer a platform for both German- and English-language contributions. In this conference volume, we collect 52 contributions from more than 20 different institutions. We are especially pleased to award the Prof. Heinrich Werner Prize for the best paper for the first time, with which we want to pay due tribute to Prof. Heinrich Werner's (1931-2022) seminal work for construction informatics. We want to express our sincere thanks to all authors and supervisors who have contributed to this conference through papers and reviews. We wish all participants an exciting conference full of stimulating discussions and impulses for further work.

F. Noichl, M. Slepicka, L. Kolbeck, S. Esser, K. Forth, J. Schlenger

Munich, September 2022

Organisation des 33. Forum Bauinformatik

Hauptorganisationsteam

Kasimir Forth
Jonas Schlenger
Florian Noichl
Sebastian Esser

Konferenzband

Martin Slepicka
Lothar Kolbeck

Welcome Evening

Kai-Uwe Bletzinger
Ann-Kristin Goldbach
Ilayda Memis
Ata Zahedi

Preise und Konferenztaschen

Fabian Pfitzner
Jiabin Wu

Session Hosts

Ata Zahedi
Jessica Bielski
Ivan Bratoev
Florian Noichl
Jan Clever
Fiona Collins
Sebastian Esser
Kasimir Forth
Chao Li
Alexander Braun
Simon Vilgertshofer

Inhaltsverzeichnis

Rahmenprogramm

Numerical modeling and simulation of lightweight structures - using the example of the Olympic Stadium in Munich on its 50th anniversary

Máté Péntek[1], Ann-Kathrin Goldbach[1], Klaus Bernd Sautter[1] and Kai-Uwe Bletzinger[1]
[1]Lehrstuhl für Statik, Technische Universtität München, Arcisstr. 21, 80333 München, Deutschland
E-mail(s): mate.pentek@tum.de, ann-kathrin.goldbach@tum.de, klaus.sautter@tum.de, kub@tum.de

Abstract: We present various aspects of numerical modeling and simulation arising from the main focus areas of the Chair of Structural Analysis at the Technical University of Munich. These include several considerations on the load-bearing behavior of lightweight structures, which are best associated with and demonstrated on the Olympic Stadium in Munich. This landmark has been an architectural and engineering challenge and a source of inspiration from its inception until now, in 2022, on its 50th anniversary. Therefore, we intend to provide a technological overview of the approaches used to model and evaluate these types of structures, clearly identifying the numerical advances and highlighting particular contributions from our institute.

Keywords: Lightweight Structures, Numerical Wind Tunnel, CAD-Integration, IBRA, CWE

1 Introduction

In structural design and analysis, lightweight constructions represent a combination of architectural aspiration and engineering challenge. Such designs allow open spaces to be covered by complex shapes, typically double-curved surfaces. They are characterized by their geometric stiffness rather than an inherent robustness from large cross sections. Due to the low thickness of the structural elements, these shapes tend to exhibit large deformations at small strains, for which geometric nonlinearities must be accounted for. Adequate stiffness is achieved through geometry (with curvature) and prestressing of certain parts or elements. Lightweight structures may be susceptible to transient effects because of their low inertia. Wind in particular, which is not only a time-dependent but also a shape-dependent load, requires careful investigation. The balance between form and force is key to the proper consideration of the effects on the structural behavior.

The study of freeform shapes and minimal surfaces using soap bubbles and fabric models represents the early and exploratory approach to lightweight design. Further experiments are measurements made in wind tunnels for appropriate load effects on the complex shapes. Lately, the appearance

of numerical methods combined with improvements in hardware enabled new possibilities for the design and analysis process. This area is the focus of our contribution, with the Olympic Stadium in Munich serving as a motivator for many further developments. We cover aspects ranging from basic mechanical prerequisites over specifics of CAD-integrated analysis and a unified workflow for the detailed simulation of coupled wind-structure behavior using the numerical wind tunnel.

Figure 1: The Olympic Stadium and its numerical structural model [1].

Fig. 1 shows the Olympic Stadium in Munich with its surroundings. A sketch of the numerical structural model is overlaid. In times of highly demanded digital twins, such models are the key to providing answers to questions directed at the actual built structure. It serves design as well as predictive analysis purposes (i.e. structural/mechanical twin) and can easily be enhanced by more properties (monitoring data, cost estimates, etc.). This idea is captured in the description of the AiCAD-concept [2].

The pioneering work on the original structure could not have been possible without many protagonists (architecture and engineering: Behnisch, Leonhardt, Otto, Schlaich; numerics: Argyris, Biguenet, Haug, Linkwitz, Schek) [3], [4]. Their contribution is further detailed in [5], as a tribute to the simulation methodology for textile lightweight structures. We build upon this knowledge base with further advances in numerical developments.

2 Design and Analysis of Lightweight Structures

We focus on the peculiarities of designing and analysing lightweight structures, where form and force are inseparable. In the case of the Olympic Stadium Roof, one can observe the series of double-curved surfaces arising from a cable net and its plexiglass cladding.

The typical design cycle is depicted in fig. 2. In the early design process, the starting point is identifying the target equilibrium shape for given prestress and boundary conditions by a formfinding analysis. However, this shape is bound to change during the iterative process of considering all design steps. This is followed by the structural analysis under relevant external loads. Other steps are related to

specifics in the manufacturing and construction staging. Cutting patterns need careful consideration, as membranes will have to be joined from flat pieces and prestressed to arrive in their designated position.

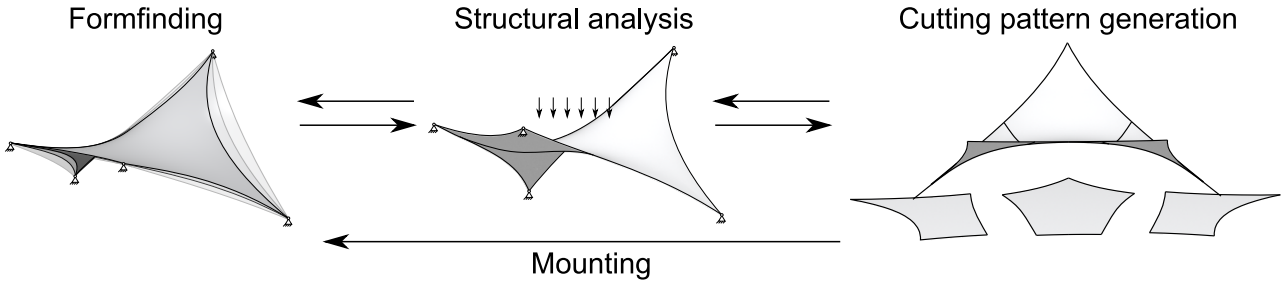

Figure 2: The design cycle of membrane structures [6].

2.1 Nonlinear Structural Analysis

Lightweight design typically considers large displacements of the structural components. Geometrically nonlinear analysis is thus needed to capture the mechanical behaviour appropriately, thoroughly motivated in [7]. This section discusses the necessary preliminaries for such considerations and points out the challenges inherent to flexible structures.

The Finite Element Method (FEM) is used to simulate the structural response to external forces and internal prestresses. The method is based on the equilibrium of virtual work. Derivation of the relations highlights two critical aspects relevant for analysis:

- There exists a non-negligible contribution of the geometry to the stiffness matrix, which implies an update and assembly of it at each iteration of a numerical process.
- For cables and membranes we need to ensure proper prestress, otherwise such elements are mechanically non-viable, leading to critical errors in a computational context.

This is in contrast with the linear theory of first order analysis, which is only valid for small deformations. For most use cases in lightweight analysis, it is a must to account for the change of shape during deformation. This is not only critical for updating the stiffness matrix, but also can be a key component in case of follower loads, such as wind. Additionally, prestress ensures proper behaviour, both from an engineering point of view as well as for numerical consideration, as respective elements lack inherent out of plane stiffness. It is evident that the formulation as well as the numerical models need to be suitable to ensure such aspects.

Thin fabrics and materials stretch considerably under such actions. How the structure is planned to behave once mounted, can be considerably different to how it is produced, transported and mounted. Consequently, the aspect of cutting pattern generation has high importance. A numerical approach enables reverse-engineering to lead from the target geometry to the cutting patterns necessary to achieve this. Figure 3 highlights this concept.

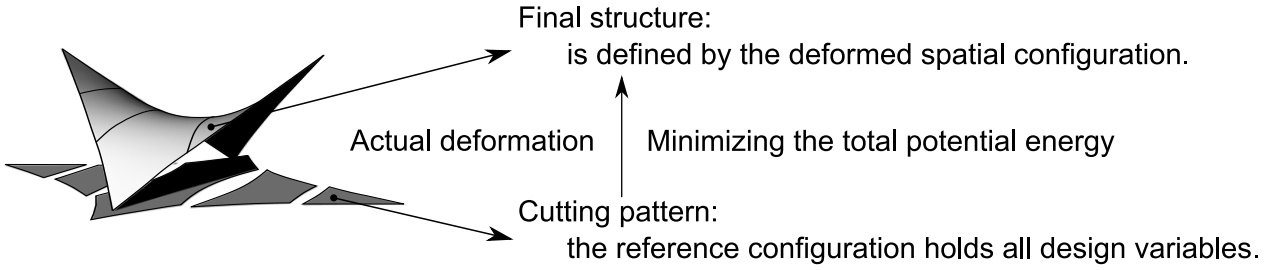

Figure 3: Cutting patterns for a hypar structure [6].

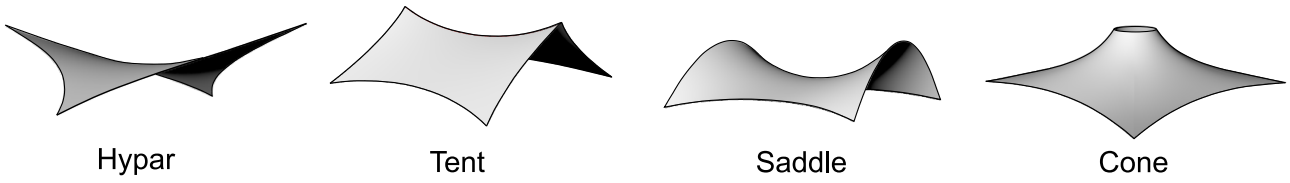

Figure 4: A selection of representative geometries for membrane structures [6].

For engineering purposes, there are certain recurring shapes, which are of utmost relevance. Figure 4 shows a collection of geometries, which will either occur alone or in certain arrays or formations. Specific modifications will lead to particular structures, such as the Olympic Stadium Roof in Munich.

2.2 The CAD-Integrated Design Cycle

The design and analysis of lightweight structures calls for a close cooperation between architects and engineers, as shown by the exemplary structures in the Olympic Park. However, the computational models are often separate and transferring data from one discipline to the other can be cumbersome. CAD-integrated analysis skips this gap by allowing all participants to work on one model for most of the design and engineering tasks. This is well in line with the topic of Building Information Modelling (BIM). However, the main link is not only to have a common format for the geometry and structural properties, but first and foremost to ensure a functional structural model, serving both computation design and analysis. This implies stringent requirements on how the model needs to be created and used.

The proposal is to use an isogeometric discretization based on Non-uniform Rational B-Splines (NURBS) instead of linear shape functions, using the inherent parametrization available in the CAD workflow. The geometry is enhanced by mechanical properties to build the structural model. As such, the Isogeometric B-Rep Analysis (IBRA, as described in [8]) combines CAD and FEM, permitting a strongly linked workflow between architects and engineers. It is also very appropriate for delicate considerations related to shape, iteration loops and exploring multiple design scenarios by utilizing parametric CAD environments, see [6] for detailed explanations and examples.

3 Wind-Structure Interaction of Lightweight Structures

Due to the interaction of form and force, the consideration of surface loads is challenging while it is especially important to capture them appropriately. The direction and intensity of wind effects (pressure and friction) will adapt to deformation, rendering them follower loads. Moreover, if lightweight structures span over large distances, potentially non-negligible amounts of air (or snow) have to be considered. Physically this leads to added mass at levels which require the detailed analysis of interaction between the construction and loading force. Such effects happening on the interface between various physical domains (in our case wind and structure) constitute a specific research area within multiphysics, in particular Fluid-Structure Interaction (FSI). We present our contributions to and recent investigations with the so-called *numerical wind tunnel*, the representative tool in Computational Wind Engineering (CWE). In [9] the potentials and challenges of this analysis tool are briefly outlined, with work since then further consolidating the research efforts. We specifically focus on enhancing the load-bearing and response behaviour of structures in wind.

3.1 Modelling Requirements of the Numerical Wind Tunnel

Investigations using the numerical wind tunnel imply multiple assumptions and have to obey various requirements. Similarly to the "traditional" (i.e. "analog") equipment, the analysis needs the definition of the relevant flow domain, generation of realistic wind conditions, the latter including various neighbouring elements and obstacles. An appropriate structural model has to be constructed as well, following the considerations presented in section 2.

Typical inflow conditions for general Computational Fluid Dynamics (CFD) investigation are well known. Additional requirements arise for wind engineering. These refer the proper metrics for the flow conditions in order to be considered realistic: the streamwise velocity component, particularly the time-averaged mean and turbulence intensity over height, supplemented by the turbulence length scale and power spectral density of the spectrum at characteristic points. This inflow condition can be created with a synthetic wind generator. Further consideration are linked to other nearby objects or terrain, which could have significant impact on the local flow conditions.

We aim to investigate the transient loading of wind on deformable structures. Consequently, both numerical models need to obey appropriate modeling best practices. A segregated approach permits applying known properties and strategies, optimal for the two domains - fluid and structure - separately. The wind flow around the target construction is recreated with the Large Eddie Simulation (LES) technology, whereas the structure is supported by a model suitable for geometrically nonlinear structural analysis.

3.2 Investigating the Olympic Stadium Roof

We focus on showcasing recent developments on the Olympic Stadium Roof. This is an ideal example of a large span lightweight construction. It is numerically modeled with plates in membrane action. The original design process in the 1960s' and 70s' used various experimental methods and analytical

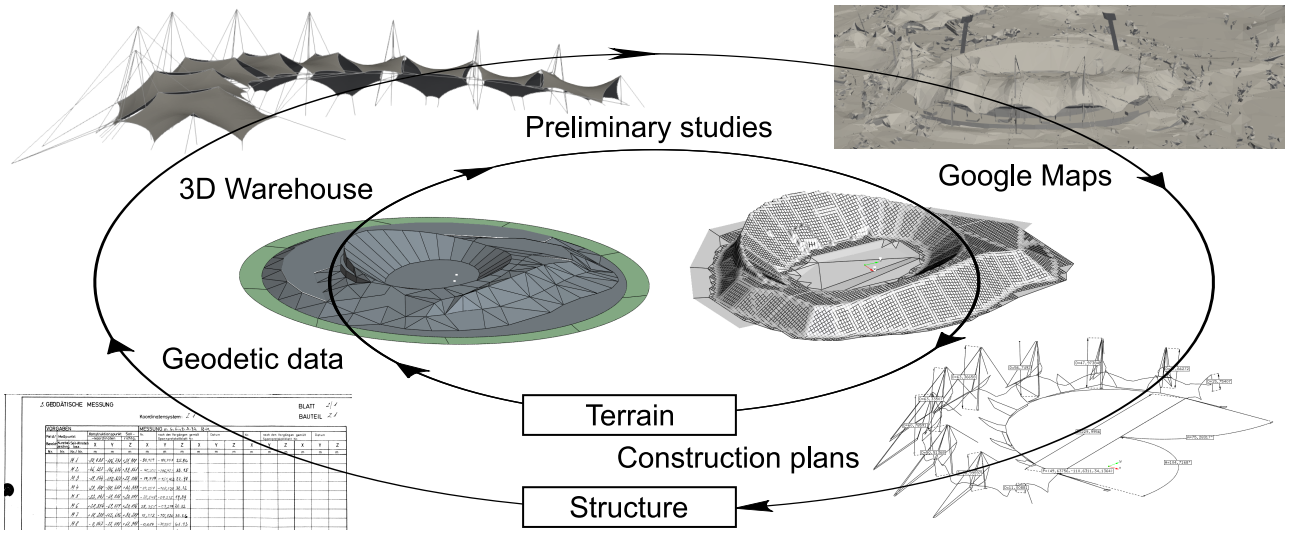

Figure 5: Model-update workflow.

considerations to arrive at this shape and respective prestress state. Due to the lack of extensive computational methods at that time, the structure is the result of ingenious engineering and is supported by the experience of all involved. Our current shows recent advances, in particular creating a viable computational model and simulation environment for the wind flow as well as structural investigations.

Apart from building appropriate numerical models for the structure of the Olympic Stadium, relevant parts of the surroundings have to be considered. For the construction we used data from building archives (based upon on-site measurements) as well as digital resources (Google Maps and 3D Warehouse). In contrast to an initial design process (such as in section 2.2) with the shape resulting from formfinding, here the shape was given. As such, We iteratively optimized the prestress state to achieve this target, under the consideration of self weight. This implies the iterative process of updating the model, as presented in fig. 5, by carefully investigating various sources.

Fig. 6 depicts the setup for the CWE-analysis used to investigate the wind-structure interaction of the stadium. The study includes the turbulent wind around the stadium and its surroundings. Not only the flow field and the aerodynamic loads are assessed, but the effect of the flexible structure in captured as well. This complexity renders such numerical simulation to be carried out on High-Performance Computing (HPC) machines. These exploit parallelism on distributed memory units based on the Message Parsing Interface (MPI).

4 Conclusion and Outlook

We showcased various developments relevant to the numerical analysis of lightweight structures. In particular, we linked multiple aspects to the example of the Olympic Stadium Roof in Munich. The necessity of considering geometrical nonlinearity was highlighted. A CAD-integrated workflow enables architects and engineers to work on one common geometric model, which is also mechanically

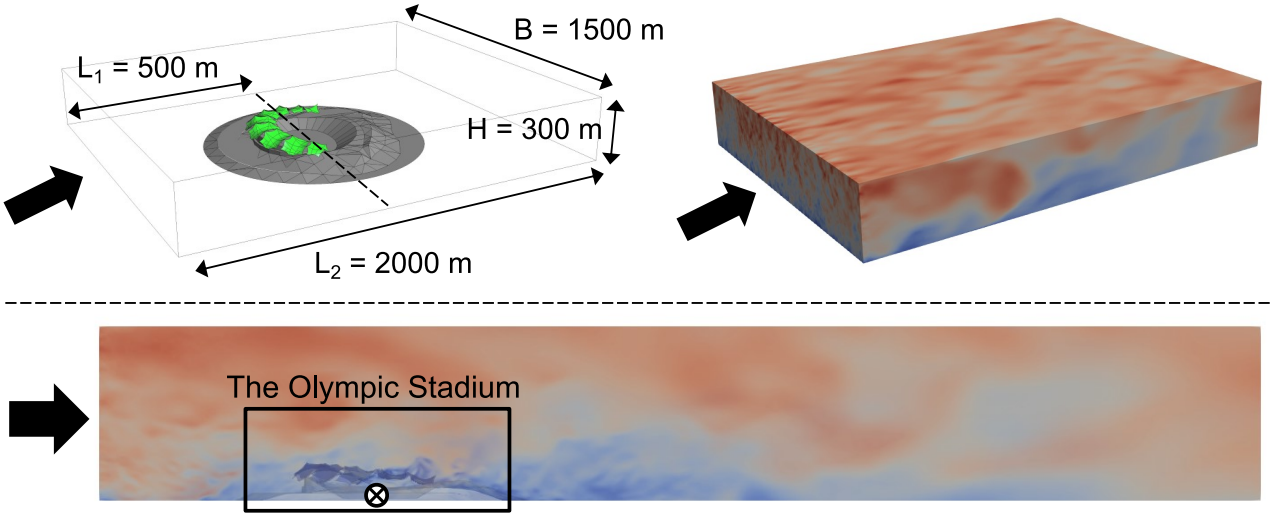

Figure 6: The CWE-model of the Olympic Stadium.

correct and ready to be used for analysis purposes. We additionally demonstrated recent capabilities in multiphysics simulations, where coupled phenomena need to be investigated. Herein the wind-structure interaction of the Olympic Stadium Roof with its surrounding was modeled and simulated. This heavily relies on adequate computational models for the simulation capabilities of the numerical wind tunnel being properly leveraged on a high performance computing environment. The outcome is a detailed flow field, the wind loads as well as their effect on the flexible structure.

The workflow can be viewed as a whole, starting with finding the appropriate shape of lightweight structures and ending with the usage of these for advanced analysis purposes, such as the action of wind. This fully-digital workflow can go well along with various advances in BIM. Yet it not only needs a common format and shared data, but requires the proper links to be made for simulation needs. Detailed and realistic numerical models are also the bases for an outlook towards digital twins. In such a context validated replicas can be paired with existing structures, where the updating of the parameters is based on monitoring data.

Acknowledgements

The authors gratefully acknowledge the Gauss Centre for Supercomputing e.V. (www.gauss-centre.eu) for funding this project by providing computing time on the GCS Supercomputer SuperMUC-NG at the Leibniz Supercomputing Centre (www.lrz.de).

References

[1] P. Bucher, M. Péntek, K. B. Sautter, R. Wüchner, and K.-U. Bletzinger, “Detailed fsi modeling and hpc simulation of the olympic stadium roof in munich under wind loading”, in *10th edition of the conference on Textile Composites and Inflatable Structures*, CIMNE, 2021. DOI: 10.23967/membranes.2021.039.

[2] B. Philipp, M. Breitenberger, I. D’Auria, R. Wüchner, and K.-U. Bletzinger, “Integrated design and analysis of structural membranes using the isogeometric b-rep analysis”, in *Computer Methods in Applied Mechanics and Engineering 303*, 2016. DOI: 10.1016/j.cma.2016.02.003.

[3] F. Leonhardt and J. Schlaich, “Weitgespannte flächentragwerke – vorgespannte seilnetzkonstruktionen: Das olympiadach in münchen”, *Sonderforschungsbereich (SFB) 64*, vol. 19, pp. 1–54, 1973.

[4] K. Linkwitz and H.-J. Schek, “Über eine methode zur berechnung vorgespannter seilnetze und ihre praktische anwendung auf die olympiadächer münchen”, *IVBH Kongressbericht*, vol. 9, 1972. DOI: 10.5169/seals-9580.

[5] K.-U.Bletzinger, “Simulationsmethoden im textilen leichtbau – die entwicklung seit 1972 und aktueller stand”, *Bautechnik*, vol. 92, no. 11, pp. 800–805, 2015. DOI: 10.1002/bate.20150008.

[6] A.-K. Goldbach, “The cad-integrated design cycle for structural membranes”, Ph.D. dissertation, Technische Universität München, München, 2021.

[7] A. M. Bauer, “Cad-integrated isogeometric analysis and design of lightweight structures”, Ph.D. dissertation, Technische Universität München, München, 2020.

[8] M. Breitenberger, A. Apostolatos, B. Philipp, R. Wüchner, and K.-U. Bletzinger, “Analysis in computer aided design: Nonlinear isogeometric b-rep analysis of shell structures”, in *Computer Methods in Applied Mechanics and Engineering 284*, 2015. DOI: 10.1016/j.cma.2014.09.033.

[9] K.-U. Bletzinger, R. Wüchner, M. Andre, M. Péntek, and A. Michalski, “Der numerische windkanal im bauwesen - potentiale und herausforderungen am beispiel flexibler tragwerke”, in *20. Dresdner Baustatik-Seminar: Realität - Modellierung - Tragwerksplanung*, T. D. Institut für Statik und Dynamik der Tragwerke, editor, 2016, pp. 5–18. DOI: 10.1002/bate.20150008.

Teil I

BIM & Planning

BIM und vorgefertigter Holzbau – Der BIMwood Referenzprozess

S. Schuster[1], J. Arnold[1] and J. Behm[2]

[1]Chair of Architecture and Timber Construction, Technical University of Munich, Arcisstraße 21, 80333 Munich, Germany

[2]Chair of Architectural Informatics, Technical University of Munich, Arcisstraße 21, 80333 Munich, Germany

E-Mails: sandra.schuster@tum.de, joh.arnold@tum.de, julia.behm@tum.de

Abstract: Der Beitrag befasst sich mit der Weiterentwicklung der Wertschöpfungskette Planen und Bauen mit Holz und beschreibt Problemlösungsansätze, die maßgeblich zu einer CO2-neutralen Bauweise beitragen: Die Nutzung des Baustoffs Holz und die industrialisierte Bauweise. Grundlage bildet das Building Information Modeling (BIM) als eine Schlüsseltechnologie in Architecture, Engineering and Construction (AEC) und die damit einhergehenden Auswirkungen auf gängige Arbeitsmethoden. Construction 4.0 als Konzept basiert auf der Digitalisierung der Bauwirtschaft einerseits und der Industrialisierung der Bauprozesse andererseits. Der moderne Holzbau ist in hohem Grad von einer industrialisierten Fertigung geprägt. Im Vergleich zu anderen ausführenden Gewerken handelt es sich bei den Holzbauunternehmen um ein planungsintensives Gewerk, das seit über 30 Jahren in der Lage ist, mit 3D (Geometrie) Modellen zu arbeiten und diese mit entsprechenden Informationen zu hinterlegen. Während im Bereich der Fertigung eine funktionierende digitale Kette existiert, wird diese im Bereich der Planung derzeit nicht durchgängig umgesetzt. Dieses Defizit führt vielfach zu einem Mehraufwand auf Seiten der Planenden. Das Forschungsprojekt BIMwood entwickelt BIM basierte Lösungen für optimierte Prozessabläufe im Holzbau. Inhalt dieses Papers ist die Beschreibung eines holzbauspezifischen BIMwood Referenzprozesses, für dessen Erarbeitung ein simulativer Methodenansatz gewählt wurde. Der BIMwood Referenzprozess beschreibt inhaltliche und prozessuale Themenfelder gleichermaßen und unterstützt damit eine optimierte integrale Planung und Koordination von vorgefertigten Holzbauprojekten. Damit fördert er die Weiterentwicklung der BIM-Methodik und BIM-Technologien im Bereich des industrialisierten Holzbaus.

Keywords: BIM, Holzbau, Vorfertigung, Referenzprozess, Construction 4.0

1 Einleitung

Der moderne Holzbau ist von einer industrialisierten Fertigung geprägt. Dieses Prinzip der Vorfertigung (Abbildung 1) und ein höherer Komplexitätsgrad der Bauteilaufbauten verlangen bereits in frühen Planungsphasen Entscheidungen und Festlegungen, welche geometrischen und alphanumerischen Informationen zu welchem Zeitpunkt in das Modell eines Holzbauprojekts einfließen.

Abbildung 1: Grad der Vorfertigung im Holzbau

Bestehende BIM Referenzprozesse haben sich entlang der Abläufe des mineralischen Bauens entwickelt, welche die spezifischen Anforderungen des vorgefertigten Holzbaus nicht berücksichtigen. Im Rahmen des Forschungsprojekts BIMwood wurde ein BIMwood Referenzprozess entwickelt, der an dieser Stelle vorgestellt wird. Der BIMwood Referenzprozess definiert neben den Informationsanforderungen die Informationstiefe in unterschiedlichen Planungsphasen unter Berücksichtigung der Spezifika des Holzbaus. Darüber hinaus werden die notwendigen Akteure und die ihnen zugewiesenen Rollen identifiziert und es wird festgelegt, über welche holzbauspezifischen Kompetenzen die beteiligten Akteure im Planungsprozess verfügen müssen. Der BIMwood Referenzprozess unterstützt damit eine optimierte integrale Planung und Koordination vorgefertigter Holzbauprojekte und stellt eine Weiterentwicklung der BIM-Methodik und BIM-Technologien im Bereich des industrialisierten Holzbaus dar.

Der BIM Projektabwicklungsplan (BAP) beschreibt in idealisierter Form alle Prozesse und die Inhalte des Informationsmanagements [1, S. 14] und definiert damit die Grundlagen einer BIM-basierten Zusammenarbeit. Das betrifft neben der Festlegung organisatorischer Strukturen und Verantwortlichkeiten auch die konkrete Beschreibung der Prozesse und Anforderungen an die integrale Kooperation der einzelnen Akteure. Darüber hinaus legt der BAP weiterhin die projektbezogenen Ausprägungen fest und definiert das Maß der Informations- und Detailierungstiefe

und deren Qualitäten [2]. Unter Einbeziehung der unterschiedlichen Möglichkeiten und Elemente der BIM-Methode wurden im Verlauf der vergangenen Jahre sogenannte BIM-Referenzprozesse entwickelt [2, 3]. Dabei beschreiben BIM-Referenzprozesse den Zusammenhang zwischen unterschiedlichen Planungs- und Projektphasen und den notwendigen Voraussetzungen an den Austausch von Informationen bzw. das Informationsmanagement. Während der BIM-Referenzablauf eine übergeordnete Betrachtung über den gesamten Lebenszyklus eines Gebäudes beschreibt, umfasst der BIM-Referenzprozess vorwiegend die Elemente des Planungsprozesses. BIM-Referenzprozesse dienen dabei für alle Projektbeteiligten als erste Referenz - beziehungsweise Grundlage - für eine kontinuierliche Verbesserung ihrer Abläufe [3]. Das Bauen mit Holz verlangt durch das Prinzip der Vorfertigung bereits in früheren Planungsphasen Entscheidungen und Festlegungen als mineralische Bauweisen [4]. Gleichzeitig bedingt der Komplexitätsgrad und das Wirkungsgefüge der Bauteilaufbauten genaue Festlegungen hinsichtlich des Zeitpunktes und des Umfangs, in dem geometrische und alphanumerische Informationen in das 3D-Modell eines Holzbauprojekts einfließen. Vor dem Hintergrund, ob die spezifischen Herausforderungen des vorgefertigten Holzbaus den etablierten Grundlagen von BIM-Referenzabläufen entsprechen, wurden folgende Fragestellungen untersucht:

- Unterscheidet sich der BIM-Referenzprozess für einen vorgefertigten Holzbau hinsichtlich der Abläufe von denen eines BIM-Prozesses für mineralische Bauweisen?
- Bedarf es im Bereich der BIM-Planung eines Holzbaus besonderer Kompetenzen der einzelnen Rollen?
- Lassen sich die geometrischen und alphanumerischen Informationen betreffend holzbauspezifischer Aspekte generieren?

Die Ergebnisse der Fragestellungen dienten der Erstellung eines BIMwood Referenzprozesses. Dieser definiert neben den Informationsanforderungen die Informationstiefe in den unterschiedlichen Planungsphasen. Ferner werden die beteiligten Akteure und die ihnen zugewiesenen Rollen überprüft und es wird festgelegt über welche holzbauspezifischen Kompetenzen die beteiligten Akteure im Planungsprozess eines Holzbaus verfügen müssen.

2 Methodischer Ansatz

Zur Erarbeitung des BIMwood Referenzprozess wurde ein handlungsorientierter, simulativer Methodenansatz gewählt, der zwei Betrachtungsebenen beinhaltet: Die prozessuale Ebene beschreibt die Austauschprozesse im Kontext der zugewiesenen Rollen (Prozess). Die deskriptive Ebene beschreibt die strukturierten, multidisziplinären Daten (Inhalte). Gemeinsam mit den am Forschungsprojekt BIMwood beteiligten Praxispartnern wurde mittels der Planung digitaler Mockups der BIMwood Referenzprozess entwickelt. Die Mockups stellen in der Annahme wesentliche Bauteile eines komplexen Holzbaus dar. Der Untersuchungsgegenstand betrifft dabei die Bauteile

Wand, Decke, Dach, Öffnung und Raum. Die für die Planung im Holzbau notwendigen Kompetenzen waren durch die am Prozess Beteiligten repräsentiert. Die Zuordnung von Rollen und Verantwortlichkeiten erfolgte vor Untersuchungsbeginn. Die Beschreibung der notwendige Holzbaukompetenz der beteiligten Rollen wurden im Laufe der Untersuchung verfeinert und definiert. Der notwendige Umfang der geometrischen und alphanumerischen Informationen zu bestimmten Planungsphasen wurde in einem dokumentierten Prozess diskutiert, beleuchtet und hinterfragt. Die dokumentierten Ergebnisse werden in einer weiteren Evaluierungsrunde mit Experten validiert.

3 Ergebnisse zum BIMwood Referenzprozess

3.1 Prozess

Hinsichtlich der Prozessabläufe wurden keine Abweichungen zu bestehenden BIM-Referenzprozessen festgestellt. Die sogenannte Leistungsphase Null als notwendige Projektvorbereitungsphase wird seit langem in unterschiedlichen Fachgremien diskutiert und als Notwendigkeit empfohlen [5, S. 62]. Sie dient der argumentierten Auswahl des Planungsteams ebenso wie der Festlegung zu erbringender Leistungen zu festgelegten Planungsphasen und definiert die Kosten- und Terminvoraussetzungen. Diese Diskussion tritt im Kontext der Beschreibung der Auftraggeber Informationsanforderungen AIA wieder vermehrt in den Mittelpunkt. Der Holzbau profitiert von der Hervorhebung der Relevanz der Leistungsphase Null im BIM Prozess [6, S. 445]. Grundsätzlich jedoch entsprechen die Abläufe der Holzbauplanung denen des BIM konformen Planens mit mineralischen Baustoffen. Die Unverzichtbarkeit notwendigen Abläufen (AIA – BAP – Projektstart) im Planungsprozess gemäß vorhandener BIM Referenzprozesse zu folgen, gilt unabhängig von den verwendeten Materialien

3.2 Holzbaukompetenz

Wesentlicher Aspekt bei der Umsetzung vorgefertigter Holzbauten ist die frühzeitige Integration der notwendigen Holzbaukompetenz [4]. Neben der Synthese holzbaugerechter Konstruktionsprinzipien und Raumbildung, bauphysikalischen Anforderungen und solchen des Brandschutzes ist eine frühe Auseinandersetzung mit dem Bauprozess notwendig, dessen besondere Anforderungen die Planungsphase hinsichtlich Ausarbeitungsdauer und -tiefe beeinflusst. Themen der Vorfertigung, Transportlogistik und Montage müssen bereits in die Planung einfließen [4]. Der Begriff Holzbaukompetenz allgemein beschreibt eine Leistungsfähigkeit aus anwendungsorientierter Sicht, die Themen des Planen und Bauen mit dem Werkstoff Holz betreffend. Neben der Festlegung und Abfrage der BIM-Kompetenzen [7, S. 19-22] ist für die Umsetzung von Holzbauprojekten im Rahmen der Zuordnung von Rollen und Verantwortlichkeiten diese Holzbaukompetenz notwendig. Eine

Konkretisierung der Holzbaukompetenz mit Blick auf Themen- bzw. Handlungsfelder erfolgte gemäß folgender Unterscheidung: Während die **allgemeine Holzbaukompetenz** das nicht fachspezifische Wissen hinsichtlich Material, Vorfertigung und Prozesse im Unterschied zum mineralischen Bauen umschreibt, impliziert die **Holzbaukompetenz der Fachplanenden** fach- und materialspezifische Kenntnisse und deren Berücksichtigung im Planungsprozess. **Prozessspezifische Holzbaukompetenz** beinhaltet fertigungsrelevantes Wissen, das von Themen der Arbeitsvorbereitung bis hin zu Elementierung, Logistik und Montage reicht.

Die im Rahmen eines BIM-Projekts notwendigen Rollen und Verantwortlichkeiten müssen vor Projektbeginn definiert und benannt sein [1, S. 9]. Gleichzeitig müssen sie von geeigneten Personen mit entsprechenden BIM- und Holzbaukompetenzen ausgeführt werden. Entsprechend ihrer jeweiligen Rollen und Verantwortlichkeiten werden im Rahmen der BIMwood Referenzablaufs den aus bestehenden BIM-Prozessen basierenden Rollen entsprechende Holzbaukompetenzen zugewiesen.

3.3 Rollen und Verantwortlichkeiten

Im Rahmen der Erarbeitung des BIMwood Referenzprozesses sind in der Rollenverteilung zwei Unterschiede im Vergleich zu der Rollenverteilung im konventionellen BIM-Referenzprozess deutlich zu identifizieren: die Integration der Holzbaukompetenz sowie die Bedeutung des Tragwerksmodells.

Um spezifischen Belange des Holzbaus (Vorfertigung, Elementierung,…) im Planungsprozess zu berücksichtigen ist es notwendig die Holzbaukompetenz in den Planungsprozess frühzeitig zu integrieren [4]. Diese Forderung wird inhaltlich bei der Planung mit BIM berücksichtigt. Um die Besonderheiten der Holzbauplanung in dem BIMwood Referenzprozess abzubilden, erhält die Holzbauplanung eine eigene Rolle im Prozess. Die Rolle der Holzbauplanung kann von verschiedenen Akteuren erbracht werden. Beispielswiese können Tragwerksplanende, gemeinsam mit Objektplanenden, mit ausreichender Holzbaukompetenz die Aufgaben der Holzbauplanung übernehmen. Alternativ kann ein/e eigenständige/r Akteur/in, wie eine Fachingenieur/in Holzbau, die Rolle ausfüllen.

Im Unterschied zum konventionellen BIM-Referenzprozess kommt dem Fachmodell der Tragwerksplanung eine besondere Bedeutung zu. In den Fallstudien und Diskussionen mit den Praxispartnern wurde die Bedeutsamkeit des Tragwerksmodells formuliert, welche im Folgenden erläutert wird: Bei der Planung mit mineralischen Baustoffen kommt es bei der Erstellung des Fachmodells der Objektplanung und der Erstellung des Fachmodells der Tragwerksplanung dazu, dass beide Fachrichtungen die gleichen Elemente planen, diese aber keinen direkten Bezug zueinander haben und es somit zu Unstimmigkeiten und unklaren Zuständigkeiten führen kann. Im BIMwood Referenzprozess bauen die Modellierung der Fachmodelle der Tragwerksplanung und der Objektplanung aufeinander auf: Der Objektplaner modelliert die Tragschicht in der Mitte der

Holzbauteile als eine Schicht. Beidseitig werden dann die spezifischen Bekleidungen (Außenwandbekleidung, Innenwandbekleidung, Deckenbeläge, Deckenbekleidungen) als Schicht differenziert dargestellt. Es entsteht für die Wand- und Deckenbauteile das 3-Schichten Modell der Objektplanung. In der folgenden Darstellung sind die drei Schichten im Modell der Objektplanung auf der linken Seite schematisch dargestellt.

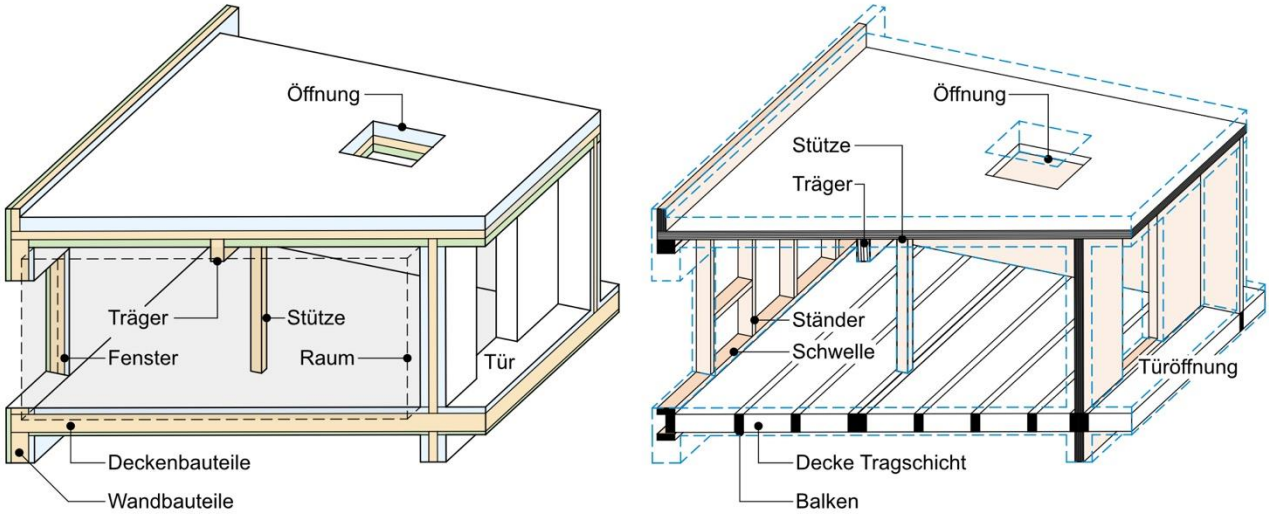

Abbildung 2: Gegenüberstellung 3 Schichten-Modell der Objektplanung (links) und Tragwerksmodell mit Überlagerung 3-Schichten-Modell (rechts)

In der Ebene der Tragschicht werden durch den Tragwerksplaner die Komponenten der tragenden Holzkonstruktion (Rähm, Schwelle, Ständer, Balken, Sperrzonen) modelliert (Abbildung 2 rechts) . Ein weiterer Unterschied zur mineralischen Bauweise ist, dass im Holzbau die tragenden Bauteile einer Holzkonstruktion aus mehreren Komponenten bestehen. Am Beispiel der Holztafelbauwand sind das Rähm, Schwelle, Ständer, die als zusammengesetzte Holzkonstruktion die Tragschicht der Wand bilden. Bei einer Betonkonstruktion besteht eine Wand aus einem Element. Die Nutzung der Tragschicht gibt der Tragwerksplanung einen Raum für die Modellierung der statisch relevanten Konstruktionselemente. Dadurch entsteht auch die Möglichkeit zur Generierung des Tragwerk-Analysemodells mit BIM.

Das Fachmodell der Tragwerksplanung ist zwar auch weiterhin in weiten Teilen deckungsgleich zu dem Fachmodell der Objektplanung. Darüber hinaus enthält es detaillierte Angaben zu den tragenden Holzbauelementen. Diese werden dementsprechend nicht im Modell der Objektplanung dargestellt. Diese Arbeitsweise ist aktuell noch nicht etabliert, jedoch so das Ergebnis der Untersuchung, verbessert diese Vorgehensweise langfristig den Planungsprozess und die Schnittstellen der Akteure. Im weiteren Planungsverlauf wird mit den Fachmodellen von Objektplanung und Tragwerksplanung eine durchgängige Kette von der Planung bis zur Ausführung initiiert. In einem Fallbeispiel wurde der Datenaustausch mit dem Praxispartner des ausführenden Holzbauunternehmens erprobt. Dabei wurde das 3-Schichtenmodell als ideale geometrische

Grundlage für die Arbeitsvorbereitung identifiziert. Die Arbeitsvorbereitung umfasst im Holzbauunternehmen die Planung der Fertigung und Montage der vorgefertigten Bauelemente und Bauteile. Die wesentlichen Informationen zur Holzkonstruktion erhält das Holzbauunternehmen durch das Tragwerksmodell.

Als sinnvolle Struktur für die Modellierung von Holzbauteilen hat sich Folgendes als zielführend erwiesen: Die Mehrschichtigkeit und Komplexität von Bauteilen in Holzbauweise kann im 3D-Modell der Objektplanung im Wesentlichen durch drei Schichten gegliedert und vereinfacht werden. Hierzu erfolgt die Zusammenfassung von mehrschichtigen Bauteilen in Tragschicht und innere und äußere Bekleidung. In sind diese 3 Schichten am Beispiel einer Außenwand dargestellt. Abbildung 3 zeigt die Tragschicht (orange), welche beidseitig von einer äußeren Bekleidungsschicht (grün) und einer inneren Bekleidungsschicht (blau) bekleidet ist.

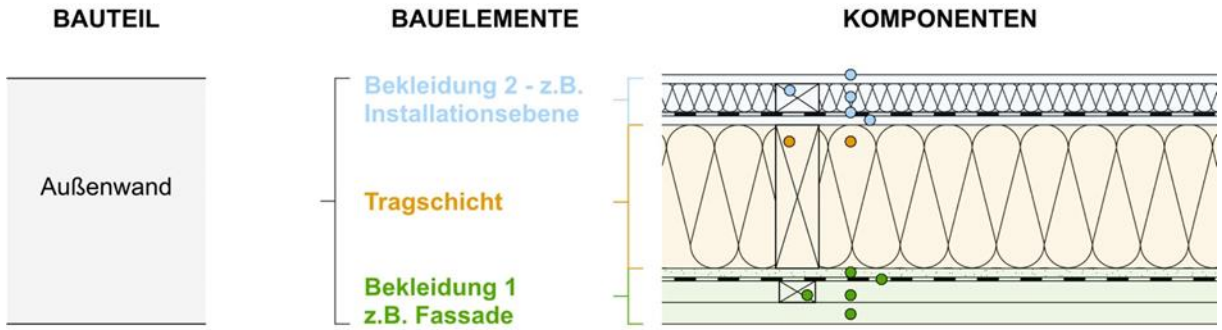

Abbildung 3: 3-Schichten-Modell am Beispiel einer Außenwand, Tragschicht (orange), äußere (grün) und innere (blau) Bekleidung mit ihren Komponenten (farbige Punkte)

Die Tragschicht beinhaltet die Komponenten der Tragkonstruktion (Abbildung 3 - dargestellt durch die farbigen Punkte). Diese kann bei einem Wandbauteil die Konstruktionsebene des Holzrahmenbaus sein oder eine massive Holzwand. Die Bekleidung fasst die Bauelemente neben der Tragschicht, welche aus mehreren Komponenten gebildet werden, zusammen. So kann, auch im Vergleich zur mineralischen Bauweise, das geometrische Modell schlank gehalten werden, obwohl die Holzbauteile wesentlich mehr einzelne Elemente enthalten. Es gibt mehr Klarheit und Überschaubarkeit der komplexen Bauweise Holz.

4 Ausblick

Vor dem Hintergrund der Construction 4.0 als Konzept, das auf der Digitalisierung der Bauwirtschaft einerseits und der Industrialisierung der Bauprozesse andererseits basiert, kommt dem Holzbau eine besondere Bedeutung zu. Die Abläufe in der Produktion und Fertigung sind, anders als beim mineralischen Bauen, weitestgehend industrialisiert. Die idealtypische Darstellung des BIMwood Referenzprozesses für den vorgefertigten Holzbau und Empfehlungen für konkrete

Anwendungsfälle dienen dazu, die digitale Kette, insbesondere an der Schnittstelle zur Ausführung zu optimieren. Die Ergebnisse haben das Potenzial wichtige Hinweise an die unterschiedlichen Stakeholder zu liefern, insbesondere an die Softwareindustrie, die für Neuentwicklungen auf die Anforderungen und Formulierung von Defiziten der holztechnischen Fachkenntnisse angewiesen ist und unterstützt in Folge die bauliche Nutzung nachwachsender Rohstoffe und damit zielgerichtet die forstbasierte Industrie. Die Entwicklung des BIMwood Referenzprozesses und die damit verbundene Weiterentwicklung der holzbasierten Prozesskette trägt dazu bei, das derzeit ungenutzte Potenzial im forstwirtschaftlichen Sektor der mehrgeschossigen Gebäude zu unterstützen und die Weltwirtschaft von der Abhängigkeit von fossilen und nicht nachwachsenden Rohstoffen zu einer nachhaltigen "Bio-based Economy" zu entwickeln. Nicht zuletzt mit Blick auf Ressourcenerhalt und Kreislaufwirtschaft, gewinnt die Nutzung von digitalen Informationsmodellen an Bedeutung. Auf Grundlage der Bauwerksmodelle können nach Jahrzehnten der Nutzung Daten und Informationen zur Weiter- und Wiederverwertung der Bauteile gewonnen werden.

Literaturverzeichnis

[1] VDI 2552 Blatt 1, VDI 2552 Blatt 1, Building Information Modeling: Grundlagen = Building information modeling : fundamentals. Berlin: Beuth Verlag GmbH, 2020.

[2] BIMiD, BIM-Referenzobjekt in Deutschland (2013-2017): Ein Praxismodellprojekt für die deutsche Bau-und Immobilienwirtschaft. [Online]. Verfügbar unter: https://www.kompetenz-zentrum-planen-und-bauen.digital/ueber-uns/bimid/projekt-bimid (Zugriff am: 27. Mai 2022).

[3] K. Hausknecht und T. Liebich, BIM-Kompendium: Building Information Modeling als neue Planungsmethode. Stuttgart: Fraunhofer IRB Verlag, 2016.

[4] H. Kaufmann, W. Huss, S. Schuster und M. Stieglmeier, leanwood - Optimierte Planungsprozesse für Gebäude in vorgefertigter Holzbauweise. [Online]. Verfügbar unter: https://mediatum.ub.tum.de/doc/1537682/1537682.pdf (Zugriff am: 4. Februar 2020).

[5] H. Lechner und D. Stifter, Kommentar zum Leistungsbild Architektur: HOAI 2013, LM.VM.2014, 3. Aufl. Graz: Verl. der Techn. Univ, 2015.

[6] H. Kaufmann, W. Huß, S. Schuster und M. Stieglmeier, „leanWOOD - Innovative und optimierte Prozesse und Kooperationsmodelle für die Planung, Produktion und den Unterhalt von Gebäuden in Holzbauweise (Forschungsbericht)“. Abschlussbericht, Technische Universität München, München, 2018. [Online]. Verfügbar unter: https://mediatum.ub.tum.de/doc/1625415/hur5rvt2kdwtgfjjyze3imj6t.leanWood_FinalReport.pdf

[7] BMDV, Konzept zur schrittweisen Einführung moderner, IT-gestützter Prozesse und Technologien bei Planung, Bau und Betrieb von Bauwerken – Stufenplan zur Einführung von BIM: Endbericht. [Online]. Verfügbar unter: https://www.bmvi.de/SharedDocs/DE/Anlage/DG/Digitales/bim-stufenplan-endbericht.html.

XML-basierte Übernahme von Inhalten der Auftraggeber-Informationsanforderungen in eine BIM-Autorensoftware

M. Mellenthin Filardo[1], C. Nürnberger[1] and H.-J. Bargstädt[1]
[1]Professur Baubtrieb und Bauverfahren, Bauhaus-Universität Weimar,
Marienstr. 7, D-99423, Weimar, Deutschland
E-mail(s): martina.mellenthin.filardo@uni-weimar.de

Abstract: In Auftraggeber-Informationsanforderungen (AIA) formulieren Auftraggebende (AG) gegenüber Auftragnehmenden (AN) projektrelevante Anforderungen an die Modellierung unter Verwendung der Building Information Modeling (BIM) Methodik. Zu diesen Inhalten gehören neben allgemeinen Informationen zum Projekt auch technische Anforderungen an die geometrische und semantische Detailtiefe, Übergabeformate und Versionen, als auch Anforderungen an die Struktur der zu erstellenden Modelle. Aktuell bedarf es meist noch eines Zwischenschritts, in dem die benötigten Informationen herausgefiltert werden müssen, um sie anschließend manuell in die BIM-Autorensoftware einzupflegen. Dazu kommt, dass viele AGs in der Regel (noch) kein tiefgreifendes BIM-Know-how besitzen oder Zugriff auf spezifische BIM-Softwareanwendungen haben, mit denen diese Problematik überwunden werden könnte. In diesem Beitrag werden am Markt verfügbare Werkzeuge zusammengefasst und ein eigener Workflow samt Prototyp zur automatisierten und maschinenlesbaren Übernahme von ausgewählten Inhalten einer AIA aus einer büroüblichen Anwendung, unter Verwendung der Auszeichnungssprache XML, in die BIM-Autorensoftware ArchiCAD vorgeschlagen und implementiert.

Keywords: BIM, AIA, Austausch-Informationsanforderungen, Auftraggeber-Informationsanforderungen, XML, AIA-Maschinenlesbarkeit

1 Einleitung

Bei der Bestellung von Planungsleistungen unter Verwendung digitaler Methoden dient die Definition der im Modell enthaltenen Informationen für ein bestimmtes Ziel bzw. für einen bestimmten Anwendungsfall einer effektiven Arbeitsweise [1]. Die Vorgabe von Informationsanforderungen, Aufgaben und Arbeitsabläufen hat sich als wesentlich für einen erfolgreichen Datenaustausch [2] und somit ausschlaggebend für eine konfliktarme Projektabwicklung gezeigt. In der Bauindustrie werden die Anforderungen an die herkömmlichen Planungs- und Ausführungsleistungen bereits minutiös spezifi-

ziert [3], [4]. Hinsichtlich der Beauftragung von Leistungen basierend auf digitalen Gebäudemodellen gibt es konkrete Ansätze, unter anderem [5]–[7]. Dass diese jedoch noch keine breite Anwendung finden, kann durch die prävalente Übergabe der von Auftraggebenden gestellten Anforderungen an die Modellierung in fließender, papierbasierter Textform [8], welche um strukturierte Typ- und Attributtabellen ergänzt werden können [1], nachgewiesen werden.

2 Background zu AIA-Inhalten

Geltende Normen und Richtlinien, hauptsächlich [7], [9], [10], bieten einen Rahmen zur Erstellung und Nutzung von Auftraggeber- bzw. Austauschinformationsanforderungen. Einen wesentlichen Vorteil der AIA-Dokumente stellt die verlässliche vertragliche Vereinbarung projektrelevanter Anforderungen dar, die von Beginn an in der Planung Berücksichtigung finden sollten. Technisch stellt die Form der AIA-Dokumente eine Herausforderung für die automatisierte Weiterverwendung dar, die der konsequenten Trennung zwischen Anforderungen an die Modellierung und an das Projekt sowie die Form solcher Dokumente - verbreitet in Fließtextform - geschuldet sind [8]. Die Erstellung von AIA-Dokumenten kann durch Dienste unterstützt werden, wie die im Anschluss erläuterten. Dabei werden modellrelevante Inhalte von AIA-Dokumenten heraus gefiltert und in maschinenlesbarer Form erzeugt.

Ein in Deutschland weit verbreiteter Dienst, BIMQ, bietet eine kostenpflichtige Lösung zur Definition von Anforderungen im Zuge eines Projekts. Dabei können diverse Formate exportiert werden, darunter (Excel-)Tabellen, Parameterdateien für Autodesk Revit (txt) und ArchiCAD (xml)[11], welche zu dem in diesem Beitrag vorgeschlagenen Workflow vergleichbar sind. Das Tool CAFM-Connect [12] ist eine für sich stehende Anwendung und besteht aus den Modulen BIM-Profile und CAFM-Connect Editor. Dort können Informationen nach vordefinierten Katalogen (DIN 277-2, DIN 276 oder GEFMA 198), teilweise mit einem inbegriffenen IFC-Mapping, in sogenannten Profilen erstellt werden. Weiterhin ist die Verknüpfung mit Dokumenten, bspw. Herstellerinformationen, möglich. Der Austausch kann über IFC-basierte Formate erfolgen (ifcXML oder ifcZIP). Der Entwickler Ekkodale stellt einen AIA-Editor zur Verfügung, welcher Autodesk Revit-kompatible Parameterdateien im Sinne von Vorgaben aus AIA-Dokumenten erzeugt. Dabei werden die von Revit gegebenen Einschränkungen berücksichtigt, wie die Trennung zwischen gemeinsam genutzten Paramentern und Projektparamentern sowie Format und Struktur der jeweiligen Parameterdatei. Der Quellcode steht nicht öffentlich zur Verfügung, jedoch kann anhand des In- und Outputs davon ausgegangen werden, dass dort - vergleichbar mit dem in dieser Arbeit vorgeschlagenen Workflow - Inhalte aus Tabellen in das von der Modellierungssoftware einlesbare Format (txt im Falle von Revit) konvertiert bzw. übersetzt werden [13]. Der Hersteller DiRoots stellt eine Sammlung an Plugins kostenfrei bereit. Darunter befinden sich auch solche, die mit der Anwendung Autodesk Revit kompatibel sind und den Im- sowie Export diverser Inhalte aus (Excel-) Tabellen erlauben, wie bspw. Typ- und Attributtabellen [14].
Hervorzuheben bleibt, dass die genannten Anwendungen an einer Marktteilhabe interessiert sind, weshalb der Quellcode der einzelnen Anwendungen nicht öffentlich zur Verfügung steht. Weiterhin handelt es sich bei den genannten Diensten teilweise um Webanwendungen, Standalone-Anwendungen oder

Add-Ons und Plugins für bestehende (Modellierungs-)Anwendungen. Modellierungsanwendungen können als Zielanwendung solcher AIA-Inhalte Umfang, Struktur und Format des einzulesenden Inhalts frei bestimmen. Entsprechend muss jeder Dienstleistende einen eigenen Workflow vorschlagen und umsetzen, da keine standardisierten Vorgaben zur maschinenlesbaren Form von AIA-Inhalten vorliegen.

3 Workflow

Ziel dieser Arbeit war die Entwicklung eines prototypischen Werkzeugs zur Unterstützung der Anforderungszusammenstellung basierend auf büroüblichen Werkzeugen, weshalb die Auswahl der Ausgangssoftware auf das weit verbreitete Excel-Tool beschränkt werden konnte. Die definierten Anforderungen sollten im Sinne einer effektiven Arbeitsweise der Planung *a priori* dienen können [15], weshalb die Zielanwendung ArchiCAD (in der Version 25) und das dort dafür verwendete Format eXtensible Markup Language (XML) gewählt wurden.

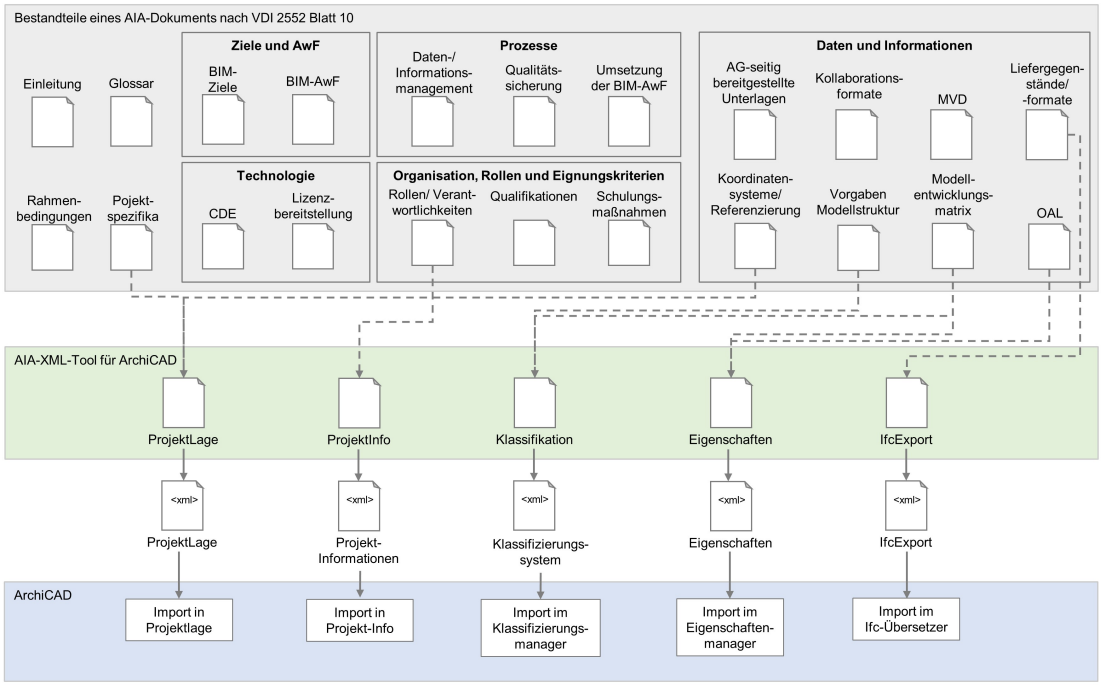

Abbildung 1: Erklärungsdiagramm zu vorgesehenen AIA-Inhalten, die mit der entwickelten Excel-Schnittstelle an die Anwendung ArchiCAD im XML-Format übergeben werden

Der in Abb. 1 dargestellte Workflow erlaubt eine anwenderfreundliche Definition von AIA-Vorgaben innerhalb einer Excel-Mappe, welche über VBA-gesteuerte Skripte (Visual Basic for Applications) von ArchiCAD 25 einlesbare XML-Dateien erzeugt. Die Auswahl und Implementierung der AIA-Inhalte ergeben sich aus den in ArchiCAD 25 bereits vorhandenen Schnittstellen, im Sinne einer Synergienutzung des Prototyps. In einer Voruntersuchung von gängigen Modellierungsanwendungen zeigte sich, das ArchiCAD im Gegensatz zu bspw. Autodesk Revit umfangreiche XML-Importfunktionen vorweist.

Die nach [10] gegliederten AIA-Inhalte wurden zunächst auf ihren Mehrwert innerhalb der Zielmodellierungsumgebung untersucht und anschließend gruppiert. Die von der ArchiCAD 25 XML-Schnittstelle unterstützten Inhalte wurden in dem entwickelten Excel-Tool angelegt. Dabei wurden die Inhalte in die Gruppen Projektlage, Projektinformationen, Klassifikationssystem, Eigenschaften und Ifc-Export sortiert. Die in Excel integrierte VBA-Schnittstelle generiert für jede Gruppe die genannte XML-Datei, welche die von ArchiCAD 25 akzeptierte XML-Formatierung berücksichtigt. Die Umsetzung dieses Prototyps soll die bereits vorhandenen Möglichkeiten einer XML-Integration darstellen und die Notwendigkeit für ein einheitliches, maschinenlesbares AIA-Format verdeutlichen.

4 Implementierung

Die Anwendung ArchiCAD 25 bietet unterschiedliche XML-Schnittstellen für den Import von Informationen zur Projektlage, zu konkreten Projektinformationen, zu Eigenschaften und Klassifikation sowie für den IfcExport. Jede Schnittstelle sieht eine eigene Struktur für die einzulesende XML-Datei vor. Eine Dokumentation dieser ist den Autor*innen nicht bekannt. Die Implementierung des Excel Tools wird anhand des Beispiels der Klassifizierungssysteme erläutert. Die Implementierung der anderen Inhalte erfolgte analog. Zunächst wird ein Einblick gegeben, wie die XML-Datei aufgebaut ist. Im Anschluss wird das VBA-Skript erläutert, welches die XML-Datei innerhalb des Excel-Tools erstellt. Abschließend wird auf die Ergebnisse eingegangen.

4.1 Von ArchiCAD unterstützte XML-Inhalte

Allgemein werden Klassifizierungen in ArchiCAD dazu genutzt, um alle in einem Projekt verfügbaren Elemente und die dazugehörigen Daten zu strukturieren. Weiterhin werden in Klassifizierungssystemen auch bestimmte Eigenschaften hinterlegt, insbesondere welche Eigenschaften für bestimmte Elemente verfügbar sein sollen. Zur Steuerung des Klassifizierungssystems in ArchiCAD wird der sogenannte Klassifizierungs-Manager genutzt. Er unterstützt neben der Erstellung von Klassifizierungssystemen auch die Anpassung von bereits vorhanden Systemen, die Zuordnung von neuen Eigenschaften und die Bearbeitung dieser.

Die für Klassifizierungen verwendeten XML-Dateien sind nicht eigenständig (Standalone), da sie sich mit den hier nicht weiter beschriebenen jedoch im Excel-Tool implementierten XML-Dateien für Eigenschaften das gleiche Wurzelelement `BuildingInformation` teilen, sodass alle definierten Eigenschaften in direkter Verbindung mit den entsprechenden Elementen aus dem Klassifizierungssystem stehen.

Da sich im Rahmen der Erstellung des Excel-Tools eine getrennte Umsetzung in Form von zwei eigenständigen Excel-Arbeitsblättern als praktikabler erwies, werden zwei getrennte XML-Dateien erstellt, jeweils mit dem Wurzelelement und dem entsprechenden Kindelement `PropertyDefinitionGroups` oder `Classification`. Dem Kinderelement `Classification` ist ein weiteres einzelnes Element namens `System` untergeordnet. Das System-Element repräsentiert das gesamte Klassifikationssystem und enthält zunächst die Kinderelemente `Name, EditionVersion, EditionDate, Description` und

`Source`. In diesen Elementen werden die Inhalte abgelegt, die ArchiCAD 25 während der Erstellung eines neuen Klassifizierungssystems abfragt. Dementsprechend sind die Inhalte der Elemente `Name`, `EditionVersion` und `EditionDate` obligatorisch.

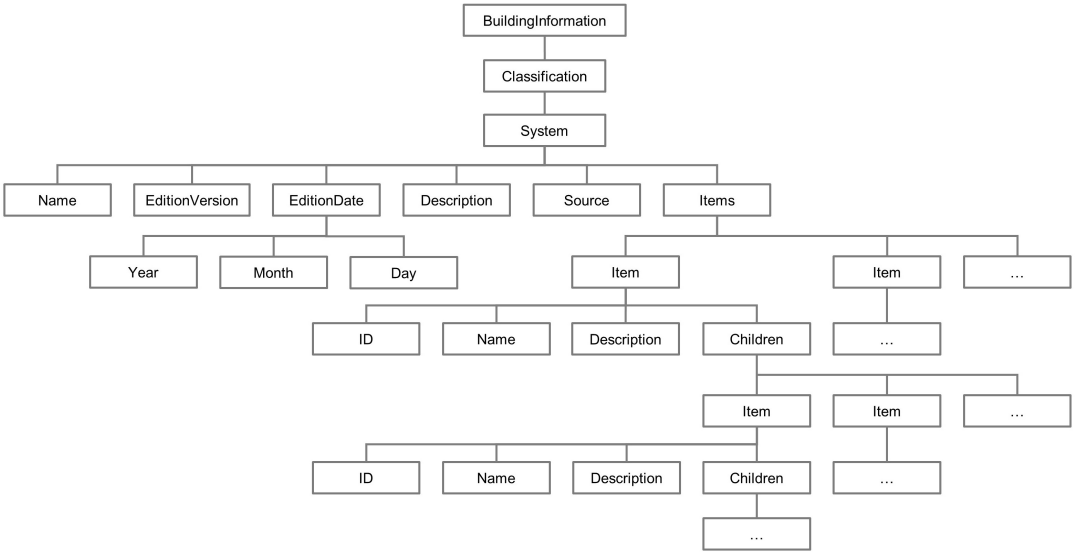

Abbildung 2: Struktur der von ArchiCAD 25 akzeptierten XML-Datei zur Definition von Klassifizierungssystemen

Das sechste und letzte Kinderelement des `System`-Elements heißt `Items`. Es enthält die gesamte vom Klassifizierungssystem eingeschlossene Klassifizierung in Form einer hierarchischen Klassenstruktur. Sie werden durch Kinderelemente namens `Item` repräsentiert und können in unbegrenzter Anzahl auftreten. Je höher der Detaillierungsgrad, desto mehr Ebene werden erstellt. Für die Erstellung des Excel-Tools wurde ein Klassifizierungssystem beispielhaft bis in die 20. Ebene geführt. In der Regel erstrecken sich Systeme für im Bauwesen übliche Projekte meist nicht weiter als zur sechsten oder siebten Ebene. Bspw. verfügt das standardmäßig vorhandene Klassifizierungssystem von ArchiCAD 25 über insgesamt sieben Ebenen.

Jedes `Item`-Element verfügt immer über genau vier Kinderelemente, `ID`, `Name`, `Description` und `Children`. Die ersten drei Elemente repräsentieren wieder die Inhalte, welche innerhalb der Erstellung einer neuen Klassifizierung durch das ArchiCAD-Dialogfenster abgefragt werden. Das letzte Element `Children` kann eine unbegrenzte Anzahl an Kinderelemente enthalten, die ebenfalls `Item`-Elemente sind und somit wieder über ein `Children`-Element verfügen. Somit können beliebig viele `Item`-Elemente hierarchisch ineinander verschaltet werden und ordnen sich je nach Wunsch des Erstellenden einem übergeordneten `Item`-Element unter. Die Struktur der erläuterten XML-Datei wird in Abb. 2 dargestellt.

4.2 Eingabe in Excel

Die als Datenquelle des Skripts definierte Excelmappe ist in die Arbeitsblätter Projektinfo, Projektlage, Klassifizierung, Eigenschaften, IfcExport, gegliedert. Aus jedem Arbeitsblatt wird von einem separaten

VBA-Skript jeweils eine separate XML-Datei erzeugt. Bei der Erstellung eines Klassifizierungssystems, wie in Abb. 3 links dargestellt, werden die vorgesehenen Elemente und Kinderelemente in dem entsprechenden Arbeitsblatt im Sinne einer Eingabemaske eingepflegt. In der Datei können die in 4.1 genannten Systeminformationen ergänzt werden. Dieser Vorgang wird für alle Arbeitsblätter wiederholt.

4.3 Visual Basic Scripting

Für die Implementierung des VBA-Skriptes wurde die XML-Exportfunktion von ArchiCAD 25 genutzt, da Graphisoft selbst keine Dokumentation zur XML-Schnittstelle von ArchiCAD bereitstellt. Aus dieser wurde eine einlesbare XML-Datei erzeugt und als strukturvorlage für das VBA-Skript verwendet. Im Folgenden wird die Logik des Skriptes zur Erzeugung der XML-Datei zum Klassifizierungssystem exemplarisch dargestellt, siehe Alg. 1. Die Steuerung des Skripts und Eingabe von AIA-Inhalten erfolgen über eine Excel-Eingabemaske.

Algorithmus 1 Pseudocode zur Logik des entwickelten VBA-Skripts

Eingabe: Excel Datei mit Items XLS
  Erstellung von Header und Metadata
  für alle Item i in XLS **mache**
    parseItem(i)
  Ende für
  Export der Datei

Funktion PARSEITEM(i)
  Auslesen von Name, ID und Beschreibung
  Wenn i hat Kinder **dann**
    für alle Kind k **mache**
      parseItem(k)
    Ende für
  Ende Wenn
  Abschließen des Items
  Rückgabe des Ergebnisses
Ende Funktion

Das Skript wird von dem Betätigen des XML-Export-Buttons in der Excel-Eingabemaske ausgelöst. Dabei wird zunächst der Dateipfad festgelegt und der notwendige XML-Header sowie Metainformationen der Datei erstellt. Anschließend wird ein `Item` (i) erzeugt. Für das `Item` werden ID, Name und Beschreibung eingelesen und Kindelemente (k) rekursiv hinzugefügt. Zum Schluss wird das Item abgeschlossen und die XML-Datei ausgeschrieben und gespeichert, sodass sie anschließend in ArchiCAD 25 eingelesen werden kann.

5 Ergebnisse: Import in ArchiCAD

Der Output des entwickelten Tools bzw. des erläuterten Skriptes kann der Abb. 3, rechte Seite, entnommen werden. Die XML-Datei wird erfolgreich in ArchiCAD durch den Klassifizierungs-Manager eingelesen und kann im Projekt bzw. von Beginn der Planung an berücksichtigt werden. Das entwickelte Tool geht so weit, dass es plattformunabhängig eingesetzt werden kann, da die Verwendung der Skripte ebenso in LibreOffice gegeben ist.

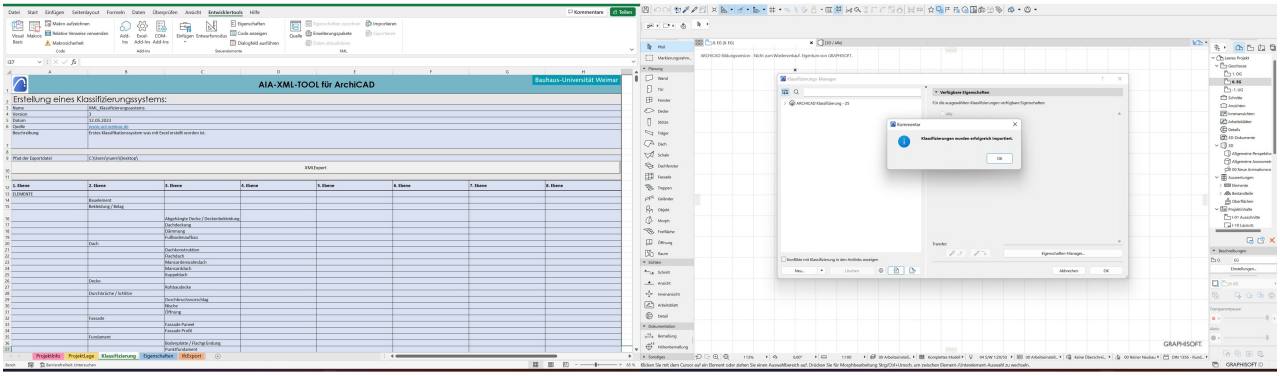

Abbildung 3: Benutzeroberflächen des Excel-Tools für die Zusammenstellung der Anforderungen an die Klassifizierung (links) und Darstellung des erfolgreichen Imports dieser in der Anwendung ArchiCAD 25 (rechts)

6 Fazit und Ausblick

Der Austausch von Anforderungen an die Modellierung im Sinne von AIA-Vorgaben wird bereits von am Markt verfügbaren Diensten mit unterschiedlichen Ansätzen adressiert. Wie der vorgeschlagene Workflow zeigt, können modellrelevante Inhalte mit geringem Aufwand und innerhalb büroüblicher Anwendungen in maschinenlesbarer Form erzeugt werden.

Da jedoch kein etablierter Standard für maschinenlesbare AIA-Inhalte existiert, geben Softwarehäuser derzeit vor, wie und wie viele Modellanforderungen eingelesen werden. Im Rahmen des vorgeschlagenen Ansatzes bedeutet dies, dass das VBA-Skript angepasst werden muss, sobald ArchiCAD nur ein Komma in der Struktur der eingelesenen XML-Dateien ändert. Der Umfang der mit dem Workflow übertragenen Inhalte deutet weiterhin auf die Notwendigkeit eines etablierten Schemas für AIA-Inhalte, um die Verwendung von standardisierten Programmierschnittstellen zu ermöglichen. Ein solches Schema sollte projekt- sowie auftraggeberspezifische Vorgaben erlauben. Eine weder in diesem Workflow noch in den marktüblichen Tools implementierte Funktion stellt die Rückkopplung von der Modellierungsumgebung zurück in die Umgebung dar, in der die Anforderungsdefinition stattfand. Eine Prüfung bzw. ein Abgleich mit den gestellten Anforderungen ist im Regelfall erst nach dem Export aus der Modellierungsumgebung möglich (Data Drop) und sollte für eine effektive Umsetzung der gestellten Anforderungen bereits während der Modellierung erfolgen können.

Literatur

[1] A. Borrmann, M. König, C. Koch und J. Beetz, Hrsg., *Building Information Modeling: Technologische Grundlagen und industrielle Praxis*, 2., aktualisierte Auflage, Ser. Springer eBook Collection. Wiesbaden: Springer Vieweg, 2021, ISBN: 9783658333614. DOI: 10.1007/978-3-658-33361-4.

[2] C. Eastman, P. Teicholz, R. Sacks und G. Lee, *BIM handbook: A guide to building information modeling for owners, designers, engineers, contractors, and facility managers*, 3. ed. Hoboken, New Jersey: John Wiley & Sons, 2018, ISBN: 978-1-119-28753-7.

[3] *HOAI 2021: Honorarordnung für Architekten und Ingenieure : Textausgabe mit Interpolationstabellen : Textausgabe mit Erläuterung der Neuerungen, Musterrechnungen und Interpolationstabellen*, 6., aktualisierte Auflage. Köln: RM, Rudolf Müller, 2021, ISBN: 9783481042011.

[4] *Musterverträge und -briefe nach HOAI und VOB*. Kissing: WEKA-Media, 2021.

[5] BuildingSMART International, *Technical Roadmap buildingSMART: Getting ready for the future*, BuildingSMART International, Hrsg., 2020.

[6] DIN Deutsches Institut für Normung e.V., *Bauwerksinformationsmodelle - Handbuch der Informationslieferungen - Teil1: Methodik und Format; DIN EN ISO 29481-1*, Berlin, 2018.

[7] DIN Deutsches Institut fuer Normung e.V., *Bauwerksinformationsmodellierung - Informationsbedarfstiefe - Teil 1: Konzepte und Grundsätze; DIN EN 17412-1*, Berlin, 2021.

[8] M. Mellenthin Filardo, »Praxisrelevante Auftraggeber-Informations-Anforderungen für Infrastrukturprojekte als Indikatoren des Einführungsgrades von BIM in Deutschland«, in *31. Forum Bauinformatik*, 2019, S. 9–16, ISBN: 978-3-7983-3105-1.

[9] DIN Deutsches Institut für Normung e.V., *Organisation und Digitalisierung von Informationen zu Bauwerken und Ingenieurleistungen, einschließlich Bauwerksinformationsmodellierung (BIM) Informationsmanagement mit BIM: Teil 1: Begriffe und Grundsätze; Normreihe DIN EN ISO 19650*, Berlin, 2019.

[10] VDI Verein Deutscher Ingenieure e.V., *Richtlinie VDI 2552 Blatt 10 Entwurf: Building Information Modeling - Auftraggeber-Informations-Anforderungen (AIA) und BIM-Abwicklungspläne (BAP)*, Berlin, 2020.

[11] AEC3, *BIMQ Centraldesk*, https://bimq.centraldesk.com/de/, Abgerufen am: 27.05.2022.

[12] K. Aengenvoort, *CAFM-Connect*, https://www.cafm-connect.org/, Abgerufen am: 27.05.2022.

[13] Ekkodale, *AIA.Editor*, https://www.ekkodale.com/tools/aiaeditor/, Abgerufen am: 27.05.2022.

[14] DiRoots Limited, *DiRoots*, https://diroots.com/, Abgerufen am: 27.05.2022.

[15] M. Mellenthin Filardo und J. Krischler, »An A Priori EIR-Compliant Modelling Approach«, in *32. Forum Bauinformatik 2021*, 2021, S. 183–191. DOI: 10.26083/TUPRINTS-00019496.

Merkmalsbasierte Kategorisierung im Building Information Model mithilfe von Machine Learning

Constantin Richter[1] and Jascha Brötzmann[1]
[1]Institut für Numerische Methoden und Informatik im Bauwesen, Technische Universität Darmstadt, Franziska-Braun-Straße 7, 64287 Darmstadt, Deutschland
E-mail(s): email@constantinrichter.de, broetzmann@iib.tu-darmstadt.de

Abstract: Einhergehend mit wachsenden Kompetenzen in der 3D-Modellerstellung ist *Building Information Modeling* durch die aktive Nutzung als Informationsträger zunehmend in den Fokus gerückt. Die Kollaboration unter Einbeziehung externer Projektbeteiligter in heterogenen Softwareumgebungen setzt ein herstellerneutrales sowie softwareunabhängiges Datenformat voraus. In der vorliegenden Arbeit werden daher die *Industry Foundation Classes* (IFC) als offene Datenstruktur und Datenformat für Bauwerksdaten in diesem Kontext besprochen. Durch die computergestützte Wissensmodellierung nehmen Anzahl und Variationen notwendiger Spezifikationen zu. Neben einer einheitlichen Struktur ist daher ein gemeinsames Verständnis von Objekten sowie eine standardisierte Terminologie Voraussetzung für eine konstruktive Zusammenarbeit. Aus diesem Grund werden hierfür Klassifikationssysteme als eines der wichtigsten Systeme zur Strukturierung von Informationen diskutiert. Hier eignet sich vor allem die VDI-Richtlinie 2552, welche die mögliche Einbindung verschiedener nationaler Klassifikationssysteme im Rahmen von IFC mithilfe von Merkmalen vorsieht. Auf dieser Grundlage wird schließlich die Möglichkeit der Automatisierung mittels Machine Learning untersucht. Der Einsatz von Decision-Tree-Algorithmen zur Unterstützung der merkmalsbasierten Kategorisierung eignet sich dabei zur Automatisierung von Klassifizierungsprozessen. Die Anforderungen an binäre Merkmale von Trainingsdaten für diese Algorithmen entsprechen im hohen Maß den Rahmenbedingungen hierarchisch numerisch strukturierter Klassifikationssysteme wie der DIN 276.

Keywords: BIM, IFC, Maschinelles Lernen, Klassifizierung

1 Einleitung

Mit der angestrebten Digitalisierung im Bauwesen wird zunehmend auf die kollaborative Planungsmethode des *Building Information Modeling* gesetzt. *Big open BIM* stärkt durch die erleichterte Interoperabilität der Projektdaten die kollaborative Zusammenarbeit der Planungs- und Bauprozesse zwischen den beteiligten Fachdisziplinen. Sowohl national als auch international wird die Einführung einer herstellerunabhängigen und fachdisziplinübergreifenden Lösung im Bauwesen angestrebt. Eine

Studie des *National Institute of Standards and Technology* von 2004 beziffert die entstandenen Mehrkosten durch fehlende Interoperabilität zwischen Softwaresystemen auf 15,8 Mrd. US-Dollar für 2002. Gut ein Drittel der verursachten Kosten fielen dabei auf die Ausführungsphase an und über die Hälfte der Kosten auf den Betrieb [1]. Das IFC-Format ermöglicht einen offenen Austausch im objektorientierten Arbeiten.

Neben dem offenen Austausch im Rahmen von *open BIM* ist zur Umsetzung von *big BIM* die Strukturierung der Informationen für eine konsistente und funktionierende Kommunikation über den gesamten Lebenszyklus eines Bauwerkes zwischen den Projektbeteiligten notwendig. Durch die digitale Wissensmodellierung nehmen die Summe an notwendigen Spezifikationen, verschiedene Informationstiefen und die Anzahl an zu berücksichtigen Kontexten stetig zu [2].

Im Gegensatz zu physischen Plänen ist der Raum zur Ansammlung von Informationen in digitalen Gebäudemodell fast unbegrenzt. Jedoch ist die reine Menge von Informationen wertlos, wenn sie sich nicht validieren lässt, effizient kommuniziert werden kann oder eventuell nicht benötigt wird. Im Folgenden werden daher mögliche Ansätze zur Organisation semantischer Daten im Rahmen von *open BIM* besprochen.

2 Organisation von Informationen

2.1 Klassifikationssysteme

Eine Klassifikation ist eine der einfachsten Möglichkeiten ein Ordnungsprinzip für Informationen mittels einer Strukturierung zu implementieren und die Kommunikation konsistent zu gestalten. Grundsätzlich wird dabei jedes Element einer Klasse zur Gliederung zugewiesen. Die verschiedenen Klassen repräsentieren die unterschiedlichen Sachverhalte des betrachteten Sachgebietes und jedes Dokumentationselement wird genau einer Klasse zugewiesen, welche die Zuweisung zu anderen Klassen ausschließen sollte. Die Klassen werden zur Übersicht meist strukturiert oder nach Themengebieten gegliedert und durch eine Notation in Form eines Index gekennzeichnet [3].

2.1.1 Hierarchische Klassifikationssysteme

Ein hierarchisches Klassifikationssystem ist die einfachste Umsetzung einer Struktur zur Klassifizierung. Eine Anordnung von Klassen in einer Baumstruktur ermöglicht die Verknüpfung verschiedener Ebenen durch die Präkombination der jeweiligen Indexierungen. Zur Anwendung ist es erforderlich, dass das genutzte Klassifikationssystem vollständig in der Lage ist, den jeweiligen Sachverhalt in seiner Gesamtheit abzubilden und jeweils einer konkreten Klasse zuzuordnen. Über die Anzahl der Klassen bestimmt sich die mögliche Genauigkeit des Systems. Der Vorteil eines monohierarchischen Klassifikationssystems ist die einfache Nutzung. Der Nachteil ist die grundsätzliche Betrachtung von nur einem einzelnen Aspekt eines Sachverhalts. Zum Ausgleich dieses Nachteils können mehrere Systeme zur Abbildung verschiedener Aspekte angelegt werden. Diese sind dann jedoch nicht inhaltlich verknüpft. Systeme mit einer hohen Genauigkeit und einer großen Varianz an Elementen werden

sehr groß und können unhandlich werden. Große Klassifikationssysteme werden heutzutage vor allem aus historisch-konservativen Gründen eingesetzt [4].

Ein Beispiel für die Verwendung eines solchen Systems in einem größeren Umfang ist das vom *Construction Specification Institute* veröffentlichte *Format for Construction Specifications*, welches seit 1978 unter dem Namen *MasterFormat* verbreitet ist. *MasterFormat* ist hierarchisch numerisch strukturiert und weist jedem klassifizierbaren Element eine sechs- bis achtstellige Ziffernkombination zu. Über die Ziffernpaare der Klassifizierung werden die entsprechenden Informationslevel zur Gliederung abgebildet [5].

2.1.2 Fassettenklassifikation

Ein Fassettenklassifikationssystem greift die Probleme der hierarchischen Klassifikation auf, indem es für jeden zu berücksichtigenden Aspekt eine eigene Klassifikation bereitstellt. Elemente erhalten für jeden Aspekt durch die jeweilige Klassifikation eine Teilnotation. Durch Zusammenfügen der einzelnen Teilnotationen der jeweiligen Aspekte zu einer Gesamtnotion wird eine Fassettenklassifikation erstellt. Somit können entgegen einer Einfachklassifikation wesentlich detailliertere Informationskombinationen bei einer geringeren Anzahl an Gesamtklassen abgebildet werden [4].

Eine erste internationale Verbreitung eines solchen Systems im Bauwesen fand der *Construction Index* des dänischen Kooperationsausschuss *Samarbetskommitte for Byggnadsfragor* (CI/SfB) basierend auf dem BS 1192-5 [6]. Das CI/SfB ist ein Fassettenklassifikationssystem mit fünf Klassifikationstabellen zu architektonischen Elementen, Formen, Materialien, Aktivitäten und der physischen Umwelt [7]. Auf dem SfB-System bauten auch andere national angepasste Klassifikationssysteme wie das französische SI/SfB oder das deutsche BRD/SfB auf [8].

Die Entwicklungen verschiedener Klassifikationssysteme mündeten 2001 in der ISO 12006 zur Standardisierung von Klassifikationssystemen im Bauwesen. Sie dient als Rahmenwerk zur Entwicklung vergleichbarer Klassifikationssysteme mit dem Ziel eines konsistenten Ansatzes zur Bauobjektklassifizierung. Dafür werden Hauptklassen definiert und in einem Grundprozessmodell in Beziehung gesetzt. Exemplarisch werden in der ISO 12006-2 Tabellen für die definierten Aspekte des Prozessmodells vorgeschlagen. Auf deren Grundlage wurden in Großbritannien *Uniclass* und in den USA das *Omniclass Construction Classification System* entwickelt. Damit bildet sie die Basis für zwei der aktuell populärsten und am häufigsten implementierten Klassifizierungssysteme im Rahmen von BIM. Beide Systeme umfassen innerhalb ihrer Klassifizierungstabellen alle gängigen Bereiche des Hochbaus und ausgewählte Bereiche des Infrastrukturbaus [9].

In Deutschland gibt es bisher kein etabliertes System, welches auf der ISO 12006 aufbaut. Daher muss abgewogen werden, ob die Zusammenführung von IFC und der ISO 12006 etwaige Vorteile birgt, die eine Neueinführung eines solchen Systems im deutschen Bauwesen rechtfertigt. IFC hat das Ziel, einen offenen Austausch von geometrischen und semantischen Daten von Bauwerksmodellen zwischen Anwendungssystemen zu ermöglichen, während die ISO 12006 ein Rahmenwerk zur Harmonisierung von nationalen und regionalen Klassifikationssystemen zur verbesserten Strukturierung

von Informationen im Bauwesen schaffen soll. Beide Systeme sollen die Kommunikation und Kooperation der verschiedenen Projektteilnehmer verbessern, um Projektergebnisse zu optimieren. Ein gemeinsames Meta-Modell würde eine grundlegende Verbesserung des Informationsmanagements bedeuten und würde den entsprechenden Mehraufwand einer Einführung in den deutschen Digitalisierungsprozess rechtfertigen. Jedoch ist das Zusammenführen der ISO 12006 und des IFC-Schemas durch die grundlegenden Unterschiede in den Strukturierungen der Grundmodelle nicht möglich. Beziehungen innerhalb des Klassifikationssystems und des Grundprozessmodells können jedoch nur behelfsweise in die IFC-Struktur implementiert werden. Die flexiblere Struktur des IFC-Schemas müsste umfangreich eingeschränkt werden und mit Bedingungen verknüpft werden, um sich dem festen Modell der ISO 12006-2 anzupassen [10]. In der Praxis werden daher beide Systeme getrennt geführt und ergänzen sich durch Verweise um semantische oder geometrische Informationen.

2.2 Begriffskombination

Neben der Implementierung einer festen Struktur zur Organisation von Informationen bieten Verwaltungssysteme eine weitere Möglichkeit zur Beherrschung größerer Informationsmengen. Eines der wichtigsten Ordnungsprinzipien ist die Begriffskombination zur Organisation großer Dokumentationen. Dabei werden Elemente durch Deskriptoren verschiedenen Äquivalenzklassen zugeordnet, welche sich im Gegensatz zum Fassettenklassifikationssystem nicht ausschließen müssen. Die Schnittmenge der indexierten Äquivalenzklassen entspricht dann dem Inhalt des Elements. Eine einfache Version der Begriffskombination ist die Schlagwortvergabe. Durch das Zuordnen beliebig vieler Schlagwörter lässt sich durch die logische Kombination von Begriffskombinationen der Inhalt gezielt abfragen [4]. Der Nachteil der Begriffskombination ist die notwendige Kenntnis und Verwaltung über die jeweiligen Merkmale zur Schnittmengenbildung. Im Gegensatz zu den Klassifikationssystemen wird es nicht durch eine vorgegebene Struktur eingeschränkt, sondern durch die Fähigkeit des Anwenders, dieses effizient zu nutzen.

Die Begriffskombination lässt sich durch Merkmale und Merkmalsets problemlos auf das IFC-Schema zur Verwaltung semantischer Informationen anwenden. Einen Ansatz zur Verwaltung der Schnittmengen der Deskriptoren liefert der Verein Deutsche Ingenieure (VDI) in Teil 9 der Richtlinienreihe 2552. Die einzelnen Begriffskombinationen der Deskriptoren im IFC-Modell werden durch etablierte Klassifikationssysteme der jeweiligen Domänen organisiert und in eine merkmalsbasierte Klassifikation überführt. Die notwendigen Merkmale werden dabei durch die jeweiligen Klassifikationsziele bestimmt [11].

3 Umsetzung mithilfe von Machine Learning

3.1 Klassifikationssystem: DIN 276

Eine mögliche Norm zur Umsetzung einer Organisation von Deskriptoren mittels einer festen Strukturierung ist die DIN 276. Durch die Verwendung langjähriger im deutschen Bauwesen etablierter Normen, wie der DIN 276, entfällt eine zusätzliche Einarbeitung in ein weiteres Klassifikationssystem.

Dies ist im Hinblick auf die Anstrengungen der Bundesregierung, die Digitalisierung im Bauwesen zeitnah voranzutreiben, ein erheblicher Faktor. Auch lässt sich diese Art des Ordnungssystems in umgekehrter Reihenfolge zur Deklaration von Instanziierungen und deren Informationsanreicherung nutzen.

Die DIN 276 ist eine der wichtigsten technischen Regeln für die Kostenplanung im Bauwesen über die gesamte Lebensdauer eines Bauwerks. Besonders bedeutend ist diese Norm, da die Honorarordnung für Architekten und Ingenieure (HOAI) seit 1976 auf sie Bezug nimmt [12]. Durch Verwendung in der HOAI wird sie zu einer verbindlichen Rechtsvorschrift. Durch die freie Verfügbarkeit und weit verbreitete Anwendung ist sie als anerkannte Regel der Technik zu betrachten. Sie strukturiert die wesentlichen Begriffe und Merkmale von Kosten im Bauwesen als Voraussetzung zum Vergleich verschiedener Kostenermittlungen im Verlauf eines Projekts sowie zwischen unterschiedlichen Projekten. Die DIN 276 ist ein hierarchisch numerisches Klassifikationssystem. Sowohl für Planer als auch für das Facility-Management kann die Norm zur Informationsstrukturierung von Bauteiltypen mit ihrer Möglichkeit zur Erweiterung eingesetzt werden.

3.2 Automatisierung der Klassifikationen

Die in der VDI 2552-9 vorgeschlagene Strukturierung von Informationen bietet sich zur Automatisierung der Informationsstrukturierung mittels Machine Learning (ML) an. ML ist ein Berechnungsmuster mit der Fähigkeit ein gegebenes Problem fallbasiert durch frühere Entscheidungen zu lösen. Über Algorithmen werden Gesetzmäßigkeiten und Muster in Daten identifiziert und Lösungsansätze entwickelt. Aus Wissen wird Erfahrung [13]. Durch die Verwendung etablierter Klassifikationsysteme können Entscheidungen auf Basis von Merkmalen anhand bestehender und bereits beendeter Projekte trainiert werden. Die Automatisierung der Klassifikation durch Algorithmen kann den zeitlichen Mehraufwand zur Organisation der Merkmale erheblich verkürzen.

Decision-Tree-Algorithmen gehören dem überwachten Lernen des ML an. Sie umfassen typische Lernalgorithmen, die vor allem zur binären Klassifikation eingesetzt werden. Dabei werden Elemente durch eine Baumstruktur mithilfe von Ästen und Verzweigungen klassifiziert. Der Endknoten eines Astes gibt dabei eine vorgegebene Klasse aus, während die Verzweigungen von Ästen für vergebene Attribute und Entscheidungen im Baum stehen sowie die zugehörigen Äste die Werte beinhalten. Bei dem Lernprozess wird die Baumstruktur selbst gebildet. Der Lernprozess erfordert, dass die Klassifikation binär lösbar ist, da an jeder Verzweigung eine positive oder negative Entscheidung getroffen wird [14].

Die Anforderungen an Merkmale von Datensätze der Decision-Tree-Algorithmen entsprechen den Rahmenbedingungen hierarchisch numerisch strukturierter Klassifikationssysteme wie der DIN 276. Durch die Begrenzung des Klassifikationsziels auf einen Gesichtspunkt, der Kostengliederung, ist die DIN 276 verhältnismäßig kompakt im Vergleich zu Systemen wie dem *MasterFormat*. Dennoch ermöglicht sie eine vollumfassende Klassifikation aller Bauelemente eines Objekts und kann bei Bedarf flexibel erweitert werden. Aufgrund der festen Einbindung in die Vergütung und Kalkulation im deutschen Bauwesen kann von einer hohen Akzeptanz ausgegangen werden. Da zum Trainieren be-

reits vorhandene Datensätze verwendet werden, ist die lange Verwendung der DIN 276 im Bauwesen von Vorteil.

Zur Aufbereitung der Trainingsdaten wird zuerst die IFC-Datei mithilfe der Open-Source-Anwendung *IfcOpenShell* [15] eingelesen und die benötigten Elemente herausgefiltert. Durch das offene Klartextformat *STEP Physical File* kann grundsätzlich jede Programmiersprache verwendet werden, die in der Lage ist, eine Textdatei auszulesen. In dieser Arbeit wird *Python* verwendet, da diese Programmiersprache vor allem in der Analyse von Datensätzen in Kombination mit der Vielzahl verfügbarer Bibliotheken eine weite Verbreitung gefunden hat. Für den Decision-Tree-Algorithmus wird die Bibliothek *scikit-learn* [16] genutzt. Die Abfrage zu klassifizierender Bauelemente kann durch die Einschränkung in Subklassen aus dem IFC-Schema, wie *IfcBuildingElements*, optimiert werden.

Für das Training des Algorithmus müssen zwei Datensätze erstellt werden, welche zum einen die klassifizierungsspezifischen Merkmale und Klassen als binäre Werte enthalten, zum anderen die zugewiesene Klassifizierung als Ergebnis. Die zugehörige Klassifikation kann aus einer *IfcClassification* oder einem *IfcPropertySet* hinterlegt und ausgelesen werden. Um den Decision-Tree-Algorithmus mit den entsprechenden Merkmalen trainieren zu können, müssen diese, sofern es sich nicht um boolsche Werte handelt, in binäre Werte umgewandelt werden. Diese Umwandlung kann mithilfe einer 1-aus-n-Codierung erfolgen. Danach kann der Algorithmus über einen *DecisionTreeClassifier* trainiert und anschließend das trainierte Modell verwendet werden. Die merkmalsbasierte Klassifikation kann durch die Verwendung eines *Random-Forest-Algorithmus* bei mehreren Modellen durch verschiedene IFC-Dateien optimiert werden.

3.3 Validierung der automatisierten Klassifikationen

Zur späteren Validierung der automatisierten Klassifikationen können die Ergebnisse an die Instanzen mittels eines *IfcPropertySingleValue* oder *IfcClassificationReference* in der Codierung der IFC-Datei hinterlegt und mithilfe eines IFC-Viewers visuell validiert werden. Sogenannte IFC-Viewer sind meist kleinere Programme, mit denen die geometrischen Modelle von IFC-Dateien und die zugewiesenen Merkmale der Bauelemente betrachtet werden. Im Gegensatz zu größeren CAD-Autoren-Programmen können IFC-Viewer meist keine Änderungen vornehmen und lediglich visuell nach Merkmalen filtern. Damit eignen sie sich besonders für eine visuelle Validierung von zugewiesen Merkmalen, in diesem Fall der zugewiesenen Klassifikation. Der Vorteil einer visuellen Validierung anhand eines konkreten Modells ist die Möglichkeit, fachspezifische Akteure einzusetzen, die durch berufliche Erfahrungen schnell die semantische Korrektheit einer Klassifizierung einschätzen können, ohne dass vertiefende Kenntnisse in CAD-Programmen oder entsprechende Nutzerlizenzen benötigt werden. Anmerkungen und Korrekturen können einfach durch das *BIM Collaboration Format* kommuniziert werden. Durch die Verwendung langjähriger im deutschen Bauwesen etablierter Normen, wie der DIN 276, entfällt eine zusätzliche Einarbeitung in ein weiteres Klassifikationssystem und es kann auf vorhandene praktische Erfahrungen zurückgegriffen werden.

4 Fazit und Ausblick

Der Einsatz nationaler Klassifikationssysteme im Zusammenhang mit IFC als Ordnungssystem steht dem Einsatz internationaler Systeme in keiner Hinsicht nach. Vielmehr kann durch die Verwendung traditioneller Systeme auf bereits bestehende Erfahrungen und Wissensbasen zurückgegriffen werden. Mithilfe von etablierten Standards und durch Algorithmen, wie dem Decision-Tree-Algorithmus, unterstützt bietet die organisierte Begriffskombination eine schnelle und übersichtliche Organisation semantischer Informationen innerhalb von digitalen Bauwerksmodellen. Der Vorteil dieser Methode besteht darin, dass eine fehlende (oder falsche) Klassifizierung bestehender Modelle im Nachhinein automatisiert durchgeführt werden kann, ohne auf ein kostspieliges Autoren-Programm zurückgreifen zu müssen. Diese Organisation und Strukturierung von Informationen könnte beispielsweise im Bereich der Kostenplanung genutzt werden.

Aufbauend auf dieser Arbeit sollte weiter untersucht werden, wie mit realen und größeren Datensätzen sowie Fehlern konkret umgegangen werden kann. Das Rauschen und die Qualität von Trainingsdaten sind der ausschlaggebende Faktor für die Implementierung einer Automation mittels ML. Anschließend an die vorliegende Arbeit sollten daher reelle Datensätze analysiert und besprochen werden. Dabei sollte der Fokus nach dem Paretoprinzip auf Modellinformationen gelegt werden, die in einer geringen Summe einen großen Einfluss auf das jeweilige Projekt haben. Eine Analyse der entsprechenden Beziehungen zwischen Menge, Qualität und Einfluss von Informationen in digitalen Bauwerksmodellen würde die weitere Arbeit zur Organisation solcher Informationen sinnvoll ergänzen.

Literatur

[1] M. Gallaher, A. O'Connor, J. Dettbarn und L. Gilday, »Cost Analysis of Inadequate Interoperability in the U.S. Capital Facilities Industry«, in *National Institute of Standards and Technology (NIST)*, 2004.

[2] A. Borrmann, *Building Information Modeling. Technologische Grundlagen und Industrielle Praxis*. Wiesbaden: Springer Fachmedien Wiesbaden GmbH, 2015, ISBN: 9783658056063.

[3] E. Hunter, *Classification made simple. 2. ed.* Hampshire: Ashgate Publishing Limited, 2005, ISBN: 97807546079537.

[4] W. Gaus, *Dokumentations- und Ordnungslehre. Theorie und Praxis des Information Retrieval*. Berlin und Heidelberg: Springer, 2005, ISBN: 9783540275183.

[5] K. R. Miller und J. S. Newitt, »MasterFormat 2004 Impact on Construction Organizations«, 2005.

[6] British Standards Institution, *BS 1192-5: Construction drawing practice. Guide for structuring and exchange of CAD data*. 2007.

[7] A. Ray-Jones und D. Clegg, *Construction Indexing Manual: CI/SfB. 3. ed.* London: RIBA Publications, 1976, ISBN: 9780900630514.

[8] K. Straub, *ISPLA Informationssystem. Planungsgrundlagen und Planungsentscheidungen mit Datenbankunterstützung durch Isplatrieve*. Frauenhofer-Informationszentrum Raum und Bau: F 1740, 1981.

[9] BIM4INFRA, *Umsetzung des Stufenplans „Digitales Planen und Bauen“. AP 5: Konzept für Datenbanken*, https://bim4infra.de/workshops/, Stand: 04.07.2022.

[10] A. Ekholm, »ISO 12006-2 and IFC - Prerequisites for coordination of standards for classification and interoperability«, 2005.

[11] Verein Deutscher Ingenieure, *VDI 2552 Blatt 9 - Entwurf: Building Information Modeling - Klassifikationssysteme*. Aug. 2020.

[12] HOAI, *Verordnung über die Honorare für Architekten- und Ingenieurleistungen*, https://www.gesetze-im-internet.de/hoai_2013/, Stand: 04.07.2022.

[13] Microsoft, *Was ist Machine Learning? Definition und Funktionen von ML*, https://news.microsoft.com/de-de/microsoft-erklaert-was-ist-machine-learning-definition-funktionen-von-ml/, Stand: 04.07.2022.

[14] T. Jo, *Machine Learning Foundations. Supervised, Unsupervised, and Advanced Learning*. Cham: Springer International Publishing, 2021, ISBN: 9783030659004.

[15] IfcOpenShell, http://ifcopenshell.org, 2022.

[16] scikit-learn, https://scikit-learn.org, 2022.

AIR-Klassifizierungssystem: Konzept eines prüfbaren Ansatzes für Bau und Betrieb

Friedrich Schroedter[1] and Nadine Wills[2]

[1] Bauhaus-Universität Weimar, Fakultät Bauingenieurwesen, Marienstr. 13, 99423 Weimar, Germany

[2] Technische Hochschule Mittelhessen, Fachbereich Wirtschaftsingenieurwesen-Immobilien, Wilhelm-Leuschner-Str. 13, 61169 Friedberg, Germany

E-Mail: friedrich.schroedter@uni-weimar.de

Abstract: Gemäß DIN ISO 19650 werden die benötigten Informationen für das Facility Management im Rahmen der Asset Informationsanforderungen (AIR) durch Informationsbesteller gefordert. Dabei werden Informationsbereitstellern regelmäßig unstrukturierte Anforderungstabellen mit teilweise inkompatiblen Mehrfachklassifizierungen vorgegeben. Eine gängige Praxis ist das Abbilden von Bauteilklassen gemäß IFC auf modellierungsinkompatible Bauteilgruppen gemäß DIN 276. Häufig treten gleiche Bauteile in verschiedenen Bauteilgruppen auf. Beim Qualitätsmanagement mit Prüfregeln können Bauteile dadurch nicht eindeutig identifiziert werden. Das Ziel dieses Beitrags ist die Definition eines Klassifikationsansatzes auf Basis des Klassifikationsmerkmals DIN 276 sowie des zu klassifizierenden Elementes nach IFC. Zunächst werden bestehende Klassifizierungsansätze analysiert. Das Ergebnis ist eine Matrix für die Klassifizierung von Bauteilen wodurch eine Verbesserung der Prüfbarkeit erreicht werden soll.

Keywords: Building Information Modeling (BIM), Facility Management (FM), Asset-Informationsanforderung (AIR), Klassifikationssystem

1 Einleitung

Die Nutzungskosten eines Gebäudes stellen mit 44 % den größten Kostenanteil im Gebäudelebenszyklus dar [1,2], wobei die Gebäudebewirtschaftung im Sinne des Facility Managements (FM) den größten Kostenfaktor darstellt [3]. Die lebenszyklusübergreifende Methode des Building Informaton Modelings (BIM) ermöglicht die Generierung FM-relevanter Daten bereits

in der Gebäudeplanungsphase [8]. BIM kann im FM zur Verfolgung von Zielen und zur Bearbeitung unterschiedlicher Aufgaben der Gebäudebewirtschaftung genutzt werden, wie der Unterstützung des Flächenmanagements, der Wartung und Instandsetzung, [8], [9], Nutzung der Planungs- und Errichtungsdaten für Ausschreibungen oder Realisierung von FM-Nachhaltigkeitszielen [4].

In BIM-Projekten definiert der Informationsbesteller sog. Asset-Informationsanforderungen (AIR), welche als Teile der Auftraggeber-Informationsanforderungen (EIR) an den Informationsbereitsteller kommuniziert werden [5]. Dabei wird definiert, welches Leistungsbild (wer) zu welcher Leistungsphase (Meilensteine) ein Informationsmodell mit welcher Informationsdichte (LOI) (was) liefern muss [6, 7]. AIR beinhalten jene Bauteile, die für den Gebäudebetrieb relevant sind und nach Inbetriebnahme in dem Asset-Informationsmodell (AIM) vorhanden sein sollen [8]. Damit die in einem AIM enthaltenen Bauteile und Anlagen zuordnungsbar sind, muss eine eindeutige Identifikation sichergestellt werden. Dazu werden sog. Ordnungssysteme [9] genutzt. Diese dienen der Informationsstrukturierung zwischen unterschiedlichen Disziplinen innerhalb eines Gebäudelebenszyklus [10]. In Ordnungssystemen enthaltene Klassifizierungsansätze folgen unterschiedlichen Logiken. Die in Deutschland derzeit am häufigsten genutzte Form der Definition von LOI in EIR stellt die holistische Kombination aus Modellentwicklungsmatritzen (MEM) und Bautteiltypenlisten nach DIN 276 dar [11]. Ziel des konventionellen Ansatzes ist es, jeder Kostengruppe (KG) alle für die Projektinformationsmodell relevanten Bauteile samt entsprechender Industry Foundation Classes (IFC)-Entität aus dem IFC Standard nach ISO 16739 zuzuordnen. Dabei werden benutzerdefinierte Parameter für die Klassifikation vereinbart, statt das Klassifikationskonzept des IFC-Standards zu nutzen. Konträr zu diesem Ansatz zielt dieser Beitrag auf einen schemakonformen, prüfbaren Klassifizierungsansatz für Informationsanforderungen unter Verzicht auf benutzerdefinierte Parameter ab. Dafür wird in einem zweistufigen Prozess auf Basis des Klassifikationsmerkmals (DIN 276) sowie des zu klassifizierenden Elements (IFC) eine Zuordnungsmatrix (Mapping-Tabelle) entwickelt. Diese wird in den Klassifizierungs-manager der BIM-Autorensoftware Autodesk Revit importiert um Bauteile zu klassifizieren. Die Funktionsfähigkeit wird im Rahmen des Qualitätssicherungsprozesses über Solibri validiert. Das Ergebnis ist ein Klassifizierungs-, Identifikations- und Prüfansatz von Bauteilen in Asset-Informationsmodellen.

2 Analyse bestehender Klassifikationssysteme

Bei BIM-Projekten werden Klassifikationssysteme im Zusammenhang mit den LOI für den Gebäudebetrieb in den AIR definiert [4]. In der Normung existieren Grundsätze für die Klassifikation von Bauteilen in der DIN 12006-2 und den VDI-Richtlinien VDI 2552-4 sowie VDI 2552-9.

Die DIN 12006 unterscheidet in Klassifizierungs- und Zusammensetzungshierarchien. Während eine Klassifizierung Klassen in Teilklassen gliedert, aggregiert eine Zusammensetzung Teile in ein Ganzes. Eine Klassifizierung kann dabei aus unterschiedlichsten Blickwinkeln und nicht nur aus Bauteilsicht erfolgen. Im Bauwesen ist beispielsweise eine Klassifizierung in Bauergebnis, -prozess und -

ressource denkbar. In gewachsenen Klassifikationen wie der DIN 276 werden häufig Klassifizierungen und Zusammensetzungen gemischt. DIN 12006-2 bezeichnet letzteres auch als Systeme. Dieser Begriff wird auch vom IFC-Schema verwendet. Bei IFC handelt es sich um einen offenen, von der Organisation buildingSMART entwickelten Standard zur Beschreibung von Klassen, Attributen, Konzepten und klassenabhängige Eingenschaften [12]. Die innere Klassifizierung erfolgt herstellerunabhängig. Externe Klassifikationen können über das Klassifizierungskonzept fast an alle Klassen angehangen werden. Dabei muss das Attribut „HasAssociation“ befüllt werden. VDI 2552-9 wurde als Anwendungshilfe für DIN 12006-2 konzipiert. Dabei weist sie eine Systematik für verschiedene Klassifikationsaspekte aus. Es sind das Klassifikationsziel, Klassen, zu klassifizierende Elemente und Klassifikationsmerkmal zu bestimmen [4]. Die VDI 2552-4 ist eine Richtlinie um Klassifikationsanforderungen nach VDI 2552-9 bzw. DIN 12006-2 vorzugeben. Es wird explizit die DIN 276 thematisiert. So werden beispielsweise im Anhang der Richtlinie Modellierungsvorschriften für Architekturmodelle vorgestellt. Um Redundanzen in Vorgaben zu vermeiden empfiehlt die VDI 2552-4 seperate Dokumente zur Klassifizierung und zur Vorgabe der LOI. Es wird zum einen die Modellentwicklungsmatrix zur Vorgabe der Klassifikation und die Bauteiltypenmatrix zur Vorgabe der eigentlichen LOI an Bauteilen ausgewiesen.

Während die Normungstätigkeiten im Bereich der Klassifizierungen bereits fortgeschritten ist, sind Defizite hinsichtlich korrekter Umsetzung in der Praxis erkennbar. Im Folgenden sollen zwei Beispielsysteme vorgestellt werden, die den Versuch unternehmen, den nach DIN 276 klassifizierenden Elementen [4] Klassifikationsmerkmalen nach IFC [13] zuzuordnen. Im Kontext des FM ist dabei CAFM-Connect zu nennen [14]. Da es sich bei KG um Gruppen, bzw. Systeme im Sinne der Zusammensetzung handelt, kommt es häufig zu unzureichenden Zuordnungen von Bauteilen. Ein weiterer Standard zur Klassifizierung FM-relevanter Bauteile stellt der IFC-Bildkommentar dar. Bei Ableitung einer Zuordnungsmatrix auf Basis dieses Standards resultieren unter Berücksichtigung der allgemeinen und spezifischen Eigenschaften des IFC-Standards zuzüglich der Identifikationseigenschaften ca. 60.000 Tabellenzeilen für die KG 300 und KG 400. Der Umfang der resultierenden Matrix ist insbesondere der permanenten Wiederholung von Bauelementen wie etwa Rohrleitungen (IfcPipeSegment) geschuldet, welche bspw. in KG 411, 431, 473 und 544 vorhanden sind. Das Problem der Wiederholung ist somit in allen holistischen Zuordnungskonzepten präsent.

Die Analyse derzeitiger Klassifizierungskonzepte zeigt, dass in der Normung bereits eine gute theoretische Grundlage zur Klassifikation besteht. Defizite jedoch hinsichtlich der Unvollständigkeit des Klassifizierungsumfangs im Gebäudekontext (IFC) oder resultierender Mehrfachklassifizierung eines Bauteils (DIN SPEC 91400 und IFC-Bildkommentar) aufweisen. Praktische Versuche, wie in CAFM-Connect und der IFC-Bildkommentar Zuordnungen zu treffen, scheitern an der Unterscheidung von Bauteilen und Systemen. In den kommenden Abschnitten soll eine Lösung dieses Problems präsentiert werden.

3 Methodisches Vorgehen

Die sich aus dem Status quo derzeitiger Klassifizierungssysteme ergebenden Defizite sollen mithilfe eines prüfbaren Klassifizierungs-, Identifikations- und Prüfansatz auf Basis einer Zuordnungsmatrix gelöst werden. Dabei wird eine alternative Kommunikation im Projekt geforderter Bauelemente gemäß dem Motto IFC-First fokussiert. Die Definition eines prüfbaren Ansatzes erfolgt zweistufig auf Basis des Klassifikationsmerkmals (DIN276) sowie des zu klassifizierenden Elements (IFC). Die technische Umsetzung erfolgt auf Basis der Struktur des Autodesk opensource Revit-Plugins „Klassifikationsmanager“. Der in diesem Beitrag vorgestellte Ansatz kann aber auch gänzlich ohne das Plugin in andere Autorensoftware implementiert werden. Der Proof of Concept erfolgt mithilfe der Software Autodek Revit und Solibri. Bauteile werden mitsamt der für die FM-Leistungserbringung relevanten Informationen in IFC exportiert. Zur validierung wird das Bauteil in der Software Solibri abgeprüft.

Nach Analyse bestehender Klassifizierungsansätze und Identifizierung des Zuordnungs-problems erfolgt zunächst die Definition einer Mappingtabelle für den Klassifikationsansatz der DIN 276, des sog. Klassifikationsmerkmals [4]. Dazu wird die (AG-seitig) definierte Zuordnungsmatrix in einer benutzerdefinierten Datenbank in Microsoft Excel angelegt, wobei grobe Layoutvorgaben des Plugins berücksichtigt wurden, um die Matrix unmittelbar in die Datenbank zu laden. Abbildung 1 veranschaulicht den Aufbau des Datenblattes der Datenbank.

TITLE	**DIN 276 A2**				
DESCRIPTION	**Klassifizierung gemäß DIN 276-2018**				
VERSION	**Version 1.0**				
FUNCTION	**Element**				
NUMBER PARAMETER					
DESCRIPTION PARAMETER	ClassificationCode				
NUMBER	**DESCRIPTION**	**LEVEL**	**REVIT CATEGORY**	**IFC 4.1 – IfcProduct Dependencies**	**IFC 4.1 – IfcGroup Dependencies**
400 - Bauwerk - Technische Anlagen	[DIN 276]400:Bauwerk - Technische Anlagen	1		N/A	
410 - ABWASSER-, WASSER-, GASANLAGEN	[DIN 276]410:ABWASSER-, WASSER-, GASANLAGEN	2		N/A	
411 - Abwasseranlagen	[DIN 276]411:Abwasseranlagen	3	-2008043	[IfcSharedComponentElements,IfcHvacDomain,IfcPlumbingFireProtectionDomain]	IfcDistributionSystem.WASTEWATER
412 - Wasseranlagen	[DIN 276]412:Wasseranlagen	3	-2008043	[IfcSharedComponentElements,IfcHvacDomain]	IfcDistributionSystem.WATERSUPPLY
413 - Gasanlagen	[DIN 276]413:Gasanlagen	3	-2008043	[IfcSharedComponentElements,IfcHvacDomain]	IfcDistributionSystem.GAS
419 - Sonstiges	[DIN 276]419:Sonstiges	3	-2008043	[IfcSharedComponentElements,IfcHvacDomain]	
420 - WÄRMEVERSORGUNGSANLAGEN	[DIN 276]420:WÄRMEVERSORGUNGSANLAGEN	2		N/A	
421 - Wärmeerzeugungsanlagen	[DIN 276]421:Wärmeerzeugungsanlagen	3	-2001140	[IfcSharedComponentElements,IfcHvacDomain]	IfcDistributionSystem.HEATING
422 - Wärmeverteilnetze	[DIN 276]422:Wärmeverteilnetze	3	-2001140	[IfcSharedComponentElements,IfcHvacDomain]	IfcDistributionSystem.HEATING
423 - Raumheizflächen	[DIN 276]423:Raumheizflächen	3	-2001140	[IfcSharedComponentElements,IfcHvacDomain]	IfcDistributionSystem.HEATING
424 - Verkehrsheizflächen	[DIN 276]424:Verkehrsheizflächen	3	-2001140	[IfcSharedComponentElements,IfcHvacDomain]	IfcDistributionSystem.HEATING
429 - Sonstiges	[DIN 276]429:Sonstiges	3	-2001140	[IfcSharedComponentElements,IfcHvacDomain]	
430 - RAUMLUFTTECHNISCHE ANLAGEN	[DIN 276]430:RAUMLUFTTECHNISCHE ANLAGEN	2		N/A	
431 - Lüftungsanlagen	[DIN 276]431:Lüftungsanlagen	3	-2001140	[IfcSharedComponentElements,IfcHvacDomain]	IfcDistributionSystem.VENTILATION
432 - Teilklimaanlagen	[DIN 276]432:Teilklimaanlagen	3	-2001140	[IfcSharedComponentElements,IfcHvacDomain]	IfcDistributionSystem.AIRCONDITIONING
433 - Klimaanlagen	[DIN 276]433:Klimaanlagen	3	-2001140	[IfcSharedComponentElements,IfcHvacDomain]	IfcDistributionSystem.AIRCONDITIONING
434 - Kälteanlagen	[DIN 276]434:Kälteanlagen	3	-2001140	[IfcSharedComponentElements,IfcHvacDomain]	IfcDistributionSystem.AIRCONDITIONING

Abbildung 1: Entwickelte Zuordnungsmatrix gem. Modellentwicklungsmatrix nach VDI 2552-4

Die derzeit praktizierte Methode, KG explizite IFC-Entitäten zuzuordnen, soll in dem entwickelten Konzept in veränderter Form beibehalten werden. Den einzelnen KG sind Hierarchieebenen, Revit-Kategorien, IFC-Datenschemata und IFC-Systemgruppen zugeordnet, wobei die Revit-Kategorien optional sind und lediglich der Filterung von Bauelementen dienen. Von Bedeutung sind die Spalten „IfcProduct Dependencies“und „IfcGroup Dependencies“. Letztere werden eingeführt, da übergeordnete Entitäten wie „IfcDistributionElement“ abstrakte Klassen für Bauelemente darstellen und daher gem. IFC-Dokumentation nicht Bauteilen zugeordnet werden dürfen. In der Praxis werden sie jedoch häufig verwendet. Vielmehr sind sie durch Gruppierungen zu Gebäudesystemen zu aggregieren. IFC sieht hierfür das „Group Assignment Concept“ vor. Durch dieses können Bauteiltypen gleicher

und divergierender Art in Gruppen, analog der DIN 276 zusammengefasst werden. Die KG 400 beinhaltet Typen von „IfcDistributionSystem“, weshalb sie in der letzten Spalte (vgl. Abbildung 1) dargestellt sind. In der Praxis werden Gruppierungen wie „IfcDistributionSystem“ bisher selten korrekt umgesetzt. Eine Empfehlung dieses Betrags besteht in der Änderung dieses Vorgehens, da in Prüfsoftware wie Solibri geeignetere Prüfregeln auf Basis von Systemen aufgestellt und die Modellqualität verbessert werden kann. Zudem entfallen die benutzerdefinierten Parameter aus DBC und CAFM Connect.

In einem zweiten Schritt wird eine IFC-Mappingtabelle analog dem Anhang der VDI 2552-9 erstellt. Die darin enthaltenen Werte (Zellen) präsentieren die IFC-Bezeichnung der Bauteiltypen wobei lediglich die IFC-Instanz, bzw. der IFC-Typ, in den Parameter „IfcExport“ geschrieben wird. Des Weiteren erfolgt die Zuordnung zu Revit-Kategorien, welche nun deutlich exakter als bei der Kostengruppentabelle darstellbar ist. Die IFC-Mappingtabelle ist in Abbildung 2 dargestellt. Die hier vorliegende Matrix kann in weiterer Forschung beliebig und eindeutig um Eigenschaften ergänzt werden. Sie entspricht der VDI 2552-4 Bauteiltypentabelle.

TITLE	**IFC Class Mappings**		
DESCRIPTION	**Class**		
VERSION	**4.1**		
FUNCTION	**Element**		
NUMBER PARAMETER			
DESCRIPTION PARAMETER	**IfcExportAs**		
NUMBER	**DESCRIPTION**	**LEVEL**	**REVIT CATEGORY**
IFC Class Mappings	**Version 4 Addendum 1**	**1**	
Gemeinsame Gebäudeelemente	IfcSharedBldgElements	2	
Balken - Unterzug	IfcBeam	3	-2001320
Balken	IfcBeamType.BEAM	4	-2001320
Unterzug	IfcBeamType.JOIST	4	-2001320
Hohlbalken	IfcBeamType.HOLLOWCORE	4	-2001320

Abbildung 2: Entwickelte IFC-Mappingtabelle

Zur Anwendung der Mappingtabelle in einer BIM-Software (hier Revit) ist es erforderlich, dass der Nutzer (in diesem Fall durch das PlugIn) die Werte in der Weise vorgibt, dass sie korrekt als „IfcClassification“ exportiert werden. Dies geschieht über den IfcSharedParameter „ClassificationCode“ in Revit. Anschließend wird die Exceldatei in den Revit Klassifizierungsmanager (PlugIn) geladen. In Abbildung 3 sind der Aufbau des Klassifikationsmanagers sowie die, in das PlugIn importierten, Klassifizierungsblätter dargestellt. Nachdem die Klassifikationen für das Bauteil ausgewählt wurden (dritte Grafik von links), sind diese in den Typen bzw. Instanz-Eigenschaften (vierte Grafik von links) ersichtlich.

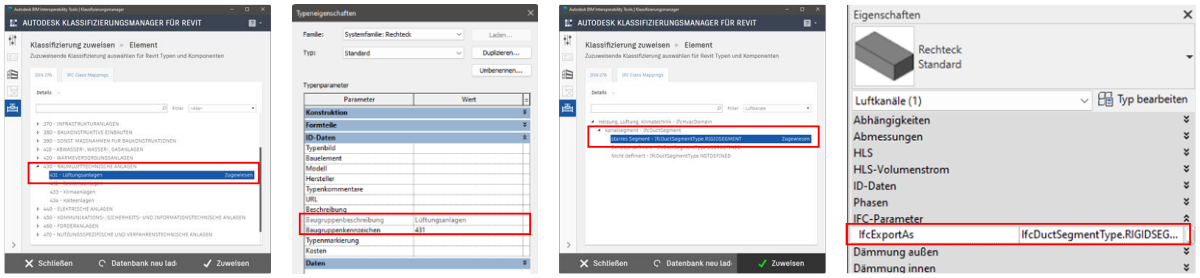

Abbildung 3: Darstellung importierter Mappingtabelle

4 Ergebnisse

Zur Validierung wurde das mittels des entwickelten Ansatzes klassifizierte Modell in IFC4 exportiert und in der Qualitätsmanagementsoftware „Solibri“ geöffnet. In dem darin enthaltenen Ruleset Manager wurden exemplarisch Prüfregeln angelegt. In erster Instanz wurden Kostengruppen allgemein abgeprüft. Sofern zuvor eine Definition der Kostengruppe als Eigenschaft und nicht als Klassifizierung erfolgte, erscheint eine Fehlermeldung. Im zweiten Schritt wurde als Beispiel für Bauelemente der KG 400 die KG 431, Lüftungsanlagen überprüft. Dazu wurden alle IfcDistributionSystem.VENTILATION mit Klassifizierung KG 431 analog der in entwickelten Zuordnungsmatrix (vgl. Abbildung 1) eingeschlossen. Aus dieser Teilmenge wurden alle Einzelbauteile auf die korrekte Klassifizierung überprüft. Zur Demonstration der Funktionsfähigkeit der entwickelten Zuordnungsmatrix wurde ein Lüftungskanal einer falschen Kostengruppe zugeschrieben. In Abbildung 4 ist ersichtlich, dass im Rahmen der Qualitätsprüfung als Ergebnis dieser inkorrekten Zuordnung eine Fehlermeldung „Falscher Wert der Eigenschaft – DIN 276 Classification 431“ erscheint.

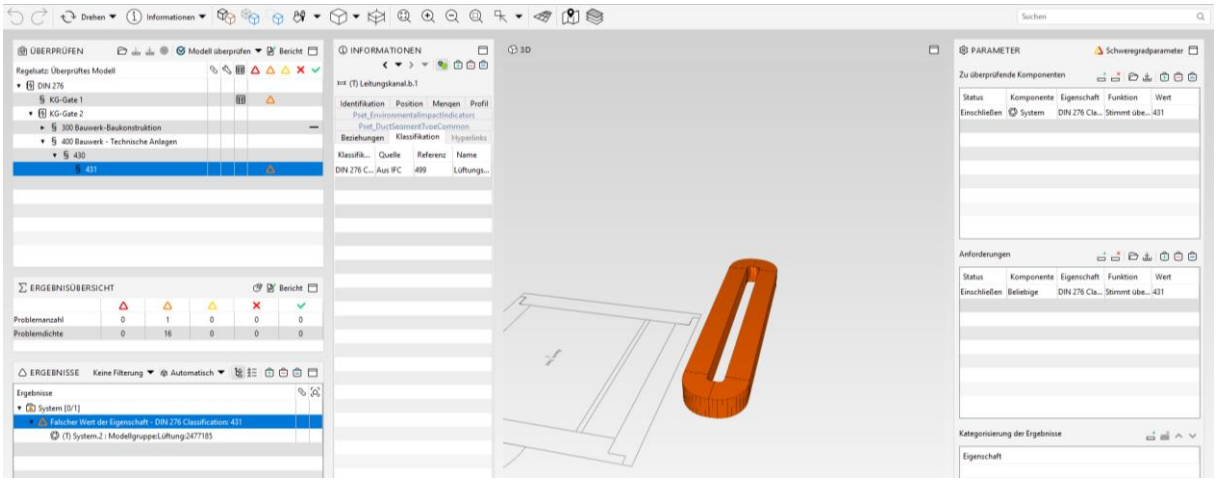

Abbildung 4: Exemplarische Überprüfung Mappingtabelle

Übergeordnet wurde eine prüfbare Mappingtabelle erarbeitet. In der Autorensoftware Autodesk Revit kann diese in das beschriebene Plugin importiert werden. Mit der Zuordnungsmatrix werden Auftraggeber in die Lage versetzt, Auftragnehmern zu modellierende Bauteile dynamisch und losgelöst von der DIN 276 vorzuschreiben, ohne jedoch völlig auf diese zu verzichten. Die im Modell enthaltenen Informationen können zudem auf Bauteiltypenebene automatisiert nachvollzogen werden.

Die Prüfung wurde mittels der Software Solibri exemplarisch durchgeführt. Der aus dem entwickelten Ansatz hervorgehende Prozess zur Modellerstellung und -prüfung ist in Abbildung 5 grafisch dargestellt.

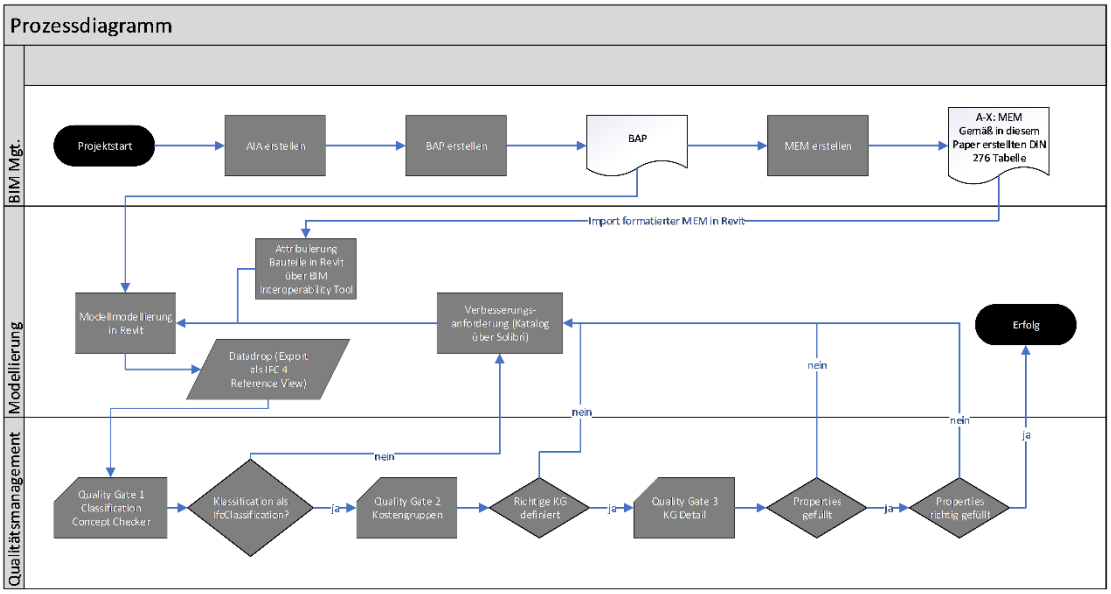

Abbildung 5: Gesamtprozess

5 Zusammenfassung und Ausblick

Die derzeit existierenden Klassifizierungskonzepte für Zuordnungsmatrizen nach Kostengruppen weisen Defizite hinsichtlich erforderlicher Bauteilidentifikation auf. Insbesondere Anlagen der KG 400, die im Gebäudebetrieb einen erheblichen Anteil der Gebäudenutzungskosten verursachen, profitieren von einer eindeutigen Identifikations-möglichkeit ihrer zugehörigen Bauteile. Im Rahmen der Modellweitergabe können diese bisher nicht vollumfänglich automatisiert hinsichtlich ihrer definierten LOI überprüft werden. In diesem Beitrag wurde ein Ansatz entwickelt, der es ermöglicht, trotz divergierender Klassifizierungssysteme eine eindeutige Bauteilzuordnug vorzunehmen. Die Ergebnisse dieses Beitrags sind theoretischer sowie technischer Natur. Theoretisch konnte dargelegt werden, weshalb das Mapping von IFC auf Kostengruppen, zumindest in der konventionellen Vorgehensweise (CAFM-Connect), ein Problem darstellt. Zudem sind benutzerdefinierte Eigenschaften zur Identifikation erforderlich, die vermieden werden sollen. Es wurde gezeigt, dass Systeme (IfcSystem) aus dem IFC-Standard eine Lösung bieten können. Technisch konnte ein Weg zur korrekten Nutzung des IFC Klassifikations-Konzeptes aufgezeigt werden. Es wurden zudem Möglichkeiten mittels des Plugins BIM Interoperability Tools der BIM-Software Autodesk Revit erörtert. Die Fokussierung auf Bauteilgruppenzuordnung statt Einzelelementzuordnung zu Bauteilgruppen ermöglicht eine Zeitersparnis auf Seiten des Qualitätsmanagements. Der entwickelte Ansatz erweist sich als vorteilhaft, da nur einige Bauteilgruppen statt einer Vielzahl Einzelelemente hinsichtlich der korrekten Kostengruppe überprüft werden müssten. Zudem können Auftraggeber ihren Auftragnehmern zukünftig flexiblere und schlankere Zuordnungsmatritzen vorlegen. Dadruch könnte zukünftig die Notwendigkeit zur

Erstellung vollumfänglicher Modellentwicklungsmatritzen, wie sie derzeit in der Praxis üblich sind, entfallen.

Die entwickelte Zuordnungsmatrix ist als Meilenstein zu betrachten, der es vereinfacht eine prüfbare Bauteilklassifizierung vorzunehmen. Außer acht gelassen ist in diesem Beitrag die Parametrisierung von Bauteilen. Künftige Forschungsarbeiten zielen darauf ab, den dargestellten Ansatz weiterzuentwicklen, um eine gleichzeitige Prüfung von Bauteilklassifikation und Parametern durchzuführen. In diesem Kontext soll zudem untersucht werden, inwiefern die hier vorgeschlagene Zuordnungsmatritzen Teil des 2021 im Forum Bauinformatik vorgeschlagenen „A Priori EIR-Compliant Modelling Approach“ sein können [5]. Dazu soll in künftigen Forschungen ein Template auf der Plattform „BIMQ“ angelegt, in verschiedenen Autorensoftwaren beispielhaft angewendet und zur Kontrolle in Solibri geprüft werden. Außerdem sollen weitere Konzepte zur exakteren Identifikation von Bauteilen untersucht werden. Denkbar wäre die Nutzung des „Port Nesting Conceptes“ um die Zusammgehörigkeit der Systeme zu validieren. Sollten diese Versuche erfolgreich sein, ist eine Veröffentlichung der vorgeschlagene Mehrfach-Klassifizierung auf bsDD geplant.

Literatur

[1] O. Litau, „Lebenszykluskosten (LzK) einer Immobilie“ in Nachhaltiges Facility Management im Wohnungsbau: Lebenszyklus - Zertifizierungssysteme - Marktchancen, Wiesbaden: Springer Fachmedien Wiesbaden, 2015, S. 23–27, doi: 10.1007/978-3-658-11352-0_5.

[2] U. Bogenstätter, Property management und facility management. München: Oldenbourg, 2008. [Online]. Verfügbar unter: http://deposit.d-nb.de/cgi-bin/dok-serv?id=3090070&prov=M&dok_var=1&dok_ext=htm

[3] U. Rotermund, „Lebenszykluskosten in der Gebäudeplanung und -nutzung: Von der Planung bis in den Betrieb“, Facility Management, Jg. 20, Nr. 05, 2020.

[4] Building Information Modeling: Klassifikationssysteme, 2552 Bl. 9, VDI Verein Deutscher Ingenieure, Berlin, Mrz. 2022.

[5] M. Mellenthin Filardo und J. Krischler, „An A Priori EIR-Compliant Modelling Approach“ in 32. Forum Bauinformatik 2021, M. Disser, A. Hoffmann, L. Kuhn und P. Scheich, 2021, S. 183–191.

[6] M. Baldwin, Der BIM-Manager: Praktische Anleitung für das BIM-Projektmanagement, 2. Aufl. Berlin, Wien, Zürich: Beuth Verlag GmbH, 2019.

[7] Building Information Modeling Begriffe, 2552 Bl. 2, VDI Verein Deutscher Ingenieure, Berlin, Apr. 2021.

[8] Building Information Modeling im Facility Management, 926, GEFMA e.V. Deutscher Verband für Facility Management, Bonn, Dez. 2019.

[9] Datenmodell, Kataloge und Ordnungsrahmen für das FM: Grundlagen und Anwendungsbeispiele, 924, GEFMA e.V. Deutscher Verband für Facility Management, Berlin, Sep. 2017.

[10] J. Beetz, „Ordnungssysteme im Bauwesen: Terminologien, Klassifikationen, Taxonomien und Ontologien“ in Building Information Modeling, A. Borrmann, M. König, C. Koch und J. Beetz, Hg., Wiesbaden: Springer Fachmedien Wiesbaden, 2015, S. 163–175, doi: 10.1007/978-3-658-05606-3_9.

[11] Building Information Modeling: Anforderungen an den Datenaustausch, 2552 Bl. 4, VDI Verein Deutscher Ingenieure, Berlin, Aug. 2020.

[12] Industry Foundation Classes (IFC) für den Datenaustausch in der Bauwirtschaft und im Anlagenmanagement – Teil 1: Datenschema (ISO16739-1:2018), 16739-1, DIN Deutsches Institut für Normung e. V., Nov. 2021.

[13] C. Richter und S. Liedtke, BKI IFC Bildkommentar nach DIN 276: Ausgewählte IFC 4 Begriffe für die BIM-Planungsarbeit gegliedert nach DIN 276. Stuttgart: BKI, 2021.

[14] CAFM Connect, CAFM-Connect BIM Profile. [Online]. Verfügbar unter: https://www.cafm-connect.org/bim-profile/ (Zugriff am: 6. April 2021).

Tracking model checks in information delivery controlling processes

Noemi Kremer[1]
[1]Design Computation, RWTH Aachen University, Schinkelstraße 1, 52062 Aachen
E-mail(s): kremer@dc.rwth-aachen.de

Abstract: While the development of checks and rule sets has been widely considered, and many contributions have been made, the process-oriented traceability of model checks has received less attention. As part of the Bundesinstitut für Bau-, Stadt- und Raumforschung (BBSR) ZukunftBau project BIM-based Information Delivery Controlling, an information delivery controlling system was developed. Part of the system is the process-oriented checking of IFC model contents with mvdXML. The model checking results are stored as BIM Collaboration Format (BCF) ZIP file. Model checking thus involves three distinct files, which have no tracked dependence on each other either before or after a model check. There is a gap in how model checks are recorded and processed in construction processes in order to reconstruct checks. This paper presents an approach on how to link model checks using open standards to enable evaluation and reconstruction capabilities in information delivery processes. Tracking files is done by storing hashes of the three files involved in the check in a database. In addition, process-related meta information of the model check is recorded. The model check tracking method is implemented and tested based on a BIM use case utilized in the Information Delivery Controlling project. Saving the hash values of the involved files enables their unique identification. Each model check can thus be individually distinguished, and duplicate checks can be recognized and avoided at an early stage. Finally, the possibilities and limitations of linked model checking in BIM use cases are discussed. Further application possibilities and challenges for linked model checking are presented.

Keywords: BIM Model Checking, Check Tracking, Information Delivery Controlling, Process Modeling

1 Introduction

In planning processes, BIM based model checks improve planning success due to the constant possibility of checking delivered information according to requirements. Process related exchange requirements at specific points of data drops in processes can be mapped with IFC elements. Developments, such as the Information Delivery Manual (IDM), support the definition of requirements on a functional and technical level. Therefore, models can be checked for exchange requirements at

defined points of data drops in processes. To perform a model check, various types of software are available, such as Solibri Model Checker [1] or Desite BIM [2].

Independently of software, model checks influence processes in the life cycle of a building, especially negative checking results can have an impact on the entire process flow, requiring a revision of the model content. For significant data drops in processes, individual model checks may have multiple iterations. Due to the importance of model checking in processes, a structured record of performed checks is essential. Recording and tracking BIM-based model checks as part of process-oriented information delivery offers a possibility to use model checking more efficiently. Model check records enable tracking and accountability of model checks within process sequences at a later date. Thus, they support the reconstruction of information delivery processes and support analyzing and assessing transactions retrospectively. Therefore, an approach is shown how BIM-based model checks can be tracked to enable evaluation and reconstruction possibilities in information delivery processes. Since model checks are highly individual, this paper presents an approach for recording model checks using the Information Delivery Controlling (ILC) project as an example.

2 Existing solutions and previous work

2.1 Model checking and data management software

BIM-based model checking is the basis for a variety of decision-making processes. Checking software such as Solibri and Desite perform BIM model checks based on IFC models. Products in the open source category mainly use open standards for checking models. For instance, the Model View Definition (MVD) Model Checker [3] from RWTH Aachen using mvdXML. Checking software stores the components of a model check within a defined project or data package: the loaded model, the defined and used rule sets, the issues found, as well as metadata. However, the storage of this information only enables the management of the files involved in the examination within the software. For example, the Solibri native format SMC is composed of geometry, sources and relationships, rule sets, results and user-defined information and can be shared within Solibri products only [4]. Open source software such as the MVD Model Checker does not offer an integrated data management option. Model checking software in general is not designed to contextualize executed model checks in information management. The focus of model checking in software products lies on rule definition and checking results saved as BCF file. Therefore, software for managing and editing BCF files, is offered by BIMcollab workflow manager [5]. Software specializing in the creation and management of exchange information requirements and quality assurance of BIM models is provided by BIMQ [6].

A Common Data Environment (CDE) defined according to ISO 19650 supports Information management and exchange processes in a common digital collaboration platform. In a CDE, processes can be created as workflows, tasks, and files can be assigned to project participants and metadata such as timestamps and progress can be recorded. However, the automated, rule-based model check is not part of the CDE. CDE software providers such as Oracle Aconex [7] or Thinkproject [8] cooperate with checking software such as Solibri and Desite BIM to enable automated model checks, but only

exchange check results so far. Reconstructing model checks is difficult since automated model checks and information management is carried out in different software.

2.2 Hashing

A hash function is the mapping of a string of characters or bytes to a numeric value or key of fixed length. The input set can be of any size and/or contain elements of different lengths. All files relevant in a model check are hashed with the standardized secure hash algorithm 256 (SHA-256) [9]. SHA-256 is also used as a cryptographic hash function and has a strong collision resistance. Hash values are composed of the content of the file, but are not influenced by metadata.

2.3 Information Delivery Manual

The information delivery manual has been introduced by buildingSMART, in order to describe process related information about who delivered what to whom at what specific point in a project life cycle [10]. According to ISO 29481-1, the basic elements of an IDM are an interaction plan/transaction diagram and/or a process diagram, and one or more information exchange requirements. In addition, there is the use case and the technical implementation as mvdXML. Since the components of an IDM are only loosely structured and hardly reusable, the third part of ISO 29481-3 defines a data schema and an XML representation, the idmXML. Each idmXML contains a fixed set of metadata, a use case, a possible process map and exchange requests [10].

2.4 ILC - Information delivery controlling project

The information delivery project supported by ZukunftBau and worked on by Bergische Universität Wuppertal(BUW), RWTH Aachen University and numerous practical partners involves the development of a tool for process-supported information control. The demonstration tool should improve digital information management in BIM processes on the client and contractor side. The developed tool, the MVD generator, is part of the ILC system (see figure 1), it enables an interoperable flow between the BUW process database and the MVD Model Checker [3] based on open standards. The process-modeling database at the University of Wuppertal has been continuously enriched with working processes from different perspectives since 2016 [11]. For each use case provided in the BUW process database, a workflow with the associated exchange requests was developed. The stored information can be retrieved as a table for further processing. The requirements for the tool were collected in a workshop with 11 practitioners from AEC industry and afterwards classified [10]. The developed tool in the ILC system consists of two subsystems, the MVD generator and the MVD checker. The MVD generator allows the generation of mvdXMLs from the corresponding tables in the process database. These can then be used to check properties of an IFC model. Results are saved as BCF file.

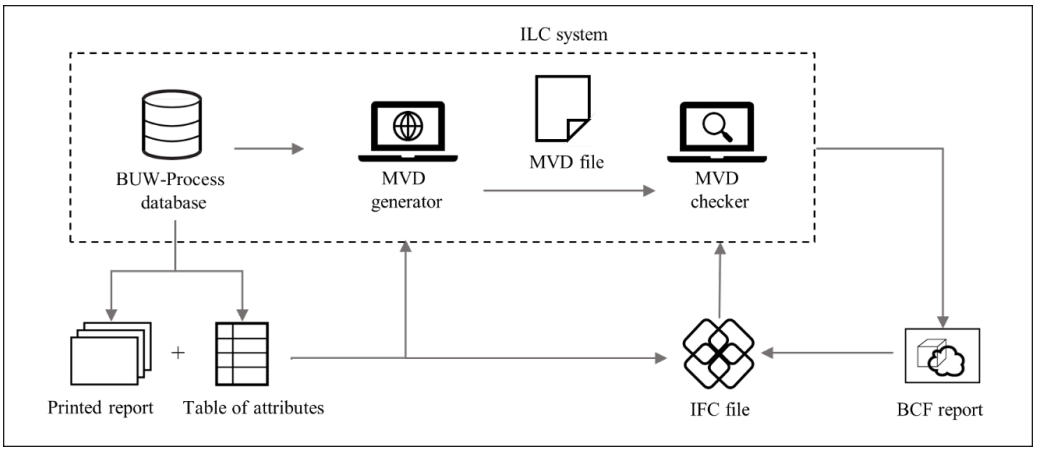

Figure 1: ILC-Project developed System [11]

3 Database - development and structure

3.1 Database development

Since model checks can be dynamic, e.g. due to iterations, the construction of a relational database is proposed. All information such as entities, attributes, and relations are represented as a collection of tuple relations, which can be thought of as tables.

To answer the question of how model checking tracking can be efficiently carried out using open standards, a combination of storing process related data and process file hashing is introduced. The development of the database is linked to the development and evaluation of the ILC system (see figure 1). Therefore, the open standards used in the ILC project and developed functional units form the basis for the structure of the database. During the development and validation of the ILC system, frequent iterations of model checks due to unspecific or incorrect rule definitions for exchange requirements and incorrect model content were necessary. A first version of the database was developed to manage these model check iterations. Since the initial situation in the ILC System contains three files: model (IFC), check file (mvdXML) and result file (BCF), the first version only stored their hash values. In order to time model checks and to identify and assign checking iterations to the model checks, further columns were added to the database. This leads to a first process-oriented sorting of model checks. Since individual model checks are assigned to process tasks, process-relevant information from the BUW-process database such as name of process owner and name of process task were added as an additional table in the database. This allows model checks to be managed by locating them in the process. The direct link to IDM was originally managed by the developed processes and exchange requirements. The database is thus closely influenced by the experiences gained in the development of the ILC system.

3.2 Database structure

The structure of the database was developed closely to content and requirements of data and tools in the ILC system. As shown in figure 2 the database consists of three tables, which are IDM, process and checking. A process defined within the IDM is broken down into individual transfer points that are assigned model checks. The central information is the hash values of the files. Furthermore, there is the process-oriented classification of the model check. In addition, there is metadata that provides additional information on data management.

The checking table consists of all information about each carried out model check. This information includes the hash values of all files required for a model check, as well as metadata about the checking process, such as iteration number and timestamp. The process table contains all information about the process. The information about the process name and the name of the person responsible for the process are part of the BUW process database. Sending and receiving person are information added from the Business Process Modeling Notation (BPMN). The additional information *has_subprocess* has been added for administrative purposes. The IDM reference table contains the associated identifiers of the IDM elements, including the unique identification name of the process. The database maps a tree structure, with the checking iterations representing individual branches.

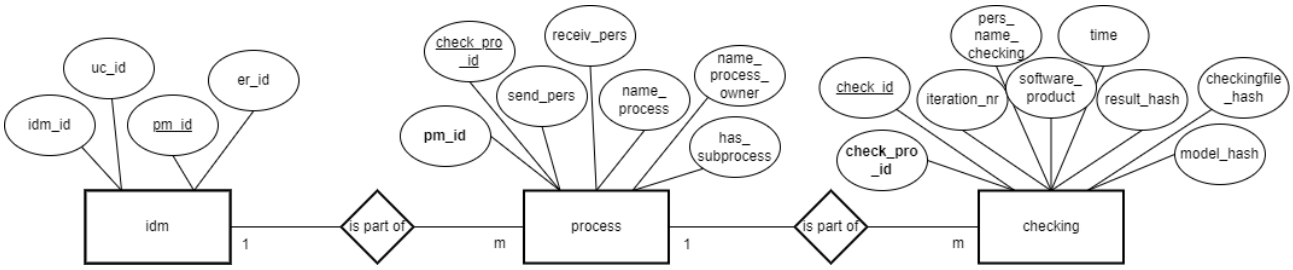

Figure 2: Structure database

4 Application of the database in the ILC project

In order to validate the advantages and disadvantages of the database, the processes of the use case *maintenance management lift system* of the ILC project was used. The predefined data provided by the BUW process database represents a process containing information transfer points and their specific exchange requirements. This information is stored in tabular form and is used to generate mvdXML. The structure of this table is subdivided into three sections, which are process information, object reference and property information. The individual sections are further subdivided. The process information contains the process name which describes the task, in the example used here such a task is: *create asset directory maintenance*. In addition, the process information also includes the process owner, in this example there are a total of three owners: *Client/owner, executing company, facility manager*. The object reference section, includes the IFC element name. The property information includes the name of the property set, the property, and the value definition.

A corresponding model is checked against the requirements, which are stored in the property information section of the table, using mvdXML. For each individual checking process, the required information is recorded (see figure 3). Part of the process-relevant information is taken from the BUW process database table, this includes the process name and person responsible for the process. For the IFC file and the mvdXML file, the corresponding hash values are generated during file upload and compared with the tuples already stored in the database. If it is determined that the check with these two files has already taken place in this exact way, the check can be cancelled or continued. If it is determined that this model checking process does not yet exist, the check is saved as a new or alternatively as an iteration of an already stored check. For the different states, different display formats can be realized for a visualized representation in the user interface. Whether a checking process is to be declared as a new check or as an iteration is decided on the basis of the known process data. Additionally, the comparison between the hash value of the uploaded mvdXML with the already stored hash values from the database. The process information extracted from the table is not stored in the database until the comparison of the process information and the hash values is complete. Since in this use case example only the data drop is relevant, the process name may be composed of several task names. This happens because more than one task can be assigned to a process owner before a data drop, and a new mvdXML is only generated after each change of a process owner.

Further information about the check such as check ID, number of iterations and timestamp are automatically generated and added to the database. Information such as the name of the person performing the check and the software product are recorded manually and stored in the database. A process ID is automatically generated and stored. The information whether there are sub-processes is recorded manually in the ILC example. An IDM assignment plays a less important role in this example, as only one use case was tested. Therefore, IDM-relevant IDs were assumed and entered manually. In general, all information to be entered manually was recorded through a user interface.

When a model check is performed for the first time, all information is recorded, automatically and manually. In iterative model checks, only the information concerning the check is recreated, the information about the process remains the same.

5 Discussion

The developed database supports the delivery processes of the ILC-system by recording data and workflow management relevant information of performed model checks in a process-oriented manner. Therefore, it presents an approach to record checks in the context of open systems over the whole process and to reconstruct checks performed when needed. It enables model checks to be reconstructed at a later point in time. Furthermore, the database supports avoiding redundancies by repeating duplicate model checks. In the context of IDMs, model checks can be assigned to individual process steps with specific meta-information. In addition, it can be traced whether, with what and by whom a model was tested at a certain point in time. However, the implementation of the database does not

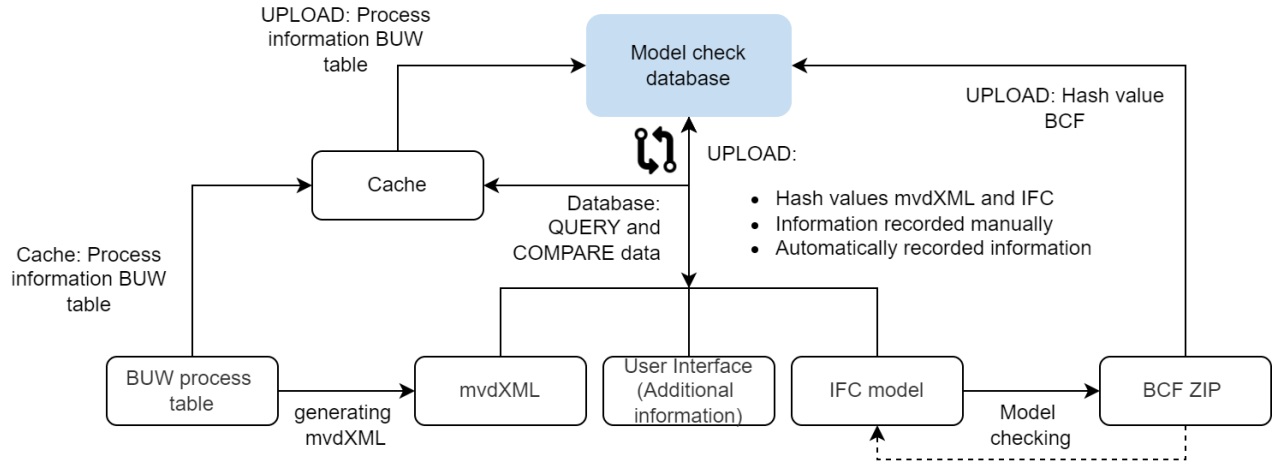

Figure 3: ILC example use case storing check information for every data drop and checking iteration in process diagram

distinguish between priorities and importance of a model check for the process flow. Model checks can also be carried out manually or semi-automatically. Within the presented use case, only automated property model checks have been recorded. In order to fully track model checks, semi-automated and manual checks must also be tracked. The database structure presented here does not necessarily have to store an IFC, mvdXML and BCF file, but has only been validated using these data files.

Since a hash value is derived from the content of the file, a new hash value will be generated if any of the file content changes. In addition to the content-dependent identification of files, a hash value requires significantly less memory than the check files used.

Potentially, a gap between data management and checking tool can be closed by recording automatic model checks. All components involved in rule-based checking are stored in addition to process-related information such as persons involved and time, as well as the associated use case. Data management and workflow management in the CDE can be enriched from this information pool and model checks can be assigned, reconstructed and retrieved.

Within the framework of the idmXML development, it will be possible to assign the definition of information delivery(s) to their delivery verification. The database developed here links to an IDM by assigning identifiers to individual components — IDM, use case, process map and exchange requirements.

6 Conclusion

This paper has presented one way to track automated, rule-based model checks in an information delivery process. The use case of tracking model checks is the ZukunftBau information delivery controlling project. It was shown how check-relevant files can be stored with hash values and enriched with process-relevant information. Particularly in the area of data and project management, this data

can help to reconstruct procedures in processes and to identify faulty files such as faulty control data records.

References

[1] S. A. N. Company. “Führend bei der qualitätskontrolle in der bauwirtschaft”. (2022), [Online]. Available: https://www.solibri.com/de/ (visited on 05/12/2022).

[2] Thinkproject. “Desite bim”. (2022), [Online]. Available: https://thinkproject.com/de/produkte/desite-bim/ (visited on 05/23/2022).

[3] J. Oraskari. “Onlinemvdxmlchecker”. (2022), [Online]. Available: https://github.com/jyrkioraskari/OnlineMvdXMLChecker (visited on 05/12/2022).

[4] S. A. N. Company. “Unterstützte dateiformate”. (2020), [Online]. Available: https://www.solibri.com/de/lernen/02-modelle-unterstuetzte-dateiformate (visited on 05/23/2022).

[5] BIMcollab. “Unterstützung aller openbim-workflows”. (2022), [Online]. Available: https://www.bimcollab.com/de/products/bcf-managers/workflow (visited on 05/12/2022).

[6] BIMQ. “Bimq intelligentes informationsmanagement von bim-projekten: Einfach, intuitiv & cloud-basiert”. (2022), [Online]. Available: https://www.bimq.de/ (visited on 05/12/2022).

[7] J. Oraskari. “Bewährte projektdurchführung und -kontrollen.” (2022), [Online]. Available: https://www.oracle.com/de/industries/construction-engineering/aconex-project-controls/ (visited on 05/23/2022).

[8] Thinkproject. “Common data environment”. (2022), [Online]. Available: https://thinkproject.com/de/produkt-familie/common-data-environment-cde/ (visited on 05/23/2022).

[9] N. N. I. of Standards and Technology. “Hash functions”. (2022), [Online]. Available: https://csrc.nist.gov/projects/Hash-Functions (visited on 05/23/2022).

[10] A. Borrmann, M. König, C. Koch, and J. Beetz, *Building Information Modeling: Technologische Grundlagen und industrielle Praxis*, ser. Springer-Lehrbuch. Wiesbaden: Springer, 2021, ISBN: 9783658333607.

[11] Z. Meng, N. Kremer, B. Klusmann, and J. Beetz, “Development of information delivery controlling tool based on process modeling”, in *Proc. of the Conference CIB W78*, vol. 2021, 2021, pp. 11–15.

Teil II

Construction Monitoring

UAV path planning for photogrammetric capture of buildings towards disaster scenarios

Betina Koleva[1], Ann-Kristin Dugstad[2] and Florian Noichl[2]
[1]Institute of Informatics, LMU Munich, Geschwister-Scholl-Platz 1, 80539 Munich, Germany
[2]Chair of Computational Modeling and Simulation, TU Munich, Arcisstr. 21, 80333 Munich, Germany
E-mail(s): betina.koleva@campus.lmu.de, ann-kristin.dugstad@tum.de, florian.noichl@tum.de

Abstract: At the scene of an emergency, first responders operate in a complex environment with limited knowledge about hazardous areas. This lack of insight is a hindrance to effective intervention. Utilizing Unmanned Aerial Vehicles (UAVs) for generating scans of the environment is one possibility to receive rapid and accurate information about hazardous conditions. Although many fields adopt UAV remote sensing, their efficient application poses a variety of research problems. Optimization of path planning for sufficient data capturing that allows 3D reconstruction is one of these problems. This paper concentrates on developing a path planning module that allows scanning the outside of the polygonal-shaped building site, considering a set of parameters, and inspecting existing strategies for outdoor UAVs. The generated module produces a path using the Traveling Salesman Problem based on the given UAV and 3D building model.

Keywords: UAV, BIM, Path Planning, Traveling Salesman Problem

1 Introduction

At a scene of an emergency, first responders often have to operate in dangerous and chaotic environments. Lack of insight into disaster scenes interferes with effective intervention. Examining the scene of an emergency with an Unmanned Aerial Vehicle (UAV) and notifying the first responders of the hazardous conditions in the operating environment allows to overcome possible overview deficiencies and respond to the hazard more rapidly and targeted. The utilization of UAVs has been widely adopted in many fields requiring remote sensing as a fundamental tool for surveying and mapping hard-to-reach locations [1]. Images captured by UAVs serve for reconstructing a point cloud, from which it is possible to generate a high-quality 3D model of the mapped area.

An efficient building examination with remote sensing is an important research problem. Many researchers focus on examining optimal scans by planning accurate paths before executing the UAV-scanning process. Inspecting optimal flight and sensor parameters and existing path planning

strategies for outdoor UAVs in the literature is the first step of this study. This literature research defines the basis for setting parameters for the path planning solution of this study with the aim to implement a path planning module for a given outdoor UAV and a 3D building model. Setting the optimal parameters can be challenging, and multiple adjustments may be needed to obtain an accurate reconstruction efficiently. Some parameters to be considered in path planning for photogrammetric reconstruction are the selection of flight altitude, flying speed, image overlap, and camera parameters, particularly spatial resolution and focal length [2]. Investigating path planning strategies in literature was conducted to support the project goal - scanning the outside of the building from above and side. The method was developed for Building Information Modeling (BIM) models in Industry Foundation Classes (IFC) format, which represents a future standard format and methodology for built environments. The tool was implemented in python and tested using a sample UAV and sample BIM-building from the TUM campus in Munich.

2 State of the Art

UAVs have become powerful remote sensing tools for investigating hard-to-reach and dangerous locations because of the flexibility, cost-efficiency, and enabled controlled flight repeatability due to improving autopilots [2]. Although widely adopted in many fields, the efficient application of UAVs is of central interest for much recent research. Planning a convenient path that considers flight efficiency remains an open research question. Utilizing a BIM model as a simulation environment helps to design a path as the model geometry of the examined building allows a collision-free flight preparation while also evaluating the visual coverage and flight safety before execution [3]. Overall, two primary difficulties regarding path planning for UAVs can be defined: setting the optimal flight and sensor parameters and choosing the algorithm for the particular mission.

A critical open question regarding setting optimal parametrization is how to define the parameters best to achieve an optimization goal. Much recent literature focuses on parameters such as altitude, image overlap, and sensor resolution for UAV-based remote sensing. For instance, Seifert et al. [4] focus on adjusting parameters to impact the generation of good quality point clouds. The study concentrates on the influence of flight and sensor parameters on the flight time, the reconstruction details and precision, and the data processing duration. A trade-off occurs between quality and processing time. The study shows that flight time is linearly related to flight height. The lower the altitude, the higher the spatial resolution for more precise 3D reconstruction, but the longer the flight time [4]. Several researchers performing urban studies suggest a 10m distance between the UAV and building from both the ground and the façade [5], [6]. Optimal data collection is also strongly affected by the photographic overlap. Maximizing forward overlap increases accuracy but results in an exponential increase in processing time and has a negative impact on flight duration [4]. However, several researchers do not recommend reducing the overlap because it positively impacts the precision and leads to significantly lower error. Several studies conclude that a fixed forward overlap above 90% yields the best reconstruction detail and accuracy [1], [4]. Few researchers have addressed a precise parametrization of camera angle and flight speed. The angle of view describes the capture of multiple objects from the camera sensor

and the determination of their distance [7]. For precise reconstruction, the captured area must be scanned from multiple angles while also considering the Field of View (FOV). Flight speed is highly influenced by the model of the UAV itself.

Finding an optimal path in a 3D model is a challenge widely addressed in the literature. An important question is defining a convenient path for a particular goal. This problem can be solved in many ways, denoted by the number of waypoints, their coordinates, and the camera orientation [3]. The literature offers a palette of examples for solving UAV path planning - from the artificial potential field to the commonly used graph search methods such as the Dijkstra and A* algorithm. A drawback of graph-based approaches is that they are time-consuming in complex environments and are prone to get trapped in the local optimum and never reach the global one [3]. Therefore, probabilistic methods such as Simulated Annealing (SA), genetic algorithms, and ant colony optimization are considered a less expensive alternative. Some literature sources interpret the UAV path planning challenge as a Traveling Salesman Problem (TSP). The fundamental characteristic of the TSP is the creation of a sequence for visiting a given list of places with the shortest distance possible [8]. For UAV path planning, the objective of the TSP is to plan a path that allows the UAV to visit all waypoints needed for scanning the object. The method for the study is developed utilizing TSP with the A* algorithm to find a path for a list of visited waypoints for scanning a building.

3 Methodology

The following chapter presents the main concept. The goal is the generation of a path planning module for outdoor UAVs that allows scanning of built environments efficiently. Figure 1 illustrates the workflow of the presented tool.

Figure 1: Workflow overview.

The first step of the method considers transforming the given BIM model in IFC format (Figure 2) to a voxel-based representation of the building (Figure 3). Calculating the bounding box from the IFC file allows obtaining an overview of the building measurements in meters for a precise voxelized representation. Therefore, a one-meter-sized voxelized model is created using the external software binvox mesh voxelizer by Patrick Min [9]. The created voxel-based data is structured in an octree, recursively subdivided into eight equal cubes until reaching the minimum voxel size. Figure 4 displays the grid resulting from a level of the octree. Each level provides different precision. A deeper level yields a more detailed vision of the building. The lowest level chosen in this study presents the voxelization of one-meter-sized cubes.

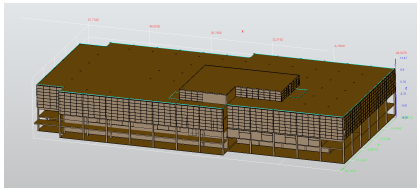

Figure 2: BIM input

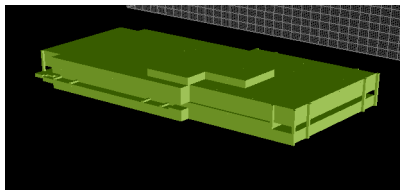

Figure 3: Voxelized model

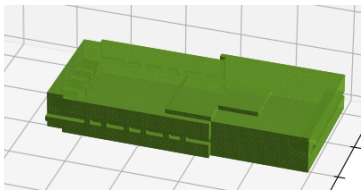

Figure 4: Octree representation

In the simplification step, the inside inaccessible voxels of the building are filtered out since they are irrelevant for outside path planning. The filling process is conducted using the flood fill algorithm. The algorithm is used to display the connected area around a given node in a multidimensional array. The flood fill algorithm allows defining the accessible voxels that can be used as waypoints in path planning by marking the outside empty voxels with the same value. Reversing the results switches the values inside and outside, meaning all inside voxels become flood-filled, which considers built environments consisting of more than one building. In the next step, a boundary box for path preparation is initialized by space extension. A building dilatation is used to guarantee a minimum distance around the building by extending the filled area with one voxel in all directions.

The simplified model is used as a basis for producing waypoints. Waypoints contain the coordinates to be visited by the UAV for scanning the building and the direction facing the building. Selecting a distance from the building aims to provide scans efficiently while considering collision avoidance. A defined maximum distance between two neighboring waypoints ensures an overlap between the two images. The distance between two waypoints is calculated using an equation that incorporates the overlap, the desired distance from waypoint to object, and the camera field of view:

$$\text{distance} = (\tan\left(\frac{\alpha}{2}\right) * \text{distance}) * 2 * \left(1 - \frac{\text{overlap}}{100}\right) \tag{1}$$

The waypoint-setting algorithm starts at a given position by collecting the coordinates of the voxels surrounding the particular node. It then iterates over the list of neighboring points until finding any neighbor on the building surface, meaning an occupied voxel at the neighbor position. The function calculates the optimal rotation matrix with the Kabsch algorithm [10] multiplied by the selected distance to align a vector between the current node and the neighbor. The coordinates of the newly created waypoint are calculated by summing up the resulting rotation matrix with the coordinates of the neighbor. A waypoint detected on the edge of the building is calculated by completely rotating over a corresponding axis using Euler angles. The waypoints are refined in the last step of the algorithm to filter the waypoints created in the direct vicinity of each other or in an inaccessible location as a consequence of the rotation process.

The TSP is a problem in combinatorial optimization, which describes the search for the most efficient path connecting a given number of cities by minimizing the cost of travel or the distance in-between. Solutions to the Traveling Salesman Problem can also be applied to the waypoint-connection problem underlying this study. The TSP is implemented with an A* algorithm to find the next nearest neighbor.

The study proposes three approaches. In the first approach, the waypoints are divided into clusters, and the TSP is performed between all elements in two neighboring clusters. The second approach takes an initial point and sorts the rest of the waypoints by distance away from it in ascending order. The closest n-points to the initial point are selected, and the TSP is performed on them to find the nearest neighbor. The last TSP is used with the cheapest insertion implementation - the algorithm places the next node in the position resulting in the cheapest possible costs.

Finally, the method performance is evaluated by assessing the coverage of the building and comparing the path planning strategies. A maximum depth distance is proposed to ensure a more accurate coverage analysis. The parameter aims to filter the visibly occupied voxels that are too far from the camera by calculating the Euclidean distance from the waypoint to the coordinates of surface points. The three presented methods regarding the TSP are analyzed by comparing the length, computational time, and path tendencies. The path length is calculated using the formula L = costs + len(waypoints), where the costs resulting from the TSP are summed up with the number of created waypoints.

4 Results

The study is tested on the BIM model of Technical University Munich Mensa. The resulting waypoints created with the tool are illustrated in Figure 5. The parameters are set to distance between the building and each waypoint of 12m, overlap of 20%, and a maximum depth distance of 20m. The coverage analysis results in a score of 85%, displayed in Figure 6. The uncovered area of the building surface is marked with red points. One limitation of the module occurs in this example. Details captured with a 20-meter-set maximum depth distance present an obstacle, as the distance from the building is fixed. One way to overcome the problem in the future is by featuring a flexible distance between the waypoints and the building.

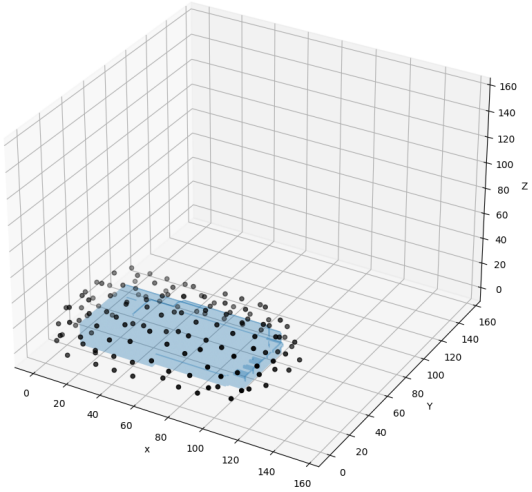

Figure 5: Waypoints with overlap 20% and distance 12 m

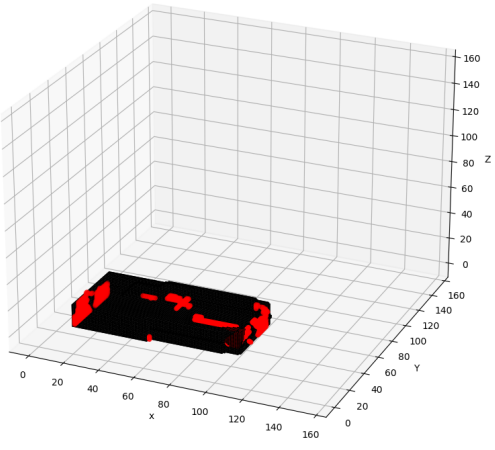

Figure 6: Coverage in black versus unseen points in red

The path planning analysis consists of the comparison of the three approaches considering TSP performed on the waypoints set. The analysis includes the processing time, the costs of the path, and the L-function, defined in Section 3. Table 1 summarizes the results of the path planning for the waypoint set selected in Figure 5. The path tendencies are visualized in Figures 7 - 9.

Table 1: Comparison of the three approaches

TSP	Number of waypoints	Processing time (s)	Costs	L
Clusters	141	106.68	2642.2	2783,5
Closest points	141	88.6	1320.9	1461.9
Cheapest insertion	141	902.8	1178.1	1319.1

The first approach is twice more expensive as the second and the last strategies and features the most randomness in the path, while the second and the third techniques have a more strict pattern yet are not perfectly aligned. The possible production of a more random path is a drawback of the discrete grid because each movement to the next point is equally expensive. Implementing a priority to one axis allows influencing a moving direction by making the cost cheaper along the particular axis. The feature helps prioritize moving along the chosen axis by equal distanced points. The study prioritizes the z-axis and x-axis. Without the priority, the first cheapest waypoint is considered a successor. This approach helps create a more consistent path, as demonstrated in the second and third approaches. The second approach has a significantly shorter processing time than the other two strategies. The cheapest costs are achieved utilizing the third approach. In the case of capturing buildings in disaster scenes, the second approach is the best because the path is produced in the shortest time. However, even this strategy should be speeded up regarding computational time in the future to provide quick results in time-pressing disaster scenarios.

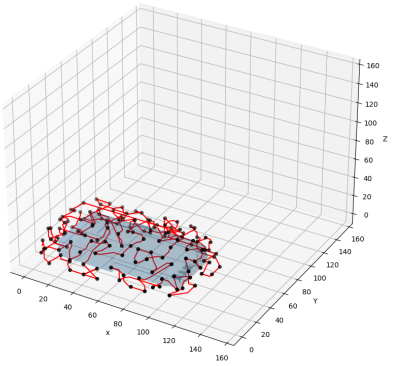

Figure 7: TSP with clusters

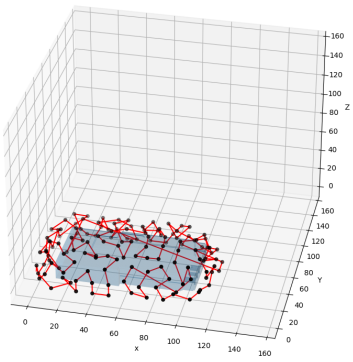

Figure 8: TSP on closest points

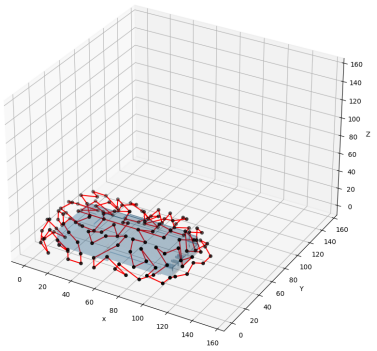

Figure 9: TSP with the cheapest insertion

Figure 10 describes the impact of the different overlaps and distances away from the building coverage. In Figure 11 logarithmic computational time is illustrated with chosen maximum depth distance of 20m and the focal length of 50mm. An overlap between 10 and 90% and a distance between 6 and 14m are the input for the analysis. A high coverage above 95% is achieved by waypoints close to the building

with the highest overlap possible. Keeping the distance short and decreasing the overlap results in a slight decrease in the gained coverage. The plot is monotonically decreasing, meaning waypoints further away from the building and lower overlap produce a lower coverage percentage. The coverage decrease is also dependent on the specified maximum depth distance. The computational time is monotonically increasing. However, a set of waypoints far from the building with a high percentage of overlap produces a sharp increase.

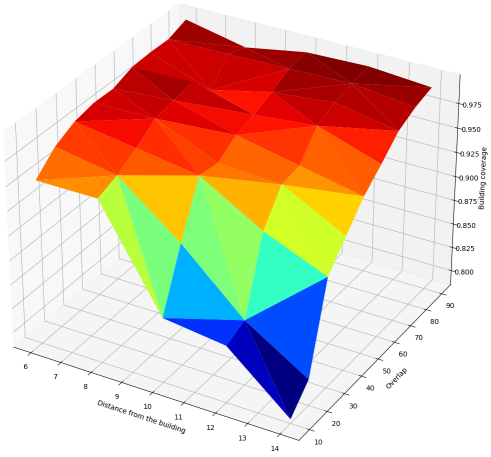

Figure 10: Gained Coverage

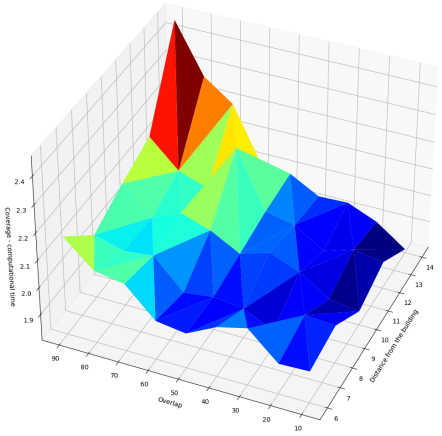

Figure 11: Computational time

5 Conclusion and Outlook

The main goal of this study was to develop a method for outdoor path planning for BIM models in IFC format, which allows for optimal scan acquisition in disaster scenarios. In the first step of the method, the input in IFC format was converted to a format that can be used for path planning. A voxel-based model was proposed, structured in an octree, and simplified with flood filled algorithm. As a next step, waypoint coordinates were defined, needed for the path planning algorithm based on the TSP with A* algorithm. The output is a resulting path consisting of a list of waypoints stored as coordinates in a JSON file. The method was tested and evaluated based on waypoints coverage and efficiency of path planning.

Based on the limitations of the developed method, a possible future work will be accelerating the path planning to adapt the module efficiently to the needs of first responders. The tool has to be adjusted concerning computational time to become applicable for disaster scenarios. One can implement a feature for distance flexibility since the fixed one is a limitation for buildings with indoor yards. Prioritization can be featured based on the current moving direction of the UAV instead of the axis.

Acknowledgements

The presented research was conducted in the frame of the project "Intelligent Toolkit for Reconnaissance and assessmEnt in Perilous Incidents (INTREPID)" funded by the EU's research and innovation funding programme Horizon 2020 under Grant agreement ID: 883345.

References

[1] D. Domingo, H. O. Ørka, E. Næsset, D. Kachamba, and T. Gobakken, "Effects of uav image resolution, camera type, and image overlap on accuracy of biomass predictions in a tropical woodland", *Remote Sensing*, vol. 11, no. 8, p. 948, 2019.

[2] L. Tang and G. Shao, "Drone remote sensing for forestry research and practices", *Journal of Forestry Research*, vol. 26, no. 4, pp. 791–797, 2015.

[3] A. Ibrahim and M. Golparvar-Fard, "4d bim based optimal flight planning for construction monitoring applications using camera-equipped uavs", in *Computing in Civil Engineering 2019: Data, Sensing, and Analytics*, American Society of Civil Engineers Reston, VA, 2019, pp. 217–224.

[4] E. Seifert, S. Seifert, H. Vogt, *et al.*, "Influence of drone altitude, image overlap, and optical sensor resolution on multi-view reconstruction of forest images", *Remote sensing*, vol. 11, no. 10, p. 1252, 2019.

[5] D. Roca, J. Armesto, S. Lagüela, and L. Díaz-Vilariño, "Lidar-equipped uav for building information modelling.", *International Archives of the Photogrammetry, Remote Sensing & Spatial Information Sciences*, vol. 45, 2014.

[6] K. Themistocleous, A. Agapiou, and D. Hadjimitsis, "3d documentation and bim modeling of cultural heritage structures using uavs: The case of the foinikaria church", *The International Archives of Photogrammetry, Remote Sensing and Spatial Information Sciences*, vol. 42, p. 45, 2016.

[7] P. M. Hell and P. J. Varga, "Drone systems for factory security and surveillance", *Interdisciplinary Description of Complex Systems: INDECS*, vol. 17, no. 3-A, pp. 458–467, 2019.

[8] P. Oberlin, S. Rathinam, and S. Darbha, "Today's traveling salesman problem", *IEEE robotics & automation magazine*, vol. 17, no. 4, pp. 70–77, 2010.

[9] P. Min, *Binvox*, 2019. [Online]. Available: https://www.patrickmin.com/binvox (visited on 09/15/2021).

[10] W. Kabsch, "A discussion of the solution for the best rotation to relate two sets of vectors", *Acta Crystallographica Section A: Crystal Physics, Diffraction, Theoretical and General Crystallography*, vol. 34, no. 5, pp. 827–828, 1978.

Object Detection of Fire Safety Equipment in Images and Videos Using Yolov5 Neural Network

H. Bayer[1] and A. Aziz[1]

[1]Chair of Computing in Engineering, Ruhr University Bochum, Universitaetsstraße 150, 44801 Bochum, Germany

E-Mails: Hakan.Bayer@ruhr-uni-bochum.de

Abstract: The whole lifecycle of building information modeling (BIM) has great potential and intersections with other emerging technologies such as Artificial Intelligence (AI). Depending on the building's life cycle phase, there are many specific AI applications to use and possibilities to investigate. In particular, facility managers are recognizing the value of AI for different maintenance tasks, especially for the field of fire safety management. Building fire safety documentation is not just for newly completed buildings but also for existing structures that have not been digitized yet. Furthermore, this documentation is usually required to be updated due to recurring maintenance work, relocations, or system changes of fire safety equipment (FSE). However, performing specific FSE inspections in the traditional way and documentation is time-consuming and error prone. The computer vision abilities in the analysis of images and videos can provide important information on the current condition of the FSE. This study investigates machine learning and computer vision methods to provide an overview of state-of-the-art detection algorithms as a first step to improving the automation level of fire safety inspections. For performing the detection of FSE objects, You Only Look Once (YOLO) v5 was considered and utilized to train a custom neural model. Additionally, transfer learning is utilized from the Microsoft COCO dataset due to limitations of the amount of available data. To address this issue, an open-source dataset was combined with self-created images. The images were classified into four object classes: fire extinguisher, emergency call point, smoke detector and fire safety blanket. Moreover, image preprocessing and augmentation techniques were applied to increase the variability of the dataset. Based on selection criteria, the pre-trained Yolov5 model was utilized and trained on different datasets. The results show a significant detection accuracy in images and live videos. In future work, the concept of this research will be extended to transfer the FSE object directly to a BIM model after detection.

Keywords: Machine Learning, Object Detection, Computer Vision, Fire Safety Equipment

1 Introduction

1.1 Problem Statement

Building Information Modeling (BIM) is enjoying increasing popularity and acceptance in the construction sector due to its numerous advantages. It serves as a shared knowledge repository for information about a facility, providing a solid foundation for decisions made throughout the building's life cycle. BIM is also an interactive computerized database that all building stakeholders involved in the design, construction, and operation phase of a facility can access. The owners, architects, engineers, contractors, and facility managers are among the stakeholders. Technical experts such as fire safety managers (FSM) are also usually involved in any construction project by ensuring and documenting fire safety aspects. By using the BIM method, an FSM can locate and share important information regarding fire protection equipment in a BIM model. Despite the use of the BIM method, inspections are still carried out manually with checklists and transferred to a BIM model afterwards. However, this documentation of fire safety equipment (FSE) is still very error-prone, time-consuming, and expensive. Therefore, this paper investigates possible methods to automatically extract the necessary information, such as the presence of FSE in images by using computer vision.

1.2 Motivation

The integration of artificial intelligence (AI) with BIM has only recently begun, and the combination of these two powerful technologies is sure to grow in the future. It will help increase productivity in construction projects. Computer vision, especially object recognition using deep learning, has had limited research in this area. Nevertheless, a few researchers have addressed object detection scenarios in the construction field using neural networks. For instance, in [1] the authors adapt a deep convolutional neural network approach using Mask R-CNN to automatically recognize and segment building objects with arbitrary shapes from images. The segmented objects are further geometrically processed and fitted to construct surface geometries and to be defined in the Industry Foundation Classes (IFC) data format. Also, in [2] one part of the study focuses on automatic semantic segmentation of building interiors from images using deep learning methods. However, also in the field of fire safety management, researchers investigated the potential of computer vision. Corneli et al. [3] investigated the detection of fire safety assets such as fire extinguishers and emergency signs using a YOLOv2 [4] algorithm. Their results showed that fire extinguishers and emergency signs can reasonably detected. Unlike the forementioned study, this research paper concentrates on implementing the latest version of the YOLO algorithm family for FSE detection – YOLOv5. Also, additional FSE object classes were included. All training models were tested on a test dataset and evaluated based on performance metrics.

2 Technical Background

The You Only Look Once v5 - YOLOv5 [5] is a natural extension of the YOLOv3 [6] and the latest version of YOLO architecture series. The detection accuracy of this network model is high, and the inference speed is fast compared to the previous versions. Also, the size of the weight file of YOLOv5 target detection network model is small, indicating that YOLOv5 model is suitable for the deployment to embedded devices to implement real-time detection. The YOLOv5 architecture contains multiple varieties of pre-trained models, specifically named YOLOv5s, YOLOv5m, YOLOv5l and YOLOv5x, respectively. The main difference between them is that the number of feature extraction modules and convolution kernels is different at specific locations in the network. The size of models and the amount of model parameters in the four architectures also increase in turn but as the models get larger the accuracy gets better. On COCO dataset [7] evaluations, YOLOv5x model performs best compared to smaller versions. Despite YOLOv5x performs slightly better than YOLOv5l on COCO dataset evaluations, it is almost two times the size of YOLOv5l and with slower inference. Considering this detail, we selected YOLOv5l for this study. The three primary pieces of the YOLOv5 architecture are the backbone for feature extraction, the head for feature fusion, and the output for object detection. The backbone network uses Darknet which is a Convolutional Neural Network (CNN) that collects and forms image features at various granularities, also includes cross stage partial network (CSPNet) [8] into its architecture, resulting in the CSPDarknet architecture. CSPDarknet handles repeating gradient information in long backbones and integrates gradient change into feature map, which speeds up inference, improves accuracy, and decreases model size by lowering parameters. The head is made up of layers that aggregate image characteristics before sending them to detection algorithm. To improve information flow, YOLOv5 uses a path aggregation network (PANet) [9] as the head. PANet uses a new feature pyramid network (FPN) topology with an improved bottom-up approach to improve low-level feature propagation. Simultaneously, adaptive feature pooling, which connects the feature grid to all feature levels, is employed to ensure that meaningful information from each feature level reaches the next subnetwork. PANet improves the use of precise localization signals in lower layers, which can significantly improve the object's localization accuracy. Finally, the output generates three distinct sizes of feature maps allowing the model to detect small, medium, and large objects.

3 Methodology

3.1 Data Acquisition and Annotation

To ensure that our models can detect different types of fire safety equipment detection tasks, we have collected self-made images of different types of buildings (university buildings, student dormitories, etc.) in Germany. Additionally, the open source FireNet dataset from University College

London [10] as used to enrich the self-made dataset. For the self-made images a mobile camera was used to capture the images with resolution of 12MP. After that we combined the self-made images with the FireNet dataset and manually separated the images into different class folders. This dataset folder contains a total of 841 images showing FSE objects such as fire extinguisher, emergency call point, smoke detector and fire safety blanket. Since the resolution of the FireNet dataset images were lower, after combining the images, the average resolution became ~9.1MP with a mean size of 2988x4032. From the main fire safety equipment dataset containing 841 images, we separated 83 images for testing purpose and the remained was used to creat two dataset: Dataset_L containing 758 images (606 train + 152 val.) and Dataset_S containing 590 images (465 train + 125 val.). Each dataset contains 80% training and 20% validation set. To label the fire safety equipment dataset we used online open-source annotation tool called Roboflow. After each annotation Roboflow automatically generates a YAML config file and one text file per jpeg image file. The text file contains the location information of the bounding box which is the center location of the rectangle (x, y), the width-height of the rectangle, and the object class in numbers.

3.2 Data Preprocessing and Augmention

After annotating all the datasets, we applied several preprocessing and augmentation techniques to reduce the training time and increase the model performance. To reduce the training time, we downsized high-resolution images to 640x640 pixels which is the default input size of YOLOv5. Two different resizing techniques were applied using the Roboflow annotation tool. In the first method, we downsized the image to 640x640 while preserving the aspect ratio and filling the padding with black pixels. In the second method, we downsized the image to 640x640 while preserving the aspect ratio and filling the padding with the reflection of the image content. To compare the effect of this preprocessing method, we also kept the images with their original size which varies based on the image. To avoid overfitting and improve our model performance, it is important to use data augmentation techniques. With each training batch, YOLOv5 passes training data through a data loader, which augments the data based on the selected hyperparameters. The data loader applies transformations to the image, such as geometric transformations like rotation, scaling, image translation and flip translation, photometric transformations like hue saturation value (hsv) and shear, image occlusion techniques like Mixup and Mosaic data augmentation. Mixup data augmentation generates weighted combinations of random image pairs from the training data. Whereas Mosaic data augmentation is used to create a new image by combining 4 training images in specific ratios into one image. As for our problem, we chose the data augmentation techniques considering different inner building conditions such as the lightening condition and the camera perspective. After preprocessing and augmentation of the images, we generated 8 different datasets using Dataset_S and Dataset_L as shown in the Table 1.

Table 1: Applied image preprocessing and augmentation parameters on different models

Model	Dataset	Preprocessing	Augmentation
Model_S_1	Dataset_S_1	Resize to 640x640 (Fit (black edges))	hsv, translate, scale, mosaic
Model_S_2	Dataset_S_2	Resize to 640x640 (Fit (reflect edges))	hsv, translate, scale, mosaic
Model_S_3	Dataset_S_3	Original size	hsv, translate, scale, mosaic
Model_L_1	Dataset_L_1	Resize to 640x640 (Fit (black edges))	hsv, translate, scale, mosaic
Model_L_2	Dataset_L_2	Resize to 640x640 (Fit (reflect edges))	hsv, translate, scale, mosaic
Model_L_3	Dataset_L_3	Original size	hsv, translate, scale, mosaic
Model_L_4	Dataset_L_4	Original size	hsv, translate, scale
Model_L_5	Dataset_L_5	Original size	None

4 Training and Evaluation of The Neural Network

After creating the datasets as shown in Table 1, we trained our models using Yolov5l coco pretrained weight with fixed input image size as 640x640, batch size of 24, with 300 epoch and learning rate of 0.01. For training the models, Google Colab Pro was utilized. Google Colab Pro runs on Ubuntu 18.04.3 and is embedded with Intel(R) Xeon(R) CPU 2.00GHz, GPU of NVIDIA Tesla T4 (16GB) and RAM of 24GB. Furthermore, we used PyTorch 1.11.0, CUDA 11.3 and Python 3.7.13. While training the model, YOLOv5 saves the best and the last trained weight after each epoch. The best weight is selected based on a fitness function. This function is a weighted combination of mAP@0.5 and mAP@0.5:0.95 which gives more weights on the mAP@0.5:0.95 side. The mAP@0.5:0.95 is also the primary metric in the COCO object detection challenge. Therefore, we preferred to use mAP@0.5:0.95 for model evaluation and selection.

5 Object Detection Results and Discussion

Table 2 shows the validation and test results of each model on all of the classes. Here it can be seen that the validation mAP@0.5 values for all models are above 91% and validation mAP@0.5:0.95 values for all models are above 80%. The top three models based on validation mAP@0.5:0.95 are respectively, Model_S_3 with 89.5%, Model_L_3 with 89.3% and Model_S_1 with 87.4%. When we look at the test metrics, we see that for all the models the test mAP@0.5 values are above 89% and the test mAP@0.5:0.95 values are above 74%. Top three models based on Test mAP@0.5:0.95 are respectively Model_L_3 with 80.1%, Model_S_3 with 79.7%, Model_L_4 with 77.1% accuracy. Model_L_3 has 0.4% better mAP@0.5:0.95 than Model_S_3 on the test dataset. Model_L_3 has higher precision than Model_L_4 in both validation and test mAP@0.5:0.95 values. This difference is due to the additional mosaic data augmentation applied on Dataset_L_3. Based on validation and test mAP@0.5:0.95, Model_L_5 performs the worst with 80.6% validation and 74.3% test precision. Model_L_3 performs 8.7% better on validation and 5.8% better at mAP@0.5:0.95 compared to Model_L_5. These results indicate that augmentation techniques are important for a proper model performance.

Table 2: Validation and test mAP results of the models

Model	Class	Validation mAP@0.5	Validation mAP@0.5:0.95	Test mAP@0.5	Test mAP@0.5:0.95
Model_S_1	all	97.3	87.4	91.2	75.9
Model_S_2	all	94.9	84	89.5	76.6
Model_S_3	all	98.4	89.5	91.7	79.7
Model_L_1	all	96.2	85.6	90.3	74.4
Model_L_2	all	95.8	85.9	91.9	76
Model_L_3	all	96.6	89.3	92.5	80.1
Model_L_4	all	94.5	86.8	89.4	77.1
Model_L_5	all	91.5	80.6	89.8	74.3

When we look at the averaged validation mAP@0.5:0.95 results of individual classes for the models we see that the fire safety blankets can be detected with 91%, fire extinguisher with 84%, call point with 73%, and detector with 73% precision. The averaged test mAP@0.5:0.95 results of individual classes for the models are for fire safety blanket with 86%, fire extinguisher with 81%, call point with

80%, and detector with 61% precision. Since we used the large version of YOLOv5 for all the datasets, we didn't observe considerable difference in object detection speeds. For the test images, the average detection speed is 43.2 FPS and for the live test video, the average detection speed is 51.5 FPS. Since the camera had a very high resolution, even the objects far from the camera could be successfully detected in a live test video. The training time of a model depends on the hardware and the preprocessing steps as well. We observed that the training duration is affected by the preprocessing step. As an example, Dataset_S_1 was downsized to 640x640, and Dataset_S_3 was kept as its original size but only downsized to 640x640 after running the algorithm. For Model_S_1 the training took 1.94 hours and for Model_S_3 8.18 hours. For Model_L_3 the training took 5 hours longer than Model_S_3. This means that the training duration is affected by preprocessing steps such as downsizing the images beforehand and the number of trained images. Even though Model_L_3 has a slightly higher test mAP@0.5:0.95 value compared to Model_S_3, the number of data it requires to train, and the training duration is much longer. To see how the models perform, object detection test results of Model_S_3 and Model_L_5 is shown in Figure 1. It is noticeable that Model_S_3 provides more precise bounding boxes with higher confidence compared to Model_L_5.

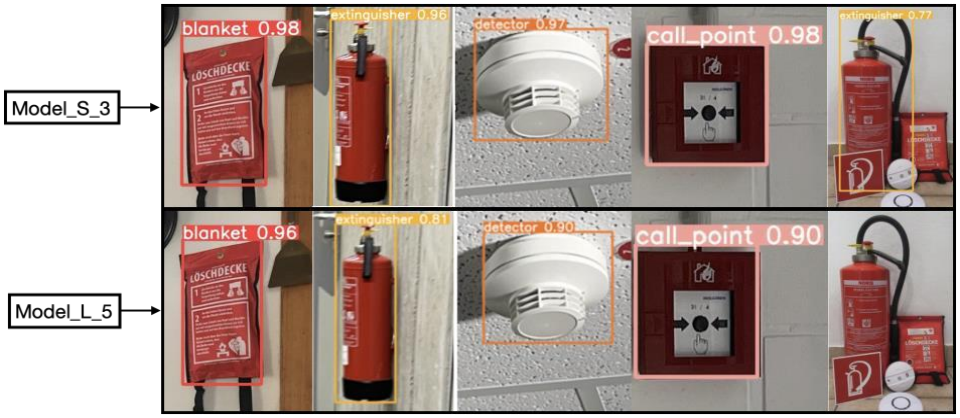

Figure 1: The detection results of model_S_3 and model_L_5 on the test dataset. The images are zoomed in for a clearer view of the bounding box and the precision.

6 Conclusion and Future Work

In this research, we utilized pretrained YOLOv5 large neural network model for fire safety equipment detection. We collected self-made images from different building types in Germany combined with an open-source dataset. We used preprocessing methods to resize the images and applied augmentation techniques to increase the performance of the models. The results showed that preprocessing techniques reduced the training time and applying augmentation techniques increased the model performances. Based on the validation and test results we concluded that YOLOv5 can successfully detect fire safety equipment with up to 80.1% of test mAP@0.5:0.95 and

up to 89.5% of validation mAP@0.5:0.95. The live video detection speed of 51.5 FPS and the performance of YOLOv5 proved that this algorithm can contribute for automated inspections in the future.

References

[1] H. Ying and S. Lee, “A mask R-CNN based approach to automatically construct as-is IFC BIM objects from digital images,” Proceedings of the International Symposium on Automation and Robotics in Construction (IAARC), 2019.

[2] E. Gülch and L. Obrock, “Automated semantic modelling of building interiors from images and derived point clouds based on Deep Learning Methods,” The International Archives of the Photogrammetry, Remote Sensing and Spatial Information Sciences, vol. XLIII-B2-2020, pp. 421–426, 2020.

[3] A. Corneli, B. Naticchia, M. Vaccarini, F. Bosché, and A. Carbonari, “Training of Yolo Neural Network for the detection of fire emergency assets,” Proceedings of the 37th International Symposium on Automation and Robotics in Construction (ISARC), 2020.

[4] J. Redmon and A. Farhadi, “Yolo9000: Better, faster, stronger,” 2017 IEEE Conference on Computer Vision and Pattern Recognition (CVPR), 2017.

[5] Ultralytics, YOLOv5 [Online]. Available: https://github.com/ultralytics/yolov5. [Accessed: 26-May2022].

[6] J. Redmon and A. Farhadi, “Yolov3: An incremental improvement,” arXiv.org, 08-Apr-2018. [Online]. Available: https://arxiv.org/abs/1804.02767. [Accessed: 27-May-2022].

[7] “Common objects in context,” COCO. [Online]. Available: https://cocodataset.org/#home. [Accessed: 31-May-2022].

[8] C.-Y. Wang, H.-Y. Mark Liao, Y.-H. Wu, P.-Y. Chen, J.-W. Hsieh, and I.-H. Yeh, “CSPNet: A new backbone that can enhance learning capability of CNN,” 2020 IEEE/CVF Conference on Computer Vision and Pattern Recognition Workshops (CVPRW), 2020.

[9] K. Wang, J. H. Liew, Y. Zou, D. Zhou, and J. Feng, “Panet: Few-shot image semantic segmentation with prototype alignment,” 2019 IEEE/CVF International Conference on Computer Vision (ICCV), 2019.

[10] J. Boehm, F. Panella, and V. Melatti, “FireNet,” figshare, 31-Jul-2019. [Online]. Available: https://rdr.ucl.ac.uk/articles/dataset/FireNet/9137798#:~:text=Fire-Net%20is%20an%20open%20ML,c lassification%20scheme%20to%20name%20objects.

Scalable construction monitoring for an as-performed progress documentation across time

Fiona C. Collins[1*] , Fabian Pfitzner[1*] and Jonas Schlenger[1*]
[1]Chair of Computational Modeling and Simulation, TU Munich, Arcisstr. 21, 80333 Munich, Germany
E-mail(s): fiona.collins@tum.de, fabian.pfitzner@tum.de, jonas.schlenger@tum.de
* all authors have contributed equally

Abstract: Compared to other industry sectors, the construction sector's productivity is relatively low. By collecting data directly from the construction site, the main bottlenecks can be identified and support decision-makers in making well-informed decisions. This is by no means a simple task because of the complexity and unpredictability of construction sites and the challenges of monitoring heterogeneous on-site data. While other researchers focus on elaborating specific steps or use-cases of the construction monitoring processes, we present a holistic workflow for scalable shell construction monitoring that uses state-of-the-art data processing techniques. The result of the proposed workflow is a per-instance database for on-site progress across time. Such a database has many possibilities for application. This can range from giving an overview to construction managers, providing a backbone for sophisticated analysis and digital twins, to the validation of computer vision approaches.

Keywords: Construction Monitoring, Image Processing, Photogrammetric Point Clouds

1 Introduction

The planning phase preceding the construction of buildings has already taken considerable steps to implement the BIM methodology fully. Conversely, the digitization of the as-performed construction process still significantly lacks behind. The absence of a common and regularly synchronized data environment fundamentally goes in hand with the risk for undocumented deviations from the project intent, resulting in extensive delays and increasing costs [1].

A construction site is a highly dynamic, complex, and chaotic environment where many parties from various disciplines simultaneously work on the same or different building components. Monitoring such environments manually for documentation is very time-intensive and error-prone, especially for big construction sites. At the same time, the number of qualified on-site personnel in the construction area is too small to meet the increasing demands of politics in respect of housing construction

[2]. Automated methods and computer vision approaches promise to significantly benefit tracking on-site assembly of construction elements in closer detail. However, the research community is limited in developing algorithms of such kinds since extensively inter-linked monitoring datasets are largely absent [3]. Therefore, a holistic, detailed, and continuous dataset of the on-site as-performed construction processes, including as-built construction products, is highly requested.

This work presents the first step of an extensive multi-sourced data-collection method for automated shell construction monitoring. The base of this work is an affordable, ready-to-use camera setup for cranes that automates RGB image acquisition. Furthermore, a complementing data pipeline is specifically designed for construction site monitoring. The introduced acquisition approach is scalable, allowing it to be easily deployed on construction sites of various sizes. Using photogrammetric reconstruction, point alignment, and projection methods, the underlying 3D reference between the images and the BIM model, is established for selected construction phases, resulting in a per-instance database for direct data consumption. RDF databases have proven their extensibility and ability to link data across domains and life cycle phases in various construction-related use cases [4]. For this reason, we have chosen an RDF database to implement the per-instance database.

In the following background section 2, we dive into the state of the art of the leading technologies and concepts employed in this work and highlight our contribution. Afterward, the proposed workflow is presented in section 3. In section 4, the presented methodology is showcased on a construction site in Regensburg, Germany. To close off, we discuss the overall results in section 5 and conclude with a summary and future works in section 6.

2 Theoretical Background

To set the theoretical background of the paper, we introduce related works in the field of construction monitoring. Moreover, established algorithms to derive a 3D reconstruction from 2D images are explained, which set the starting point for the present paper. Finally, with the shortcomings of existing approaches, we state our contribution to the current state of the art.

2.1 Construction Monitoring

Previous research in construction monitoring has shown serious potential in documenting the as-performed construction process. Various monitoring systems have been used on construction sites targeting different purposes. Existing approaches focus on investigating construction sites, including safety management [5], vehicle and resource detection [6], and construction activities [3]. In addition, other studies focus on generating as-built models by continuously monitoring the construction site [7].

However, research approaches shown above [3], [5], [6] can barely be used to fulfill the need to generate large-scale datasets of construction sites. This is due to several points: First, the introduced methods manually and statically generate data. Here the data acquisition depends, e.g., on LiDAR scans, resulting in considerable efforts. Yet, a dynamic and automatic data acquisition method is needed to compare target vs. actual over time steadily. Second, less focus has been put on the

acquisitions for as-planned vs. as-performed comparison. This research area is still in its infancy. Third, many studies only focused on monitoring one specific construction site, not proving their scalability. Undoubtedly, there is a need for a generalized scalable approach for generating extensive datasets across various construction sites. The link between the data and the as-planned information lies there while at the center of attention.

2.2 3D reconstruction for facilitated progress track

As opposed to conventional construction progress track such as with means of textual logs, graphical representations have become indispensable. The reconstruction of the 3D space gives additional meaning to the recorded images and notes and offers stakeholders a unique way of localizing recorded events. At the core of the linkage between recorded images and the as-planned BIM model is the extraction of 3D information from a 2D image - a topic that has received much attention from the computer vision community. Researchers have chosen different methods to achieve the linkage [6]. The directest way is achieved if the camera's extrinsic and intrinsic parameters are known. In this case, the 2D-pixel to 3D-point correspondence can be found. However, this method is susceptible to errors if outdoor cameras are moved by wind or rotated by a crane. Repeated calibration would be needed. Perspective-based methods use a set of key points, lines, and/or surfaces to register the image information to the BIM [8]. A common way to reconstruct 3D information from images is to match unique feature points previously defined by specialized algorithms such as Scale Invariant Feature Transform (SIFT). Matches are generated between similar feature points of overlapping views taken from different viewpoints. Finally, the depth and normal information are computed for every pixel with triangulation. The final 3D point cloud is achieved by fusing depth and normal information of multiple images. In recent years AI has been shown to estimate the needed camera parameters well enough to perform single image registration [9]. This method is, however, still suspected to show limitations in highly chaotic scenes such as construction sites.

2.3 Contribution

Our work makes an essential step toward an automated continuous event monitoring of construction sites and offers significant value by tracking all structural elements in the shell assembly phase. Using multidisciplinary technologies along the workflow allows us to present an end-to-end solution: from construction-site events to a historical database queryable for each structural element given in the planning model. Additionally, the provided result is use case agnostic, provides a sound basis for automated reasoning, e.g., progress tracking or construction safety, and was designed with the potential for extensibility.

3 Proposed Workflow / Methodology

In this section, we first put light on the continuous data-acquisition setting and hardware systems mounted on the construction site before we dive deeper into the post-processing steps.

3.1 Hardware setup

The camera monitoring system is designed for various building construction sites and can be deployed flexibly, considering the following aspects: First, the number of monitoring systems installed at the construction site is determined by the number of cranes. Second, the system is crane agnostic, which is usable for bottom and top-slewing cranes. Third, the critical requirement for installing the system is the power supply at the bottom of the crane, which makes this system easy to install since there are no existing network requirements. The key components of the setup are the router, the Virtual Private Network (VPN), the Power over Ethernet (PoE)-Switch, the cameras, the local server, and the remote server, illustrated in fig. 1. The outdoor-proof router enables a local network with an independent mobile internet connection. The router and the Raspberry Pi, configured with VPN services, build a gateway to the setup allowing remote configurations. Water-sensitive systems, the VPN, PoE, and the local server are sealed in a water-proof box. The PoE-Switch supplies all devices with internet and power.

On each crane, three outdoor-proof surveilling cameras are placed. The location and orientation of the cameras depend on the crane type and the construction project, covering large areas of the site. Cameras take pictures every thirty seconds and send them directly to the local FTP server,

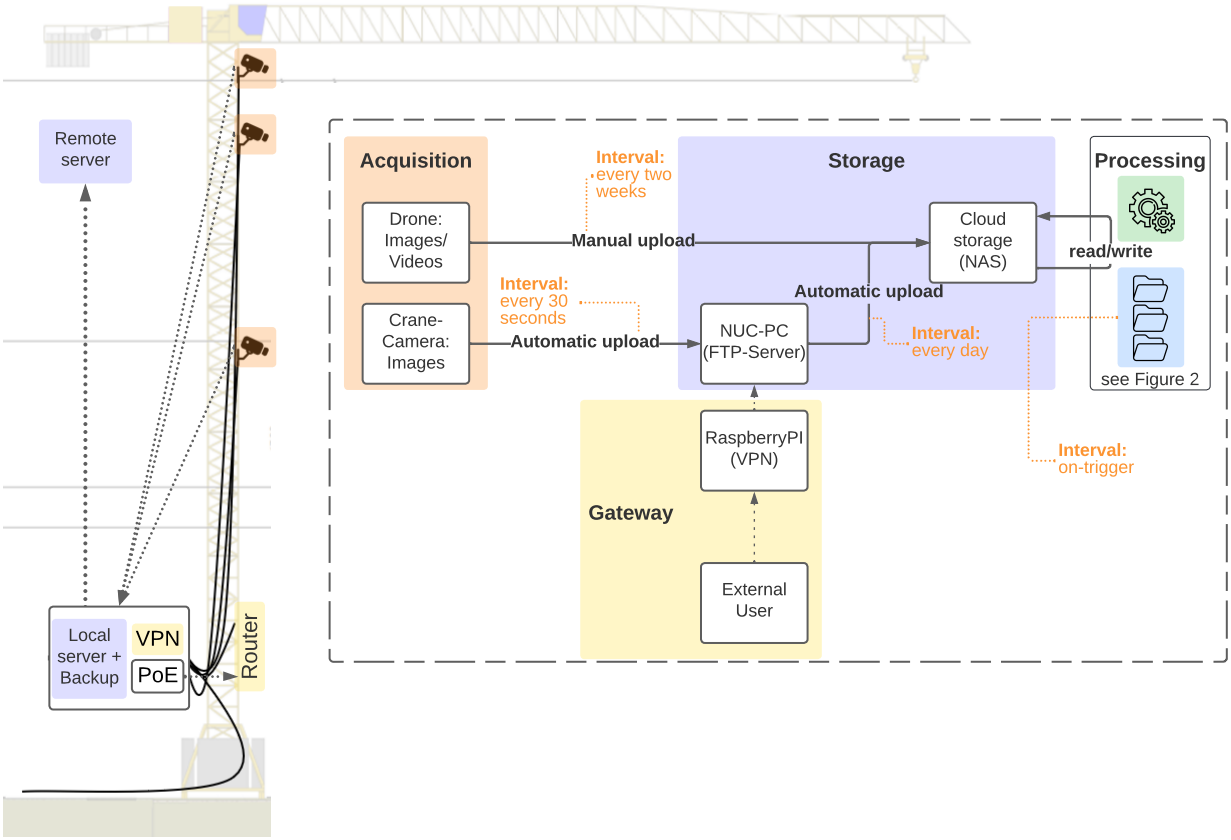

Figure 1: Hardware setup of the image acquisition

the NUC-PC. The continuous data acquisition enables steady documentation of the as-performed construction progress. The server processes the images by creating a backup and uploading the pictures to the remote server once a day. The remote server has extensive storage capabilities and is the system's endpoint. The processing of the images takes place on the remote server on-demand. The following sections will explain a technical workflow to treat the extensive data.

3.2 Data processing

This section presents all steps of the data processing pipeline: Starting from the input data to the 3D reconstruction, the point cloud alignment, and projection onto the BIM model to the final linked database. Figure 2 shows the overall technical workflow for processing the input data and structures this section.

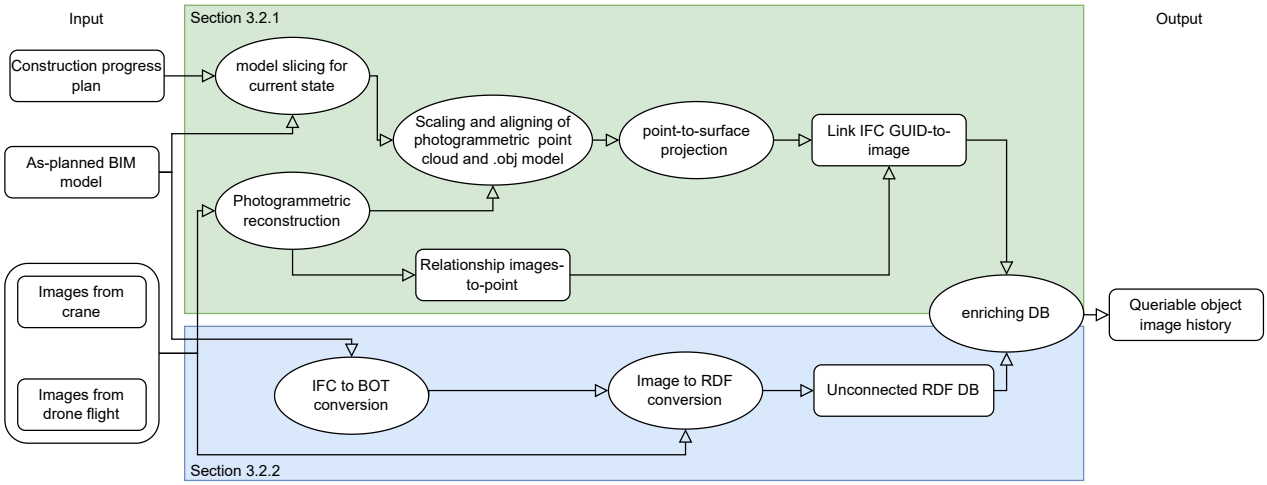

Figure 2: Technical workflow for data processing. Round shapes denote processes whereas rectangles denote states of data.

3.2.1 Linking images to BIM elements

A 3D reconstruction of the images taken from the construction site is needed to register the images to the 3D BIM model objects. To that end a photogrammetric reconstruction process is deployed using Colmap [10]–[12]. To minimize false matches due to weather effects (e.g. shadows) the images should ideally be chosen selectively, this however was set out of scope in this research. It is hypothesized that the construction progress within a short time range in the early morning or late afternoon is not considerable enough to impede SfM from matching feature points in pair images. The result is a 3D point cloud lacking absolute scale and orientation. Depending on the set-up, namely the number of cranes and cameras, the crane viewpoints alone might not cover enough view angles for the reconstruction to work well. In such cases, drone imagery is occasionally used to generate additional point references. For each reconstructed point, the initial overlapping and matched images used for its calculation are known. The point cloud is then aligned and scaled manually to overlay

with the BIM model. Outlier removal and noise removal are common ways to reduce the scattering of photogrammetric point clouds, and both are applied here.

Once the as-is acquisition is located in the proximity of the corresponding as-designed, an iterative projection algorithm is used to find the closest IFC element to each point. The projection combined with the image-to-point relationship yields the final link between IFC GUID and image ID. The reconstruction process would be performed at a given interval according to the needed granularity of process monitoring. The database described in the next section is hence continuously updated.

3.2.2 RDF Per-Instance Database

An RDF database is created to uniformly access and query multi-sourced data from the design and construction phase. For the present use case, information from the BIM model is connected with the image data captured on the construction site. Since existing ontologies can describe the topology of buildings, images, and sensor data, the data modeling is limited to combining already defined ontologies. The applied ontologies are BOT, a well-established ontology to describe the topological structure of buildings [13], and Dublin Core Terms to describe pictures and their metadata [14].

For the conversion of the IFC to RDF, the IFCtoLBD converter by Bonduel, Oraskari, Pauwels, *et al.* [15] is used. This translates the fundamental structure of the building with its stories, rooms, and building elements into its BOT representation. This structure serves as a starting point to connect data from the construction site to the corresponding building elements and spaces. Afterward, a self-implemented algorithm steps through the repository with all construction site images and translates their metadata to Dublin Core terminology. Since the pictures themselves can not be adequately represented in RDF format, only the file's location within the repository is referenced in the graph. Finally, the links between the pictures and the building elements that are visible on them, as obtained by the method described in section 3.2.1, are added explicitly to the RDF graph.

With the resulting RDF graph and SPARQL queries, extracting information related to a specific building element or picture instance, e.g., requesting the most recent picture of a building element, becomes a simple task. Overall, such an RDF database is a solid base for further analysis that can easily be enriched with additional data because of the flexible RDF structure.

4 On-site showcase

We conduct a first roll-out of the described method on a construction site in Regensburg, Germany with a footprint of 1200m^2. The carcass construction was performed with one bottom slewing crane from July to December 2021. The images were taken at an interval of 1/minute from 3 camera positions (1 on the cantilever and the two others at different heights from the tower). The diverse view angles and scene overlaps required for the optimal photogrammetric reconstruction are only partially satisfied in Regensburg since 1. the crane stands on one side of the construction site and 2. the crane movements are faster than what is mapped between the minute interval. Due to these limitations, the presented method is extended to include a series of drone images from the corresponding flight and acquisition

dates to improve the overall result. The subset of crane images of all three cameras is combined with a few snapshots of the drone camera. Detailed analysis of how many images of either source were needed is out of scope for this contribution. The photogrammetric reconstruction results in point clouds accurate enough to perform the link between images and points, see figure fig. 3a. The deviation between the as-planned BIM model and the as-performed construction is assumed to be slight enough for the process to work. This reconstruction has been performed for two selected construction stages to showcase the usability: once the beams and walls in the underground storey are just completed (see fig. 3a) and in the other stage, the slab structure and stair elements are added.

The RDF database created from the described data is queriable with SPARQL query language, as fig. 3b shows. The query returns the most recent image linked to the selected BIM instance. The result of querying the database for the wall element highlighted in fig. 3a is shown in fig. 3c. It includes images of the same wall element, both sourced from the crane cameras and the drone flights from two separate dates. More complex queries are possible to receive more meaningful as-performed construction information.

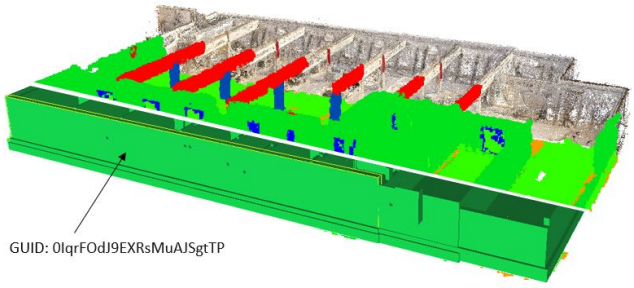

(a)

```
SELECT ?img ?loc ?date
WHERE {
    ?img bot:containsElement
            inst:element_0IqrFOdJ9EXRsMuAJSgtTP .
    ?img dct:created ?date .
    ?img dct:location ?loc .
}
ORDER BY DESC(?date)
LIMIT 1
```

(b)

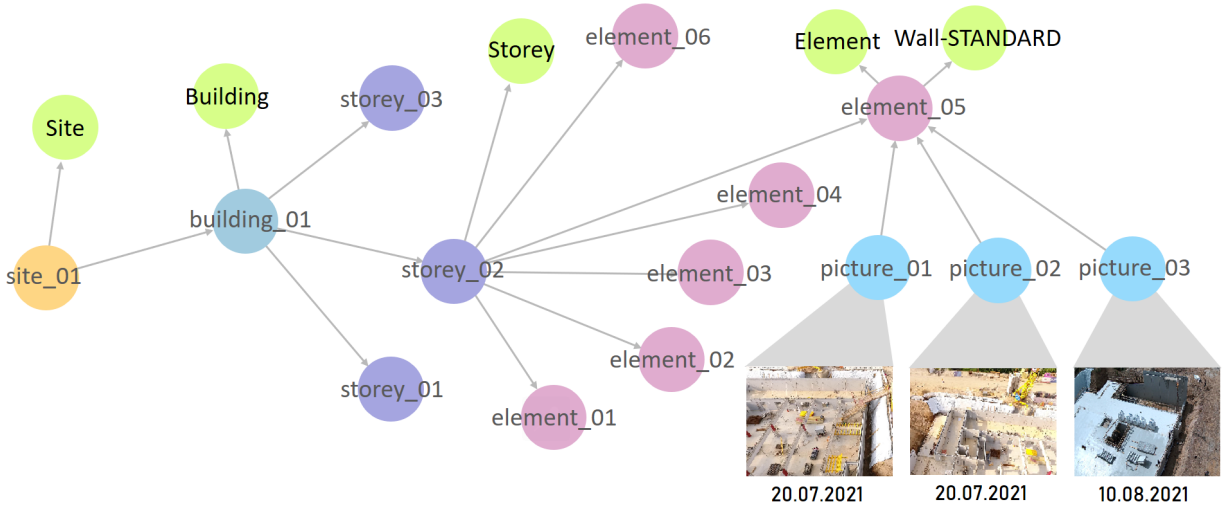

(c)

Figure 3: From point cloud to queryable database: a) BIM-to-cloud correspondence and projection for underground storey b) query that returns all elements linked to the specific BIM GUID c) excerpt from resulting RDF graph

5 Discussion

The developed camera system proved robust straightforward to install in the first roll-out and is already beeing tested on other construction sites. It allows us to generate extensive image data sets of construction sites at a low cost. Thereby, continuous and automated documentation of the as-performed progress is enabled. Regarding the data processing pipeline, a few limitations need additional attention. In this case, we addressed the limitations of too few view-angles and too little overlap in images with additional drone-sourced images. Still, we will further investigate this in future construction sites by equipping multiple cranes with the camera setup systems and increasing the frame rate to have more overlap between images. Alternatively, neighboring buildings or movable cameras offer additional placement and coverage possibilities. Given the setup's objective of monitoring shell construction only, it is acceptable to notice that the monitoring only covers the outside top-most elements. To go beyond this, additional indoor surveying must be performed with movable camera systems and registered with the outdoor images.

One short manual step is included in the pipeline, namely the point cloud to BIM model alignment and scaling. This is currently impeding the full scalability of the database updates and suggests further investigation. Furthermore, the computation times of the data processing are resource-intensive, especially for the photogrammetric reconstruction step, and suggest an analysis for alternative pipelines touching aspects highlighted in section 2. The quality of the photogrammetric reconstruction (e.g., amount of noisy points) directly influences the linking accuracy in the final database. Any little error in the image matching process will lead to erroneous links. A quantitative analysis of the error rate would require a manual detection of construction instances in images and lies beyond the scope of this work. Finally, it must be said that the images linked to the instances are, especially in early phases, still taken from far distance making the element appear only amongst many others. An additional mask could be laid on the images to show which pixels have been used to reconstruct the point in question.

6 Conclusion

With the proposed method, we achieve a continuous yet low-cost data acquisition of the shell construction processes by documenting the assembly steps taken from the crane's field of view. The image registration to the BIM objects using photogrammetric reconstruction, alignment, and point projection is successful; each BIM element is linked to the corresponding images if sufficient capturing overlap from sufficient view angles is given. We then apply SWT to store this information in an RDF database using established ontologies and allow for a quick query-based process investigation. The use case agnostic database might benefit managers for verifying safety compliance or verifying schedules or future research methods that can profit from the BIM links to enhance computer vision-based image interpretation.

The goal of the workflow presented in this article demonstrated viability as a whole and scalability in the data acquisition phase. Yet, the processing requires time-intensive intermediate steps and a

manual one. In the future, we plan to investigate further and optimize the scalability and full automation of the data processing steps. More specifically, this encompasses more optimal camera placement and frame rates, an image classification prior to reconstruction to prevent unsharp or irrelevant images from causing noise in the point cloud, or an analytical comparison to other 2D-3D reconstruction methods. The publishing of our dataset is planned for a future point in time. Conclusively, our approach shows an autonomous way for future construction supervision using state of the art processing steps, enabling on-demand documentation for construction managers and researchers.

Acknowledgements

We thankfully acknowledge Innovation Management Bau for their financial support and for providing us access to multiple construction sites to conduct case studies. Further, we thank the chair of geodesy at OTH Regensburg for letting us use their Faro laser scanner and supporting us with their expertise on the construction site, and the MINT-Labs for allowing us to install cameras on their roof.

References

[1] R. Sacks, I. Brilakis, E. Pikas, H. S. Xie, and M. Girolami, “Construction with digital twin information systems”, *Data-Centric Engineering*, vol. 1, e14, Nov. 2020, ISSN: 2632-6736. DOI: 10.1017/dce.2020.16. [Online]. Available: https://www.cambridge.org/core/product/identifier/S2632673620000167/type/journal_article.

[2] G. Zika, T. Maier, A. Mönnig, *et al.*, “Die folgen der neuen klima-und wohnungsbaupolitik des koalitionsvertrags für wirtschaft und arbeitsmarkt”, 2022.

[3] G. Torabi, A. Hammad, and N. Bouguila, “Two-dimensional and three-dimensional cnn-based simultaneous detection and activity classification of construction workers”, *Journal of Computing in Civil Engineering*, vol. 36, 4 Jul. 2022, ISSN: 0887-3801. DOI: 10.1061/(ASCE)CP.1943-5487.0001024.

[4] P. Pauwels, S. Zhang, and Y. C. Lee, “Semantic web technologies in AEC industry: A literature overview”, *Automation in Construction*, vol. 73, pp. 145–165, 2017, ISSN: 09265805. DOI: 10.1016/j.autcon.2016.10.003.

[5] T. Cheng and J. Teizer, “Real-time resource location data collection and visualization technology for construction safety and activity monitoring applications”, *Automation in Construction*, vol. 34, pp. 3–15, 2013, ISSN: 09265805. DOI: 10.1016/j.autcon.2012.10.017.

[6] J. Xue, X. Hou, and Y. Zeng, “Review of image-based 3d reconstruction of building for automated construction progress monitoring”, *Applied Sciences (Switzerland)*, vol. 11, no. 17, 2021, ISSN: 20763417. DOI: 10.3390/app11177840.

[7] S. Tuttas, A. Braun, A. Borrmann, and U. Stilla, “Acquisition and consecutive registration of photogrammetric point clouds for construction progress monitoring using a 4d bim”, *PFG–journal of photogrammetry, remote sensing and geoinformation science*, vol. 85, no. 1, pp. 3–15, 2017.

[8] K. Asadi and K. Han, “Real-Time Image-to-BIM Registration Using Perspective Alignment for Automated Construction Monitoring”, no. March, pp. 388–397, 2018. DOI: 10.1061/9780784481264.038.

[9] D. Acharya, R. Tennakoon, S. Muthu, K. Khoshelham, R. Hoseinnezhad, and A. Bab-Hadiashar, “Single-image localisation using 3D models: Combining hierarchical edge maps and semantic segmentation for domain adaptation”, *Automation in Construction*, vol. 136, p. 104 152, 2022, ISSN: 09265805. DOI: 10.1016/j.autcon.2022.104152. [Online]. Available: https://doi.org/10.1016/j.autcon.2022.104152.

[10] J. L. Schönberger and J.-M. Frahm, “Structure-from-motion revisited”, in *Conference on Computer Vision and Pattern Recognition (CVPR)*, 2016.

[11] J. L. Schönberger, E. Zheng, M. Pollefeys, and J.-M. Frahm, “Pixelwise view selection for unstructured multi-view stereo”, in *European Conference on Computer Vision (ECCV)*, 2016.

[12] J. L. Schönberger, T. Price, T. Sattler, J.-M. Frahm, and M. Pollefeys, “A vote-and-verify strategy for fast spatial verification in image retrieval”, in *Asian Conference on Computer Vision (ACCV)*, 2016.

[13] M. H. Rasmussen, M. Lefrançois, G. F. Schneider, and P. Pauwels, “BOT: The building topology ontology of the W3C linked building data group”, *Semantic Web*, vol. 12, no. 1, pp. 143–161, 2020, ISSN: 22104968. DOI: 10.3233/SW-200385.

[14] K. Coyle and T. Baker, *Guidlines for dublin core application profiles*, 2009. [Online]. Available: https://www.dublincore.org/specifications/dublin-core/profile-guidelines/ (visited on 05/25/2022).

[15] M. Bonduel, J. Oraskari, P. Pauwels, M. Vergauwen, and R. Klein, “The IFC to linked building data converter - Current status”, in *6th Linked Data in Architecture and Construction Workshop*, vol. 2159, 2018, pp. 34–43.

Multi-Sensor Fusion for a UAV/USV Tandem System for Spatial Data Collection of Waterways

Louis Makiello

Geodetic Institute and Chair for Computing in Civil Engineering & Geo Information Systems, RWTH Aachen University, Mies-van-der-Rohe-Straße 1, 52074 Aachen

E-Mails: Louis.Makiello@gia.rwth-aachen.de

Abstract: The aim of the RiverCloud research project is to develop an autonomous and networked unmanned tandem system consisting of an unmanned aerial vehicle (UAV) and an unmanned surface vehicle (USV) for the collection and provision of spatially and temporally high-resolution data for the development and maintenance of waterways and to support waterway management. The collected data will be analyzed by fusion with existing macroscale data and the results will be integrated into the models and workflows of users from the water management sector. An essential task to be solved for the practical use of the tandem system is the multi-sensor fusion for exact position and orientation estimation, especially of the USV, and for georeferencing of all collected data. For this purpose, data from GNSS, IMU and cameras are to be fused by means of dynamic state estimation. In this contribution the UAV/USV tandem system is presented. Particular attention is paid to the developed sensor fusion algorithm and the implementation using ROS.

Keywords: Multi-sensor fusion, visual odometry, ROS, UAV, USV

1 Introduction

1.1 Project overview

The RiverCloud research project brings together seven partner organisations to develop and evaluate a novel method of holistically monitoring inland water bodies as well as storing acquired data and making it available to stakeholders.

Data acquisition is to be carried out by two vehicles: a USV (unmanned surface vessel) and a UAV (unmanned aerial vehicle), operating either together (tandem mode) or alone. Four missions are to be undertaken:

- The first is carried out either by the USV alone or by the USV aided by the UAV. It consists of recording underwater topography using a multibeam echo sounder as well as flow velocity via ADCP (acoustic doppler current profiler) and water quality using a multiparameter sensor. All three sensors are mounted on the USV. A visual target is mounted on the USV and a camera mounted on the UAV is used to track the visual target. This will allow improved positioning of the USV in areas with poor GNSS signal.
- The second is carried out by the UAV alone. It consists of recording underwater topography using a bathymetric LiDAR. A camera placed on the UAV may also be used to record the surface flow velocity. This can be used to estimate river discharge.
- The third is to produce a Digital Terrain Model using a digital camera mounted on the UAV.
- The fourth is to record shore vegetation types using the panoramic camera mounted on the USV.

1.2 UAV/USV tandem mode

Before the River Cloud project, a similar project called “RiverView” was carried out with the goal of monitoring water parameters and depth as well as acquiring 360°-panorama images [1]. It was found that in certain circumstances, GNSS positioning accuracy was seriously affected by features such as tall buildings and trees on the shore or the presence of bridges. Overcoming this issue required the use of a total station placed on the shore and a prism placed on the USV. Although this solution provides optimal accuracy, it presents drawbacks and limitations. Using a total station, range is limited to line of sight locations and a single stretch of river may require the total station to be repositioned several times, resulting in a much slower survey process. Moreover, in certain situations, It may not be possible to find a suitable location for the total station due to terrain, obstructions or property law.

The RiverCloud project requires the presence of a UAV (Unmanned Aerial Vehicle) to fulfill certain missions such as aerial photogrammetry and river flow velocity measurement. When the USV is required to perform surveys in areas with poor GNSS signal, it is therefore possible to use the UAV equipped with a camera as well as visual markers placed on the USV to deduce the position of the USV using data from sensors placed aboard the UAV as well as the images taken by the camera. To achieve this, the UAV must fly while the USV carries out it’s surveying task. This is referred to as “tandem mode”. As result, the position of the USV can be calculated in real-time. In addition to enabling autonomous operation of the UAV, this eliminates the need to save the image data from the tracking camera, the size of which could grow to be very large.

An estimate of the position and state of the USV in real-time is to be further refined by fusing data from sensors onboard the USV. These include a dual antenna GNSS system, inertial measurement unit (IMU) and one or more stereo camera systems. For improving positioning in post-processing it is possible to use image data from a panoramic camera. The goal of real-time state estimates for

several vehicles simultaneous can be achieved by using a Robot Operating System (ROS) network connecting both vehicles with a Ground Control Station (GSC).

2 ROS – Robot Operating System

The Robot Operating System (ROS) is a flexible framework for writing robot software. It is a collection of tools, libraries and conventions that aim to simplify the task of creating complex and robust robot behaviour across a wide variety of robotic platforms. The ROS framework allows research groups and individuals to make use of each other's work. ROS is not an operating system in the traditional sense. Rather, it provides a structured communications layer above the host operating system for a heterogeneous compute cluster [2]. ROS was originally designed to meet the challenges faced by researchers at Stanford University and Willow Garage when developing service robots. It has since been shown to be applicable to a range of challenging endeavours such as autonomous drone flight, Autonomous Surface Vessels (ASVs), self-driving cars and robotic industrial manufacturing.

3 USV – Unmanned Surface Vehicle

The Hydrosurv Reav-16 USV is equipped with various sensor for autonomous positioning as well as for data collection of the water body both above and under water.

3.1 Sensors

The Sonic 2020 multibeam echosounder (MBES) manufactured by R2Sonic is used to measure bathymetry. This MBES has a resolution of 2°x2°at 450kHz and 4° x 4° at 200kHz. The speed of sound at different depths needs to be measured in order to produce accurate survey data in bodies of water with variations in temperature and/or salinity at different depths. To determine this, a Swift Sound Velocity Profiler (SVP) is used. The speed of sound can be both directly measured using transducers or inferred from measurements of pressure, temperature and conductivity.

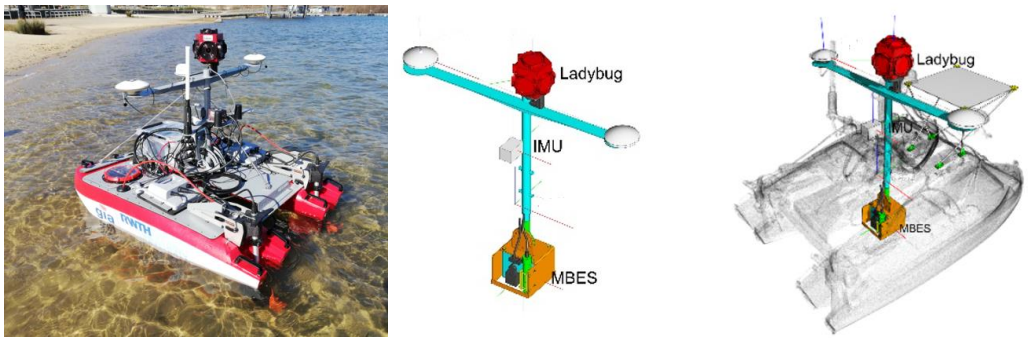

Figure 1: USV at the testing ground (left); Sensor configuration (middle & right)

The Novatel CPT7 combines an RTK-capable OEM7 dual antenna GNSS with a Honeywell HG4930 Micro Electro Mechanical System (MEMS) Inertial Measurement Unit (IMU). It can provide centimeter-level positional accuracy when GNSS signal is of sufficent quality. In the presence of poor GNSS conditions, it combines GNSS measurements with IMU measurements to provide a filtered state estimate. It also provides a heave estimate.

The Ladybug 5 panoramic camera combines six global shutter 5MP Sony ICX655 CCD sensors with fisheye lenses in a single housing. It can be connected to a computer via a single USB3 cable.

Figure 1 shows sensors installed onboard the USV.

Another camera system that is to be used additionally for position estimation purposes when GNSS is not usable is omited in Figure 1 as it is still under development and not yet installed. The stereo system uses two OnSemi, global shutter 0.3MP MT9V022 sensors with 2.8mm or 6mm lenses both triggered simultaneously by an ARM Cortex-M4-based microcontroller. It is connected to a single board computer via two USB cables. The baseline between the cameras can be modified to be either 0.1m, 0.2m or 1m. Figure 2 shows a schematic of the stereo system.

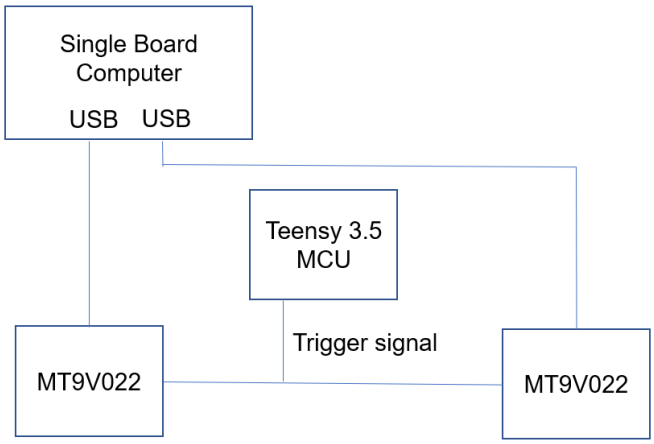

Figure 2: Stereo system diagram

3.2 Software

Qinsy is a survey planning, data acquisition, and real-time hydrographic data processing software package produced by Dutch company QPS. In order to acquire bathymetric data, Qinsy is interfaced with the MBES and Novatel GNSS+INS. This setup has the capability to measure bathymetry as well as provide data regarding river bed morphology and water column characteristics.

Teledyne FLIR, the manufacturers of the Ladybug 5 camera, provide the LadybugCapPro software. This application can be used to modify setting, record data and perform post processing tasks such as image rectification, image quality optimisation and image stiching.

In order to use images from the panoramic camera within the ROS network, a custom node is able to read the timestamps of the trigger pulses, convert the relevant images into ROS format and publish them on the ROS network.

4 UAV – Unmanned Aerial Vehicle

The Avartek boxer hybrid UAV is equipped with an RTK-capable Emlid M2 GNSS module and a Cube Orange IMU/barometer. For the purpose of tracking the USV, a Ximea 20MP camera is mounted on a Gremsy T7 gimbal. For photogrammetry missions, a Phase One ix M100 camera is used. For aerial bathymetric mapping, a Riegl BDF-1 can be deployed.

5 Simultaneous operation of USV and UAV

During tandem mode operation, an ix M100 camera located on the UAV is pointed towards nadir with the help of a gimbal. A Xavier NX computer located on the UAV detects two AprilTag markers placed on the USV and directs the UAV to fly vertically above the USV. Using the AprilTag markers in the image and the sensors on the UAV, the USV position is estimated.

For testing, a STIL (Software in the loop) simulator is initially used to simulate the UAV's Arducopter flight controller. The boat tracker node runs on the Xavier NX's GPU which is directly connected to the camera in order to speed up image processing. This node detects the markers and estimates the range to the USV as welll as the position and attitude of the USV.

6 Inter-vehicle communication

In tandem mode, the surveying system consists of a UAV, a USV and a single GCS (ground control station). Command and Control of both vehicles as well as monitoring data acquisition is carried out from the laptop, which acts as the GCS.

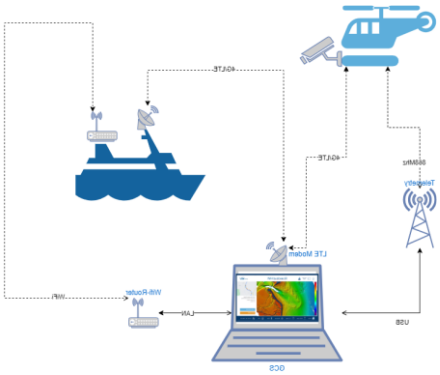

Figure 3: Diagram of inter-vehicle communication

Figure 4 shows the communication methods between the UAV, the USV and the GCS (ground control station). The UAV communicates with the GCS through an LTE modem and a 868Mhz telemetry link. In addition, a 2.4GHz Herelink system is used by the UAV pilot for video transmission and remote control. The USV communicates to the GCS through both an LTE modem and a Wifi connection. The wifi router allows multiple laptops to be connected simultaneously if necessary. There is no direct data link between the UAV and the USV.

7 Sensor fusion algorithm

Use of a ROS network facilitates the implementation, modification and testing of various existing algorithms. Methods tested so far include “Robot Localization”, which is a collection of Kalman Filters, “Rovio”, “ORB-SLAM2” and “ORB-SLAM3” which are visual odometry/SLAM algorithms and the “Aruco”, “Alvar” and “AprilTag” visual marker generation and detection methods. [3]

In the absence of the UAV, the position estimate of the USV is to be performed using “Robot Localization” and “ORB-SLAM3” [4]. In the presence of the UAV, an additional Marker detection algorithm based on AprilTag is used.

“Robot Localization” [5] is a ROS package created to estimate the state of robots through sensor fusion. It is versatile and has been applied to drones [6], deep sea Remotely Operated Vehicles (ROVs) [7] and bathymetric survey vessels [8]

The Robot Localization package contains an implementation of an Extended Kalman Filter (EKF). An unlimited number of inputs from multiple sensors can be fused using this package. It supports position, orientation, linear velocity, angular velocity and linear acceleration inputs. The package’s output is an estimation of the robot’s position, attitude, velocity and angular velocity.

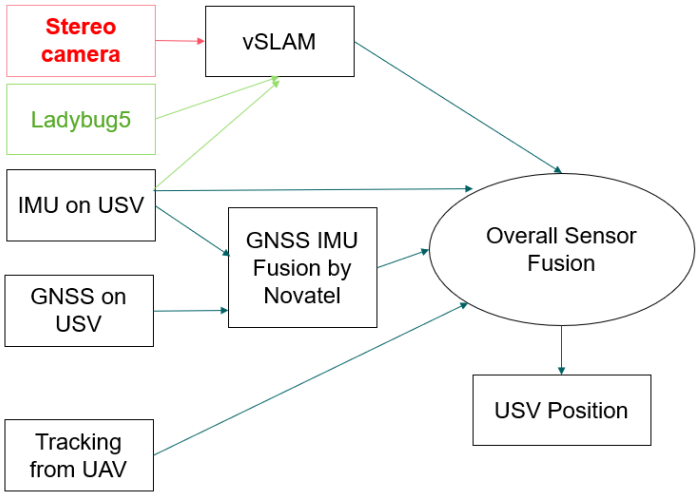

Figure 4: Sensor fusion methods using stereo (red) and monocular (green) visual odometry

The ORB-SLAM3 package is able to perform visual, visual-inertial and multi-map SLAM with monocular, stereo and RGB-D cameras, using pin-hole and fisheye lens models. Experiments performed by the ORB-SLAM3 authors have shown that, in all sensor configurations, ORB-SLAM3 is as robust as the best systems available in the literature and significantly more accurate. We shall be testing the stereo version of ORB-SLAM3 using lenses with various focal lengths incl. 6mm and 2.8mm as well as various baselines between the two cameras incl. 10cm, 20cm and 1m. Another possible sensor fusion method involves using images from the panoramic camera to perform monocular visual odometry and scaling the resultant track using data from other sensors such as the IMU. Figure 6 shows monocular visual odometry on a test dataset using images from the panoramic camera.

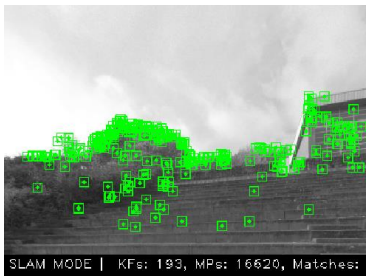

Figure 5: Monocular visual odometry test using panoramic camera

Two separate EKFs run onboard the UAV. One is used for estimating the state of the UAV and fuses data from two GNSS sensors, an IMU and a barometer. A second EKF is used to estimate the position and orientation of the camera. In addition to using the output of the previously described EKF, it integrates data from the gimbal encoders, the gimbal IMU and optical flow data derived from the camera.

8 Evaluation

Various surveys with only the USV were conducted on a lake near Aachen. These tests confirmed that the bathymetric survey system operated as expected (Figure 7). It also confirmed that it was possible to access data from the Novatel IMU through a ROS network running on a laptop with Ubuntu 18 and ROS Melodic. It was possible to create a rosbag file on the laptop.

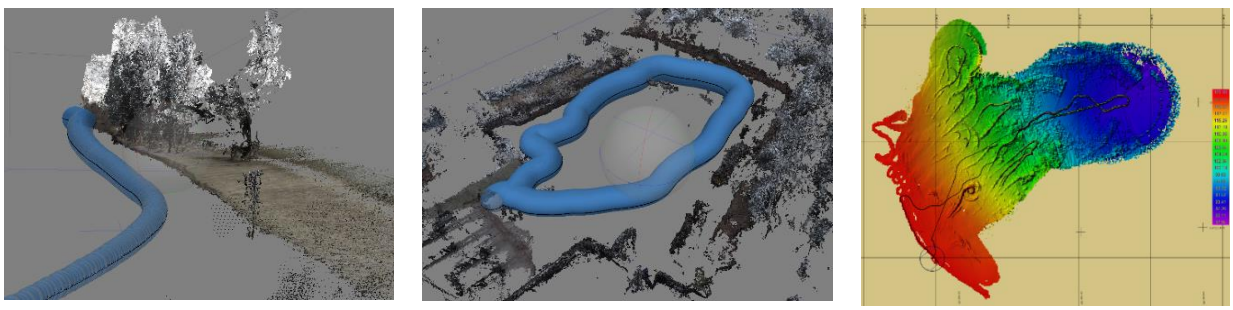

Figure 6: Pointclouds created (left & middle); Bathymetric map created using MBES (right)

Acknowledgement

This research is funded by the German Federal Ministry of Digital and Transport, research initiative mFund, grant number: 19F2121A. We would like to thank you for the good cooperation at our project partners: Forschungsinstitut für Wasser- und Abfallwirtschaft e. V, IAV GmbH Ingenieurgesellschaft Auto und Verkehr, SEBA Hydrometrie, Orthodrone, Bundesanstalt für Gewässerkunde, Bundesanstalt für Wasserbau.

References

[1] R. Schwermann, C. Effkemann, N. Hein, G. Kutschera, J. Blankenbach, “Riverview - Monitoring of water parameters in small and medium-sized water bodies using USV”, 126. 136-146. 10.5675/HyWa_2018.6_5.

[2] Quigley, Morgan & Conley, Ken & Gerkey, Brian & Faust, Josh & Foote, Tully & Leibs, Jeremy & Wheeler, Rob & Ng, Andrew. (2009). “ROS: an open-source Robot Operating System. ICRA Workshop on Open Source Software. 3.”

[3] Olson, Edwin. (2011). “AprilTag: A robust and flexible visual fiducial system. Proceedings - IEEE International Conference on Robotics and Automation.” 3400 - 3407. 10.1109/ICRA.2011.5979561.

[4] Campos, Carlos & Elvira, Richard & Gómez Rodríguez, Juan & Montiel, José & Tardós, Juan. (2020). “ORB-SLAM3: An Accurate Open-Source Library for Visual, Visual-Inertial and Multi-Map SLAM.”

[5] T. Moore and D. Stouch, “A Generalized Extended Kalman Filter Implementation for the Robot Operating System”, Proceedings of the 13th International Conference on Intelligent Autonomous Systems (IAS-13), 2014

[6] F. Kucuksubasia and A.G. Sorguc, “Transfer Learning-Based Crack Detection by Autonomous UAVs”, 35th International Symposium on Automation and Robotics in Construction, 2018

[7] Mueller et al., “Dexterous Undersea Interventions with Far Distance Onshore Supervision: the DexROV Project”, IEEE Robotics & Automation Magazine Volume: 25, Issue: 4, Dec. 2018

[8] Makiello, “Using a ROS-based low-cost system for bathymetric surveys”, Hydrographische Nachrichten Ausg. 116, 2020

Teil III

Semantic Web Technologies

Inferential Reasoning in Co-Design Using Semantic Web Standards alongside BHoM

Diellza Elshani[1], Alessio Lombardi[2], Al Fisher[2], Steffen Staab[3,4] , Daniel Hernández[3] and Thomas Wortmann[1]

[1]Chair for Computing in Architecture (CA), Institute for Computational Design and Construction (ICD), Faculty of Architecture and Urban Planning, University of Stuttgart, Keplerstraße 11, Stuttgart, 70174, Germany

[2]Buro Happold, 17 Newman St, London, W1T 1PD, United Kingdom

[3]Department for Analytic Computing (AC), Institute for Parallel and Distributed System (IPVS), University of Stuttgart, Universitätsstraße 38, Stuttgart, 70174, Germany

[4]Electronics and Computer Science, University of Southampton, University Road, Southampton, SO17 1BJ, United Kingdom

E-Mail: diellza.elshani@icd.uni-stuttgart.de

Abstract: Design or construction constraints are often considered only in later phases of a linear design process, which leads to costly revisions during construction. Knowledge bases can include logic rules to check constraints and are a powerful tool for representing knowledge on the Semantic Web. Knowledge bases contain facts and rules. The Buildings and Habitats object Model (BHoM) framework, similarly separates objects from methods that assist in deriving knowledge. This paper evaluates data validation, knowledge inferring, and reasoning methods in the Architecture, Engineering, and Construction (AEC) industry. It argues that augmenting BHoM KBs with Semantic Web rules and roles would increase the usage of KBs in the AEC industry by assisting design decisions through inferential reasoning.

Keywords: BIM, Semantic Web, Reasoning, Data Validation, Knowledge Bases

1 Introduction

In current architectural practice, constraints arising from involved disciplines are considered only in later phases of a linear design process. This late consideration often leads to costly revisions shortly before or even during construction. Instead, constraints should be considered as early as possible, which requires representations and reasoning patterns across different kinds of data models[1].

The Semantic Web Ontology Language (OWL) has a rich expressivity and is supported by several reasoning tools [2]. OWL allows for describing the data in terms of concepts and relationships between concept individuals. Furthermore, there are also Semantic Web rule languages which define the operations over the knowledge. While OWL does not define operations because the inference is done by algorithms that have to satisfy the semantics of the ontology, rules indicate explicitly how to perform the inference. These descriptions and rules can be used to check the consistency of the knowledge base and to infer new knowledge. In the Architecture, Engineering and Construction (AEC) industry, the inferred knowledge would recognize design constraints from involved disciplines from early design stages. A Knowledge Base (KB) adds a semantic model to the data by using ontologies and rules for interpreting the data. KBs contain a set of terminological statements (TBox), a set of assertional statements (ABox), and the set of roles defined in the role box (RBox).

The Linked Building Data-Community Group (LBD-CG) [3] is using Semantic Web standards as an open and decentralized alternative to the existing centralized and file-based approaches to storing and sharing data [4]. Many AEC ontologies exist in research and industry, including ifcOWL [5], the OWL representation of the Industry Foundation Classes (IFC) schema [6]. Even though IFC is available in Semantic Web standards and can represent data as a knowledge graph, the support for AEC knowledge graphs and linked data in tool development remains insufficient [7]. In addition, the IFC schema's specification is not based on a logic theory as it was not designed to be translated into rule checking environments [8].

The open-source Buildings and Habitats object Model (BHoM) [9] framework consists of BHoM object models, BHoM Engines, adapters (to map data across design platforms), and user interfaces. Even though BHoM uses an object-oriented data model, its approach to separating objects from functions makes it compatible with ontologies [10]. Whereas BHoM objects (classes and instances) describe facts about the building, which in a knowledge graph corresponds to the facts on TBox and ABox, methods and functions under BHoM Engine can be used to derive knowledge (e.g. properties about object models), which can be found on an RBox in a knowledge graph (Table 1.). Previous research presented the conversion of BHoM object models to knowledge graphs [10]. In this paper, we investigate methods to define axioms constraining roles on BHoM object models based on existing BHoM Engine functions using Semantic Web standards. This investigation requires a comparison of Semantic Web rules that assist to infer new knowledge, roles that define the

relationships between objects and properties, and BHoM Engine methods that assist in deriving knowledge from BHoM objects.

Table 1: Similarity of the structure of Knowledge Bases (KB) and BHoM

Knowledge Bases (KB)	**BHoM**
TBox - Terminological Box	BHoM Classes and properties
ABox – Assertional Box	BHoM Instances and property values
RBox – Role box	BHoM Engine

This paper reviews some of the key approaches to data validation and reasoning in the AEC Industry. It discusses the reasoning and data validation methods using Semantic Web technologies as well as derived knowledge from BHoM objects using BHoM Engine methods. Additionally, it argues the rule forms in both approaches, including their syntax and structure. The evaluation and proposal section exemplifies BHoM rules using Semantic Web languages, making BHoM information compatible with OWL reasoners. We apply a semantic reasoner to the resulting graph to discover new facts about the given objects. We conclude by discussing the advantages and limitations of describing BHoM derived properties in Semantic Web languages and present future work possibilities.

2 Review of some approaches to data validation and reasoning in the AEC Industry

In building design processes, designers from different disciplines such as architecture, structure and sustainability collaborate to meet a variety of building performance objectives and constraints [11]. Such objectives and constraints include an appropriate provision of spaces, safety, resource efficiency (e.g., in terms of embodied and emitted carbon dioxide), aesthetics and ease of construction. To consider such performance objectives and constraints as early as possible in design processes, data from different disciplinary data models must be integrated [12]. In the following subsections, we discuss IFC data validation methods, reasoning and data validation using Semantic Web technologies, and the ability to derive knowledge from BHoM objects using BHoM Engine.

2.1 IFC Data Validation

The standard methodology for defining the data exchange requirements and rule constraints for Building Information Models is the Model View Definition (MVD) [13]. MVD specifies the subsets of an Industry Foundation Classes (IFC) schema, including entity, attribute, and geometry representation constraints. BuildingSMART recommends the use of mvdXML as a formal representation format for MVDs. Model Checking in BIM includes (1) BIM validation which checks modelling attributes and procedures, (2) clash detection, i.e. interference check; and (3) code

checking, verifying compliance with the correspondent regulation. While MVD checking focuses on fast validation of data structures and values in raw IFC data, semantic rule checking methods for BIMs focuses on enriching geometry calculation and semantic inferencing [8]. Model Checking in BIM using the IFC standard might be very powerful in documenting and storing design data; however, IFCs' hierarchical, heavy and monolithic data model makes it complex to be used during the design phase. However, the most critical decisions in building design are made in the conceptual design phase, and they influence not only construction costs but also building energy consumption [1]. Lack of data validation and reasoning during the whole design phase, including the early stages of design, may prevent the recognition of violated design constraints until it is too late, i.e., until construction has already started. Additionally, when considering a logic-based rule checking environment for the AEC industry, one must consider its source of information first [8]. The IFC schema's specification is not based on a logic theory because it was not specifically designed for import into rule-checking environments [8].

2.2 Reasoning and Data Validation Using Semantic Web Technologies

Instead of relying on document-based building models, a promising approach for enhancing interoperability with integrated data is the use of the Semantic Web, [14] ,[3]. Semantic Web technologies allow for cross-domain linking, advanced regulations and rule set checking as well as reasoning on data.

The Semantic Web covers a set of technologies; the standard data model of the Semantic Web technology stack is the Resource Description Framework (RDF) [15]. In 2017, the W3C proposed Shapes Constraint Language (SHACL) [16], as the language to validate data in the RDF model [Check]. SHACL defines the shape of the RDF data. SHACL define constraints with expressions called shapes. Each shape consists of a name, a restriction, and an expression determining a set of resources in the data that have to satisfy the shape. OWL is a formal language for authoring ontologies [2]. OWL allows for expressing complex concept definitions, relations between concepts and roles, and inferring new knowledge from these definitions. SHACL covers data validation and constraints and is one of the Semantic Web technologies that assume a closed world [16].With a Closed World Assumption (CWA), any statement that is not known to be true is considered false. Many conventional design software applications adopt a CWA, including BIM tools and common database systems [17]. OWL assumes an open world, where missing information is simply unknown. For instance, with the aforementioned axioms (2) and (3) and the assertion stating that rp is a RoofPanel (i.e., ClassAssertion(RoofPanel rp)), if rp has no explicit ID, a reasoner my produce a new element rpID to represent the identifier of rp (i.e., the assertions ObjectPropertyAssertion(hasID rp rpID) and ClassAssertion(Identifier rpID) are inferred). While SHACL constrains data to follow a schema, OWL provides additional inferencing. In other words, reasoning allows inferring new knowledge, and data validation with SHACL allows seeing inconsistencies by indicating that there

are design violations. Ontology reasoners can assist in ontology consistency, class satisfiability, classification, instance checking, and conjunctive query answering.

The Semantic Rule Language (SWRL) is a W3C standard that combines OWL and the Rule Markup Language (RuleML). In SWRL rules are expressed in terms of OWL concepts, including classes, properties, and individuals. Rules define new assertions as a consequence of previous assertions. For example, the rule:

$$\text{hasColumns}(?x,?y) \wedge \text{columnsMaterialIsTimber}\ (?y,?z) \Rightarrow \text{isTimberBuilding}(?x,?z)$$

says that if an object ?x has columns ?y and these columns ?y are of timber material ?z, then ?x is a timber building of material ?z.

2.3 Deriving knowledge from BHoM objects using BHoM Engine methods

Although BHoM employs an object-oriented data model, its separation of object models from data-processing functions brings it closer to ontologies and knowledge bases [10]. All functionality applicable to the *object models (oM)* types is isolated, and it is primarily grouped in C# Projects called *Engines*. Similarly to *oM* projects, engine projects target a specific domain, use specific namespaces and are suffixed with "*Engine*", e.g. methods for Structural Engineering are placed in the *Structure_Engine* under namespaces starting with *BH.Engine.Structure*. Engines are essentially collections of five different kinds of static classes (Table 2.), which are used as groups for the methods. Each function must clearly target one main input type, and methods are to be written as extension methods, so they are available throughout the framework as an extension to the type. This makes the oM C# classes work in a manner that is closer to dynamically typed languages (e.g. Python) than statically typed languages, and is a design choice that simplifies contribution and scalability. Each oM type can effectively be augmented with precise functions included in Engines. BHoM objects describe facts about the building, which correspond to TBox and ABox axioms in a knowledge graph. BHoM Engine methods and functions can be used to derive knowledge, such as properties about object models, from an RBox in a knowledge graph. Query methods in *BHoM_Engine* are qualified as derived properties and also check certain rules. For example, the centreline of a Bar is an example of a derived property of a Bar. The Bar does not have a Centreline as a declared property (directly defined in the Bar class), but it has *StartNode* and *EndNode*. The centreline can therefore be derived from a function that returns the centreline of the Bar as the line between the *StratNode* and *EndNode* (See Fig. 1). This function is a function that lives under the BHoM Engine. Similarly to other properties, for example, the extrusion is a derived property. Given the declared properties, it is possible to first compute the *Centreline* of the bar, then using its cross-section property one can extrude the cross-section along the centreline, getting the extrusion.

Table 2: BHoM Engine Classes

Create class	To instantiate types (similarly to a singleton pattern)
Modify methods	Operate on the data stored on instances
Query	To retrieve derived data from the types
Convert	Changes a type for another
Compute	Hosts computationally intensive function

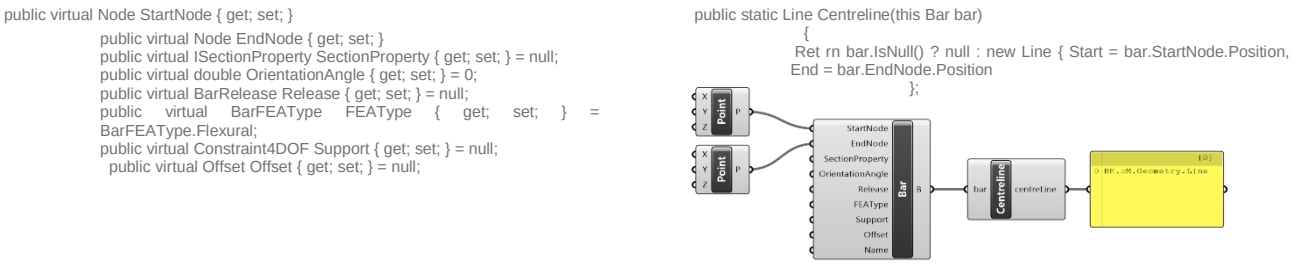

Figure 1: (Left) A bar, structural namespace of the BHoM object models; (right) the function to derive its centerline as a derived

3 Evaluation and Proposal

In this section, we evaluate the usage of Semantic Web standards to validate data and infer knowledge in AEC and BHoM Engine that similarly assist in deriving new knowledge from objects.

3.1 Evaluation of reasoning and data validation in AEC

Using Semantic Web technologies, one can validate data through schemas or apply to reason about a given knowledge base. While the term linked data is closer to "web of data", the term "Semantic Web" encompasses all aspects of the Semantic Web stack, SHACL, OWL, rules, proofs, and truth [17]. The linked data principles of Berners-Lee [18] provide a solid ground for data interoperability for heterogeneous data sources and allow for querying complex questions. However, the principles do not include ontologies, rules and proofs. Consequently, the linked data emerging out of this proposal leaves aside some Semantic Web technologies [17]. This neglect might have caused a low usage of reasoning and methods in applications of linked data. Current building data, rules and restrictions for data validation (e.g. MVDs) do not rely on the same environments, so interoperability problems between tools often hinder reasoning and data validation. Such data validators are usually used only at the end of design processes. Using Semantic Web standards to link data, designers could benefit from the power of knowledge graphs, including discovering new knowledge, reasoning, and data validation. In short, the potential of Semantic Web is not fully unlocked in the AEC industry. Since BHoM provides user interfaces in many design software, using BHoM to model data and define specific rules that can infer new knowledge and convert it to Semantic Web standards would make

knowledge graphs more accessible to architectural designers. With such infrastructure, designers could validate design options in real-time, and design with ontologies and rule-checking constraints in their design platforms (e.g. Grasshopper 3D). BHoM allows integration of both OWA as well as CWA. While OWA should reflect the incremental nature of design processes, (partial) CWA reasoning should allow for discovering lacking specifications. Beetz emphasized that as long as the geometric information is not used in a logical inference process, an RDF representation of the building information is inefficient and does not add much additional value [20]. BHoM allows geometric representation of building elements using primitive data types (e.g. it represents NURBS curves using the coordinates of control points). Introducing algebraic formulas for geometries and adding rules that define the relations between these geometries will make a step forward towards using geometric information in logical inferences. Therefore, integrating geometric information in logical inferences is possible with BHoM.

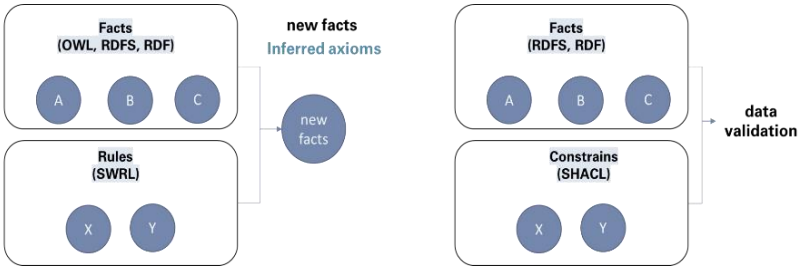

Figure 2. Left: Inferring new knowledge with reasoning; Right: validating data with SHACL shapes.

3.2 Example: Using Semantic Web rules with BHoM Engine methods

BHoM information can be converted to SWRL as well as SHACL, based on the purpose of the design. For example, calculating a centerline length of a bar from its Start Node and End node using SWRL language could be described as follows:

Column (c1) ∧ StartNode (c?, ?p1) ∧ EndNode (?c, ?p2) ∧ subtract (?Length, ?p2, ?p1) ⇒ Length (?c, ?length).

With a reasoner one can infer the length of the centerline, based on the given StartNode and EndNode variables. In the given example, for simplicity, we do not show the datatypes of the SartNode and EndNode, and consider that they are xsd:dobule. On the other hand, if we want to make sure that every bar has at least one start node, we could use SHACL:

```
BhomBarShape a sh:NodeShape; sh:targetClass :Bar ; sh:property [ sh:path :hasStartNode ; sh:minCount 1 ; sh:node :StartNodeShape.
```

Both approaches could support the BHoM knowledge graph and allow one to infer new knowledge with reasoning mechanisms or validate data against SHACL definitions to satisfy a given set of requirements.

4 Conclusion and future work

This paper discusses and evaluates data validation and reasoning methods in the AEC industry. It discusses how to integrate explicit knowledge and implicit building information (rules) into a KB. It also presents the advantages and potentials of BHoM ontologies, operators and reasoning methods, which could offer a novel knowledge representation framework for co-design processes in the AEC industry. We conclude that there are several approaches to append new information on a BHoM KB using either BHoM Engine, RBox roles, or Semantic Web rules. Future work will analyse when one or the other of these approaches should be used by providing advantages and disadvantages of each approach based on the tasks that need to be completed. Combining the BHoM framework with Semantic Web standards can increase the use of knowledge graphs in the AEC industry, by not only improving data interoperability but also assisting design decisions through inferential reasoning.

Acknowledgements

Partially supported by the Deutsche Forschungsgemeinschaft (DFG, German Research Foundation) under Germany's Excellence Strategy - EXC 2120/1 - 390831618 and COFFEE - STA 572_15-2.

References

[1] D. Elshani, T. Wortmann, and S. Staab, “Towards Better Co-Design with Disciplinary Ontologies: Review and Evaluation of Data Interoperability in the AEC Industry.,” Linked Data in Architecture and Construction 2022 ESWC, 2022.

[2] P. Hitzler, M. Krötzsch, B. Parsia, P. F. Patel-Schneider, and S. Rudolph, “OWL 2 Web Ontology Language Primer” W3C Recommendation, 2021. https://www.w3.org/TR/owl2-primer/

[3] P. Pauwels, A. Costin, and M. H. Rasmussen, “Knowledge Graphs and Linked Data for the Built Environment,” in Industry 4.0 for the Built Environment, vol. 20, M. Bolpagni, R. Gavina, and D. Ribeiro, Eds. Cham: Springer International Publishing, 2022, pp. 157–183

[4] P. Poinet, D. Stefanescu, and E. Papadonikolaki, “Collaborative Workflows and Version Control Through Open-Source and Distributed Common Data Environment,” in Proceedings of the 18th International Conference on Computing in Civil and Building Engineering, vol. 98, E. Toledo Santos and S. Scheer, Eds. Cham: Springer International Publishing, 2021, pp. 228

[5] P. Pauwels and W. Terkaj, “EXPRESS to OWL for construction industry: Towards a recommendable and usable ifcOWL ontology,” Automation in Construction, vol. 63, pp. 100–133

[6] buildingSMART.“Industry Foundation Classes.bSI Standards”n.d. buildingsmart.com

[7] P. Pauwels, S. Zhang, and Y.-C. Lee, “Semantic web technologies in AEC industry: A literature overview,” Automation in Construction, vol. 73, pp. 145–165, 2017

[8] P. Pauwels et al., “A semantic rule checking environment for building performance checking,” Automation in Construction, vol. 20, no. 5, pp. 506–518, Aug. 2011

[9] “BHoM. The Buildings and Habitats object Model,” https://bhom.xyz/, n.d.

[10] D. Elshani, A. Lombardi, A. Fisher, D. Hernandez, S. Staab, and T. Wortmann, “Knowledge Graphs for Multidisciplinary Co-Design: Introducing RDF to BHoM,” Linked Data in Architecture and Construction 2022, ESWC 2022.

[11] T. Wortmann and G. Nannicini, “Introduction to Architectural Design Optimization,” in City Networks, vol. 128, A. Karakitsiou, A. Migdalas, S. Th. Rassia, and P. M. Pardalos, Eds. Cham: Springer International Publishing, 2017, pp. 259–278.

[12] T. Wortmann and B. Tunçer, “Differentiating parametric design: Digital workflows in contemporary architecture and construction,” Design Studies, vol. 52, pp. 173–197, Sep. 2017

[13] H. Liu, G. Gao, H. Zhang, Y.-S. Liu, Y. Song, and M. Gu, “MVDLite: a Fast Validation Algorithm for Model View Definition Rules.” arXiv, 2019.

[14] A. Hogan et al., “Knowledge Graphs,” Synthesis Lectures on Data, Semantics, and Knowledge, vol. 12, no. 2, pp. 1–257, Nov. 2021

[15] D. Brickley and R. V. Guha, “RDF Schema 1.1.” 2014. [Online]. Available: https://www.w3.org/TR/2014/REC-rdf-schema-20140225/

[16] H. Knublauch, “Shapes Constraint Language (SHACL),” 2017. https://www.w3.org/TR/shacl/

[17] P. Pauwels, S. Zhang, and Y.-C. Lee, “Semantic web technologies in AEC industry: A literature overview,” Automation in Construction, vol. 73, pp. 145–165, Jan. 2017

[18] T. Berners-Lee, “Note on Linked Data,” 2006. https://www.w3.org/DesignIssues/LinkedData.html

Aufbau und Erweiterung eines Wissensbasis-gestützten Datenmodells mit Semantic Web Technologie und Verarbeitung natürlicher Sprache im Kontext vom Multiprojektmanagement im Verkehrswasserbau

Jiuru Huang[1]

[1]Bundesanstalt für Wasserbau

Kußmaulstraße 17, 76187 Karlsruhe, Germany

E-Mails: jiuru.huang@baw.de

Abstract: Im Bereich des Verkehrswasserbaus entsteht aktuell das Informationssystem „Multiprojektmanagement der Wasserstraßen- und Schifffahrtsverwaltung des Bundes (WSV)“, welches einen aktuellen und umfassenden Überblick aller projektrelevanten Informationen von Baumaßnahmen bieten soll. Dabei bezieht das Informationssystem die Daten aus den anderen etablierten Informationssystemen. Diese Daten werden jedoch in heterogener Art und Qualität gespeichert und für unterschiedliche Nutzungsanforderungen verwertet. Der Überführung relevanter Informationen in maschinenlesbare und -verarbeitbare Daten kommt künftig aber mehr Bedeutung zu. In einem Forschungs- und Entwicklungsprojekt der Bundesanstalt für Wasserbau wird der Ansatz der Semantic Web Technologie (SWT) zum Aufbau eines Wissensbasis-gestützten Datenmodells zur Integration der heterogenen Daten untersucht. Im Zuge dessen wurde ein Ansatz zur Verarbeitung natürlicher Sprache (engl. Natural Language Processing, kurz NLP) verwendet, um neue Entitäten für die Wissensbasis aus den Daten der natürlichen Sprache zu gewinnen. Verschiedene Techniken der NLP, wie z. B. Erkennung bekannter Entitäten (engl. Named Entity Recognition, kurz NER), wurden auf die zuvor erstellte Wissensbasis angewendet, um z. B. in einem vortrainierten Modell neues Vokabular zur Verarbeitung hinzuzufügen. Der Beitrag zeigt exemplarische Ergebnisse dieses Ansatzes und schließt mit einer fachlichen Evaluation.

Keywords: Wissensbasis, SWT, NLP, NER, Verkehrswasserbau

1 Problemstellung und Motivation

Die IT-Anwendungslandschaft in der Wasserstraßen- und Schifffahrtsverwaltung des Bundes (WSV) ist aufgrund ihrer langen Entwicklungshistorie technologisch heterogen. Es entsteht aktuell das Informationssystem “Multiprojektmanagement der WSV”, welches einen aktuellen und umfassenden Überblick aller projektrelevanten Informationen von Baumaßnahmen bieten soll. Dabei bezieht das Informationssystem die Daten manuell aus den anderen etablierten Informationssystemen. Diese Daten werden jedoch in heterogener Art und Qualität gespeichert und für unterschiedliche Nutzungsanforderungen verwertet. Der Überführung relevanter Informationen in maschinenlesbare und -verarbeitbare Daten kommt künftig aber mehr Bedeutung zu. Ein Informationsmodell, das eine effizient vernetzte IT-Landschaft zur optimalen Bedienung der Informationsanforderungen der Nutzer bündelt und integriert, existiert nicht. In einem Forschungs- und Entwicklungsprojekt der Bundesanstalt für Wasserbau (BAW) wird der Ansatz der Semantic Web Technologie (SWT) zum Aufbau eines Wissensbasis-gestützten Datenmodells zur Integration der heterogenen Daten untersucht. In Huang [1] wurde dieser Ansatz hierzu bereits erläutert. In diesem Beitrag werden die Fortführung sowie der aktuelle Stand dieser Entwicklung vorgestellt.

In der vorherigen Untersuchung in Huang [1] wurde festgestellt, dass die SWT für die Integration der Daten in der Qualität eines Datenbanken-ähnlichen Systems einerseits geeignet ist und andererseits liegen größtenteils relevante Informationen in Daten der natürlichen Sprache, wie z. B. Dokumente, Entwürfe, vor. Basierend auf dieser Feststellung wird ein kombinierter Ansatz – SWT mit Unterstützung von Methoden des maschinellen Lernens (ML) – angestrebt. Mit der Entwicklung des ML kommen Sprachmodelle zur Verarbeitung natürlicher Sprache (engl. Natural Language Processing, kurz NLP) zum Einsatz, welche anhand großer Datensätze trainiert wurden und an den Domänenbereich benutzerdefiniert angepasst werden können [2, 3]. Verschiedene Techniken der NLP sollen auf die zuvor erstellte Wissensbasis angewendet werden, um z. B. in einem vortrainierten Modell neues Vokabular zur Verarbeitung hinzuzufügen und neue Entitäten für eine Wissensbasis aus den Daten zu gewinnen. Kapitel 2 führt die Modellierungsmethode der SWT ein und erläutert den aktuellen Stand des Wissensbasis-gestützten Datenmodells. Im Kapitel 3 wird der kombinierte Ansatz mit NLP zur Erweiterung der Wissensbasis prinzipiell demonstriert. Der Beitrag schließt mit einer fachlichen Evaluation und Disskusion.

2 Datenmodell als Wissensbasis

2.1 Modellierung der Wissensbasis

In Huang [1] wurde die Modellierungsmethode zur Überführung relevanter Informationen in Daten mit SWT bereits beschrieben, welche zum besseren Verständnis im Folgenden zusammengefasst wird:

Es wird ein Domänenbereich, in dem die Wissensbasis aufgebaut werden soll, festgelegt. Es werden Abfragen, die das Datenmodell bedienen sollen, als Anwendungsszenarien definiert. Auf diesen Abfragen aufbauend wird ein Assoziationsnetz als Entwurf für die Wissensbasis konzipiert, welches die im Datenmodell befindlichen Klassen bildet. Die Bestandteile der Wissensbasis werden in formaler Sprache mittels der Methode SWT definiert. Diese Definitionen werden durch eine umfangreiche Recherche der Verwaltungsvorschriften und der Regelwerke widerspruchfrei mit Quellenangaben belegt. Das entstandene Datenmodell wird fortlaufend konsistent und kohärent gehalten. Anschließend werden Quellspeicherorte der Wissensbasis und deren Datenstrukturen in den Datenbeständen der verteilten IT-Systeme analysiert, um die Durchsuchungsmöglichkeit der vorhandenen IT-Systeme über die Wissensbasis zu skizzieren. Final soll eine Wissensbasis entstehen, in der alle integrierten Daten mit der Sprache SPARQL abgefragt werden können. Die technologischen Grundlagen sind in Hitzler et al. [4] beschrieben.

2.2 Stand der Wissensbasis

Es wurde eine Wissensbasis für das Informationssystem Multiprojektmanagement der WSV konzipiert. Darin wurden sukzessiv Entitäten nach festgelegten Anwendungsszenarien definiert. Aktuell befinden sich in der Wissensbasis 397 Klassen, welche über 17 Properties miteinander in Beziehungen gesetzt wurden. Davon sind 132 Klassen von Bauwerken und Bauteilen, 99 Klassen von Maßnahmen, 47 Klassen von Wasserstraßen. Organisationen, abstrakte Personen, Bauwerksinspektionsnoten, sowie beschreibende Klassen wie Funktion und Zweck der Bauwerke und der Wasserstraße sind enthalten. Abbildung 1 zeigt den in WebVOWL [5] visualisierten Stand der Wissensbasis, deren Individuen nach und nach in das Datenmodell integriert werden.

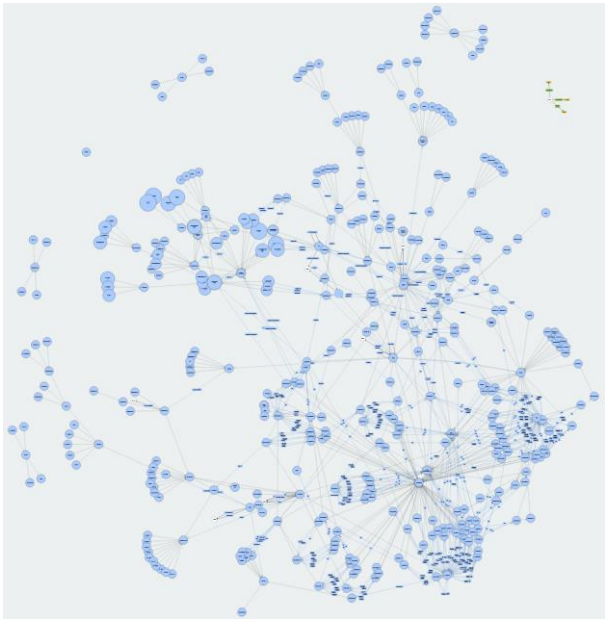

Abbildung 1: Visualisierung der Wissensbasis in WebVOWL [5]

Diese Wissensbasis wird laufend durch das Programm “Debugger” von Protégé auf Konsistenz und Kohärenz geprüft. Die Datenintegration betrifft sowohl die Klassen und Properties als auch die Individuen und deren Datenwerte. Eine Datenbestandsanalyse dient dazu, das Vorhandensein und die Qualität der Daten, die als Klassen, Properties, Individuen vorfinden, zu dokumentieren. Die in Quelldatenbanken befindlichen Daten werden als Klasse, Property oder als Individuum in der Wissensbasis definiert. Bei der Integration müssen die Daten in der Wissensbasis und in den Quellsystemen eindeutig annotiert sein, sodass diese über Application Programming Interface (API) ausgetauscht werden können. Oftmals stellen Quellsysteme kein API zur Verfügung und diese Daten sind nicht identifiziert, d. h. uneindeutig oder widersprüchlich. Um das Problem zu lösen, muss eine Festlegung der Identifikation der zu integrierenden Daten getroffen werden, um die Daten mit einer eindeutigen Kennung zu annotieren. Z. B. wird für jeden Schaden die Schadensnummer, adiert mit Objektidentnummern zwecks eindeutiger Identifikation vergeben – eine Art der Datenveredelung. Der obengenannte Prozess wird derzeit noch manuell bearbeitet. Ein Konzept zur automatisierten Datenkonvertierung wird aufgestellt. Die Datenumwandelung soll so programmiert werden, dass die Daten unabhängig von den Quellsystemen und aus den Quellsystemen direkt automatisch konvertiert und aktualisiert werden, ohne die Quelldaten zu verändern.

Zwei ausgewählte Beispiele demonstrieren das Prinzip einer Wissensbasis. Abbildung 2 stellt die Klasse Projektklasse “Fischpass Wehr Synergie” und ihre Klassenbeziehungen und Abbildung 3 stellt das Individum Wasserstraße “Rhein, Wehrarm Burkheim” dar. Beide sind in WebProtégé [6] visualisiert.

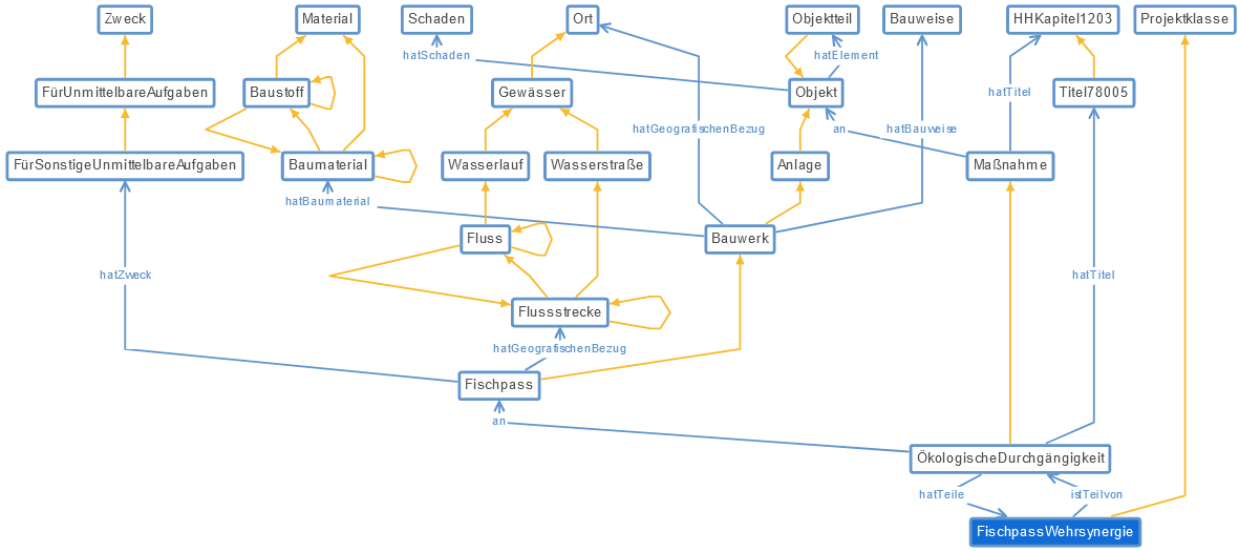

Abbildung 2: Klasse Projektklasse “Fischpass Wehr Synergie” und ihre Klassenbeziehungen dargestelt in WebProtégé [6]

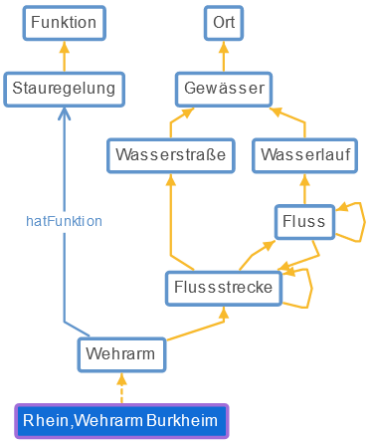

Abbildung 3: Individuum Wasserstraße “Rhein, Wehrarm Burkheim” und seine Klasse sowie Klassenbeziehungen, dargestellt in WebProtégé [6]

2.3 Anwendung der Wissensbasis

Die Wissensbasis kann recherchiert, durchsucht und kollaborativ via Web Protégé [6] editiert werden. Mit den Abfragesprachen DL Query und SPARQL Query können alle in der Wissensbasis befindenlichen Informationen, wie Individuen bestimmter Klasse oder abgeleitete Klassen, abgefragt werden.

Zwar erfüllt der Ontology-Editor Protégé die Grundvoraussetzung eines Datenbankensystems, um relevante Informationen in Daten zu speichern, zu ändern und abzufragen, ist solch eine Nutzung jedoch abhängig vom Programm Protégé und damit auch nur eingeschränkt bei der Fortschreibung und Pflege der darin befindlichen Daten. Eine unabhängige Programmierung bis hin zum Lizenzmodell mit Zugriffssystem ist daher notwendig, um eine breite Anwendung zu gewährleisten. Eine Webanwendung für die Nutzung der Wissensbasis u. a. in Datenformaten RDF/OWL (auch triplestore genannt) wird derzeit umgesetzt.

3 Wissensbasis zur Verarbeitung natürlicher Sprache

3.1 Einführung

Die manuelle Erstellung einer Wissensbasis ist aufwendig. Mit der Entwicklung im Bereich des maschinellen Lernens (ML) sind neue Technologien entstanden – u. a. NLP, die für die Daten der natürlichen Sprachen speziell entwickelt ist [2, 3]. Es existieren bereits vortrainierte Sprachmodelle, z. B. spaCy [7], die einige Entitäten in solch beliebigen Daten mit hoher Genauigkeit erkennen können [8]. Daher wird diese Technologie im Hinblick auf die Frage untersucht, in wieweit diese zur Unterstützung der Erstellung einer Wissensbasis angewendet werden können. Ziel ist es, die

Erkennung relevanter Entitäten und Relationen aus Daten für die Wissensbasis zu automatisieren. Zunächst wird ein vortrainiertes Sprachmodell gewählt, dann die erste manuell erstellte Wissensbasis für das Hinzufügen von Vokablen verwendet. Die Trainingsdaten werden anhand der Wissensbasis generiert und anschließend zum Erlernen des neuen Modells in den maschinellen Lernprozess eingegeben. Das erlernte Modell, welches spezielle Vokabeln der Wissensbasis erkennt, kann anschließend auf weitere Daten zur Erkennung von Entitäten und Relationen eingesetzt werden, welche durch Domänenexperten geprüft der erweiterten Wissensbasis hinzugefügt werden.

3.2 Anwendungsbeispiele

Nachfolgend werden die untersuchten Techniken der NLP anhand der Algorithmen 1-3 erläutert. Zunächst wurde das Python-Paket der Organisation spaCy importiert, dann das auf den deutschen Nachrichten trainierte mittelgroße Sprachmodell [9] geladen. Ein paar eigene Muster und ein Wörterbuch wurden zu dem Modell hinzugefügt, um die Named Entity Recognition (NER) auf die ausgewählten Datensätzen mit angepassten benutzerdefinierten Attributen anzuwenden.

Algorithmus 1: Hinzufügen von Mustern und Wörtern

```
1  import spacy
2  nlp = spacy.load("de_core_news_md")
3  ruler = nlp.add_pipe("entity_ruler")
4  patterns = [{"label": "ORG", "pattern": "Generaldirektion
   Wasserstraßen und Schifffahrt"},{"label": "ORG", "pattern":
   "Wasser- und Schifffahrtsdirektion Mitte"}]
5  ruler.add_patterns(patterns)
6  DICTIONARY = {"GDWS":"Genernaldirektion Wasserstraßen und
   Schifffahrt","WSD Mitte":"Wasser- und Schifffahrtsdirektion
   Mitte"}
```

Algorithmus 2: Erkennen von bekannten Entitäten mit Named Entity Recognition (NER)

```
1  text = ("current_dataset")
2  doc = nlp(text)
3  for entity in doc.ents:
   print(entity.text,entity.label_,spacy.explain(entity.label_))
```

Algorithm 3: Inspizieren von Nominalphrasen und Verben mit Part-of-speech Tagging (POS)

```
1   print("Noun phrases:", [chunk.text for chunk in
    doc.noun_chunks])
    print("Verbs:", [token.lemma_ for token in doc if token.pos_ ==
    "VERB"])
```

Die Ausgabe der Algorithmen 1-3 auf den ausgewählten Datensätzen ist in Abbildung 4 zu sehen. Abbildung 5 stellt die von spaCy visualisierten NER dar. Die Dependenz, visualisiert in Abbildung 6, kann für das Finden von Subjekt-Objekt-Beziehungen (S-P-O) verwendet werden. Die gefundenen S-P-O können der Wissensbasis hinzugefügt werden und als Trainingssatz zum maschinellen Lernprozess dienen. Dabei werden die Nominalphrasen mit den dazugehörigen Verben markiert. Im Beispielsatz lauten die S-P-O "WSA Verden"-"aufstellen"-"Entwurf-AU" und "WSD Mitte"-"genehmigen"-"Entwurf-AU". Alle richtig erkannten Entitäten und S-P-O sind potenziell die neuen Kandidaten der Klasse und Properties in der Wissensbasis.

```
Entwurf-AU Nr. I 3312.000.2013.05.A.23 MISC Miscellaneous entities, e.g.
events, nationalities, products or works of art
Mittelwesennrehren Petershagen, Schlüsselburg und Lang-wedel LOC Non-GPE
locations, mountain ranges, bodies of water
WSA Verden ORG Companies, agencies, institutions, etc.
WSD Mitte ORG Companies, agencies, institutions, etc.
Noun phrases: ['Der Entwurf-AU', '3312.000.2013.05.A.23', 'den Ersatz',
'der Laufeinrichtungen', 'den Mittelwesennrehren Petershagen', 'Schlüsse
lburg', 'Lang-wedel', 'WSA Verden', '15. April', 'der WSD', 'Mitte', '2
5. Juni']
Verbs: ['aufstellen', 'genehmigen']
```

Abbildung 4: Ausgaben der ausgeführten Algorithmen 1-3 auf Beispiel-Datensätzen

```
displacy.render(doc, style='ent', jupyter=True)
```

Die Sohlsicherung im Bereich der Flügelwand LOC bestand nicht gemäß der Planunterlagen aus einem Deckwerk, sondern die ca. 2m dicke Betonsohle der Wehranlage würde bis an die Flügelspundwand LOC herangeführt. Hierdurch entstand erheblicher Mehraufwand durch Abbrucharbeiten unter Wasser um die Rammtrasse der neuen Spundwand zu räumen. Der Entwurf für die Sanierung der Flügelspundwand am Wehr im Unterwasser LOC links im Bereich des WSA Verden, ORG vom WSD Verden ORG am 14.05.2015 aufgestellt, von der Generaldirektion Wasserstraßen und Schifffahrt (ORG GDWS) am 11.06.2014 genehmigt, beinhaltet folgende Einzelmaßnahmen.

Der Entwurf-AU Nr. I 3312.000.2013.05.A.23 MISC für den Ersatz der Laufeinrichtungen an den Mittelwesennrehren Petershagen, Schlüsselburg und Lang-wedel LOC wurde vom WSA Verden ORG am 15. April 2010 aufgestellt und von der WSD Mitte ORG am 25.Juni 2010 genehmigt.

Abbildung 5: Visualisierung der erkannten Entitäten

```
displacy.render(doc, style="dep")
```

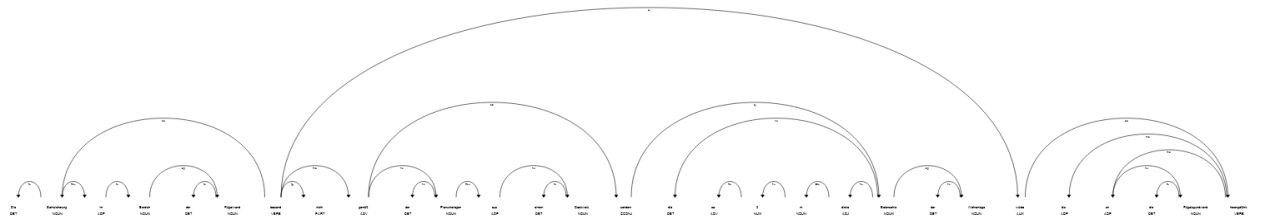

Abbildung 6: Visualisierung der Dependenz der Tokens

4 Fachliche Evaluation, Diskussion und Fazit

Dieser Beitrag zeigt den kombinierten Ansatz mit SWT und NLP. Die SWT ist nützlich für die Erstellung einer Wissensbasis für den Domänenbereich mit Datenbanken-ähnlichen Daten. Diese Wissensbasis enthält relevante Informationen, die auf eine machinenlesbare Art und Weise spezifiziert wurden. Die Herausforderung besteht darin, die Daten in den Quellsystemen eindeutig zu identifizieren, sodass diese mit der Wissensbasis verbunden und von der Wissensbasis abgefragt werden können. Dadurch wird eine Durchsuchung der IT-Landschaft möglich. Bis jetzt wurde die NER der NLP mit angepassten Attributen, d. h. ohne das Modell zu trainieren, angewendet. Erkannt wurden auf den Testdatensätzen insgesamt Organisationen (ORG), Orte (LOC) und sonsitge Begriffe (MISC). Die im Kapitel 2 gezeigten Klassen (z. B. Wasserstraße, Bauwerk, Maßnahme und abstrakte Person) werden als neue Muster oder Wörter für das Modell hinzugefügt. Die hinzugefügten benutzerdefinierten Muster und Wörter wurden richtig erkannt. Fehl- und Falscherkennungen sind vorhanden. Um eine Domänen-spezifische Genauigkeit der NER festzulegen, bedarf es mehr Testdaten. Diese Untersuchung soll durchgeführt werden, um im nächsten Schritt das angepasste Sprachmodell auf größeren Datensätzen anzuwenden. Die Generierung der neuen Wissensbasis und des Trainingssatzes wurden vorgestellt. Eine Automatisierung soll diese Prozesse beschleunigen.

Literatur

[1] J. Huang, „Datenabfrage und -integration im Kontext vom Multiprojektmanagement im Verkehrswasserbau mit Semantic Web Technologie“ in *32. Forum Bauinformatik 2021*, S. 157–165. [Online] Verfügbar unter: https://hdl.handle.net/20.500.11970/108246.

[2] T. Hoppe, *Semantische Suche*. Wiesbaden: Springer Fachmedien Wiesbaden, 2020.

[3] W. Ertel, *Grundkurs Künstliche Intelligenz*. Wiesbaden: Springer Fachmedien, 2021.

[4] P. Hitzler, M. Krötzsch, S. Rudolph und Y. Sure, *Semantic Web: Grundlagen*. Springer-Verlag Berlin Heidelberg, 2008.

[5] *WebVOWL: Web-based Visualization of Ontologies.* [Online] Verfügbar unter: http://vowl.visualdataweb.org/webvowl.html. Zugriff am: 6. Juli 2022.

[6] *The WebProtege site.* [Online] Verfügbar unter: https://webprotege.stanford.edu.

[7] *Industrial-Strength Natural Language Processing in Python.* [Online] Verfügbar unter: https://spacy.io/. Zugriff am: 6. Juli 2022.

[8] *Facts & Figures: The hard numbers for spaCy and how it compares to other tools.* [Online] Verfügbar unter: https://spacy.io/usage/facts-figures. Zugriff am: 6. Juli 2022.

[9] *Available trained pipelines for German: de_core_news_md.* [Online] Verfügbar unter: https://spacy.io/models/de#de_core_news_md. Zugriff am: 6. Juli 2022.

Conversion of XML Property Schema according to ISO 23386 into RDF Graphs

Kilian Kandt[1] and Sven Zentgraf[1]
[1]Chair of Computing in Engineering, Ruhr University Bochum, Universitätsstraße 150, 44801 Bochum, Germany
E-mail(s): kilian.kandt@rub.de, sven.zentgraf@rub.de

Abstract: A fundamental part of the infrastructure is civil engineering. Due to its huge economic and resource relevance optimizing the resource efficiency in this sector has high societal relevance. The German research project RekoTi is initiated to increase this efficiency by closing the mineral material cycle in municipal civil engineering. The project aims to create resource strategies with stakeholders from different disciplines using BIM. In terms of resource aspect, the description of objects in BIM models needs to be formulated in a standardized, maintainable, and exchangeable way. ISO 23386 defines such a data format and methods, for combining information from different sources. As XML is an established format for describing data, the underlying structures of the developed resource efficiency strategies are modeled in XML compliant with ISO 23386. To provide the modeled data in a more queryable way it should be converted into a graph-based representation. So this paper aims to transform XML documents, compliant with ISO 23386, into RDF/XML documents. This is done by examining the current research to find a suitable variant for this transformation. The result of this study is a concept for transforming XML documents conform to ISO 23386 utilizing the XSLT framework. Saved into a database the transformed RDF/XML data is queried to evaluate the resulting data quality and thereby the validity of the created stylesheet.

Keywords: BIM, RDF/XML, XSLT, Resource Efficiency, Energy Simulation

1 Introduction

The central part in infrastructure is the civil engineering, due to its huge economical and resource relevance. Therefore, optimizing the resource efficiency in this sector has a high societal relevance. To increase resource efficiency by closing the mineral material cycle in municipal civil engineering, the German research project Ressourcenplan kommunaler Tiefbau (RekoTi) was formed. The project examines how resources can be used efficiently through the entire life cycle of the infrastructure, regarding the legal and administrative requirements. Subsequently, the results of this investigation

should be analyzed with focus on the deficits and potentials about their possibilities to increase the resource efficiency in the mineral material cycle.

For creating resource strategies, Building Information Modeling (BIM) is of immense relevance, as it acts as a linking instrument between stakeholders from different disciplines. The key stakeholders in planning, building, operating and maintaining infrastructure projects are the public authorities. To describe the properties of objects in BIM models, e.g. in terms of resource aspects, in a standardized way, a data format for describing, maintaining, and exchanging information is needed. ISO 23386 defines such a data format and methods, especially for combining information from different sources or stakeholders [1]. Within this data format, information is recorded in properties that are themselves organized in a tree-shaped group of properties hierarchy.

An established format to describe data in a standardized manner is eXtensible Markup Language (XML). This data representation makes the gathered data human and machine-readable and is easily maintainable, and exchangeable. Thus, the underlying structures of the developed resource efficiency strategies are modeled in XML complaint with ISO 23386. A problem in modeling the data in this structure is that the queryability of XML is neither efficient nor feasible. To overcome this issue, Semantic Web technologies can be used. Resource Description Framework (RDF) is an easy queryable graph-based data representation that describes resources (metadata), is the basis of the Semantic Web and offers an XML-based data serialization the RDF/XML format [2].

This paper aims to transform XML documents, which are defined compliant with ISO 23386, into RDF/XML documents efficiently. An ontology that maps the data format of the standard and introduces the functionalities to attach the created properties to a Feature of Intrest (FOI) is presented in [3]. Therefore, the converted documents should conform with this ontology. A concept to convert XML serialized documents into RDF/XML serialized documents is presented. For this purpose, the current research is examined to find suitable variant for this transformation (c.f section 2). In section 3 the results of this research are analyzed first, and the most suitable technology is selected. With a focus on the syntactic structure of the input data given, a concept for the conversion process from XML to RDF/XML is presented. Finally, the results are present and evaluated by reviewing the created eXtensible Stylesheet Language Transformations (XSLT) stylesheet and querying the transformed RDF/XML data(see section 4). A conclusion and further outlook are given in section 5.

2 Background

This section emphasizes the main terms, concepts, and previous research relevant to the subsequent conceptualization. ISO 23386 introduces a methodology adopted by the International Organization for Standardization (ISO) to describe, manage and maintain properties in a linked data network in construction [1]. Through this standard, the groups of properties and properties that are important for the description of resource efficiency parameters can be divided and described unambiguously in a standardized way [1]. However, this methodology is still rarely used in the infrastructure area. Alani, Dawood, Rodriguez, *et al.* [4] implemented a framework based on Semantic Web technologies

to convert Product Data Templates (PDTs) into a graph-based representation and used the ISO 23386 data model to support the linked data creation in the water infrastructure sector. The authors emphasize the need for a standardized description format for describing building elements in this sector. In addition, the authors recommend manufacturers and suppliers in the construction industry provide their PDTs in RDF-based formats in accordance with the ISO 23386. Furthermore, buildingSmart international, which is focused on the standardization process in the construction industry, provides an online service for classifications, standards, dictionaries, and their properties, referred to as buildingSMART Data Dictionary (bsDD) [5]. buildingSmart announced that bsDD will support the ISO 23386 data model as an export format soon. This extension enables BIM modelers to enrich their models with properties modeled complaint to the standard.

RDF is a World Wide Web Consortium (W3C) framework for representing resources (metadata) in triples (subject, predicate, object). In these, a predicate relates a subject representing a resource and an object representing a resource or a literal. RDF can be complemented through vocabularies such as the Web Ontology Language (OWL) to represent ontologies and can be serialized in different formats such as RDF/XML, Turtle, or N-Triples. RDF/XML allows RDF graphs to be represented in an XML-based serialization.

XML is a widely used text-based format for representing ordered information in a logical tree structure [6]. One extension is the XSLT based on the so-called *stylesheet*, in which the desired output format is described in references to the original XML document [7]. With XSLT stylesheets, tags and their contents from the XML document are localized by XPath expressions, a language for navigating to specific tags within XML documents [8], and placed in a new context. Templates can be used to describe a default structure that is called each time the tag belonging to the template occurs in the XML document.

The conversion of XML documents, which are clearly defined by XML Schema, into documents in RDF/XML format is gaining a broad range of applications in research due to the increasing use of Semantic Web technologies. The Gleaning Resource Descriptions from Dialects of Languages (GRDDL) working group from the W3C is working on the process of *lifting* XML data [9]. The Term *Lifting* describes the process of converting XML to RDF/XML data. For these transformations the GRDDL group uses XSLT since it was developed to express transformations between XML formats such as RDF/XML.

Bohring and Auer [10] proposed a transformation from XML to OWL data. They make the assumption that an XSD document must first be generated from their XML document to derive an OWL model as well as a suitable XSLT stylesheet from this schema. Here, it was noticed that the transformation from XML to OWL using XSLT, which can be seen as a similar process to the transformation from XML to RDF/XML, can produce an uncertain result, especially in the absence of a schema. The assumption XSLT may provide a less accurate result is also confirmed in [11] and [12]. However, Akhtar, Kopecký, Krennwallner, *et al.* [11] also indicate that since XSLT is Turing-complete, this uncertainty can be removed by describing the transformation in more detail in the stylesheet. Bischof, Decker, Krennwallner, *et al.* [12] also notes that *lifting* can be done precisely with XSLT, but that

the underlying stylesheet must become correspondingly more detailed. Both papers address XML Query Language SPARQL RDF Protocol and Query Language (XSPARQL) as an alternative for XSLT conversion. XSPARQL is supposed to be a combination of XQuery and SPARQL. XQuery and SPARQL are both database query languages, with XQuery used for queries and transformations within XML documents and SPARQL used for querying RDF documents. Components of SPARQL have been subsumed into XQuery, and thus should guarantee error-free lifting [12].

3 Concept

This paper focuses on the conceptualization of a transformation process of XML documents compliant to ISO 23386 into RDF/XML documents. As denoted in section 2, XSLT and XSPARQL are two possible frameworks for fulfilling this task. XSPARQL offers in comparison to XSLT a better time complexity, resulting from embedded XML Query Language (XQuery) functionalities [13]. Compared with XSLT, XSPARQL is less prone to errors whenever the structure of the input documents differs. Therefore, the transformation with XSPARQL is a bit more robust against deviations in the input data [12]. This robustness can be considered subordinate because the input data is always first validated against the standard's data format and then transformed after the validation was successful. The validation in advance guarantees the correctness of the input data. A limitation of XSPARQL is its much higher complexity compared to XSLT resulting in a higher workload. Based on these considerations, both technologies can be used for transforming XML documents to RDF/XML. Nevertheless, XSLT is used within this paper, as it provides a more straightforward approach for the transformation and is more suitable for small to medium data sets according to Sherman [13], which are the main data sets used in this project.

An XSLT transformation relies on an underlying XSLT stylesheet that interprets an XML document and transforms its content into the desired format. If the given XML document contains an XML tag, which is defined in the stylesheet, an eXtensible Stylesheet Language (XSL) template is applied to convert the XML tag from the input format to the output format. To support the conversion of the input XML documents into RDF/XML documents using an XSLT stylesheet, it was necessary to analyze the structure of the input data.

The analysis of the underlying XML format showed that there are three basic types of data descriptions used within the input data. These are plain literals, elements that refer to resources like properties, and collections of literals. For each type a basic template concept is created. The resulting templates than can easily be reused by adjusting the according attribute names.

Most attributes in the input XML represent plane literals. These elements are converted with the template shown in listing 1. The shown example implements the transformation of the Globally Unique Identifier (GUID) attribute of a group of properties.The template consists of an XML Path Language (XPath) expression that reads out the value stored in the `match`-path and places it in the corresponding `value-of` tag in the RDF/XML representation.

Listing 1: XSL template for transforming literals using the example of the GUID attribute

```
<xsl:template match="Container/propertyGroup/guid">
    <bimstruct:GloballyUniqueIdentifier>
        <xsl:value-of select="."/>
    </bimstruct:GloballyUniqueIdentifier>
</xsl:template>
```

The second group of attributes represents dependencies between properties or groups of properties instances. For the transformation of these elements the GUIDs stored in the corresponding XML tag forms the basis of a new Uniform Resource Identifier (URI) which references the `rdf:resource` the dependency points to. All relationships specified in the data format of the standard can be transformed in RDF/XML accordingly.

The last template type is used for literals appearing as a list within properties and group of properties. Because they appear several times in an object, they are placed within `Collection` tags in the RDF/XML document. In addition, it is important that every element of the collection still can be uniquely identified to make appropriate querying possible after the transformation. Therefore a new identifier is created out of the GUID of the corresponding parent object and the position of the element in the list. An example for transforming the `namesInLanguage` collection of a property is shown in listing 2.

In summary, all attributes of the XML documents conforming to the standard can be converted to RDF/XML using the conceptualized templates, with one exception. For the transformation of the optional attribute `BoundaryValues` the `Collection` template has to be extended. This adaptation will not be discussed further in this work.

Listing 2: XSL template for transforming a list of literals using the example of the *Names in Language* list of a property

```
<xsl:template match="Container/property/namesInLanguage">
        <xsl:variable name="nameCounter">
                <xsl:value-of select="count(preceding-sibling::namesInLanguage)"/>
        </xsl:variable>
        <xsl:variable name="GUID">
                <xsl:value-of select="../guid"/>
        </xsl:variable>
        <bimstruct:NameInLanguage rdf:ID="NameInLanguage_{$GUID}_{$nameCounter}">
                <bimstruct:Name>
                        <xsl:value-of select="./name"/>
                </bimstruct:Name>
                <bimstruct:Language>
                        <xsl:value-of select="./language"/>
                </bimstruct:Language>
        </bimstruct:NameInLanguage>
</xsl:template>
```

4 Evaluation

In the following, the created XSLT stylesheet is presented and evaluated. The stylesheet converts XML documents based on the data model of ISO 23386 into a graph-based representation in RDF/XML format. The conversion of an XML document compliant with the standard can be performed with the implemented templates introduced in section 3. The Evaluation has shown that checking the XML document in advance syntactically makes the implemented XSLT robust against deviations in the document structure. One issue that occurs while testing is the possibility of empty lists in the input documents. The attribute list `descriptionsInLanguage` for example is denoted as optional in the standard and can be omitted in properties in the input document. The current version of the stylesheet converts such documents without any error but produces empty collection elements in the output data. These empty collection elements don't lead to errors but consume disk space without offering any value. Therefore this issue needs to be fixed in future work.

The Resulting RDF/XML documents are inserted into a graph database to make them queryable and thus attachable to FOIs to use them for rule checking, quantity or cost estimations, or validation purposes. Therefore, in figure 1, a query for gathering the names of groups of properties is presented. Within the SPARQL query, all objects were collected belonging to the `rdf:type bimstruct:GroupOfProperties`. In the next step the literals `bimstruct:GloballyUniqueIdentifier` and `bimstruct:VersionNumber` are gathered for each object. The consecutive step searches for the related `bimstruct:NamesInLanguage` collection and extracts the first name out of it. The corresponding result of the query is shown at the bottom of figure 1. One limitation that became apparent when querying the data was that converted dependencies pointing to resources that do not exist result in errors. Such an error can occur if mistakes arise when creating references between properties and groups of properties. From this, it can be concluded that the input data also needs to be checked for semantic correctness before the transformation. However, this cannot be realized within the XSLT stylesheet and must therefore be validated in advance similar to the syntactic validation. In summary, the evaluation states that the data converted with the developed XSLT stylesheet is suitable to describe resource efficiency specific BIM objects. However, future testing using data from real infrastructure projects must further examine the suitability and robustness of the system.

5 Conclusion

This paper provides a conceptualization for the transformation of XML documents containing properties according to ISO 23386 into the RDF/XML format to support the description of objects in BIM Models through properties, e.g. in terms of resource aspects, in a standardized way. Possible technologies to realize the transformation of XML documents are considered from literature according to the robustness, accuracy, complexity, and performance of the different approaches. As a result of this consideration, the XSLT framework was determined as the most suitable. Requirements from the XML document structure based on the standards data format were systematically analyzed to identify patterns within the data to improve the XSLT template creation by defining reusable patterns for the

```
PREFIX rdf: <http://www.w3.org/1999/02/22-rdf-syntax-ns#>
PREFIX bimstruct: <http://www.bimstruct.de/v0/bimstruct-schema#>
SELECT ?guid ?name ?version
WHERE
{
   ?propGroup rdf:type bimstruct:GroupOfProperties.
   ?propGroup bimstruct:GloballyUniqueIdentifier ?guid.
   ?propGroup bimstruct:VersionNumber ?version.
   ?propGroup bimstruct:NamesInLanguage ?namesInLanguage.
   ?namesInLanguage rdf:first ?nameInLanguage.
   ?nameInLanguage bimstruct:Name ?name.
}
Limit 3
```

QUERY RESULTS

Showing 1 to 3 of 3 entries

Search: Show 50 entries

	guid	name	version
1	"422B41EA-C177-4798-874E-36D4E0256435"	"ATB-BeStra_08"	"1"^^xsd:integer
2	"67BB1B2F-9F88-4700-B49C-8B6D56FFF279"	"Ausstattung"	"1"^^xsd:integer
3	"227FE59D-124F-48FD-89ED-0BE244F03EF4"	"Fahrbahn"	"1"^^xsd:integer

Showing 1 to 3 of 3 entries

Figure 1: Example SPARQL Query for getting all groups of properties with their `guid`, `name` and `version` and the corresponding results from the database

transformation. Out of this analysis three basic templates were created to transform plane literals, dependencies and lists of literals (cf. listing 1 and 2). The result of the concept's implementation is an XSLT stylesheet for transforming XML documents containing properties according to ISO 23386 into semantic graphs in RDF/XML format.

The feasibility of the XSLT stylesheet concerning the requirements is successfully demonstrated by querying a transformed data set (see figure 1). The assignment of queried properties to BIM Objects for describing and maintaining information about e.g. resource aspects can be done according to Zentgraf, Hagedorn, and König [3]. Although it was proven that the developed stylesheet is feasible for the desired use case, the limitations regarding the processing of empty lists and the semantic stability must be improved in the future. An evaluation of the XSLT stylesheet with complex data from real worlds infrastructure projects is still pending and needs to be done in further research.

References

[1] ISO 23386, *Building information modelling and other digital processes used in construction*, Vernier, Geneva, 2020. (visited on 11/24/2021).

[2] P. Pauwels, A. Costin, and M. H. Rasmussen, "Knowledge Graphs and Linked Data for the Built Environment", in *Industry 4.0 for the Built Environment*, Cham: Springer International and Springer International Publishing, 2022, pp. 157–183, ISBN: 978-3-030-82430-3. DOI: \url{10.1007/978-3-030-82430-3_7}.

[3] S. Zentgraf, P. Hagedorn, and M. König, “Multi-requirements ontology engineering for automated processing of document-based building codes to linked building data properties”, in *Proceedings 39th CIB W78 Conference 2022*, ser. CIB W78 Proceedings, 2022. DOI: accepted.

[4] Y. Alani, N. Dawood, S. Rodriguez, and H. Dawood, “Whole life cycle construction information flow using semantic web technologies: A case for infrastructure projects”, in *Proceedings 37th CIB W78 Conference 2020*, ser. CIB W78 Proceedings, 2020, pp. 141–155. DOI: 10.46421/2706-6568.37.2020.paper011.

[5] buildingSMART, *Bsdd buildingsmart data dictionary (bsdd)*, buildingSMART, editor, 2021. [Online]. Available: https://github.com/buildingSMART/bSDD (visited on 11/29/2021).

[6] L. R. Quinn, *Xml essentials*, 2015. [Online]. Available: https://www.w3.org/standards/xml/core.html.

[7] Kay, Michael, *XSL Transformations (XSLT) Version 3.0 W3C Recommendation*, 2012. [Online]. Available: https://www.w3.org/TR/2017/REC-xslt-30-20170608/ (visited on 11/14/2021).

[8] Clark, James and DeRose, Steve, *XML Path Language (XPath) Version 1.0*, 2016. [Online]. Available: https://www.w3.org/TR/1999/REC-xpath-19991116/ (visited on 11/13/2021).

[9] Hazaël-Massieux, Dominique and Connolly, Dan, *Gleaning Resource Descriptions from Dialects of Languages (GRDDL) W3C Recommendation*, 2007. [Online]. Available: https://www.w3.org/TeamSubmission/2005/SUBM-grddl-20050516/ (visited on 11/17/2021).

[10] H. Bohring and S. Auer, “Mapping xml to owl ontologies”, in *Marktplatz Internet: Von e-Learning bis e-Payment, 13. Leipziger Informatik-Tage (LIT 2005)*, K. P. Jantke, K.-P. Fähnrich, and W. S. Wittig, editors, Bonn: Gesellschaft für Informatik e. V., 2015, pp. 147–156.

[11] W. Akhtar, J. Kopecký, T. Krennwallner, and A. Polleres, “Xsparql: Traveling between the xml and rdf worlds – and avoiding the xslt pilgrimage”, in *The Semantic Web: Research and Applications*, Berlin, Heidelberg: Springer Berlin Heidelberg, 2008, pp. 432–447, ISBN: 978-3-540-68234-9.

[12] S. Bischof, S. Decker, T. Krennwallner, N. Lopes, and A. Polleres, “Mapping between rdf and xml with xsparql”, *Journal on Data Semantics*, vol. 1, no. 3, pp. 147–185, 2012.

[13] G. Sherman, “A critical analysis of xslt technology for xml transformation”, Citeseer, Tech. Rep., 2007.

Linking ontology metrics with BIM modeling stages

Silke Dierssen[1], Mario Cichonczyk[1], Uwe Weitkemper[1] and Dominic Becking[1]
[1]Bielefeld University of Applied Sciences, Campus Minden
E-mail(s): sdierssen,mcichonczyk,uweitkemper,dbecking@fh-bielefeld.de

Abstract: Before starting a project, stakeholders of the Architecture, Engineering and Construction (AEC) industry aim to agree on common requirements, such as which information and geometry should be provided at any given stage of the engineering process. In particular, this consensus includes the geometric depth of the processed building information model and its enhancement with information artifacts. A suitable determination of a categorical standard can be achieved on the basis of Level of Geometry (LOG) and Level of Information (LOI). Since no international standard exists for these qualifiers, individual catalogs and checklists are currently used, which often do not allow an unambiguous classification. Given the subjective interpretability of existing methods, a more explicit and objective way of categorization would be beneficial.
The purpose of this paper is to investigate whether this process can be supported by a mathematically rigorous methodology. If LOG and LOI could be determined by a formal computational process, the influence of subjectivity would be reduced to introduce a more objective categorization. With the proposed method, stakeholders can achieve a more reliable assignment of criteria and a common understanding.
We examine whether the Resource Description Framework (RDF) representation of a building information model in Industry Formation Classes (IFC) format allows conclusions about categorization levels. Existing metrics for the analysis of ontologies are applied to RDF graphs. We then assess their correlation with LOG and LOI levels. Finally, we evaluate these mathematically objective qualifiers in terms of their relevance to the AEC domain. Our results show a promising framework for further exploration of a new class of BIM tools that facilitate collaboration and standardization.

Keywords: BIM, IFC, Ontology Metrics, Level of Development (LOD), Level of Information (LOI)

1 Introduction

For any construction project that uses a Building Information Model (BIM), project stakeholders must agree on the level of elaboration of the included model objects. This is usually done by specifying the elaboration via the classification into a Level of Development (LOD). The specified LOD usually

includes requirements for geometric detailing (LOG) and alphanumeric information content (LOI). The classification into the individual levels is mostly done for LOG via textual description in combination with a visual illustration of the individual elements. For the LOI, predefined sample checklists are common. For this purpose, numerous concepts, catalogs and publications exist to facilitate the application process and to achieve a standard. For example, a well-known and often used guideline is the *Level of Development Specification* from BIMForum [1]. These publications provide a suitable guide but still leave much room for interpretation. Since the given definitions are ambiguous, users have to make subjective decisions about what a particular LOD exemplifies and what graphical representation and information to include in the model. Abualdenien and Borrmann [2] highlight discrepancies, misunderstandings and misinterpretations that practitioners face when following the definitions of the various LOD specifications and the need to standardize the different concepts internationally. The concept of LOD itself has been established in the AEC industry, but lacks a formal method. An approach that provides a more objective and reproducible categorization would be beneficial.
Our hypothesis is that the established approach to represent IFC data as an RDF graph lends itself for further analysis beyond model enrichment and querying. Based on the fact that ontological representations have been studied thoroughly in the semantic web domain [3], we assume that the interpretation of a given BIM model only as an abstract ontological construct in a superordinate sense holds information centric value. Viewed from an ontology theoretic perspective, a BIM model can be regarded as a knowledgebase describing a graph realization of an abstract information schema. This analogy arises from the observation that IFC files constitute an object-based instance collection of the IFC entity relationship model. As such, generic semantic analyses produce valid results if applied to BIM applications. We demonstrate that inherent properties of the internal graph topology spanning an IFC instance can be linked to abstract concepts like LOD and LOI. The very same structure originates the visual renderings that would otherwise be interpreted subjectively in e.g. quality control. Therefore, we test whether existing ontology metrics can be applied for the same assessment.

2 Background

Opposed to conventional CAD drawings, digital building models do not have a measurement scale which has a significant influence on the degree of elaboration. Other regulations must be made regarding the specificity of the model for the individual project phases. This can be determined with the Level of Development, a combination of specifications for the geometric representation (LOG) and the alphanumeric information to be provided (LOI) which comprises five levels ranging from LOD100 and reaching up to LOD500. Approaches have been developed to automate the classification of model objects into LOD categories. Abualdenien and Borrmann [2][4] have shown that features which exploit the geometric surface complexity of primitives composing an assembly are useful for ensemble learning methods. For a quality check and model analysis, there are a number of software tools that can automatically validate the model according to predefined rules. These are suitable for verifying information contained in the model, but checks have to be defined manually.
It has become a common approach in the AEC domain to make use of ontologies, the Resource

Description Framework (RDF) and other semantic web technologies to represent knowledge and information in a machine-readable form for reuse and processing. Information is formulated as directed graphs (e.g. RDF graphs). By applying ontological linkages to this information, semantic relations and interconnections can be encoded. Content can be queried using a query language, e.g. SPARQL. The application of these technologies is often used as a complement to existing BIM software. This is mainly done to overcome the problem of interoperability of different software tools within individual disciplines, to establish connections between different application areas in order to integrate unused, valuable resources and to make use of the intrinsic logical features of semantic technologies [3]. For these purposes, a universal entity relationship model is described by the Industry Foundation Classes schema, itself representing a highly descriptive ontology.
Deeper formal analysis using tailored metrics have been accepted as necessary means for ontological quality control and evolution tracking during development and application [5]. Based on the propositions of Franco, Vivo, Quesada-Martínez, *et al.* [6], within the scope of this work, metrics for ontology engineering are understood as objective and reproducible measuring instruments which asses quantitative and qualitative criteria of a structured information corpus adhering to the definition described in [7]. As Gangemi, Catenacci, Ciaramita, *et al.* [8] point out, different dimensions for ontology measurement can be quantified. We loosely summarize potential dimensions as follows [9]:

- **Schema Metrics:** Aspects of ontology design are measured. The correct modeling of intended knowledge cannot be ascertained given an ontology, but its semantic potential to do so is measurable [10].
- **Graph Metrics:** The ontology is viewed as an information *object*. The metric space is defined as a function of its topology and logical syntax [8].
- **Knowledgebase Metrics:** Describe the way in which knowledge is placed within an ontology as a whole and its effectiveness to encapsulate information [10].
- **Class Metrics:** Relate defined classes provided by the schema with their utilization in the knowledgebase [10].

Chosen mathematical quantifiers from these dimensions are being tested for their explanatory capabilities in the context of semantic building representations.

3 Method

To test the explanatory capability of standard criteria from the semantic web domain for model quality assessment, we applied different ontology and graph metrics to a selected set of IFC files. These sample files have been derived from a pre-existing building information model by successively reducing first the geometric complexity and thereafter the information content to obtain 7 different models of the same building in total (LOG100-LOG400, LOI100-LOI300, LOI400 being equivalent to LOG400). The model and all related data artifacts will be released as a reference data set in a separate publication. Figure 1 shows the incremental LOG stages. Table 1 gives a short excerpt

over the specified information artifacts for each LOI level. These levels have been declared for the entity set {*IfcWall, IfcDoor, IfcColumn, IfcRoof, IfcWindow, IfcSlab, IfcStair, IfcBeam, IfcCurtainWall, IfcBuildingElementProxy, IfcRailing*}.

Figure 1: Sample IFC models.

Table 1: Example of LOI specification

Element type	LOI 100	LOI 200	LOI 300	LOI 400
...				
Walls	Name	+ is external	+ load-bearing	+ thermal transmittance
Window	Name	+ is external		+ thermal transmittance
...				

Our test sample is a 3-story office building in solid construction with a flat roof, built in the year 2018. All sample IFC files were exported from Autodesk Revit 2021 in IFC4 Design Transfer View and afterwards converted to RDF graphs in Turtle format using the IFCtoRDF[1] converter. This approach was chosen to transform the IFC representation into a more flexible, fully interoperable ontology that supports semantic analysis. The underlying EXPRESS schema has limited functionality beyond descriptive capabilities [11][12] and our analysis requires the custom implementation of metrics as well as graph query methods [13].
We specifically focused on quantifiers which give weight to topological and taxonomical dimensions to prevent indirect benchmarking of the IFC schema itself. As our interest lies in the metric behaviour of the test sample as a specific realization of the schema, we have selected a set of promising quantifiers from graph and knowledge base analytics to illustrate the process (see Table 2). These metrics were implemented as either graph operations or SPARQL queries and then applied to our 7 sample IFC files.

4 Results

After conversion to RDF, the different modeling stages of our IFC sample set exhibit topological graph properties as listed in Table 3.

[1] Pieter Pauwels: https://github.com/pipauwel/IFCtoRDF

Table 2: Tested metrics.

Metric	Description	Formula
Density	Measures how connected a graph is. Defined as the relationship between all theoretically possible connections in V and the observed edges E.	$D = \frac{2\|E\|}{\|V\|*(\|V\|-1)}$
Degree Centrality	The degree d(v) of a node v is equal to the sum of all edges incident upon that node. Degree centrality is the mean degree contained in V.	$DC = \frac{\sum_{v_i}^{V} d(v_i)}{\|V\|}$
Degree Centrality stdev.	Introduced to capture the second statistical moment of the dispersion properties of DC. Commonly calculated as the root of the variance.	$\sigma = \sqrt{\frac{\sum_{v_i}^{V} \|d(v_i)-DC\|^2}{\|V\|}}$
Average Population	Indicates how extensively populated a knowledgebase is. Calculated through the ratio between the number of instances I provided by the knowledgebase divided by the number of classes C defined in the ontology schema [10].	$AP = \frac{\|I\|}{\|C\|}$
Class Richness	Represents a percentage indicating how well a knowledgebase exemplifies the potential knowledge in the schema. Calculated by dividing the cardinality of the set of all classes C' within the knowledgebase by the total number of classes C defined in the ontology [10].	$CR = \frac{\|C'\|}{\|C\|}$

Table 3: Modeling stages graph topology.

	Nodes	Edges	Pendants		Nodes	Edges	Pendants
LOG 100	2888	6525	732	**LOI 100**	275818	778128	20206
LOG 200	8857	23295	1457	**LOI 200**	298321	833729	27510
LOG 300	221009	627970	20686	**LOI 300**	298325	834046	27511
LOG 400	298412	834687	27537	**LOI 400**	298412	834687	27537

On average, graph density decreased by –61.6% per LOG stage. Degree centrality behaves accordingly but exerts an average decrease in standard deviation by –40.8%. Average population increased 9.8-fold with the most significant change between LOG200 and LOG300, demonstrating a median increment of 254.4%. Class richness expanded by 20.7%, mostly saturating at the LOG300-LOG400 level.

For LOI, density decreased by –2.9% on average. The main contribution can be observed at the transition from LOI100 to LOI200 at –8.4% and stabilizing thereafter. Again, degree centrality mirrors this behavior. Standard deviation is reduced by –3.4% presenting a median rate of change with –0.04%. Average population saturates after LOI200 and gains 2.0% on average. Likewise, class richness does not increase significantly after LOI200 with a pronounced difference of 6.6% before saturation.

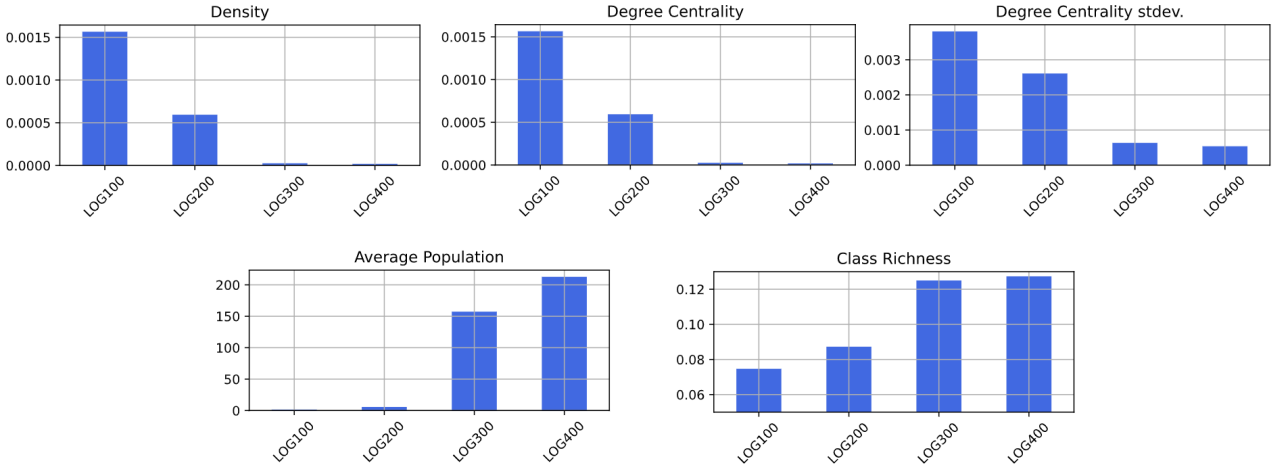

Figure 2: Metrics calculation for LOG stages.

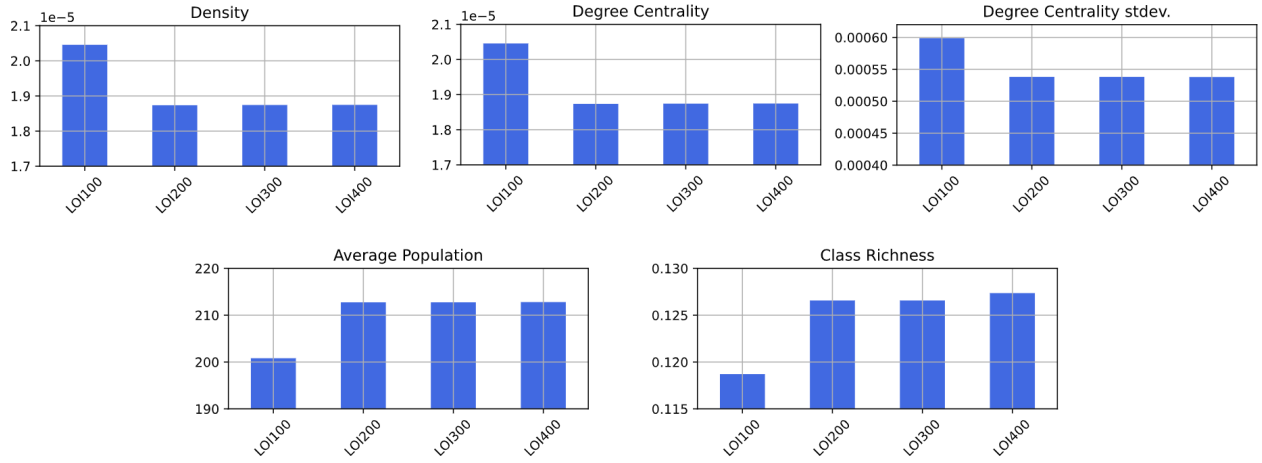

Figure 3: Metrics calculation for LOI stages.

5 Discussion and Future Work

We conclude that generically defined ontology metrics can correlate with BIM modeling stages. The quantifiers we have chosen respond more noticeably to Level of Geometry than Level of Information. We assume this to be an effect of LOI being a more semantically complex categorization, which is predominantly defined by specific IFC classes and their meaning, e.g. *IFCPropertySet*. Once these instances exist within the knowledgebase, the given metrics tend to react less to them as the general ontological topology remains largely unchanged when adding more information afterwards.

We emphasize that ontology metrics are at the center of an active field of research. Existing quantifiers are improved upon and new ones with more specialized purposes are constantly being added. Therefore, many more metrics can be investigated using the presented method.

Our test case has shown the potential value which an ontology theoretic view of an IFC file can add, but measured properties of the underlying RDF graph are bound to the specific model. Future work should aim to find generalizing patterns by testing a wide variety of IFC samples beyond the presented

case. If a large enough sample base is evaluated using our method, converging components of different metrics can be identified. Such patterns would normalize the metric space across all domains and could be universally applied in BIM quality control and replace subjective interpretation providing a vital step towards standardization between BIM stakeholders.
Currently, a BIM quality check can only verify whether previously defined rules have been adhered to. If the requirements for the model change, new agreements and constraints must be defined. Without a requirements catalog, an automated model check is therefore difficult using available tools. However, an initial automated assessment of Level of Development in the event of renovation or redevelopment could be helpful and a significant economic advantage.
We are currently investigating which properties a metric needs for such a purpose and test different custom metric designs against the needs of BIM. We observe that transforming IFC models into RDF representations is a beneficial step in this line of research because it enables querying and semantic enrichment for an increase in metric precision.
Lastly, if the behavior of ontology metrics can be understood in such depth that their measurement can be linked to actual meaning in the context of the AEC industry beyond LOG and LOI, machine-aided control and optimization of complex goal-functions in the planning and design space become viable. The same advantage applies to Scan2BIM for validation of automatically reconstructed semantic models.

Acknowledgements

The project on which this report is based was funded by the German Federal Ministry of Education and Research under the funding code 13FH554IX6 and actively and generously supported by our partners HOCHTIEF ViCon GmbH and Pape Architekten AG. The responsibility for the content of this publication lies with the authors.

References

[1] BIMForum, *Level of development specification*, https://bimforum.org/lod/, Stand: 2022-05-18, 2021.

[2] J. Abualdenien and A. Borrmann, “Levels of detail, development, definition, and information need: A critical literature review”, *Journal of Information Technology in Construction*, vol. 27, pp. 363–392, Apr. 2022. DOI: 10.36680/j.itcon.2022.018.

[3] P. Pauwels, S. Zhang, and Y.-C. Lee, “Semantic web technologies in aec industry: A literature overview”, *Automation in Construction*, vol. 73, pp. 145–165, 2017, ISSN: 0926-5805.

[4] J. Abualdenien and A. Borrmann, “Formal analysis and validation of levels of geometry (log) in building information models”, in *EG-ICE 2020 Workshop on Intelligent Computing in Engineering*, Universitätsverlag der TU Berlin, 2020, p. 33.

[5] D. Vrandečić and Y. Sure, “How to design better ontology metrics”, in *The Semantic Web: Research and Applications*, E. Franconi, M. Kifer, and W. May, editors, Berlin, Heidelberg: Springer Berlin Heidelberg, 2007, pp. 311–325, ISBN: 978-3-540-72667-8.

[6] M. Franco, J. M. Vivo, M. Quesada-Martínez, A. Duque-Ramos, and J. T. Fernández-Breis, “Evaluation of ontology structural metrics based on public repository data”, *Briefings in Bioinformatics*, vol. 21, no. 2, pp. 473–485, Feb. 2019, ISSN: 1477-4054.

[7] R. Hoehndorf, P. N. Schofield, and G. V. Gkoutos, “The role of ontologies in biological and biomedical research: A functional perspective”, *Briefings in bioinformatics*, vol. 16, no. 6, pp. 1069–1080, 2015.

[8] A. Gangemi, C. Catenacci, M. Ciaramita, and J. Lehmann, “A theoretical framework for ontology evaluation and validation.”, in *SWAP*, vol. 166, 2005, p. 16.

[9] B. Lantow, “Ontometrics: Application of on-line ontology metric calculation.”, in *BIR Workshops*, vol. 1684, 2016, pp. 1–12.

[10] S. Tartir, I. B. Arpinar, M. Moore, A. P. Sheth, and B. Aleman-Meza, “Ontoqa: Metric-based ontology quality analysis”, 2005.

[11] E. van den Bersselaar, J. Heinen, M. Chaudron, and P. Pauwels, “Automatic validation of technical requirements for a bim model using semantic web technologies”, English, 1st 4TU/14USA research day on Digitalization in the Built Environment ; Conference date: 01-04-2022, 2022.

[12] J. Beetz, J. van Leeuwen, and d. Vries, “Ifcowl: A case of transforming express schemas into ontologies”, *AI EDAM*, vol. 23, pp. 89–101, Feb. 2009. DOI: 10.1017/S0890060409000122.

[13] E. Tauscher, H.-J. Bargstädt, and K. Smarsly, “Generic bim queries based on the ifc object model using graph theory”, in *Proceedings of the 16th International Conference on Computing in Civil and Building Engineering, Osaka, Japan*, 2016, pp. 6–8.

Teil IV

Inspection & Defects

Automatisierte Schadstellenermittlung aus Bildaufnahmen von Bauwerken mit Hilfe von Deep Learning

David Crampen

Geodätisches Institut und Lehrstuhl für Bauinformatik & Geoinformationssysteme

RWTH Aachen University, Mies-van-der-Rohe Straße 1, 52074 Aachen

E-Mail: crampen@gia.rwth-aachen.de

Abstract: Die Instandhaltung von Bestandsbauwerken ist einer der wichtigsten Aspekte im Gebäudelebenszyklus. Die bei Begehungen durch den Bausachverständigen gesammelten Bilddaten zu Schäden haben das Potenzial den Prozess der Schadensdokumentation zu transformieren. Für die Adaption des vorgestellten digitalen Ansatzes für die Schadensdokumentation ist eine Minimierung des durch die neue Methodik entstehenden Mehraufwands, aufgrund des engen Kostenrahmens, in dem sich Bauleistungen und Maßnahmen zur Instandsetzung bewegen, bedeutsam. Darüber hinaus kann die Digitalisierung von analogen Prozessen zum einen zur Entlastung von Akteuren und zum anderen zur Strukturierung von Abläufen führen. Durch die Nutzung von ohnehin anfallenden Schadstellenbildern können unter Einsatz von maschinellen Lernverfahren zusätzliche Daten generiert und der Prozess der Schadensbewertung unterstützt werden. Im Beitrag wird eine bildbasierte Methode zur Erkennung von Schadstellen an Bauwerken vorgestellt. Zur Schätzung der Fläche der segmentierten Schäden wurde ein Referenzgerät entwickelt, das zur Herstellung eines optischen Maßstabs direkt bei der Aufnahme von Schäden eingesetzt wird. Für die Segmentierung kommt das faltende neuronale Netzwerk Mask-R-CNN zum Einsatz, das für jeden erkannten Schaden Einzelinstanzen generiert, sodass multiple Schäden in einem Bild separat verarbeitet werden können. Der für das Training eingesetzte Datensatz wurde speziell für den Anwendungsfall manuell generiert. Es konnten vielversprechende Ergebnisse erzielt und eine Basis für weiterführende Forschung geschaffen werden.

Keywords: Automation, Neuronale Netzwerke, Instanz-Segmentierung, Bauwerksschäden

1 Einführung

Der Einsatz von künstlicher Intelligenz dringt seit Jahren in nahezu alle Bereiche des Ingenieurwesens vor. Dabei verspricht der Einsatz von künstlicher Intelligenz eine flexible Möglichkeit für das Lösen einer großen Bandbreite von bestehenden Problemen. Bei ausreichender Datenverfügbarkeit stellt Deep Learning einen leistungsfähigen Ansatz für die Automatisierung von verschiedensten Aufgaben dar. Vor allem im Teilbereich „Computer-Vision“ wurden zuletzt Meilensteine in der Zuverlässigkeit und Verarbeitungsgeschwindigkeit von neuronalen Netzwerken zur Bilderkennung erreicht. Dazu kommen im Regelfall faltende neuronale Netzwerke zum Einsatz, die aufgrund ihres zweidimensionalen Schichtaufbaus die Positionen einzelner Bildpixel verarbeiten können. [5]

Bei den Modelltypen wird zwischen Klassifizierungsmodellen, Objekt-Detektionsmodellen wie Fast-RCNN [3] und Faster-R-CNN [6], Modellen zur semantischen Segmentierung und Instanz-Segmentierungsmodellen unterschieden [1]. Bei der Instanz-Segmentierung wird jede Objektklasse auf Pixelbasis in Einzelinstanzen zerlegt. Neben U-Net [7] ist die Mask-R-CNN Architektur [4] eine der erfolgreichsten Architekturen zur Segmentierung von Einzelinstanzen. Die Mask-R-CNN Architektur wird im vorgestellten Ansatz für die Segmentierung von Schäden genutzt.

Im Bauwesen findet die automatisierte Schadenserkennung unter Einsatz von Deep Learning heute vor allem im Infrastrukturbau Anwendung. Die Möglichkeit mit speziell aufgerüsteten Fahrzeugen schnell ganze Straßenzüge aufnehmen zu können, führt zu einer soliden Datenbasis, auf der robuste Modelle trainiert werden können. Generell ist die Risserkennung ein besonders stark beforschter Bereich, zum Beispiel werden in Tang, Mao et al. [9] Risse auf Betonoberflächen wie Dämmen erkannt. Bei der Schadensaufnahme wird, neben der Messung der Rissbreite, in der Regel ein Maßstab in den Schadensbildern aufgenommen, um das ungefähre Schadensausmaß dokumentieren zu können. Eine einfache Variante für einen solchen Maßstab sind Messmarken. Diese werden auf der Wand aufgeklebt und zusammen mit dem Schaden im Bild erfasst. Der Nachteil dieser Methode ist der erhöhte Aufwand für das Befestigen der Marken und die geringe Effizienz einer Marke. Ein besserer Ansatz verwendet einen Entfernungsmesser, der zusammen mit den spezifischen Eigenschaften der eingesetzten Kamera in einen Maßstab umgerechnet werden kann. Dazu muss zwar nichts an der Wand selbst befestigt werden, jedoch erfordert dieser Ansatz die Kopplung bzw. Zuordnung von Entfernungsmesser und Bild, was den Aufwand im post-processing erhöht. Die neu entwickelte Methode stellt einen hybriden Ansatz aus visuellem Maßstab und flexibler Aufnahme aus der Ferne dar. Inspiriert von Chang, Lin et al. [2] wurde ein Referenzgerät aus vier parallelen Lasern entwickelt, das ein quadratisches Objekt auf die Schadensebene projiziert und in der Bildaufnahme platziert wird. Mit diesem Ansatz sind alle notwendigen Informationen in einer Datenquelle (Bild) enthalten, wodurch ein Umformen oder Matching von unterschiedlichen Datenquellen umgangen wird, während der Aufwand für das manuelle Befestigen von Maßstäben vermieden wird.

2 Methoden

Im Folgenden wird die entwickelte Methodik zur Segmentierung und Flächenschätzung von Schadstellen vorgestellt. Dazu wird in 2.1 zunächst der Prototyp des Referenzsystems vorgestellt. In 2.2 wird auf den verwendeten Datensatz eingegangen. In 2.3 wird die Strategie zur Optimierung der Hyperparameter der verwendeten Deep Learning-Architektur beschrieben.

2.1 Referenzsystem

Für die Referenzierung der Schadenstellenbilder, sind die Eigenschaften Flexibilität und Geschwindigkeit von besonderer Bedeutung. Darüber hinaus ist die Minimierung der Kosten zur Erstellung des Referenzsystems von Interesse. [2] lieferten die Inspiration für die Entwicklung des Referenzlasers. Das System besteht aus einem Kunststoffgehäuse, das im 3D-Druckverfahren hergestellt wurde und vier Laserdioden. Dadurch konnten die Herstellungskosten minimiert werden und eine Herstellung nach dem „Rapid-Prototyping-Prinzip“ durchgeführt werden, was gerade in frühen Phasen, in denen Vor- und Nachteile von verschiedenen Lösungen geprüft werden, von Vorteil ist. Das resultierende Gerät ist in Abbildung 1 dargestellt. Durch die I-Form des Gerätes lässt sich ein Smartphone direkt an dem Gerät befestigen, wodurch die relative Position des projizierten Referenzobjektes in den aufgenommenen Bildern weitgehend fixiert werden kann.

Abbildung 1: Referenzgerät zur Erzeugung eines optischen Maßstabs

Die Fläche des Referenzmaßstabs auf der Wand beträgt ca. 150cm². Der Vorteil der parallel angeordneten Laser, ist die Unabhängigkeit vom Abstand zu einer flachen Oberfläche. Dafür müssen die Laser jedoch orthogonal zur Schadensebene ausgerichtet sein. Das Gerät kann über einen externen Schalter ein- und ausgeschaltet werden. Die Sammlung der Daten für den Datensatz wurde mit dem vorgestellten Referenzgerät und einer Smartphone-Kamera durchgeführt.

2.2 Datensatz

Der vollständige Datensatz besteht aus insgesamt 1800 Schadensbildern. Davon stammen ca. 500 Bilder aus dem Internet und 1300 Bilder wurden manuell aufgenommen. Die eigenen Aufnahmen bilden ausschließlich den Außenbereich zu unterschiedlichen Jahreszeiten ab. Die Häufigkeitsverteilung der Objektklassen in den Aufnahmen ist weitestgehend ausgewogen. Die im Datensatz vorhandenen Objektklasssen sind: Riss, Abplatzung, freiliegender Stahl und Referenzobjekt. Letzteres ist auf jedem der 1300 selbst aufgenommenen Bilder bei unterschiedlichen Lichtverhältnissen abgebildet. Die Dauer für die Aufnahme eines Schadens mit dem Referenzobjekt belief sich auf ca. 2-6 Sekunden für ein Bild. Für die Kalibrierung und Validierung der im späteren Verlauf vorgestellten Flächenschätzung wurden 50 Schadstellen manuell aufgemessen. Die zeitlichen Dimensionen des Dokumentationsprozesses mit dem Referenzgerät und die der manuellen Dokumentation zu Kalibrierungszwecken lassen sich vergleichen und zeigen das Potenzial zur Beschleunigung des Prozesses, das durch den Einsatz der vorgestellten Methodik nutzbar gemacht wird, denn das manuelle Vermessen ist von Form und Komplexität der Schadstelle abhängig und nahm in vielen Fällen mehrere Minuten in Anspruch, wohingegen der vorgestellte Ansatz unabhängig vom Schadensausmaß ist.

2.3 Deep Learning-Modell

Mask-R-CNN wurde als Architektur für die Schadenssegmentierung ausgewählt. Es nutz ein FPN (feature pyramid network), das Objekteigenschaften in verschiedenen Auflösungen und unterschiedlichen Größen erlernen kann. Dieser Aspekt unterstützt die Flexibilität der Anwendung, da es zur Erkennung von Objekten keines fixen Abstandes zum Schaden bedarf.

Die „RoI-Align-Layer“ in Mask-R-CNN ermöglicht eine Segmentierung auf Pixelbasis, sie ersetzt die im Vorgänger Faster-R-CNN genutzten RoI-Pooling-Layer und befähigt das Netzwerk erst eine Klassifizierung auf Pixelbasis zu vollziehen. In der Konfiguration von Mask-R-CNN wird ResNet101 als backbone des Netzwerks ausgewählt.

Aufgrund der Zielsetzung der Flächenschätzung ist es von besonderem Interesse, dass das resultierende Modell möglichst präzise Objektmasken erzeugt. Aus diesem Grund wird die im Training relevante Verlustfunktion angepasst, indem der Verlustparameter Validation-mask-loss mit dem Faktor zehn übergewichtet wird. Dies führt zu einer stärkeren Modellanpassung im Falle einer unpräzise prädizierten Instanz-Maske.

Die Optimierung der Hyperparameter wird manuell durchgeführt. Da das Training eines Modells in 100 Epochen auf der verfügbaren Hardware jeweils ca. neun Stunden dauert und Mask-R-CNN die Anpassung von vielen Hyperparametern erlaubt, würde ein Grid-Search-Ansatz zur Optimierung der Hyperparameter den zeitlichen Rahmen sprengen. Die Optimierung folgt einer selbst festgelegten heuristischen Hierarchie mit Baumstruktur, bei der auf jeder Ebene ein Parameter verändert wird.

Als entscheidungsrelevantes Kriterium für die Fortsetzung des Entscheidungsbaums fungiert die mean Average Precision. Diese stellt die durchschnittliche Präzision der Detektion über alle Objektklassen dar. Die mAP wird indirekt über die IoU (Intersection over Union) berechnet, die einen notwendigen Parameter für die Berechnung von Precision und Recall darstellt. Die IoU fungiert als Schwellenwert für die Ähnlichkeit der Objekt Bounding Boxes zwischen Detektionen und Validierungsdaten, über den ein tp (true positive) bestimmt wird. Die mAP kann sowohl auf Basis der Mask-IoU als auch basierend auf der Bounding-Box-IoU bestimmt werden. Generell ist die Bounding-Box-IoU der Standardparameter für den Vergleich verschiedener Modelle, was hauptsächlich in der Verbreitung von Objekt-Detektionsmodellen begründet ist. Modelle zur Instanz-Segmentierung werden jedoch ebenfalls regelmäßig über die mAP der Bounding Box verglichen. Aus diesem Grund wird für den vorliegenden Ansatz ebenfalls die mAP der Bounding Boxes herangezogen.

Für das Training eines Deep Learning Modells im Bereich der Computer-Vision ist es üblich vortrainierte Modellgewichtungen zu verwenden. So kann sehr viel Zeit eingespart werden, weil das Modell lediglich „umtrainiert“ werden muss, statt die Fähigkeit der Bilderkennung von Grund auf zu erlernen. Stufe 1 der Optimierung stellt die Wahl der vortrainierten Gewichtungen dar. Auf Stufe 2 steht die Wahl des Optimizers, der die Hauptkomponente für die Anpassung der Modellgewichtungen nach jeder Iteration durch das Netzwerk übernimmt. In Stufe 3 wird die Lernrate, also das Ausmaß der Anpassung der Gewichtungen optimiert. Die Gradient-Clip Norm auf Stufe 4 stellt einen Schwellenwert für das Ausmaß der Anpassungen in Folge von besonders großen Fehlern innerhalb einer Trainingsiteration dar. Das Lernmomentum wird in Stufe 5 angepasst und beeinflusst die Konvergenz der Lernrate im Lernprozess. Das RoI-Positive-Ratio auf Stufe 6 regelt das Verhältnis von im Training eingesetzten positiven und negativen Samples. In der letzten Stufe 7 werden verschiedene Verfahren der Data Augmentation verglichen, um die Robustheit des Modells zu erhöhen und ein overfitting zu vermeiden, welches bei einem kleinen Datensatz wie dem verwendeten, eine große Gefahr für die Modellperformance darstellt. Overfitting bezeichnet die zu starke Anpassung des Modells an die Trainingsdaten, was zu einer verringerten Generalisierbarkeit und damit auch zu einer schlechten Performance gegenüber neuen Daten führt.

3 Ergebnisse

Im Folgenden werden die Ergebnisse der Untersuchungen zur Modelloptimierung, dann die Ergebnisse der Detektion veranschaulicht und das Ergebnis der Flächenschätzung vorgestellt.

Die Optimierung der Hyperparameter resultierte wie bereits beschrieben in einem Entscheidungsbaum. Als beste Konfiguration stellte sich der Einsatz der COCO-Weights als Basis für das Transferlernen auf Stufe 1 heraus. Die Wahl des Optimizers fiel auf Adam (Adaptive Moment Estimation). Darüber hinaus schnitt die Standardkonfiguration am besten ab. So wurde auf dem eigenen Datensatz eine mAP von 0,46 erreicht.

Für die weitere Optimierung durch den Einsatz von Data Augmentation wurde zunächst geprüft, ob eine Nutzung von Data Augmentation ab Trainingsepoche 1 oder erst in späteren Epochen bessere Ergebnisse erzielt. Das Resultat dieser Prüfung ist eine bessere Modellperformance bei bereits frühem Einsatz von Data Augmentation. Zur weiteren Optimierung wurden verschiedene Data Augmentation Verfahren kombiniert, dazu zählten Rotationen, Spiegeln, Offset, Cutout, Farbänderungen, Gaußfilter und Skalierungen [8]. Die mAP konnte durch den Einsatz von Data Augmentation von 0,46 auf 0,49 gesteigert werden.

3.1 Detektionsergebnisse & Flächenschätzung

Bei der visuellen Begutachtung der prädizierten Schäden wurden verschiedene Modelle miteinander verglichen ein Beispiel für die Ergebnisse von verschiedenen Detektionsmodellen ist in Abbildung 2 dargestellt. Anhand der Ergebnisse zeigt sich, dass der Einsatz von zu viel Data Augmentation das Modell „verwirren“ kann, was dazu führt, dass Objekte wie Schotter o.ä. als Abplatzung segmentiert werden.

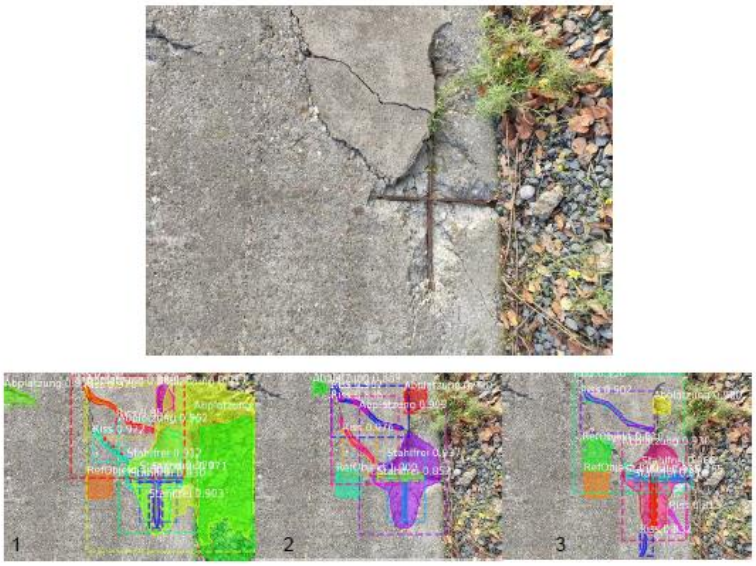

Abbildung 2: Prädizierte Schäden unterschiedlicher Modelle (1 geometrische Data Augmentation, 2 keine Data Augmentation, 3 netzbasierte Data Augmentation

Die Flächenschätzung erfolgt durch die Umrechnung von der Pixelmaske des Referenzobjektes und den realen Maßen des projizierten Quadrates in einen Umrechnungsfaktor, über den die Masken der Schadstellen in reale Maße umgerechnet werden können. Die Kalibrierung der Flächenschätzung gestaltet sich schwierig, da keine Metrik für die Bewertung der Präzision der manuell vermessenen Schäden existiert. Es wurde zunächst angenommen, das die 50 Kalibrierungsdaten korrekt vermessen wurden. Trotz der Kalibrierung verbleibt eine mittlere Abweichung der Fläche von 20% für Risse, 11% für Abplatzungen und 9% für freiliegenden Stahl.

4 Diskussion

Im Folgenden wird zunächst auf den Nutzen und die Kritik an dem entwickelten Workflow eingegangen, bevor auf die Erkenntnisse und Ideen zur Verbesserung eingegangen wird.

Der Mehrwert des entwickelten Workflows liegt in der Beschleunigung und Verbesserung der Schadensdokumentation. Darüber hinaus kann die digitale Darstellung von Schäden in digitalen Bauwerksmodellen die Schadensbewertung verbessern, was positiven Einfluss auf den Instandhaltungsprozess nehmen würde. Der Prozess der Schadensaufnahme kann beschleunigt und seine Ergebnisse digital nutzbar gemacht werden, sofern der Workflow in Zukunft zuverlässig eingesetzt werden kann. Außerdem ist der Ansatz flexibel in Innenräumen einsetzbar. Zusätzlich könnte die Entwicklung von Schäden in Zeiträumen zwischen zwei Aufnahmen analysiert werden.

Um das Verfahren in der Praxis einsetzen zu können, müssen jedoch noch einige Aspekte verbessert werden. Die herausgearbeiteten Kritikpunkte am aktuellen Status liegen in der begrenzten Verfügbarkeit von Daten, was zu großen verbleibenden Unsicherheit des Modells für den Anwendungsfall führt. Zudem setzt sich die Ungenauigkeit der Flächenschätzung aus Ungenauigkeiten der Erkennung des Schadens und zusätzlich Ungenauigkeiten in der Detektionsmaske des Referenzobjektes zusammen. Ein weiterer Kritikpunkt ist die Genauigkeit des entwickelten Gerätes selbst, dieser Kritikpunkt wurde bereits bei den Überlegungen in der frühen Phase der Entwicklung in Kauf genommen, da es sich zunächst nur um einen Prototyp handelt und die Kosten für die Entwicklung möglichst gering sein sollten.

Aus den Kritikpunkten ergibt sich auch das Verbesserungspotenzial für den vorgestellten Ansatz. Ein größerer Datensatz wird die Robustheit des Modells steigern, ein präziseres Referenzgerät wird die Abweichungen der Projektion auf der Schadensebene minimieren. Dazu könnte konkret ein starreres Gehäuse genutzt werden, zudem würde die Möglichkeit zur Nachjustierung der Laser ebenfalls die Genauigkeit des projizierten Objekts steigern. Eine kleinschrittigere Differenzierung der Objektklassen abhängig vom aufgenommenen Material oder die Differenzierung von Rissen nach Rissbreiten könnte potenziell ebenfalls die Detektion verbessern und würde den Informationsgehalt der Dokumentation erhöhen.

5 Fazit & Ausblick

Zusammenfassend lässt sich feststellen, dass der vorgestellte Ansatz ein großes Potenzial für die Vereinfachung der Schadensaufnahme und Dokumentation bieten kann. Dazu muss jedoch die Genauigkeit und Robustheit des entwickelten Models zur Segmentierung der Schäden verbessert werden. Das Übertragen der Ergebnisse der Detektion in digitale Planungsmodelle ist bereits jetzt möglich, im Rahmen des Projektes DigiPark [10] wurde die Möglichkeit zur automatischen Positionierung der Schäden im digitalen Bauwerksmodell geschaffen, was in Kombination mit dem

verbesserten vorgestellten Ansatz zukünftig einen automatischen Workflow möglich machen wird. Der Ansatz ist schnell und vor allem einfach, weshalb eine Adaption in der Praxis, nach der Verbesserung der in 4.2 beschriebenen Aspekte denkbar ist. Zukünftig könnte der Ansatz durch Tiefendaten erweitert werden, was die Bewertung von Schäden in digitalen Modellen möglich machen und damit die generelle Qualität der Schadensbewertung verbessern könnte.

Literatur

[1] Aggarwal, Charu C. (2015): “Data Mining”, Springer International Publishing.

[2] Chang, Wen-Yi; Lin, Franco; Liao, Tai-Shan; Tsai, Whey-fone (2019 - 2019): “Remote Crack Measurement Using Android Camera with Laser-Positioning Technique” in 4th International Conference on Control, Robotics and Cybernetics (CRC) Tokyo, Japan, 9/27/2019 - 9/30/2019: IEEE, S. 196–200.

[3] Girshick, Ross (2015): “Fast R-CNN” in Proc. IEEE Int. Conf. on Comput. Vis. (ICCV), Dec. 2015, pp. 1440–1448.

[4] He, Kaiming; Gkioxari, Georgia; Dollár, Piotr; Girshick, Ross (2017): “Mask R-CNN” in Proc. IEEE Int. Conf. on Comput. Vis. (ICCV), Oct. 2017, pp. 2961–2969.

[5] O'Shea, Keiron; Nash, Ryan (2015): “An Introduction to Convolutional Neural Networks”, Department of Computer Science, Aberystwyth University, Ceredigion, SY23 3DB 2015.

[6] Ren, Shaoqing; He, Kaiming; Girshick, Ross; Sun, Jian (2015): “Faster R-CNN: Towards Real-Time Object Detection with Region Proposal Networks” in Proc. IEEE Transactions on Pattern Analysis and Machine Inteligence (TPAMI) 2015.

[7] Ronneberger, Olaf; Fischer, Philipp; Brox, Thomas (2015): “U-Net: Convolutional Networks for Biomedical Image Segmentation” in Navab, N., Hornegger, J., Wells, W., Frangi, A. (eds) Medical Image Computing and Computer-Assisted Intervention – MICCAI 2015. MICCAI 2015.

[8] Shorten, Connor; Khoshgoftaar; Taghi M. (2019): “A survey on Image Data Augmentation for Deep Learning” in J Big Data 6, 60 2019.

[9] Tang, Jianghong; Mao, Yingchi; Wang, Jing; Wang, Longbao (2019): “Multi-task Enhanced Dam Crack Image Detection Based on Faster R-CNN” in IEEE 4th International Conference on Image, Vision and Computing, July 5-7, 2019.

[10] Blut, Christoph; et. al. (2021): “DigiPark - Digitalisierung in der Bauwerksinstandsetzung” in 7. Kolloquium Erhaltung von Bauwerken : Fachtagung zur Beurteilung, Instandhaltung und Instandsetzung von Bauwerken 2021, pp. 91-100.

Coupling physics-based models with wireless sensor networks for structural health monitoring

Kosmas Dragos

Institute of Digital and Autonomous Construction, Hamburg University of Technology

email: kosmas.dragos@tuhh.de

Abstract: In wireless structural health monitoring (SHM) systems, the over-the-air transmission of large data sets – apart from being unreliable – may drastically reduce the power autonomy of wireless sensor nodes, thus raising the need for continuous power supply, which effectively cancels the “wireless” nature of the sensor nodes. To address the aforementioned shortcomings, this paper reports on advantageously utilizing the embedded computing capabilities of wireless sensor nodes for extracting information on the structural properties on board, i.e. without resorting to centralized data acquisition. Drawing from emerging paradigms associated with the digitalization of physical processes, e.g. using digital twins, the embedded physics-based modeling concept presented herein couples physics-based models of structures with wireless sensor networks. In particular, physics-based models, which are frequently adopted in SHM for mapping the outcome of (typically model-agnostic) data analysis to structural behavior phenomena perceivable by structural engineers, can be embedded into wireless sensor nodes, facilitating advanced local autonomous data analysis on board the sensor nodes. The embedded physics-based modeling concept is validated via simulations, showcasing the capability of the embedded physics-based models to yield information on the structural properties. The results of the proposed concept are expected to align SHM practices with digitalization paradigms that form the backbone of Industry 4.0.

Keywords: Structural health monitoring, wireless sensor nodes, embedded computing, physics-based models

1 Introduction

The importance of predictive structural maintenance of the built environment has been gaining growing traction with the civil engineering community, following the recent devastating effects of climate change on aging civil infrastructure [1]. Representing a subsidy to traditional nondestructive evaluation (NDE), conducted within the framework of predictive structural maintenance, structural health monitoring (SHM) has been proven a reliable strategy for extracting information on structural conditions [2]. By providing abundant structural response data, typically on a long-term basis, SHM aims to cover the discontinuities resulting from the periodicity of traditional NDE methods, such as visual inspections [3]. Moreover, the “digital” nature of SHM, largely involving data analysis and artificial intelligence techniques [4], aligns well with emerging digitalization paradigms that have been infiltrating physical processes across a wide spectrum of activities, such as traffic management and building energy management, which form the backbone of Industry 4.0 [5, 6].

In recent years, SHM has been implemented in several structures that mostly comprise parts of critical civil infrastructure [7]. However, SHM strategies are still limited to structures with high impact on public safety and well-being or to structures of strong academic interest. The widespread adoption of SHM is significantly hindered by the high installation costs of cable-based sensor networks, which are required to collect structural response data [8]. The advances in wireless sensing technologies have been able to partly address the high budgetary requirements, owing to the low cost of wireless sensor nodes and the elimination of cabling [C9]. Nevertheless, practitioners have not been expressing the same trust in wireless SHM systems as in cable-based SHM systems, especially for long-term SHM, due to the limited reliability and robustness of wireless communication as well as to the limited power autonomy of wireless sensor nodes. As a result, the modern SHM landscape involves well-established cable-based strategies and sporadic wireless strategies, usually decided on the basis of cost-benefit analyses conducted by stakeholders of critical infrastructure [10].

In an attempt to boost the adoption of wireless technologies for SHM, researchers have been targeting the shortcomings of wireless sensor networks [11]. Specifically, the embedded computing capabilities of wireless sensor nodes have advantageously been used to embed data analysis algorithms to avoid wirelessly transferring structural response data to centralized servers. With embedded data analysis, wireless sensor nodes are tasked to autonomously extract the information on structural conditions locally (i.e. on the on-board processors), and only communicate the results of data analysis. However, since the computational resources of wireless sensor nodes can hardly support on-board numerical analysis, most embedded data analysis approaches have been based on model-agnostic data-driven modeling methods [12, 13]. Despite its efficiency, data-driven modeling is only capable of yielding global information on structural conditions (e.g. sparse experimental mode shapes), which may be less sensitive to structural damage compared to the rich information obtained from physics-based modeling.

Aiming to advance embedded data analysis, this paper presents a concept for coupling physics-based modeling with wireless sensor networks. In particular, the proposed concept seeks to enable wireless sensor nodes to leverage the descriptive and predictive capabilities of physics-based models on board for extracting richer information from structural response data as compared to data-driven modeling. Each wireless sensor node is tasked with analyzing its structural response data using a partial physics-based model of the monitored structure, corresponding to the surroundings of the sensor node, which is created using substructuring. Thereupon, the complete picture of the structural condition is obtained by collaborative analysis of the results of individual wireless sensor nodes. The validity of the embedded physics-based modeling concept is showcased via simulations on a shear frame structure. In what follows, Section 2 presents the theoretical foundation of the embedded physics-based modeling concept, and Section 3 covers the simulations, serving as validation of the proposed concept. The paper ends with a summary and conclusions as well as with a brief discussion on follow-on future research.

2 Mathematical background of the embedded physics-based modeling approach

In this section, the mathematical background of the proposed embedded physics-based modeling concept is shown via a simple example of a multi-degree-of-freedom (MDOF) oscillator. For the sake of simplicity, the oscillator used in this section follows the “stick” model paradigm, i.e. only translational degrees of freedom are considered. The MDOF oscillator is essentially an assembly of n lumped masses m_i ($i = 1\ldots n$) on n beam elements with stiffness k_i ($i = 1\ldots n$) and damping values c_i ($i = 1\ldots n$), as shown in Figure 1.

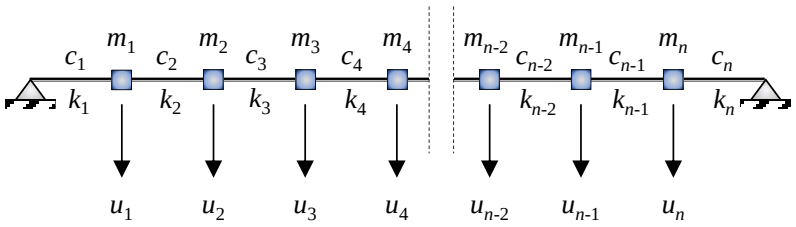

Figure 1: Multi-degree-of-freedom oscillator.

Under the effect of loading conditions P_i ($i = 1\ldots n$), the structural response is approximated using the equations of motion:

$$\mathbf{M}^{n\times n}\ddot{\mathbf{u}}^{n}(t)+\mathbf{C}^{n\times n}\dot{\mathbf{u}}^{n}(t)+\mathbf{K}^{n\times n}\mathbf{u}^{n}(t)=\mathbf{P}^{n}(t). \tag{1}$$

In Equation 1, $\mathbf{M}$, $\mathbf{C}$, $\mathbf{K}$ are the $n\times n$ mass matrix, damping matrix and stiffness matrix, respectively, of the oscillator. The structural response (displacement) is expressed by the n-sized $\mathbf{u}$ vector, and $\dot{\mathbf{u}}$ and $\ddot{\mathbf{u}}$ represent the velocity vector and the acceleration vector, respectively. Finally, t denotes time. The basis of the embedded physics-based modeling concept lies in the ability of individual wireless

sensor nodes to analyze data locally collected, using the physics-based models without extensive wireless communication with the rest of the network. However, the inherently coupled nature of the equations of motion prevents directly embedding the physics-based models into the sensor nodes, because any mathematical operation using the models (e.g. applying equations of motion) would require extensive data exchange with neighboring sensor nodes. Instead, prior to embedding the physics-based model, the monitored structure is segmented into substructures, each containing internal degrees of freedom and interfaces, as shown in Figure 2.

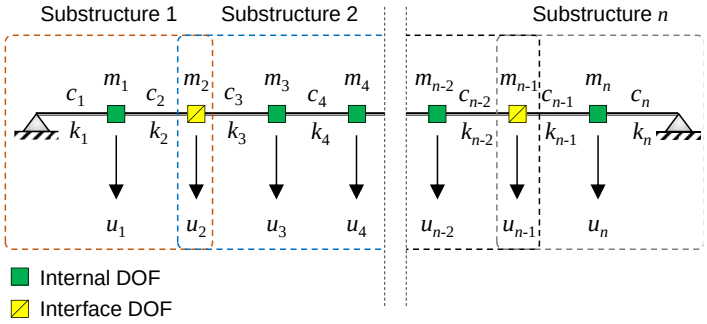

Figure 2: Substructuring of the physics-based model.

As a result of the substructuring, the oscillator physics-based model is segmented into n partial models. Each partial model, corresponding to one substructure, can then be embedded into the wireless sensor nodes that measure the internal degrees of freedom of the substructure. As will be shown below, using the equations governing the oscillation of the internal degrees of freedom, estimates on the acceleration response of the interfaces can be obtained. Specifically, considering substructure 1 from Figure 2, the equation of motion of DOF 1 under the effect of load $p_1(t)$ is:

$$m_1\ddot{u}_1(t)+(c_1+c_2)\dot{u}_1(t)+(k_1+k_2)u_1(t)-c_2\dot{u}_2(t)+k_2u_2(t)=p_1(t). \tag{2}$$

Transforming Equation 2 into the frequency domain (e.g. via fast Fourier transform [14]) results in:

$$m_1\ddot{U}_1(\omega)+(c_1+c_2)\dot{U}_1(\omega)+(k_1+k_2)U_1(\omega)-c_2\dot{U}_2(\omega)+k_2U_2(\omega)=P_1(\omega). \tag{3}$$

In Equation 2, ω is the natural frequency, and $\ddot{U}$, U and U are the frequency-domain representations of the acceleration, the velocity and the displacement, respectively. In the frequency domain, the accelerations, velocities and displacements are related to each other with the following expressions:

$$\dot{U}(\omega)=\frac{\ddot{U}(\omega)}{\omega i} \qquad U_1(\omega)=-\frac{\ddot{U}(\omega)}{\omega^2}, \tag{4}$$

with the help of which, Equation 3 becomes:

$$\ddot{U}_2(\omega)=\frac{P_1(\omega)+\left(\frac{k_1+k_2}{\omega^2}-\frac{c_1+c_2}{\omega i}-m_1\right)\ddot{U}_1(\omega)}{\frac{k_2}{\omega^2}-\frac{c_2}{\omega i}}. \tag{5}$$

Considering that for broadband quasi-white-noise excitation the contribution of $\ddot{U}_1(\omega)$ is much larger than the contribution of the load $P_1(\omega)$ around frequencies that dominate the structural response, Equation 5 serves essentially as a transfer function between the internal DOF of substructure 1 and the interface DOF 2. Following the exact same reasoning, the equation of motion of DOF 3 (substructure 2) may be written as:

$$\ddot{U}_2(\omega) = \frac{P_3(\omega) + \left(\frac{k_3 + k_4}{\omega^2} - \frac{c_3 + c_4}{\omega i} - m_3\right)\ddot{U}_3(\omega) + \left(\frac{c_4}{\omega i} - \frac{k_4}{\omega^2}\right)\ddot{U}_4(\omega)}{\frac{k_2}{\omega^2} - \frac{c_2}{\omega i}}. \tag{6}$$

From Equations 5 and 6, it is evident that two independent estimates can be obtained for the acceleration response of interface DOF 2, which, by extension, entails that two independent estimates can be obtained for every interface of the oscillator. Subsequently, the estimates can be compared to the actual acceleration responses of interface DOF 2, and, in case of discrepancies, the partial model that is no longer capable of describing the structural condition is detected. In the next section, simulations on a 4-DOF oscillator are performed to showcase the validity of the proposed concept using acceleration response data.

3 Simulations on a 4-DOF oscillator

The proposed embedded physics-based modeling concept is validated through simulations on a 4-DOF oscillator. The simulations involve two scenarios: scenario 1, with the oscillator intact, and scenario 2, with slight damage induced as a small change in stiffness. The oscillator comprises four lumped masses on 4 beam elements, as shown in Figure 3a. The dynamic behavior of the oscillator is assumed to be characterized by translational degrees of freedom solely, i.e. following the “stick” model paradigm. The oscillator is segmented into two substructures with one interface, as shown in Figure 3b. For scenario 1 (no damage), the oscillator is subjected to white-noise excitation $P_n(t)$ ($n = 1\ldots4$), and its acceleration response data are calculated through time-history analysis, using the Newmark-β integration algorithm:

$$\begin{aligned} \dot{u}_{m+1} &= \dot{u}_m + (1-\gamma)\Delta t \cdot \ddot{u}_m + \gamma \Delta t \cdot \ddot{u}_{m+1} \\ u_{m+1} &= u_m + \Delta t \cdot \dot{u}_m + \tfrac{1}{2}(\Delta t)^2\left[(1-2\beta)\cdot \ddot{u}_m + 2\beta \cdot \ddot{u}_{m+1}\right]. \end{aligned} \tag{7}$$

In Equation 7, subscript m represents the mth time interval of the time-history analysis, and γ and β are integration coefficients, whose values in this study are set equal to $\gamma = 0.5$ and $\beta = 0.25$. The duration of the time interval is denoted as Δt. The total duration of the time-history analysis is $3{,}600$ s, and the acceleration response data is calculated with a sampling rate equal to $f_s = 100$ Hz.

Following the substructuring, the partial model of substructure 1 and the partial model of substructure 2 will be used to estimate the acceleration response $\ddot{U}_2$ of interface DOF 2, using Equations 5 and 6. The

acceleration response data is split into 21 windows of 16,384 points length, and for each window, Equations 5 and 6 are applied for each substructure, yielding estimates $\ddot{U}_{2,1}(\omega_j)$, from substructure 1, and $\ddot{U}_{2,2}(\omega_j)$, from substructure 2, respectively, over a range of 20 dominant natural frequencies ($j = 1\ldots20$). Finally, the root mean squared error (RMSE) values (ε) between estimates $\ddot{U}_{2,1}(\omega_j)$, $\ddot{U}_{2,2}(\omega_j)$ and $\ddot{U}_2(\omega_j)$ are computed over the range of the 20 natural frequencies. The RMSE values for the 21 windows are plotted in Figure 4; since responses in the frequency domain are complex numbers, the errors are plotted separately for the real parts and the imaginary parts of $\ddot{U}_{2,1}(\omega_j)$, $\ddot{U}_{2,2}(\omega_j)$ and $\ddot{U}_2(\omega_j)$.

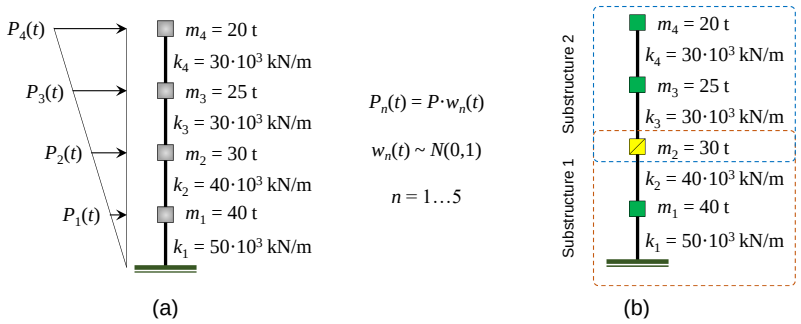

Figure 3: 4-DOF oscillator used for the simulations.

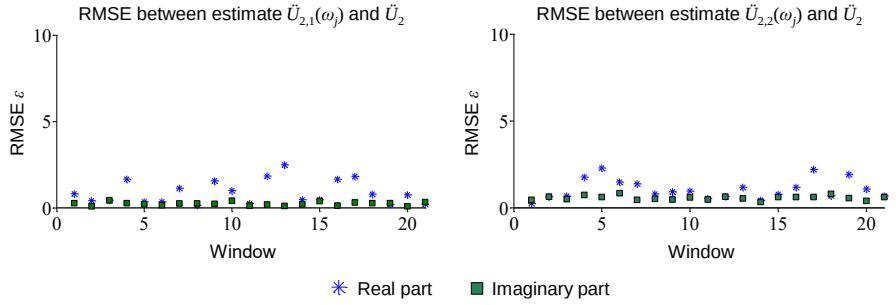

Figure 4: RMSE between estimates $\ddot{U}_{2,1}(\omega_j)$, $\ddot{U}_{2,2}(\omega_j)$ and responses $\ddot{U}_2(\omega_j)$ (Scenario 1).

As shown in Figure 4, the RMSE values between the estimates yielded by the substructures and the actual acceleration responses at the interface are relatively low, showcasing the capability of the partial models to provide information on the structural behavior. To highlight the sensitivity of the estimates to damage, scenario 2 involves a second time-history analysis with a slight change in stiffness k_1, which is reduced to $k_1' = 45{\cdot}10^3$ kN/m. Upon completing the second time-history analysis, the estimates are calculated anew using the original model parameters (i.e. with $k_1 = 50{\cdot}10^3$ kN/m), as shown in Figure 5.

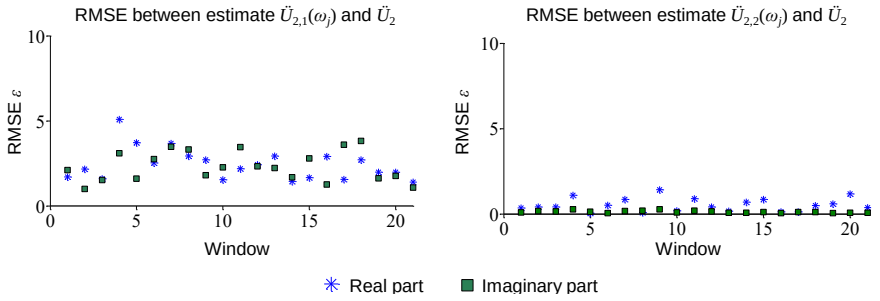

Figure 5: RMSE between estimates $\ddot{U}_{2,1}(\omega_j)$, $\ddot{U}_{2,2}(\omega_j)$ and responses $\ddot{U}_2(\omega_j)$ (Scenario 2).

The significant error values in the left plot of Figure 5 are indicative of the capability of the embedded physics-based modeling concept to yield richer information about damage on the monitored structure than global data-driven methods. Specifically, the inability of the partial model corresponding to substructure 1 to provide correct estimates of the acceleration response of interface DOF 2 indicate the location where changes in structural stiffness have occurred. By contrast, the estimates obtained from substructure 2 for scenario 2 are low, thus indicating that the model parameters of substructure 2 have remained unaffected.

4 Summary and conclusions

This paper has reported on an embedded physics-based modeling concept for wireless structural health monitoring, to enable wireless sensor nodes to analyze data locally with physics-based models. Using substructuring, the embedded physics-based modeling concept foresees the segmentation of an overall physics-based model of the monitored structure into partial models, each corresponding to one substructure, which comprises internal degrees of freedom and interfaces with neighboring substructures. Thereupon, functioning as transfer function, each partial model is used to obtain estimates of acceleration responses in the frequency domain at the interfaces of the corresponding substructure, using equations of motion at internal degrees of freedom. By comparing the estimates of the acceleration responses to the actual acceleration responses at the interfaces, conclusions are drawn on the structural condition, and, particularly, on the capability of the partial models (and, by extension, of the overall physics-based model) to describe the structural condition. The embedded physics-based modeling concept has been validated through simulations on a 4-DOF oscillator showcasing the capability of the concept to accurately describe the current structural condition both in the presence and in the absence of damage. Future work will focus on considering more elaborate physics-based models as well as applying the concept to real-world SHM systems.

Acknowledgments

The authors gratefully acknowledge the support offered by the German Research Foundation (DFG) through grant SM 281/20-1. Any opinions, findings, conclusions, or recommendations expressed in this paper are those of the author and do not necessarily reflect the views of the DFG.

References

[1] Willbanks, T.J. & Fernandez, S.J., 2014. Climate change and in-frastructure, urban systems, and vulnerabilities. Technical Report for the US Department of Energy in support of the National Climate Assessment. Washington, DC, USA: Island Press.

[2] Agdas, D., Rice, J.A., Martinez, J.R. & Lasa, I.R., 2016. Comparison of visual inspection and structural health monitoring as bridge condition assessment methods. Journal of Performance of Constructed Facilities 30(3): 04015049.

[3] Dragos, K. & Smarsly, K., 2017. Decentralized infrastructure health monitoring using embedded computing in wireless sensor networks. In: Sextos, A. & Manolis, G. D. (eds.). Dynamic Response of Infrastructure to Environmentally Induced Loads. Pp. 183-201. Cham, Switzerland: Springer International Publishing.

[4] Smarsly, K. & Law, K. H., 2013. Advanced Structural Health Monitoring based on Multi-Agent Technology. In: Zander, J. & Mostermann, P. (eds.). Computation for Humanity: Information Technology to Advance Society. Pp. 95-126. Boca Raton, FL, USA: CRC Press.

[5] Dragos, K. & Smarsly, K., 2015. A comparative review of wire-less sensor nodes for structural health monitoring. In Proc. of the 7th International Conference on Structural Health Monitoring of Intelligent Infrastructure, Turin, Italy, 01/07/2015.

[6] Smarsly, K., Law, K. H. & Hartmann, D., 2013. A Cyberinfrastructure for Integrated Monitoring and Life-Cycle Management of Wind Turbines. In: European Group for Intelligent Computing in Engineering. Proc. of the 20th International Workshop on Intelligent Computing in Engineering 2013. Vienna, Austria, 07/01/2013.

[7] Nagarajaiah, S. & Erazo, K., 2016. Structural monitoring and identification of civil infrastructure in the United States. Smart Monitoring and Maintenance 3(1): 51-69.

[8] Farrar, C.R. & Worden, K., 2010. An introduction to structural health monitoring. In Deraemaeker & Worden (eds), New Trends in Vibration Based Structural Health Monitoring: 1-17. Udine, Italy: Springer.

[9] Smarsly, K., Law, K. H. & König, M., 2011. Autonomous Structural Condition Monitoring based on Dynamic Code Migration and Cooperative Information Processing in Wireless Sensor Networks. In: Proc. of the 8th International Workshop on Structural Health Monitoring 2011. Stanford, CA, USA, 09/13/2011.

[10] Smarsly, K. & Hartmann, D., 2010. Agent-Oriented Development of Hybrid Wind Turbine Monitoring Systems. In: Proc. of ISCCBE International Conference on Computing in Civil and Building Engineering and the EG-ICE Workshop on Intelligent Computing in Engineering. Nottingham, UK, 06/30/2010.

[11] Smarsly, K. & Petryna, Y., 2014. A Decentralized Approach towards Autonomous Fault Detection in Wireless Structural Health Monitoring Systems. In: Proc. of the 7th European Workshop on Structural Health Monitoring. Nantes, France, 07/08/2014.

[12] Smarsly, K. & Tauscher, E., 2016. Monitoring information modeling for semantic mapping of structural health monitoring systems. In: Proceedings of the 16th International Conference on Computing in Civil and Building Engineering. Osaka, Japan, 07/06/2016.

[13] Zimmerman, A., Shiraishi, M., Swartz, R.A. & Lynch, J.P., 2008. Automated modal parameter estimation by parallel processing within wireless monitoring systems. Journal of Infrastructure Systems 14(1): 102-113.

[14] Smarsly, K., Dragos, K., & Kölzer, T., 2022. Sensorintegrierte digitale Zwillinge für das automatisierte Monitoring von Infrastrukturbauwerken. Bautechnik 99(2022).

Automated Detection of Cracks based on Statistical Analysis of Image Histograms

Lea Jutz and Baris Özcan

Chair for Computing in Civil Engineering & Geo Information Systems, RWTH Aachen University,

Mies-van-der-Rohe-Straße 1, 52074 Aachen, Germany

E-Mails: oezcan@gia.rwth-aachen.de

Abstract: Damage detection on technical components, such as crack detection on concrete surfaces, is an important task in the life cycle of structures. Currently, this is mainly done manually by the human operator, which is time-consuming and cost-intensive as well as error-prone. Automating the process therefore promises considerable advantages. The documentation of damage by means of photographs represents an established procedure, so that these can provide a valuable basis for greater automation in damage evaluation. A major challenge in the automated detection of damage in images, however, is the diversity of damage, but also of surfaces itself. Thus, due to their generalization capability, machine learning methods are increasingly being used in this context. However, these have the crucial disadvantage that they require a considerable amount of training data. In particular, supervised machine learning requires additional annotations (labels) to the image data for the training process, which are often very elaborate to create. In this paper, we present an approach for automated damage detection using traditional image analysis methods like histogram analysis. Thus, compared to machine learning, this method has the significant advantage of being rule-based and therefore does not require training data. The first results on a reference dataset show a classification accuracy of around 99%, which is very promising.

Keywords: Crack detection, Histogram analysis, Image processing, Gaussian Mixture Model

1 Introduction

Cracks are among the most common types of damage occuring in concrete structures, as a variety of factors can promote their formation. From the initial installation throughout the entire life cycle of a concrete structure, a wide variety of weather conditions influence its strength behavior. While

cracking is desirable in the composite material reinforced concrete so that the reinforcement can absorb the tensile stresses in the concrete, the formation of cracks itself carries the risk of corrosion by allowing chlorides and other contaminants from the surroundings to penetrate through them into the structural component. In the case of exposed concrete, the formation of cracks is additionally unfavorable for aesthetic reasons.

For these reasons, it is crucial to detect damage to concrete components at an early stage in order to be able to take appropriate remedial measures. In practice, the detection, analysis and documentation of cracks are usually still mainly done manually. Commonly used methods are, for example, crack width gauges, strain gauges or ultrasonic measuring methods. An overview of numerous manual methods is given by Lange and Benning in [1]. These manual procedures, however, suffer from several issues. They are prone to errors, time-consuming and consequently cost-intensive, especially in the case of larger structures, and are generally subject to subjective assessment or evaluation. In addition, humans can only detect cracks up to a certain size with the naked eye, but the finest microcracks can also lead to major damage.

Since damages are usually documented by photographs during periodical inspections, these can serve as a data basis for automating the detection and assessment of damages. In the context of automation, methods of machine learning are often used, however, these have the major flaw of requiring large amounts of training data with annotated labels.

In this paper, we propose a rule-based method based on statistical analysis of the image histograms. The objective is the classification of images into two classes, specifically intact concrete surfaces and concrete surfaces containing cracks. Our study is further based on the assumption that the frequency distribution of the grayscale values of both object types, concrete surfaces and cracks, is normal distributed. The classification is performed considering different decision criteria of the estimated parameters of the distributions.

2 Related Work

There is a vast number of approaches for detecting damage in concrete, which can basically be divided into methods based on machine learning, as well as methods based on traditional image analysis. In this regard, a comprehensive review of 50 research papers is provided by Mohan [2].

A holistic approach for the detection of pavement damages using machine learning has been presented by Sesselmann et al. [3]. They use the mobile mapping system I.R.I.S., which contains a multi-sensor integrated navigation system and captures the roads during the journey by a 3D laser scanner and a surrounding camera. For georeferencing, the 3D measurements obtained by the laser scanner are fused with the images captured by the camera. They exploit a sliding-window approach in combination with a Convolutional Neural Network (CNN) developed for multi-target classification to detect different classes in the images, such as cracks, potholes, patches, road markings and intact

asphalt. For large-area damage classes, such as patches, they could not achieve satisfactory results. For rather linear shaped classes, such as cracks or road markings, on the other hand, their model delivered moderate to good results.

In the field of damage detection using traditional image analysis methods, a wide variety of image processing methods come into use. An example is the digital image correlation, which enables the detection of the crack behavior of concrete components by means of a camera-based deformation measurement [4]. This method can also be extended by other measurement techniques such as acoustic emission technique [5] to determine other crack parameters. In common, most of the methods based on image processing have a similar procedure. First of all, the images are pre-processed, for example converted to grayscale or processed by image filtering, in order to subsequently apply the crack detection mechanism. Ultimately, determination of further features of the detected cracks, such as dimensions or density, can be performed [6].

3 Histogram-based Detection of Cracks

3.1 Dataset

The examinations in this paper are based on the open-source dataset of Özgenel et al. [7]. This dataset consists of 458 images taken on the same day and under similar lighting conditions from buildings on the Middle East Technical University (METU) campus in Ankara. From these images, 40,000 patches of uniform size (227 x 227 pixels) were created, visually inspected for cracks, and accordingly classified into intact ("negatives") and cracked ("positives") surfaces. Apart from this classification, the images have not been subjected to any further processing.

The dataset is characterized by a variety of surfaces and by clear visibility and different sizes and patterns of the cracks. In Figure 1, a selection of images is presented with their corresponding histograms:

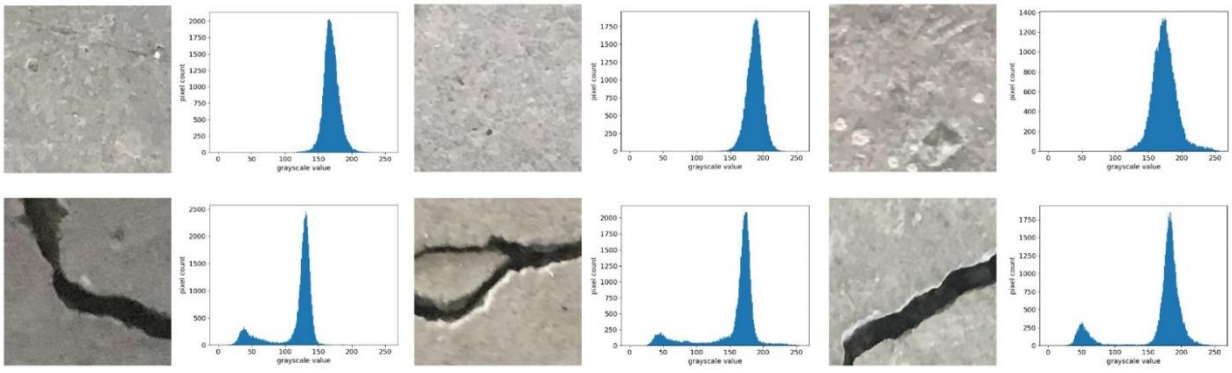

Figure 1: Examples of intact (top) and cracked surfaces (bottom) with associated histograms.

3.2 Parameter estimation of a Gaussian distribution

Following the assumption that the frequency of grayscale values of intact concrete surfaces behaves normally distributed, the corresponding parameters can be estimated from the image histograms. For our study, we consider the first two moments of a random variable, which are the expected value μ and variance σ². These can be determined by the following well-known expressions:

$$\mu = \frac{\sum_{i=1}^{n} x_i}{n}, \quad \sigma = \sqrt{\frac{\sum_{i=1}^{n} (x_i-\mu)^2}{n}}. \tag{1}$$

Given a histogram of an image, these parameters can be approximated by the arithmetical mean $\bar{x}$ and the empirical standard deviation s of the sample. To determine the goodness of fit of the Probability Density Function (PDF) with the estimated parameters μ and σ, the coefficient of determination is used:

$$r^2 = 1 - \frac{\sum_{i=1}^{n} \left(y_i - \hat{y}(x_i)\right)^2}{\sum_{i=1}^{n} \left(y_i - \bar{y}\right)^2}. \tag{2}$$

with r^2 the coefficient of determination, y_i the given frequency and $\hat{y}(x_i)$ the estimated frequency of the grayscale value x_i and $\bar{y}$ the sample mean.

3.3 Parameter estimation of a Gaussian Mixture Model using EM algorithm

Due to the presence of multiple object types in a crack image (crack and surface), the grayscale values of the image originate accordingly from different populations. Given the assumption that both populations follow a normal distribution, whose parameters are in general unknown, this is commonly referred to as a Gaussian Mixture Model (GMM). In the histogram of crack images, this fact is usually reflected as a bimodal distribution, caused by a mixture of two Gaussian distributions.

The parameter estimation of a GMM, however, is not as straightforward as in the case of a Gaussian distribution. For the data points (in our case the grayscale values), it is typically unknown from which population they originate. Neither is there any information about the parameters of the underlying distributions in the GMM. A solution for this, however, is the Expectation-Maximization (EM) - algorithm. EM is an iterative algorithm for clustering and parameter estimation of GMM based on two steps. It requires the number of Gaussian distributions and initial guesses for the parameters.

The Expectation-step estimates the probabilities of the data points to originate from the individual distributions based on the given parameters and thus assigns each data point proportionally to the single distributions. Based on these assignments, the Maximization-step recalculates and updates the parameters of the distributions. These two steps are repeated for a predefined number of iterations or until converge is reached. The pseudocode for EM is given in Algorithm 1.

Algorithm 1: EM algorithm

1 p ← Data points
2 N ← Number of distributions, here: N = 2
3 α ← Proportion of distribution to total distribution
4 μ ← Expected values of the probability functions
5 σ^2 ← Covariances of the probability functions
6
7 Input: p, N
8 Random estimates of μ, σ^2, α
9 for t=1:T with T: maximum number of iterations
10 //Expectation-step
11 for k=1:K with K: number of data points
12 for n=1:N
13 $$P(x_{kn}) = \frac{\alpha_n K(p_k \mid \mu_n,\ \sigma_n^2)}{\sum_{i=1}^{n} \alpha_i K(p_k \mid \mu_i,\ \sigma_i^2)}$$
14 end
15 end
16 //Maximization-step
17 for n=1:N
18 $$\mu_n = \frac{\sum_{k=1}^{K} P(x_{kn}) p_k}{\sum_{k=1}^{K} P(x_{kn})}$$
19 $$\sigma_n^2 = \frac{\sum_{k=1}^{K} P(x_{kn})(p_k - \mu_n)(p_k - \mu_n)^T}{\sum_{k=1}^{K} P(x_{kn})}$$
20 $$\alpha_n = \frac{1}{K} \sum_{k=1}^{K} P(x_{kn})$$
21 end
22 end
23 Output: Expected values μ, covariances σ^2 und proportions α

The algorithm finally provides an output of estimates for the parameters of the underlying normal distributions, such as the expected values μ_i and covariances σ_i^2, as well as the proportions of the individual distributions α_i in the overall distribution. Furthermore, the assignment of the data points to the distributions are associated with probabilities, which is why the method is also referred to as soft-clustering. Figure 2 shows an example of a crack image with estimated parameters.

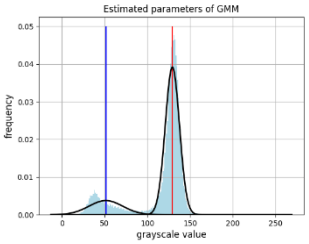

Figure 2: Example of an image containing a crack with estimated parameters of a GMM

3.4 Decision Criteria for Classification

For a robust classification of the concrete images, we formulated multiple decision criteria based on parameter estimations of Gaussian distributions (section 3.2) and of the GMM (section 3.3).

The first criterion is based on the coefficient of determination r^2 of the estimated Gaussian distribution. In case of the coefficient approaching 1, it can be concluded that the estimated Gaussian PDF is fitting the underlying sampling distribution very accurately and thus it can be assumed that there is only one significant texture present in the image, which can only be the surface itself. We found a threshold of 0.975 to be suitable for the coefficient. Thus, images with a lower coefficient of determination undergo the following two criteria whilst the others are excluded since it is assumed there are no cracks in these images.

As second criterion, the estimated expected values μ_1, μ_2 of the GMM are used. Cracks are generally significantly darker in the images than the rest of the surface, leading to the expected values μ_1, μ_2 to differ as correspondingly strong. Therefore, we adopt a threshold of 20 grayscale values for the difference between the two expected values (based on the observation of the current dataset). If the difference of the expected values is smaller than the threshold, the respective image is also considered as "intact" and the remaining images are subjected to the next criterion.

The third criterion involves the proportions of the two mixed Gaussian distributions in the GMM. Cracks in the image usually constitute a smaller part than the intact surface itself, which is also reflected in the proportions of the distributions accordingly. As ratio between the proportions, we found that 0.7 represents a suitable threshold value. Therefore, if the proportion of the distribution with the lower expected value is lower than 0.3, the image is considered to include a cracked surface.

Only if all three criteria are fullfilled, we classify the respective image as a cracked surface (Fig. 3). In all other cases, the image is considered to be of an intact concrete surface.

Figure 3: Criteria for classification of concrete images into intact and cracked surfaces

4 Results

Testing the entire dataset of 40,000 images based on the introduced decision criteria shows a good classification accuracy especially for images containing cracks. For intact surfaces, the number of images classified incorrectly as images containing cracks is slightly higher than the number of images containing cracks classified incorrectly as intact. For crack images, this gives us a rate of 99.995%, while for images of intact surfaces it is 97.58%. The overall classification accuracy is therefore about 98.79%. Figure 4 shows the results in a confusion matrix.

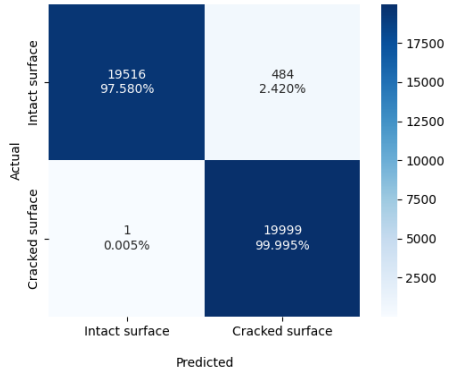

Figure 4: Results obtained for the reference dataset

5 Discussion

The presented method shows an appropriate classification performance on the dataset used. However, it has to be taken into account that the methodology was developed and tested using only this dataset and is therefore only representative to a certain extent.

It is noticeable that intact surfaces are classified generally worse than ones with cracks. A reason for this might be the diversity of the surfaces and the presence of blobs and spots in the surfaces, which lead to the formation of two peaks, similar to the cracked surfaces, which in turn leads to a bimodal distribution. In practice, however, this constellation is less critical, since it would be much riskier to classify a cracked image as intact than the other way around.

Contrary to other algorithms like k-means clustering, the EM algorithm performs a soft-clustering of data points by assigning probabilities to the points for belonging to the individual populations. These probabilities in turn could be further considered in classification process.

The grayscale values of both surfaces and cracks were assumed to be normally distributed and independent. However, these are actually based on visual assessment and must first be verified.

Up to now, we only considered two moments of a random variable, specifically the expected values and variances. However, the frequency distributions of the grayscale values could also involve other significant moments, such as skewness or kurtosis, which should be taken into account.

6 Conclusion

In this paper, we presented a method for binary classification of images to intact and cracked surfaces based on three decision criteria. The results on the reference dataset used show an appropriate classification accuracy. The presented methodology thus forms a baseline approach to serve a basis for further research.

The proposed method could be extended for image segmentation by adapting a sliding-window approach, as presented by Sesselmann [3]. This in turn could be used to measure the crack width.

References

[1] J. Lange and W. Benning, „Verfahren zur Rissanalyse bei Betonbauteilen“, DGZfP-Berichtsband 100-CD, 2006.

[2] A. Mohan und S. Poobal, „Crack detection using image processing: A critical review and analysis“, Alexandria Engineering Journal, Jg. 57, Nr. 2, S. 787–798, 2018, doi: 10.1016/j.aej.2017.01.020.

[3] M. Sesselmann und Stricker, R., Eisenbach, M., „Einsatz von Deep Learning zur automatischen Detektion und Klassifikation von Fahrbahnschäden aus mobilen LiDAR-Daten/ Deep Learning for Automatic Detection and Classification of Road Damage from Mobile LiDAR Data“, AGIT Journal, Nr. 5, S. 100–115, 2019.

[4] N. Gehri, J. Mata-Falcón und W. Kaufmann, „Automated crack detection and measurement based on digital image correlation“, Construction and Building Materials, Jg. 256, S. 119383, 2020, doi: 10.1016/j.conbuildmat.2020.119383.

[5] S. Y. Alam, A. Loukili, F. Grondin und E. Rozière, „Use of the digital image correlation and acoustic emission technique to study the effect of structural size on cracking of reinforced concrete“, Engineering Fracture Mechanics, Jg. 143, S. 17–31, 2015, doi: 10.1016/j.engfracmech.2015.06.038.

[6] H. S. Munawar, A. W. A. Hammad, A. Haddad, C. A. P. Soares und S. T. Waller, „Image-Based Crack Detection Methods: A Review“, Infrastructures, Jg. 6, Nr. 8, S. 115, 2021, doi: 10.3390/infrastructures6080115.

[7] Ç. F. Özgenel und A. G. Sorguç, „Performance Comparison of Pretrained Convolutional Neural Net-works on Crack Detection in Buildings“ in 34th International Symposium on Automation and Robotics in Construction, Taipei, Taiwan, 2018, doi: 10.22260/ISARC2018/0094.

Enabling object-based documentation of existing bridge inspection data using Linked Data

Anne Göbels[1]
[1]Chair of Design Computation, RWTH Aachen University, Schinkelstraße 1,52062 Aachen, Deutschland
E-mail(s): goebels@dc.rwth-aachen.de

Abstract: Digital Twins (DTs) of existing bridges can provide a reliable data basis for predictive maintenance needed to ensure an operational infrastructure as the number of bridges in critical condition increases. An essential data source for a DT is the existing construction and inspection documentation stored in Germany in the relational database system *SIB-Bauwerke*. However, SIB-Bauwerke does not support object-specific documentation of inspection data, making it challenging to retrieve the condition of individual components and to link the data appropriately with other data sources of the DT. To address these issues, we present an automatic transmission of the existing SIB-Bauwerke data into an object-oriented structure, allowing detailed recording and analysis of inspection data and precise linking to external data objects. Based on a previously developed conversion of the inspection data into Linked Data graphs, we enhance the converted data by introducing direct links between components and damages and defining damaged areas. The newly implemented structure allows sophisticated and detailed statements about the condition of individual components or areas and can be easily linked at the object level with other resources of the DT.

Keywords: Infrastructure Maintenance, Digital Twin, Linked Data, SIB-Bauwerke, ASB-ING

1 Introduction

Bridge maintenance is currently performed reactively based on detected deficiencies during a manual inspection. However, as the number of bridges in critical condition increases, a predictive maintenance strategy is needed that ensures a sustainable working infrastructure through reliable predictions and preventive measures.

A prerequisite for predictive maintenance is a comprehensive and reliable data basis on which analyses can be performed. In this context, the TwinGen research project investigates how Digital Twins (DTs) of existing bridges can be generated using automated methods. The DT (in the project's scope) is a semantic-geometric model that represents a precise digital replica of a bridge. It is based on a geometry model linked on the object-level with complementary, external data sources, including point

clouds data, damage pictures, construction plans, and inspection reports. Linked Data methods are used to achieve expressive and accurate links between these heterogeneous and distributed data sources.

Existing bridge documentation and inspection data are essential data sources to represent a bridge's entire lifespan as they provide information on the construction, previous maintenance, and the current condition. In Germany, this data is documented in *SIB-Bauwerke*, a documentation program that works with a relational database, whose structure is defined in the national data model *ASB-ING* [1]. This database is not object-oriented and only allocates damage information to the individual components via textual descriptions. Thus, it is challenging to assess individual components' conditions and to link the inspection information of SIB-Bauwerke appropriately to external data, such as IFC model elements.

To address these issues, we developed an automated transmission of the existing SIB-Bauwerke data into an object-oriented documentation structure, allowing precise linking and analyzing of the data. In prior work, we converted the inspection data into a Resource Description Format (RDF) graph [2] using the previously developed ASB-ING Ontology [3] . However, the graph still contains the same information and detail depth as the original data. In the work presented in this paper, we use Linked Data functionalities, such as SPARQL queries and the inclusion of external ontologies, to transform the implicit information about damage to components into explicit objects and links. We improve damage documentation by introducing precise linking between damages and individual components and defining damaged areas. At the same time, the original, mandatory data structure of the ASB-ING is maintained to ensure backward compatibility.

2 Related research activities

Representing and processing building and maintenance data using Linked Data technologies is subject to several research and development efforts. The ifcOWL Ontology [4] is the RDF-compatible version of the IFC schema, thus enabling the representation of IFC models in Linked Data. Bridge structures can be represented in Linked Data using the Bridge Ontology (BROT) [5]. It enables to describe bridge zones and components, including their topological relations. It is a generic, modular ontology that allows for domain-specific extension, e.g., building materials or component details.

The Damage Topology Ontology (DOT) [6] of Hamdan and Scherer provides classes and properties to document and classify damage elements or patterns and assign them to building elements. To highlight the specific damaged area of an element, they developed the Area of Interest (AOI) Ontology [7]. The AOI Ontology contains classes that subdivide an element into defined areas (e.g., bottom, top, horizontal/vertical center, peripheral areas, or external/internal area). The classes and properties of the AOI Ontology can be used in addition to other ontologies, such as the DOT Ontology, to provide a more detailed location of the damage.

An approach by Liu et al. presented in [8] also addresses the interlinking of BIM models and SIB-Bauwerke data using Linked Data. They store newly acquired element condition grades linked to

model elements in an Information container for linked document delivery (ICDD) [9]. The BOT Ontology is used to represent the model elements, and the ASB-ING Condition Ontology [2] to store the condition grades compatible to SIB-Bauwerke in Linked Data. With a custom mapping ontology, the data of the ICDD gets transferred into the database tables of SIB-Bauwerke, by automatically generated SQL commands. However, their approach deals with newly acquired data and only covers a small part of the entire SIB-Bauwerke data. Nevertheless, the derivation of SQL commands from Linked Data graphs can support the backward compatibility of our approach.

Since the presented approaches and ontologies mainly focus on processing and storing new acquired (inspection) data, the applicability of existing data to the proposed methods is not addressed. However, we present in this paper how existing data can also benefit from these developments.

3 Background and previous work steps

The *Anweisung Straßeninformationsbank – Teilsystem Bauwerksdaten* (ASB-ING) (engl.:Instruction road database - subsystem structural data) [1] is the national data model for infrastructure documentation. It specifies how information on the structure and inspection must be recorded, including condition assessments, damages, and maintenance measures. To ensure uniform documentation, the ASB-ING provides predefined values stored in extensive key-value tables containing, e.g., possible component-, damage-, or material specifications.

The ASB-ING is implemented in the *Straßeninformationsbank- Bauwerke* (SIB-Bauwerke) (engl.:Road information database - structures), a relational database application that stores the inspection results and structural data of a bridge since its construction. According to the ASB-ING structure, the bridge documentation is separated into tables, covering different subjects. The structural data is divided into component groups (e.g., superstructure, substructure, bearings, coverings, etc). These groups are used for damage assignments, by which a condition grade is calculated for each component group following a defined algorithm [10]. These grades lead to the overall bridge condition assessment. Textual descriptions assign damages to individual components, but these are only intended to retrieve the damage on site.

The management of data that gets updated at each inspection (damages, measures, inspection report) is handled by using two tables for each topic. One table contains the current data of the latest inspection, and another table archives all previous information. For example, a damage existing for five years has been documented at each inspection and is finally stored once in the current data table and four times in the previous data table. These damage versions are indirectly linked by having the same Damage-ID.

The current published version of the ASB-ING is from 2013, but recently, there has been ongoing development of a new version to update the data structure and content, provided as a UML model. It

[2] https://roadotl.eu/static/eurotl-ontologies/testontologies/Germany/asb-ing-condition_doc/index-en.html

defines the content of the ASB-ING using 120 classes, 80 datatype definitions, and 500 properties. By converting this new ASB-ING UML model, we created the *ASB-ING Ontology* [3] [3].

The ASB-ING Ontology is the basis for converting the inspection data sets of SIB-Bauwerke into RDF, as it provides the required ontological framework to represent the data. Combined with mapping tables between the ASB-ING 2013 and the new version (provided by the official migration project), we enabled an automatic conversion process of the SIB-Bauwerke datasets into RDF graphs [2].

After converting the data, the graph of each bridge data set reflects the same information structure and quality as the original data. It records individual construction components and detailed damage documentation, but these are not linked, thus preventing an object-based organization of inspection data. In addition, the method of updating damage data leads to data repetition and makes it challenging to track damage conditions.

4 Methodological approach

A review of the current damage documentation of SIB-Bauwerke identifies its weaknesses. Each damage object contains information about the affected component group, element type, and the location of the element and/or damaged area. In addition, it provides information about the damage type and size, the damage ID, and the impact of the damage on the stability, traffic safety, and durability of the bridge.

This method of damage documentation merges many different types of information into one data object. These data types can be broadly categorized into static and dynamic/variable data. The static data, such as the description of the affected component and the damage ID, stays the same over time, while the variable data can change at each inspection. The combination of these data types in one object leads to repetition, ineffective data processing, and complicates the proper handling of the data concerning an object-based organization.

Thus, we split the static data into separate elements, each containing only one type of information. The separation allows independent and flexible processing of the different information.The new elements were defined using additionally developed classes of the ASB-ING Ontology (prefix: asb) or existing classes of the DOT and AOI Ontology. Thus, they also express a more specific semantic meaning.

Figure 1 shows a (simplified) example of an original damage object of our sample data set from SIB-Bauwerke after the conversion into RDF. The figure indicates how the damage information is separated and stored as new objects. We introduce a new class (*asb:SchadenObjekt*) for creating a parent damage object that serves as a container for the individual damage versions (the original damage objects). This parent damage object takes the damage ID of the original damage and is used as a reference for linking the damage to the component. Thus, only one link between the component and the damage object must be created instead of duplicated links for each damage version.

[3] https://w3id.org/asbingowl/core

```
@prefix asb: <https://w3id.org/asbingowl/core#> .
@prefix asbkey: <https://w3id.org/asbingowl/keys#> .
@prefix asbkey13: <https://w3id.org/asbingowl/keys/2013#> .

:NY0LZ32M_Schaden a                                  asb:Schaden ;
  asb:ASBING13_Bauteil (Component)                   asbkey13:130011911000000_Wand ; (Wall)
  asb:ASBING13_Bauteilergaenzung (Supplement)        asbkey13:130031100000000_Beton ; (Concrete)   (sub structure)
  asb:ASBING13_Bauteilgruppe (Component group)       asbkey13:390021200000000_BauteilgruppeUnterbau ;
  asb:ASBObjekt_Systemdatum                          "2020-05-07"^^xsd:date ;
  asb:PruefungUeberwachung_Pruefjahr (Year)          2019 ;
  asb:ObjektMitID_hatObjektID                        [ asb:ObjektID_ID "NY0LZ32M" ];
  asb:ASBObjekt_Textfeld (free text field)           "Tropftülle wasserführend." ; (drip spout water leading)
  asb:Schaden_AllgemeineMengenangabe (size)          asbkey:kleineSchadensausbreitung_eineStelle ; (small)
  asb:Schaden_Schaden (type)                         asbkey:Wasserschaden_feuchteStelle ; (water damage)
  asb:Schaden_Foto (picture)                         "SCHADEN 21.JPG" ;
  asb:Schaden_ID-Nummer-Schaden (damage ID)          21 ;
  asb:Schaden_Ortsangabe (location specifications)
    [ asb:Ortsangabe_Ortsangabe                      asbkey:Widerlager_WiderlagerVorn ] , (front abutment)
    [ asb:Ortsangabe_Ortsangabe                      asbkey13:130115000000000_Unten ], (bottom)
    [ asb:Ortsangabe_Ortsangabe                      asbkey13:130101100000000_Links ] ; (left side)
  asb:Schaden_Schadensbeispiel (damage example)      asbkey13:021-06_Schadensbeispiel ;
  asb:Schaden_BewertungDauerhaftigkeit               2 ; (durability grade)
  asb:Schaden_BewertungStandsicherheit               0 ; (stability grade)
  asb:Schaden_BewertungVerkehrssicherheit            0 ; (traffic saftey grade)
  asb:associatedWith                                 :7936662_0_Teilbauwerk .
```

Related Element Description → asb:BauteilDefiniton (component definiton)

Metadata

Damage type and size

Name of related picture

Overall Damage-ID → asb:SchadenObjekt (overall damage object)

Location of component → asb:BauteilDefiniton (component definiton)

Location of damage → aoi:AreaOfInterest

Impact on bridge condition

Teilbauwerk Assignment → asb:SchadenObjekt (overall damage object)

Figure 1: Example of an SIB-Bauwerke damage object after conversion into RDF and its separation

The properties that describe the component and its location are summarized with the new class *asb:BauteilDefinition* (Component definition). The location of the damage on the component is defined as an *aoi:AreaOfInterest*, according to the AOI Ontology of Hamdan and Scherer [7].The variable data stays in the original data objects (damage version) that remain unchanged to maintain compatibility with the original SIB-Bauwerke structure.

The interlinking of the new implemented elements using self-defined, and existing properties of the AOI and DOT Ontology, can be seen in figure 2. The damage versions are connected to the new parent object that is linked to the component definition and the area of interest. We retrieve the individual component in another process based on the component definition (see section 4.1). The component is then linked to the parent damage object or the area of interest. Thus, we achieved detailed and precise object-oriented documentation allowing direct and unambiguous assignment of damages to individual components.

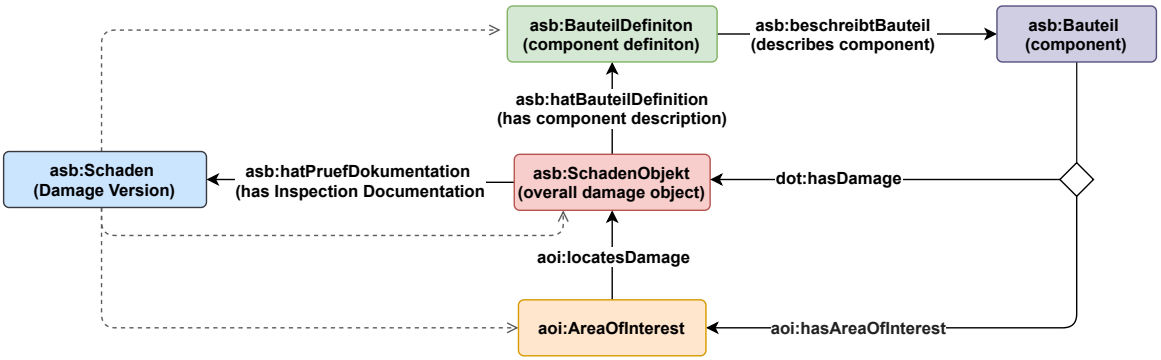

Figure 2: Proposed object-oriented structure for damage documentation

4.1 Implementation process

The implementation was tested on a dataset of SIB-Bauwerke containing the construction documentation and the inspection reports of a multi-span girder bridge from 2002 with 40 damages.The current code of the implementation process can be found at GitHub [4].

The starting point for implementing the proposed structure is the creation of the parent damage objects by querying the graph for all distinct damage IDs. Next, a component definition (*asb:BauteilDefinition*) is developed for each parent damage object, reusing the original damage version's component group and type specification (see rows 4 and 2, figure 1).

Adding the individual location to the component definition needs an intermediate step. The original structure does not distinguish between component locations and damage areas. Both are values of the property *asb:Schaden-Ortsangabe* (location specification) (see rows 13-16, figure 1). The meaning of location terms also depends on the component type, e.g., "left" can describe the left area of an abutment wall, but also the whole left cap. Thus, we developed a table that defines the meaning per location term and component type. Based on this table, the location information is either added to the component definition or used to create a damage area (area of interest).

Next, each parent damage object is related to a component definition via *asb:hatBauteilDefinition* and optionally to an area of interest via *aoi:locatesDamage* (see Figure 2).

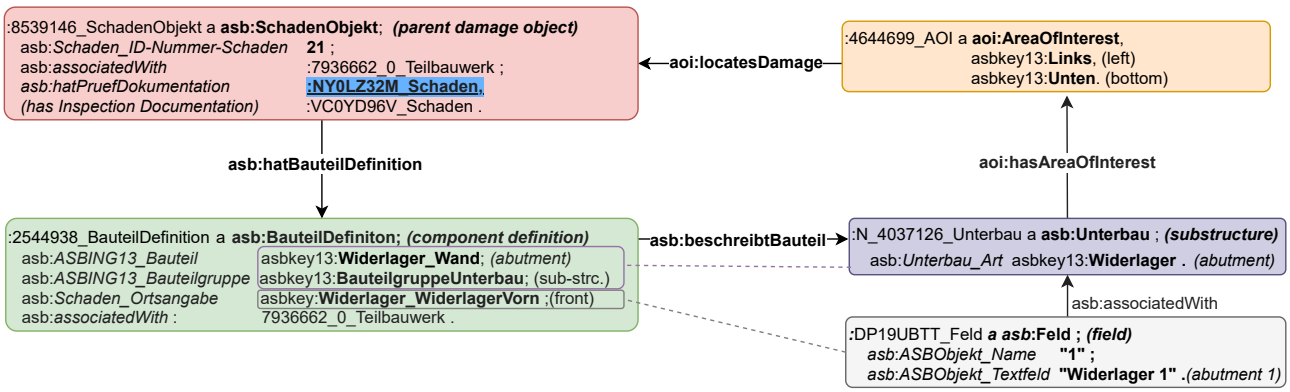

Figure 3: Implementation of the object-oriented structure for an example damage

The retrieval of the individual components based on the component definitions is done by comparing specific properties of both objects using SPARQL queries. Figure 3 shows the implemented structure for the damage object introduced in figure 1. In this example, the component definition is related to the front abutment because its component group and type (group: substructure, type: abutment wall) corresponds to the individual component's class and type (class: substructure, type: abutment). The location of "Front Abutment" of the component definition matches the values "1. Field" resp. "Abutment 1" of the field object associated with the abutment component. The relation between both objects is stored using *asb:beschreibtBauteil* (describes component).

[4] https://github.com/AnneGoebels/SIB-Bauwerke-To-Linked-Data

Thus, broadly defined, the value of the component group property matches the components' class, but all further details depend on the component type, which leads to individual handling in the script for each type. In the sample data set, this method was able to find most of the described components, except for smaller equipment, such as pipes and drains. Finally, the retrieved individual components are linked to the corresponding parent damage objects using *dot:hasDamage*, or to the area of interest, using *aoi:hasAreaOfInterest*. After this process is completed, the component definitions do not appear to be needed, but they can be used as a substitute for components that could not be found or are not present as individual components in the SIB-BW data set.

5 Conclusion

We achieved an automatic transformation of the existing inspection data from SIB-Bauwerke into an object-oriented structure. This structure enables precise linking with other object-based data models such as IFC models, allowing efficient use of existing inspection data in digital twins. Moreover, it is now possible to query for damages to individual components and most damaged areas of components or a bridge. If many SIB-Bauwerke data sets were converted using this process, an extensive knowledge database could be created to provide information about which component (area) is most affected by which type of damage and how they progress. The object-oriented structure also enables a detailed condition assessment of the bridge. Currently, an algorithm [10] is used in which the worst grade of a damage determines the grade of the component group. The worst component group determines the grade of the entire bridge. Applying this algorithm to individual components (i.e., the damage determines only the grade of the affected component) can lead to more precise, tailored, and efficient maintenance measures.

However, the process still needs to be tested on more data sets. Especially the assignment of component definitions to the components is currently highly adapted to one sample data set that describes a simple bridge construction with comparatively few damages. The extent to which this procedure can be generalized to more complex data sets needs to be investigated. In ongoing work, we are using the presented developments to enable an automatic linking of the components of SIB-Bauwerke to elements of the IFC model. Based on that, we create a prototypical viewer that can visualize the geometry model and the linked inspection data, including spatial representations of the damages. It will be able to perform space-, time-, and object-based queries to get new insights into the data.

Acknowledgements

We thank the German Federal Ministry for Digital and Transport (BMDV) for their support in funding the TwinGen research project and the Autobahn GmbH des Bundes - Niederlassung Südbayern for providing us the SIB-Bauwerke data set.

References

[1] Bundesministerium für Verkehr, Bau und Stadtentwicklung, Abteilung Straßenbau., *ASB-ING 2013 Anweisung Straßeninformationsbank Segment Bauwerksdaten*. 2013.

[2] A. Göbels, “Conversion of infrastructure inspection data into Linked Data models”, in *32. Forum Bauinformatik 2021*, Darmstadt, 2021.

[3] A. Göbels and J. Beetz, “Conversion of legacy domain models into ontologies for infrastructure maintenance”, in *Proceedings of the 9th Linked Data in Architecture and Construction Workshop - LDAC 2021*, vol. 3081, Luxembourg: CEUR-WS, 2021, p. 12.

[4] J. Beetz, J. van Leeuwen, and B. de Vries, “IfcOWL: A case of transforming EXPRESS schemas into ontologies”, en, *Artificial Intelligence for Engineering Design, Analysis and Manufacturing*, vol. 23, no. 1, pp. 89–101, Feb. 2009.

[5] A.-H. Hamdan and R. J. Scherer, “Integration of BIM-related bridge information in an ontological knowledgebase”, in *Proceedings of the 8th Linked Data in Architecture and Construction Workshop - (LDAC)*, CEUR-WS, 2020, pp. 77–90.

[6] A.-H. Hamdan, M. Bonduel, and R. J. Scherer, “An ontological model for the representation of damage to constructions”, in *Proceedings of the 7th Linked Data in Architecture and Construction Workshop - (LDAC)*, Lisbon: CEUR-WS, 2019, pp. 64–77.

[7] H. Al-Hakam and R. J. Scherer, “Areas of Interest - Semantic description of component locations for damage assessment”, en, in *EG-ICE 2020 Proceedings: Workshop on Intelligent Computing in Engineering*, Berlin, Jul. 2020.

[8] L. Liu, P. Hagedorn, and M. König, “BIM-Based Organization of Inspection Data Using Semantic Web Technology for Infrastructure Asset Management”, in *Proceedings of the 1st Conference of the European Association on Quality Control of Bridges and Structures*, C. Pellegrino, F. Faleschini, M. A. Zanini, J. C. Matos, J. R. Casas, and A. Strauss, editors, vol. 200, Cham: Springer International Publishing, 2022, pp. 1117–1126.

[9] “ISO 21597-1:2020 Information container for linked document delivery - Exchange specification - Part 1: Container”, International Organization for Standardization, Geneva, Standard, 2020.

[10] P. Haardt, *Algorithmen der Zustandsbewertung von Ingenieurbauwerken*. Bergisch Gladbach, 1999.

Teil V

Data Management

Research data management of large scale projects and a reference model of data life cycle for dynamic DMPs

Syed Ashfaq Hussain Shah

Chair of Architectural Informatics, Technical University of Munich, Arcisstraße 21, 80333 Munich, Germany

E-Mails: syed.hussain@tum.de

Abstract: Good research data management (RDM) is an integral part of high quality modern research activities. It is not only crucial for the ongoing research and its claims but also for the future uses of the same data and its understanding by the other users. RDM also helps to achieve transparency, repeatability, and reusability goals. FAIR is one of the set of principles to instruct good data management. Different systems and services are being developed and proposed to comply with such principles. The data and its metadata are often handled in file system like structures. The information relating to the data handling are documented in data management plan (DMP). DMPs are made available in editable document formats as well as online free-text editable forms which users are required to keep updating manually. DMP is also usually managed in the similar file structures and it has no common understanding and consistency. It also lacks machine readability. In this paper the case of research data management of large scale interdisciplinary projects of architecture and civil engineering is being presented. This paper also presents a reference model of data lifecycle for dynamic data management plans. The presented approach enables modularisation of DMPs as well as mapping between the data and the corresponding DMP to assist users.

Keywords: RDM, dDMP (dynamic Data management plan), Data life cycle, VRE.

1 Introduction

Increasing dependence of science on digital means and data driven proves of hypothesis are raising the bar of RDM practices. Consequently, researchers are required for example by funding agencies like German Research Foundation to conduct good RDM practices while adopting appropriate RDM systems [1].

RDM refers to the activities relating to the storage, organisation, documentation and dissemination of research data. These are continuous activities which are needed to be performed during the duration of the research project [2]. However, in order to comply with modern scientific practices these activities should adhere to the requirements of stake holders e.g., subject-specific standards, advices of funding agencies, or generally to the FAIR Data Principles. Since the 'good data management' is largely undefined, FAIR Principles provide guidelines about four foundational principles i.e., Findability, Accessibility, Interoperability, and Reusability of data and the information that lead to that data to guide data producers and publishers [3]. The information relating to the data management are documented in data management plan (DMP). A **DMP** consists of questions relating to the data and its handling and dissemination. DMPs are considered as key elements of good data management [4]. The process of DMP authorship starts with the explanations that how the data will be managed during the proposed research work. However, once the research starts DMP turns into a document that needs to be updated by documenting the ongoing practices [5]. But, there are no clear guidelines which could describe what and when it should be updated e.g., "Revisit your plan frequently and update it if necessary" [6]. During a research process data goes through different phases. Each phase consists of processes carried out by different users over data. This journey of data is usually modelled as data life cycle [7]. A **data lifecycle model** offers a graphical high-level overview of the stages and processes. Different systems, services and models are being developed and proposed to facilitate researchers to accomplish these challenging goals of RDM.

This paper presents the case of RDM of Collaborative Research Centre Transregio 277 Additive Manufacturing in Construction (AMC). AMC was started in the beginning of 2020. It is a trans-regional centre hosted by TU Munich and TU Braunschweig, while the scientists and labs are situated at different locations. The research of AMC is grouped in three focus areas i.e., Area A: Materials and Processes, Area B: Computational Modelling and Control, and Area C: Design and Construction [8].

2 Requirements elicitation for a university hosted platform

It was required to foster internal and external research collaborations that documents and data together with related information must be managed in a controlled and organised manner across several subprojects and research institutions. Apart from file like data handling and related metadata, the selected platform should offer further custom development on demand, scalable storage

capacity, scheduled data backup and archiving, archiving of data for long terms i.e., at least for 10 years, customisable access rights, institution independent ID management, standard protocol support for data synchronisation and additional features of project management e.g., project pages, appointment and calendar management. Based on the requirements, TUM Workbench was selected as Virtual Research Environment (VRE). Next section summarises already offered and further developed features for organising research data of AMC.

3 TUM Workbench

TUM Workbench offers data management coupled with research project/subproject management and communication tools with customisable access rights. Other than file and folder like structure handling, notable project management tools in TUM Workbench are calendar, note/lab book, task and task management, commenting and notifications. These tools are termed as elements. All elements could be divided into two categories based on their composition i.e., simple element and composite element. Simple element does not contain or depend upon other elements for its representation e.g., File. Whereas, composite element is an element which could contain other elements and act as a container for those elements e.g., Folder. As such, it requires other elements to complete its body of information.

TUM Workbench offers namespace concept where users and projects are the main spaces. Elements can be assumed based on flat architecture i.e. elements not only can be created in their containing spaces but also in user space. Access and rights management can be realised by inviting and assigning a role to the participating users in a project. Roles are inherited to the subprojects and translated to the default access rights for containing elements. Rights can also be customised for elements on individual basis as illustrated in figure 1. Information and data can be registered by means of online forms and files. Apart from basic operations over data i.e., create, read, update and relocate, TUM Workbench also offers link/ unlink operation to create a simple association between elements e.g., to associate data and corresponding DMP, to signify the origin of the file. Custom DMP templates can also be created. Then a DMP from a template can be created and manage as online free-text editable form. All the elements are assigned unique ID and are versioned. Thus contain change logs. Apart from DataCite support as basic metadata, further metadata fields can also be described. For user interaction it offers graphical user interface. It also supports WebDAV and CalDAV protocols for synchronisation with compliant systems. REST API is offered for machine-based communication and its functionality can be extended by taking advantage of plug-in support.

TUM Workbench is being developed and maintained by the TUM Library. It is also available as an open source software [9]. Its technological backend including data backup and archive services are being supported by the Leibniz-Supercomputing Centre (LRZ).

4 The case of research data management of AMC

To ensure best practices, a policy of RDM for AMC was designed. The structure for the organisation of data was defined in TUM Workbench as per their proposals. A profiling system was developed to create profiles of exiting data. Storage systems for each project were allocated and verified based on the profiles. Then the users and data migration process was initiated.

Research data management policy: In order to govern and align with highest standards of research and RDM practices a policy was drafted. In this policy the definition of research data and related information, platform and information infrastructure, categories of roles and responsibilities of the participants, types of research outcomes and publications, file formats to communicate research outcomes, naming and versioning conventions, and initial metadata standard were defined. The policy was made applicable for all the participants of AMC.

Elements for data organisation and documentation: Based on the analysis of the proposed tasks and anticipated work of the researchers, selection of the elements of TUM Workbench was initially made to avoid complexity of the work for RDM related tasks. Therefore, Project, Storage, File, Appointment, Calendar and DMP were determined as mandatory elements. Whereas, researchers were free to take advantage of rest of the elements available in TUM Workbench.

Metadata and context management: To maintain context and related information of data which might be created in response of a task, work package or even project, all the main projects were defined as work packages of the parent project by taking advantage of hierarchical association offerings of TUM Workbench. At the level 1 parent project was representing the whole AMC. All the projects of AMC were defined at the level 2 where they share the same level of hierarchy. Each project further has multilevel work packages defined in the hierarchy from level 3 onward as shown in figure 1. Additionally, each project and work package might also have associated elements e.g. storages, files and DMP.

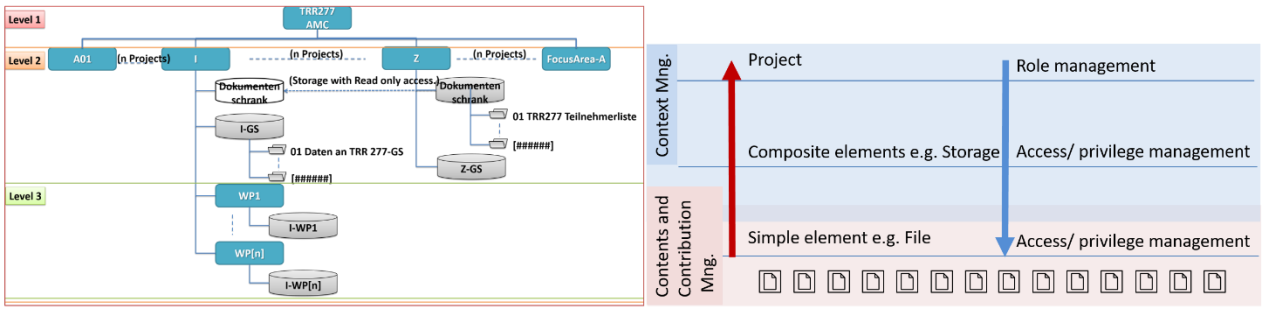

Figure 1: Organisation of projects and data (left), Context and role/ access management (right).

File-like data organisation: Storages in TUM Workbench are soft representations of partitions of a drive to represent independent organisations of their containing data. It was defined that one Storage will represent data of one research activity. Based on the analysis of the data that might be

generated, used and published by the researchers the data was categorised by defining four main folder structures i.e., code, data, publications and resources. **code** for any kind of piece of software/ executable script. **data** for all the static data e.g., datasets, images, audio/visual record. These are non-executable scripts and contents. **publications** for paper, presentation, report, template, form etc., which will be made public within or outside of AMC. Lastly, **resources** for any code, data or publication which is not actually the work of the current research activity but the current research activity needs that to get the work done. The contents of this main folder were also suggested to be organised under subfolders code, data and publications.

Naming and versioning convention: The patterns of naming elements were defined to make them identify by human and machine readable. They were defined for naming project, work package, storage, file, DMP as well as code and variable in the files. Use of blank spaces and diacritic letters/ special language characters were made prohibited. The use of special strings e.g. workspace, draft, release, were suggested to differentiate between copies of same element for different purposes. Semantic versioning scheme [10] was adopted to signify the state of data when it evolves.

5 Reference model of data lifecycle for dynamic data management plans (dDMP)

DMP is created to document information about the handling of data when it goes through different processes. A life cycle reference model was deemed necessary to reflect information that need to be filled in DMP as well as the information that data should accompany to fulfil the requirements of DMP. This approach of representation helps users/ researchers to easily identify the stages, corresponding actions and information. In this research work a dDMP is defined as a plan which can adopt or suggest user based on the information available on the associated data part, and vice versa.

5.1 Related work

A moderate search and analysis of existing life cycle models for RDM revealed that existing models are using either single layered approach or concentrated more towards data archiving and long term curation activities or are based on institutional solutions e.g., [11, 12]. To present users, actions and processes of an ongoing data intensive research in a collaborative environment like VRE, there was a need of a data lifecycle which could prescribe information based on the actions and user domains from a DMP perspective. So that an actionable procedure could be advised to the DMP users.

5.2 Methodology

Based on the problem definition first the nature of expected data, user domains, actions which a user can perform and the properties that need to be associated with data in terms of metadata were identified. Existing DMP templates e.g., for H2020 projects, CLARIN-D, were analysed. Then the workflows that can be adopted for the transitions of data in TUM Workbench were determined. The whole process was aligned with the guidelines of DFG, AMC and hosting institutions. As a result, a custom DMP template and associated data lifecycle was defined. Since the provision of metadata and information in DMP is an incremental process, the need of recording such an information arises depending on the change of information which might occur on either plan or data part. Therefore, the questions of DMP were arranged and grouped in a way that they could be modularised when it comes to automation of the processes. A multi-layered approach was adopted to draw the life cycle.

5.3 Reference model of data lifecycle

Suggested reference model consists of user domains, processes or actions, and the complied information for DMP as well as for the corresponding data. In real-time this representation assumes two-way communication between DMP and the corresponding data or the glossary. The flow of data based on actions and between user domains is represented with arrow signs. The requirements of data features/ properties before and after a transition are sumarised in dialog signs. The components of the lifecycle are being further explained in the following sections.

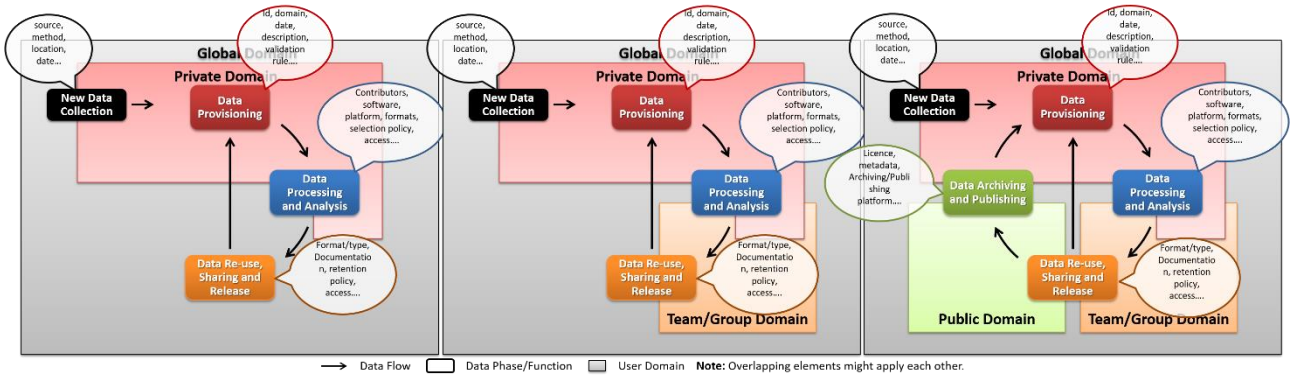

Figure 2: Data life cycle reference model complete (right), team based (center), Individual (left).

5.4 Definition of User domains

The user domains are classified in following four core domains where two or more domains can also coincide and form new domain, e.g., Private and Team domains can form a Private Team domain.

Global Domain: It is the parent domain of all the known and unknown domains. It includes any external system or source from where data can be received or collected. A classic example could be the real world from where user collects new data by means of interviews etc.

Private Domain: A domain which is restricted and only privileged user can access. An example could be a local system or a storage space in cloud accessable only with user access credentials.

Team/ Group Domain: It represents a domain which is accessible by more than one users in a controlled way. But limited to the known number of users. Example could be a shared system or storage space in the cloud, publishing platforms. Access to this space may vary depending on role.

Public Domain: It represents a domain which is available to the public as a whole. The access is not restricted. A classic example could be open data and publishing platforms.

5.5 Explanation of actions/ states

During a research, depending upon the role, user performs different tasks and activities relating to the data. In order to accomplish a task, user performs different series of actions. Each action usually has some pre and post requisites. Actions are being explained in the following section. The information/ metadata relating to each action is depicted in figure 2.

New Data Collection: The action of collecting data to make it available for the current task for the first time. The new data could be the data which is newly collected e.g., by interview in the Global Domain, or it could be an extracted/ selected data from an existing dataset from the Private Domain.

Data Provisioning: The action of making data available for the task. At this state provenance/ basic information of the data is known and data is considered valid for the research activity.

Data Processing and Analysis: This represents the actions when the data is further processed and analysed. From this state most of the information are required to be provided by the user.

Data Reuse, Sharing and Release: These set of actions focus on the release of data, e.g., after a milestone was achieved by individual/ team, and the data is ready for next iteration of tasks by the same team, for other teams or even for future projects i.e., for a different context etc.

Data Archiving and Publishing: These actions relate to long term preservation/ publication of the work. These are usually carried out at the end of the set of series of the tasks, research project or when a publication is made e.g. for the general public, publishing authorities, research groups, etc.

6 Conclusion and future work

In this paper the case of research data management of AMC using TUM Workbench is presented. The first part presents that how project hierarchal and element association models can be used for RDM activities. The second part presents the life cycle model of the data for a dynamic DMP. It is assumed that this approach can be adopted for the data which is managed in VRE like environments. The design of the model and custom template of DMP for AMC was the first step towards the realisation of a dynamic DMP. In future, apart from AMC specific use cases, recently developed application profile by the DMP Common Standards working group of RDA could also be consulted for the standardisation process and the evaluation of the adopted aproaches will be carriedout. This paper describes only the adopted features of TUM Workbench for AMC. Therefore, it cannot be considered as a detailed paper about TUM Workbench for RDM activities. TUM Workbench is also going through a continuous development and improvement process.

Acknowledgement

The work presented in this paper is being conducted as part of the collaborative research centre ‘Additive Manufacturing in Construction - The Challenge of Large Scale,’ funded by the German Research Foundation (DFG), within the I - Information Infrastructure Project. The project is supervised by Prof. Dr.-Ing. Frank Petzold (AI, TUM) and Prof. Dr.-Ing. André Borrmann (CMS, TUM). The work preseented in this paper has also been made possible with the cooperation of Mr. Robert Strötgen from the library of TU Braunschweig and Mr. Manuel Hora from the library of TUM.

References

[1] DFG. "Handling of research data." DFG. https://www.dfg.de/download/pdf/foerderung/grundlagen_dfg_foerderung/forschungsdaten/forschungsdaten_checkliste_en.pdf (accessed 27.05.22.)

[2] J. A. Borghi, S. Abrams, D. Lowenberg, S. Simms, and J. Chodacki, "Support Your Data: A Research Data Management Guide for Researchers," *Research Ideas and Outcomes,* vol. 4, 2018.

[3] M. D. Wilkinson *et al.*, "The FAIR Guiding Principles for scientific data management and stewardship," *Scientific Data,* vol. 3, no. 1, p. 160018, 2016/03/15 2016.

[4] E C. "Data management." European Commission. https://ec.europa.eu/research/participants/docs/h2020-funding-guide/cross-cutting-issues/open-access-data-management/data-management_en.htm (accessed 27.05.22.)

[5] T. Miksa, S. Simms, D. Mietchen, and S. Jones, "Ten principles for machine-actionable data management plans," *PLOS Computational Biology,* vol. 15, no. 3, p. e1006750, 2019.

[6] nature. "Data management made simple." nature. https://www.nature.com/articles/d41586-018-03071-1 (accessed 27.05.22.)

[7] T. Weber and D. Kranzlmüller, "Methods to Evaluate Lifecycle Models for Research Data Management," *Bibliothek Forschung und Praxis,* vol. 43, no. 1, pp. 75-81, 2019.

[8] AMC. "Additive Manufacturing in Construction TRR277." https://amc-trr277.de/ (accessed 27.05.22.)

[9] UB TUM. "eWorkbench." https://github.com/eworkbench/ (accessed 27.05.22.)

[10] T. Preston-Werner. "Semantic Versioning Specification." https://semver.org/ (accessed 27.05.22.)

[11] S. Higgins, "The dcc curation lifecycle model," presented at the Proceedings of the 8th ACM/IEEE-CS joint conference on Digital libraries, Pittsburgh PA, PA, USA, 2008.

[12] DataONE. "Data Life Cycle." https://old.dataone.org/data-life-cycle (accessed 27.05.22.)

Integration of BIM and Industry 4.0 - approach for rapid deployment of digital twins for modular construction

Jan Hendrik Heinbach[1], Bennet Hülsmann[1] and Simon Kosse[1]
[1]Chair of Computing in Engineering, Ruhr University Bochum, Universitätsstraße 150, 44801 Bochum, Germany
E-mail(s): jan.heinbach@ruhr-uni-bochum.de, bennet.huelsmann@ruhr-uni-bochum.de, simon.kosse@ruhr-uni-bochum.de

Abstract: The automation of production processes has made enormous progress in recent years through modern communication and information technologies. Through continuous intelligent networking of components, machines, and processes in Industry 4.0 (I4.0), the production of precast concrete elements can be carried out more efficiently in terms of both time and costs. The digital twin, as a central information container, is a fundamental concept in I4.0 that collects and provides relevant data and information across all lifecycle phases of a component. As an established tool for the planning and design phase, Building Information Modeling (BIM) focuses on designing and describing buildings and infrastructure. However, BIM models are not suitable for communication and interaction in cyber-physical systems and real-time data integration. The aim, therefore, must be to combine current BIM concepts with methods from I4.0, which enable self-organized and decentralized production. For this, suitable interfaces must be developed that ensure a continuous flow of information across all lifecycle phases. This paper presents an approach for digital twins' rapid and automated creation based on implementing the asset administration shell, a digital twin framework known from I4.0. In the presented approach, an administration shell template of a component, which already contains the necessary semantic data structures, is instantiated with a corresponding BIM model's design and construction data. The concept is demonstrated and validated using a virtual precast concrete column as an example. The proposed approach thus combines BIM with I4.0 methods and ensures a continuous flow of information between planning and production.

Keywords: Digital Twin, Building Information Modelling (BIM), Industry 4.0, Modular Construction, Automation

1 Introduction

The construction industry is at the beginning of a digital transformation that will change how we plan, build and operate buildings and infrastructure. Advances in sensor technology, connectivity, cloud computing, Internet of Things (IoT) and artificial intelligence enable the built environment to become a dynamic network in which smart objects can exchange data and information. In the manufacturing industry, IoT technologies are referred to as Industry 4.0 (I4.0) and enable the networking of products, machines, and processes to realize decentralized production. In the sense of I4.0, smart products seek an optimal path through production systems by communicating and interacting autonomously with their environment. In contrast, the production of precast concrete elements resembles a roofed construction site with only a few digitalized or automated processes. The implementation of digital twins is an essential component of I4.0 for the collection, evaluation, and provision of data along the entire value chain. First works are already successfully applying the concepts of I4.0 to the construction industry, where the application of I4.0 methods is also referred to as Construction 4.0.

In construction, Building Information Modelling (BIM) is an established tool for the digital description of structures and infrastructure during the planning and construction phase. BIM models contain the logical structure of the building and other semantic properties and attributes. However, using BIM models as digital twins is a heavily debated topic in many studies. The digital models created as part of the BIM process are intended for the planning and construction phases in which mainly static data is handled. Furthermore, BIM models are not designed for human-machine and machine-machine interaction. Both of these are elementary functionalities of the digital twin in I4.0 and are indispensable for implementing cyber-physical systems. In the context of I4.0, the administration shell was developed as an information container that provides methods for interaction in cyber-physical systems, which can be used for data management and distribution. Initial applications to the industrialization of the production of precast concrete parts show that the technology can also contribute to the digital transformation of manufacturing in the construction industry. By combining BIM and the digital twin from the context of I4.0, a unique symbiotic approach can be created. However, the ultimate goal in construction must be that the flow of information remains continuous and does not become further fragmented.

This paper presents a concept for integrating IFC-based BIM models into the administration shell of Industry 4.0 in the industrialized production of precast concrete elements. BIM models contain various data that are important for creating digital twins. With regard to the industrialized production of precast concrete elements, these are mainly general dimensions as well as data on material, reinforcement, and quality of the element. These data can be used to model digital twins and enable automated, rapid deployment on completion of the BIM process and at the start of production. The concept is validated in a case study in which an implementation of the approach is first proposed and finally applied to a virtual precast concrete column.

2 State of the Art

2.1 Digital Twin in Construction

Since the introduction of the digital twin, the concept has been adopted by many industries. As a result, many different definitions exist, each differentiating between industry-specific characteristics. Boje, Guerriero, Kubicki, *et al.* [1] propose a definition for the construction industry based on the digital twins' original definition by Michael Grieves. In this definition, the digital twin consists of physical and virtual space as well as a data link connecting the two. A characteristic of a digital twin is a bidirectional data link between the physical and virtual space. In a literature review, Sepasgozar [2] examine applications of digital twins regarding their data exchange capabilities. Their analysis shows that many published implementations of the digital twin do not qualify as such but rather as digital shadows for which only unidirectional data exchange is needed. The role of BIM in digital twins is a question on which there is still no consensus in the construction industry. In the literature, the digital twin is described as either an evolution, complementary, or independent of BIM [3]. According to Davila Delgado and Oyedele [4], both concepts are unique approaches that respond to different industry needs. In general, BIM is designed to improve the efficiency of design and construction. In contrast, the digital twin is designed to accurately represent the current state during manufacturing and operations, mainly through real-time data enabling data-driven decision-making and the simulation of what-if scenarios [3]–[5]. Shahzad, Shafiq, Douglas, *et al.* [3] state in their work that the data contained in BIM can be of great use to the digital twin if integrated appropriately.

2.2 Industry 4.0 & the Asset Administration Shell

I4.0 is the digitalization of production by linking the real and virtual space by connecting products, machines, and processes through innovative communication and information technologies to cyber-physical production system [6]. Smart products know their status and can independently find their optimal path through intelligent production systems by communicating and interacting with the machines and processes. Essential to the implementation of cyber-physical systems in the sense of I4.0 is the fully automated collection of the underlying process data and the evaluation, quantification, and analysis of the collected data. I4.0 is being driven forward in Germany by the *Industrie 4.0* project initiated by the Federal Ministry of Education and Research. The asset administration shell is considered the technical implementation of the digital twin in *Industrie 4.0*. It consists of many submodels that form an overall digital representation, each submodel representing an aspect or use case. The submodels contain all relevant data required by the asset through all life cycle phases. Essential for the autonomous exchange of data between Industry 4.0 components is the unambiguous interpretability of the data by both humans and machines. For this purpose, concept descriptions are specified that clearly define the semantic meaning of the data enabling machine-readability. Semantic descriptions of the data can also be provided by external repositories such as E-CLASS. Machine readability makes it possible to transfer data autonomously in machine-to-machine communication. A special I4.0 language is used for this purpose [7].

3 Concept

During the digital BIM planning process, a central digital model is created that, in addition to a simple geometric model, contains further data and information that are added to the components in the form of properties and attributes. The level of detail of this data depends heavily on individual project requirements. However, it can be assumed that at least data regarding geometric dimensions, materials, and reinforcement will be captured as part of the detailed design. For the industrialized production of precast concrete elements, these data represent a subset of the data requirements (cf. [8]). The data captured in the BIM model can be used to create digital twins, ensuring a continuous flow of data between the design phase and production and avoiding further fragmentation. In addition, the often cumbersome and tedious modeling process is simplified and enables digital twins to be made available quickly. The approach presented in this paper integrates an IFC-based BIM model into the digital twin for the industrialized production of precast concrete parts based on the administration shell of *Industrie 4.0*. The paper builds on the extensive preliminary work of [8], who developed data requirements and an administration shell template for precast concrete parts which are used as a basis for the presented approach.

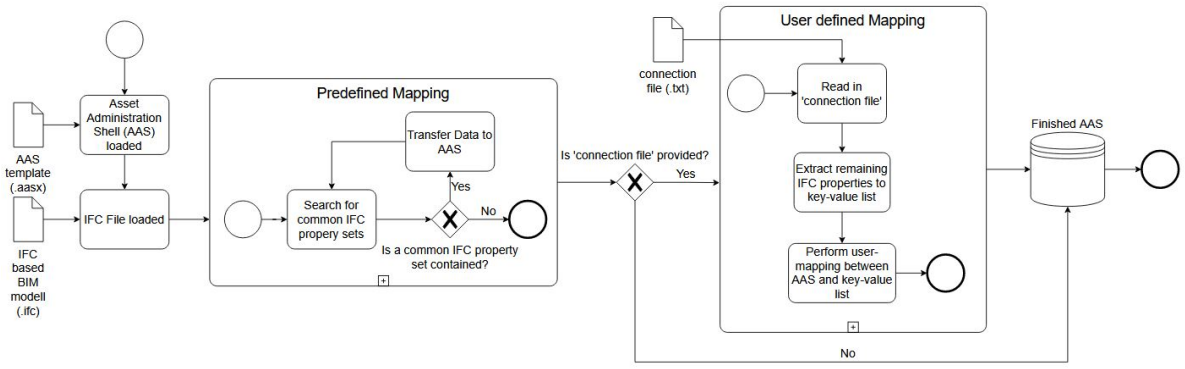

Figure 1: BPMN diagram of the proposed approach

The Industry Foundation Classes (IFC) are an open, vendor-neutral data format for the geometric and semantic description of a building. An IFC model consists of many hierarchically organized entities that model the logical structure of a building. These entities can be assigned properties that are defined as static properties directly in the schema of the IFC model or as dynamic properties that the user can freely assign. Dynamic properties are defined via a name-value-datatype list and combined into property sets which are then assigned to objects [9]. The properties of the IFC-based BIM model must be mapped to the properties contained in an administration shell-based digital twin. The prerequisite for this is an administration shell template with a data structure that conforms to the specific application requirements. Although an IFC-based BIM model cannot cover the entire data requirements of the digital twin, the data significantly contributes to simplifying and automating the deployment process. Data related to production processes and machine parameters are usually not captured in a BIM model. Therefore, they must be modeled manually or added to the administration shell by adding other external sources.

4 Case Study

As part of a case study, a Java-based implementation has been developed for the presented concept. The developed application assigns the properties in an IFC-based BIM model to the corresponding properties in the administration shell. The application is validated using the example of a precast concrete column.

4.1 Implementation

The developed application (see fig.1) consists of two components processing an IFC-based BIM model on the one hand and an administration shell on the other. The apstex IFC framework is used to evaluate the IFC files. For processing the administration shells, the BaSyx middleware from the Eclipse Foundation is used. Basyx has a Java-based SDK enabling reading and writing of administration shells. The prerequisite for the application is an IFC file and administration shell template, both being passed to the application as input. In this case study, the administration shell template developed by Kosse, Vogt, Wolf, *et al.* [8] is used. The application's functionality includes mapping material and reinforcement data and the addition of the reference to the underlying IFC file. To ensure the availability of attributes and properties, MVD's can be used. In the context of the prototypical implementation presented in this work, the availability of the properties is assumed without prior checking. The mapping is performed in two steps. The application first evaluates all statically defined IFC properties before evaluating user-defined properties. For this purpose, a mapping file is defined that is passed to the application.

Mapping of properties specified in the IFC data schema
The IFC file format provides statically defined property sets for the material and reinforcement data. These properties are mapped to properties in the administration shell. In the administration shell, data relating to material and reinforcement are available in a structured manner in submodel element collections. A submodel element collection exists for each unique element containing the properties and attributes. Especially for the data concerning reinforcement, grouping and aggregation of reinforcement types are performed prior to the mapping.

User-defined mapping
Dynamically specified properties can be used to transfer information such as production data and machine parameters, provided they have been assessed as part of the BIM process. A mapping file ('connection file') is required that specifies the assignment of the user-defined properties to the data structure of the administration shell. The mapping is specified via a text file by indicating the property name and the associated property in the administration shell, separated by a colon. Instead of the unique GUID of a property in the administration shell, the more readable idShort is used to simplify the application. To ensure a unique mapping, information on the position within the hierarchy of the administration shell is added to the mapping (e.g., Production-Transport-Transport company-Address). Before the mapping is performed, a key-value list, containing all unused IFC properties, is created.

This list is then used to perform the actual mapping (between AAS and key-value list). This procedure enables the flexible addition of information from other sources.

The progress of the process and any errors that occur are logged in a corresponding file. At the end of the process, the user receives a log containing information about the transferred data and a list of missing data.

4.2 Results

The validation of the proposed implementation is performed using the precast concrete column shown in fig 2 and 3. The column has a cast-on foundation and bracket support. The geometric dimensions can be taken from fig. 3. An IFC-based BIM model exists for the component, which, in addition to a geometric model, also contains data on material and reinforcement.

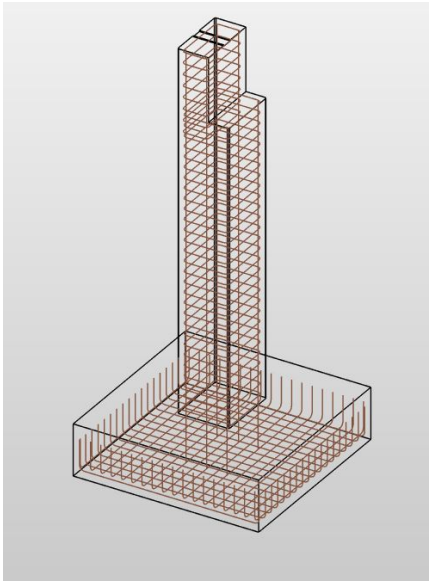

Figure 2: precast concrete column with foundation

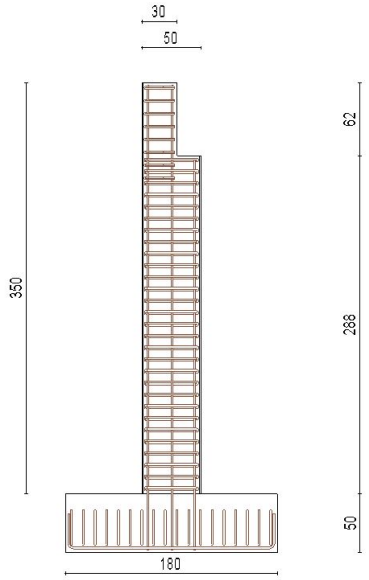

Figure 3: Dimensions of the precast concrete column with foundation

Figure 4 and 5 show the asset administration shell after successful application of the presented tool. The administration shell of the precast concrete column now contains data regarding material, reinforcement, and a reference to the IFC-based BIM model. A submodel element collection was created for each reinforcement type.

5 Discussion & Conclusion

The construction industry's digital transformation is characterized by the introduction of modern information and communication technologies. By introducing Internet of Things technologies, the built environment is interconnected to form cyber-physical systems in which participants can exchange data and react intelligently to one another. Essential for implementing cyber-physical systems is the digital

Figure 4: Instantiated Administration shell material SMC

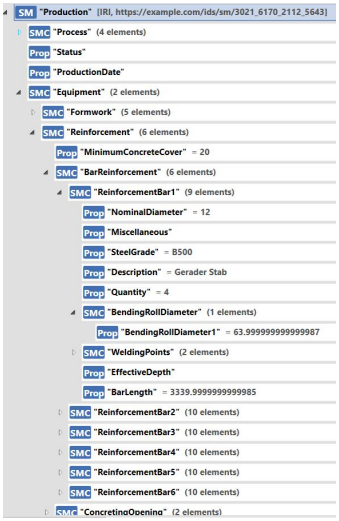

Figure 5: Instantiated Administration shell reinforcement SMC

twin. BIM is a proven and established tool for the digital description of buildings and infrastructure during the planning phase. However, due to insufficient integration of real-time data and a lack of interaction capabilities, BIM is unsuitable as a platform for an IoT digital twin. The digital twin, on the other hand, is by no means an evolution of BIM, but should rather be seen a complementary. Integrating BIM into digital twins allows for a digital model that uses current data models in construction and at the same time is able to participate in data exchange in cyber-physical systems. The approach presented in this work integrates BIM as a data basis for the creation of digital twins enabling the rapid provision of digital twins and, at the same time, contributes to keeping the flow of information continuous preventing further fragmentation. Furthermore, it is scalable and can be applied to entire buildings. An administration shell is created for each precast concrete element, which combines to form the administration shell of the entire building. Future research will extend the presented approach by a visualization component in which data is presented interactively to the user. Furthermore, the addition of further sources is planned.

Acknowledgements

This research is funded under Grant No. 423963709 by the German Research Foundation as part of the priority program “SPP2187 - Adaptive modularized constructions made in flux.”

References

[1] C. Boje, A. Guerriero, S. Kubicki, and Y. Rezgui, “Towards a semantic construction digital twin: Directions for future research”, *Automation in Construction*, vol. 114, p. 103 179, 2020, ISSN: 09265805. DOI: 10.1016/j.autcon.2020.103179.

[2] S. M. E. Sepasgozar, “Differentiating digital twin from digital shadow: Elucidating a paradigm shift to expedite a smart, sustainable built environment”, *Buildings*, vol. 11, no. 4, p. 151, 2021. DOI: 10.3390/buildings11040151.

[3] M. Shahzad, M. T. Shafiq, D. Douglas, and M. Kassem, “Digital twins in built environments: An investigation of the characteristics, applications, and challenges”, *Buildings*, vol. 12, no. 2, p. 120, 2022. DOI: 10.3390/buildings12020120.

[4] J. M. Davila Delgado and L. Oyedele, “Digital twins for the built environment: Learning from conceptual and process models in manufacturing”, *Advanced Engineering Informatics*, vol. 49, p. 101 332, 2021, ISSN: 14740346. DOI: 10.1016/j.aei.2021.101332.

[5] S. H. Khajavi, N. H. Motlagh, A. Jaribion, L. C. Werner, and J. Holmstrom, “Digital twin: Vision, benefits, boundaries, and creation for buildings”, *IEEE Access*, vol. 7, pp. 147 406–147 419, 2019. DOI: 10.1109/ACCESS.2019.2946515.

[6] H. Kagermann, W. Wahlster, and J. Helbig, *Securing the future of german manufacturing industry : Recommendations for implementing the strategic initiative industrie 40: Final report of the industrie 4.0 working group*, Forschungsunion im Stifterverband für die Deutsche Wirtschaft e.V., Berlin, editor, 2013.

[7] Plattform Industrie 4.0, “Verwaltungsschale in der praxis: Wie definiere ich teilmodelle, beispielhafte teilmodelle und interaktion zwischen verwaltungsschalen (in german) (version 1.0)”, 2020. [Online]. Available: https://www.plattform-i40.de/IP/Redaktion/DE/Downloads/Publikation/2020-verwaltungsschale-in-der-praxis.html (visited on 01/26/2022).

[8] S. Kosse, O. Vogt, M. Wolf, M. König, and D. Gerhard, “Digital twin framework for enabling serial construction”, *Frontiers in Built Environment*, no. 8, 2022. DOI: 10.3389/fbuil.2022.864722.

[9] A. Borrmann, M. König, C. Koch, and J. Beetz, *Building Information Modeling*. Cham: Springer International Publishing, 2018, ISBN: 978-3-319-92861-6. DOI: 10.1007/978-3-319-92862-3.

Experiment proposal for data quality assessment in construction management

Raphael Hippe[1], Marco Binninger and Olli Seppanen[1]
[1]Department of Civil Engineering, Aalto University, Otakaari 5A, 02150 Helsinki, Finland
E-mail(s): raphael.hippe@aalto.fi, marco.binninger@googlemail.com, olli.seppanen@aalto.fi

Abstract: In recent years the usage of digital tools in construction management has increased, and with it the need for automation and applications of *Artificial Intelligence* (AI). The basis for AI to work properly is clean and meaningful data. However, several publications have appeared in recent years documenting the lack of good data in the construction industry. Most of the previous studies discussing the use of AI in construction management do not take into account the assessment or definition of data quality. Therefore, this paper presents an experiment to measure data quality of three construction management methods: *Critical Path Method* (CPM), *Location Based Management System* (LBMS) and *Takt Planning and Takt Control* (TPTC). Since location-based techniques (LB), such as LBMS and TPTC, require information on a higher level of detail for input than activity-based techniques—especially in terms of connecting processes, times, and locations—the expectation is that they also provide better data as output. This lead to the following hypothesis: construction projects using TPTC or LBMS provide a higher data quality for AI than projects using CPM. The proposed experiment consists of five phases: Project Definition, Project Planning, Tool Selection, Data Entry & Export, and Evaluation. The experiment was carried out to find LB methods do indeed provide a higher score across all defined evaluation metrics. However, the authors identified several limitations for the presented results, with the strongest one being a small sample size of evaluated software solutions, which leads to a strong bias towards the individual implementations. Therefore, the next stage of the authors' research will be a more thorough execution of the experiment to verify the results.

Keywords: Data Quality, Artificial Intelligence, Construction Management, CPM, LBMS, TPTC

1 Introduction

There has been a growing interest in the usage of digital tools for construction management. Great effort has been devoted to the study of using *Artificial Intelligence* (AI) to automate processes within the construction industry. As reported by Abioye, Oyedele, Akanbi, *et al.* [1] the amount of papers published on *Machine Learning* (ML), Computer Vision and especially Optimisation has increased drastically over the last two decades. They reported that limitations in construction for those subfields

of AI, amongst others, are issues like incomplete data, scalability, and dealing with high-dimensional data. Further, Sacks, Girolami, and Brilakis [2] studied the use of *Building Information Modelling* (BIM) and AI in construction management and identified several challenges, which need to be overcome before AI can be widely used in the industry. AI solutions often are discipline-specific and lack multi-discipline collaboration. Many object relations and properties are not well defined in BIM and human intelligence is required in order to make sense of them. They discovered that data structures and representations often are optimised for the respective application to run and not for the use of AI [2]. To solve the issue of lacking data in construction management, Delgado and Oyedele [3] developed autoencoders to augment their data sets, which increased their model score by up to 11.5%.
Although several studies have indicated that data quality in construction is a limiting factor in terms of AI development and usage, little attention has been given to assessing and thus systematically increasing data quality in construction management [1]–[3]. In order to analyse this, it is important to know how construction projects are planned and managed. Olivieri, Seppänen, Alves, *et al.* [4] conducted a survey about the usage of the *Critical Path Method* (CPM), the *Last Planner System* (LPS), as well as *location-based techniques* (LB) in construction management across four countries and 532 projects. Their results show that CPM is the most used system for planning and controlling construction projects with a representation of 71%. However, the interest of LB systems has been growing and they were used in 40% of all considered projects. In recent years popular LB methods have been *Location-Based Management System* (LBMS) and, *Takt Planning and Takt Control* (TPTC) [5]–[7]. Figure 1 highlights, in (a) and (b) for LBMS and TPTC respectively, the structure created when adding the location information to time and process. Both LB methods have clear rules on how to integrate the locations of a construction site and how to connect it to all other relevant data points [5], [8]. While it is possible to add the location information when using an activity based method, like CPM, there is no clear procedure on how to select locations or on how to connect them to tasks or resources and thus there is no clear structure provided by the method itself.

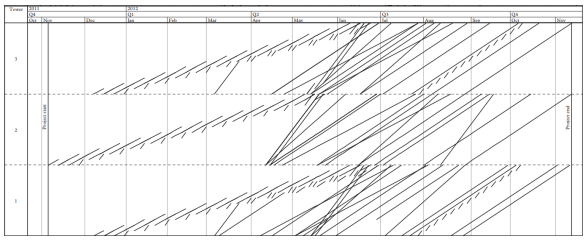

(a) LBMS flowlines by Olivieri, Seppänen, and Denis Granja [5]

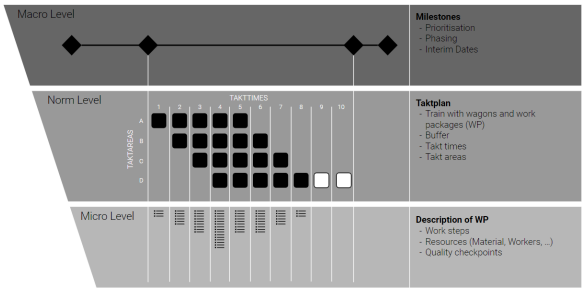

(b) Three levels of TPTC by Binninger [6] and Dlouhy, Binninger, Oprach, *et al.* [7]

Figure 1: Structure of LB methods LBMS and TPTC

Publications on the usage of AI in construction indicate that data quality in construction is a limiting factor. However, to the authors best knowledge, the impact of construction management methods on data quality has been scarcely investigated from the point of view of AI applications. Therefore, this work presents a method to assess data quality of construction management methods for AI

applications. Because of the stricter rules on connecting data points by LB methods, this work further proposes the following hypothesis: construction projects using TPTC or LBMS provide a higher data quality for AI than projects using CPM.
The remainder of the paper is organized as follows: section 2 describes the method used to assess the data quality of construction management methods. Tentative results are presented in section 3 and section 4 concludes with a summary.

2 Method

This work presents an experiment to determine the data quality produced by construction management methods, which is illustrated in Figure 2. The experiment consists of five phases: *Project Definition*, *Project Planning*, *Tool Selection*, *Data Entry & Export*, and *Evaluation*. During the *Project Definition*

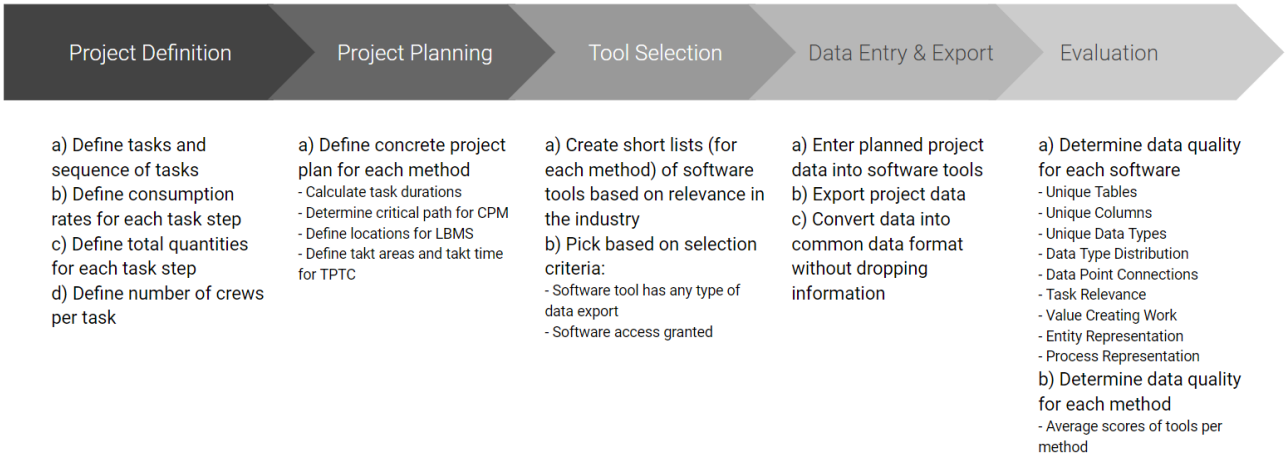

Figure 2: Experiment setup

phase, one project is defined as a foundation for the experiment. Therefore tasks and their sequence have to be set. The sequence of tasks describes the fixed order the tasks need to be executed in. To calculate the duration of each task, tasks should consist of at least one or more task steps, with each task step having a consumption rate, some quantity of materials, and a number of crews working on this task. Next, in the *Project Planning* phase, the base project has to get prepared for each construction management method. This means that the exact duration for each task is calculated, using the consumption rates, quantities, and number of crews. For CPM, the critical path needs to be identified by using the sequence of tasks. Additionally, the locations for LBMS, as well as the takt areas for TPTC, have to be defined. The third phase—*Tool Selection*—has the purpose of identifying software tools, which are used in practice to run construction projects using either CPM, LBMS or TPTC. Therefore, short lists of software solutions for each construction management method have to be created using search engines. Finally, the desired amount of software tools are selected from the short lists by applying the following selection criteria: the software tool has any type of data export, and it is possible to receive access to the software solution. Both criteria are necessary conditions, because otherwise there would be no data to evaluate. *Data Entry & Export* is the fourth phase and

describes the process of using the previously selected software tools to plan the project according to the preparations done in phase one and two. Next, the project data has to be exported from the tools using their defined export functions. The authors suggest to convert all data sets into a shared data format, such as CSV, to simplify the evaluation phase. Finally, the *Evaluation* phase uses dimensions, elements as well as indicators, presented by Cai and Zhu [9], to determine the data quality. Cai and Zhu [9] defined five dimensions of data quality: *Availability*, *Usability*, *Reliability*, *Relevance*, and *Presentation Quality*. However, they argue from a computer science point of view for the goal of optimizing software solutions in the big data era, whereas this work aims to assess data quality created by construction management methods. Thus, several of their dimensions are being dismissed in the evaluation process, because they are only affected by the implementation of a software solution. The authors found the following elements to be relevant for this work: *Accuracy*, *Integrity*, and *Completeness* from the *Reliability* dimension, *Fitness* from *Relevance* dimension, and *Readability* and *Structure* from the *Presentation Quality* dimension. Cai and Zhu [9] describe the *Accuracy* element as a measurement of how well the data compares to actual reference values. Additionally, in the authors' opinion, this is reflected by the level of detail used by the data set. The *Integrity* of data is displayed by how precisely tasks, as well as definitions and relations of entities, on the construction site are represented. This is further supported by the *Completeness* element, which indicates, whether the data set describes the actual components in their totality. Indicators such as how much has the data already been summarized, or are appropriate data types being used, are important factors for AI applications. They stem from the *Fitness*, *Readability*, and *Structure* elements. Table 1 provides an overview of the Data Quality Elements and their respective Evaluation Questions and Metrics. Since the answers to those questions are very complex, subjective, and not very tangible,

Table 1: Evaluation Questions and Evaluation Metrics

Data Quality Elements	Evaluation Question	Evaluation Metrics
Accuracy, Completeness, Fitness, Structure	How precisely are the tasks described?	Unique Tables, Unique Columns
Accuracy, Completeness	How accurate are tasks linked to the actual work?	Task Relevance, Value Creating Work
Accuracy, Completeness, Integrity	How accurate are tasks linked to entities on site?	Entity Representation
Accuracy, Completeness, Integrity	How much of the actual process on site is represented in the data?	Process Representation
Structure, Fitness, Readability	How is the representation of data types?	Data Type Distribution
Structure, Fitness, Readability, Integrity	How well are data points connected to each other?	Connections

the authors derived eight metrics from evaluation questions. The metrics *Unique Tables* and *Unique Columns* simply represent the number of exported tables and columns. Which is supported by the basic idea of more columns means more information, which allows for more AI use cases. The *Task Relevance* metric describes the amount of features, which contribute to describing the broader tasks in a meaningful way. All value creating activities that are described by the data are counted in the *Value Creating Work* metric. All columns, which represent any entities on the construction site, such as locations, workers, or materials, are added up in the *Entity Representation* metric. More columns for those metrics, imply a higher level of detail and less abstraction, which provides more opportunities for feature engineering and thus richer AI solutions. The *Data Type Distribution* metrics provides an overview of all data types used in the data set. Finally, the *Connections* metric indicates how many references between data points can be found in a data set. All metrics are defined so that higher results mean higher data quality.

3 Results

The experiment described in section 2 has been conducted for the three construction management methods CPM, LBMS and TPTC. During the *Project Definition* phase a project for a six storey building consisting of seven tasks has been defined, which is displayed in Table 2. The tasks have been enriched by steps, consumption rates, quantities, and number of crews. Note that the consumption rates and quantities for this project are not taken from a real project.

Table 2: Project Definition: Tasks, Consumption Rates, Quantities, and Crews for a 6 storey building. *(*Reinforce and pour slab on metal deck)*

Subcontractor	Task	Steps	Consumption Rate [hrs]	Quantity [LF/SF]	Crews
Concrete	R/P SOMD*	Concrete	0.0219	60000	10
Concrete	R/P SOMD*	Reinforcement	0.0219	6000	10
Drywall	LAYOUT TOP TRACK	Layout Top Track	0.0073	60000	4
Drywall	LAYOUT TOP TRACK	Install Top Track	0.0073	6000	4
MEP	OVERHEAD MEP	OH MEP INSTALL	0.032	12000	2
Drywall	STUDS	2nd Pass Int Walls	0.0138	60000	3
MEP	In-Wall MEP Rough-in	Rough Inwall	0.016	60000	6
Drywall	Drywall Install	Hang Drywall	0.032	60000	10
Finishes	Finishes	Finish Materials	0.128	60000	15

Next, the project has been prepared for the three construction management methods. For CPM the initial task sequence has been selected as the critical path, since each task depends on the previous one. Locations and takt areas have been identified for LBMS and TPTC respectively. Building storeys have been selected as locations for LBMS. Since TPTC typically uses smaller locations, the authors decided on using 18 takt areas with a takt time of 4 days.
During the *Tool Selection* phase three short lists were created. While the short list of CPM contained 15 software solutions, both LB methods found less results, with LBMS only providing three, and TPTC only nine options. A few software solutions had to be discarded, because they did not provide a data export option. Others could not be considered for this experiment due to the lack of accessibility. However, one tool per method was found, matching all criteria.
The described project data has been entered and exported from all three software solutions. The LBMS tool required a data set conversion from XML to CSV. The other tools exported to CSV directly. The evaluation metrics, defined in Table 1 have been applied to all exported data sets. Therefore, tables and columns meeting the respective evaluation metric criteria, have been counted. The *Connection* metric takes all columns into account, which create a relation between data points. All columns, which contribute to describing the tasks, defined during the first two phases of the experiment, are summed up in the *Task Relevance* metric. This includes all processes on the construction site, which are relevant to the respective task, e.g. design or logistic. Next, the *Value Creating Work* metric adds up all columns of a data set, which describe the actual tasks and task steps. The *Entity Representation* metric counts all columns representing entities like workers, materials, or tools on the construction site. All features expressing ongoing processes on the construction site, such as the state of the tasks are added up in the *Process Representation Metric*. Finally, the *Data Type Distribution* metric accounts for all different data types used in a data set.

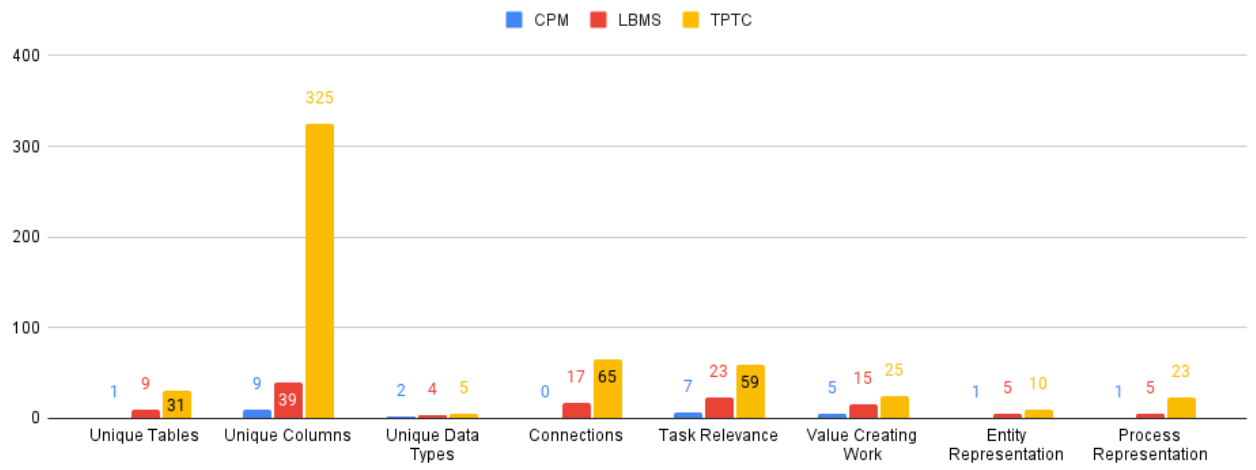

Figure 3: Results of Evaluation Metrics for one CPM, LBMS, and TPTC software solution respectively

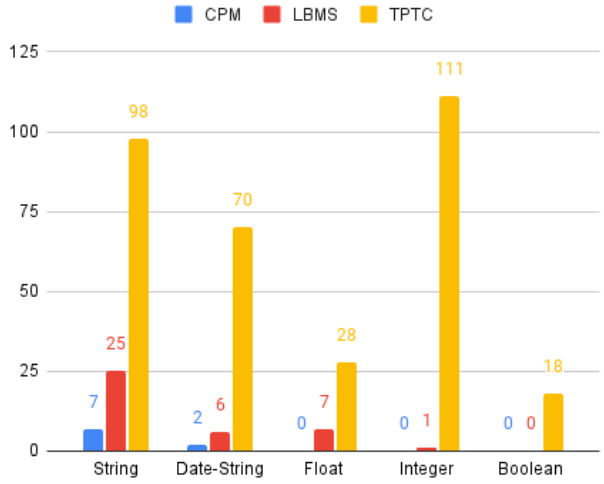

Figure 4: Results of Data Type Distribution evaluation metric for one CPM, LBMS and TPTC software solution respectively

Figure 3 presents the results of eight evaluation metrics for one CPM, LBMS, and TPTC software tool respectively. From this figure it can be seen that both LBMS and TPTC software scored higher than the CPM tool in every metric. Especially the results of *Unique Tables*, *Unique Columns*, and *Connections* indicate the structural differences of activity-based and location-based methods. The higher level of detail provided by LBMS and TPTC software, which was assumed based on Figure 1, can be seen through the better results in the *Task Relevance*, *Value Creating Work*, *Entity Representation* and *Process Representation* metrics. LBMS and TPTC tools also show a higher *Data Type Distribution* score than the CPM software solution, which can be found in Figure 4. Striking is the complete lack of numerical data in the data set of the CPM tool, which is preferential to categorical data.

While the results are a good first indication to support the hypothesis, the evaluation is only based on a single project and a single software tool per construction method. Thus the results are extremely

biased towards the individual implementation of the respective software applications. Nonetheless, the results of this experiment support the proposed hypothesis—construction projects using TPTC or LBMS provide a higher data quality for AI than projects using CPM—to be true.

4 Conclusion

Based on the results, it can be concluded that the research into assessing data quality in construction management has been very successful and data quality of construction management applications can be measured. The proposed experiment works as a method for assessing data quality and the first performance of the experiment clearly shows differences between the data quality of projects using LBMS or TPTC over CPM. However, generalized conclusions cannot be drawn based on one software solution per construction method. Additional projects as well as expanding the experiment to include project controlling, would further strengthen the experiment. On the basis of the promising findings presented in this paper, work on the remaining issues is continuing and will be presented in future papers.

References

[1] S. O. Abioye, L. O. Oyedele, L. Akanbi, *et al.*, “Artificial intelligence in the construction industry: A review of present status, opportunities and future challenges”, *Journal of Building Engineering*, vol. 44, p. 103 299, 2021.

[2] R. Sacks, M. Girolami, and I. Brilakis, “Building information modelling, artificial intelligence and construction tech”, *Developments in the Built Environment*, vol. 4, p. 100 011, 2020.

[3] J. M. D. Delgado and L. Oyedele, “Deep learning with small datasets: Using autoencoders to address limited datasets in construction management”, *Applied Soft Computing*, vol. 112, p. 107 836, 2021.

[4] H. Olivieri, O. Seppänen, T. d. C. Alves, *et al.*, “Survey comparing critical path method, last planner system, and location-based techniques”, *Journal of construction engineering and management*, vol. 145, no. 12, p. 04 019 077, 2019.

[5] H. Olivieri, O. Seppänen, and A. Denis Granja, “Improving workflow and resource usage in construction schedules through location-based management system (lbms)”, *Construction management and economics*, vol. 36, no. 2, pp. 109–124, 2018.

[6] M. Binninger, *Untersuchungen zum arbeitsfluss in getakteten bauproduktionssystemen aus perspektive von generalunternehmern*, 2022.

[7] J. Dlouhy, M. Binninger, S. Oprach, and S. Haghsheno, “Three-level method of takt planning and takt control–a new approach for designing production systems in construction”, *Proceedings (IGLC 24). Boston, USA*, 2016.

[8] J. Dlouhy, S. Oprach, M. Binninger, T. Richter, and S. Haghsheno, “Using takt planning and takt control in production projects–comparision of construction and equipment phases”, in *Proceedings of the 26th Annual Conference of the International Group for Lean Construction, Chennai, India*, 2018, pp. 16–22.

[9] L. Cai and Y. Zhu, “The challenges of data quality and data quality assessment in the big data era”, *Data science journal*, vol. 14, 2015.

Verwendung und Einbindung von Open-Data-Schnittstellen am Beispiel der Bundes-APIs

Tim-Jonathan Huyeng[1]
[1]Technische Universität Darmstadt, Institut für Numerische Methoden und Informatik im Bauwesen
E-mail(s): huyeng@iib.tu-darmstadt.de

Abstract: Aggregation von Daten mittels API-Request ist eine verbreitete Methodik zur Abfrage von Informationen aus verschiedenen Datenquellen, welche zum Beispiel in einer Applikation dargestellt werden können. Üblicherweise werden dabei die Daten für eine Anwendung in einem speziell hierfür implementierten Backend mit einer eigenen API zur Verfügung gestellt. Mit der Verabschiedung des *Zweiten Open-Data-Gesetzes* 2021 wird die Menge an Daten von Bundesbehörden und öffentlichen Einrichtungen, welche frei verfügbar sind, noch deutlich gesteigert werden. Die sogenannte *Bundesstelle für Open Data* (*BundDEV*) hat sich zur Aufgabe gemacht, diese Daten bzw. deren API-Spezifikationen zu veröffentlichen und einfach zugänglich zu machen. Dabei wird auf den weit verbreiteten *OpenAPI*-Standard bei der Beschreibung der APIs gesetzt. Im Rahmen des Papers wird analysiert, inwiefern diese Initiative bzw. die dokumentierten APIs für Anwendungen einfach verwendet werden können. Es wird beispielhaft der Prozess für verschiedene Ausgangslagen von APIs dargelegt und beschrieben. Als Beispielanwendungsfälle werden unter anderem der Hochwasserschutz sowie dazu passende APIs herangezogen. Die öffentliche Bereitstellung von API-Spezifikationen sowie die automatische Generierung von Client-Tools ist ein weiterer Baustein für die einfache Nutzung von öffentlichen Daten. Dabei liefert der *OpenAPI*-Standard eine einfache und maschinenlesbare Möglichkeit verschiedene APIs und deren Parameter zu beschreiben.

Keywords: Open-Data, APIs, Hochwasserschutz, Automatisierung

1 Einleitung

Daten sowie die Verfügbarkeit von Daten sind wichtige Bestandsteile in den Digitalisierungsstrategien von vielen Bereichen [1, S. 34]. Dies gilt ebenfalls für die Bauindustrie, in der die Verwendung und Analyse von Datenquellen aufgrund des technologischen Fortschritts in den letzten Jahren ein zentraler Baustein geworden ist. Neben privaten und proprietären Daten hat die Verwendung öffentlich verfügbarer Informationen ein großes Potenzial. Neben den technischen Weiterentwicklungen im

Bereich der Datenerfassung gibt es zudem auch politische Motivation und entsprechende Gesetze, die insbesondere öffentliche Einrichtungen bei der Bereitstellung der Daten mehr in die Pflicht nehmen.

Damit die Daten von Anderen verwendet werden können, werden diese entweder zum Download bereitgestellt oder mittels einer Schnittstelle (API - Application Programming Interface) über das Web zur Verfügung gestellt. Die Bereitstellung mittels einer API ist vor allem sinnvoll, wenn aktuelle (live) und nicht nur historische Daten zur Verfügung gestellt werden und eine Anbindung der Daten an andere Tools oder Webservices ermöglicht werden soll. Im Rahmen des Papers werden daher nur Schnittstellen nicht aber die einfache Bereitstellung als Datei-Download beachtet. Die Dokumentation von APIs ist auf verschiedene Art und Weisen möglich und an den Anspruch sowie die Möglichkeiten des Anbieters gebunden. Ist es ein konkretes Ziel der Betreiber Daten anderen Personen zur Verfügung zu stellen, ist meist eine ausführliche Dokumentation oder Anleitung zur Verwendung der API vorhanden. Diese können entweder als reine Textdokumentation oder auch über sonstige maschinenlesbare Formate (z.B. *OpenAPI*) bereitgestellt werden. Üblicherweise werden die Routen, die Parameter sowie die zu erwartenden Antworten beschrieben. Ist es vom Betreiber nicht vorgesehen, oder hat der Betreiber kein gesteigertes Interesse an einer einfachen Nutzung seiner Schnittstelle ist es möglich, dass keine Dokumentation zur Verfügung steht. Durch Reverse Engineering und die Verwendung von verschiedenen Tools ist es allerdings dennoch möglich die API-Struktur nachzuvollziehen und sich darauf aufbauend eine Dokumentation zu erstellen. Diese kann anschließend anderen Personen öffentlich zur Verfügung gestellt werden. Im Rahmen des Papers wird für diese Möglichkeiten jeweils ein Beispiel beschrieben.

Als einheitliches Dokumentationsformat für die im Folgenden beschriebenen APIs wird das *OpenAPI*-Format verwendet. Dieses Format wird von der *OpenAPI*-Initiative (OAI) [2], welche der *Linux Foundation* untergeordnet ist, stetig weiterentwickelt und standardisiert. In diesem textbasierten Format (*JSON oder YAML*) werden Informationen zu den einzelnen Routen, Parametern sowie Antworten gespeichert. Überdies können zusätzliche Beschreibungen, Informationen sowie Beispiele die Verwendung der API vereinfachen.

2 Aktueller Stand von Open-Data-Schnittstellen

Wie in der Einleitung beschrieben sind in den letzten Jahren die Möglichkeiten der Verwendung von öffentlichen Daten gestiegen. Dies liegt neben den bereits beschriebenen Gründen auch an Initiativen, welche sich zur Aufgabe gemacht haben Daten bzw. die Datenschnittstellen öffentlich zu dokumentieren. Zudem wird die Nutzbarkeit sowie Verfügbarkeit von öffentlichen Daten durch verschiedene Gesetze weiter gestärkt und vereinfacht [3]. So sind zum Beispiel die Behörden des Bundes durch das *Zweite Open-Data-Gesetz* [4] dazu verpflichtet eine öffentliche Schnittstelle über Netze zum Datenabruf bereit zustellen [5, §12a, (1)]. Neben Behörden gilt das Gesetz unter anderem auch für Unternehmen mit öffentlichen Aufträgen sowie Hochschulen und Forschungseinrichtungen.

Das Gesetz konkretisiert dies wie folgend: *„[...] Daten [sind] elektronisch und in nach den anerkannten Regeln der Technik offenen, maschinenlesbaren, zugänglichen, auffindbaren und interoperablen*

Formaten zusammen mit den zugehörigen Metadaten bereitzustellen“ [6, §7, (2)]. Dabei muss dies nicht erfolgen, wenn für die Behörde oder zuständige Stelle ein unverhältnismäßiger Aufwand entstehen würde. Wie der Aufwand und die daraus resultierenden Veröffentlichungen von Daten bewertet wird, muss sich in den nächsten Jahren zeigen. Untersuchungen wie zum Beispiel von Schmietendorf [7] zeigten dabei 2020 noch einige Lücken und Probleme auf.

Das Gesetz ist Teil der Digitalisierungsstrategie des Bundes, zu der auch das Portal *GovData* gehört [8]. Das Portal soll einen einfachen Zugang zu Daten und Dokumenten der öffentlichen Hand bieten. Dabei ist es möglich nach Datensätzen zu suchen und sich die entsprechenden Metadaten in den jeweils verfügbaren Formaten anzeigen zu lassen. Die Daten sowie Datenschnittstellen werden dezentral von den jeweiligen Anbietern zur Verfügung gestellt. *GovData* wurde vom IT-Planungsrat ins Leben gerufen und wird somit direkt von der öffentlich Hand betreut. Neben öffentlich gestützten Angeboten zur Sammlung von Schnittstellenbeschreibungen gibt es auch andere Initiativen nicht öffentlicher Stellen. Eine Initiative ist *BundDEV* [9], welche unter anderem von Lilith Wittmann ins Leben gerufen wurde. Die Initiative *BundDEV* soll laut den Gründern vor allem zeigen, was aktuell in den Behörden nicht umgesetzt wird und wie die Verwendung von öffentlichen Daten beschleunigt werden kann [10]. Eines der ersten Beispiele war die API-Dokumentation für das Katastrophenwarnsystem NINA [11]: Sowohl die Daten als auch die Schnittstelle zum Zugriff waren zwar seit einiger Zeit verfügbar, dies war aber mangels offizieller Unterstützung und Dokumentation kaum bekannt. Als Basis der Beschreibung wird der *OpenAPI*-Standard verwendet. *BundDEV* stellt zur Beschreibung von Schnittstellen inzwischen auch ein Template auf GitHub zur Verfügung. Mithilfe des Templates und den bereits vorhandenen Beispielen sind Beteiligungen von weiteren Personen auch ohne Expertenwissen möglich. Aktuell sind über 30 APIs dokumentiert und öffentlich einsehbar [9].

3 Konzept zur Verwendung und Einbindung von Open-Data

Die Initiative *BundDEV* zeigt, wie einfach es sein kann Schnittstellen zu dokumentieren und hierdurch für die breite Masse nutzbar zu machen. Im folgenden Kapitel soll der Workflow von Schnittstellen bis zur Verwendung dieser erläutert werden um zu zeigen, wie bei verschiedenen Ausgangslagen vorgegangen werden kann. Es werden hierfür folgende drei Ausgangslagen definiert:

Tabelle 1: Übersicht über die beschriebenen Ausgangslagen

	Dokumentation	Spezifikation
A-1	✗	✗
A-2	✓	✗
A-3	✓	✓

Hierbei ist zu beachten, dass bei der Ausgangslage `A-3` die Spezifikation maschinenlesbar vorliegen muss, bei `A-2` kann es möglich sein, dass die Dokumentationen auch maschinell und automatisch ausgelesen werden können, wenn sie zum Beispiel als Textdokumentation vorliegen. Nachfolgend werden

die einzelnen Ausgangslagen und die jeweilige Vorgehensweise zur Erstellung einer Dokumentation erläutert.

3.1 A-1: keine Dokumentation der API vorhanden

Ist zu einer Datenschnittstelle keinerlei Dokumentation vorhanden, gibt es verschiedene Wege diese zu erstellen. Wird die API zum Beispiel bereits auf einer anderen Webseite als Datenquelle für zum Beispiel Kartendarstellungen verwendet, können die einzelnen Requests im Browser nachvollzogen werden. Hierbei bieten sich die üblichen Entwicklertools der jeweiligen Browser an. Abhängig vom verwendeten Browser gibt es eine Ansicht, welche die einzelnen Anfragen und deren Antworten darstellt. In dieser Ansicht lassen sich Abfragen zu einer API auch mithilfe von Filtern einfach ausfindig machen und analysieren. Wird *Firefox* verwendet, ist es möglich die identifizierten Abfragen zu verändern und anschließend erneut zu senden. Mit dieser Methode können schnell und einfach Abfrageparameter getestet werden. Neben dieser sehr simplen Lösung gibt es auch weitere Tools, die bei diesem Prozess unterstützen können. Der *Swagger Inspector* [12] oder auch das von goofmint [13] entwickelte Tool *„cURL to Swagger“* ermöglichen das Erzeugen von *OpenAPI*-Spezifikationen anhand einer Abfrage. Auch können Webtools wie *Postman* o.ä. zum Testen und Analysieren von Abfragen und deren Antworten verwendet werden. Unabhängig davon, wie hier konkret vorgegangen wird, ist das Ziel eine *OpenAPI*-Spezifikation zu erhalten, welche entweder im YAML- oder im JSON-Format gespeichert werden kann.

3.2 A-2: Dokumentation vorhanden, aber keine API-Spezifikation

Diese Ausgangslage ist insbesondere bei älteren Schnittstellen öfters der Fall. Dies kann zum Beispiel daran liegen, dass zum Zeitpunkt der Implementierung der Schnittstelle der *OpenAPI*-Standard noch nicht verbreitet war. Dokumentationen können in unterschiedlichster Qualität und Form vorliegen. Sind bei einer Dokumentation zum Beispiel neben der reinen Beschreibung auch Beispiele angegeben, erleichtert dies die Konstruktion der *OpenAPI*-Spezifikation deutlich. Eine automatische Auswertung mithilfe von Webcrawlern ist nur sinnvoll, wenn die Schnittstelle sehr umfangreich ist oder sich das hierfür entwickelte Tool auch bei anderen Schnittstellen verwenden lässt. Ist dies nicht der Fall wird empfohlen die *OpenAPI*-Spezifikation händisch anhand der Dokumentation zu erstellen.

3.3 A-3: API-Spezifikation vorhanden

Liegt eine API-Spezifikation vor, kann diese direkt im nachfolgend beschriebenen Workflow verwendet werden. Mithilfe von verschiedenen Tools wie zum Beispiel einem YAML/JSON-Linter [14] kann die *OpenAPI*-Spezifikation auf mögliche Fehler untersucht werden. Dabei ist es prinzipell unerheblich, ob die Spezifikation von dem Anbieter der Schnittstelle oder von einer anderen Person geschrieben wurde. Anschließend kann eine Dokumentation mithilfe der *Swagger UI* im Browser zur Verfügung gestellt werden. Wird die Spezifikation in einem GitHub-Projekt verwaltet, kann z.B. *GitHub-Pages* zum Hosting der Dokumentation verwendet werden. In der webbasierten Darstellung können Abfragen ebenfalls getestet werden.

Nach Bearbeitung der jeweiligen Schritte ist das Ziel somit eine API-Spezifikation. Im hier vorgestellten Konzept ist diese in Form einer *OpenAPI*-Spezifikation gefordert. Anhand dieser Spezifikation kann dann mithilfe von Generatoren Client-Quellcode generiert werden (siehe Abb. 1).

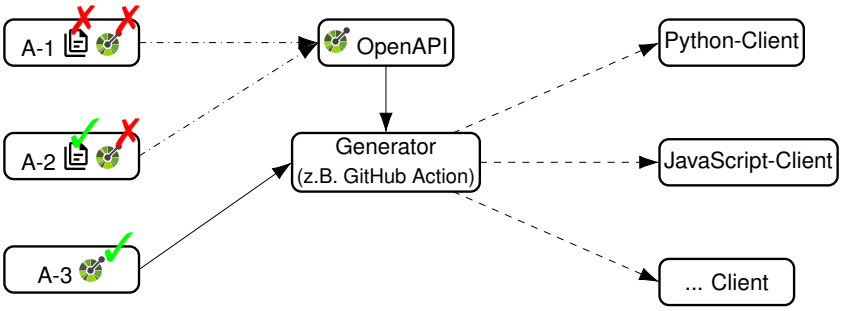

Abbildung 1: Darstellung des Workflows auf Basis der verschiedenen Ausgangslagen

4 Exemplarische Umsetzung für die verschiedenen Ausgangslagen

Die im vorherigen Kapitel beschriebene automatische Generierung des jeweils geforderten Client-Quellcodes wird in diesem Kapitel anhand einer hierfür erstellten GitHub-Action erläutert. Dabei wurde sich an der GitHub-Action, welche von *BundDEV* eingesetzt wird, orientiert [15].

4.1 A-1: Länderübergreifendes Hochwasserportal (LHP)

Als Beispiel für diesen Fall wird die API des Länderübergreifenden Hochwasserportals (LHP) verwendet. Auf der Webseite hochwasserzentralen.de werden länderübergreifende Informationen zu Pegel- und Hochwasserwarnungen zusammengefasst und auf einer Karte dargestellt. Um die Daten auf einer Karte darzustellen, werden die Informationen von einer eigenen API zur Verfügung gestellt. Hierbei werden verschiedene Datenquellen der Bundesländer und anderen öffentlichen Stellen im Backend zusammengefasst und gebündelt veröffentlicht. Im engen Sinne existiert momentan keine API, welche für die Öffentlichkeit zur Verfügung gestellt werden soll. Da die Webseite allerdings über Requests die erforderlichen Daten abfragt, kann dies auch zur Anbindung an eigene Applikationen genutzt werden. Die Dokumentation wurde hier anhand einer Request-Analyse mittels Reverse Engineering erstellt. Die zum jetzigen Zeitpunkt noch nicht vollständige Dokumentation ist auf GitHub veröffentlicht [16].

4.2 A-2: PEGELONLINE API

Die von der Wasserstraßen- und Schifffahrtsverwaltung des Bundes (WSV) zur Verfügung gestellte API für Pegel in Deutschland ist in einer umfangreichen HTML-Dokumentation beschrieben [17]. Anhand dieser Dokumentation wurde eine *OpenAPI*-Spezifikation erstellt. Diese Spezifikation ist auf GitHub veröffentlicht und ist Teil des *BundDEV*-Projekts. Die API liefert umfangreiche Daten wie zum Beispiel die Wasserstände, Abflussparameter oder Wasserparameter für die überwachten Gewässer. Da diese API für den öffentlichen Zugriff entwickelt wurde bestehen aktuell keinerlei

Limitierungen oder notwendige Authentifizierungen. Abbildung 2 zeigt eine beispielhafte Anbindung über ein *Vue.js*-Frontend sowie eine Visualisierung der Daten mittels *Leaflet.js*.

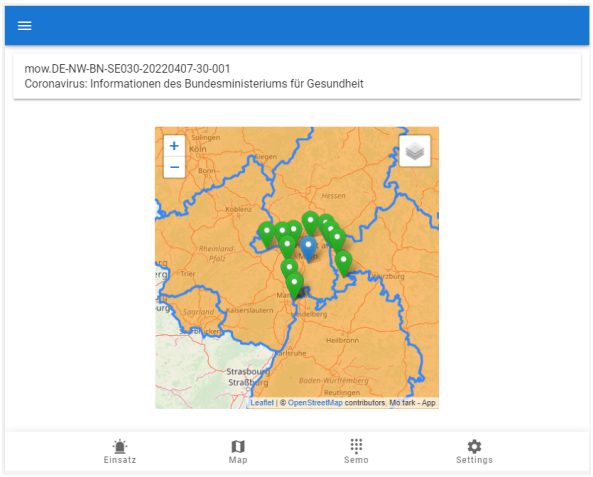

Abbildung 2: Beispielhafte Verwendung der PEGELONLINE-API in einem Frontend

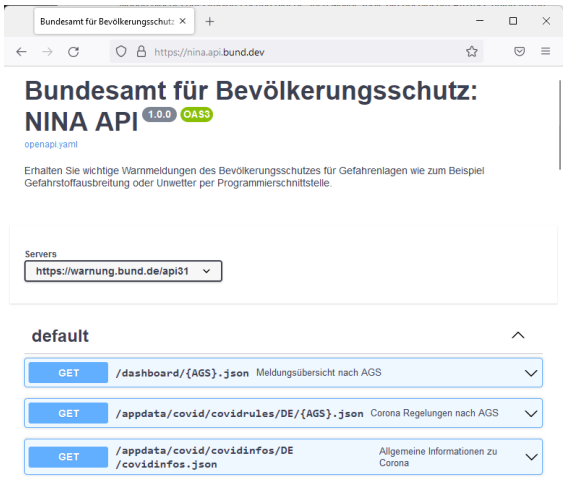

Abbildung 3: Swagger UI am Beispiel der NINA API

4.3 A-3: NINA API

Ist eine Spezifikation bereits vorhanden, kann diese direkt als Grundlage für weitere Anbindungen verwendet werden. Dabei ist es prinzipiell unerheblich, ob die Beschreibung von einer Community oder vom Anbieter der Schnittstelle zur Verfügung gestellt wird. Am Beispiel der NINA API [11] kann gezeigt werden, dass öffentliche Daten mithilfe dieser Dokumentation sehr einfach verwendet werden können. Erstaunlich ist hierbei besonders, dass für die Daten, welche zur Warnung der Bevölkerung verwendet werden, keine Dokumentation seitens des öffentlichen Anbieters existiert. Die von der Community erstellte Spezifikation ist unter nina.api.bund.dev einsehbar (siehe Abb. 3).

4.4 Automatische Generierung von Client-Code mittels GitHub-Action

Die implementierte GitHub-Action ist öffentlich verfügbar und kann dem jeweiligen Projekt einfach hinzugefügt werden. Anschließend erzeugt die Action abhängig von der Einstellung nach jedem Push oder durch manuelles Triggern aktuellen Client-Quellcode. Damit das ursprüngliche Projekt übersichtlich bleibt wird der generierte Quellcode in einen gesonderten Branch gepusht. Aktuell wird ein JavaScript- sowie ein Pythonpackage erzeugt [18].

5 Zusammenfassung und Ausblick

Die öffentliche Bereitstellung von API-Spezifikationen sowie die automatische Generierung von Client- oder Server-Tools ist ein weiterer Baustein für die vereinfachte Nutzung von öffentlichen Daten. Dabei liefert der *OpenAPI*-Standard eine einfache und maschinenlesbare Möglichkeit verschiedene APIs und deren Parameter zu beschreiben.

Im Rahmen des Papers konnte ein Workflow für die Anbindung und Verwendung von Open-Data-Schnittstellen gezeigt werden. Dieser Workflow basiert auf einer *OpenAPI*-Spezifikation der Schnittstelle und automatisch generiertem Client-Quellcode. Die Einbindung von Open-Data wird in den nächsten Jahren deutlich zunehmen, insbesondere wenn die entsprechenden Gesetze in den Behörden mehr und mehr Umsetzung finden. Dies bedeutet neben der Bereitstellung von Daten und Schnittstellen auch eine Dokumentation. Zusätzlich zu den hier gezeigten Beispiel-Schnittstellen ist davon auszugehen, dass weitere APIs mit Baubezug in den nächsten Jahren wachsen. Zum Beispiel setzt *buildingSMART* auch bei der Dokumentation des BCFs auf die *OpenAPI*-Spezifikation [19]. Da sich der Ansatz auf einheitliche Dokumentation stützt, ist dies aber auch als mögliche Schwäche zu benennen, da diese Dokumentationen teilweise erst aufwendig erstellt werden müssen. Wenn die Dokumentation zudem von der Community und nicht vom Anbieter der Schnittstelle erstellt wird, ist es möglich, dass Veränderung der API nicht direkt in der Dokumentation widergespiegelt werden.

Zudem besteht nicht bei allen Anbietern ein intrinsisches Bestreben nach einer hohen Verbreitung einer der einer Schnittstelle. Wird eine Schnittstelle umfangreich öffentlich dokumentiert, kann dies zu einer vermehrten Nutzung und damit gleichzeitig zu einem steigenden Server- und Wartungsbedarf führen.

Literatur

[1] Bundesministerium des Innern, »Open Government Data Deutschland«, Eine Studie zu Open Government in Deutschland im Auftrag des Bundesministerium des Innern, Studie, Juli 2012.

[2] The Linux Foundation. »OpenAPI Initiative«, OpenAPI Initiative. (2022), Adresse: https://www.openapis.org/ (besucht am 30. 03. 2022).

[3] BMI. »Open Data«, Bundesministerium des Innern und für Heimat. (2021), Adresse: https://www.bmi.bund.de/DE/themen/moderne-verwaltung/open-government/open-data/open-data-node.html (besucht am 30. 03. 2022).

[4] *Entwurf eines Gesetzes zur Änderung des E-Government-Gesetzes und zur Einführung des Gesetzes für die Nutzung von Daten des öffentlichen Sektors*, unter Mitarb. von Bundesregierung.

[5] *Gesetz zur Förderung der elektronischen Verwaltung (E-Government-Gesetz - EGovG)*, 25. Juli 2013. Adresse: https://www.gesetze-im-internet.de/egovg/ (besucht am 10. 05. 2022).

[6] *Gesetz für die Nutzung von Daten des öffentlichen Sektors (Datennutzungsgesetz - DNG)*, 16. Juli 2021. Adresse: https://www.gesetze-im-internet.de/dng/ (besucht am 26. 05. 2022).

[7] A. Schmietendorf, »Öffentlich angebotene Daten und Funktionen (Open Data/Open APIs) als Rückgrat des digitalen Wandels in den deutschen Behörden – eine Bestandsaufnahme«, in *Verständliche Verwaltungskommunikation in Zeiten der Digitalisierung*, R. Fisch, Hrsg., Nomos Verlagsgesellschaft mbH & Co. KG, 2020, S. 63–76, ISBN: 978-3-7489-0284-3.

[8] IT-Planungsrat. »GovData - Datenportal für Deutschland«. (2022), Adresse: https://www.govdata.de (besucht am 06. 04. 2022).

[9] bundDEV. »Entwicklungsportal - API Übersicht«, Bundesstelle für Open Data - Verwaltung Digital. (2022), Adresse: https://bund.dev/ (besucht am 30. 03. 2022).

[10] L. Wittmann. »Wenn die Zivilgesellschaft bei Open Data hilft«, Medium. (2021), Adresse: https://lilithwittmann.medium.com/wenn-die-zivilgesellschaft-bei-open-data-hilft-905add0aa21b (besucht am 28. 03. 2022).

[11] bundDEV. »Bundesamt für Bevölkerungsschutz - NINA API«. (2021), Adresse: https://nina.api.bund.dev/ (besucht am 29. 03. 2022).

[12] SmartBear Software. »Swagger Inspector«. (2022), Adresse: https://inspector.swagger.io/builder (besucht am 12. 05. 2022).

[13] goofmint. »cURL to Swagger«. (2022), Adresse: https://goofmint.github.io/cURLtoSwagger/ (besucht am 01. 05. 2022).

[14] Stoplight. »Spectral - Open Source API Description Linter | Stoplight«. (2022), Adresse: https://stoplight.io//open-source/spectral (besucht am 02. 05. 2022).

[15] wirthual, *deutschland-generator-action*, 2021. Adresse: https://github.com/wirthual/deutschland-generator-action (besucht am 09. 05. 2022).

[16] T.-J. Huyeng. »Hochwasserzentralen - OpenAPI Documentation«. (2022), Adresse: https://t-huyeng.github.io/hochwasserzentralen-api/ (besucht am 25. 05. 2022).

[17] Wasserstraßen- und Schifffahrtsverwaltung des Bundes (WSV). »PEGELONLINE REST-API Dokumentation«. (2022), Adresse: https://www.pegelonline.wsv.de/webservice/dokuRestapi (besucht am 12. 05. 2022).

[18] T.-J. Huyeng. »GitHub OpenAPI Action«. (2022), Adresse: https://github.com/t-huyeng/openapi-action (besucht am 07. 06. 2022).

[19] buildingSMART, *BCF REST API*, 13. Feb. 2022. Adresse: https://github.com/buildingSMART/BCF-API (besucht am 09. 05. 2022).

Teil VI

Visualization & Topology

BIM and AR in Factory Planning: a Combination of Techniques from Architecture, Computer Science and Factory Planning

Sofia Lampe[1] and Julian Böck[2]

[1]Chair of Architectural Informatics, Technical University of München, Arcisstraße 21, 80333 Munich, Germany

[2]Fraunhofer Institute for Casting, Composite and Processing Technology IGCV, Am Technologiezentrum 10, 86159 Augsburg, Germany

E-Mails: sofia.lampe@tum.de, julian.boeck@igcv.fraunhofer.de

Abstract: Companies have to constantly adapt their products to the needs of an increasingly global, rapidly changing market. The production environment needs to change accordingly and factory planning thus becomes a continuous cycle. Plans for existing factory buildings are often not entirely available or outdated. In addition, diverse and incompatible planning tools lead to deficits in collaboration between the planning specialists. These circumstances may cause errors when implementing adaptions. This paper examines how digitalization as well as the use of Building Information Modeling (BIM) and Augmented Reality (AR) can improve the factory planning process by unifying data on the factory building and the production system to grant planners intuitive access to the data. This paper proposes a link-based integration of production data from existing databases into the open-source BIM server to create a single source of truth containing all relevant data for the factory planning process. In addition, we utilize AR to visualize the data on the shop floor for easy and intuitive access.

Keywords: Building Information Modeling, Augmented Reality, Factory Planning

1 Introduction

Today, manufacturing companies compete in an increasingly global and dynamic market [1]. Especially for small to medium-sized enterprises, this can be challenging because new product

iterations are required in shorter time spans [2]. To adapt to these shorter product lifecycles and still produce efficiently, manufacturing companies have to optimize their production facilities frequently [3]. Consequently, the factory planning process transforms into a continuous cycle instead of a one-time task [4].

Optimizing existing facilities is considered brownfield planning. Plans of the factory building are often scarce, outdated and only available in 2D. Planning tools are as diverse as the domains of the participating specialist planners. Fuzzy planning data may lead to errors and delays when realizing projects [5]. In order to structure the required data, Building Information Modeling (BIM) offers promising potentials. As an increasingly widespread methodology in architectural building planning, BIM coordinates the different domains and includes centralized data storage based on 3D models. [6]. BIM is not yet commonly used in factory planning, and therefore few factory planning tools support BIM formats.

In the ongoing research project ARBIM4Factory, we examined if a combination of techniques from architecture, computer science and factory planning can be utilized to improve the continuous factory planning process. This paper presents an approach to unifying factory building data and data from the production system using BIM. We propose a link-based integration of production data into an open-source BIM server to create a single source of truth containing all relevant data for the factory planning process. The main goal is to enable collaborative planning of the building and the production system. This collaborative approach ensures that planning errors can be identified earlier. Additionally, we explore possible use cases for AR to help visualize specific information stored within the BIM model to better leverage the model's advantage in the factory's operational phase.

2 Challenges in the Current Factory Planning Process

The factory planning process is composed of two main domains, the production system and the building planning. While the planning of the production system focuses on the value creation in the factory, the building planning forms the envelope. Following classical planning procedures as described in the VDI guideline 5200 1, the processes of both domains run in parallel [7], [8]. This causes problems such as poor synchronization and communication as well as a lack of early collision detection [9], often resulting in schedule delays or costly reconstruction efforts shortly after project completion. Using the methodology of BIM could help to overcome these problems by creating a collaborative planning procedure with consistent and up-to-date data [7], [10]. However, only a few factory planning projects with BIM are known so far.

In factory planning the most common planning cases are development planning and replanning. In development planning projects, a factory is built on a greenfield site, whereas in replanning projects the factory already exists. The so-called brownfield projects are the most common planning cases

and the restrictions of the existing facilities must be taken into account, which poses a special challenge. [8], [11]

In most brownfield projects the available planning data is very limited. There are many different data sources, e.g. plans and software systems, which are often not consistent, complete and up-to-date. Since the building and production system are often planned individually, even existing BIM models do not include models of the production system. Therefore one of the first steps is always to digitize the entire factory and prepare the data in a structured way. If this preparation is carried out directly in a BIM model for the production system and building, the data and information can be presented transparently for every planner. This leads to a so-called single source of truth. To alleviate the described problems, we combine techniques from the fields of architecture, computer science and factory planning. We hypothesize that the consistent use of BIM and AR facilitates a faster, more collaborative process by providing each planning expert easy access to the information needed for their specific domain. Thus, experts can communicate and collaborate more effectively.

3 Centralised Data Storage using BIM

The goal is to create a system where all the information relevant to the factory planning process is stored centrally. The data on the building and the production system are pulled together from various sources and consolidated in a single source of truth by either entering it directly into the BIM model or by linking the data from external sources. Traditionally, data of different planning departments is stored decentralized and often analog. When collaborating for projects this often leads to data loss and errors resulting in additional work through the re-entering of data [6]. When using a single source of truth instead, every planner is provided with up-to-date data on the facility and thus changes to the building and the production system can be planned collaboratively.

The benefits of BIM include the continuous use and maintenance of digital data throughout the planning process and the lifecycle of a building. Open data standards simplify collaboration as well as data exchange between teams and enable model checking for planning errors and inconsistencies. A high-quality BIM model can also provide the basis for data-based applications such as simulations [6], [12]. These aspects can be applied to solve factory planning issues as well.

If no models are available, a digital representation of the factory needs to be created in the first step. This can be done by laser scanning the factory and subsequently modelling the building and the production system based on the resulting point cloud. BIM models unify geometric information with alphanumeric data. The resulting geometric models are thus combined with alphanumeric information from existing plans and data lists. A BIM server stores the models and allows remote access to them.

In the case of factory planning, the model must also contain data from the production environment. Existing databases such as Manufacturing Execution Systems (MES) already contain a large

quantity of data on the production system such as live sensor data. Many manufacturing companies are using some form of these tools. To harness these data pools, we propose to utilize a prototypical broker where users can set up links between these systems and a database on the BIM server. The broker synchronizes between the database and data sources at regular intervals.

Linking information from the database ensures that the model files do not become too large and thus slow down the server, which can occur when data is entered directly into the model. Automating this data integration eliminates the risk of input errors by humans and guarantees that the various databases stay consistent.

After digitalizing two of our partners' factories, we populated the resulting BIM models with the needed data to realize the most relevant use cases. We used the open-source BIM server by the BIM collective [13] in our research project, as it allows for extension via its Application Programming Interface (API). An overview of the system setup can be seen in Figure 1.

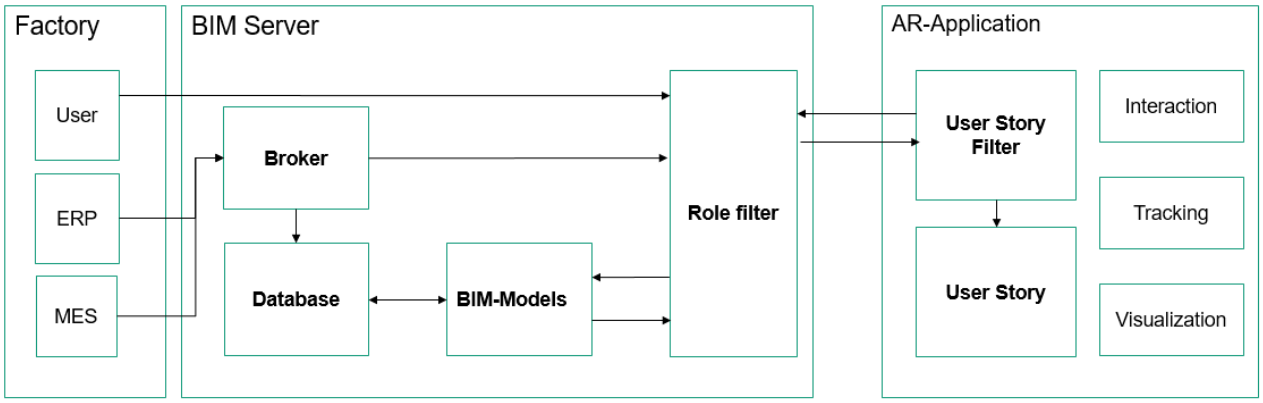

Figure 1: Ideal system uniting databases from the factory, BIM building data and a representation via an AR application.

We encountered problems with loading the BIM model into the AR app in real-time, such as a missing interface between BIM server and the game engine Unity. Thus, the BIM models were loaded directly into Unity using the PiXYZ plugin, with some of the meta data included in the model as well as the possibility to load them from a database.

4 Augmented Reality for On-Site Data Accessibility

The single source of truth contains or links to the available information on the factory building and the production system. Navigating a large system like this can be challenging when searching for a dataset. To make the information on the factory more accessible and transparent for staff on-site, we utilize AR. Therefore the advantages of BIM can still be leveraged after the planning phase. Overlaying virtual models with reality allows not only for comparison between the two but also to enrich the real facilities with information from their digital representation. AR aims to present

information that is directly registered to the physical environment. AR goes beyond mobile computing by bridging the gap between virtual world and real world, both spatially and cognitively. With AR, the digital information appears to become part of the real world, at least in the user's perception [14]. This is often done by rendering digital objects on top of a view of the user's real environment. Azuma [15] defines three characteristics of AR: it combines real and virtual, is interactive in real-time and the content is registered in 3D.

This project aims to display the information contained in the single source of truth using AR, forming the interface between the data system and the user. To implement AR, we first identified the appropriate tracking methodology and then developed visualization concepts for different use cases.

4.1 Augmented Reality in Factory Planning

AR as a visualization technique is quite versatile and can be applied to various use cases. In the case of factory planning, there are a few matters of import. The tracking methods need to work in the factory environment. We found marker-based tracking using QR codes, markerless tracking such as simultaneous localization and mapping (SLAM) and point cloud-based tracking to be suitable for use within the factory. Most alternatives do not provide the necessary level of accuracy or impose technical requirements which lead to high acquisition cost. The user interaction needs to fit the work environment as well. Head-mounted displays (HMDs) such as the HoloLens are controlled via gestures, view direction and voice commands [16], which can be challenging for users but allow for hands-free operation. Contrarily, touch screen interaction is familiar to most users but users need to hold and operate it with their hands.

In factory planning, multiple specialists collaborate to optimize the factory layout. On-site AR visualizations facilitate communication between specialist planners of different domains [17]. The AR visualization needs to be tailored to the user's needs and provides additional role-specific information to these planners, like datasets that vary depending on the user's area of expertise, or pieces of information that require specific levels of security clearance to view.

One of the main goals of this research project is to support collaboration between different specialist planners like architects and production system planners. On-site access to the central data source allows planning teams to work more effectively. We chose a tablet as the end device, as it offers better opportunities for collaboration than an HMD since multiple people can view and use the device simultaneously without having to switch HMDs or connect the devices via networking.

4.2 Prototype Concepts

After determining common problems in the factory planning process, we analyzed user scenarios and defined two basic modules: visualizing alphanumeric data contained in the BIM model and

displaying 3D models of machines at their designated locations in the factory. By combining these functionalities, the app supports various scenarios, e.g., highlighting necessary connections for new machines to showing sensor data on existing ones. One of the selected user scenarios is checking if a planned location for a machine fulfills the machine's prerequisites, such as connections for high-voltage current, water or compressed air. The lines often run under the ceiling and connectors are provided on pillars at regular intervals. We use color-coded highlights to visualize which requirements the current location fulfills and where the connections are located. For example, the position of available power connections is visualized by green dots next to the connections. Occupied connections are marked with a red dot (see Figure 2, left). We expand the collision detection to take the production system into account. Clashes in the geometry and the semantic information, such as lack of media supply in the surrounding area, can thus be detected and visualized in the app, alerting the planners to problems in the placement.

Another user scenario is accessing alphanummeric data via the AR app. Using the tracking methods, the machine is identified by, e.g., scanning a QR code on the machine. The app then selects the corresponding 3D model in the BIM model, filters the information based on the user's domain and displays static information and live sensor data (see Figure 2, right).

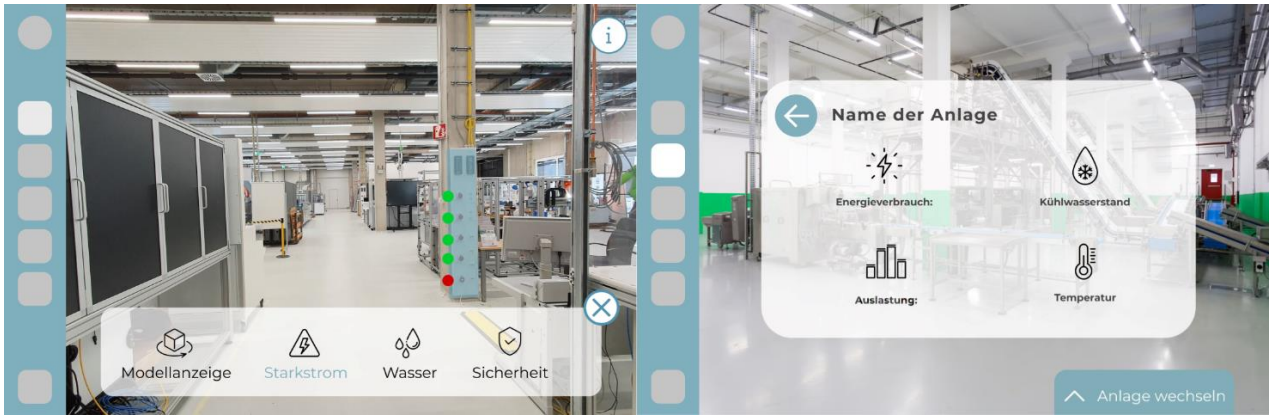

Figure 2: Concept of an AR visualization showing a machine's required connections (left) and the template to show live sensor data (right).

5 Conclusion

Digitalization offers immense opportunities for manufacturing companies when it comes to factory planning. Unifying factory data and accessing it on-site has the potential to improve the factory planning process to be more collaborative and efficient in terms of cost, time and resources. The next steps in this project are the implementation of the AR application and testing it in practice to evaluate the actual impact on the factory planning process of real manufacturing companies.

However, some companies already incorporate practices such as laser scanning and subsequent modelling into their planning procedure, but the usage of the resulting models has to be extended over the entire building lifecycle to exploit their full potential. Since the operational phase accounts for the majority of the life cycle, one model can be used as the basis for all planning measures and facility management during this phase. The biggest challenges are the constant adaptions to the factory and the continuous updating of the BIM model, which is often neglected, leaving the models outdated. Information on the production system is often updated automatically, there are however properties that are not observed by sensors, such as repositioning of machines, which have to be recorded manually and repeatedly in the BIM model. Further research is needed to find ways to simplify or, at best, automate the updating process for these properties.

Acknowledgements

This project was funded by the KME – Kompetenzzentrum Mittelstand GmbH.

References

[1] E. Abele and G. Reinhart, Zukunft der Produktion: Herausforderungen, Forschungs-felder, Chancen. s.l.: Carl Hanser Fachbuchverlag, 2011. [Online]. Available: http://www.hanser-elibrary.com/action/showBook?doi=10.3139/9783446428058

[2] G. Pawellek, Ed., Ganzheitliche Fabrikplanung. Berlin, Heidelberg: Springer Berlin Heidelberg, 2014.

[3] H.-P. Wiendahl, J. Reichardt, and P. Nyhuis, Handbook factory planning and design. Heidelberg: Springer, 2015. [Online]. Available: http://search.ebscohost.com/login.aspx?direct=true&scope=site&db=nlebk&AN=984764

[4] G. Schuh, A. Kampker, and C. Wesch-Potente, “Condition based factory planning,” Prod. Eng. Res. Devel., vol. 5, no. 1, pp. 89–94, 2011, doi: 10.1007/s11740-010-0281-y.

[5] S. Hawer, P. Ilmer, and G. Reinhart, “Classification of Fuzzy Planning Data for Facility Planning,” Zeitschrift für wirtschaftlichen Fabrikbetrieb, vol. 110, no. 6, pp. 348–351, 2015, doi: 10.3139/104.111339.

[6] A. Borrmann, M. König, C. Koch, and J. Beetz, Eds., Building Information Modeling: Technology Foundations and Industry Practice. Cham: Springer International Publishing, 2018.

[7] T. Neuhäuser et al., Collaborative Factory Layout Planning With Building Information Modeling: Hannover: Institutionelles Repositorium der Leibniz Universität Hannover, 2021. [Online]. Available: https://www.repo.uni-hannover.de/handle/123456789/11378

[8] VDI 5200 Blatt 1: Fabrikplanung - Planungsvorgehen: VDI 5200 Blatt 1, VDI 5200 Blatt 1, VDI-Gesellschaft Produktion und Logistik, Feb. 2011. [Online]. Available: https://www.vdi.de/richtlinien/details/vdi-5200-blatt-1-fabrikplanung-planungsvorgehen

[9] C. Reinema, A. Pompe, and P. Nyhuis, “Agiles Projektmanagement,” (in 108), Zeitschrift für wirtschaftlichen Fabrikbetrieb, vol. 108, no. 3, pp. 113–117, 2013. [Online]. Available: https://www.degruyter.com/document/doi/10.3139/104.110903/html

[10] T. Neuhäuser, Q. Chen, M. Rösch, A. Hohmann, and G. Reinhart, “Building Information Modeling im Fabriklebenszyklus,” Zeitschrift für wirtschaftlichen Fabrikbetrieb, vol. 115, s1, pp. 66–69, 2020.

[11] M. N. Loos, J. Ovtcharova, and S. Heinz, “Fabrikplanung im Fokus,” Bautechnik, vol. 89, no. 4, pp. 257–263, 2012, doi: 10.1002/bate.201201547.

[12] L. Hovestadt, U. Hirschberg, and O. Fritz, Atlas of digital architecture: Terminology, concepts, methods, tools, examples, phenomena. Basel: Birkhäuser, 2020.

[13] Open source BIM collective, The open source BIM collective. [Online]. Available: https://github.com/opensourceBIM (accessed: Jul. 5 2021).

[14] D. Schmalstieg and T. Höllerer, Augmented reality: Principles and practice. Boston: Addison-Wesley, 2016.

[15] R. T. Azuma, “A Survey of Augmented Reality,” Presence: Teleoperators & Virtual Environments, vol. 6, no. 4, pp. 355–385, 1997, doi: 10.1162/pres.1997.6.4.355.

[16] Microsoft, HoloLens 2—Overview, Features, and Specs | Microsoft HoloLens. [Online]. Available: https://www.microsoft.com/en-us/hololens/hardware (accessed: Jul. 5 2021).

[17] D. Donath, J. Beetz, K. Grether, E. Kruijff, F. Petzold, and H. Seichter, “Cooling Factory, a concrete project to test new architectural applications for augmented reality,” in EUROIMAGE ICAV3D 2001: Int. Conf. Augmented, Virtual Environments and Three-Dimensional Imaging, Mykonos, Greece, Brussels: European Project INTERFACE IST, May 30 - June 1 2001, pp. 14–17

Indoor Navigation with Augmented Reality and BIM: A Marker-Based Approach for Locating Logistics Areas on Construction Sites

Maximilian Gehring[1] und Pascal Mosler[1]

[1]Institute of Numerical Methods and Informatics in Civil Engineering, Technical University of Darmstadt, Franziska-Braun-Str. 7, 64287 Darmstadt, Germany

E-Mails: gehring@iib.tu-darmstadt.de, mosler@iib.tu-darmstadt.de

Abstract: A significant part of the working time on a construction site is spent searching for materials. Unnecessary distances are covered because the logistics areas for storing components are distributed over several floors and areas, depending on the size of the construction site. This paper proposes an augmented reality logistics app for smartphones that navigates a user to a desired logistics area on a construction site. The logistics app was developed with the Unity game engine based on the augmented reality framework ARFoundation and ZXing, a library for recognising QR codes. Solely the BIM model of the building to be constructed, which contains the 3D geometry as well as the position of the logistics areas and the QR codes, serves as the data basis for navigation. Since no further processing is necessary, the logistics app can be easily adapted to new building conditions. The demonstrated linking of BIM with marker-based indoor navigation and augmented reality facilitates the targeted search for material on the construction site and improves the logistical information flow on a construction site.

Keywords: BIM, Construction Logistics, Indoor Navigation, Augmented Reality, QR Code

1 Introduction

Construction logistics deals with the planning, control and monitoring of material and information flow on a construction site [1]. It is an important discipline in the realisation of construction projects and contributes significantly to the efficient and effective implementation of construction projects [2]. In the context of increasing cost pressure, the lack of skilled workers and the increasing specialisation of the companies involved, it is important to increase the productivity of the industrial workers and to

improve the cross-trade information flows on the construction site. According to [3], around 25% of the working time in building construction is spent on avoidable activities such as manual transport, searching for materials and unnecessary routes. The high number of involved companies leads to vertical and horizontal breaks in the value chain [4]. This favours the loss of logistically relevant information.

This paper aims to improve the flow of information in construction logistics by linking augmented reality (AR)-based indoor navigation with Building Information Model (BIM) planning data. A developed logistics app reduces unnecessary travel times on the construction site when searching for materials.

2 Technical Basics

2.1 Augmented Reality

Augmented Reality (AR), like Virtual Reality (VR), is a form of Extended Reality.

Regarding the distinction between AR and VR, [5] states that AR "is a variant of Virtual Environments (VE) or Virtual Reality as it is more commonly called. VE technologies fully immerse the user in a synthetic environment. While immersed, the user cannot see the real world around them. In contrast, AR allows the user to see the real world, with virtual objects superimposed on or merged with the real world. Therefore, AR complements reality rather than replacing it completely." [5].

[6] distinguish between six different types of AR and classifies them as "triggered" as well as "view-based". Trigger-based AR, for instance, relies on markers or objects and GPS positioning, which initiates the visualisation of augmented objects. In contrast, with "view-based" AR, there is no matching between the real world and the augmented objects.

2.2 Indoor Navigation

There are various approaches to indoor navigation with AR. Depending on the use case, different positioning methods are conceivable. They are divided into three categories by [7]: marker-based methods, 2D image recognition-based methods and 3D space recognition-based methods. Marker-based methods aim at synchronising between reality and the augmented objects to be placed. For example, QR codes can be used to achieve such synchronisation by placing QR codes in the real world and linking them in the AR application.

With 2D image recognition-based methods, the real environment is screened for distinctive objects. If the position of possible objects to be recognised is known in a stored model, the location is determined if the recognition is successful. [7] note that this approach has weaknesses in the case

of many and very similar objects. In addition, external factors play a role (angle of view of the image, distance to the object, moving objects).

Methods for 3D spatial recognition are used to capture spaces and match them with the cubature of stored spaces. For instance, a recording is made as a point cloud model. This approach is considered accurate, but also time-consuming and inflexible. If a location is heavily frequented or if individual rooms are very furnished, methods for 3D spatial recognition reach their limits.

[8] summarise the use of common positioning systems for indoor navigation (GPS, infrared, Wi-Fi, Bluetooth, ZigBee, NFC). They differ in terms of accuracy, operating location (indoor, outdoor), power consumption and costs. Only with NFC (near field communication) is it possible to determine a location with an accuracy of a few centimetres. Otherwise, the range is between 1m (infrared, Wi-Fi) and 10m (GPS).

2.3 Using Augmented Reality for Indoor Navigation in Buildings

In the scientific literature, very different proposals for using AR in buildings can be found, especially public buildings with much public traffic such as hospitals and shopping centres. As early as 2014, using the example of a hospital, [9] showed that navigation using AR is faster than orientation using maps or floor plans. [10] use the SLAM algorithm (Simultaneous Localisation and Mapping) to create and match point clouds. In contrast, [11] and [12] deposit two-dimensional maps in the application to enable pathfinding. [8] combine both approaches by initially creating a point cloud model and entering it into a content management system. There, navigation points are added and floor plans are exported. The data can be accessed from a cloud and coordinates are exchanged as JSON files. [7] propose a marker-free system by attaching Bluetooth transmitters (beacons) to the ceiling. All applications have a similar user interface. The user selects one of several predefined destinations on his smartphone, then his location is determined and his path is indicated by augmented lines or arrows on the floor.

At present, AR does not play a significant role in construction logistics. Nevertheless, approaches to simplify the process of component delivery through digital methods have existed for a few years. For example, the start-up Schüttflix [13] provides a GPS tracking system for delivering building materials. The unloading location is identified using a photo. The construction company Strabag uses a specially developed digital component tracking system based on QR codes [14]. Each component is marked with a corresponding QR code. The element status can be recorded and changed via an app. Contract documents, deadlines, etc. can be viewed for each component on an online platform. This makes it possible to compare the actual and target status.

3 Requirements for the logistics app

[4] mention the following particularities of construction logistics that need to be considered:

There are limited possibilities for storing material on the construction site. For this reason, the aim is to deliver building materials to the construction when they are needed. Before placement, the delivered building material should be stored as close as possible to the placement site, considering assembly, construction and movement areas. Thus, in building construction, the material is distributed over several floors and building areas. For construction logistics and executing companies, it is consequently not possible to maintain a simple visual overview of the material stored on the construction site. The individuality of construction projects (individual production and temporary location) and daily changing construction conditions make orientation on large construction sites difficult, as walkways and storage areas change regularly during the course of the project. To reduce the time spent searching for materials, it is therefore advisable to support the project participants with an indoor navigation tool. Due to planning changes during the construction phase, the basis of such an indoor navigation tool must be based on current planning data. The fluctuating availability of materials and construction personnel leads to unpredictable changes in the construction process, which influence the data basis of the indoor navigation tool. Furthermore, the highly fragmented industry structure results in many different project participants who need to be supplied with information as efficiently as possible. On the one hand, the logistics app should be as intuitive to use as possible and the information should be presented in a way that is as easy to understand as possible. On the other hand, no additional effort should be required on the part of the logistics planners or site managers to maintain the content.

This leads to the following requirements for the logistics app:

- Increasing productive working time by reducing search and travel times
- High topicality of the used data basis
- Low implementation effort, e.g. through the use of BIM data
- Low training costs

4 Logistics app to support construction logistics

Based on the requirements for the logistics app, an application concept was developed. It supports the project participants in their search for building materials or logistics areas on a construction site. The use of mobile phone-based AR techniques enables a widely accessible and easy-to-understand navigation in the building.

A logistics server will provide the navigation data for the logistics app. In addition to the building geometry and semantic component information from the BIM, this server contains current planning data for the construction process and logistics planning as well as the status data of the suppliers who deliver to the construction site. It is assumed that the logistics planning created has been adapted to the conditions of the different construction stages and also considers temporary assembly and construction areas. Through the use of the logistics server or an extended BIM platform, the app has an up-to-date and shared data source. This improves the exchange of information between the project participants. Via a web API, the logistics app can query the required data and update its data status (see Figure 1).

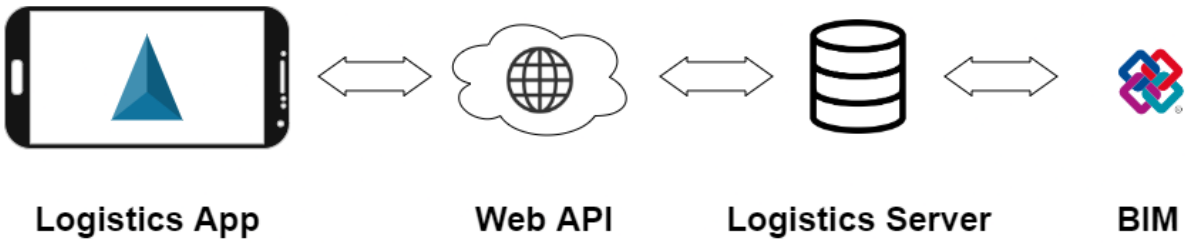

Figure 1: Components of the Logistics App

4.1 Combining BIM and Indoor Navigation

The basic research showed that various possibilities for indoor navigation and positioning using AR exist. This application uses a marker-based approach with QR codes, as the locations of the QR codes and the logistics areas can be implemented directly in the BIM software used and then imported into Unity. Even though, for example, [7] mention the disadvantages of QR code markers such as the lack of protection against the weather, the productive application of QR codes even under weather conditions by Strabag [14] shows that QR code markers are robust enough. Moreover, in the present application, they are used exclusively for positioning and can therefore be attached to fixed, immovable construction elements such as columns or walls. Another argument against the use of 2D- or 3D-based positioning methods and in favour of the marker-based approach is that due to the construction progress and the rapidly changing local conditions, point cloud models, for instance, quickly become outdated and would have to be updated in a time-consuming manner. For these reasons, a construction site does not offer any meaningful clues for image recognition either.

The logistics app was implemented as a demonstration application using the Unity game engine. The AR tracking is carried out via the AR Foundation Framework. This framework makes it possible to track the position of an AR device in the real world via acceleration sensors and recorded camera images and to pass this information on to the AR application. A comparable concept for indoor navigation with Unity, but based on AR-Core, was pursued by [15]. The library of ZXing [16] is used for QR code recognition.

The BIM planning data is integrated using scripts that assign the necessary semantic content to the imported 3D geometry in the FBX format. Thus, the logistics storage areas are stored as target locations in the navigation and calibration locations previously defined in the BIM are stored as entry points in the logistics app. To use the application on the construction site, the defined calibration locations must also be marked in the real world using QR markers. Components that remain unchanged over several construction stages, e.g. Kanban-Boards are suitable for this purpose, which are used in Lean Construction Management to visualize the work at various stages on site.

4.2 User Interface of the Logistics App

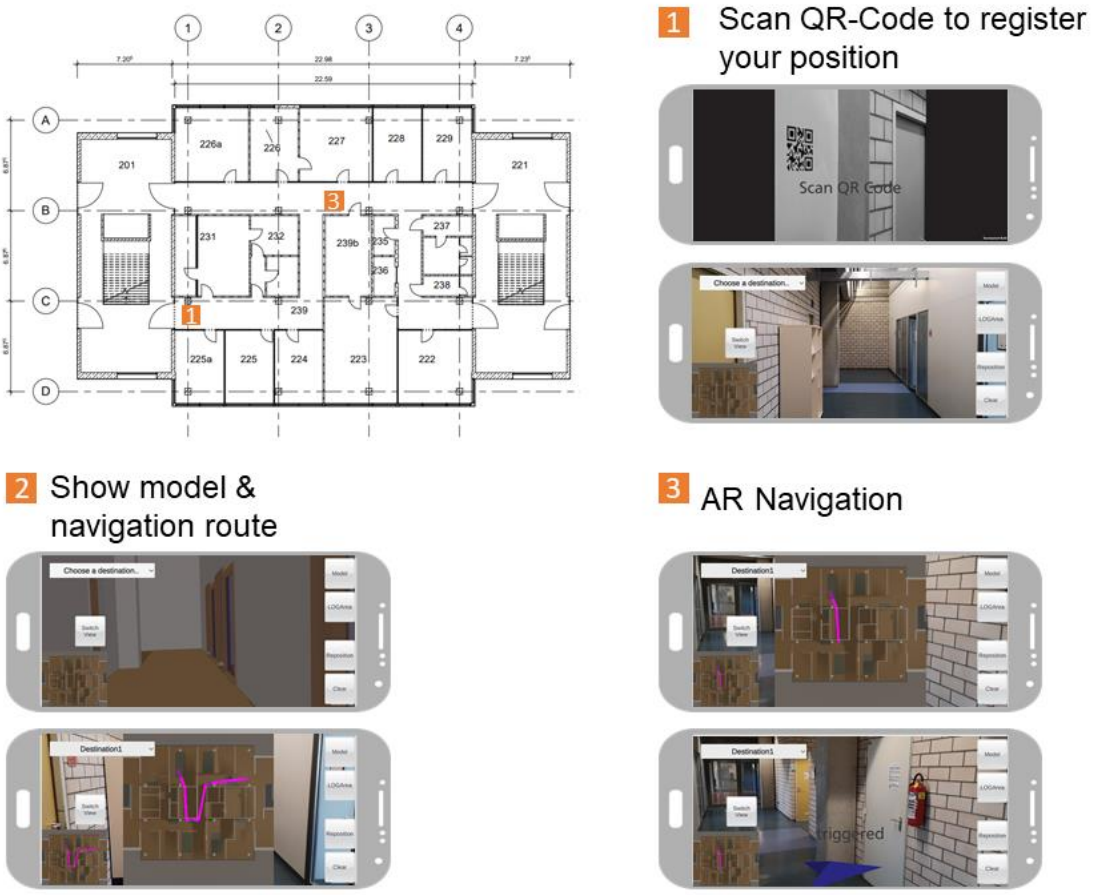

Figure 2: Exemplary Usage of the Logistics App

In the following, two application scenarios are outlined for the usage of the logistics app:

In the first case, a construction site logistics employee receives the delivery of materials. According to the stock planning, this material delivery is to be distributed to the logistics areas on the individual floors. To support the employee in finding the correct logistics areas, he can scan a unique component code on the material packaging and is guided to the correct storage area by the logistics app with the help of augmented arrows (see Figure 2).

In the second case, an employee of an executing company is in the building and is looking for more material to be installed. The logistics app shows the delivery status of the ordered materials and the storage location on the construction site. The logistics app directs the employee to the logistics area with the materials she is looking for in the building (see Figure 2).

5 Conclusion and Outlook

The logistics app shows that a BIM-based AR application for indoor navigation simplifies the search for materials and logistics areas on the construction site. In practice, only an occasional "drifting" of the AR camera in the application occurred, which was due to inaccurate positioning. This could be circumvented with more recalibration points, but this means more "maintenance effort" on the construction site.

Furthermore, temporary "blockages" of the paths in the building by supports or similar have not yet been considered when navigating to the desired logistics area. In future, it should be investigated how such closures can be noted in the logistics app and shared with the other project participants via the logistics server.

To provide a comprehensive assessment of the choice and use of a suitable tracking technology on a construction site, a systematic consideration of these technologies should be carried out in perspective. Against the background of different local conditions and construction states, aspects of the integration of outdoor navigation should also be considered.

References

[1] R. Jünemann and A. Beyer, Steuerung von Materialfluss- und Logistiksystemen. 1998. Accessed: 27. Mai 2022. [Online]. Available: https://doi.org/10.1007/978-3-642-72225-7

[2] C. Motzko et al., „Baubetrieb und Bauverfahrenstechnik“, in Bauwirtschaft und Baubetrieb, C. J. Diederichs and A. Malkwitz, Hrsg. Wiesbaden: Springer Fachmedien Wiesbaden, 2020, p. 489–614. doi: 10.1007/978-3-658-27916-5_13.

[3] G. Girmscheid, „Phasen des Angebotsmanagements“, in Angebots- und Ausführungsmanagement-prozessorientiert, Berlin, Heidelberg: Springer Berlin Heidelberg, 2015, p. 9–13. doi: 10.1007/978-3-642-55291-5_2.

[4] W. Günthner and A. Borrmann, Hrsg., Digitale Baustelle- innovativer Planen, effizienter Ausführen. Berlin, Heidelberg: Springer Berlin Heidelberg, 2011. doi: 10.1007/978-3-642-16486-6.

[5] R. T. Azuma, „A Survey of Augmented Reality“, p. 48.

[6] A. Edwards-Stewart, T. Hoyt, and G. M. Reger, „Classifying Different Types of Augmented Reality Technology“, p. 4.

[7] B.-C. Huang, J. Hsu, E. T.-H. Chu, and H.-M. Wu, „ARBIN: Augmented Reality Based Indoor Navigation System“, Sensors, Vol. 20, No. 20, p. 5890, Oct. 2020, doi: 10.3390/s20205890.

[8] P. Verma, K. Agrawal, and V. Sarasvathi, „Indoor Navigation Using Augmented Reality“, in Proceedings of the 2020 4th International Conference on Virtual and Augmented Reality Simulations, Sydney NSW Australia, Feb. 2020, p. 58–63. doi: 10.1145/3385378.3385387.

[9] M. Gheisari, G. Williams, B. N. Walker, and J. Irizarry, „Locating Building Components in a Facility Using Augmented Reality vs. Paper-Based Methods: A User-Centered Experimental Comparison“, in Computing in Civil and Building Engineering (2014), Orlando, Florida, United States, June 2014, p. 850–857. doi: 10.1061/9780784413616.106.

[10] W. Chidsin, Y. Gu, and I. Goncharenko, „AR-Based Navigation Using RGB-D Camera and Hybrid Map“, Sustainability, Vol. 13, No. 10, p. 5585, May 2021, doi: 10.3390/su13105585.

[11] G. Gerstweiler, „Guiding People in Complex Indoor Environments Using Augmented Reality“, in 2018 IEEE Conference on Virtual Reality and 3D User Interfaces (VR), Tuebingen/Reutlingen, Germany, March 2018, p. 801–802. doi: 10.1109/VR.2018.8446138.

[12] D. N. Mohd Nizam, L. W. Shin, Z. H. A. Sani, P. Thamrongrat, and N. Mohd Tuah, „An Indoor Navigation Support for the Student Halls of Residence using Augmented Reality: A Design Perspective“, Pertanika J. Sci. Technol., Vol. 29, No. 4, Oct. 2021, doi: 10.47836/pjst.29.4.23.

[13] „Schüttflix“, Schüttflix. https://www.schuettflix.de/de/de/ (Accessed 27. May 2022).

[14] „Digitales Bauteil-Tracking“, Innovation bei STRABAG. https://innovation.strabag.com/projekt/digitales-bauteil-tracking/ (Accessed 27. May 2022).

[15] R.-H. Patronoudis, „Creating an ARCore powered indoor navigation application in Unity“, Raccoons. http://raccoons-5252152.hs-sites.com/blog/arcore-powered-indoor-navigation-unity (Accessed 27. May 2022).

[16] zxing/zxing. ZXing Project, 2022. Accessed: 27. May 2022. [Online]. Available: https://github.com/zxing/zxing

Topological queries in a space partitioning model: Definition, visualization and exports of results

Amelia Städtler[1] and Maximilian Sternal[1]
[1]Chair of Computing in Civil Engineering, Technische Universität Berlin, Germany
E-mail(s): amelia@die-fabelhafte-welt-der-amelia.de, maximilian.sternal@tu-berlin.de

Abstract: A modern building model is usually digital (BIM) and contains the geometry of the elements and spaces. The topological relationships of their elements, on the other hand, are often insufficiently described. However, many civil engineering applications do rely on the topological relationships between modeled elements. Two examples for that being energy modeling and the computer assisted navigation through indoor spaces. This paper investigates how topological queries can be run on an exemplary polyhedral space partitioning model. Therefore, a brief introduction to the principles of polyhedral space partitioning is presented. Current research approaches for topological models, spatial information and graph-based building models are reviewed. Topological queries are presented that derive neighboring relations from the investigated polyhedral space partitioning model. These queries are subsequently used deriving and visualization graph models that represent the full topology of the space partitioning model. Finally, the topologic information stored in the space partitioning model is exported into data structures with a focus on topological aspects: the Building Topology Ontology (BOT) and the OGC IndoorGML standard. Benefits and limitations of the space partitioning model, in regard to the export to such data structures, are discussed. And outlook is given on future possibilities of connecting geometric description, semantic data and topological and spatial information based on polyhedral space partitioning.

Keywords: Data Modeling, Topological Data Structures, Building Topology Ontology (BOT), IndoorGML

1 Introduction

Digital building models include geometric and semantic information of various kinds, for example materials and technical features. The topological relationships of their elements, on the other hand, are often insufficiently described. This is pointed out, for example, by Diakité and Zlatanova [1], for the prominent BIM standard Industry Foundation Classes (IFC). However, many civil engineering applications do rely on the topological relationships between modeled elements. One example for that being the computer assisted navigation through indoor spaces [2]. Graph-based models are an essential tool for describing relationships in digital workflows in the architecture and engineering

industry (AEC). One relationship, investigated in this paper, is the spatial configuration of “topological primitives” like edges or cells. Such objects are part of geometric descriptions in geo-information-systems (GIS) and building information models (BIM), but the neighbourhood configurations between objects are often insufficiently described. However, it is possible to model a holistic geometry including topological relationships using a polyhedral space partitioning (*PPSpace*).

The *PPSpace* [3] project comprises a modeling kernel that creates and modifies a polyhedral space partitioning model, explicitly storing neighborhood relations of topological objects. Queries are implemented and described in this paper for a *PPSpace* space partitioning model. An example for such a query would be: “Return all cells that are neighbors of and share a face with this cell”. It shall be shown that, based on these queries, the export of a *PPSpace* space partitioning model to existing topological data structures in a civil engineering context, such as *BOT*, is possible.

This paper demonstrates how topological information can be exported from such a partition model to existing graph data structures. In the following chapter, the background for graph-based application models in AEC is outlined and related work of topological data structures for computational geometry is reviewed. Central features of the presented polyhedral space partitioning approach are introduced. It is shown how queries to the space partition can return topological relations and how these can be used to build graphs. Subsequently, these queries are used to export topological information, with a minimal subset of semantics, from a partition model to established topological data models of the AEC industry. Finally, an outlook to future applications and extensions to this concept is given.

2 Topological Queries

Topological queries are traditionally performed over spatial databases, which store primarily "regions" as two-dimensional geometry [4]. Spatial predicates can be computed by testing to regions against each other. Romanschek et al.[5] presented a novel approach based on space partition in the two-dimensional space. While this concept has been proven to be robust and extensible to the three-dimensional space [6], [7], the data structure used in this paper is not computed from an existing B-Rep, but constructed from scratch and topological queries can be performed without geometrical computation. The following chapters describe related approaches to topological information and introduces the main features of the *PPSpace data model* and its relations.

2.1 Related Work

Topology, as described by Paul [8], stems from the mathematical theory of continuous functions and denotes the connectivity between, for example, the rooms of a building and their links like doors or walls. Paul outlines the connection between CAD applications and the underlying topological concepts of topological space and homeomorphism of spatial data. A very similar approach is taken by the *topologic.app* tool [9]. It provides methods for visual programming to evaluate non-manifold cell complexes in terms of topological relationships.

For geo-information models, Clementini et al. [4] identify the need for GIS databases to be able to process queries with “topological constraints”. Daum and Borrmann [10] have presented a spatial query language that is based on the well-known 9-intersection matrix to analyse a given boundary representation using geometric calculations in order to describe e.g. "touch" and "contain" relationships between objects. However, such computations are complex and must be performed again after every modification. Research projects for 3D cadastral models have recently presented approaches for including spatial configurations, e.g. [11]–[13], which highlights the existing need for better capabilities or representing topology in AEC on the building and city scale.

2.2 Polyhedral Space Partition

The *PPSpace data model*, presented in [3], is a polyhedral space partitioning that structures the point set of Euclidian space. This point-set topology can be modified using atomic merge and split operators [14]. The partition system consists of two parts, an non-oriented user model and a core model. The user model represents a point-set topology and consists of nodes, edges, faces and cells, each defined by their boundaries. These domains represent manifolds that can be non-convex, multiply-connected and unbounded, as the Euclidean space is unbounded as well. The geometry of this model is specified by point coordinates, directions and planes. The core model is oriented and stores topological references. This concept builds upon existing approaches such as Radial Edge[15], Partial Edge[16] and Dual-Half Edge[2] and thereby combines features of space partitioning and topological data structures. Oriented "arrow bundles" and "twin facets" provide links to compute outer and inner polygons, radial and dihedral cycles and neighbouring or consisting cells.

2.3 Relations

Through the internal structure of the core model, topological information can be derived directly, without any geometric calculations. This is supported by the separation of geometrical and topological data, which are each represented by a different sub-model. Queries can be run on a partition model that identify neighboring relations between user model elements. The actual topological relations are determined in the core model, while the super-ordinate queries on the user model serve as an interface for other applications and tasks.

Comic and de Floriani [17] exhaustively describe existing topological data structures and relations. A relation is classified $R_{j,k}(P)$, where P is the parameter to start the query, e.g. an edge or cell, j and k indicate the dimension of the start and target of the relational contact query. A contact query for *adjacent* domains of the same dimension (j = k) would be to return all cells in contact with one specific cell ($R_{3,3}(C)$). The implementation in this paper extends this concept by defining an additional dimension for the contact, to obtain also all cells that share at least one edge $R^1_{3,3}(C)$ or node $R^0_{3,3}(C)$. Furthermore, queries for *boundary* relations (j < k) are specified to return, e.g. all nodes in the boundary of a face $R_{2,0}(F)$ or all edges *connected* (j > k) through a node $R_{0,1}(N)$.

Contact queries are often describe to only return elements that are in contact with the parameter. However, during the export of graph data structures the need arose to also obtain the model elements

through which contact elements are connected to the parameter, because this information is right at hand when the query is run, but difficult to obtain later.

3 Export

Based on the implemented topological queries (as described in section 2), links and paths within the model can be calculated. A partition model can be translated to a graph that contains topological information. This is achieved by translating model objects to graph vertices. Topological relations between these model objects are represented by graph edges, which connect the parameter object of a topological query to its result objects. Because the user model serves as an interface of the space partition, graphs are determined only for user model objects while the calculation relies on the links in the underlying core model.

Figure 1 shows an example of adjacent boxes (A-E), surrounded by two other cells (X-Y) that are eventually embedded in a partitioned unbounded outer space (c0X). The graph in figure 2 symbolizes the topological relations of connected cells. The generic open-source graph framework *JGraphT* is used to export and visualize semantic-free *GraphML* graphs. The following chapter will extend this concept by mapping and classifying cells according to existing engineering standards.

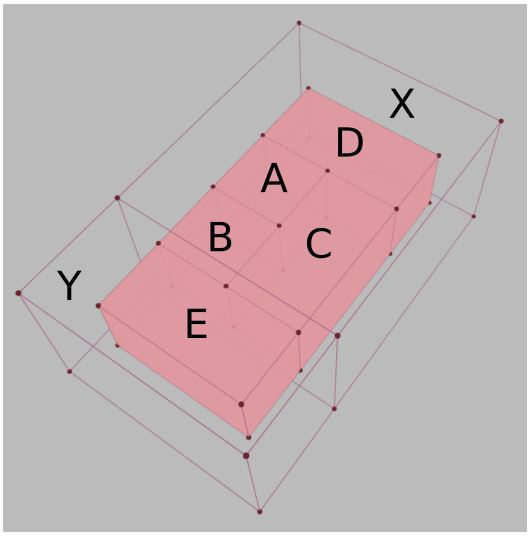

Figure 1: A test fixture for the derivation of graphs. The boxes A, B, C, D and E are encased in the boxes X and Y.

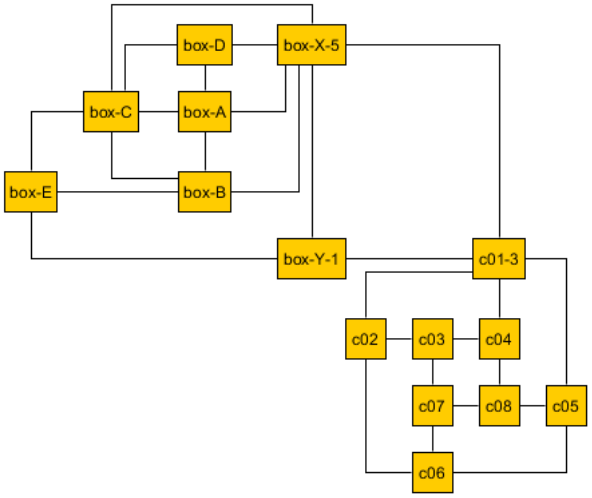

Figure 2: A graph representing topological relations of the test fixture. The graph vertices represent cells, a graph edge implies a common face. $R^2_{3,3}$

3.1 Building Topology Ontology

The *Building Topology Ontology* (BOT) is an *OWL* ontology that describes topological relationships specifically in a building context [18]. As an ontology, BOT represents semantic information. A *PPSpace* partition model contains geometrical and topological information about its objects, but it cannot be inferred if the object represents a building element, a building space or something completely

different. It is therefore necessary to wrap a partition model in an export model that contains the BOT classifications for the relevant partition model objects. The BOT classes [18] considered in this paper are:

- **Space**: has a 3D extend with physical or conceptual meaning
- **Element**: building elements like walls, beams etc.
- **Interface**: qualifies the relationships of Spaces and Elements

BOT furthermore defines properties, which mostly describe topological relations between classes and entities [18]. The partition model contains such information. This paper investigates how these properties can be automatically derived from a partition model. Adjacency, expressed by the properties *adjacentZone* and *adjacentElement*, can be derived from a partition model through topological queries. The result of a topological query are partition model objects that are adjacent to the parameter object.

A partition model object separately refers to its inner boundary elements by referencing a single element of each inner region in the core model. Therefore, containment, expressed by the properties *containsZone, hasSpace, hasElement and containsElement*, can also be inferred from the partition model. The other elements belonging to an inner region can be determined through model traversal, for example a depth-first search. In a partition model, contained elements are always also adjacent elements. This is acceptable because adjacency and containment properties are not disjoint in BOT. However, an element that is connected to the boundary of its encasing element is considered adjacent, but not contained. This might not always be a good estimation, especially in civil engineering where, for physical reasons, everything is usually connected to the floor (for example a column in a room).

Intersection, expressed by the properties *intersectsZone* and *intersectingElement*, is strictly excluded from a partition model and can therefore not be exported to BOT. An implementation is introduced that derives a BOT ontology from a *PPSpace* partition model, according to the ideas presented above. The BOT ontology is written to a Turtle file. Figure 3 shows the visualization of a partition model. Figure 4 shows a graph visualization of the BOT ontology that was derived from this partition model, using the implementation. The graph visualization was produced using the *SPARQL* visualizer provided by Mads Holten Rasmussen [19].

This shows that the topological relations defined as properties in BOT, particularly adjacency and containment, can be automatically exported from a *PPSpace* partition model, using the implemented topological queries. Intersection cannot be exported, because it is not covered by the partition model. However, a valid BOT ontology can still be created without.

3.2 IndoorGML

IndoorGML is an ‘open data model and XML schema for indoor spatial information’. It features a cellular space model with additional semantic, geometrical and topological information [20]. The cellular space consists of identifiable cells that do not intersect, which resembles the structure of the partition model. The central aspect of an IndoorGML model is the *Structured Space Model (SSM)*. A graphical representation is depicted in figure 6. The SSM distinguishes between the primal and the

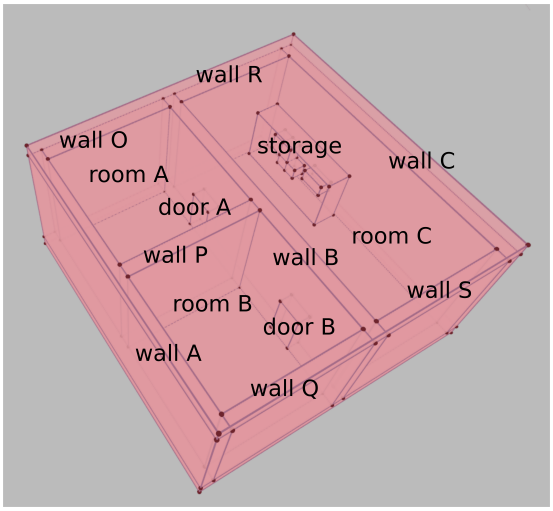

Figure 3: A visualization of the model for testing the BOT export.

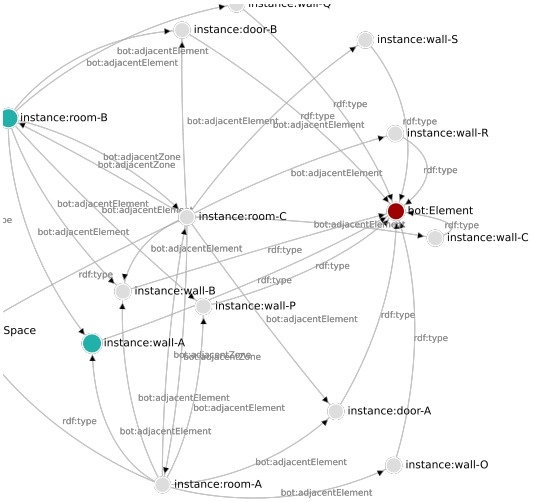

Figure 4: The exported ontology, loaded in the *SPARQL* visualizer tool.

dual space, and therein between geometrical and topological data. The primal geometry is stored in the polyhedral partition model. The dual space is represented by Node Relation Graphs (NRG). A NRG is based in the Poincaré-duality and represents three-dimensional objects through nodes and their common boundaries through edges [20]. Figure 5 shows a prototype visualization of primal and dual geometry for the special case of convex polytopes.

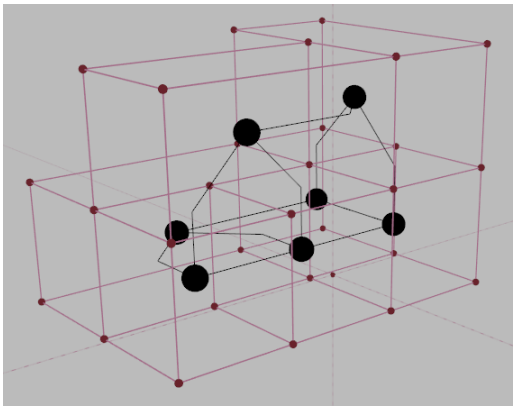

Figure 5: Primal and dual geometry of a test fixture.

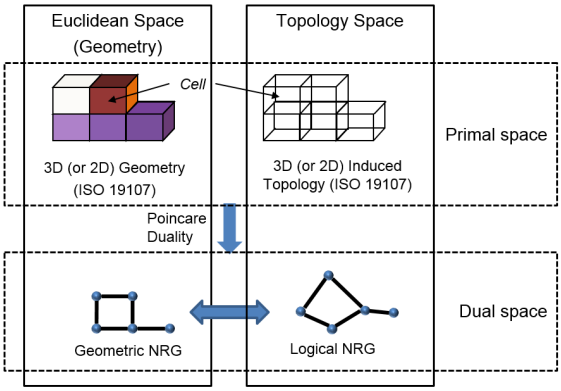

Figure 6: An overview over the Structured Space Model, as employed by *IndoorGML*. From: [20])

The dual topology, represented by a 'logic NRG', can be inferred from a *PPSpace* partition model. using the concepts for graph derivation presented in chapter 2. Contact queries $R_{3,3}(C)$ are able to determine cells that share a common boundary with the parameter *'C'*.

4 Outlook

The implemented topological queries are able to derive topological information from a partition model without geometrical calculations. A large number of related applications can be based on the topological queries. The export to BOT and IndoorGML is generally possible and convenient when topological queries are used to derive topological information from the partition model. Currently, only test models have been analyzed and only a subset of its classes and properties have been considered in the export to BOT. Further implementation and validation of exported models must be performed to assess the usability of the presented approach. Open questions regarding geometrical robustness are investigated in current research.

As space partitioning maps the complete space including unbounded domains, this approach would be able to connect indoor and outdoor models. Several research projects aim to align building standards such as the IFC with urban models and navigation [1], [13], [21]. Multiple shortcomings of topological relations and geometric inconsistencies have been found and any alignment can benefit strongly from a holistic modeling of space and its relations.

References

[1] A. Abou Diakité and S. Zlatanova, “Valid Space Description in BIM for 3D Indoor Navigation:” *International Journal of 3-D Information Modeling*, vol. 5, 2016.

[2] P. Boguslawski and C. Gold, “The Dual Half-Edge—A Topological Primal/Dual Data Structure and Construction Operators for Modelling and Manipulating Cell Complexes”, en, *ISPRS International Journal of Geo-Information*, vol. 5, no. 2, 2016.

[3] P. J. Pahl, “Polyhedral Partition of Euclidean Space”, TU Berlin, (draft), 2021.

[4] E. Clementini, J. Sharma, and M. J. Egenhofer, “Modeling Topological Spatial Relations: Strategies for Query Processing”, en, p. 15, 1994.

[5] E. Romanschek, C. Clemen, and W. Huhnt, “A Novel Robust Approach for Computing DE-9IM Matrices Based on Space Partition and Integer Coordinates”, *ISPRS International Journal of Geo-Information*, vol. 10-11, 2021.

[6] J. Vetter and W. Huhnt, “Accuracy Aspects when Transforming a Boundary Representation of Solids into a Tetrahedral Space Partition”, in *Proceedings of the EG-ICE 2021 Workshop on Intelligent Computing in Engineering*, 2021.

[7] M. W. Jahn and P. E. Bradley, “A Robustness Study for the Extraction of Watertight Volumetric Models from Boundary Representation Data”, *ISPRS International Journal of Geo-Information*, vol. 11, no. 4, 2022, Publisher: MDPI.

[8] N. Paul, “Applications of continuous functions in topological CAD data”, *arXiv:1308.0256 [cs]*, [Online]. Available: http://arxiv.org/abs/1308.0256 (visited on 12/08/2021).

[9] W. Jabi and A. Chatzivasileiadi, “Topologic: Exploring Spatial Reasoning Through Geometry, Topology, and Semantics”, in *Formal Methods in Architecture, Springer*, 2021.

[10] S. Daum and A. Borrmann, “Processing of Topological BIM Queries using Boundary Representation Based Methods”, *Advanced Engineering Informatics*, vol. 28, 2014.

[11] U. Ujang, F. Anton Castro, and S. Azri, “Abstract Topological Data Structure for 3D Spatial Objects”, *ISPRS International Journal of Geo-Information*, vol. 8, 2019.

[12] L. Knoth, B. Atazadeh, and A. Rajabifard, “Developing a new framework based on solid models for 3D cadastres”, *Land Use Policy*, vol. 92, 2020.

[13] R. Jaljolie, K. Riekkinen, and S. Dalyot, “A topological-based approach for determining spatial relationships of complex volumetric parcels in land administration systems”, *Land Use Policy*, vol. 109, 2021.

[14] V. Galishnikova and W. Huhnt, “Polyhedral space partitioning as an alternative to component assembly”, in *ECPPM 2021 – eWork and eBusiness in Architecture, Engineering and Construction*, CRC Press, 2021.

[15] K. J. Weiler, *Topological structures for geometric modeling (Boundary representation, manifold, radial edge structure)*, Aug. 1986.

[16] S. H. Lee and K. Lee, “Partial entity structure: A compact non-manifold boundary representation based on partial topological entities”, en, in *Proceedings of the sixth ACM symposium on Solid modeling and applications - SMA ’01*, Ann Arbor, Michigan, United States: ACM Press, 2001.

[17] L. Čomić and L. D. Floriani, “Modeling and manipulating cell complexes in two, three and higher dimensions”, in *Digital Geometry Algorithms*, Springer, 2012, pp. 109–144.

[18] M. H. Rasmussen, M. Lefrançois, G. F. Schneider, and P. Pauwels, “BOT: The building topology ontology of the W3C linked building data group”, *Semantic Web*, vol. 12, pp. 143–161, 2021, Publisher: IOS Press.

[19] Rasmussen, Mads Holten. “Sparql-visualizer | bot: The basics”. (2021), [Online]. Available: https://w3c-lbd-cg.github.io/bot/tutorial/ (visited on 12/12/2021).

[20] J. Lee, K.-J. Li, S. Zlatanova, *et al.*, “Ogc® indoorgml 1.1”, Open Geospatial Consortium, Tech. Rep. 19-011r4, version 1.1, 2020. [Online]. Available: http://www.opengis.net/doc/IS/indoorgml/1.1 (visited on 12/29/2021).

[21] J. Yan, S. Zlatanova, and A. Diakité, “A unified 3D space-based navigation model for seamless navigation in indoor and outdoor”, *International Journal of Digital Earth*, vol. 14, 2021.

Immersive Teaching of AEC Construction Details using Virtual Reality

Dr.-Ing. Michael A. Kraus, M.Sc. (hons)[1] and Dr. Romana Rust[1]
[1]Design++ Initiative and Immersive Design Lab, ETH Zurich, Stefano-Franscini-Platz 5, CH-8093 Zurich, Schweiz
E-mail(s): kraus@ibk.baug.ethz.ch, rust@arch.ethz.ch

Abstract: Designing basic construction details of buildings is a fundamental part in the course of educating students of architecture and civil engineering during their first year. To meet current challenges in education, this research is concerned with investigating the benefits of advancing VR technology for knowledge gain and supporting the understanding process for the students for teaching construction details. The objective of this research is twofold: (i) develop a VR-workflow for construction detail analysis, and (ii) conduct a survey amongst lecturers, students and laypersons to measure the acceptance, ergonomics and learning impact of the developed VR application for a prototypical construction detail. This is investigated through a VR-demonstrator, which comprises of an interactive 3D model of a construction detail of a basement wall and two different modes (*inspection* and *quiz* mode). To verify our hypothesis of a significant benefit in students' learning through the interactive and intuitive nature of VR, a pilot study with a panel consisting of 41 participants was conducted. A control group used 2D paper drawings of the basement construction, which was labelled exactly as in the VR model. It was concluded that for participants with a professional background in the AEC industry, there was no significant advantage of using VR over 2D drawings. For students without much prior knowledge VR learning was more effective. The results support the authors' core assumption for the use of VR in teaching: the presentation of contextual 3D models to illustrate content is a promising approach. To that end, VR technology will augment traditional teaching formats in architecture and civil engineering in the near future.

Keywords: Education in Architecture and Engineering, Immersive Teaching, Virtual Reality

1 Introduction

With Extended Reality (XR) and especially Virtual Reality (VR) technologies becoming more affordable, the dissemination of this technology increases steadily and hence promises new opportunities and use cases. The majority of higher education institutions in the architecture, engineering and construction (AEC) sector however have not yet adopted new digital learning technologies and XR in particular, or

have done so only to a relatively small extent. Based on our previous work [1], [2] on using Augmented and Mixed Reality applications for developing novel workflows in teaching structural engineering, this paper presents a workflow for teaching construction details with VR. The findings of our past studies are in accordance with the findings in literature [3], which proof, that virtual learning environments enhance, motivate and stimulate students' understanding for the construction and analysis of AEC problems.

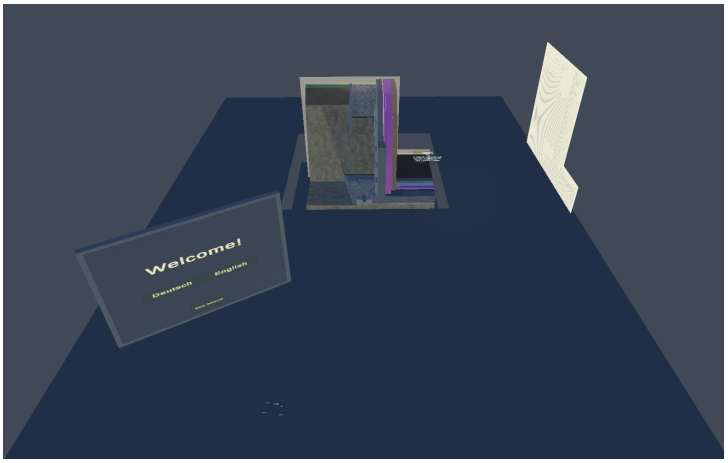

Figure 1: Total view of the VR scene: Tutorial (left), 3D construction detail (centre), and 2D detail (right)

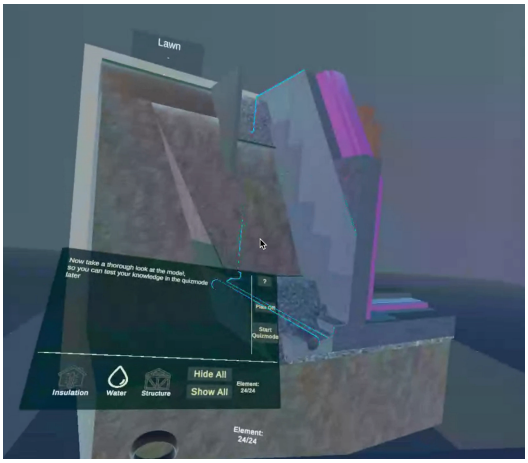

Figure 2: Tablet that enables to highlight the water-dissipating layers

The content of introductory and fundamental lectures on design and analysis of structures and the built environment demands advanced analytical thinking and abstraction abilities for students in order to understand the content of lectures and the principles of the profession. Especially for students in architecture and civil engineering with little professional experience, this abstraction in lectures is a hurdle. A prototypical example problem category is construction detailing, where students are taught principles of functional, reliable and efficient construction details. Today, the method of conveying the content uses instructor-centred lectures together with exercises and textbooks upon two-dimensional drawings of the 3D construction elements. The content to be learned consists of considerations towards geometry, adjacency, functionality and construction sequences as construction details are usually fabricated in a complex joined fashion. Due to time, cost and availability constraints, construction site visits are hardly part of today's teaching in order to supplement the lecture material and to provide students with the real 3D content of construction details. Elgewely, Nadim, ElKassed, *et al.* [4] even state, that occasional site visits are not sufficient to establish students' understanding about construction details or their 3D configuration. In summary, the status-quo of teaching construction details in AEC actually triggers students to rather memorise the 2D representation than really gaining insight and understanding of the construction detail, its functionality and composition sequence.

To that end, the objective of this research is twofold: (i) develop a workflow for embedding construction detail analysis content into a VR application, and (ii) conduct a survey amongst lecturers, students and laypersons to measure the acceptance, ergonomics and learning impact of the developed VR

application for a prototypical construction detail. All code produced within this publication is freely available and open access, see [5].

2 Related Work and Literature Review

Over the past years, some research was dedicated to assess effectiveness of XR methods in the AEC domain and relevant teaching. However, given the brevity and scope of this paper, only VR-related literature in AEC and teaching is considered.

A VR interface for developing construction plans of a nuclear power plant within an hour was implemented by Messner, Yerrapathruni, Baratta, *et al.* [6] and assessed in undergraduate AEC programs. The study showed, that immersive VR displays are beneficial for this type of lecture and the technology allowed an understanding for planning issues beyond their prior knowledge and visualisation capacities concerning buildings and infrastructures. Liarokapis [7] provides an educational XR application to enable user interaction with 3D content via web technology and AR/VR techniques. Häfner, Häfner, and Ovtcharova [8] curated a university-level course for teaching students the use of VR hardware, software and applications in engineering, where the study found a higher motivation with the students at given tasks when VR was used. Dinis, Guimaraes, Carvalho, *et al.* [9] developed VR and AR applications for students of an introductory class of the Integrated Masters in Civil Engineering and tested those in two trials. Further successful development of VR applications in design and education tasks are reported by Sampaio and Martins [10] and Wolfartsberger [11].

A VR application created by Maghool, Amir, Moeini, *et al.* [12] enables architecture students to experience a construction site, closely investigating details, and testing their knowledge. The study revealed, that a significant proportion of learners have been left out in the current teaching system. They showed, that a VR teaching method is superior compared to traditional means since it allows for problem-based and experiential learning. The paper concludes learning construction details in VR to carry notable benefits for the students and in addition will be part of future education. Elgewely, Nadim, ElKassed, *et al.* [4] also observe a lack of experiential learning in current architectural education. The study relates this mainly to the low number of site visits as an important extension of classroom activity. An educational VR experience with BIM integration hence was developed. Further potentials beyond regular site visits were seen in the more engaging teaching styles enabled by VR. While Maghool, Amir, Moeini, *et al.* [12] concluded that integrating models into the VRE is time consuming and tedious, Elgewely, Nadim, ElKassed, *et al.* [4] take BIM models and databases as a source of technical information. Finally, Kraus, Custovic, and Kaufmann [1] take a different approach, where instead of simulating construction sites, the lecture is complemented by Augmented Reality (AR) applications. AR apps allow students to conduct in-depth and true-scale assessments of 3D structural engineering details with interactive supplemental information. With this approach, the advantages of both teaching modes are harnessed. Statistical evaluation of the conducted surveys amongst students and lecturers revealed, that XR technologies possess great potential for improving effectiveness of teaching by displaying environments and associated information in an intuitive way similar to real

objects. In addition, they observed that users reported higher enjoyment of the learning process when using XR technology.

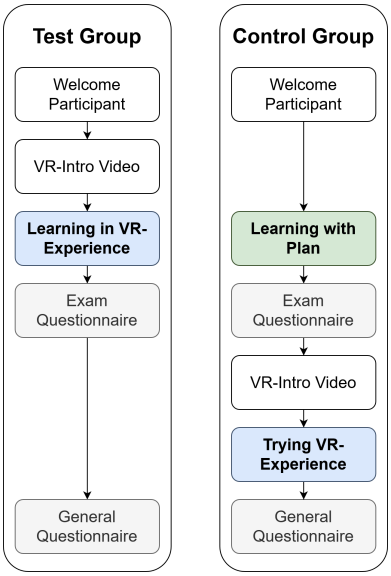

Figure 3: Different study journeys of the participants.

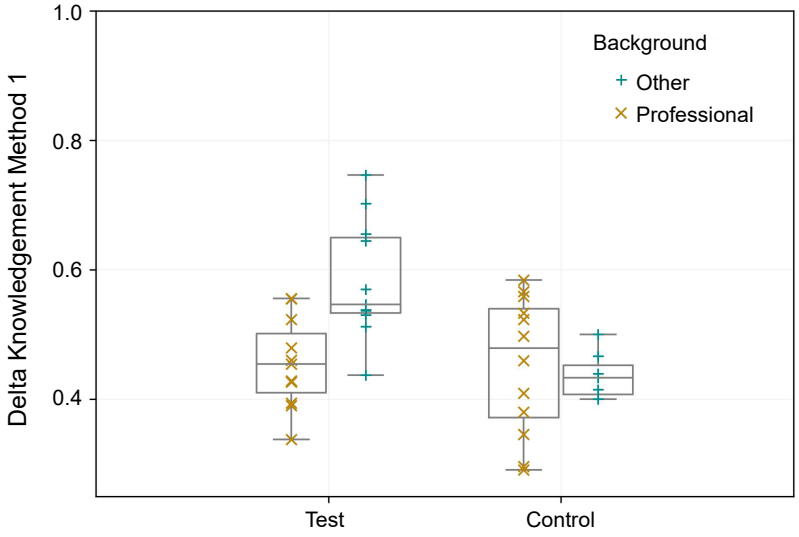

Figure 4: Measured knowledge gain conditioned on professional background and group

3 Methods

This research developed a Virtual Reality Environment (VRE) experience and subsequently assessed the novel method with a pilot study. We used a basement wall construction detail as prototypical content of a construction detail and deploy it as a learning task to a panel, which is split into a test group (using the VRE) and a control group (employing 2D drawings).

3.1 Virtual Reality Environment (VRE) and its components

The VRE is conceived as a medium sized room, where users can freely navigate using the controller buttons or a teleportation ray (cf. Fig. 1). This study employed the Oculus Quest 2. The means of displaying the construction detail are (i) traditional construction detail displayed as a 2D section, and (ii) as an interactive 3D model with augmented information. Within the VRE, the user can inspect the model from different angles, and the controllers allow the user to rotate and lift the model. In addition, the construction sequences together with explanations on functionalities and properties of the respective building component are available, where the 3D model can be assembled or disassembled element by element. A functionality to highlight certain groups of construction elements further improves the understanding of the construction and their relation. Most functionalities described so far are accessible from the controllers as these are required a great number of times. Other less often consulted functions are sourced to a screen (called the 'Tablet', see Fig. 2), which hosts a number of buttons as well as a text field. The buttons enable interaction for the user with higher-

level functionalities, e.g. highlighting certain element groups. A text field on the tablet enables communication between app and user.

The user experience within the VR follows the steps of (i) tutorial, (ii) learning phase, and (iii) examination through a *quiz* mode. As we expect many panellists to be unfamiliar with VR, an introductory tutorial for explaining the most important functionalities to use the VRE is provided. The learning phase is student-centred, where the described functionalities can be used to learn about the construction detail and explore it. To make the learning experience interactive, we introduce the *quiz* mode, where users are provided multiple choice or written-answer questions about the construction. The knowledge of the users is hence tested while at the same time we receive feedback on what has been learned so far.

3.2 Examining Effectivity of the VRE

This study was conducted with 41 participants, who were randomly divided into the test and control group. During a predefined time frame of at least 3 minutes, the participants were asked to learn about the construction detail employing either the VRE (test group) or a 2D drawing (control group). After the learning phase, both groups were examined. After the exam, participants in the control group had the opportunity to test the VRE as well. The study finally provided a survey to the panellists to gather information about their background and opinions towards learning with VR. The whole process is illustrated in Fig. 3.

The aim of this study is to assess whether the VRE provides a better learning experience and outcome than the traditional way of learning about construction details. To assess this, we compare the exam-score with the score for pre-existing knowledge (PEK) s_{PEK}. The exam-score measures the participant's exam performance, where s_{exam} is calculated by:

$$s_{exam} = \frac{n_{ex,correct} - 0.5 \cdot n_{ex,total}}{0.5 \cdot n_{ex,total}} \tag{1}$$

with $n_{ex,correct}$ is the number of correctly answered exam questions and $n_{ex,total}$ is the total number of question in the exam. Half of the maximum score is deducted from the actual score to account for the bias mentioned above. Since the exam questions possess a binary answer space (true/false), filling it at random would on average lead to 50% of the possible points. Therefore, the exam score is mapped accordingly by half of the maximum score. The pre-existing knowledge is assessed by eighth questions with a score between 0 (no preexisting knowledge) to 1 (good knowledge). The pre-existing knowledge score s_{PEK} is computed as the mean of the obtained answers. Measuring the pre-existing knowledge enables then to account for the prior knowledge bias for the learning increment.

To define a measure for the learning increment $\partial_{knowledge}$, the pre-existing knowledge score s_{PEK} is compared to the achieved exam score s_{exam} by:

$$\partial_{knowledge} = 0.5 \cdot \frac{1 + s_{exam}}{1 + s_{PEK}} \tag{2}$$

This measure, equal s_{PEK} and s_{exam} yield a $\partial_{knowledge}$ of 0.5 (i.e. the person did not learn anything). For $s_{exam} > s_{PEK}$, the result are in the interval from 0.5 to 1, indicating the person to have learned something. Otherwise, $\partial_{knowledge}$ lies in the interval between 0.25 and 0.5, indicating that the person's pre-existing knowledge was higher than they performed in the exam.

Table 1: Mean values for the most relevant variables

	All	**Test**	**Control**	**Test Professional**	**Control Professional**	**Test Other**	**Control Other**
$N_{participants}$	41	22	19	11	12	11	7
s_{exam} [-]	0.726	0.734	0.715	0.769	0.820	0.699	0.551
s_{PEK} [-]	0.471	0.384	0.572	0.622	0.727	0.145	0.308
$\partial_{Knowledge}$	0.485	0.519	0.445	0.454	0.450	0.584	0.436
VR Quiz Score [-]	0.666	0.619	0.740	0.659	0.750	0.591	0.722
VR PEK [-]	0.372	0.466	0.263	0.420	0.271	0.511	0.250

4 Results

The panel consisted of mostly students or recently graduated professionals. 23 persons had a AEC background ("professionals"), while the remaining 18 persons came from various fields ("Other"). Division into test and control group happened at random. The results for the most important variables are shown in Tab. 1, where a conditioning w.r.t. the background as well as being in test and control group is made.

Tab. 1 reveals, that test and control group performed very similarly on the exam, however when conditioning w.r.t. to professional background performed better on the exam. The exam score amongst professionals is surprisingly higher in the control group than in the test group, but the prior knowledge score is also higher in the control group amongst professionals. While $\partial_{Knowledge}$ is similar for the groups amongst professionals, for participants from other backgrounds the values differ significantly. The control group scored higher on the VR quiz, which is not surprising as they learned the detail on paper and filled out an exam before taking the VR quiz. The VRE user experience and the liking of the VRE and whether VR was deemed useful for education were all rated similarly amongst the different groups. The time spent in the VRE was slightly higher for the test group.

Considering the average score achieved by each participant during the exam, it can be observed, that these values lie above 0.5 for all participants. As pointed out earlier, this can be expected as filling out the exam at random would still achieve 0.5 points on average. Therefore s_{exam} is calculated acc. to Eq. 2. Further investigation of $\partial_{Knowledge}$, as provided graphically in Fig. 4, delivers a mean amongst the test group at 0.52 and 0.44 for the control group. Non-professional participants of this study achieve a clearly higher mean of $\partial_{Knowledge}$ in the test group.

In addition to the quantitative evaluation of the knowledge increase, participants were surveyed towards the usefulness of functionalities of the app and enjoyment of the VRE. The highest rated features are

those related to the model and corresponding labels. Both professionals and others rated features similarly in most cases. Most users gave a high overall rating towards their enjoyment of the VRE.

5 Discussion and Conclusions

This study elaborated a workflow for augmenting existing construction lectures with VR content to deepen students' learning. The effect of the VR in gained knowledge $\partial_{\text{Knowledge}}$ about the construction detail was statistically investigated. From the results of the tests we can conclude, that the learning effect is pronounced for non-professionals but not significant for the professional group. However, the scores for professionals are more widely distributed (cf. Fig. 4) in the control group. The data furthermore indicate that although on average they did not learn more with VR, their performance became more streamlined. From this it can be deduced, that prior knowledge did not play much of a role in the test group than in the control group. Furthermore a larger learning effect occurred for professionals in the test group compared to the control group.

In total, the study proved VRE to support learning more significantly for participants with limited to no prior knowledge, which is especially the case for students and laypersons. Therefore the VRE is a suitable medium for augmenting teaching of AEC students about construction details in their early studies. Through conversations after the VR experience, we observed, that most participants see clear advantages in learning with VR. However, when asked whether the VRE would be useful as the main means of teaching without an accompanying lecture series, some strongly disagreed and on average the answer was somewhere between neutral and agreement. Furthermore, the participants on average agreed that VR is a better means than 2D drawings for displaying construction details. Surprisingly the participants had a different view when asked whether VR was better for learning than 2D drawings as the average response was between neutral and agreement. Interestingly, professionals did not learn better in the VRE than on paper, which we mainly reason given their significant prior knowledge about construction details and reading 2D drawings. Regardless of the learning outcome, the users might prefer VR technology for learning as it is more entertaining and engaging. Combined with technological advancement in XR and sinking costs for implementing VR technology, this will lead to the introduction and application of VR into more areas within education in general and AEC education in particular. However in our perspective, any XR method will rather augment the teaching than completely replace it.

Acknowledgements

The authors thank Design++ for providing facilities and equipment to conduct the studies as well as Prof. Daniel Hall and our Master student Maximilian Rietschel for valuable support with this study.

References

[1] M. Kraus, I. Custovic, and W. Kaufmann, “Struct-mrt: Immersive learning and teaching of design and verification in structural civil engineering using mixed reality”, *arXiv:2109.09489*, 2021.

[2] M. Kraus, I. Čustović, and W. Kaufmann, “Mixed reality applications for teaching structural design”, in *Structures Congress 2022*, pp. 283–295.

[3] Z. Pan, A. D. Cheok, H. Yang, J. Zhu, and J. Shi, “Virtual reality and mixed reality for virtual learning environments”, *Computers and Graphics (Pergamon)*, vol. 30, no. 1, pp. 20–28, 2006.

[4] M. H. Elgewely, W. Nadim, A. ElKassed, M. Yehiah, M. A. Talaat, and S. Abdennadher, “Immersive construction detailing education: building information modeling (BIM)–based virtual reality (VR)”, *Open House International*, vol. 46, no. 3, pp. 359–375, Jan. 2021.

[5] *Weburl for code access:* https://github.com/mkrausAi/mkrausAI.github.io/tree/main/lectures/2021_XR/VR. (visited on 05/09/2022).

[6] J. Messner, S. Yerrapathruni, A. Baratta, and V. Whisker, “Using virtual reality to improve construction engineering education”, in *2003 Annual Conference*, 2003.

[7] F. Liarokapis, “Web3d and augmented reality to support engineering education”, en, *World Trans. Eng. Technol. Edu*, vol. 3, no. 1, pp. 11–14, 2004.

[8] P. Häfner, V. Häfner, and J. Ovtcharova, “Teaching methodology for virtual reality practical course in engineering education”, in *Procedia Computer Science*, vol. 25, Elsevier B.V., 2013, pp. 251–260. DOI: 10.1016/j.procs.2013.11.031.

[9] F. M. Dinis, A. S. Guimaraes, B. R. Carvalho, and J. P. P. Martins, “Virtual and augmented reality game-based applications to civil engineering education”, in *IEEE Global Engineering Education Conference, EDUCON*, IEEE, 2017, pp. 1683–1688.

[10] A. Z. Sampaio and O. P. Martins, “The application of virtual reality technology in the construction of bridge: The cantilever and incremental launching methods”, *Automation in Construction*, vol. 37, pp. 58–67, 2014.

[11] J. Wolfartsberger, “Analyzing the potential of virtual reality for engineering design review”, *Automation in Construction*, vol. 104, no. April, pp. 27–37, 2019.

[12] H. Maghool, S. Amir, S. H. Moeini, and Y. Arefazar, “An educational application based on virtual reality technology for learning architectural details: Challenges and benefits”, *Archnet-IJAR*, vol. 12, no. 3, pp. 246–272, 2018.

BIMGaze - Eine Versuchsumgebung zur datenanalytischen Beobachtung von BIM-Modellierungsprozessen

Torsten Niemeier[1], Mario Cichonczyk[1], Silke Dierssen[1], Uwe Weitkemper[1] and Dominic Becking[1]
[1]Bielefeld University of Applied Sciences, Campus Minden
E-mail(s): [tniemeier1, mcichonczyk, sdierssen, uweitkemper, dbecking]@fh-bielefeld.de

Abstract: In der vorliegenden Arbeit wird die technische Versuchsumgebung *BIMGaze* vorgestellt, welche die experimentelle Beobachtung von Modellierer:innen bei der Erstellung von Building Information Models erlaubt. Für Untersuchungen zum Verständnis der Schnittstelle zwischen Mensch und Maschine haben sich Eyetracking-Systeme bewährt. Insbesondere Usability-Tests und Interaktionsanalysen werden mit dieser Technologie erfolgreich durchgeführt und generieren quantitativ auswertbare Forschungsdaten. Das System *BIMGaze* überträgt diesen Ansatz auf Forschungsfragen der AEC-Branche, die bisher hauptsächlich qualitativ behandelt wurden, sodass mit diesem innovativen System neue Erkenntnisse für die Automatisierung des BIM-Prozesses möglich werden. *BIMGaze* simuliert hard- und softwareseitig eine 3D-CAD-Arbeitsumgebung zur Erstellung von Bestandsmodellen. Kombiniert mit einem Trackingsytem, werden dem Nutzer Bestandsdaten in Form von 2D-Plänen und 3D-Punktwolken bereitgestellt. Dessen Interaktion mit diesen Informationsquellen wird bei der Modellierung eines Gebäudes in Revit detailliert automatisch protokolliert. Somit lassen sich vom Modellierer angewandte Suchstrategien und die damit verknüpfte Aufmerksamkeitssteuerung erfassen und untersuchen. Die quantitative Auswertung dieser kognitiven Vorgänge wird durch *BIMGaze* ermöglicht und einer breiteren Forschergruppe zur Analyse zugänglich. Es wird dargelegt, wie die gewonnenen Rohdaten aufbereitet werden und eine intuitive Visualisierung der Ergebnisse erfolgen kann. Dazu wird mittels 2D-Heatmaps und 3D-Heatclouds die Aggregation der Points of Interest des Nutzers durchgeführt. Anschließend erfolgt in einer grafischen Oberfläche die zeitliche Gegenüberstellung der Aggregationen mit den sukzessiv durchgeführten Modellierungsschritten. Zudem wird die Aufmerksamkeitsverteilung des Probanden über die Zeit der Versuchsdauer illustriert. So können Einblicke in Lösungsstrategien und den Workflow der BIM-Modellierung gewonnen werden. Ein eigenes Datenschema erlaubt die einfach auswertbare Archivierung der erhobenen Forschungsartefakte und Protokolle sowie deren Wiederverwendung in weiterführenden Untersuchungen.

Keywords: Eyetracking, Datenaufnahme, Laserscan, BIM

1 Einführung

Während Neubauten zunehmend mittels moderner Methoden wie Building Information Modeling geplant und realisiert werden, ist diese Technologie bei geplanten Baumaßnahmen im Bestand nur mit erhöhtem Aufwand nutzbar, da aktuelle Gebäudemodelle selten vorliegen. Es hat sich als Praxis etabliert, Modelle betroffener Gebäude nachträglich zu erstellen, um die Vorteile von BIM auch im Bestand nutzen zu können. Grundlage zum Aufbau eines solchen Modells stellen in der Regel die Pläne des Gebäudes (Papierform oder 2D-CAD-Daten) sowie ein Laserscan des Bauwerkes dar. Um ein qualitativ angemessenes BIM-Modell zu erstellen, bedarf es aufgrund mangelnder Informationsbestände des Wissens und der Erfahrung eines Bauingenieurs, Statikers oder Tragwerkmodellierers. Dieser kann unvollständige Informationen durch Schlussfolgerungen ergänzen, die situativen Gegebenheiten durch sein technisches Wissen interpretieren und einen Lösungsvorschlag erdenken. Je nach Projektgröße ist dieser Prozess umfangreich, ressourcenintensiv und schwierig skalierbar.
Diese Aufgabenstellung einer Automatisierung näherzubringen, ist im zentralen Fokus aktueller Forschung. Den bestehenden Trend wollen wir mit dem System *BIMGaze* unterstützen, welches das Wirken impliziten Erfahrungswissens beim Modellierungsprozess und menschliche Suchstrategien in komplexen Domänendatensätzen erforschbar macht. Quantitativ analysierbare Daten können generiert werden, wenn Ingenieure (Tragwerksmodellierer, Statiker) sensorgestützt dabei beobachtet werden, wie sie aus vorgegebenen zwei- und dreidimensionalen Daten eine BIM-Rekonstruktion durchführen. Aus den Beobachtungen können Erkenntnisse gewonnen werden hinsichtlich der tatsächlich verwendeten Datenteilmenge und -quelle, der Strategie des Modellaufbaus und der angewandten Lösungsansätze beim Auftreten von Anomalien. Darüber hinaus können die gewonnenen Daten Einsichten liefern, wie sich die spezifische oder zeitliche Berufserfahrung der Probanden auf deren Arbeitsweise auswirkt.
Vergleichbare Untersuchungen in anderen Disziplinen haben bereits Erkenntnisse liefern können. Dazu wurden Eyetracker eingesetzt, um während eines solchen Versuches die Fixationen, Sakkaden und Regressionen der Probanden aufzuzeichnen und daraus visuelle Aufmerksamkeitsstrategien abzuleiten [1], [2]. Bednarik [1] konnte bei der Beobachtung des Arbeitsprozesses von Softwareentwicklern mit einem Eyetracker signifikante Verhaltensunterschiede in Relation zur Berufserfahrung identifizieren. Weiterhin konnte deren Auswahlpräferenz hinsichtlich gegebener Datenquellen festgestellt werden. Drew, Vo, Olwal u. a. [2] konnten vergleichbare Erkenntnisse mit unterschiedlich erfahrenen Medizinern generieren. In einer Versuchsgruppe wurden zwei unterschiedliche aber vorherrschende Suchstrategien identifiziert, die bei der Interpretation von dreidimensionalen Lungenbildern angewendet wurden. *BIMGaze* überträgt diese bereits etablierte Forschungsmethodik auf Modellierungsprobleme im AEC-Umfeld, um Erfahrung als wissenschaftliche Ressource zugänglich zu machen und die Forschung an Automatisierungssystemen zu unterstützen. Ziel der Entwicklung ist es, analytisch rekonstruieren zu können, wann während des Modellierungsprozesses welche Informationen herangezogen werden. Zu diesem Zweck werden aus aufgezeichneten Aufmerksamkeitspunkten eines Eyetrackers zweidimensionale Heatmaps auf PDF-Plänen und dreidimensionale Heatclouds in Laserscans generiert.

2 Versuchsumgebung

Um Probanden möglichst wenig mit neuen Eindrücken von der experimentellen Aufgabenstellung abzulenken, entspricht die Versuchsumgebung einem üblichen CAD-Arbeitsplatz mit zwei Monitoren (siehe Abbildung 1). Auf dem rechten Bildschirm soll die Versuchsperson das BIM-Modell erstellen (d), auf der linken Seite werden mittels zweier angepasster Anzeigewerkzeuge die Ausgangsdaten in Form von PDF-Unterlagen (b) und Laserscans (c) zur Verfügung gestellt. Die Art und Weise, wie die Probanden die vorliegenden Daten inspizieren, wird durch den Eyetracker (a) aufgezeichnet, der die Blickerfassung der Versuchsperson auf dem linken Monitor überwacht.

Abbildung 1: Versuchsumgebung (a: Eyetracker, b: PDF-Viewer, c: Pointcloud-Viewer, d: BIM-Software)

2.1 Hardware

Die einzige Hardware der Versuchsumgebung, die über die normale Ausstattung eines CAD-Arbeitsplatzes hinausgeht, ist der Eyetracker. Bei der Auswahl eines geeigneten Gerätes war das primäre Ziel, die normale Handlungsweise der Probanden möglichst nicht zu beeinflussen. Ein tragbares Gerät in Bauform einer Brille wurde aus diesem Grund nicht in Betracht gezogen. Allerdings sollte auch ein stationärer Eyetracker optisch möglichst unauffällig sein, eine eventuell benutzte Sehhilfe der Versuchsperson tolerieren können und eine freie und möglichst großzügige Kopfbewegung während des Versuchsablaufs ermöglichen. Ausgewählt wurde das Gerät Tobii Pro Fusion[5]. Dieses schmale, leistenförmige System ist für wissenschaftliche Anwendungen konzipiert und wurde in mehreren, aktuellen Untersuchungen [3], [4] bereits erfolgreich verwendet. Das Tobii Software Development Kit ermöglicht die für *BIMGaze* erforderliche Messdatenaufzeichnung und angepasste Kalibrierungssequenz.

2.2 Software

Bei der Auswahl eines geeigneten PDF-Viewers kam es vorrangig auf die Möglichkeit der nachträglichen Implementierung einer Logging-Funktionalität an. Es war zwingend erforderlich, dass während

[5]Tobii Pro Fusion, https://www.tobiipro.com/de/produkte/fusion/

der Benutzung des Programms die angezeigte Datei, die angezeigte Seite, die verwendete Blattrotation und der Zoomstatus protokolliert werden konnten, denn nur so würden die Gaze-Points des Eyetrackers auch einem zugehörigen Punkt auf der PDF-Zeichnung zugeordnet werden können. Da keine Software gefunden werden konnte, die im Urzustand über ein solches Feature verfügt, wurde eine Open-Source-Lösung ausgewählt und angepasst. Weiterhin sollte der PDF-Viewer vorzugsweise nur diejenige Funktionalität besitzen, um einen digitalisierten Gebäudeplan in einer wählbaren Konfiguration (Seite, Rotation, Vergrößerung) darzustellen. Jedes weitere Feature (z.B. Seitenlauf, Inhaltsverzeichnis, Kommentarfunktion) wäre für die Versuchsumgebung ablenkend, würde das Logging verlangsamen und die spätere Auswertung erschweren. Ausgewählt wurde hier der Dokumentenbetrachter Sumatra PDF[6]. Dieser Viewer ist eine freie Software, die unter den Lizenzbedingungen der GNU General Public License Version 3 angeboten wird. Innerhalb des Sourcecodes (C++) konnte hier das erforderliche Logging des Anzeigestatus implementiert werden. Zusätzlich wurden bei der eingesetzten Version des Programms einige nicht benötigte Features deaktiviert.
Bei der Evaluierung eines geeigneten Pointcloud-Viewers wurde ebenfalls auf die Open-Source-Eigenschaft Wert gelegt, da erhebliche Anpassungen vorgenommen werden mussten. Hier ist die zeitliche Aufzeichnung der benutzten Dateien und des Anzeigestatus (Zoom, Blickrichtung/View Matrix) ergänzt worden. Gewählt wurde dazu der ccViewer. Diese Software ist aus dem CloudCompare-Projekt[7] als ressourcenschonender und schneller Betrachter für Punktwolken entstanden. Das Programm unterliegt den Lizenzbestimmungen der GNU General Public License, Version 2 und folgende. Der ccViewer verfügt im Vergleich zu CloudCompare bereits über einen reduzierten Funktionsumfang, der für den Versuchsablauf ausreichend ist. Eine Implementierung des Loggings der Benutzeraktionen (Zoomen, Pannen und Rotieren) sowie die Bereitstellung einer Messfunktion wurden der Versuchsversion des Programmes hinzugefügt. Nicht benötigte Einstellungsmöglichkeiten wurden aus der Benutzeroberfläche entfernt.
Zur Durchführung der BIM-Modellierung auf dem rechten Bildschirm wurde Autodesk Revit gewählt. Dieses Softwarepaket ist aufgrund seiner Funktionsvielfalt und der starken Umsetzung des BIM-Konzepts in der Informationsmodellierung von Gebäuden weit verbreitet [5]. Weiterhin wird angenommen, dass die meisten Probanden mit dem Werkzeug bereits hinreichend vertraut sind. Anders als für die Darstellung der Ausgangsinformationen wurde für die eigentliche BIM-Modellierung kein Eyetracking vorgesehen, da hier nicht die Informationsaufnahme, sondern die durchgeführten Arbeitsschritte im Fokus der Beobachtungen liegen. Einige Arbeiten aus dem BIM-Umfeld verwenden in solchen Fällen die Revit-Journaldateien, um das Verhalten der Anwender zu untersuchen [6], [7]. Es erwies sich für *BIMGaze* zielführender, mittels des Revit Application Programming Interface ein C#-Plugin zu entwickeln, welches auf jede Modelländerung als EventHandler reagiert. Hinzugefügte, geänderte und gelöschte Elemente werden protokolliert und darüber hinaus für jeden solchen Modellierungsschritt ein IFC-Modell als visueller Zwischenstand exportiert. Auf diese Weise ergibt sich sowohl eine automatisch schriftlich protokollierte Aufzeichnung aller durchgeführten Benutzeraktionen als auch eine Abfolge von IFC-Modellen, welche die Zwischenschritte im *BIMGaze Visualizer* über die gesamte Versuchsdauer hinweg anzeig- und auswertbar macht.

[6] Sumatra PDF, https://www.sumatrapdfreader.org/
[7] CloudCompare, https://www.danielgm.net/cc/

2.3 Datenauswertung

Während der Versuchsdurchführung werden Messwerte und Logs aus vier unterschiedlichen Quellen generiert: Eyetracking, PDF-Viewer, Pointcloud-Viewer und BIM-Software. Um aus diesen Rohdaten darstellbare Ergebnisse (Heatmaps, Heatclouds und visualisierte Arbeitsabläufe) zu generieren, bedarf es einer eigenen Prozess-Pipeline (Abbildung 2). Die Heatmap-Verteilungen auf den PDF-Zeichnungen zu einem gegebenen Zeitpunkt des Versuchsablaufs werden aus den akkumulierten Blicktreffern des Probanden innerhalb des PDF-Viewers berechnet (Abbildung 3, links). Bei der Betrachtung der Punktwolken ergibt sich durch die beim ccViewer verwendete Parallelprojektion ein Blickzylinder des Probanden durch den 3D-Raum, welcher eine Heatcloud-Kollision der vom Zylinder eingeschlossenen Punkte bewirkt (Abbildung 3, mittig).
Der benutzte Eyetracker arbeitet mit einer maximalen Aufzeichnungsfrequenz von 120 Hz, womit sich pro Versuchssekunde 120 unterschiedliche Heatmaps oder Heatclouds ergeben können. Des Weiteren erzeugen unterschiedliche Einstellungen zur Gazepointgröße potenziell voneinander abweichende Heatmaps und Heatclouds. Eine vorberechnete Auswertung der Rohdaten bis zu jeder möglichen und darstellbaren Heatmap beziehungsweise Heatcloud ist daher nicht sinnvoll. Die Erzeugung dieser Grafiken wurde deshalb in die Visualisierungssoftware ausgelagert und dort anhand des gewählten Zeitpunktes und der getätigten Einstellungen vom Visualizer ad-hoc berechnet. Die Rohdaten werden

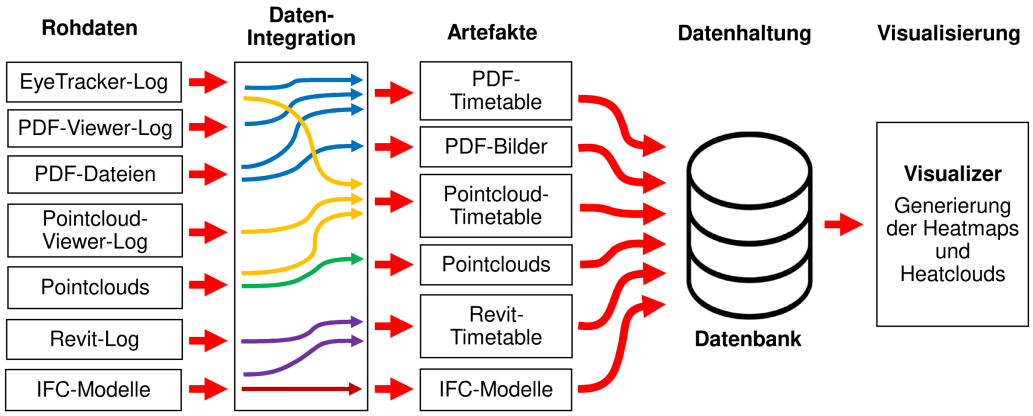

Abbildung 2: Darstellung der Auswertungspipeline

innerhalb des Systems zu einer Datenstruktur integriert, die wir als *Timetable* bezeichnen. Hierbei handelt es sich um Datentabellen, welche die Rohdaten in die drei Hauptbereiche PDF, Pointcloud und Revit kategorisieren. Die PDF-Timetable besteht aus Einträgen mit Timestamps, in denen der Gazepoint des Probanden den PDF-Viewer getroffen hat, ergänzt um den zu diesem Zeitpunkt vorliegenden Anzeigestatus (Dateiname, Zoom, Rotation und Seitennummer) der benutzten PDF. Die Pointcloud-Timetable verhält sich dazu analog. Hier werden dem Eintrag noch die Indizes der Laserscanpunkte hinzugefügt, die innerhalb des größten annehmbaren Blickzylinders des Probanden liegen. Zusätzlich übernimmt die Datenintegration die Generierung von Rastergrafiken aus den benutzten PDF und eine Bereinigung der protokollierten IFC-Modelle, falls Modellstände ohne nennenswerte Veränderung erzeugt wurden. Die so generierten Artefakte haben einen geringen Datenumfang und erlauben eine angemessen schnelle Endauswertung durch den Visualizer.

3 Ergebnisvisualisierung

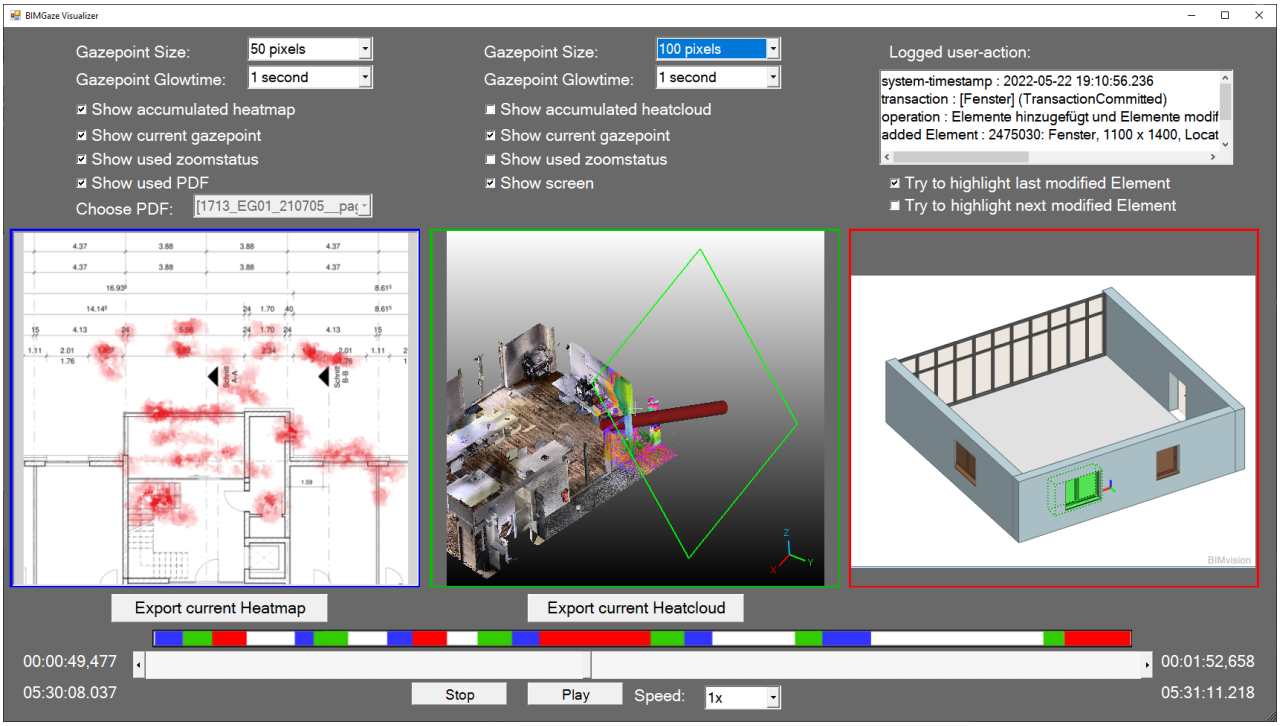

Abbildung 3: Ergebnisvisualisierung

Die entwickelte Software zur Visualisierung der Versuchsergebnisse *BIMGaze Visualizer* (C#) entspricht einem Mediaplayer mit drei Ausgabefenstern. Im unteren Bereich ist die Zeitsteuerung angeordnet, mit der ein Abspielen des Versuchsablaufs oder auch ein Springen zu bestimmten Zeitpunkten der Versuchsdurchführung ermöglicht wird. Oberhalb des Zeitbalkens wird eine Aktivitätsleiste angezeigt, welche die zeitliche Verteilung der Benutzeraktionen darstellt und mit einer Farbmarkierung die angesehene Datenquelle zum jeweiligen Zeitpunkt illustriert. Die Visualisierung der Timetables erfolgt zeitsynchron in den getrennten Bereichen für PDF-, Pointcloud- und BIM-Daten. Jeder dieser Bereiche verfügt über verschiedene Einstellmöglichkeiten zur Form der Darstellung. PDF- und Pointcloud-Bereich erlauben die Anzeige der bis zum aktuellen Zeitpunkt akkumulierten Heatmaps/Heatclouds, anpassbar an die Bedürfnisse der durchgeführten Analyse. Im Pointcloud-Bereich ist zudem eine freie Anzeige der Punktwolke möglich. In diesem Anzeigemodus wird die Bildebene des Probanden als grün markiertes Rechteck stilisiert eingezeichnet und der Zylinder am aktuellen Gazepoint orthogonal dazu im 3D-Raum verortet (Abbildung 3, mittig). Die Visualisierung im PDF-Bereich (blau) erfolgt auf der Basis der zuvor aus den benutzten PDF generierten Rastergrafiken, damit die Inhalte der benutzten PDF-Dateien bei Bedarf mit den generierten Heatmaps überblendet werden können (Abbildung 3, links). Zur Darstellung der Pointclouds/Heatclouds (grün) wird ein eingebetteter Prozess des ccViewer benutzt, in diesem Fall in einer Konfiguration, die der Software das Lesen der Timetables und das Empfangen von Interprozessnachrichten (Timestamps und aktuelle Einstellungen) aus dem übergeordneten Visualisierungsprogramm ermöglicht. Die Darstellung der aufgezeichneten IFC-Modelle (rot)

übernimmt eine Instanz des Programms BIMvision[8]. Hier sorgt ein für diesen Zweck entwickeltes PlugIn dafür, dass dieser Viewer Steuernachrichten aus dem übergeordneten Fenster empfangen, die richtigen Modelle laden und die gewünschten Modellelemente markieren kann (Abbildung 3, rechts). So kann der Modellierungsfortschritt parallel zur Interpretation von PDF und Laserscan nachvollzogen werden.

4 Fazit und Ausblick

Die in dieser Arbeit vorgestellte Versuchsumgebung *BIMGaze* hat die Aufgabe, als wissenschaftliches Capture System für weitergehende Untersuchungen zu dienen und die Messergebnisse anschaulich darzustellen. Die Visualisierung der Messdaten gibt einen Einblick in das Verhalten der Probanden und geht dabei über eine reine Darstellung der Blickerfassung hinaus, da auch sämtliche Zoom- und Rotationsaktionen angezeigt werden können und die visuelle Aufmerksamkeit zeitsynchron den getätigten Modellierungsschritten gegenübergestellt wird. Die Aktivitätsleiste erlaubt einen Überblick über die Aufmerksamkeitsverteilung während einzelner Versuche. Generierte Heatmaps und Heatclouds können für jeden Versuchszeitpunkt exportiert werden und als Basis für folgende Forschungsarbeiten dienen. Weiterhin sind die intern verwendeten Timetables als einfache Datenstrukturen auch direkt auswertbar, um beispielsweise Aufmerksamkeitsmuster über ganze Versuchsreihen mit vielen Probanden zu evaluieren.

BIMGaze ist darauf vorbereitet, als Grundlage für Erweiterungen durch andere Forschende zu dienen. Der Funktionsumfang des gewählten Eyetrackers übersteigt die für unsere Zwecke verwendeten Parameter. Das Gerät protokolliert nicht nur die Gazepoint-Position auf der Bildschirmebene, sondern auch Pupillengröße und räumliche Position der Augen. Mehrere Arbeiten beschäftigen sich damit, aus solchen Messwerten Rückschlüsse auf Emotionen, Wahrnehmung, Aufmerksamkeit und Entscheidungsfindungsprozesse der Versuchspersonen zu ziehen [8], [9]. Hier bieten das dargestellte System und die damit erhebbaren Daten Potenzial für weiterführende Untersuchungen.

Wir planen *BIMGaze* zur Untersuchung des Wirkens von Expertenwissen bei der BIM-Modellierung einzusetzen. Vor dem Hintergrund der Unterstützung von Mustererkennungsverfahren durch ontologisch formulierte Expertise wird im nächsten Schritt eine Studienreihe mit Domänenexperten aus der Industrie durchgeführt. Die denkbare Nutzung der Systemarchitektur ist aber nicht auf diesen Fall beschränkt. Mit entsprechenden Anpassungen ließe sich das Konzept auf eine Vielzahl von Anwendungsfeldern übertragen, bei denen ein Proband aus visuellen Informationen ein Ergebnis generieren soll. Die Sourcecodes der Versuchssoftware, Verarbeitungspipeline und des Visualizers können im BIMGaze GitHub Repository[9] abgerufen werden. Die Programme werden laufend weiterentwickelt.

[8] Homepage BIMvision, https://bimvision.eu/de/
[9] BIMGaze GitHub, https://github.com/TorstenNiemeier/BIMGaze

Danksagung

Das diesem Bericht zugrunde liegende Vorhaben wurde mit Mitteln des Bundesministeriums für Bildung und Forschung unter dem Förderkennzeichen 13FH554IX6 gefördert und aktiv unterstützt durch unsere Projektpartner HOCHTIEF ViCon GmbH und Pape Architekten AG. Die Verantwortung für den Inhalt dieser Veröffentlichung liegt bei den Autoren.

Literatur

[1] R. Bednarik, »Expertise-dependent visual attention strategies develop over time during debugging with multiple code representations«, in *Int. J. Human-Computer Studies 70 pp.143–155*, 2012.

[2] T. Drew, M. L. H. Vo, A. Olwal, F. Jacobson, S. E. Seltzer und J. M. Wolfe, »Scanners and drillers: characterizing expert visual search through volumetric images«, in *Journal of vision, 13(10), 3-3*, 2013.

[3] S. Schreiter, M. Vogel, M. Rehm und T. Dörfler, »Die Rolle des Wissens angehender Mathematiklehrkräfte beim Diagnostizieren schwierigkeitsgenerierender Aufgabenmerkmale. Erkenntnisse aus Eye-Tracking Stimulated Recall Interviews.«, in *Journal für Mathematik-Didaktik, 43(1), 101-133*, Springer, 2022.

[4] R. Cheng, J. Wang und P. C. Liao, »Temporal Visual Patterns of Construction Hazard Recognition Strategies«, in *International Journal of Environmental Research and Public Health, 18(16), 8779*, MDPI, 2021.

[5] E. Ignatova, S. Zotkin und I. Zotkina, »The extraction and processing of BIM data«, in *IOP Conference Series: Materials Science and Engineering. Vol. 365. No. 6.*, IOP Publishing, 2018.

[6] L. Zhang, Y. Pan, X. Wu und M. J. Skibniewski, *Artificial intelligence in construction engineering and management*, Ser. Lecture Notes in Civil Engineering. Springer Singapore, 2021, ISBN: 978-981-16-2841-2.

[7] E. Forcael, A. Martínez-Rocamora, J. Sepúlveda-Morales, R. García-Alvarado, A. Nope-Bernal und F. Leighton, »Behavior and Performance of BIM Users in a Collaborative Work Environment«, in *Applied Sciences, 10(6), 2199*, 2020.

[8] M. Zhao, H. Gao, W. Wang, J. Qu und L. Chen, »Study on the identification of irritability emotion based on the percentage change in pupil size«, in *Proceedings of the 2020 2nd International Conference on Image, Video and Signal Processing (pp. 20-24)*, 2020.

[9] M. T. Kucewicz, J. Dolezal, V. Kremen u. a., »Pupil size reflects successful encoding and recall of memory in humans«, in *Scientific reports, 8(1), 1-7*, 2018.

Towards Real-time Image Localization with BIM models

Rafaella Dantas[1], Simone Peter[1], Xingzhou Wang[1], Miguel Vega Torres[1] and Ann-Kristin Dugstad[1]
[1]Chair of Computational Modeling and Simulation, TU Munich, Arcisstr. 21, 80333 Munich, Germany
E-mail(s): miguel.vega@tum.de

Abstract: In der vorliegenden Arbeit wird die technische Versuchsumgebung *BIMGaze* vorgestellt, welche die experimentelle Beobachtung von Modellierer:innen bei der Erstellung von Building Information Models erlaubt. Für Untersuchungen zum Verständnis der Schnittstelle zwischen Mensch und Maschine haben sich Eyetracking-Systeme bewährt. Insbesondere Usability-Tests und Interaktionsanalysen werden mit dieser Technologie erfolgreich durchgeführt und generieren quantitativ auswertbare Forschungsdaten. Das System *BIMGaze* überträgt diesen Ansatz auf Forschungsfragen der AEC-Branche, die bisher hauptsächlich qualitativ behandelt wurden, sodass mit diesem innovativen System neue Erkenntnisse für die Automatisierung des BIM-Prozesses möglich werden.
BIMGaze simuliert hard- und softwareseitig eine 3D-CAD-Arbeitsumgebung zur Erstellung von Bestandsmodellen. Kombiniert mit einem Trackingsytem, werden dem Nutzer Bestandsdaten in Form von 2D-Plänen und 3D-Punktwolken bereitgestellt. Dessen Interaktion mit diesen Informationsquellen wird bei der Modellierung eines Gebäudes in Revit detailliert automatisch protokolliert. Somit lassen sich vom Modellierer angewandte Suchstrategien und die damit verknüpfte Aufmerksamkeitssteuerung erfassen und untersuchen. Die quantitative Auswertung dieser kognitiven Vorgänge wird durch *BIMGaze* ermöglicht und einer breiteren Forschergruppe zur Analyse zugänglich. Es wird dargelegt, wie die gewonnenen Rohdaten aufbereitet werden und eine intuitive Visualisierung der Ergebnisse erfolgen kann. Dazu wird mittels 2D-Heatmaps und 3D-Heatclouds die Aggregation der Points of Interest des Nutzers durchgeführt. Anschließend erfolgt in einer grafischen Oberfläche die zeitliche Gegenüberstellung der Aggregationen mit den sukzessiv durchgeführten Modellierungsschritten. Zudem wird die Aufmerksamkeitsverteilung des Probanden über die Versuchsdauer illustriert. So können Einblicke in Lösungsstrategien und den Workflow der Bestandsmodellierung gewonnen werden. Ein eigenes Datenschema erlaubt die einfach auswertbare Archivierung der erhobenen Forschungsartefakte und Protokolle sowie deren Wiederverwendung in weiterführenden Untersuchungen.

Keywords: Eyetracking, Datenaufnahme, Laserscan, BIM

1 Introduction

The replacement of human workload by computational support is a recurring request during the last decades. Especially the monitoring of indoor construction progress is nowadays usually conducted manually, leading to error-prone comparisons between the acquired data and actual construction progress.

The enhancement of indoor monitoring progresses with automatic data acquisition and alignment in real-time is thus a promising step towards a dynamic, less error prone and automated construction procedure. Existing approaches require a time consuming Structure from Motion (SfM) procedure to find the correct camera pose in the BIM-coordinate system. This paper aims to overcome this drawback by proposing a method that combines point cloud acquisition with SLAM, perspective detection in BIM view and keyframes and localization improvement to discover the fine camera poses.

The paper is structured as follows: Related work is presented in Section 2. The steps of the proposed concept are described in Section 3. The approach was tested in a case study involving a rectangular-shaped corridor. Results and analysis are presented in Section 4. Section 5 concludes this work.

2 Related Research

Some studies have use the BIM model for *global localization* (without estimate about its initial position) or to solve the *kidnapped robot problem* (in which you know where the robot was but lost communication for a moment).

Acharya, Khoshelham, and Winter [1] introduced BIM-PoseNet, which leverages a deep CNN that uses synthetic images obtained from the 3D indoor model to regress the camera pose without an accurate initial position, achieving an accuracy of 2 m. Haque, Elsaharti, Elderini, *et al.* [2] locate an UAV in the BIM coordinate system by detecting doors and windows in a sequence of images. They use YOLO to detect bounding boxes of these objects in the RGB images captured with a depth camera. This camera simultaneously generates a 3D map with ORB-SLAM2, allowing them to project the detected objects in 3D. Once a sufficient number of doors and windows are detected and localized, they can match with the BIM model. However, once the robot finds its location on the reference map (in this case, the BIM model), the problem is a *pose tracking* task, in which the location and orientation of the robot want to be known all the time while the robot moves. This problem is of more practical importance since while the approximate or corrected starting position could be provided manually, tracking the robot's pose is a problem that the robot itself should be able to perform automatically in order to navigate effectively in an environment autonomously.

To address this problem with the help of a BIM model, Kropp, Koch, and König [3] carried out a study on image to 4D BIM registration using camera pose discovery for each image frame concerning the BIM coordinate system. This method uses line segments as the features. Although the initial registration needed manual intervention, the consecutive images were registered automatically. However, since an

SfM algorithm was used for the rough camera motion estimation, the whole registration pipeline is not applicable in real-time. Asadi, Ramshankar, Noghabaei, *et al.* [4] propose an augmented monocular SLAM algorithm achieving real-time localization performance. They do so iteratively reducing the distance between vanishing points and lines in the image frames and their corresponding BIM views.

Boniardi, Valada, Mohan, *et al.* [5] propose a method that can deal with clutter environments leveraging a convolutional neural network for layout prediction, a particle filter algorithm and a floor plan. Winter, Acharya, M.Ramezani, *et al.* [6] introduced BIM-Tracker, a model-based visual tracking framework, achieves an accuracy of more than 10 cm in environments where even dynamic agents are present, however, there is not much clutter present on their tests.

3 Methodology

The proposed methodology can be divided into three main steps: 1. Point cloud acquisition with SLAM; 2. Perspective detection in the BIM view and in keyframes, and 3. Localization improvement to find the fine camera poses. An overview of the workflow can be seen in Figure 1.

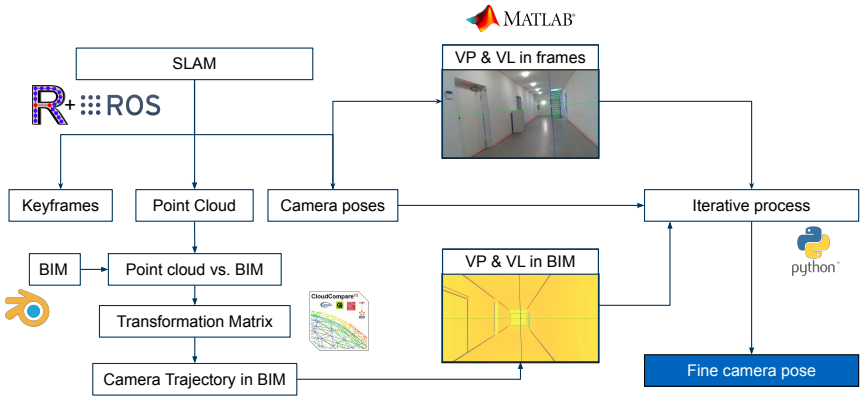

Figure 1: Proposed workflow for fine camera pose correction with a BIM model.

3.1 Point Cloud Acquisition and First BIM Alignment

In order to obtain the rough camera poses, a point cloud acquisition was performed using a RealSense D435i camera with the RTAB-Map SLAM framework [7]. Once a bag file is recorded, a database is created with the help of the “2019-UGRP-DPoom” project [8].

The point cloud database is then opened in RTAB-Map where the poses in the trajectory are optimized, and from where the final rough camera poses and frames can be exported. Besides that, creating a point cloud database is important since it will later be used as one part of the input data in *CloudCompare* (CC) for the alignment between the point cloud and the BIM model.

In order to find the camera poses in the BIM coordinate system the resulting point cloud has to be aligned with the model. This first alignment is done in a semi-automatic manner using *CC*.

The BIM model, originally in IFC format, needs to be saved as an STL file, which can be conducted using Revit. Afterward, the BIM model can be imported into *CC*. Additionally, to render the BIM keyframes, the model is imported into Blender, where the camera object and scripting tools are primarily used. The keyframes are frames extracted every second from the video stream.

The transformation matrix that aligns the point cloud with the BIM ensures that the initial BIM keyframe of the executed trajectory is in the scope of the one from SLAM.

The alignment in *CC* is conducted after manually selecting three reference points in the point cloud and their correspondences in the BIM model. Finally, a transformation matrix from point cloud to BIM is obtained.

Once the correct transformation matrix and scale of the point cloud are found with *CC*, the coordinates of the rough camera trajectory obtained previously with RTAB-Map are transformed to the BIM coordinate system.

3.2 Perspective Detection

One significant task in the computer vision community is to extract 3D information from two-dimensional (2D) images [4]. The estimation of vanishing points (VPs) is important to perform the localization improvement step. In this paper, the algorithm proposed in [9]was applied in order to conduct this step. The vanishing points are points on the image plane, where 2D perspective projections of mutually parallel lines in 3D space intersect. Hedau, Hoiem, and Forsyth [9] propose to compute the parallel lines by the edge detection approach. Afterward, the triplet of orthogonal vanishing points and two vanishing lines are calculated.

In order to obtain the VPs and VLs in the BIM view, a virtual camera is simulated in Blender at the rough camera poses. The parameters of the camera object are set according to the intrinsic parameters of the D435i real depth camera. To be able to generate frames in the BIM view directly in Python and avoid a manual step in Blender, an adaptor was written. Blender is called in the background using the command line rendering.

The script extracts the location, rotation and frame destination from the passed command and renders the respective keyframe in Blender. Then, the module “Data Access” is used to obtain Blender’s internal data and set the new camera information.

3.3 Image Localization improvement

The localization improvement is based on the distance error and the angular error (see Δd and $\Delta\theta$ respectively in eq. 3 between the VPs and VLs of the keyframe and BIM, which are depicted in Figure 2.

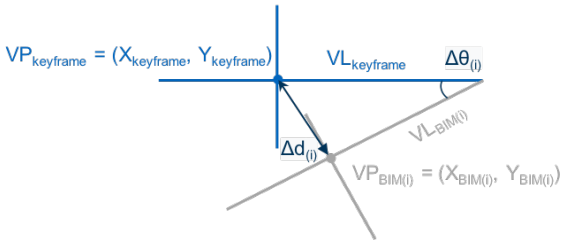

Figure 2: Distance error Δd and angular error $\Delta\theta$ between the VPs and VLs of the current key frame and the corresponding BIM frame. The BIM frame has to be corrected until it matches the current real-world frame, in this way the real camera pose is found in the BIM coordinate system (own illustration based on [4]).

$$\begin{aligned} \Delta d &= \sqrt{(X_{BIM} - X_{keyframe})^2 + (Y_{BIM} - Y_{keyframe})^2} \\ \Delta\theta &= \tan^{-1}\left(\frac{VL_{BIM} - VL_{keyframe}}{1 + VL_{BIM} * VL_{keyframe}}\right) \end{aligned} \tag{1}$$

At first, the location values of the camera poses are corrected. The two corresponding VPs located in the image frame are backward projected from 2D pixel (u, v) to 3D camera coordinates (X_C, Y_C, Z_C) using the intrinsic parameters of the camera.

A correction based on the obtained difference is applied. However, it turns out that the influence on the VPs is relatively small compared to the influence of the VLs. The second part is the improvement of the rotation angles, based on the definition by Euler.

This step is conducted by an iterative, stepwise correction process until a defined threshold is reached. The Euler rotation around the y-axis, also referred to as *pitch*, is directly related to the in-plane computed angle $\Delta\theta$, so that it can be directly applied as a correction for this value.

The *yaw* rotation around the z-axis mainly influences the x-coordinate of the VP.

This coordinate is changed stepwise until a threshold of 3 % for the difference between the x-coordinates of both VPs is reached.

After each correction step, a new BIM frame is generated with Blender. The VPs and thereby the updated distance and angular error are computed. A similar approach is used for the y-coordinate and the *roll* rotation around the x-axis.

4 Results and Analysis

To test the image localization system, a section of an uncluttered corridor was selected. The resulting point cloud and the corresponding BIM model are illustrated in Figures 3 and 4, respectively.

Figures 5 and 6 show the angular and translational errors of the initial rough camera poses (estimated with RTABMAP), and the improved errors after the proposed image localization pipeline is executed. Figure 7 presents the average computational time of each step of the pipeline.

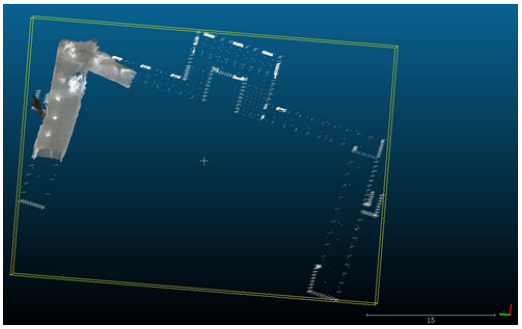

Figure 3: Sparse point cloud reconstructed with RTAB-MAP for a corner with the real-world camera frames used to evaluate the proposed image localization system.

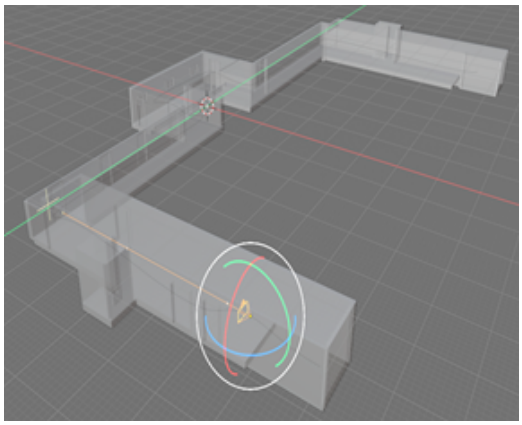

Figure 4: Corresponding BIM model of the whole corridor.

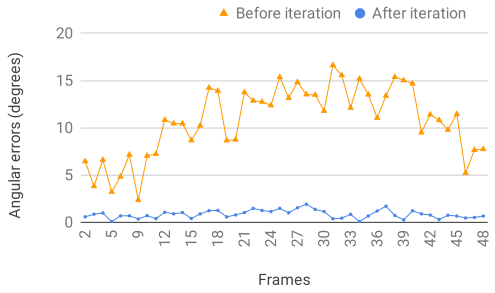

Figure 5: Performance of the image localization system angular errors in degrees.

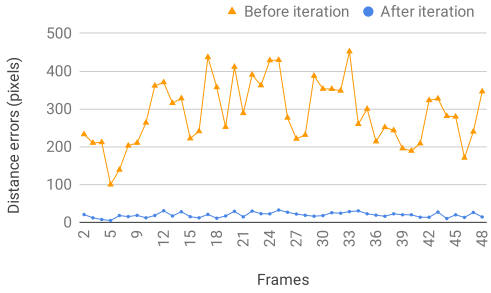

Figure 6: Corresponding distance errors in pixels.

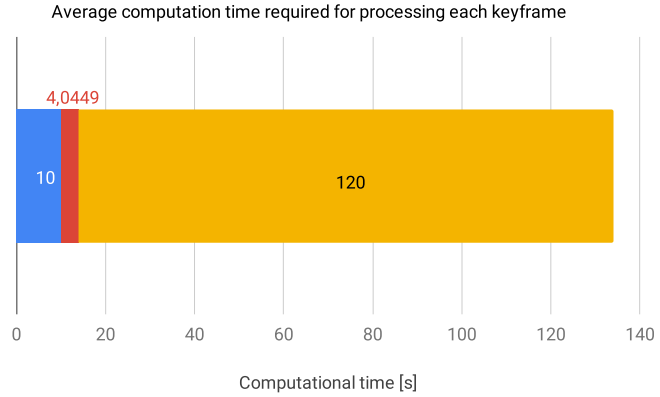

Figure 7: Average computational time performance of the image localization system. In red the time for estimating the rough camera pose with SLAM, in blue for perspective detection (computation of VPs and VLs) and in yellow the time to recover the fine camera pose through localization improvement.

The proposed image localization algorithm achieved a reduction of the average distance error between the VPs of the video and BIM of 93 % and of the average angular error of 92 %, with an average processing duration of 134 s) per frame.

5 Conclusions and Future Work

The experimental results show that the proposed method has a significant potential to improve the camera pose by leveraging an existing BIM model and perspective detection.

The foremost limitation lies in the computational time. By definition, if the speed of processing each keyframe is higher than the speed of the frame sampling, the process can be considered real-time. The proposed method requires, on average, 134 s to process one keyframe. As it can be seen in Figure 7, it does not work in real-time (considering each keyframe is extracted every 1 s). Nonetheless, it is important to consider that the required time per frame varies depending on the quality of the initial pose estimation.

A larger step size or the implementation of the code on a statically typed programming language like C++ could increase the performance of the method substantially.

In addition, this method is based on the computation of VPs. If the algorithm can't detect enough edges required for this computation, which might happen around a corner, close to the wall, in the non-usual case of rounded walls, or in a cluttered room, the VPs cannot be obtained accurately. Consequently, the technique will fail in such cases. One possible solution is to take advantage of other approaches based on plane detection or layout predition instead of only the VP calculation, as it is done in [6] or [5].

Furthermore, a more accurate transformation of the point cloud to the BIM coordinate system could be useful to generate a more precise initial keyframe in the BIM view. For this, visual-based *global localization* or algorithms based on Machine Learning, for example *PoseNet* like in [1], [10], can be implemented, which could serve to partially omit the manual step in CloudCompare. Another possibility is to use a more precise point cloud, which can be generated with the help of other SLAM algorithms such as ORB-SLAM3 [11].

Acknowledgements

The presented research was conducted in the frame of the project "Intelligent Toolkit for Reconnaissance and assessmEnt in Perilous Incidents" (INTREPID) funded by the EU's research and innovation funding programme Horizon 2020 under Grant agreement ID: 883345.

References

[1] D. Acharya, K. Khoshelham, and S. Winter, “Bim-posenet: Indoor camera localisation using a 3d indoor model and deep learning from synthetic images”, *ISPRS Journal of Photogrammetry and Remote Sensing*, vol. 150, pp. 245–258, 2019, ISSN: 09242716. DOI: 10.1016/j.isprsjprs.2019.02.020.

[2] A. Haque, A. Elsaharti, T. Elderini, M. A. Elsaharty, and J. Neubert, “Uav autonomous localization using macro-features matching with a cad model”, *Sensors (Basel, Switzerland)*, vol. 20, no. 3, 2020. DOI: 10.3390/s20030743.

[3] C. Kropp, C. Koch, and M. König, “Interior construction state recognition with 4d bim registered image sequences”, *Automation in construction*, vol. 86, pp. 11–32, 2018.

[4] K. Asadi, H. Ramshankar, M. Noghabaei, and K. Han, “Real-time image localization and registration with bim using perspective alignment for indoor monitoring of construction”, *Journal of Computing in Civil Engineering*, vol. 33(5), 2019. DOI: https://doi.org/10.1061/(ASCE)CP.1943-5487.0000847.

[5] F. Boniardi, A. Valada, R. Mohan, T. Caselitz, and W. Burgard, *Robot localization in floor plans using a room layout edge extraction network*, Mar. 5, 2019. [Online]. Available: http://arxiv.org/pdf/1903.01804v2.

[6] S. Winter, D. Acharya, M.Ramezani, and K. Khoshelham, “Bim-tracker: A model-based visual tracking approach for indoor localisation using a 3d building model.”, *ISPRS Journal of Photogrammetry and Remote Sensing.*, 2019. DOI: 10.1016/j.isprsjprs.2019.02.014.

[7] M. Labbé and F. Michaud, “Rtab-map as an open-source lidar and visual simultaneous localization and mapping library for large-scale and long-term online operation”, *Journal of Field Robotics*, vol. 36, no. 2, pp. 416–446, 2019.

[8] Shinkansan, “Slam - 2019-ugrp-dpoom”, *GitHub - https://github.com/shinkansan/2019-UGRP-DPoom/blob/master/SLAM*, 2021.

[9] V. Hedau, D. Hoiem, and D. Forsyth, “Thinking inside the box: Using appearance models and context based on room geometry”, in *European Conference on Computer Vision*, Springer, 2010, pp. 224–237.

[10] D. Acharya, R. Tennakoon, S. Muthu, K. Khoshelham, R. Hoseinnezhad, and A. Bab-Hadiashar, “Single-image localisation using 3d models: Combining hierarchical edge maps and semantic segmentation for domain adaptation”, *Automation in Construction*, vol. 136, p. 104 152, 2022, ISSN: 09265805. DOI: 10.1016/j.autcon.2022.104152.

[11] C. Campos, R. Elvira, J. J. Gomez, J. M. M. Montiel, and J. D. Tardós, “ORB-SLAM3: An accurate open-source library for visual, visual-inertial and multi-map SLAM”, *IEEE Transactions on Robotics*, vol. 37, no. 6, pp. 1874–1890, 2021.

Teil VII

Thermal Comfort & Resource Efficiency

Development of a microcontroller-based interactive monitoring system for indoor environmental quality

Qirui Huang[1] and Marc Syndicus[1]
[1]Institute of Energy Efficiency and Sustainable Building (E3D) RWTH Aachen University, Mathieustr. 30, 52074 Aachen, Germany
E-mail(s): qirui.huang@e3d.rwth-aachen.de, syndicus@e3d.rwth-aachen.de

Abstract: A holistic determination and improvement of the quality of the indoor environment includes, in addition to the "classic" parameters such as air temperature and humidity, other influencing variables such as air quality, noise, and lighting conditions (brightness, color temperature). Since Covid-19, air quality came back into focus. The interaction of these factors in their entirety has an effect on people and significantly determines their well-being and performance. This paper presents the implementation of a monitoring system for these indoor comfort variables (temperature, humidity, wind speed, CO_2, VOC, lighting, and noise) based on the Arduino microcontroller ecosystem and corresponding sensor technology. This setup is complemented by the development of a graphical user interface (GUI) with an interactive feedback system. Via touchscreen or the accompanying app for desktop PCs, users can monitor real-time measurements and change settings such as the model of thermal comfort, algorithm parameters that are used to predict comfort indices, database connection, application programming interface, or the language of the software. Feedback can be augmented by using system notifications, color notifications in the GUI, and changeable animated images according to user preferences. Furthermore, user tests were conducted to investigate the system usability and to explore the differences between these two interaction possibilities. During the user testing phase (N = 4), two questionnaires based on the usability metric for user experience lite (UMUX-LITE) and the system usability scale (SUS) proved the high usability of this monitoring system. Additionally, it was found that users increasingly prefer to use the touchscreen as the testing phase progressed.

Keywords: Indoor Climate, Indoor Environment, Indoor Environmental Quality, Indoor Air Quality, Sensors, Monitoring, Interaction, Internet of Things, Microcontroller, Arduino

1 Introduction

Humans spend nearly 90% of their time indoors, and since Covid at the latest, the indoor environmental quality (IEQ), particularly indoor air quality (IAQ), usually measured by CO_2 concentration, has come back into focus [1]–[4]. At the same time, given the growing interest in human's productivity, well-being, and health, the indoor environment has also received increasing attention in recent years [1], [5], [6]. The use of low-cost sensor technology to monitor IEQ, especially IAQ, has come a long way in the last decade, particularly after 2017 [6]. Chojer et al. [6] reviewed 35 relevant projects from 2012 to 2019. The monitored indoor environment parameters vary from study to study. Most projects only include sensors to monitor temperature, relative Humidity, and CO_2, as showed in Figure 1. Only very few studies monitored the wind speed, the acoustic and visual environment.

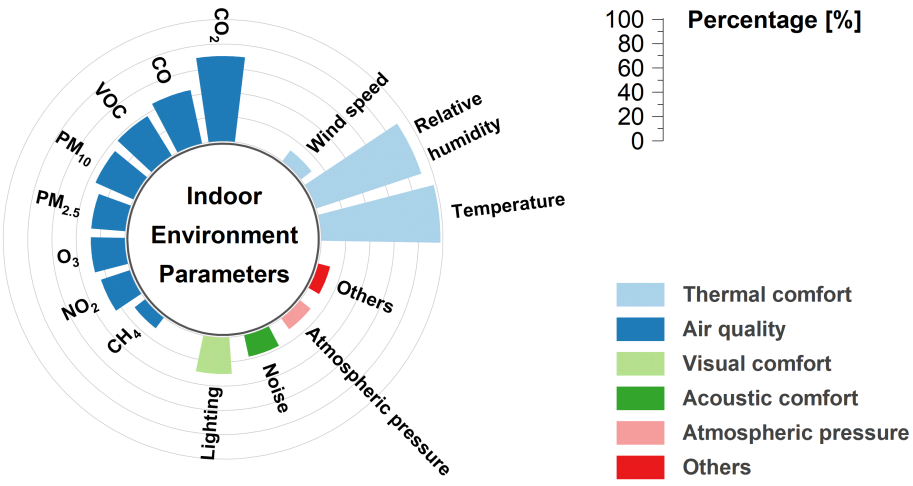

Figure 1: Monitoring parameters of the sensors used in the relevant projects, based on [6]

Most systems in these projects support both real-time access to sensor data and access to historical data [6]. The project of Tiele, Esfahani, and Covington [7] provides the user with real-time IEQ assessment on the hardware display, but beyond that, no software has been developed to view and analyze historical data. Only Parkinson et al. [8] developed both the hardware and software for the end user and offered the analysis and evaluation of IEQ.

The aim of this work is to develop a microcontroller-based monitoring system including hardware, software for the monitoring of the IEQ parameters (temperature, humidity, air pressure, wind speed, CO_2, VOC, lighting, and noise) using Arduinos and the corresponding sensor technology. Since there are very few IEQ algorithms that take all these parameters into account, the development of a new algorithm for the indoor environmental quality index (IEQI) in multi domain by integrating and extending existing algorithms is also an important goal of this work. In this paper, we propose a new multi-domain IEQI algorithm, a highlight of which is that the counterweight can be adapted to various populations in different domains.

2 Materials and Methods

As the central component, the Arduino Nano microcontroller (MC) controls all sensors and actuators. In addition, the MC organizes the communication of the measurement device with the computer and the touchscreen. A Nextion 3.5" touchscreen (NX4832K035) is used to display the GUI.

2.1 Sensors

In order to control all components in the best possible way and for meaningful monitoring, the status of the system must be known at all times, which means that the IEQ needs to be continuously monitored, not just a single measurement at a certain point in time. The MC can retrieve the system status in real time using the sensors and display it in the GUI.

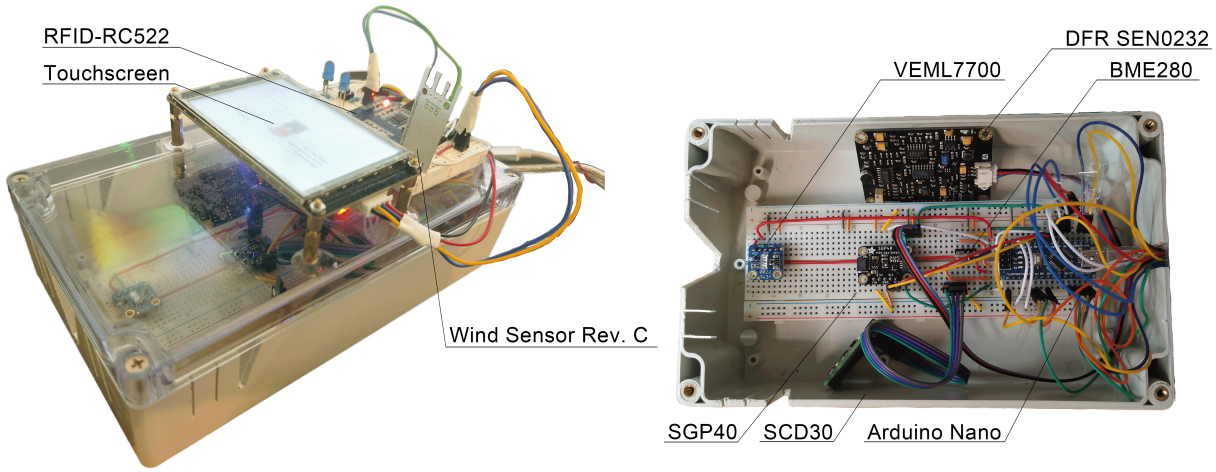

Figure 2: Prototype of the monitoring system

2.2 Algorithms

In this work, the IEQI consists of the thermal comfort index (TCI), acoustic comfort index (ACI), barometric comfort index (BCI), visual comfort index (VCI), and indoor air quality index (IAQI). To allow an individual comfort prediction, the constant k_i is used to facilitate adaptation by the user.

$$IEQI = \frac{k_{TCI} \cdot TCI + k_{ACI} \cdot ACI + k_{BCI} \cdot BCI + k_{VCI} \cdot VCI + k_{IAQI} \cdot IAQI}{k_{TCI} + k_{ACI} + k_{BCI} + k_{VCI} + k_{IAQI}} \quad (1)$$

The default value for the constant k_i is 1.0 with value range from 0 to 3. A larger value of k_i means that the index accounts for a larger percentage of the IEQI, which means that it is more important for the user. To predict the thermal comfort, the user has a choice of two thermal comfort models, the static PMV (predicted mean vote) / PPD (predicted percentage of dissatisfied) model according to ISO 7730 standard [9] and the adaptive model according to DIN EN 16798 [10]. For both models, the algorithm from the Python package pythermalcomfort developed by Tartarini and Schiavon [11] was used in this work. The PMV/PPD model outputs the PMV index values directly, while the adaptive model only

gives threshold values of categories I - IV. Therefore, it is necessary to subdivide and define them uniformly. In this work, a total of four comfort zones were defined, as shown in Table 1. Each zone has a corresponding PMV/PPD interval and thresholds for the different categories of DIN EN 16798 [10].

Table 1: Definition of the comfort zones for TCI

Zone	PPD	PMV	Threshold value	Definition
1	≤ 6	$\lvert PMV \rvert \leq 0.2$	Category I	very comfortable
2	≤ 25	$\lvert PMV \rvert \leq 0.7$	Category III	comfortable
3	≤ 70	$\lvert PMV \rvert \leq 2.0$	Category III $\pm$ 2 °C	uncomfortable
4	> 70	$\lvert PMV \rvert > 2.0$	-	extremely uncomfortable

For ACI, BCI, VCI and IAQI, similar classification criteria were used to calculate the corresponding comfort index (CI) and quality index (QI), respectively, by setting the corresponding thresholds for each zone. To compare indoor environment data more intuitively, the PMV index and sensor data are converted to CI and QI, see the equations 2 to 6.

$$TCI_{PMV/PPD} = 3 - |PMV| \tag{2}$$

$$TCI_{adaptiv}, BCI = \begin{cases} 3 - \dfrac{|x - \frac{x_{1,max} + x_{1,min}}{2}| \cdot 2}{x_{1,max} - x_{1,min}} & \text{if } x_{1,min} \leq x < x_{1,max} \\ I_{i,max} - |x - x_{i-1,min}| \cdot \dfrac{I_{i,max} - I_{i+1,max}}{x_{i-1,min} - x_{i,min}} & \text{if } x_{i,min} \leq x < x_{i-1,min} \text{ for i = 2 and 3} \\ I_{i,max} - |x - x_{i-1,max}| \cdot \dfrac{I_{i,max} - I_{i+1,max}}{x_{i,max} - x_{i-1,max}} & \text{if } x_{i-1,max} \leq x < x_{i,max} \text{ for i = 2 and 3} \\ 0 & \text{if } x < x_{3,min} \text{ or } x \geq x_{3,max} \end{cases} \tag{3}$$

$$ACI,\ IAQI_{VOC/CO_2} = \begin{cases} 3 - |x| \cdot \dfrac{3 - 2.8}{x_{1,max}} & \text{if } x < x_{1,max} \\ I_{i,max} - |x - x_{i-1,max}| \cdot \dfrac{I_{i,max} - I_{i+1,max}}{x_{i,max} - x_{i-1,max}} & \text{if } x_{i-1,max} \leq x < x_{i,max} \text{ for i = 2 and 3} \\ 0 & \text{if } x \geq x_{3,max} \end{cases} \tag{4}$$

$$IAQI = \frac{IAQI_{VOC} + IAQI_{CO_2}}{2} \tag{5}$$

$$VCI = \begin{cases} 0 & \text{if } x < x_{3,min} \\ I_{i,max} - |x - x_{i-1,min}| \cdot \dfrac{I_{i,max} - I_{i+1,max}}{x_{i-1,min} - x_{i,min}} & \text{if } x_{i,min} \leq x < x_{i-1,min} \text{ for i = 3 and 2} \\ 3 & \text{if } x \geq x_{1,min} \end{cases} \tag{6}$$

Where:

x	data value from sensor
$I_{i,max}$	maximum index value of comfort zone i, with $I_{1,max} = 3.0, I_{2,max} = 2.8, I_{3,max} = 2.3, I_{4,max} = 1.0$
$x_{i,min/max}$	minimum / maximum threshold of zone i, the thresholds can be adjusted in the settings page of the software

Once all CI and QI are calculated, user comfort can be predicted. Due to the veto power of thermal and acoustic comfort [5], user comfort is deemed uncomfortable if TCI or ACI is below 2.3.

2.3 User test

Users were asked to fill out a questionnaire every evening. To avoid too many questions repeatedly each day, a questionnaire based on the usability metric for user experience lite (UMUX-LITE) was used [12]. At the end of the test, a 20 minute interview was conducted in which the users were asked to complete a more detailed questionnaire based on the system usability scale (SUS) developed by Brooke [13]. To ensure the validity of the collected data and to avoid the effects of different operating systems on the data mentioned by Lewis [14] in his study, all test users used the Windows 10 operating system with a screen resolution of 1080p. There were also no additional instructions for the test users. They were only informed about how to power the monitoring system and where to find the manual.

3 Results and Discussion

As shown in Figure 2, a touchscreen is installed on the box, which includes a total of four screens (see Figure 3). As Figure 4 shows, the accompanying desktop app provides the information on user comfort prediction, system status, outdoor weather, indoor environment analysis, and the level system. The desktop app performs an analysis of all sensor data collected since the app was launched and makes appropriate suggestions to the user to improve comfort, depending on the state of the indoor environment. Also, the desktop app will inform the user via the notification center which parameters of the current indoor environment have exceeded the threshold value. The user does not have to constantly keep an eye on the data. In addition to comfort prediction, it is also important to provide feedback and interaction to the user. Depending on how long the user has been using the app and what the current state of the indoor environment is, the level system gives the user the appropriate experience points (EXP). When the EXP reaches the pre-set threshold, the user's level will increase and the content of the animated images will become more varied and have more detail at the same time.

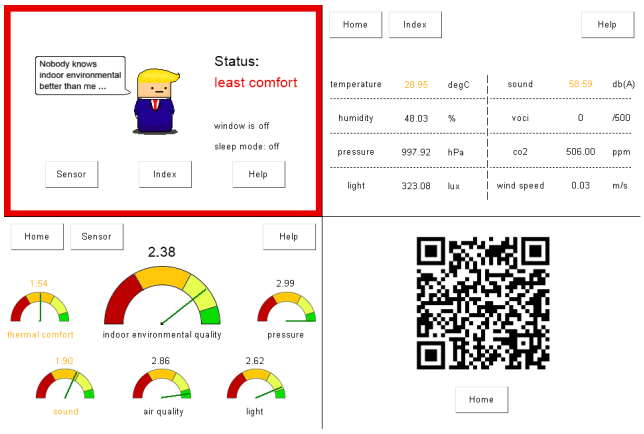

Figure 3: Top: home screen (left) and sensor screen, bottom: index screen (left) and help screen

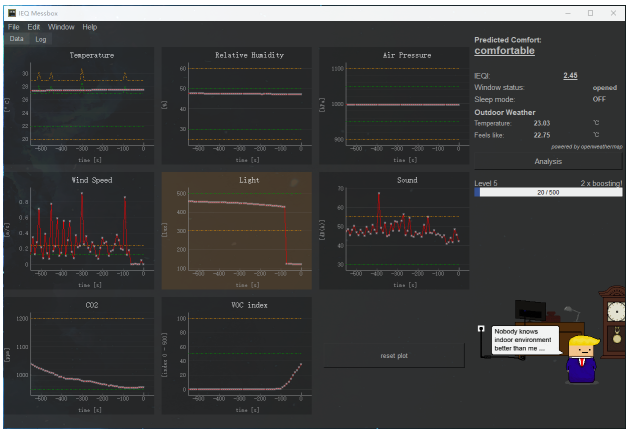

Figure 4: GUI of the accompanying desktop app

However, it should be noted that since the system only implements monitoring functions and is not connected to other personalized conditioning systems, although it can provide users with predictions of comfort and tips of how to improve the indoor environment, users still need to decide whether and to what extent to change the current environment.

Four testers used the monitoring system for five days each. The average usage time is 3.8 hours per day, but differed strongly between users (Figure 5). With regard to usage habits, it can be seen from the user responses to the question "I use display on the box more often than the desktop app" in Figure 6 that the longer the test users use the monitoring system, the longer they use the touchscreen.

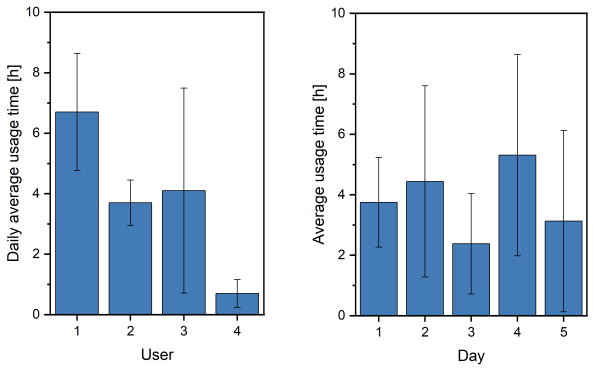

Figure 5: Average usage time incl. standard deviation, left: for each test user, right: for each day

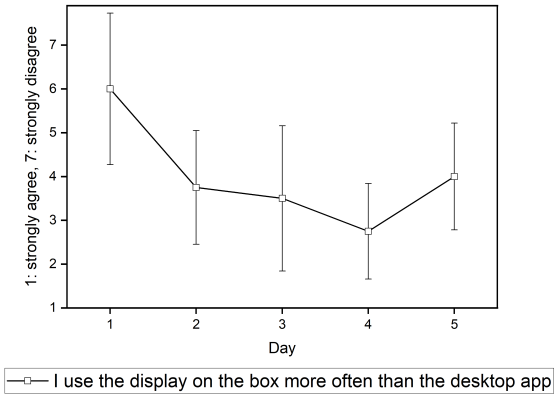

Figure 6: Responses to display vs. desktop app use (error bars show standard deviation)

This could indicate that experienced users prefer faster and easier access to basic IEQ data, and that the desktop app enables users to understand the system faster. This does not mean that touchscreen is a better solution for human-machine interaction. Three test users stated in the interview that they liked some functions offered by the desktop app, such as the notification function running in the background. Touchscreen and desktop app should be complementary: The touchscreen can offer simpler interaction possibilities, while the accompanying desktop app offers more complex and more

extensive functions. Although all four test users rated the monitoring system very positively, the prototype still has some shortcomings, e.g., the GUI of the desktop app should be optimized, because the 4th tester used the app very little due to the frequent notifications, and this user did not know that the notification interval can be changed in the settings. Three users did not change the default settings because they were too complex. This may affect the accuracy of the comfort predictions, especially when using the PMV/PPD model, which requires the current clothing insulation value.

4 Conclusion and Future Work

In this work, a monitoring system including a new algorithm for IEQI was developed to monitor IEQ. Four users participated in the test phase, and the UMUX-LITE and SUS surveys indicated high usability of the system. However, it should not be overlooked that the prototype still needs improvement in some areas. Future work will be focused on minimizing the number of elements that need to be set manually by the user, as well as on associating the system with personalized climate equipment thus achieving a high degree of automation and intelligence for the entire system. The number of test users can also be further extended to obtain more accurate and reliable results. Lastly, environmental parameters are measured only at one room position. The influence of vertical temperature difference, radiation asymmetry, and measurement location is not taken into account. Therefore, how to include 3D spatial information into the system is also a focus of future work.

References

[1] N. E. Klepeis, W. C. Nelson, W. R. Ott, *et al.*, “The national human activity pattern survey (nhaps): A resource for assessing exposure to environmental pollutants”, *Journal of Exposure Science & Environmental Epidemiology*, vol. 11, no. 3, pp. 231–252, 2001.

[2] K. Azuma, U. Yanagi, N. Kagi, H. Kim, M. Ogata, and M. Hayashi, “Environmental factors involved in sars-cov-2 transmission: Effect and role of indoor environmental quality in the strategy for covid-19 infection control”, *Environmental Health and Preventive Medicine*, vol. 25, no. 1, p. 66, 2020, ISSN: 1347-4715. DOI: 10.1186/s12199-020-00904-2. [Online]. Available: https://doi.org/10.1186/s12199-020-00904-2.

[3] A. Ahlawat, A. Wiedensohler, S. K. Mishra, *et al.*, “An overview on the role of relative humidity in airborne transmission of sars-cov-2 in indoor environments”, *Aerosol and Air Quality Research*, vol. 20, no. 9, pp. 1856–1861, 2020.

[4] Z. Peng and J. L. Jimenez, “Exhaled co2 as a covid-19 infection risk proxy for different indoor environments and activities”, *Environmental Science & Technology Letters*, vol. 8, no. 5, pp. 392–397, 2021. DOI: 10.1021/acs.estlett.1c00183.

[5] L. Huang, Y. Zhu, Q. Ouyang, and B. Cao, “A study on the effects of thermal, luminous, and acoustic environments on indoor environmental comfort in offices”, *Building and Environment*,

vol. 49, pp. 304–309, 2012, ISSN: 0360-1323. DOI: https://doi.org/10.1016/j.buildenv.2011.07.022. [Online]. Available: https://www.sciencedirect.com/science/article/pii/S0360132311002368.

[6] H. Chojer, P. Branco, F. Martins, M. Alvim-Ferraz, and S. Sousa, "Development of low-cost indoor air quality monitoring devices: Recent advancements", *Science of The Total Environment*, vol. 727, p. 138 385, 2020, ISSN: 0048-9697. DOI: https://doi.org/10.1016/j.scitotenv.2020.138385. [Online]. Available: https://www.sciencedirect.com/science/article/pii/S0048969720318982.

[7] A. Tiele, S. Esfahani, and J. Covington, "Design and development of a low-cost, portable monitoring device for indoor environment quality", *Journal of Sensors*, 2018. DOI: https://doi.org/10.1155/2018/5353816.

[8] T. Parkinson, A. Parkinson, and R. J. de Dear, "Continuous ieq monitoring system: Context and development", *Building and Environment*, vol. 149, pp. 15–25, 2019, ISSN: 0360-1323. DOI: https://doi.org/10.1016/j.buildenv.2018.12.010. [Online]. Available: https://www.sciencedirect.com/science/article/pii/S0360132318307467.

[9] DIN EN ISO 7730, *Ergonomie der thermischen umgebung – analytische bestimmung und interpretation der thermischen behaglichkeit durch berechnung des pmv- und des ppd-indexes und kriterien der lokalen thermischen behaglichkeit*, Norm, 2005.

[10] DIN EN 16798-1, *Energetische bewertung von gebäuden – lüftung von gebäuden – teil 1: Eingangsparameter für das innenraumklima zur auslegung und bewertung der energieeffizienz von gebäuden bezüglich raumluftqualität, temperatur, licht und akustik*, Norm, 2019.

[11] F. Tartarini and S. Schiavon, "Pythermalcomfort: A python package for thermal comfort research", *SoftwareX*, vol. 12, p. 100 578, 2020, ISSN: 2352-7110. DOI: https://doi.org/10.1016/j.softx.2020.100578. [Online]. Available: https://www.sciencedirect.com/science/article/pii/S2352711020302910.

[12] J. R. Lewis, B. S. Utesch, and D. E. Maher, *UMUX-LITE: When There's No Time for the SUS*. Association for Computing Machinery, 2013, ISBN: 9781450318990. [Online]. Available: https://doi.org/10.1145/2470654.2481287.

[13] J. Brooke, *SUS: A 'Quick and Dirty' Usability Scale*. London: Taylor and Francis, 1996, ISBN: 978-0748404605.

[14] J. R. Lewis, "Measuring perceived usability: The CSUQ, SUS, and UMUX", *International Journal of Human–Computer Interaction*, vol. 34, no. 12, pp. 1148–1156, 2018. DOI: 10.1080/10447318.2017.1418805. eprint: https://doi.org/10.1080/10447318.2017.1418805. [Online]. Available: https://doi.org/10.1080/10447318.2017.1418805.

Automatisiertes Behaglichkeitsmonitoring mit Hilfe von IoT-Technologien

Carlos Federico Chillón Geck

Institut für Digitales und Autonomes Bauen, Technische Universität Hamburg, Blohmstraße 15, 21079 Hamburg

E-Mail: carlos.chillon.geck@tuhh.de

Abstract: Thermische Behaglichkeit ist zu einem Schlüsselelement moderner und umweltfreundlicher Gebäudeplanung geworden. Üblicherweise wird die thermische Behaglichkeit entweder anhand von Umfragen in Papierform, die von den Gebäudenutzenden ausgefüllt werden, oder durch die Erfassung von Umgebungsdaten, die in mathematische Modelle wie das Predicted Mean Vote (PMV) einfließen, bewertet. Derzeit ist die Durchführung von digitalen Umfragen und manuellen Übertragungen der erhobenen Daten zwischen verschiedenen Software- und Datenformaten sehr zeitaufwändig, fehleranfällig und umständlich. Zudem führen sie oft zu Informationsverlusten. Um die genannten Nachteile zu beheben, wird in diesem Beitrag ein automatisiertes Behaglichkeitsmonitoringsystem vorgestellt, das mittels IoT-Technologien automatisch Daten für die Bewertung der thermischen Behaglichkeit sammelt. Eine digitale Umfrage zur thermischen Behaglichkeit ergänzt die Umgebungsdaten mit Feedbacks der Gebäudenutzenden. Das automatisierte Behaglichkeitsmonitoringsystem wurde in einem Praxistest validiert, bei dem intelligente Sensorknoten kontinuierlich die Umgebungsdaten in einer Büroumgebung aufzeichnen, während die Gebäudenutzenden die digitale Umfrage zur thermischen Behaglichkeit ausfüllen. Die Ergebnisse des Praxistests und weitere Anwendungsfälle des Monitoringsystems sowie zukünftige Arbeiten werden am Ende des Beitrages diskutiert.

Keywords: Thermische Behaglichkeit, Internet of Things (IoT), Smart Building, drahtlose Sensornetzwerke, Gebäudeautomation

1 Einleitung

Die thermische Behaglichkeit, d.h. die Zufriedenheit mit der thermischen Umgebung, ist in den letzten Jahrzehnten zu einem wichtigen Forschungsgebiet geworden, was auf die zunehmende Bedeutung der allgemeinen Behaglichkeit für die Gebäudenutzenden zurückzuführen ist [1]. Obgleich die automatisierte Analyse von Umgebungsdaten für die Bewertung der thermischen Behaglichkeit nützlich ist, liefern Umfragen unter den Gebäudenutzenden wertvolle Informationen für eine ganzheitlichere Bewertung. Traditionell wurden Umfragen zur thermischen Behaglichkeit manuell durchgeführt. Mit den Fortschritten in Sensor-, Monitoring- und IoT-Technologien [2] wurden in den letzten Jahren Werkzeuge bereitgestellt, mit denen das Feedback der Gebäudenutzenden in das Monitoring der thermischen Behaglichkeit einbezogen werden kann, sodass Studien, die nur die Umgebungsparameter in Innenräumen messen, überholt sind [3]. IoT-basierte, mobile Anwendungen und digitale Umfragen wurden implementiert, um Rückmeldungen zu thermischen Empfindungen und Präferenzen der Gebäudenutzenden zu erfassen [4]. Trotz der neuen IoT-gestützten Möglichkeiten zur Automatisierung von Erhebungen der thermischen Behaglichkeit [5] ist die Entwicklung einer Umfrage der thermischen Behaglichkeit, die aussagekräftige Daten sammelt, keine triviale Aufgabe [6]. Ein vollständig digitalisierter und automatisierter Arbeitsablauf, der sowohl Umgebungsdaten als auch Feedbacks von Gebäudenutzenden aus digitalen Umfragen zur thermischen Behaglichkeit integriert, würde den Datenverlust, den Aufwand und die Kosten für die zukünftige Bewertung der thermischen Behaglichkeit deutlich reduzieren.

In Anbetracht des Trends zu kosteneffizienter Hardware und der Beteiligung von Gebäudenutzenden am effektiven Monitoring der thermischen Behaglichkeit stellt dieser Beitrag ein automatisiertes *Behaglichkeitsmonitoringsystem* vor, das die Erfassung von Umgebungsdaten durch intelligente drahtlose Sensorknoten mit dem Feedback der Gebäudenutzende durch eine digitale Umfrage zur thermischen Behaglichkeit ergänzt. Die automatische Datenerfassung soll die Probleme verringern, die beim Austausch von Daten zwischen verschiedenen Software- und Datenformaten auftreten, was zu zeitaufwändigen, fehleranfälligen und mühsamen Aufgaben führt, die oft Informationsverluste zur Folge haben. Zunächst werden die Entwicklung der intelligenten drahtlosen Sensorknoten und die digitale Umfrage beschrieben. Daraufhin wird das Behaglichkeitsmonitoringsystem durch einen Praxistest in einer Büroumgebung validiert und die Ergebnisse der Umfrage und der Erfassung von Umgebungsdaten werden vorgestellt. Der Beitrag schließt mit einer Zusammenfassung der Studie und möglichen neuen Aspekten im Forschungsfeld der thermischen Behaglichkeit.

2 Entwicklung des automatisierten Behaglichkeitsmonitoringsystems

Das hier vorgestellte automatisierte Behaglichkeitsmonitoringsystem basiert auf einer vierschichtigen IoT-Architektur [7] und macht sich moderne Konzepte des Monitorings [8],

eingebetteter Systeme [9] und intelligenter Sensorik zunutze [10]. Das System umfasst eine thermische *Behaglichkeitsstation* und eine *digitale Umfrage* zu thermischer Behaglichkeit, die von Gebäudenutzenden ausgefüllt wird. Die Behaglichkeitsstation besteht aus einem drahtlosen Sensorknoten, der aus kosteneffizienten Hardwarekomponenten zusammengesetzt ist. Die Software, die in dieser Studie entwickelt wurde, integriert Echtzeit-Sensorik, eingebettete Datenverarbeitung und IoT-Konnektivität. Die Aufgabe des Systems ist es, die Erfassung von Umgebungsdaten zu automatisieren und sie mit der digitalen Umfrage zur thermischen Behaglichkeit zu ergänzen, um genügend Daten für eine effektivere Bewertung der thermischen Behaglichkeit erfassen zu können. In diesem Abschnitt wird die Systemarchitektur erläutert (2.1), gefolgt von einer Einführung in die Hardware- (2.2) und Softwarekomponenten (2.3) sowie Anmerkungen zur digitalen Umfrage (2.4).

2.1 Systemarchitektur

Die Architektur des Behaglichkeitsmonitoringsystems (Abbildung 1) besteht aus vier Schichten, (i) einer Anwendungsschicht, (ii) einer Verarbeitungsschicht, (iii) einer physischen Schicht und (iv) einer zusätzlichen Sicherheitsschicht, die im folgenden skizziert werden. Die Gebäudenutzenden interagieren mit der *Anwendungsschicht* über ein Dashboard, das in einer Webschnittstelle verwaltet wird. Das Dashboard bietet eine Echtzeit-Visualisierung der Umgebungsdaten und enthält die digitale Umfrage zur thermischen Behaglichkeit. Die *Verarbeitungsschicht* enthält einen mobilen Server auf der Basis eines Raspberry Pi. Der Raspberry Pi verwaltet die Backend-Dienste des Systems mit Hilfe des Node-RED-Entwicklungstools, das visuelle, flussbasierte Programmierung für die Entwicklung der Backend-Systemlogik bietet. Node-RED empfängt das Feedback der Gebäudenutzenden von der Anwendungsschicht und speichert die Ergebnisse der Umfrage sowie die Umgebungsdaten, die von der physischen Schicht erfasst werden. Die *physische Schicht* des automatisierten Behaglichkeitsmonitoringsystems besteht aus einem intelligenten drahtlosen Sensorknoten, der Daten aus dem Innenbereich sammelt, d.h. Lufttemperatur, relative Luftfeuchtigkeit, mittlere Strahlungstemperatur (mean radiant temperature, MRT) und Luftgeschwindigkeit. Darüber hinaus verfügt der drahtlose Sensorknoten über die nötige Rechenkapazität, um die Rohdaten der Umgebung mit Hilfe eingebetteter Algorithmen zu verarbeiten. Die verarbeiteten Daten werden über eine http-Verbindung zur Datenspeicherung und Visualisierung an die Verarbeitungsschicht gesendet. Die *Sicherheitsschicht*, die Authentifizierungsdienste für den Datenschutz und die Sicherheit aller Schichten bereitstellt, verläuft transversal zu den anderen Schichten.

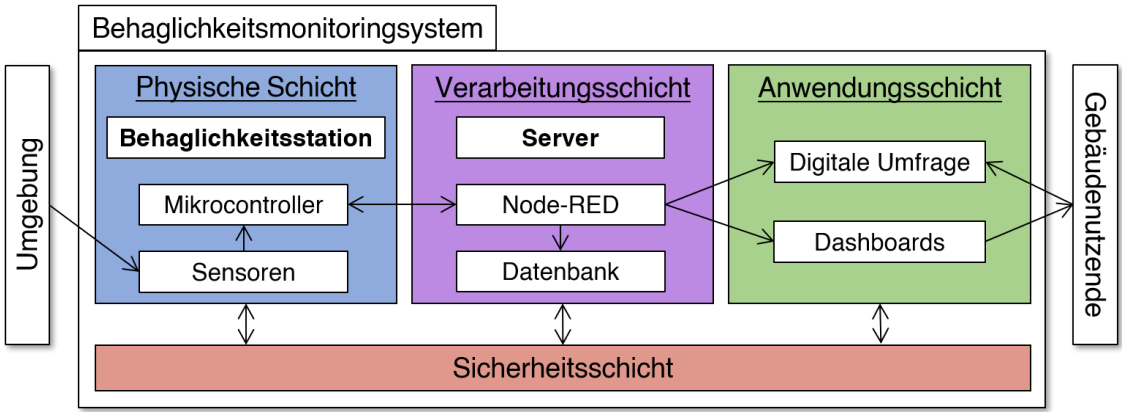

Abbildung 1: Vierschichtige IoT-Architektur des automatisierten Behaglichkeitsmonitoringsystems.

2.2 Hardwarekomponenten

Die Behaglichkeitsstation, als eine Komponente des Behaglichkeitsmonitoringssystem umfasst drei Sensoren, (1) einen kombinierten Sensor, der Lufttemperatur und relative Luftfeuchtigkeit misst, (2) einen Luftgeschwindigkeitssensor und (3) einen Lufttemperatursensor, der in einem schwarz lackierten Tischtennisball eingebaut wird, um ein Globe-Thermometer zu bilden, mit dem die mittlere Strahlungstemperatur berechnet wird. Ein Mikrocontroller des Typs ESP32 WROOM-32 sorgt für die Verarbeitung der Rohdaten der Umgebung und sendet die Daten in regelmäßigen Abständen über Wi-Fi an die Verarbeitungsschicht. Zum Schutz der Hardware und zur Wärmeisolierung der einzelnen Komponenten wurde ein 3D-gedrucktes Gehäuse gebaut. Alle Komponenten sind auf einer Leiterplatte verdrahtet und verlötet. Abbildung 2 zeigt die Hardwarekomponenten der in dieser Studie entwickelten kostengünstigen und intelligenten Behaglichkeitsstation. Die Komponenten wurden nach den folgenden Kriterien ausgewählt: Niedriger Preis, geringer Stromverbrauch, Genauigkeit, Größe und Funktionsfähigkeit bei 5 V.

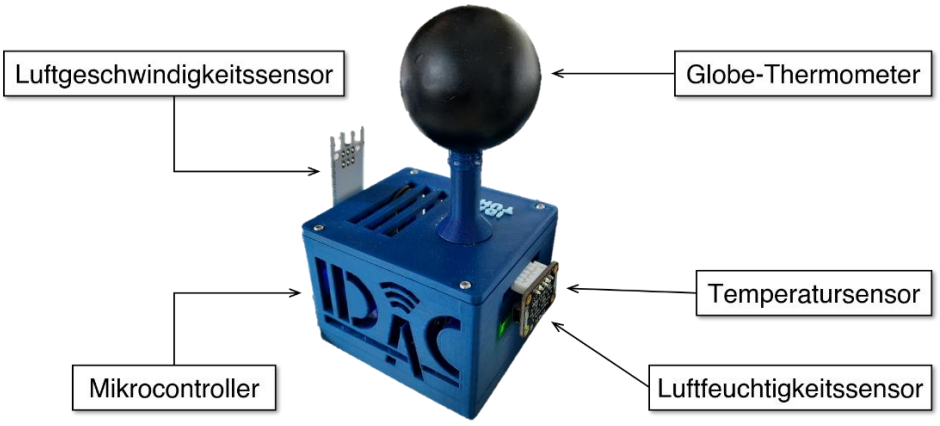

Abbildung 2: Die Behaglichkeitsstation.

2.3 Softwarekomponenten

Der ESP32-Mikrocontroller enthält ein eingebettetes Softwareprogramm, das es ermöglicht, Sensordaten zu sammeln sowie Daten vom Server zu senden und zu empfangen. Darüber hinaus berechnet das eingebettete Softwareprogramm den PMV-Index (Predicted Mean Vote), d. h. einen Index der thermischen Behaglichkeit, der die durchschnittliche thermische Behaglichkeit einer Gruppe von Personen in Innenräumen vorhersagt. Der Algorithmus zur Berechnung des PMV-Index ist in [1] beschrieben und wurde in dieser Studie in Arduino-Programmiersprache übersetzt und übertragen. Die Eingaben zur Berechnung des PMV-Index sind die von der Behaglichkeitsstation gemessenen Umgebungsparameter sowie zwei persönliche Parameter, die die Kleidung und Aktivität (z. B. Sitzen und Schreiben) der Gebäudenutzenden quantifizieren. Die Ausgabe des PMV-Index entspricht einem Wert auf der 7-Punkte-Skala des ASHRAE-55-Standards, wobei -3 für „extremes“ Kälteempfinden und +3 für „extremes“ Wärmeempfinden steht. Ein Index von 0 drückt die „optimale“ thermische Behaglichkeit aus.

Node-RED empfängt die Messungen der Umgebungsparametern und den PMV-Index und zeigt sie in Echtzeit in den Dashboards der Anwendungsschicht an. Gleichzeitig füllen die Gebäudenutzenden die Umfrage zur thermischen Behaglichkeit aus, die auf dem Dashboard angezeigt wird. Die Echtzeit-Diagramme und die digitale Umfrage, die zur Anwendungsschicht gehören, sind in Abbildung 3 dargestellt. Die digitale Umfrage ist so konzipiert, dass die Datenerfassung maximiert und der Aufwand der Gebäudenutzenden beim Ausfüllen der Umfrage minimiert wird.

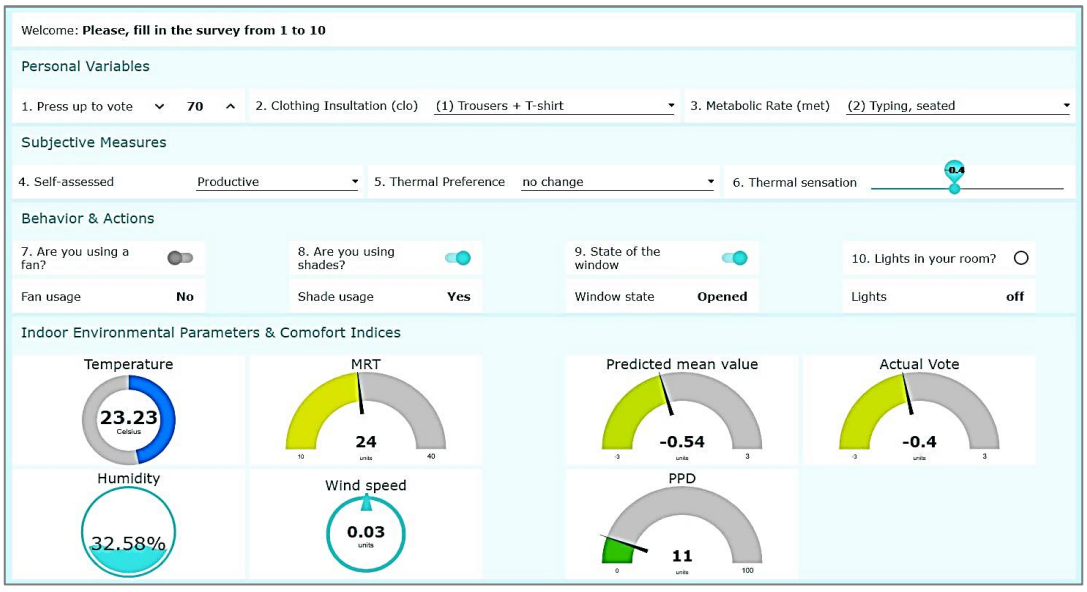

Abbildung 3: Dashboard mit Echzeit-Visualisierung der Umgebungsparameter und digitale Umfrage.

2.4 Digitale Umfrage

Die Umfrage besteht aus drei Arten von Messungenund sammelt eine Reihe von Parametern, die in [6] vorgeschlagen werden. Erstens werden persönliche Variablen von den Gebäudenutzenden erfasst, z.B. Kleidung und Aktivität, die für die korrekte Berechnung des PMV-Indexes benötigt werden. Zweitens wird das Verhalten der Gebäudenutzenden in der Umfrage erfasst; so können die Gebäudenutzenden beispielsweise das Öffnen und Schließen der Fenster und den Zustand der Jalousien aktualisieren. Schließlich werden subjektive Messwerte erfasst, wie z.B. die Bewertung des thermischen Empfindens, d.h. wie die Gebäudenutzenden sich auf der 7-Punkte-Skala für thermische Behaglichkeit fühlen und wie sie selbst ihre Produktivität einschätzen. Demzufolge werden die Umgebungsdaten und die Ergebnisse der Umfrage zusammengeführt und in einer Datei gespeichert. Für jede neue Datenzeile in der Datei wird ein Zeitstempel hinzugefügt, sodass ein Datensatz entsteht, der für weitere Anwendungen analysiert werden kann.

3 Praxistest

Zur Validierung des Behaglichkeitsmonitoringsymstems wurde ein Praxistest in Büroräumen durchgeführt. Die Validierung zielt darauf ab, die Leistung des Systems unter realen Bedingungen zu bestimmen, d.h. welches die Reaktion der Gebäudenutzenden auf die Untersuchung der thermischen Behaglichkeit ist und wie effektiv die intelligente drahtlose Behaglichkeitsstation die Umgebungsdaten erfasst und den PMV-Index berechnet. Anschließend wird der PMV-Index mit dem Feedback der Gebäudenutzenden zum thermischen Empfinden während des Praxistests verglichen.

Der Praxistest wurde in den Monaten April und Mai 2022 durchgeführt. Im Praxistest wurden in fünf Büros des Instituts für Digitales und Autonomes Bauen der Technischen Universität Hamburg fünf intelligente Behaglichkeitsstationen platziert, die im Abstand von 5 Sekunden Messungen von Umgebungsparametern durchführten. Zusätzlich wurde jeder Person ein Dashboard zugewiesen, um die digitale Umfrage ausfüllen und das Echtzeit-Dashboard mit den Umgebungsdaten visualisieren zu können. Der Server empfängt die Messungen der Umgebung, aktualisiert die Dashboards und speichert die Daten in formatierten Dateien. Abbildung 4 zeigt die gemessenen Lufttemperaturen aller Behaglichkeitsstationen (CS01 bis CS05) über den Verlauf eines Arbeitstages. Durch das vorübergehende Öffnen der Fenster im Raum sinkt die Lufttemperatur während des Beobachtungszeitraums erheblich. Durch das Aufzeichnen der Daten ist es außerdem möglich, Sensorfehler zu erkennen, wie z.B. bei der Behaglichkeitsstation Nummer 2 (CS02). Die frühzeitige Erkennung von Sensorfehlern ist wichtig, um aussagekräftige Ergebnisse bei der Bewertung der thermischen Behaglichkeit zu erhalten und Informationsverluste zu vermeiden.

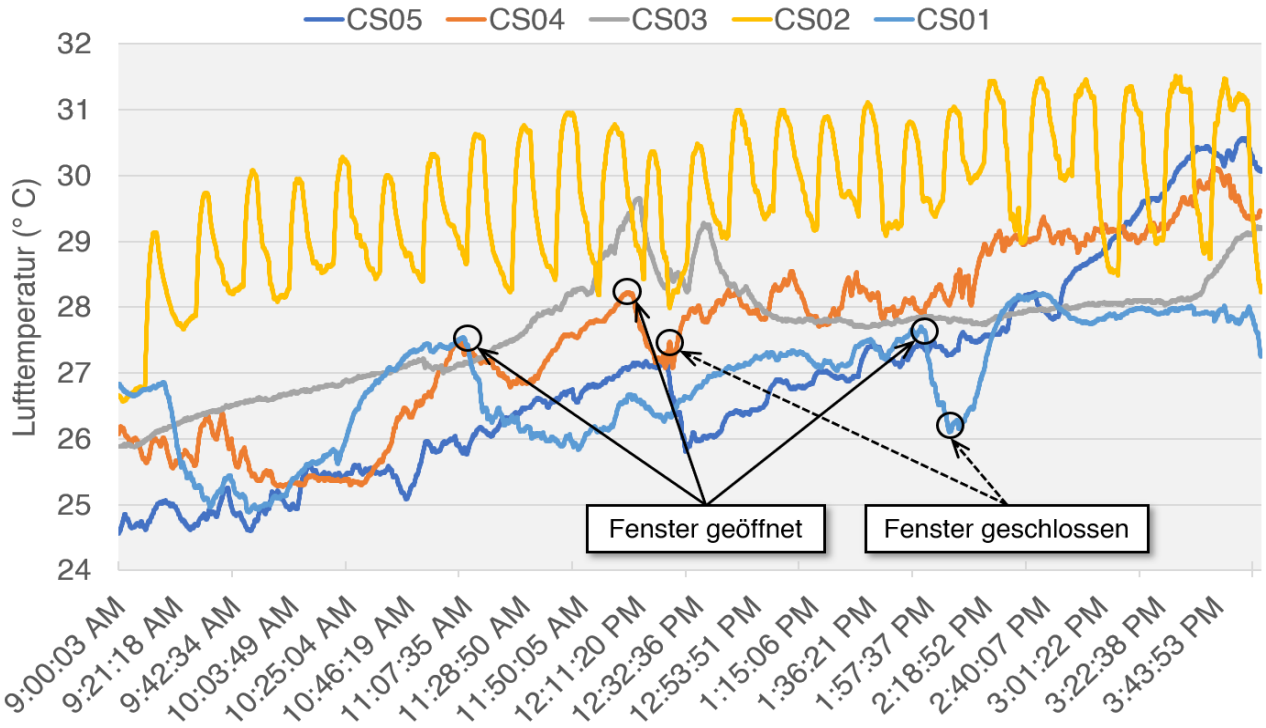

Abbildung 4: Messung der Lufttemperatur während eines Zeitraums des Praxistests.

Darüber hinaus bieten die Ergebnisse der Umfrage Informationen über die Interaktion der Gebäudenutzenden mit der Umgebung, z.B. wann Fenster geöffnet oder Jalousien geschlossen wurden und wie sich diese Veränderungen auf den PMV-Index und die Bewertung der thermischen Behaglichkeit auswirken. Die Beobachtungen können dazu beitragen, die Eignung von Indizes für die thermische Behaglichkeit, hier dem PMV-Index, in bestimmten Umgebungen zu untersuchen. Der Vergleich des kalkulierten PMV-Index und der subjektiv wahrgenommenen Behaglichkeit sind in Tabelle 1 dargestellt. Wie aus den Ergebnissen der Tabelle hervorgeht, kann das System zur Validierung eines Modells der thermischen Behaglichkeit, wie z. B. des PMV-Modells, in einer bestimmten Umgebung und für bestimmte Gebäudenutzenden verwendet werden. Darüber hinaus können die gesammelten Daten dazu verwendet werden, persönliche Profile zu erstellen, die Präferenzen der Gebäudenutzenden enthalten, z. B. wie lange sie am Tag ein Fenster oder eine Jalousie geschlossen halten und wie sich dies auf ihr Wärmeempfinden auswirkt.

Tabelle 1: Vergleich des kalkulierten PMV-Index und der subjektiv wahrgenommenen Behaglichkeit.

PMV-Index	Bewertung der Behaglichkeit	Differenz	Fenster	Jalousie
0,73	0,90	0,17	Geschlossen	Geschlossen
0,53	1,10	0,57	Geschlossen	Geöffnet
0,79	0,40	0,39	Geschlossen	Geschlossen

-0,43	0,10	0,53	Geöffnet	Geöffnet
0,37	0,50	0,13	Geöffnet	Geschlossen
1,02	1,00	0,02	Geschlossen	Geöffnet

4 Fazit

Dieser Beitrag beschreibt die Entwicklung eines automatisierten Behaglichkeitsmonitoringsystems auf der Grundlage einer vierschichtigen IoT-Architektur. Der Entwurf des Behaglichkeitsmonitoringsystems und die Verwendung der eingesetzten Tools zielen darauf ab, die Geschwindigkeit und Genauigkeit der Datenerfassung zu erhöhen, die durch manuelle Erhebungen verursachten Fehler zu reduzieren und sicherzustellen, dass etwaige Fehler im Behaglichkeitsmonitoringsystem durch visuelle Inspektionen der Echtzeit-Dashboards erkannt werden, bevor ein bedeutender Datenverlust auftritt. Zur Validierung des Behaglichkeitsmonitoringsystems wurde ein Praxistest durchgeführt. Die Ergebnisse des Praxistests zeigen, dass das System kontinuierlich und zuverlässig Daten zur thermischen Behaglichkeit erfasst. Die Verwendung des Systems soll der Forschung im Gebäudesektor helfen, die Interaktion zwischen Menschen und Gebäuden sowie das Wohlbefinden der Gebäudenutzenden weiter zu untersuchen. In zukünftigen Forschungsarbeiten ist geplant, das Behaglichkeitsmonitoringsystem über Aktorik mit Kontrollsystemen wie z.B. Luftbefeuchtern zu koppeln, um die Möglichkeiten der Gebäudeautomatisierung zu erweitern und damit insgesamt die Behaglichkeit in Innenräumen verbessern zu können.

Referenzen

[1] ANSI/ASHRAE Standard 55, 2017. Thermal environmental conditions for human occupancy. Atlanta, GA: American Society of Heating, Refrigeration and Air Conditioning Engineers, Inc.

[2] Smarsly, K. & Petryna, Y., 2014. A Decentralized Approach towards Autonomous Fault Detection in Wireless Structural Health Monitoring Systems. In: Proceedings of the 7th European Workshop on Structural Health Monitoring (EWSHM) 2014. Nantes, France, 07/08/2014.

[3] V. Tomat, A. P. Ramallo-González, and A. F. Skarmeta Gómez, 2020. A Comprehensive Survey about Thermal Comfort under the IoT Paradigm: Is Crowdsensing the New Horizon? Sensors 20(16), 4647.

[4] A. Sanguinetti, M. Pritoni, K. Salmon, A. Meier, and J. Morejohn, 2017. Upscaling participatory thermal sensing: Lessons from an interdisciplinary case study at University of California for improving campus efficiency and comfort. Energy Research & Social Science, 32(2017), pp. 44-54.

[5] T. Parkinson, A. Parkinson, and R. de Dear, 2019. Continuous IEQ monitoring system: Context and development. Building Environment, 149, pp. 15–25.

[6] F. Nicol, M. Humphreys, and S. Roaf, 2012. Adaptive Thermal Comfort: Principles and Practice (1st ed.). London, UK: Routledge.

[7] Peralta, J. & Smarsly, K., 2021. Internet of Things frameworks for smart city applications – a systematic review. In: Proceedings of the 2021 ASCE International Conference on Computing in Civil Engineering (I3CE). Orlando, FL, USA, 09/14/2021.

[8] D. Legatiuk and Smarsly, K., 2018. An abstract approach towards modeling intelligent structural systems. In: Proceedings of the 9th European Workshop on Structural Health Monitoring (EWSHM). Manchester, United Kingdom, 07/10/2018.

[9] K. Dragos and K. Smarsly, K., 2017. Decentralized infrastructure health monitoring using embedded computing in wireless sensor networks. In: Sextos, A. & Manolis, G. D. (eds.). Dynamic Response of Infrastructure to Environmentally Induced Loads. Pp. 183-201. Cham, Switzerland: Springer International Publishing AG

[10] Dragos, K. & Smarsly, K., 2016. A hybrid system identification methodology for wireless structural health monitoring systems based on dynamic substructuring. In: Proceedings of the SPIE Smart Structures/NDE Conference: Sensors and Smart Structures Technologies for Civil, Mechanical, and Aerospace Systems. Las Vegas, NV, USA, 03/24/2016.

A data-driven approach for predicting occupant thermal comfort in offices

Fatma Deghim[1], Farzan Banihashemi[1], Sebastian Koth[2] and Werner Lang[1]
[1]Institute of Energy Efficient and Sustainable Design and Building, TU Munich, Munich, Germany
[2]Chair of Building Technology and Climate Responsive Design, TU Munich, Munich, Germany
E-mail(s): [fatma.deghim, farzan.banihashemi, sebastian.koth, w.lang]@tum.de

Abstract: Since people spend most of their time in indoor environments, working on thermal comfort is of increasing interest to researchers. Indoor thermal comfort is currently modeled using knowledge-based methods such as the predicted mean vote (PMV) model. The PMV model was developed by averaging the feedback of large groups of people on thermal comfort in laboratory studies. Hence the model is limited when predicting the thermal comfort of individuals. Researchers investigated new approaches to model individual-specific thermal comfort responses that showed high potential such as the Personal Comfort Models (PCM). In this paper, we evaluated different machine learning (ML) classifiers predicting personal thermal comfort in offices. Our final model performed 30% better than PMV in predicting thermal sensation votes (TSV) on the ASHRAE Global Thermal Comfort Database II. We performed a case study to evaluate the trained models, where we obtained comparable F1-scores between the PMV model and the trained models. This result on the case study is explained by the mild environment in the conducted experiment and the imbalanced data with high presence of the neutral thermal sensation vote. This work exemplifies the potential and the limitations of using classifiers trained on the ASHRAE dataset to predict TSV on a real use case.

Keywords: Thermal sensation, group-based personal comfort modeling, data-driven, PMV, ASHRAE Global Thermal Comfort Database II

1 Introduction

Generally Heating, Ventilation and Air Conditioning (HVAC) systems are used to ensure thermal comfort in indoor environments based on standards such as ASHRAE 55 [1]. With predefined setpoints, current HVAC systems provide a "one-size fits all" environment, thereby ignoring that comfort is subjective and can differ from one person to another depending on several environmental and personal factors. Apart from the high energy consumption to provide this defined comfortable environment, studies showed that people do not necessarily feel comfortable at the end [2]. Thus, with the emergence of the Internet of Things (IoT), the importance of developing intelligent HVAC

systems that correctly predict the thermal sensation of individuals increased. These systems will learn from users real-time feedback and adapt the environmental parameters of the room to make it more comfortable accordingly. A better understanding of occupants' behavior in indoor environments will help fill the performance gaps of the PMV and adaptive models and provide better individual indoor conditions that are not only comfortable but also healthy [3], [4].
Several researchers have used data-driven methods to predict individuals' feedback on thermal comfort. This approach is called personal comfort modeling (PCM) and was discussed and reviewed in detail by Kim [5] and Martins [6]. The models use real-time sensor data combined with personal information and individuals' feedback obtained from surveys. The objective and subjective data are used to train ML models in predicting individual' thermal sensations and preferences. The sensor data typically include indoor and outdoor environmental parameters: indoor and outdoor air temperature, indoor mean radiant temperature, relative humidity, and air velocity [5], [6]. Certain studies like the done by Lee (2021) [7] used physiological parameters, including skin temperature from different body parts and heart rate using thermal cameras or wearable devices. Other studies started using data from Personal Comfort Systems (PCS) to learn individual thermal preferences[8]. Additional to sensor data, personal information such as age, sex, clothing, and metabolic rate were used to build the models using ML.
Various ML algorithms have been evaluated with the goal of improving thermal sensation predictions. Prominent examples include: Random Forest [9], [10], Classification Trees [9], Gaussian process classification [7], Gradient Boosting Method [11], Support Vector Machine [10]–[12], K-Nearest Neighbors [10], [11], and Artificial Neural Networks [10]. Although previous studies showed the high potential of the PCMs in predicting thermal comfort of individuals especially compared to the PMV or adaptive method, these Blackbox models lack transparency when it comes to evaluating them on real use cases or reproducing them. In fact, in previous research, mainly data from own experiments was used to develop PCMs using ML [7], [9], [10]. Others used the ASHRAE database to create thermal comfort models but did not test them on real use cases for example [12]. Any change in the data, be it only the combination of input parameters or using a completely different training data set implies adaptations to the model properties and therefore its capabilities. This research paper aims to answer the following research question: Can data-driven models trained on an open-source dataset accurately predict the thermal sensation of new individuals compared to conventional methods?

2 Methodology

The proposed approach for predicting individuals' TSV includes three steps: (1) data preprocessing of the ASHRAE dataset, (2) model development using ML algorithms, and (3) model evaluation on collected data from experiments at the Technical University of Munich, as seen in Figure 1.

2.1 Data preprocessing

The open-source database ASHRAE Global Thermal Comfort Database II was launched in 2014. This database comprises 81,846 rows of raw data divided into measured environmental parameters

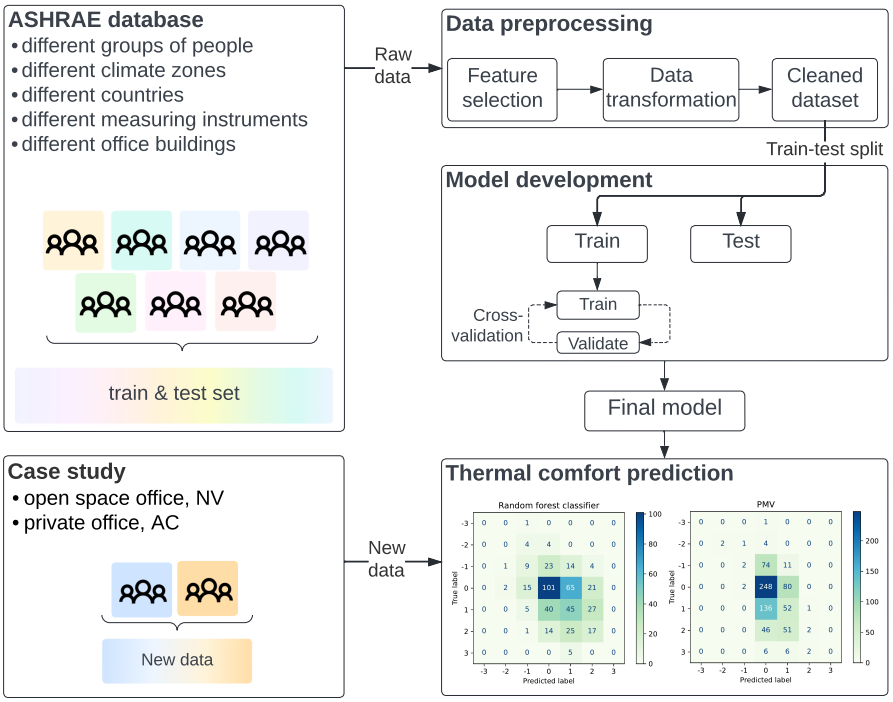

Figure 1: Proposed methodology

and subjective user feedback collected between 1995 and 2016 on different continents according to predefined data collection requirements. The database furthermore comprises several “building categories” such as classrooms, multi-family houses, offices and “building types” that concern cooling strategies [13]. Within the framework of this paper, the data was filtered to only include data from offices which results in a raw dataset with 61,691 rows.

Data preparation: First, the features vector x and the target vector y are selected. As stated before commonly three types of parameters were used for PCM development: (1) indoor environmental features, (2) outdoor environmental features, and (3) personal features. The ASHRAE dataset only provides the monthly outdoor temperature. Hence, it was excluded from model training. In this study, we use additional features such as the country, the climate zone, the season, and the building type. The target value is the individual’s Thermal Sensation Votes (TSV), which is an occupant’s feedback on thermal sensation at the moment of the survey and is given on a 7-point scale corresponding to the categories: -3 (cold), -2 (cool), -1 (slightly cool), 0 (neutral), 1 (slightly warm), 2 (hot), 3 (warm). The rows with null values and errors in the target column are removed. Moreover, the climate zones are grouped to the five main groups according to Köppen climate classification: A tropical, B dry, C temperate and D continental. The E polar group was absent in the dataset. Figure 2 depicts the TSV distribution in the cleaned data set. **Encoding**: The selected features are a mixture of numerical and categorical data. Since most of ML algorithms can not handle categorical values, these must be converted to numerical values. The preprocessing method from python scikit-learn “One hot encoding” is used for this purpose. **Data scaling**: Feature values in the dataset show wide ranges, for example, indoor air temperature ranges between 13.4 and 37.6℃ and air velocity ranges between 0.01 and 0.5 m/s, which can lower the model performance and its learning speed. Feature scaling is a good practice

in this case. The most common techniques of feature scaling are Normalization and Standardization [14]. In the realm of this work standardization was used. **Data resampling:** Figure 2 shows the class imbalance in the dataset where the classes -1 and 1 represent the majority of the TSVs. To deal with the problem of data imbalance, researchers combined classes together and worked with a 3 or 5-point scale TSV [9]. In this study, the 7-point scale TSV is kept to consider the nuances in an individual's TSV. The "RepeatedStratifiedKFold" cross-validation with 10 folds and 3 repetitions as well as other algorithm-specific hyperparameters are used to overcome the problem of imbalanced data. After data preparation, the obtained dataset had a total of 9,070 valid rows further summarized in Table 1.

Table 1: Features used for model training (ASHRAE) and evaluation (case study)

Feature type	Feature name	Range of values (ASHRAE)	Range of values (Case study)
Indoor environment	Indoor air temperature (℃)	[13.4, 37.6]	[19.51, 30.8]
	Air velocity (m/s)	[0.01, 0.51]	[0, 0.39]
	Relative humidity (%)	[15.5, 88.8]	[23.84, 74.47]
Personal information	Age	[10, 75]	[25, 39]
	Sex	Female, male	Female, male
	Clothing insulation (clo)	[0.3, 2.2]	[0.23, 1.75]
	Metabolic equivalent of task (Met)	[0.8, 6.8]	[1.1, 5.3]
Additional features	Climate zones	A, B, C	C
	Country	Australia, Brazil, Iran, India, Germany	Germany
	Season	Summer, autumn, winter, spring	Winter, spring
	Building type	Naturally ventilated (NV), air-conditioned (AC), mixed mode (MM)	NV, AC

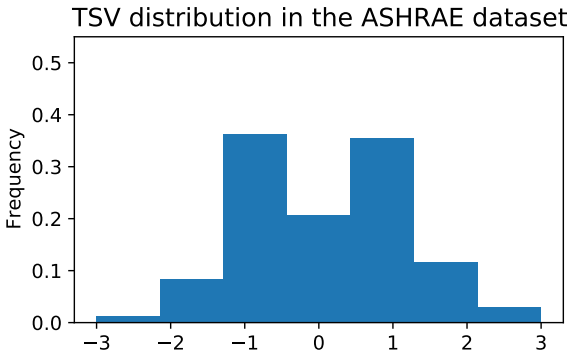

Figure 2: Label distribution (ASHRAE dataset)

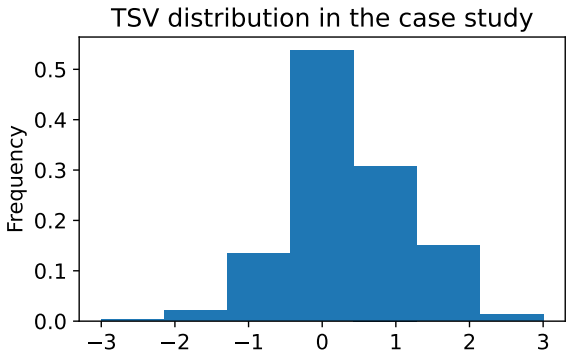

Figure 3: Label distribution (case study)

2.2 Model development

The dataset is split in an 80% train and a 20% test set using stratified train-test split for imbalanced data. Four ML classifiers were trained: Support Vector Machine (SVM), Random Forest (RF), Gradient Boosting (GB) and K-Nearest Neighbors (KNN). The hyperparameters were tuned using gridSearchCV from python scikit-learn and the BayesianOptimazationOracle Tuner in Keras.Tuner [15] and showed comparable results with the Keras.Tuner being computationally more effective. The best parameter

search was conducted using the Bayesian optimization with a Gaussian Process model with defining the maximum number of trials. The RepeatedStratifiedKFold was used to evaluate the algorithms during hyperparameter tuning with 10 folds and 3 repetitions. The hyperparameter tuning was done with the goal of maximizing the mean f1-score across all folds and all runs. This cross-validation method has, compared to simple cross-validation, the advantage of keeping the same percentage of each class in every iteration by stratification and the cross-validation being repeated, allows a more accurate evaluation of the algorithm. After hyperparameter tuning, the following models were developed using the ASHRAE dataset. The RF was trained with 300 trees and a max_depth of 16 using a balanced subsample. The GB was trained with 200 boosting stages, a max_depth of 6 and a learning rate of 0.01. The KNN was trained with 26 nighbors and leaf_size 25 and using the distance weights methods for points. The SVM was trained using C=10, an 'rbf' kernel and a gamma of 0.1.

2.3 Thermal comfort prediction - case study

The case study consists of two field studies conducted in two types of offices: one naturally ventilated open space office and one air-conditioned single office. For the first experiment, a survey was conducted at the Institute of Energy Efficient and Sustainable Design and Building during the winter and spring 2022. For three weeks in February and in May, 12 healthy individuals, 8 females and 4 males, participated in the survey. The participants answered questions about their (1) clothing, (2) activity level in the last 30 minutes before taking the survey, (3) current thermal sensation and (4) current thermal preference. The participants were asked to take the survey two to three times per week and three times a day: in the morning, before lunch break, and in the afternoon. For the second experiment, the survey was conducted in the Senselab from the Chair of Building Technology and Climate Responsive Design, Prof. Dipl-Ing. Thomas Auer, TUM [16] over six weeks in October and November 2021. 10 healthy participants, 6 females and 4 males, participated in the survey and answered the same questions as in the first experiment several times a day. Each participant did the experiment for two days in the survey period. In addition to the survey data, the case recorded the office environmental parameters with measurement boxes situated near to the participants. Indoor air temperature, relative humidity, and air velocity were recorded at the time of the survey. The clothing insulation and the metabolic rate of each participant were calculated according to the ASHRAE 55 [1]. The metabolic rate was calculated by averaging the activity levels in the last 30 minutes before the survey.

3 Results and discussion

In this study we developed ML models to predict the TSV of a group of individuals based on the ASHRAE database. These models were then evaluated on previously unseen data in a case study. Additionally, the PMV index is computed using pythermalcomfort package [17] according to the ASHRAE standard [1] to compare the ML models and the conventional comfort model. All six parameters for PMV calculation (indoor air temperature, mean radiant temperature, relative humidity, air velocity, metabolic rate, and clothing insulation) are known. The calculated PMV indices are

converted to integers between -3 and 3 to allow a precise comparison to the personal TSVs [12]. Table 2 summarizes the performance of the proposed classifiers as well as the PMV on the ASHRAE test set and the case study. In general, the four classifiers performed similarly in predicting the TSV on the test set and showed better results than the PMV with F1-scores of 0.49 and 0.47 compared to 0.17. The models were further evaluated on the unseen data of the case study. For this specific case, where the indoor environment was relatively mild and people tend to feel neutral, the PMV showed comparable F1-score and accuracy to the ML models. The RF, GB and the PMV were the top three best models with F1-scores of 0.37 and 0.39. The two-dimentional confusion matrices of these three models in Figures 4 and 5 show the actual class (rows) and prediction value (column). Due to data imbalance and despite the different techniques used to overcome this problem, we can see that the labels -1, 0 and 1 are the most predicted classes for the trained models followed by the class 2. These classes are in fact the most present classes in the training set 2, whereas the PMV model predicted mainly the classes 0 and 1 with higher correct prediction for the class 0 which represented more than half of the TSVs in the case study (Figure 3). 80% of the values of the class 0 were correctly predicted by the PMV but only for this class the PMV showed this high true positive prediction. Cheung [2] stated in his study as well that the PMV showed high accuracies in predicting the neutal TSV 0. The Mean Absolute Errors (MAE) between prediction and actual values range between 0.66 and 0.92 for all the models. The MAE were less than 1 which means that the models predict in average one level higher or lower than the person really feels.

Table 2: Classification model performances on test set (ASHRAE) and on new data (case study)

Classification models	Test set (ASHRAE)				New data (Case study)			
	F1-score	Accuracy	Precision	Recall	F1-score	Accuracy	Precision	Recall
RF	0.49	0.5	0.5	0.5	0.39	0.39	0.39	0.39
KNN	0.47	0.5	0.48	0.49	0.37	0.36	0.39	0.39
GB	0.47	0.49	0.47	0.49	0.37	0.38	0.39	0.38
SVM	0.47	0.49	0.47	0.49	0.21	0.27	0.46	0.27
PMV	0.17	0.22	0.33	0.22	0.37	0.45	0.42	0.45

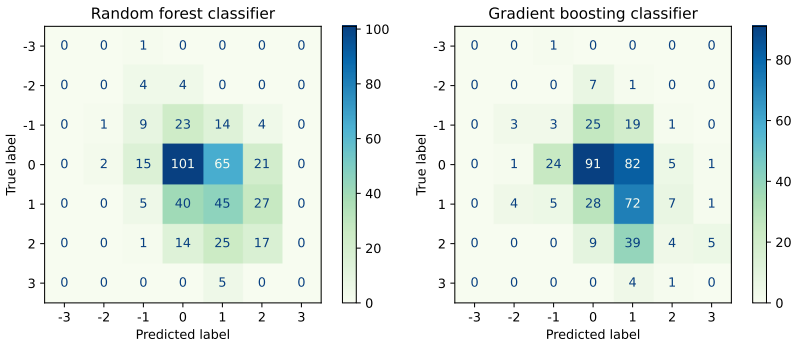

Figure 4: Random forest and gradient boosting classifier confusion matrix (case study)

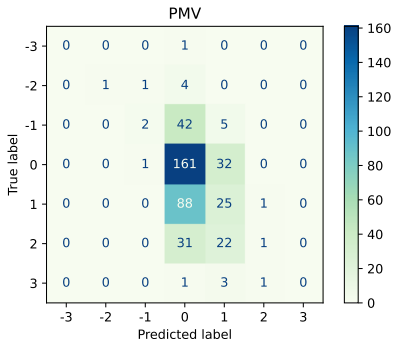

Figure 5: PMV confusion matrix (case study)

4 Conclusions

This study used the ASHRAE dataset to develop thermal comfort models that learn from different groups of individuals to predict individual thermal sensation of a specific group of people. The ASHRAE dataset is the only database of this kind that aggregates a significant number of measured and reported information from individuals from different continents. Nevertheless, in this considerable amount of data coming from different studies, the quality of the measured data should be questioned. The method performed sufficiently well and the model predicted new individuals' TSVs correctly almost 40% of the time. Due to the small number of participants in the experiments and the mild indoor environment of the case study, the collected data was less rich and diverse than the ASHRAE dataset which can be assumed to have led to the poor prediction of some of the TSV classes. This context lacks extreme indoor conditions which also allowed the PMV to perform as good as the data-driven models in this specific case but not on the ASHRAE test set where the PMV failed in predicting 80% of the votes. This method exemplifies limitations directly related to the data quality, its diversity, and its distribution in the training set and in the evaluation set. For a better understanding of people's thermal sensation, physiological data and behavioral data recorded on long time periods are essential. This time-dependent high amount of data will not only allow training models that predict personal thermal sensation with higher accuracies, but also allow understanding the underlying physiological properties of the different thermal sensations over time. Additionally, this data type is user independent and will therefore reduce uncertainties and inconsistencies of surveys.

Acknowledgements

This work was conducted as part of the research project "NuData Campus" funded by the Federal Ministry of Economics Affairs and Climate Action (BMWK). The authors are grateful to the BMWK for its support. The authors are grateful to the Senselab team (Building Technology and Climate Responsive Design, Prof. Dipl-Ing. Thomas Auer, TUM) and all the participants in the case study.

References

[1] ASHRAE, "Standard 55-2013 - thermal environmental conditions for human occupancy", 2013.

[2] T. Cheung, S. Schiavon, T. Parkinson, P. Li, and G. Brager, "Analysis of the accuracy on pmv–ppd model using the ashrae global thermal comfort database ii", *Build Environ*, 2019.

[3] A. Warthmann, D. Wölki, H. Metzmacher, and C. Van Treeck, "Personal climatization systems—a review on existing and upcoming concepts", *Applied Sciences*, 2018.

[4] W. van Marken Lichtenbelt, M. Hanssen, H. Pallubinsky, B. Kingma, and L. Schellen, "Healthy excursions outside the thermal comfort zone", *Build Res Inf*, 2017.

[5] J. Kim, S. Schiavon, and G. Brager, "Personal comfort models – a new paradigm in thermal comfort for occupant-centric environmental control", *Build Environ*, 2018.

[6] L. A. Martins, V. Soebarto, and T. Williamson, “A systematic review of personal thermal comfort models”, *Build Environ*, 2022.

[7] J. Lee and Y. Ham, “Physiological sensing-driven personal thermal comfort modelling in consideration of human activity variations”, *Build Res Inf*, 2021.

[8] A. Aryal, B. Becerik-Gerber, G. M. Lucas, and S. C. Roll, “Intelligent agents to improve thermal satisfaction by controlling personal comfort systems under different levels of automation”, *IEEE Internet Things J*, 2020.

[9] A. Aryal and B. Becerik-Gerber, “Thermal comfort modeling when personalized comfort systems are in use: Comparison of sensing and learning methods”, *Build Environ*, 2020.

[10] S. Liu, S. Schiavon, H. P. Das, M. Jin, and C. J. Spanos, “Personal thermal comfort models with wearable sensors”, *Build Environ*, 2019.

[11] W. Jung, F. Jazizadeh, and T. E. Diller, “Heat flux sensing for machine-learning-based personal thermal comfort modeling”, *J Sens*, 2019.

[12] X. Zhou, L. Xu, J. Zhang, *et al.*, “Data-driven thermal comfort model via support vector machine algorithms: Insights from ashrae rp-884 database”, *Energy Build*, 2020.

[13] V. F. Ličina, T. Cheung, H. Zhang, *et al.*, “Development of the ashrae global thermal comfort database ii”, *Build Environ*, 2018.

[14] A. Burkov, *The hundred-page machine learning book*. A. Burkov Quebec City, Canada, 2019.

[15] T. O’Malley, E. Bursztein, J. Long, F. Chollet, H. Jin, L. Invernizzi, *et al.*, *Kerastuner*, https://github.com/keras-team/keras-tuner, 2019.

[16] B. Kobas, S. C. Koth, K. Nkurikiyeyezu, G. Giannakakis, and T. Auer, “Effect of exposure time on thermal behaviour: A psychophysiological approach”, *Signals*, 2021.

[17] F. Tartarini and S. Schiavon, “Pythermalcomfort: A python package for thermal comfort research”, *SoftwareX*, 2020.

IFC-based variant analysis considering multi-criterial sustainability analysis of buildings

Benjamin Lammers[1] and Kasimir Forth[2]
[1]Technische Universität München, Arcisstr. 21, 80333 München, Deutschland
[2]Lehrstuhl für Computergestützte Modellierung und Simulation, Technische Universität München, Arcisstr. 21, 80333 München, Deutschland
E-mail(s): b.lammers@tum.de

Abstract: Economic, social, and environmental aspects are the foundation for holistically measuring sustainability in construction projects. However, combining different indicators of these aspects is not common practice, yet. Especially not in early design phases. At the same time, Building Information Modeling (BIM) enables an interdisciplinary and integrated design approach for comparing variants and helping design decision support in early design stages. Therefore, this paper aims to enable a framework of an automated, multi-criteria sustainability assessment by combining the methods of life cycle assessment (LCA) and life cycle cost (LCC) with BIM. Using the open BIM approach and its data exchange format Industry Foundation Classes (IFC), the proposed method is applicable to all project stakeholders. Design variants can be compared by combining relevant information from the IFC model and several LCA and LCC databases. A combined database framework is created using relational databases and SQL to provide a single source for LCA and LCC data. As a result, an automated holistic assessment of sustainability using BIM and a component database is possible in an early design stage, without manually adding any LCA and LCC information to the BIM model.

Keywords: BIM, IFC, Life Cycle Assessment, Life Cycle Costs

1 Introduction

The building sector is responsible for 38% of the global CO_2 emissions, including the manufacturing, transportation and use of construction materials, which is the highest total level recorded until 2020 [1]. To assess the ecological and economical impact of buildings, standardized methods have been established, such as LCA and LCC.

At the same time, the building sector is in a transition phase of digitization. New processes and methods, such as BIM, are introduced and used. Combining BIM and the stated sustainability analysis has beneficial synergies. A wide variety of information can be stored in the semantic 3D building model.

Therefore, the extraction of cost estimates, and improvements in energy efficiency and sustainability with the help of design alternatives is an arising potential. Additionally, the early-design stages are getting more important, as more information is available using BIM. As the use of BIM is assumed to be very common for future building projects, automated assessments based on the information of a BIM model can present a huge chance [2].

This study tackles the challenge of combining multi-criteria sustainability analysis and automating the process based on BIM models as the data input.

2 State of the Art

For early design stages, different international standards and norms are available, which define building projects to phases or stages. The established methods are either focusing on organizing building project phases, like RIBA in the UK, or defining cost groups, like HOAI in Germany. However, conventional design processes are mainly linear, without enabling iterations for changes early into the project [3].

2.1 Building Information Modeling

In 2008, several committees of the American Institute of Architects (AIA) have adopted the concept Level of Development (LOD). The same standard was taken over by the BIMForum in 2013 and will be used for this study [4].

The standard itself consists of five basic LOD's, from Level 100 to 500. The early design stages are defined as the phases from the pre-draft or preparation to the first design draft [3]. Concerning the definitions of LOD's, these phases correspond to LOD 100 to 300. Despite being vague in an overall description of LOD, the standard defines precisely what information is included for the different object types, e.g. external wall, door etc. [4].

For the proposed methodology, the difference of open and closed BIM is relevant. The controversy describes the restrictions when relying on closed software systems and exchange formats. To make the process available for all stakeholders and independent of software systems, an open BIM approach is chosen. This corresponds to the exchange format of IFC, which can be written and read by every software product commonly used in BIM. Therefore, IFC is used as the exchange format for this study [5].

2.2 Sustainability Assessment

The process of calculating LCA is standardized in the ISO 14040 [6]. Because not all life cycle modules are considered as being representative for an early design phase estimation, the assessed modules encompass A1-A3, B4 and C3-C4. In this study, only the construction, but not the operation of buildings is considered. The use of module D is controversial and highly individual, since it relies on factors like the location of the building site and the recycling possibilities in the future [7].

To use an open and flexible approach, serveral environmental databases are linked together. Those encompass the Ökobaudat from Germany [8], the swiss KBOB [9] as well as the international Ecoinvent [10]. The environmental impact indicators, such as Global Warming Potential (GWP), Ocean Depletion Potential (ODP), etc., used for this study are limited to the lowest common denominator of the selected LCA databases. By combining theses databases, the overlapping, remaining indicators are GWP and Primary Energy total (PE).

Additionally, LCC is an established method to calculate the cost of a project over the whole life-cycle. In this study, only the construction phase is assessed. Similar to the environmental assessment, several databases are combined to assess the costs. These include the *DBD* [11] and *BKI* [12]. All used databases refer to prices in Euros (€).

In contrary to environmental data, which is mostly coherent on a material level, the cost data is assigned to components. To classify costs for building projects in Germany, the DIN 276 [13] has categories for all occurring cases. This system is used to group materials to building component categories and add the costs.

2.3 Literature Review of BIM-based LCA and LCC

The combination of sustainability analyses using BIM is not a totally new approach. An overview of the current research is given through the literature review made by Forth [14]. The aim of analyzed research encompasses the topics BIM, BIM-LCA integration and LCA. Several exchange formats for accessing building information through BIM are common, with IFC being the most adopted technology for open BIM applications. Additionally, the BIM-integrated LCC approach is investigated through the review by Santos [15]. It integrates several sustainability criteria, such as LCA and LCC. Information for combined analysis can either be stored in a specialized database or directly in the building model. A combination of both is often used as well. The first approach relies on exporting a Bill of Quantities (BoQ) from the model and combining that with cost and environmental data [16]. The second is enriching either the model or the resulting IFC-structure [7]. A third approach can be identified as adding an interface to an external software. This software uses the information for further calculations, but might also need separate inputs besides the model [16]. This leads to the existing gap, of using one combined database framework for LCA and LCC information to balance the often scarce information incorporated in an early-phase model.

3 Methodology

3.1 Framework

The goal of this paper is to propose a methodology, which combines two sustainability analysis methods with information input from an early design stage BIM model.

The methodology, including a bigger framework, is displayed in Figure 1. The red bounding box includes the complete project framework. Outside of the bounding box are either data sources or

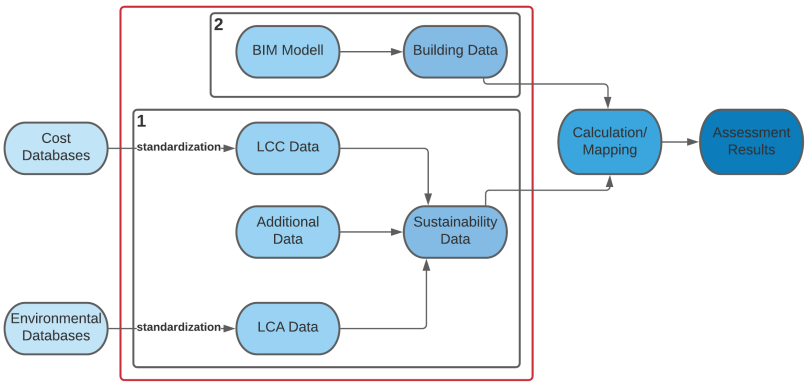

Figure 1: General framework represented as a flow chart, including the project boundary and the separation for first and second part.

additional steps for an automated calculation of design variants. For example, the mapping of building data to material data is not scope of this paper, but will be performed manually for the case study. The process inside the frame is split into two separate sub-parts. Both parts are described in more detail in the following sections.

3.2 Combined Sustainability Database

The first part is about transforming data from different databases and storing it in a useful way. Therefore, the input must be unified, and the structure must take all reference units into account. For cost data, building parts are mostly measured in square meters, which is why the environmental data is also transformed to this unit. That means materials have to be linked together to building parts before matching them with the cost data. The database structure is derived from different levels of complexity, moving up from single materials to whole building components. The material level contains the indicator information, in this case GWP and PE. On the component level, information like cost, replacement rates and layer thickness are added. By enriching the database with most of the calculation crucial information, the BIM-based model can be used without adding additional attribute information. The database is modelled in MySQL Workbench and then accessed and further processed through a python environment.

3.3 Model requirements and preparation

The challenge of using an early phase BIM-based model is the amount of information included. As previously identified, the model components have to be LOD 200 in early design stages. Therefore, the information for automatic matching of components or even materials might not always be included. The component classification is based on the DIN 276 cost groups. Subsequently, the BoQ is derived from the exported IFC-file with the help of IFCOpenShell, an open-source package for parsing IFC files in Python. For the multi-criteria calculation, model information is then matched manually with component information. Each cost group is mapped to a component group, e.g. outer walls, inner

walls or roof. Subsequently, the standardized calculation process regarding the LCA and LCC is used. This integrates the stated modules from production, end-of-life and the replacements in between.

4 Implementation and Validation

4.1 Case Study

To validate the proposed methodology, a case study is used to compare a conventional workflow with the proposed one. Figure 2 shows the model of the case study. The building consists of two floors, one of which represents a basement. The following component types are represented: load bearing and non-load bearing inner and outer walls as well as windows, inner doors, and one outer door on the ground floor. Windows and doors are essential for the example calculation because the LCC calculation is based on a different reference unit. Walls, floors, ceilings, and roofs are calculated by area, whereas the reference unit of windows and doors is the quantity. The maturity of the model is aimed to be LOD 200, which is neither at the beginning of the process nor does it stretch the definition of early design stages. A list of all building components is derived from the model, including their associated component type, cost group and the area. In this BoQ, the IFC-file provides the reference unit square meters, which is needed for the cost and environmental impact calculation.

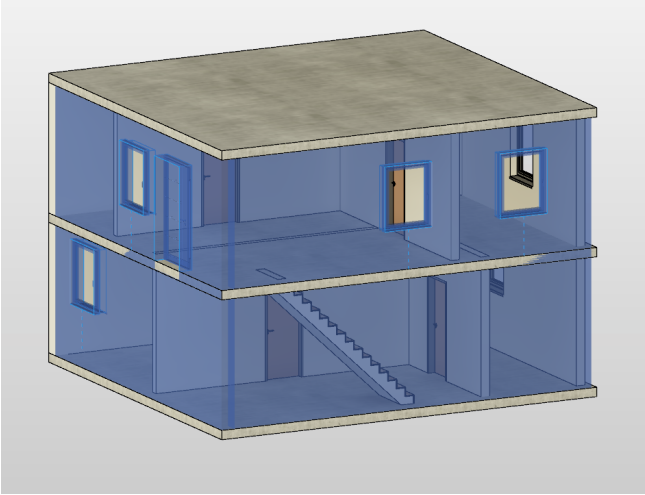

Figure 2: Case study building modelled in AutoDesk Revit.

Other reference units can be used by selecting different output parameters for the BoQ. This possibility is helpful if the LOD of the model changes. For example, thickness or other material information could be included, and therefore the pre-established template would not need to include this information separately. This flexibility ensures a robust methodology.

For each of the component types included in the model, several component variants are established. Components from the cost databases are used as templates, from which several alternatives are created. Different materials are selected as the core layer for different variants. Wooden, concrete and brick walls are chosen. The majority of material datasets is derived from Ökobaudat, with a few

representing KBOB and ecoinvent. Datasets from different sources are not combined to represent a single value, but modules can contain materials from different databases. Therefore, the benefits of several databases can be utilized without compromising their correctness. This enables to choose from a wider variety of datasets.

4.2 LCA and LCC Results

Three variants are established with the described materials and components to be compared to each other in both environmental and cost perspectives. Variant 1 (load-bearing concrete walls, non-load bearing wood and brick walls, all outer walls insulated) represents the thickest walls and overall most volume of materials. Variant 2 (core material bricks) is much lighter, concerning the number of different layers and materials. Variant 3 (concrete walls, no insulation) features similar materials to variant 1 but without insulation.

Additionally to the automated calculation of the proposed methodology, the three variants are calculated manually with an excel sheet to validate the results. The areas for the manual calculation are extracted directly from Revit. The components are established in a spread sheet which is linked to the environmental databases. The costs are added to the spread sheet manually from the cost databases.

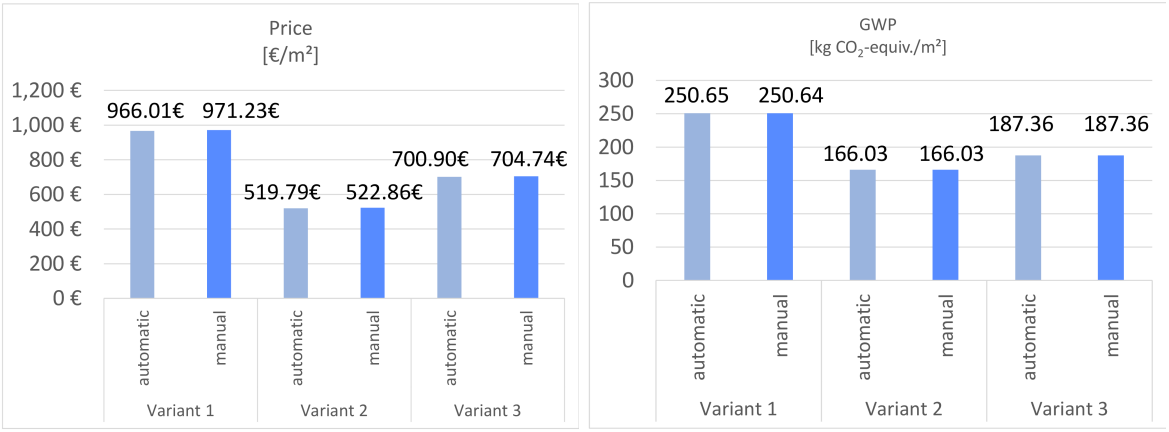

Figure 3: LCC and LCA calculation results per m².

Both automatic and manual calculation results are displayed in Figure 3. Apart from some minor deviations in the costs, which is due to rounding errors of currencies, the results are the same. The results are showing the correctness of the automatic calculation.

Comparing the calculation results to the different components, the outcome is reasonable. Basically, more material results in a higher price and higher GWP. Also, the variants differ similar to each other for all calculated variants. This calculation is comparing the whole building in three variants using different component settings. Nevertheless, the method can be used to compare different components on a building scale.

5 Discussion and Outlook

For early design stage building models, a method of using an enriched database to automatically calculate LCA and LCC without enriching IFC-files is proposed and verified. One requirement for the established method is to manually design a component catalogue. Once established, it is viable to be used in many projects. This compensates the work done manually once. Another requirement is that the component matching was done manually, because it is out of scope for this paper. The needed information could be included in the model, by providing model requirements beforehand.

Some challenges still remain about the implementation of the combined sustainability database, such as the high inconsistency of the input databases. Compensating these inconsistencies requires a high amount of manual work. If some values, e. g. for a specific concrete, are completely missing, the data-set cannot be used for a holistic calculation. Also in the second part some problems have occurred. Even though IFC is defined through a standard, exports from different modeling software products can vary strongly. This can be tackled by defining a robust quantity take-off algorithm, which adapts to the exporting software. Nevertheless, appropriate model requirements should always be defined beforehand.

As a conclusion, a multi-criteria variant comparison using the open BIM methodology is possible. However, further steps have to be taken for being applied in the decision process. First of all, to make a useful decision, it is not sufficient to only assess the construction and demolishing phases of buildings. Energy and costs during the operation phase have to be assessed as well and should be included in future research. Secondly, the shown case study aimed at a very rudimentary comparison. For real projects, the complexity of models and components will be notably higher, incorporating also a broader variety of component types. Nevertheless, the proposed methodology proved to be applicable. By extending this approach in the future accordingly, the goal of automated and holistic LCA and LCC analysis can be realized.

References

[1] United Nations Environment Programme, “Global Status Report of Buildings and Construction: Towards a Zero-emission, Efficient and Resilient Buildings and Construction Sector”, 2020.

[2] R. Sacks, C. Eastman, G. Lee, and P. Teicholz, *BIM Handbook: A Guide to Building Information Modeling for Owners, Designers, Engineers, Contractors, and Facility Managers*, 3rd ed. John Wiley & Sons, Ltd, 2018, ISBN: 9781119287568. DOI: 10.1002/9781119287568.

[3] P. Schneider-Marin and J. Abualdenien, “A framework to facilitate an interdisciplinary design process using BIM”, Sep. 2019.

[4] BIMForum, “Level of Development (LoD) specification Part I & Commentary”, Tech. Rep., Dec. 2020.

[5] T. Liebich, C.-S. Schweer, and C. Dubler, *Auswirkungen der Planungsmethode Building Information Modelling (BIM) auf die Leistungsbilder und Vergütungsstrukturen für Architekten*

Architekten und Ingenieure sowie auf die Vertragsgestaltung. Research Initiative ZukunftBAU, Federal Institute for Research on Building, Urban Affairs and Spatial Development, 2011.

[6] DIN EN ISO 14040, “Umweltmanagement – Ökobilanz – Grundsätze und Rahmenbedingungen”, standard specification, Feb. 2021.

[7] C. LLatas, B. Soust-Verdaguer, A. Hollberg, E. Palumbo, and R. Quiñones, “Bim-based lcsa application in early design stages using ifc”, *Automation in Construction*, vol. 138, p. 104 259, 2022, ISSN: 0926-5805. DOI: https://doi.org/10.1016/j.autcon.2022.104259.

[8] BMI. “Ökobaudat”. (2021).

[9] KBOB. “Ökobilanzdaten im Baubereich 2009/1:2016”. (2016).

[10] ecoinvent Association. “Ecoinvet.org”. (Oct. 2021).

[11] DBD, “Dynamische BauDaten”, 2021. [Online]. Available: https://www.dbd.de/ (visited on 07/13/2021).

[12] BKI, “BKI Kostenplaner”, 2021. [Online]. Available: https://www.bki.de/ (visited on 07/13/2021).

[13] DIN 276, “Kosten im bauwesen”, standard specification, 2018.

[14] K. Forth, J. Abualdenien, A. Borrmann, S. Fellermann, and C. Schunicht, “Design optimization approach comparing multicriterial variants using BIM in early design stages”, Nov. 2021.

[15] R. Santos, A. Aguiar Costa, J. Silvestre, and L. Pyl, “Integration of LCA and LCC analysis within a BIM-based environment”, *Automation in Construction*, vol. 103, pp. 127–149, Jun. 2019. DOI: 10.1016/j.autcon.2019.02.011.

[16] K. Lu, X. Jiang, J. Yu, V. W. Tam, and M. Skitmore, “Integration of life cycle assessment and life cycle cost using building information modeling: A critical review”, *Journal of Cleaner Production*, vol. 285, p. 125 438, 2021, ISSN: 0959-6526. DOI: 10.1016/j.jclepro.2020.125438.

Geometrische Transformation von IFC-Raumbegrenzungsflächen für die normkonforme thermische Gebäudesimulation

Alex Junck[1], Veronika Richter[1], Eric Fichter[1], Jérôme Frisch[1] and Christoph van Treeck[1]
[1]Lehrstuhl für Energieeffizientes Bauen (E3D), RWTH Aachen University, Mathieustr. 30, 52074 Aachen, Deutschland
E-mail(s): alex.junck@rwth-aachen.de, richter@e3d.rwth-aachen.de, fichter@e3d.rwth-aachen.de

Abstract: Im Rahmen der fortschreitenden Digitalisierung des Baugewerbes setzt sich Building Information Modeling (BIM) zunehmend durch und ermöglicht die vereinfachte Integration der thermischen Gebäudesimulation in den Planungsprozess. Im herstellerunabhängigen openBIM-Planungsprozess liegen die Daten zur Gebäudegeometrie dabei im offenen Austauschformat IFC vor. Die darin beschriebenen und für die Simulation benötigten thermischen Raumbegrenzungsflächen sind entgegen verschiedener normativer Vorgaben auf den Bauteiloberflächen positioniert. Die in diesem Paper vorgestellte Methode transformiert die Raumbegrenzungsflächen aus einer IFC-Datei so, dass anschließend eine regelwerkskonforme BIM-basierte thermischen Gebäudesimulation durchgeführt werden kann. Die Methode wurde prototypisch implementiert und getestet.

Keywords: OpenBIM, IFC, Geometrische Transformation, Thermische Gebäudesimulation, Normen

1 Einleitung

Um die Interoperabilität im openBIM-Planungsprozess sicherzustellen, werden Bauteile und Anlagen der unterschiedlichen Gewerke semantisch und geometrisch im offenen Datenaustauschformat IFC (Industry Foundation Classes) abgebildet. Die Geometrien der Instanzen der IFC-Klasse *IfcRelSpaceBoundary2ndLevel* (kurz. SB, dt. Raumbegrenzungsfläche) modellieren die Wärmeübertragungsflächen zwischen den thermischen Zonen und werden demnach auf der Bauteiloberfläche positioniert [1], [2]. Die SBs sind als Beziehungsobjekte definiert, welche das Verhältnis zwischen einem IfcSpace (Attribut *RelatingSpace*, dt. „Raumeinheit“) und einem Bauteil (Attribut *RelatedBuildingElement*) beschreiben. Im Umkehrschluss ist ein IfcSpace durch die SBs der angrenzenden Bauteile vollständig umschlossen, wobei jede SB nur einem IfcSpace zugehörig sein kann. Die Normalvektoren der SBs zeigen definitionsgemäß aus dem IfcSpace heraus [3].

Objekte der Klasse *IfcRelSpaceBoundary2ndLevel* können in zwei Typen 2a und 2b unterteilt werden. Diese unterscheiden, ob ein IfcSpace (2a) oder ein weiteres Bauteil (2b) jenseits des von der SB referenzierten Bauteils liegt. Schemakonforme SBs sind Polygone, weshalb die SBs gekrümmter Bauteile oft segmentiert werden. Alle relevante Attribute der *IfcRelSpaceBoundary2ndLevel*-Klasse werden in Tabelle 1 aufgegriffen.

Tabelle 1: Auswahl der Attribute von *IfcRelSpaceBoundary2ndLevel* und deren Beschreibung

Attribut	**Beschreibung**
Description	Angabe zu Typ 2a oder 2b
RelatingSpace	Angrenzende Raumeinheit (thermische Zone)
RelatedBuildingElement	Referenziertes Bauteil, auf dem die SB liegt
PhysicalOrVirtualBoundary	*PHYSICAL*, falls physisches Bauteil referenziert, sonst *VIRTUAL*
InternalOrExternalBoundary	*INTERNAL*, falls Referenzbauteil kein Fassadenobjekt, sonst *EXTERNAL*
ParentBoundary	SBs von Fenster und Türen referenzieren die zugehörige SB der Wand
CorrespondingBoundary	Gegenüberliegende SB (2a), die die wärmeübertragende Gegenseite bildet

Zur thermischen Bemessung von Gebäuden kann zwischen quasi-stationären und dynamischen (Simulation) Rechenverfahren unterschieden werden. Beide Verfahren sind durch Normen und Richtlinien geregelt (Tabelle 2, Abbildung 1a-1d) [4]–[8]. Dynamische Rechenverfahren betrachten die Randbedingungen, wie bspw. Wetterdaten (Außentemperatur, Solarstrahlung), im Gegensatz zu stationären Methoden nicht als konstant und erreichen eine höhere zeitliche Auflösung der Berechnungsgrößen. SBs nach normativer Vorgabe befinden sich, im Gegensatz zur Definition in IFC, zumeist in der Bauteilmitte oder auf der Außenkante der Fassadenbauteile. Diese Diskrepanz hat zur Folge, dass die berechneten Raumhüllflächen und -volumina verschieden sind, bei der Simulation abweichende Ergebnisse entstehen und somit kein normkonformer Nachweis besteht.

Tabelle 2: Positionierung der SBs je nach Regelwerk

Regelwerk	**Positionierung der SB**
DIN EN 12831-1	Allg. Innenwände und -decken: *Bauteilmitte*
DIN V 18599-1	Bauteile mit Transmissionswärmeverlusten (Außenwand, Innenwand zu Raum mit $\theta \leq 15$ °C): *Außenmaße in horizontaler Richtung, Oberkante bis Oberkante in vertikaler Richtung*
VDI 6020	Adiabates Bauteil: *Bauteiloberfläche*. Nicht adiabates Bauteil: *Bauteilmitte* in horizontaler Richtung, *Oberkante bis Oberkante* in vertikaler Richtung
VDI 2078	Innenbauteile: *Bauteiloberfläche*, Außenbauteile: *Bruttoaußenmaße*
ASHRAE 140-2020	Innenbauteile: *Bauteilmitte* in horizontaler Richtung, *Oberkante bis Oberkante* in vertikaler Richtung, Außenbauteile: *Bauteilinnenseite*

Zur Lösung dieser Problemstellung soll die Umsetzung eines allgemeingültigen geometrischen Transformationsverfahrens erörtert werden. Unter Angabe eines Regelwerks werden die SBs einer IFC4-Datei automatisch angepasst. Dieses Vorgehen trägt zur Vereinfachung des openBIM-Workflows bei.

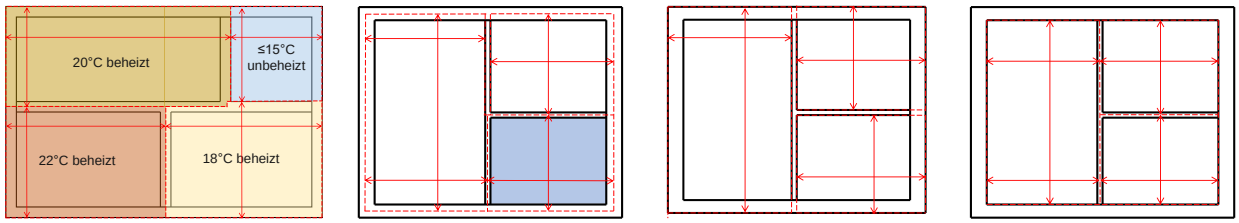

(a) DIN EN 12831-1/ DIN V 18599-1 (b) VDI 6020 (c) VDI 2078 (d) ASHRAE 140-2020

Abbildung 1: Positionierung der Raumbegrenzungsflächen in den unterschiedlichen Normen

2 Stand der Technik und der Forschung

Für die vorhandene Problematik bestehen bereits Algorithmen, welche eine geometrische Transformation der SBs nach unterschiedlichen nationalen Regelwerken vornehmen. Das Verfahren nach Ladenhauf sieht die Positionierung der SBs (IFC2x3) nach österreichischer Norm vor [9], [10]. Hierbei werden für jeden IfcSpace zunächst die jeweiligen SBs ermittelt. Anschließend werden die gegenseitigen Beziehungen der IfcSpaces untersucht, indem nach korrespondierenden SBs gesucht wird. Ladenhauf betrachtet dabei das Attribut *CorrespondingBoundary* nicht, da dies erst mit IFC4 eingeführt wurde. Bedingung für die Flächenpaarbildung ist, dass beide SBs dasselbe *RelatedBuildingElement* sowie einen unterschiedlichen *RelatingSpace* besitzen und dass beide Flächen kongruent sind. Ein solches Flächenpaar bildet nach Verschiebung auf ihren mittleren Abstand eine *INTERNAL* SB, welche beiden IfcSpaces angehört. Bei den übrigen SBs handelt es sich um *EXTERNAL* SBs. Zur Schließung entstandener Lücken werden die SBs mit ihren benachbarten SBs verschnitten.

Im Projekt BIMxBEM wird die Schweizer Norm SIA 380:2015 angewandt [11]. Diese sieht dieselbe Positionierung wie das österreichische Regelwerk vor. Das Vorgehen zur Transformation unterscheidet sich insbesondere bei der Identifikation der erforderlichen Verschiebung der SBs. Zunächst wird die Bauteildicke aus der IFC-Datei berechnet und anschließend mit einem Faktor multipliziert, der aus den Attributen *InternalOrExternalBoundary* und *RelatedBuildingElement* abgeleitet wird. Dies entspricht dann der erforderlichen Translationslänge entlang der Flächennormalen. Zum Schließen der Lücken wird die nächste Kante einer SB gesucht und die Fläche bis in deren Ebene erweitert. Anschließend kann das geometrische Modell in das Simulationsprogramm Lesosai [12] importiert werden, um dort Gebäudezertifizierungen auszustellen, bzw. Öko- und Energiebilanzen anzufertigen.

Die Software IDA ICE [13] erlaubt es IFC2x3-Dateien ohne transformierte SBs zu importieren, da vorrangig *IfcSpace*- und Bauteil-Instanzen verwendet werden [14]. IDA ICE interpretiert diese und passt die entsprechenden Raumumhüllungsflächen normgerecht an. Somit ist keine vorangehende Transformation der SBs erforderlich und IDA ICE führt sofort Normnachweise für die Gebäudezertifizierung oder eine dynamische Gebäudesimulation durch.

3 Methodik des Algorithmus

Im Beispiel in Abbildung 2 werden die vorzunehmenden Schritte am Beispiel der VDI 6020 dargestellt. Da die Räume R1 und R2 unterschiedlich temperiert sind, gilt die trennende Wand als nicht adiabat. Dementsprechend müssen die SBs in die Mitte des Bauteils verschoben werden.

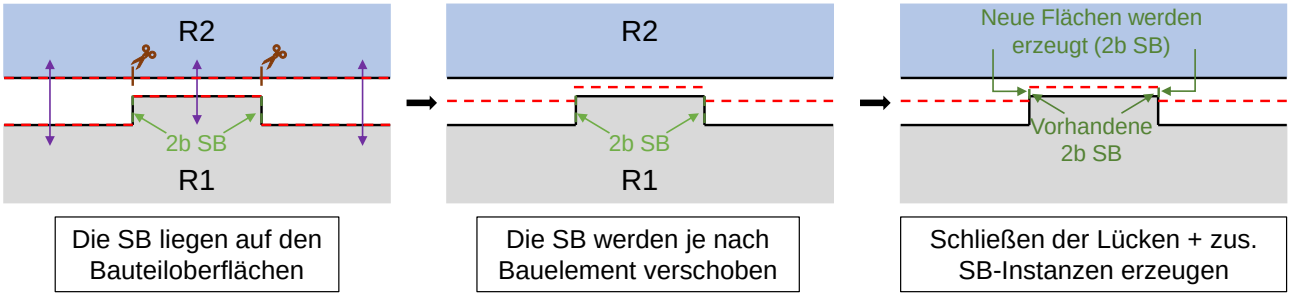

Abbildung 2: Programablauf anhand eines Beispiels

Um die Transformation eindeutig zu beschreiben, werden folgende Annahmen für den entwickelten Algorithmus getroffen:

- 2b SBs (weiteres Bauteil jenseits des ref. Bauteils) werden nicht vor dem Verschieben aufgeteilt und werden immer verschoben, wenn mindestens eine der benachbarten komplanaren SBs auch verschoben wird. Ihre Verschiebung entspricht der maximalen Verschiebung ihrer Nachbar-SBs.
- Wenn zwei aneinandergrenzende SBs derselben Bauteiloberfläche (also komplanar und in gleicher Ebene) unterschiedlich verschoben werden, entsteht eine neue Fläche senkrecht zu den Ursprungsflächen, welche diese verbindet.
- Wenn neue Flächen erzeugt werden, handelt es sich dabei um 2b SBs, auch wenn diese dann in manchen Fällen augenscheinlich eine *CorrespondingBoundary* haben (vgl. Abbildung 2).

Durch den soeben abgesteckten Programmablauf, die getroffenen Annahmen und die Tatsache, dass die SBs planar sind, bietet es sich an, die SB-Instanzen in Ebenen zu definieren, welche dann in ihre endgültige Lage transformiert werden. Anschließend können diese mit ihren zuvor ermittelten Nachbar-SB verschnitten werden, um so die neuen SB-Flächen zu bestimmen. In manchen Fällen entstehen neue SB-Instanzen.

3.1 Erfassung der Randbedingungen

Um die normkonforme Transformation durchführen zu können, müssen in erster Linie die Gegebenheiten an den SBs ermittelt werden. Dazu gehören bspw. die Bauteildicke und die thermischen Randbedingungen (d.h. Raumtemperaturen) der angrenzenden Zonen. Erstere kann für alle 2a SBs (IfcSpace jenseits des ref. Bauteils) entweder anhand der IFC-Datei über das *RelatedBuildingElement* ermittelt werden oder anhand des Abstandes zwischen den *CorrespondingBoundaries*. Um die thermischen Randbedingungen zu erhalten, müssen die Temperaturen der *RelatingSpaces* von den *CorrespondingBoundaries* verglichen werden, welche direkt aus der IFC-Datei extrahiert werden können. In manchen Fällen bietet es sich auch an, das Attribut *InternalOrExternalBoundary* zu betrach-

ten. Zusammen mit dem Bauteiltyp und dessen Orientierung (Normalvektor) kann die erforderliche Verschiebung der SB bestimmt werden.
Da die Transformation anhand der Verschneidung der SB in ihrer neuen Lage erfolgt, muss für jede SB die Abfolge der Nachbar-SBs entgegen dem Uhrzeigersinn ermittelt werden. Dabei gilt eine SB als Nachbar-SB einer Ausgangs-SB, wenn diese sich mindestens einen Abschnitt einer Kante teilen und den gleichen *RelatingSpace* besitzen. Dazu bieten sich zwei unterschiedliche Verfahren an. Die »Punkt-Methode« kann angewandt werden, wenn sich Kanten unterschiedlicher SBs auf deren ganzen Länge überlagern. Dazu müssen zwei aufeinanderfolgende Eckpunkte der potenziellen Nachbar-SB in umgekehrte Ordnung mit denen der Ausgangs-SB identisch sein. Falls dieses Verfahren für eine Kante der Ausgangs-SB keine Nachbar-SB identifizieren kann, wird die »Puzzle-Methode« angewandt. Dabei handelt es sich um ein iteratives Verfahren, welches bis zu einem Grenzwert nach weiteren Nachbar-SBs entlang der gefragten Kante sucht. Bedingung ist, dass die Kanten der Ausgangs- und Nachbar-SB sich berühren und deren Vektoren parallel (für erste Nachbar-SB entlang dieser Kante zusätzlich entgegengerichtet). Wie in Abbildung 3 erkennbar, gilt die gemeinsame Kantenlänge als Vergleichswert, welche nicht größer als die Kantenlänge der Ausgangs-SB werden darf.

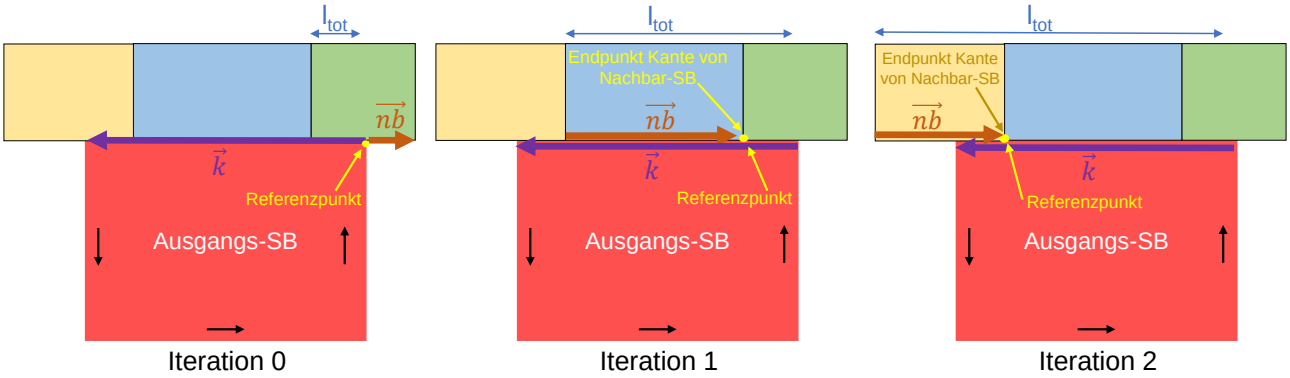

Abbildung 3: Anwendung der »Puzzle-Methode«

Die Verschiebung der 2a SBs (IfcSpace jenseits des ref. Bauteils) kann anhand der zuvor ermittelten Bauteildicke in Multiplikation mit einem Faktor, der sich aus dem angewandten Regelwerk und der Bauteilbedingungen ergibt, bestimmt werden. Die Verschiebung der 2b SBs (weiteres Bauteil jenseits des ref. Bauteils) entspricht der maximalen Verschiebung ihrer Nachbar-SBs. Da die Verschiebung der 2b SBs sich ggf. gegenseitig bedingen, muss dieses Verfahren zweimal durchgeführt werden.

3.2 Transformationsfunktion

Darüber hinaus muss für jede Nachbar-SB die Orientierung und dessen Verschiebung im Verhältnis zur Ausgangs-SB betrachtet werden, damit im Anschluss die SBs richtig untereinander verschnitten werden können. Dabei wird unterschieden, ob die SBs nicht komplanar sind (Fall 0), komplanar sind und gleich verschoben werden (Fall 1) oder komplanar sind und unterschiedlich verschoben werden (Fall 2). Je nach Fall können dann die endgültigen Verschneidungsebenen für jede SB ermittelt werden. Für Fall 0 wird die verschobene Ebene der Nachbar-SB herangezogen, wohingegen für die Fälle 1 und 2 eine neue Ebene zum Verschneiden erstellt wird, welche senkrecht zur Ausgangs-SB ist und in

der jeweiligen Kante liegt. Bei Fall 2 entsteht dabei eine ergänzende SB-Instanz, welche zwischen den unterschiedlich verschobenen, komplanaren Nachbar-SBs aufgespannt wird (vgl. Abbildung 4). Zusätzlich werden zwischen allen nebeneinanderliegenden, komplanaren Verschneidungsebenen (anhand von Nachbar-SB mit der »Puzzle-Methode« ermittelt) eingefügt, damit die Entstehung von neuen Kanten aufgrund von ergänzenden SB-Instanzen berücksichtigt werden kann. Bevor die zusätzlichen SB-Flächen endgültig bestimmt werden können, muss für jede SB geprüft werden, ob nebeneinanderliegende Verschneidungsebenen nicht komplanar sind: Ist dies der Fall, muss eine dieser Verschneidungsebenen gelöscht werden, damit die Schnittpunkte immer eindeutig ermittelt werden können.
Anschließend können die Eckpunkte der neuen SB-Flächen ermittelt werden. Für alle Eckpunkte wird die Schnittmenge der verschobenen SB-Ebene und zwei nebeneinanderliegenden Verschneidungsebenen berechnet. Am Ende liegen somit alle Eckpunkte für jede transformierte SB vor, welche somit zur Erstellung der SB-Flächen benutzt werden können (vgl. Abbildung 5). Alle Eckpunkte, welche in Verbindung mit einer Verschneidungsebene, mit Ursprung in einer Nachbar-SB aus Fall 2, erzeugt wurden, können außerdem zur Erstellung der ergänzenden SB-Instanzen benutzt werden. Diese Punkte treten in der Regel paarweise auf und können mit zusätzlichen Attributen wie bspw. dem *RelatingSpace*, Normalvektor der Verschneidungsebene und der Lage der Verschneidungsebene assoziiert werden. Anschließend können diese Punktpaare zur Erstellung der neuen SB-Instanzen kombiniert werden. Bedingung hierzu sind unter anderem, dass die Normalvektoren parallel sind, die Ebenen ineinander liegen (Abstand gleich null) und die Punktpaare den gleichen IfcSpace referenzieren.

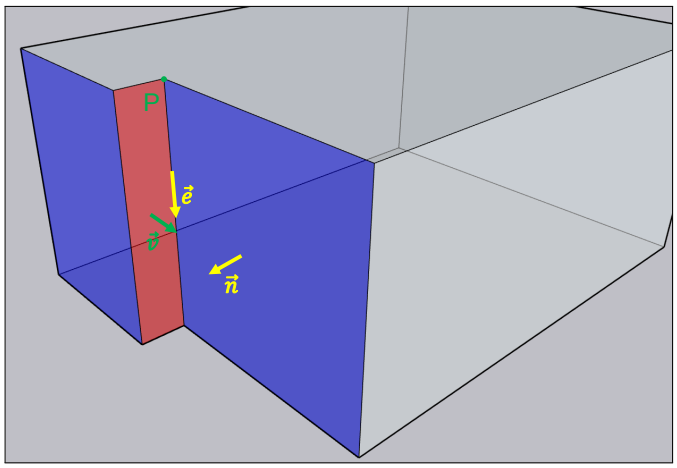

Abbildung 4: Erstellung der Verschneidungsebenen im Fall 1 und 2

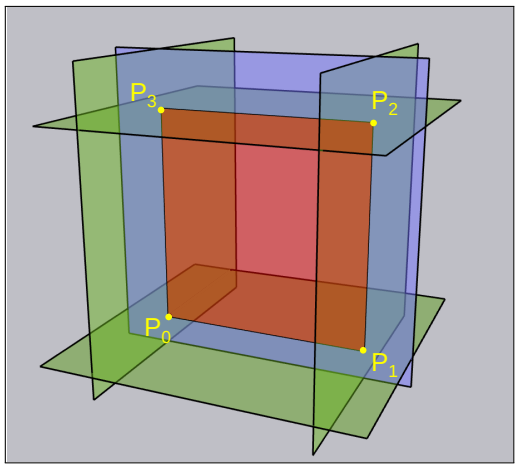

Abbildung 5: Erstellung der neuen SB-Flächen mittels Ebenenverschneidung

4 Anwendung

Die prototypische Implementierung der Methode erfolgte in der Programmiersprache Python. Die Bibliothek `IfcOpenShell` [15] wurde für die Interpretation und Manipulation der IFC-Dateien, insbesondere der *IfcRelSpaceBoundary2ndLevel*-Instanzen verwendet. Als geometrischer Rechenkern kam `pythonOCC` (`OpenCascade`) [16] zum Einsatz. Während des Entwicklungsprozesses wurde die

IFC4-Datei des zweigeschössigen Einfamilienhauses »FZK-Haus« (IAI, Karlsruher Institut für Technologie) verwendet, welche zuvor mit *IfcRelSpaceBoundary2ndLevel*-Instanzen nach Fichter, Richter, Frisch u. a. [17] angereichert wurde. Dementsprechend liegen die Attribute *ParentBoundary* und *CorrespondingBoundary* vollständig vor. Die Implementierung wurde anhand der in Tabelle 2 aufgeführten Regelwerke für das FZK-Haus umgesetzt. Die resultierenden, transformierten SBs sind in Abbildung 6a-6f dargestellt. Ein Vergleich der Flächeninhalte ergibt, dass die Gesamtfläche der SBs um 9 bis 15% größer ist. Die genauen Werte sind in Tabelle 3 aufgeführt.

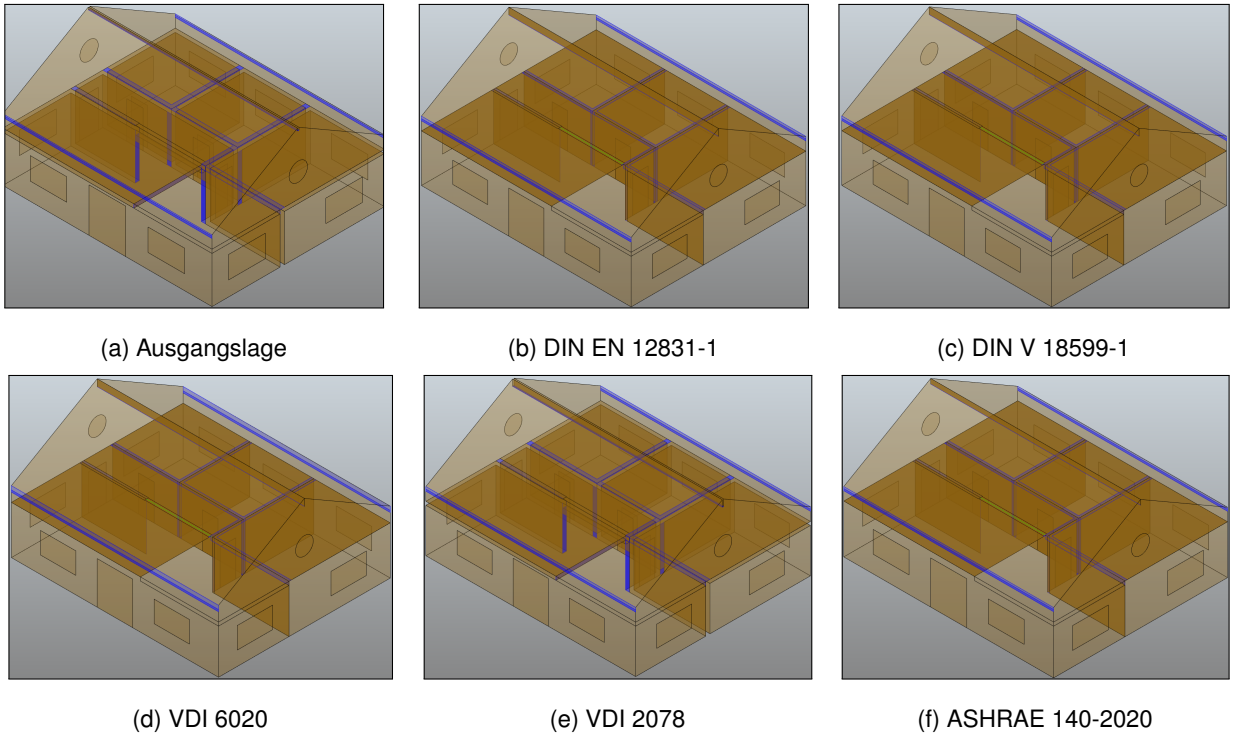

(a) Ausgangslage (b) DIN EN 12831-1 (c) DIN V 18599-1

(d) VDI 6020 (e) VDI 2078 (f) ASHRAE 140-2020

Abbildung 6: Regelwerkskonforme Transformation der SBs bei Anwendung der präsentierten Methodik

Tabelle 3: Vergleich der Flächeninhalte der SBs je nach Regelwerk

SB-Typ	Ausgangslage	DIN 12831-1/DIN V 18599-1	VDI 6020/VDI 2078	ASHRAE 140-2020
INTERNAL	316.17 m^2	15.2 %	10.6 %	9.7 %
EXTERNAL	408.53 m^2	14.0 %	10.1 %	8.9 %

Zur Überprüfung der transformierten und neu erstellten SB-Instanzen kann in erster Linie eine visuelle Prüfung der SBs anhand deren geometrischen Darstellung in 3D erfolgen. Beispielsweise müssen die SBs, die im Inneren eines Bauwerkes liegen, nach der DIN EN 12831-1 aufeinander liegen (in Bauteilmitte, bzw. Innen-/Außenkante, falls ein Raum nicht beheizt). Darüber hinaus ist es auch möglich visuell grob zu beurteilen, ob die SBs für alle IfcSpaces eine geschlossene Hülle bilden. Zusätzlich sind noch weitere Kriterien formuliert, die nicht direkt visuell überprüft werden können, wie bspw. die korrekte Orientierung der Normalvektoren. Für eine detaillierte Dichtheitsprüfung der IfcSpaces können die Funktionen von `pythonOCC` genutzt werden. Zur Prüfung der Dichtheit können die SBs eines IfcSpaces miteinander vernäht werden, um anschließend das zusammenhängende

Objekt auf eine geschlossene Hülle zu testen. Auch die Orientierung der Normalen ist in `pythonOCC` zu überprüfen. Für beide Problemstellungen kann ein entsprechendes Validierungstool [18] eingesetzt werden, welches soeben aufgeführte Kriterien und Prinzipien aufgreift. Während die Transformation der bereits vorhandenen SB-Instanzen zuverlässig durchgeführt wird, muss insbesondere die Erstellung der zusätzlichen SB-Instanzen überarbeitet werden: Die Orientierung deren Normalvektoren ist teilweise fehlerhaft, da diese mit den bislang definierten Kriterien von der Reihenfolge der Kombination der Punktpaare abhängig ist.

5 Zusammenfassung

IFC-SBs müssen für die normkonforme Simulation geometrisch transformiert werden. Das erarbeitete Verfahren ergänzt und verbessert hierfür bestehende Methoden. Jedoch stellt es höhere Anforderungen in Bezug auf die Input-Datei, die aktuell nicht flächendeckend erfüllt werden und es dementsprechend ggf. einer zusätzlichen Anreicherung mit *IfcRelSpaceBoundary2ndLevel*-Instanzen bedarf. Das entwickelte Tool ermöglicht es vorhandene SB-Instanzen zuverlässig zu transformieren. Des Weiteren werden Lücken mit ergänzenden SB-Instanzen geschlossen, wobei das Verfahren anhand weiterer Beispiel-Dateien verfeinert werden kann. Infolgedessen können transformierte IFC-Gebäudemodelle in entsprechende Simulationssoftware importiert werden. Zukünftig wird die SB-Klasse weiter ausgebaut, sodass deren Instanzen vielfältiger eingesetzt werden und und für neue Use Cases herangezogen werden können.

Literatur

[1] M. Weise, T. Liebich, R. See, V. Bazjanac, T. Laine und B. Welle, *Implementation Guide: Space Boundaries for Energy Analysis*, http://www.blis-project.org/IAI-MVD/documents/Space_Boundaries_for_Energy_Analysis_v1.pdf, Stand: 2022-04-07, 2011.

[2] buildingSMART, *IFC4_ADD2_TC1 - 4.0.2.1 [Official]*, https://standards.buildingsmart.org/IFC/RELEASE/IFC4/ADD2_TC1/HTML/, Stand: 2022-04-07, 2020.

[3] K.-H. Häfele und T. Liebich, *IFC Implementation Agreement Space Boundary: Overview on the common agreements for implementing space boundaries*, 2009.

[4] Deutsches Institut für Normung, DIN EN 12831-1, *Energetische Bewertung von Gebäuden - Verfahren zur Berechnung der Norm-Heizlast - Teil 1: Raumheizlast, Modul M3-3; Deutsche Fassung EN 12831-1:2017*, Berlin, 2017.

[5] Deutsches Institut für Normung, DIN V 18599-1, *Energetische Bewertung von Gebäuden - Berechnung des Nutz-, End- und Primärenergiebedarfs für Heizung, Kühlung, Lüftung, Trinkwarmwasser und Beleuchtung - Teil 1: Allgemeine Bilanzierungsverfahren, Begriffe, Zonierung und Bewertung der Energieträger*, Berlin, 2018.

[6] Verein Deutscher Ingenieure, VDI 2078, *Berechnung der thermischen Lasten und Raumtemperaturen (Auslegung Kühllast und Jahressimulation)*, Düsseldorf, 2015.

[7] Verein Deutscher Ingenieure, VDI 6020, *Anforderungen an thermisch-energetische Rechenverfahren zur Gebäude- und Anlagensimulation*, Düsseldorf, 2016.

[8] American Society of Heating, Refrigerating and Air-Conditioning Engineers und American National Standards Institute, *Method of test for evaluating building performance simulation software*, Washington, D.C., 2021.

[9] D. Ladenhauf, R. Berndt, U. Krispel u. a., »Geometry Simplification According to Semantic Constraints«, *Comput. Sci.*, Jg. 31, Nr. 3, S. 119–125, Aug. 2016. Adresse: https://doi.org/10.1007/s00450-014-0283-7.

[10] D. Ladenhauf, K. Battisti, R. Berndt u. a., »Computational geometry in the context of building information modeling«, English, *Energy and Buildings*, Jg. 115, S. 78–84, März 2016.

[11] C. Waechter und S. Le Corre, *BIMxBEM: GitHub Repository*, https://github.com/ENAC-CNPA/BIMxBEM/blob/master/freecad/bem/boundaries.py, Stand: 2022-04-07, 2022.

[12] E. S. SA, *Lesosai*, https://lesosai.com/?lang=de, Stand: 2022-04-07, 2022.

[13] E. S. T. Group, *IDA ICE*, https://equa.se/de/ida-ice, Stand: 2022-04-07, 2022.

[14] ——, *BImport of IFC BIM models to IDA Indoor Climate and Energy 4*, http://www.equaonline.com/iceuser/pdf/IFC_Import.pdf, Stand: 2022-04-07, 2022.

[15] IfcOpenShell, *the open source ifc toolkit and geometry engine*, http://ifcopenshell.org/, 2022.

[16] OpenCASCADE Technology, *Collaborative development portal*, https://dev.opencascade.org/, Stand: 2022-04-07, 2022.

[17] E. Fichter, V. Richter, J. Frisch und C. van Treeck, »Automatic generation of second level space boundary geometry from IFC models«, in *Proceedings of Building Simulation 2021: 17th Conference of International Building Performance Simulation Association, Bruges, 1-3 September*, 2021.

[18] V. Richter, A. Malhotra, E. Fichter, A. Hochberger, J. Frisch und C. van Treeck, »Validation of IFC-based Geometric Input for Building Energy Performance Simulation: To be published«, in *Proceedings of 2022 Building Performance Modeling Conference and SimBuild co-organized by ASHRAE and IBPSA-USA: To be published*, IBPSA USA, Hrsg., 2022.

BIM-basierte Ressourceneffizienzberechnung mittels LCA-Integration anhand parametrischer Infrastrukturmodelle

Jonas Maibaum[1] and Marlena Block[1]
[1]Lehrstuhl für Informatik im Bauwesen, Ruhr-Universität Bochum, Universitätsstraße 150, 44803 Bochum, Deutschland
E-mail(s): Jonas.Maibaum@rub.de, marlena.block@rub.de

Abstract: Die Erstellung eines parametrischen Infrastrukturinformationsmodells (IIM), welches es ermöglicht verschiedene Anwendungsfälle im Rahmen der Integration der Ökobilanz in die BIM-Methodik durchzuführen, gilt als Motivationsgrundlage für diesen Beitrag. Dabei werden geometrische Abhängigkeiten, Querschnitts-, Aufbau- und Materialparameter sowie Ressourceneffizienkriterien in einem Infrastrukturmodell implementiert. Veranlasst wird die Methodik durch den signifikanten Rohstoff- und Energieverbrauch im Infrastruktursektor und dem damit verbundenen Ausstoß von umweltschädlichen Gasen, die eine Quantifizierung dieser und ein holistisches Bauwerks-Monitoring erfordern. Die in Anlehnung an nationale Konstruktionsrichtlinien erstellten parametrischen Infrastrukturmodelle werden dabei mit den spezifischen Materialkennwerten aus einer öffentlichen Produktdatenbank für verschiedene Standardaufbauten verknüpft. Im Rahmen der darauf aufbauenden Ökobilanz werden die erfassten Indikatorwerte für verschiedene Infrastrukturmaßnahmen und Aufbauten verglichen. Das übergeordnete Ziel ist es möglichst automatisiert und transparent Lebenszyklusdaten mit einem parametrischen Infrastrukturmodell zu verknüpfen und die Auswirkungen eines Bauprojekts auf die Umwelt über verschiedene Lebenszyklusphasen zu bestimmen. Weiter können durch den Vergleich unterschiedlicher Baumaterialien und -verfahren sowie Planungsvarianten Potenziale zur effizienteren und nachhaltigeren Gestaltung von Baumaßnahmen aufgedeckt werden. Der Ansatz ist insbesondere auf den kommunalen Straßenbaubereich und den dort vorzufindenden baulichen Gegebenheiten ausgerichtet und legt den Fokus dazu auf Parametrik und Adaptierbarkeit.

Keywords: BIM, LCA, parametrisches IIM (Infrastructure Information Model), Ressourceneffizienz

1 Einleitung

Bei der Realisierung eines Bauvorhabens werden große Mengen an Primär- und Sekundärmaterialien benötigt. Zudem sind Herstellung, Transport, Einbau, Wartung, Rückbau und Recycling mit einem

hohen Energieaufwand verbunden. Zusätzlich entstehen bei den einzelnen Prozessen über den gesamten Lebenszyklus betrachtet große Mengen an Gasen und Abfallprodukten, welche die Umwelt in einem erheblichen Maße negativ beeinträchtigen [1]. Aktuell nimmt der Abbau und die Nutzung von Ressourcen und die damit verbundenen negativen Umweltauswirkungen weltweit weiter zu. Gerade im Bausektor würde eine Steigerung der Ressourceneffizienz zu deutlichen Einsparungen beim Ressourcenverbrauch führen [2]. Hierbei nimmt insbesondere die Erhaltung kommunaler Straßen einen wesentlichen Anteil ein, da auf Kommunen mehr als 60% der Gesamtlänge des deutschen Straßennetz entfallen. Um geeignete Maßnahmen zur Steigerung der Ressourceneffizienz anwenden zu können, muss diese adäquat anhand verschiedener Indikatoren wie dem Material- und Energieverbrauch quantifiziert werden [3]. Zur Erfassung und Bewertung der Nachhaltigkeit, der Ressourceneffizienz oder der Umwelteinwirkung gibt es mehrere einheitliche und standardisierte Analysemethoden, wie das Durchführen einer Ökobilanz.

Die Ökobilanz ist ein strukturiertes Verfahren zur Bereitstellung von Informationen über Umweltauswirkungen innerhalb eines festgelegten Untersuchungsrahmens. Die Komplexität der zu verarbeitenden Informationen variiert mit der Anzahl der berücksichtigten Ressourceneffizienz-Indikatoren und der Größe, dem Detaillierungsgrad und Diversität der Informationen innerhalb des betrachteten Objekts. Um mehr Aspekte bewerten zu können, ist eine angemessene digitale Unterstützung erforderlich. Trotz des kontinuierlichen Fortschritts der Digitalisierung und der Anwendung der Methode des Building Information Modeling (BIM) im Straßenbau ist deren Verbreitung derzeit noch begrenzt. Auch die Integration der Ökobilanz in die BIM-Methodik steht bislang noch am Anfang [4].

Es zeichnet sich ab, dass die ganzheitliche Betrachtung von Umweltverträglichkeitsaspekten insbesondere bei Straßenbauprojekten zukünftig weiter an Relevanz gewinnt. Derzeit ist die Verfügbarkeit von BIM-Anwendungen die LCA integrieren noch gering. Ebenso werden Umweltproduktdeklarationen (hier: Environmental Product Declaration, EPD), die für den Infrastruktursektor geeignet sind in geringem Maße zur Verfügung gestellt. Es besteht daher ein hoher Handlungs- und Forschungsbedarf in diesem Bereich. Vor diesem Hintergrund ist eine Methode erstellt worden, die das Ziel verfolgt, für parametrische Infrastrukturmodelle eine modellbasierte Ökobilanz durchzuführen.

Im Abschnitt 2 werden die relevanten Grundlagen im Rahmen der BIM-basierten Ressourceneffizienzbetrachtung erläutert. Darauf aufbauend stellt Abschnitt 3 das Konzept der erstellen Methode vor. Dieses wird im Abschnitt 4 modellhaft angewendet. Abschnitt 5 fasst die Ergebnisse zusammen, stellt die Limitationen dar und gibt einen Ausblick auf mögliche Entwicklungsschritte.

2 Ressourceneffizienz im Kontext von BIM

Neben dem Nutzen der digitalen Bauwerksplanung und einer holistischen Bauwerksbetrachtung wird für den konzipierten Ansatz nachfolgend im Kontext von Umweltprodukdatenbanken der Ablauf der Ökobilanz zusammengefasst und mögliche Integrationsparadigmen der BIM- und LCA-Methoden angeführt (vlg. Abschnitt 2.2).

2.1 Ökobilanz und EPD-Datenbanken

Bei der Ökobilanz (hier: Life Cycle Assessment, LCA) handelt es sich um einen vierstufigen, iterativen Prozess. In einem ersten Schritt wird das Ziel und der Umfang der Ökobilanz festgelegt. Es folgen die Schritte der Sach- (Life Cycle Inventory, LCI) und Wirkungsbilanz (Life Cycle Impact Assessment, LCIA). Eine anschließende Interpretation der LCIA-Daten ist derzeit für den Infrastruktursektor lediglich vermindert möglich. Der Begriff LCI umfasst die Erfassung der gesamten In- und Outputströme, eine Quantifizierung des Bestands, der direkten Umweltauswirkungen, des Abfallaufkommens und des Energie- und Rohstoffverbrauchs. Im Rahmen des auf der LCI aufbauenden LCIA-Schritts werden die erfassten Umweltauswirkungen kategorisiert und charakterisiert [5][6]. Es wird zudem ein standardisierter Aufbau für EPDs vorgeschlagen. Hierbei wird ein einheitliches Datenformat empfohlen, dieses ermöglicht die Darstellung von Ökobilanzergebnissen in Form eines einheitlichen und prüfbaren Dokuments. Auf europäischer Ebene sind die zentralen Produktkategorieregeln für EPDs von Produkten im Bausektor in der EN 15804 beschrieben [7].

EPD-Datensätze können als kleinste Modellierungseinheit in einer LCI angegeben werden [8]. Mehrere dieser Datensätze, die auch als Prozesseinheiten bezeichnet werden, werden in einem Lebenszyklusmodell zusammengefasst. Dabei reicht das Spektrum von Datensätzen, welche lediglich Umweltproduktdaten der Produktionsphase (cradle-to-gate) beinhalten bis zu Datensätzen, welche zusätzlich die Bau- , Unterhaltungs-, Rückbau- und Recyclingphase (cradle-to-cradle) berücksichtigen. Neben einer transparenten Darstellung der verschiedenen In- und Output-Flüsse eines Datensatzes sollte eine Umweltprodukt-Datenbank einen konsistenten Modellierungsansatz, eine einheitliche Namensgebung und eine vollständige Dokumentation der Datensätze bereitstellen [9]. In Abhängigkeit von der jeweiligen Datenbank werden Prozesseinheiten und Modellierungseinheiten entweder einzeln oder aggregiert angeboten. Zu den umfangreichsten Datenbanken zählen EcoPlatform EPD, IBU, INES, das GaBi, OKOBAUDAT, Ecoinvent und das internationale EPD-System [7][10].

2.2 BIM-LCA-Integration

Grundsätzlich werden von Wastiels und Decuypere fünf verschiedene Integrationsmöglichkeiten unterschieden. Dabei werden LCA und BIM unterschiedlich kombiniert. Drei dieser Verfahren sehen eine sequenzielle Bearbeitung vor. Auf Basis bestehender BIM-Software werden Leistungsverzeichnisse (1) oder IFC-Modelle (2) generiert, die dann entweder direkt oder im Falle eines Modells mittels der Nutzung in einem BIM-Viewer (3) und der Ableitung relevanter Größen innerhalb des LCA-Tools als Berechnungsgrundlage herangezogen werden. Zudem kann die LCA mittels eines Plugins in die BIM-Software integriert sein (4) oder innerhalb der BIM-Software werden ausschließlich Objekte benutzt, die bereits LCA-Profile aufweisen (5). Dies erleichtert die anschließende LCA-Berechnung, dieser Ansatz ist sowohl mit (2) als auch mit (4) kombinierbar. [11]

Durch die Integration von BIM und LCA kann ein Bauwerk nachhaltiger geplant werden, indem während der frühen Planungsphasen Umweltbelastungsschwerpunkte ermittelt werden können. Mit Hilfe dieser Ergebnissen ist es schließlich möglich Entwurfsvarianten und Verfahren mit geringer Umweltbelastung zu identifizieren und vorzuziehen. Weiter wird in diesem Kontext die Verwendung

von konzeptionellen BIM-Modellen und visuellen Skripten empfohlen, um eine Vielzahl von designspezifischen Umweltbelastungsschwerpunkte bei der Durchführung von LCAs zu untersuchen [12]. In diesem Rahmen wurde bereits die programmatische Realisierung eines Prozesses zur Ökobilanz für den Indikator Emissionen in einem BIM-Modell mit Autodesk Civil 3D umgesetzt [13].

3 Konzept der BIM-basierten Ressourceneffizienzberechnung

Hinsichtlich der in Abschnitt 2.2 angeführten BIM-LCA-Integrationsmöglichkeiten entspricht der konzipierte Ansatz im Allgemeinen dem Konzept der Plug-in basierten LCA-Durchführung. Weiter wird in Abschnitt 2.2 zudem bereits dargelegt, dass die Integration von BIM und LCA besonders für frühe Planungsphasen vorteilhaft ist, da eine ökologische Entscheidungsfindung bei der Betrachtung der Ressourceneffizienz eines Bauwerks forciert wird. Abbildung 1 veranschaulicht hierzu, welche für die Umsetzung des erstellten Ansatzes notwendigen Prozessschritte der jeweiligen Methodik zugeordnet werden können. Auf Basis des Modells (links) wird die LCA (rechts) durchgeführt. Die generierten Daten werden wiederum mit dem Modell verknüpft. Nach einer Änderung im Modell muss die LCA erneut angestoßen werden und die Modelldaten aktualisiert werden. Die technische Umsetzung erfolgt mittels visueller Programmierung, hierzu wird Dynamo von Autodesk verwendet. Die Methodik folgt dabei einem mehrstufigen Modellierungsprozess (vgl. Abb. 2).

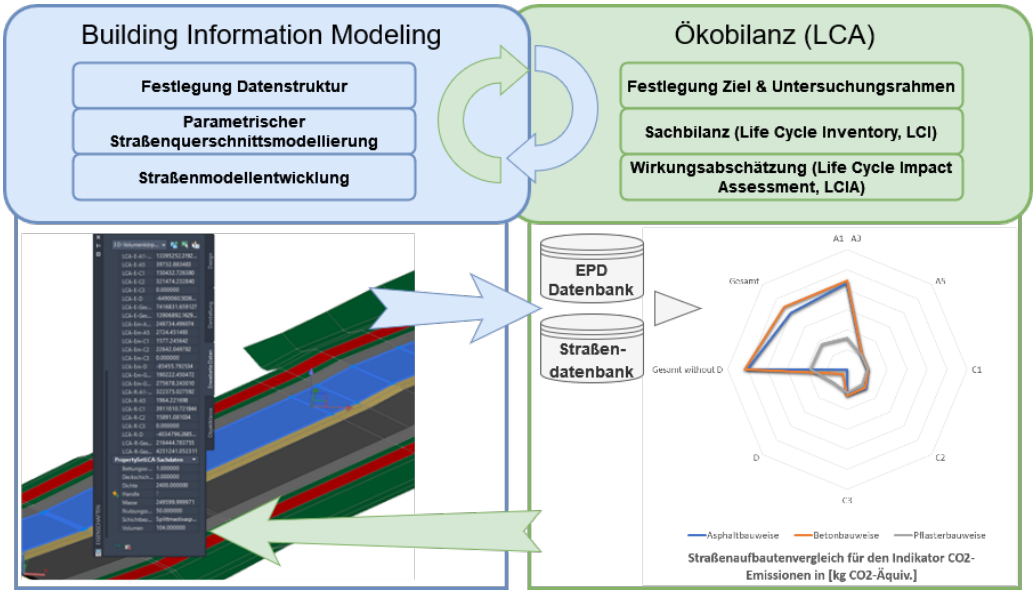

Abbildung 1: Angewandte Verknüpfung des BIM-Modells und LCA-Daten für die erstellte Methodik (Es werden exemplarisch die Lebeszyklusphasen A1-A3 - Herstellung, A5 - Einbau, C1-C3 - End-of-Life und D - Recycling dargestellt)

In einem ersten Schritt ist es notwendig den derzeitigen Status quo der Datenstrukturierung zu quantifizieren und Eingabedaten und benötigte Parameter entsprechend dem Anwendungsfall zu definieren und anzupassen.

Die Querschnittsmodellierung erfolgt graphbasiert und ermöglicht es transparent parametrische Straßenmodelle zu erstellen. Parameter, Abhängigkeiten und Attribute sind so gewählt, dass die Modellierung möglichst variabler und vielfältiger Straßenaufbauten realisierbar ist. Dadurch ist das Anwenden der Methode für Straßen, welche Querschnittsaufweitungen und Fahrbahnsanierungen ausweisen, möglich. Insbesondere wird damit eine Adaptierbarkeit für die Erfordernisse im kommunalen Straßenbau ermöglicht, da häufig davon ausgegangen werden muss, dass unkonventionelle und nicht Richtlinien-konforme Aufbauten vorliegen.

Die Verknüpfung von Modelldaten und EPDs erfolgt über einen Mapping-Algorithmus. Dabei wird in Abhängigkeit des Materials jeder einzelnen Modellschicht ein entsprechender Datensatz aus der verknüpften Umweltproduktdatenbank anhand des Materialnamens oder der Material-ID zugeordnet. Darauf aufbauend werden die aus dem Modell abgeleiteten Mengen, Massen und Volumina mit den EPDs im Rahmen der Sachbilanz und Wirkungsabschätzung verrechnet. Angeknüpft an die Berechnung der Ökobilanzwerte werden die generierten Daten im BIM-Modell integriert, sodass dieses für weitere Modellierungsschritte und Analysen genutzt werden kann. Durch die Rückführung in das Modell wird es zudem möglich den Export in das neutrale IFC-Format (Industry Foundation Classes) auszuführen. Es wird somit ein Modell zur transparenten Darstellung und Übergabe von ressourcenrelevanten Eigenschaften erzeugt. Ein Überblick über die definierten Prozesse, den angewandten Techniken und denen zur Implementierung genutzten Software ist in Abbildung 2 gegeben.

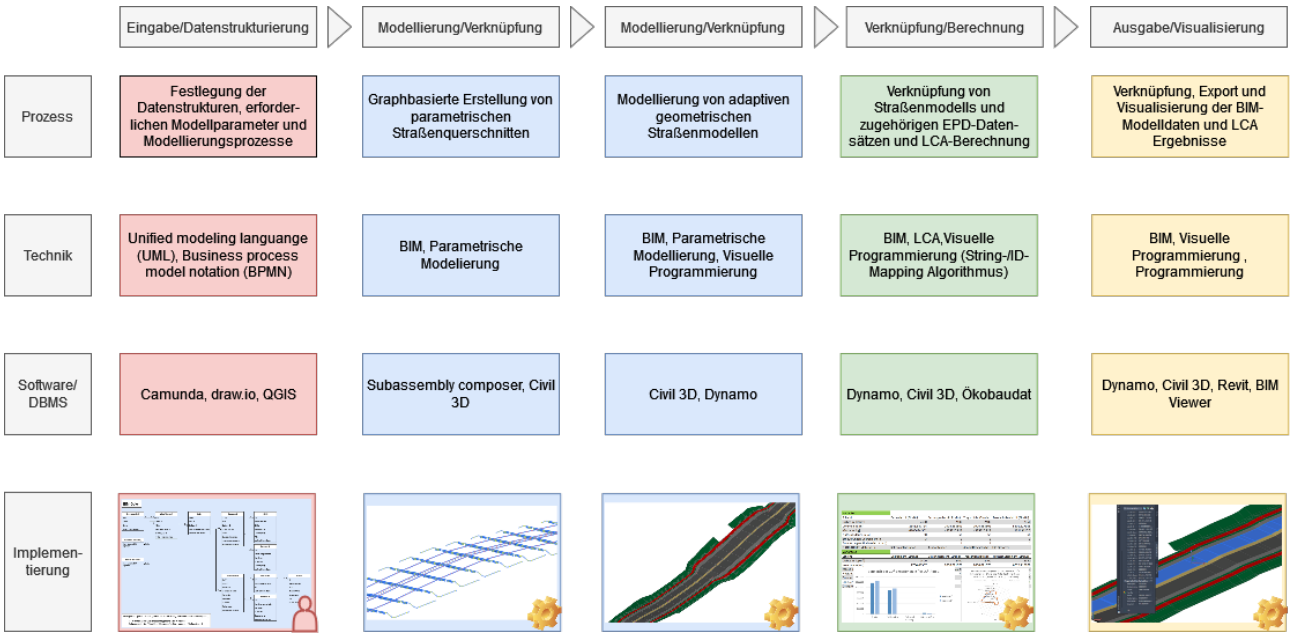

Abbildung 2: Granulare Übersicht der definierten Prozesse, angewandten Techniken, genutzten Software und Implementierungsvisualisierung dieser für die verschiedenen Modellierungsschritte von der Dateneingabe bis zur Modellausgabe

4 Demonstrator

Für die technische Umsetzung sind die in Abbildung 2 angeführten Techniken und Software genutzt worden. Dazu wurde zunächst ein digitales Geländemodell eingeladen. Mittels des in Civil 3D enthaltenden Subassembly-Composer-Plug-in sind darauf basierend die parametrischen Straßenquerschnitte erzeugt und in der Civil 3D Umgebung importiert worden. Unter Anwendung des visuellen Programmierungstools Dynamo, welches ebenfalls bereits in Civil 3D enthalten ist, sind achsbasiert und entsprechend des Längsschnitts die parametrischen Straßenmodelle erstellt worden. Diese konnten über die graphische Benutzeroberfläche weiter spezifiziert werden. Ebenfalls mit einem Dynamo-Skript, wurden die Schritte der Ökobilanz und Modellweitergabe umgesetzt. Dazu wurden verschiedene Dynamo-Funktionen verwendet, welche das Modell auswerten und mit externen Datenquellen verknüpfen. Neben Import und Export-Funktionen beinhaltet Dynamo eine Reihe von vorprogrammierten Blöcken (nodes), die zahlreiche mathematische und geometrische Operationen auf Basis des digitalen Modells erlauben. Die dabei genutzte deutsche Ökobaudat-EPD-Datenbank beinhaltet mit über 1400 frei erhältlichen EPD-Datensätzen bereits eine Reihe von Datensätzen, welche sich mit dem Infrastruktursektor befassen.

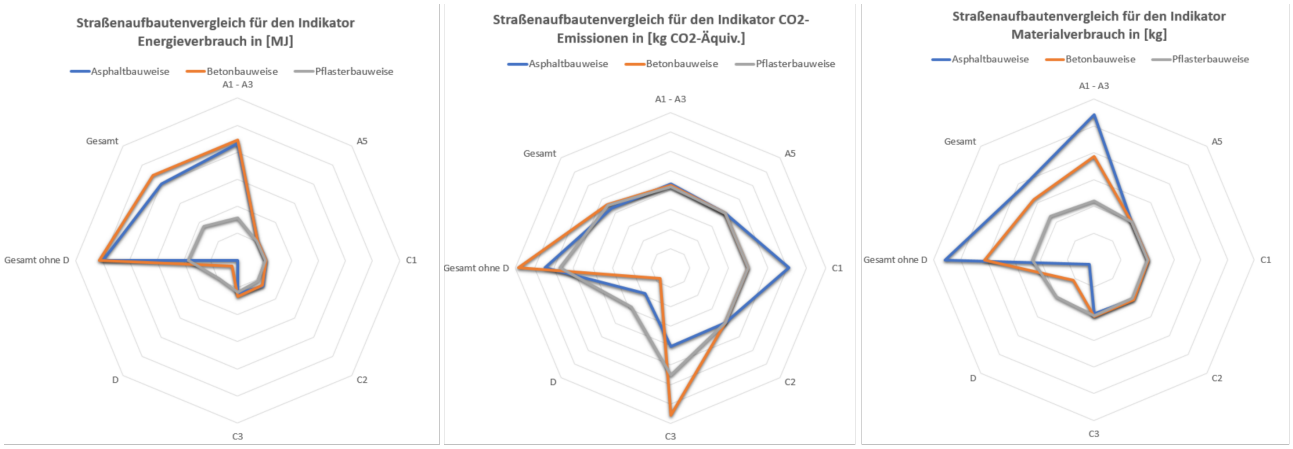

Abbildung 3: LCA Ergebnisgegenüberstellung der drei Ressourceneffizienzindikatoren Materialverbrauch, Treibhausgase und Energieverbrauch anhand eines Deckschichtaufbaus aus Asphalt, Beton und Pflaster (Dabei wurden die Lebeszyklusphasen A1-A3 - Herstellung, A5 - Einbau, C1-C3 - End-of-Life und D - Recycling berücksichtigt)

Das modellierte parametrische und mit Ökobilanzdaten angereicherte Straßenmodell eignet sich insbesondere für den Aufbau- und Trassenvergleich in frühen Planungsphasen. In Abbildung 3 werden gemäß der vorgestellten Methodologie die drei üblichen Straßenaufbauten Asphalt, Beton und Pflaster entsprechend der RStO12 einander gegenübergestellt [14]. Mittels dem modellbasierten Aufbautenvergleich können unterschiedliche Materialien und Aufbauformen transparent miteinander verglichen werden. Durch die Einbeziehung von spezifischen Straßenschicht-Parametern wie unter anderem Lebensdauer, Anzahl Deckschichterneuerungen und Schichtdicke können in frühen Planungsphasen Materialien erfasst werden, welche besonders umweltbelastend sind. Neben dem Vergleich von Straßenaufbauten wurden zusätzlich verschiedene Trassierungsoptionen miteinander verglichen. Dabei

konnten ressourcenintensive Trassierungsvarianten identifiziert werden. Sowohl beim Aufbautenvergleich als auch bei der Gegenüberstellung verschiedener Varianten können modellbasiert Ergebnisse der Ökobilanz visualisiert dokumentiert werden.

5 Zusammenfassung, Limitationen und Ausblick

In diesem Beitrag werden die Besonderheiten des kommunalen Straßenbaus bei der Betrachtung der Ressourceneffizienz berücksichtigt. Daher wurde eine Methode entwickelt, die zum einen eine hohe Anpassungsfähigkeit des parametrischen Straßenquerschnitts ermöglicht und zum anderen Ressourceneffizienzdaten transparent berechnet und mit dem Infrastrukturmodell verknüpft. Durch die Kombination bestehender Tools und offener Datensätze konnten die Vorteile durch eine Anwendung der BIM-Methodik mit der Methodik der Ökobilanz verbunden werden.

Bei der Berechnung der einzelnen LCA-Werte sind die hinterlegten EPD-Datensätze von besonderer Bedeutung. Derzeit sind für den Bereich des Infrastrukturbaus lediglich rudimentäre EPD-Datensätze verfügbar. Diese EPD-Datensätze müssen daher entsprechend eingeordnet werden, da Unsicherheiten und Berechnungseigenheiten vorhanden sind. Dies gilt insbesondere für die End-of-Life-Daten, da nicht nachvollziehbar zu differenzieren ist, welche Informationen bei der Erstellung berücksichtigt wurden. Hier sind die Anbieter gefordert, ihre Datensätze und verwendeten Methoden transparent zu dokumentieren. Dennoch bieten diese Datensätze eine Möglichkeit die Ressourceneffizienz vergleichbar darzustellen, insbesondere wenn unterschiedliche Trassierungsoptionen abgebildet werden sollen. Um auf veränderte Angebote bezüglich der EPD-Daten zu reagieren muss die dargestellte Methode in Richtung einer kontinuierlichen Integration neuer (verbesserter) EPDs weiterentwickelt werden. Dieses kann prozessual erfolgen oder durch die Integration einer Programmierschnittstelle (API) zum Beispiel in Form eines Plugins.

Ausblickend sind nach derzeitiger Einschätzung unterschiedliche Anknüpfungspunkte als Erweiterungen für die konzipierte Methodik denkbar wie die Ausweitung des Ansatzes auf weitere Infrastrukturbereiche. Dies könnte dabei helfen Baumaßnahmen unterschiedlicher Maßnahmenträger oder Fachbereiche (z.B. Straßensanierung nach Belastung, Eingriff durch Telekommunikationsunternehmung, turnusmäßige Erneuerung tiefer liegender Schichten) besser aufeinander abzustimmen und auf diese Weise überflüssige Straßenaufbrüche zu vermeiden. Außerdem ist dadurch ein verbesserte Erfassung des anthropogenen Materiallagers möglich, sodass Stoffströme vollständiger abgebildet werden können. Eine weitere Erweiterungsmöglichkeit stellt das Anwenden des derzeit Objekt-basierten Ansatzes auf der Ebene des Straßennetzes dar. Durch diesen Ansatz können Ressourceneffizienzdaten für zusammenhängende Quartiere (bspw. einer Kommune) bestimmt werden. Unter anderem dieser Ansatz wird auch im Rahmen des mit diesem Beitrag zusammenhängenden RekoTi-Projekts verfolgt (Ressourceneffizienz im kommunalen Tiefbau).

Literatur

[1] J. G. Backes und M. Traverso, »Application of Life Cycle Sustainability Assessment in the Construction Sector: A Systematic Literature Review«, *Processes*, Jg. 9, Nr. 7, S. 1248, 2021.

[2] UNEP, *Global Environment Outlook – GEO-6: Healthy Planet, Healthy People*, Cambridge University Press, Hrsg., Cambridge, UK, 2019.

[3] M. Hirschnitz-Garbers, F. Montevecchi und A. Martinuzzi, »Resource Efficiency«, in *Encyclopedia of corporate social responsibility*, Springer, 2013, S. 2018.

[4] T. Dalla Mora, E. Bolzonello, C. Cavalliere und F. Peron, »Key Parameters Featuring BIM-LCA Integration in Buildings: A Practical Review of the Current Trends«, *SUSTAINABILITY*, Jg. 12, Nr. 17, S. 7182, 2020.

[5] ISO, *ISO 14040:2006: Environmental management - Life cycle assessment - Principles and framework*, Juli 2006.

[6] ——, *ISO 14044:2006: Environmental management - Life cycle assessment - Requirements and guidelines*, Juli 2006.

[7] F. Pagnon, A. Mathern und K. Ek, »A review of online sources of open-access life cycle assessment data for the construction sector«, *IOP Conference Series: Earth and Environmental Science*, Jg. 588, S. 42 051, 2020.

[8] M. Pasetto, E. Pasquini, G. Giacomello und A. Baliello, »Life-Cycle Assessment of road pavements containing marginal materials: comparative analysis based on a real case study«, 2017.

[9] J. Olivier, M. Saadé-Sbeih, S. Shaked, A. Jolliet und P. Crettaz, *Environmental life cycle assessment*. Boca Raton: CRC Press, 2015.

[10] A. Takano, S. Winter, M. Hughes und L. Linkosalmi, »Comparison of life cycle assessment databases: A case study on building assessment«, *Building and Environment*, Jg. 79, 2014.

[11] L. Wastiels und R. Decuypere, »Identification and comparison of LCA-BIM integration strategies«, *IOP Conference Series: Earth and Environmental Science*, Jg. 323, Nr. 1, S. 012 101, 2019. DOI: 10.1088/1755-1315/323/1/012101.

[12] M. Röck, A. Hollberg, G. Habert und A. Passer, »LCA and BIM: Integrated Assessment and Visualization of Building Elements' Embodied Impacts for Design Guidance in Early Stages«, *Procedia CIRP*, Jg. 69, S. 218–223, 2018.

[13] R. Slobodchikov, K. Lohne Bakke, P. Ragnar Svennevig und R. O'Born, »Implementing climate impacts in road infrastructure in the design phase by combining BIM with LCA«, *IOP Conference Series: Earth and Environmental Science*, Jg. 323, S. 012 089, 2019.

[14] FGSV, *RStO 12: Richtlinien für die Standardisierung des Oberbaues von Verkehrsflächen*, 2012.

Teil VIII

Machine Learning & Artificial Intelligence

Machine-Learning Methoden zur frühzeitigen Prognose von Bewehrungsstahlmengen im Stahlbetonhochbau

Marcel Heiß[1]

[1]Institut für Numerische Methoden und Informatik im Bauwesen, Technische Universität Darmstadt, Franziska-Braun-Straße 7, 64287 Darmstadt, Deutschland

E-mail(s): heiss@iib.tu-darmstadt.de

Abstract: Zum Arbeitsalltag von Ingenieuren und Architekten gehören immer noch viele sich wiederholende Arbeitsprozesse, welche einen hohen Zeitbedarf einnehmen. Dies hat zur Folge, dass die kreative Lösung von Problemen oftmals in den Hintergrund gerät. Abhilfe leisten können KI-basierte Assistenzsysteme, welche in der Planung die Entscheidungsfindung unterstützen und Arbeitsprozesse automatisieren. Mit dem Einsatz von BIM-Daten in Machine-Learning Methoden zur frühzeitigen Prognose von Bewehrungsstahlmengen im Stahlbetonhochbau wird ein möglicher Anwendungsfall für ein KI-basiertes Assistenzsystem in der Tragwerksplanung hinsichtlich seiner Potentiale und Grenzen im Detail untersucht. Hierbei werden entsprechende Daten aus BIM-Modellen gewonnen und diese für das Machine-Learning vorverarbeitet. In einem Vergleich unterschiedlicher Machine-Learning Algorithmen werden deren Leistungsfähigkeit beurteilt und vielversprechende Lernmodelle werden nochmals optimiert. Ziel ist die Entwicklung eines Machine-Learning Algorithmus, welcher in der Entwurfsplanung die Bewehrungsstahlmenge eines Gebäudes automatisiert auf Basis eines BIM-Modells der Tragwerksplanung entsprechend gewisser Vorgaben genau bestimmt. Die Ergebnisse zeigen, dass dieser Ansatz bereits mit einer geringen Menge an zu Verfügung stehenden Daten und Informationen unter Einschränkungen möglich ist und außerdem noch weitere Potentiale birgt.

Keywords: Building Information Modeling, Datenaufnahme/ Data Mining, Machine Learning und KI

1 Einführung

Bauwerke stellen im Regelfall Unikate dar, weswegen zu Planungsbeginn die Baukosten und die Bauzeit immer neu abgeschätzt werden müssen. Die Kostenberechnung in der Entwurfsplanung verwendet die Entwurfszeichnungen und sich daraus ergebenden Mengen zu Bauteilen wie Wänden als Grundlage hierfür. In diesem Projektstadium erschweren jedoch viele weitere noch unbekannte Planungsgrößen eine zuverlässige Prognose der Kosten. Dies bedeutet für alle Beteiligten eine

Planungsunsicherheit und damit ein gewisses Risiko in jedem Bauprojekt. Eine in einem Stahlbetonhochbauprojekt erst spät in der Planung bekannte Größe ist die Bewehrungsmenge. Diese wird erst mit Abschluss der Bewehrungsplanung durch die Tragwerksplanung in Leistungsphase 5 gemäß Anlage 14 der HOAI [1] bekannt. Die Bewehrungsmenge hat jedoch Einfluss auf die Kosten und den Ablauf eines Stahlbetonbauprojektes. Deswegen ist eine Grundleistung der Leistungsphase 3 im Rahmen der Tragwerksplanung eine überschlägige Ermittlung der Betonstahlmenge eines Projektes vor der eigentlichen Statik und Bewehrungsplanung. Hierzu wird oftmals auf den Baustoffkennwert Bewehrungsgrad [2] zurückgegriffen, welcher durch den Quotienten aus **Bewehrungsmenge ($BW_{M,i}$)** und **Betonmenge ($BT_{M,i}$)** definiert wird. In der bisherigen Praxis finden u.a. Werte für den **Bewehrungsgrad einzelner Bauteile ($bw_{g,bt,i}$)** aus unterschiedlichen Literaturen wie [3], eigene Erfahrungswerte und mittels einer überschlägigen Bemessung für einzelne Bauteile ermittelte Werte Anwendung. Wissenschaftliche Veröffentlichungen wie [4] beschäftigen sich mit der Validierung von Werten aus etablierten Literaturen und der Herleitung eigener, statischer Werte auf Basis statistischer Auswertungen analoger Unterlagen wie Bewehrungsplänen und statischen Bemessungen. Unter Mittelwertbildung werden dabei abhängig des Bauteiltyps und davon abhängenden, identifizierten Einflussgrößen wie Belastung, Beanspruchung oder Spannweite Werte für den Bewehrungsgrad ermittelt . In der Praxis muss der Ingenieur aufwändig Planungsunterlagen wie 2D-Pläne oder BIM-Modelle sichten, für die ermittelten Bauteile individuelle Bewehrungsgrade schätzen und daraufhin die benötigte Bewehrungsmenge hochrechnen. Je nach Größe und Komplexität des Gebäudes kann die überschlägige Ermittlung der Bewehrungsmenge in der Entwurfsplanung jedoch sehr aufwendig werden und bietet dabei nur eine geringe Sicherheit bezüglich der Genauigkeit der Prognose.

2 Konzept

Zur datengestützten Optimierung dieses Prozesses können Machine-Learning Methoden zu dieser überschlägigen Bewehrungsermittlung Anwendung finden. **Maschinelles Lernen** (engl. machine learning) (ML) ist ein Ansatz aus dem Gebiet der **künstlichen Intelligenz** (KI) und beschreibt die Fähigkeit von Systemen und Algorithmen, Fertigkeiten zu erlernen ohne dafür explizit programmiert zu sein und damit Wissen zu erzeugen [5] . Die Ansammlung der für den Einsatz von ML oftmals notwendigen großen Datenmengen wird durch die starke Fragmentierung der Bauwirtschaft erschwert, weswegen noch keine Anwendungen zur Automatisierung von Planungsprozessen, zu denen auch der vorgestellte Prozess der Bewehrungsermittlung zählt, ihren Weg in die Praxis gefunden haben. Das Forschungsprojekt „Smart Design and Construction (SDaC)“ [6] beschäftigt sich mit dem vorangestellten Problem und u.a. mit dem Einsatz von KI zur Planungsautomatisierung. Spezifische Anwendungsgebiete im Stadium der Forschung sind der Einsatz von KI im Designprozess der Architektur wie in [7] und bei der Dimensionierung von Bauteilen im Rahmen der Tragwerksplanung wie in [8]. Die Verwendung von überwachtem maschinellem Lernen zur Bewehrungsermittlung hat eine Automatisierung des Prozesses und eine höhere Sicherheit bezüglich der Genauigkeit der Prognose zum Ziel. Zielgröße des überwachten Lernens stellt der Bewehrungsgrad einzelner Stahlbetonbauteile dar, welcher auf Basis sogenannter Merkmale (engl. Features) wie Bauteiltyp, Abmessungen und Ma-

terialeigenschaften prognostiziert wird. Die **Gesamtbewehrungsmenge eines Bauwerks ($BW_{M,bwk}$)** ergibt sich aus der Iteration über alle Bauteile eines Bauwerks (n) gemäß Gleichung (1).

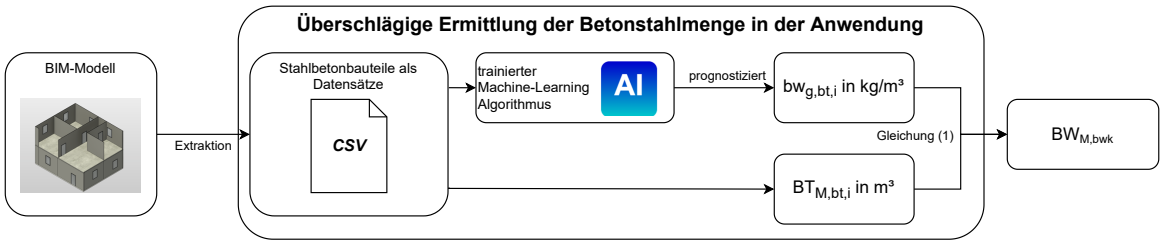

Abbildung 1: Prozess der überschlägigen Ermittlung der Betonstahlmenge mit ML in der Entwurfsplanung auf Basis eines BIM-Modells

$$BW_{M,bwk} = \sum_{i=0}^{n} BW_{M,bt,i} = \sum_{i=0}^{n} BT_{M,bt,i} \cdot bw_{g,bt,i} \tag{1}$$

3 Rohdaten, Datenaufbereitung und Datenanalyse

Die notwendigen Rohdaten zu den einzelnen Bauteilen können durch die Planungsweise des **Building Information Modellings** (BIM) automatisiert aus abgeschlossenen Projekten gewonnen werden. Die in BIM modellierten Bauteile besitzen neben den geometrischen Informationen des 3D-Körpers zusätzliche Informationen wie beispielsweise zu dem Bauteiltyp, dem Material oder der Betongüte in Form von angehängten Attributen. Die verwendeten Rohdaten stammen aus BIM-Modellen der Tragwerksplanung, welche die Extraktion der in Tabelle 1 dargestellten Features und des Zielwertes ermöglichen. Die Extraktion der Daten ist direkt aus dem Autorensystem Allplan 2019 des Herstellers Nemetschek erfolgt. Eine mittels einer Schnittstelle entwickelte Erweiterung ermöglicht den Zugriff auf alle Bauteile und deren Informationen und das Überführen dieser in Datensätze, welche in einer csv-Datei gesammelt werden. Die Information über den Bewehrungsgrad ist nur implizit in den BIM-Modellen vorhanden. Die semantisch unabhängige Modellierung von Bauteilen und Bewehrung macht eine nachträgliche Berechnung des Bewehrungsgrades der Bauteile mittels Algorithmen erforderlich, welche sich die eindeutige Positionierung von Bewehrung und Bauteilen im Raum zunutze macht. Zur Erhöhung der Qualität für das ML wird zunächst eine **Datenvorverarbeitung** durchgeführt, in welcher unter anderem fehlerhafte Werte in Datensätze korrigiert werden. Außerdem werden Features, welche mehrere oder implizite Informationen enthalten, in gesonderte Features überführt. Im Rahmen dieses Prozesses wird die Anzahl der zu Verfügung stehenden Datensätzen von 7042 auf 4901 reduziert. In der anschließenden **Feature Transformation** wird eine Kodierung der kategorischen, ordinalen und binären Features in ganze Zahlen vorgenommen. Die Features werden normalisiert um einen wertebedingten Einfluss in auf Ähnlichkeitsmessungen basierenden Lernmodellen zu verhindern.

Im Rahmen einer Datenanalyse werden die auftretenden Häufigkeiten der unterschiedlichen Ausprägungen in den einzelnen ordinalen und kategorischen Features mittels Histogrammen auf Un-

ausgeglichenheit untersucht. Eine gewisse Verteilung der Werte der Features ist in den meisten Fällen gegeben. Die Verteilung des Features Projekttyp zeigt dabei eine starke Konzentration der Daten auf dem Wohnungsbau. Von den insgesamt 48 ausgewerteten Projekten sind nur 7 dem Wohnungsbau zuzuordnen. Demnach enthalten die ausgewerteten Wohnungsbauprojekte immer eine hohe Anzahl an Bauteilen. Gleiches gilt für die Projekte aus dem Parkhausbau, jedoch nicht für die Projekte aus dem Industriebau. Im Allgemeinen sind in allen Features, welche direkt oder indirekt in eine statische Bemessung einzelner Stahlbetonbauteile mit eingehen, Informationen zum Bewehrungsgrad eines Bauteils zu vermuten. Generell richtet sich die Bemessung nach dem genauen Bauteiltyp, welcher auch in bisherigen Literaturen als einziges Kriterium für den Bewehrungsgrad eines Bauteils verwendet wird. Das Feature Projekttyp kann implizit Informationen zu Lastannahmen und Gebäudestruktur, welche beispielsweise Spannweiten von Decken beeinflussen, enthalten. Mit dem Feature Material gehen oftmals besondere Anforderungen an die Bewehrung des Bauteils, wie zur Betondeckung, einher. Die Druckfestigkeitsklasse in dem Feature Betongüte kann Hinweise zur generellen Beanspruchung des Tragwerks geben, da hohe Betongüten bei starken beanspruchten Tragwerken Einsatz finden. Die Abmessungen eines Bauteils geben Aufschluss über die Geometrie, welche in einer Bemessung eine maßgebliche Größe darstellt, aber unter Umständen auch über statische Randbedingungen wie Spannweiten. Außerdem geht das Volumen des Bauteils direkt in die Berechnung des Bewehrungsgrades eines Bauteils ein und bestimmt diesen daher mit.

Tabelle 1: Entwicklung der Daten im Rahmen der Datenvorverarbeitung

Features der Rohdaten	Features nach Datenverarbeitung	Featuretyp	Wertebereich
Projektbezeichnung	Bauherr	kategorisch	Bauherr A, Bauherr B, und Weitere
	Projekttyp	kategorisch	Wohnungsbau, Industriebau, Parkhausbau
Bauteiltyp Funktion	Bauteiltyp	kategorisch	Stütze, Wand, Decke und Weitere
Material	Material	kategorisch	Stahlbeton, wasserundurchlässiger Stahlbeton, flüssigkeitsdichter Stahlbeton
Betongüte	Betongüte	ordinal	C 25/30, C 30/37, C 35/45, höhere Betongüte
Außenbauteil	Außenbauteil	binär	Ja, Nein
Statisch Tragend	Statisch Tragend	binär	Ja, Nein
3D-Kordinaten des Bauteilmittelpunktes	x-Koordinate	kontinuierlich	-
	y-Koordinate	kontinuierlich	-
	z-Koordinate	kontinuierlich	-
Abmessungen des Bauteils	Länge	kontinuierlich	-
	Breite	kontinuierlich	-
	Höhe	kontinuierlich	-
Nettovolumen	Nettovolumen	kontinuierlich	-

4 Training und Validierung

Die vorverarbeiteten Daten werden an ausgewählte Lernmodelle übergeben und deren Lernerfolg anhand von Metriken betrachtet. In der praktischen Anwendung erhält der Algorithmus ein neues Projekt mit beliebig vielen Bauteilen in Form von Datensätzen. Um diesen Anwendungsfall auch in der Validierung zu beachten, erfolgt die Einteilung in Trainings- und Testdaten in Form einer k-fachen Kreuzvalidierung. Dabei ist k gleich der Anzahl an verfügbaren Projekten. So werden immer die Datensätze eines Projektes zum Testen zurückgehalten, während die Datensätze aller anderen Projekte zum Trainieren verwendet werden. Metriken erlauben dann einen Vergleich der Lernmodelle zwischen einander. Jedoch wird durch diese nicht deutlich ob das letztendliche Ziel, die Ermittlung der Gesamtbewehrungsmenge, eines Bauwerks ebenfalls erreicht ist. Deswegen wird außerdem die Gesamtbewehrungsmenge jedes Bauwerks ermittelt und der tatsächlichen Gesamtbewehrungsmenge gegenübergestellt. Es werden die fünf Lernmodelle k-Nearest-Neighbor, Gradient Boosting, Random Forest, Support Vector und Neuronale Netze herangezogen. Als Metrik dient der mittlere absolute Fehler (MAE), welcher dieselbe Einheit wie die Zielgröße ausweist. Zur Beurteilung des Lernerfolgs werden zum einen der Mittelwert und die Streuung des MAE und zum anderen der Mittelwert und die Streuung bezüglich der Abweichung von der Gesamtbewehrungsmengen herangezogen. Während für den MAE keine Zielwerte definiert werden können und dieser daher nur relativ betrachtet werden kann, sind Abweichungen von der tatsächlichen Gesamtbewehrungsmenge unter 20 % als Ziel fest definiert.

5 Ergebnisse

Beim Training der unterschiedlichen Lernmodelle unter den zu Verfügung stehenden Daten zeigt sich früh, dass die erzielten Resultate der Lernmodelle vom Projekttyp abhängen. Deswegen erfolgt die Auswertung der Resultate der Lernmodelle getrennt für die unterschiedlichen Projekttypen. Während alle Lernmodelle im Wohnungsbau hinsichtlich der gesetzten Kriterien aussichtsreiche Ergebnisse liefern, schwanken die Ergebnisse im Industriebau je Projekt unabhängig des Lernmodells sehr stark. Dies kann auf die starke Variation der kleinen Industriebauprojekte und den wenigen zu Verfügung stehenden Datensätzen aus diesem Bereich im Vergleich zum Wohnungsbau zurückgeführt werden. Sowohl bei den Wohnungsbauprojekten als auch bei den Parkhausprojekten handelt es sich um große Bauwerke, welche eine starke Ähnlichkeit untereinander hinsichtlich der Bauweise aufweisen, und einen Großteil der Daten ausmachen. Das Gradient Boosting erweist sich unter den zu Verfügung stehenden Daten sowohl im Wohnungsbau als auch im Parkhausbau als aussichtsreichstes Lernmodell und die Ergebnisse zum Wohnungsbau sollen im Folgenden genauer vorgestellt werden. In diesem Fall wird ebenfalls eine k-fache Kreuzvalidierung angewendet, bei der jedoch k gleich der Anzahl an Wohnungsbauprojekten zuzüglich eins ist. Es ergeben sich deswegen sieben Folds, von denen sechs die sechs Wohnungsbauprojekte darstellen, welche auch als Testdatensätze verwendet werden. Eine erneute Feature Transformation muss nicht erfolgen, da auf Entscheidungsbäumen basierende Lernmodelle kategorische und ordinale Features ohne eine aufwendige Kodierung verarbeiten

können. Außerdem ist keine Skalierung notwendig. Eine erste Lernkurve des Gradient Boosting in Abbildung 4 zeigt einer Annäherung der beiden Scores. Dies deutet eine sich ausbildende Generalisierungsfähigkeit des Modells an. Der Score (MAE) für die Trainingsdaten weist im Vergleich zu dem Cross-Validation Score eine wesentlich geringe Streuung und einen wesentlich geringeren Wert für den MAE auf, wodurch eine Überanpassung des Modells an die Trainingsdaten und damit die Erzeugung eines zu komplexes Modell deutlich wird. Um den Effekt der Überanpassung zu reduzieren wird auf die Erzeugung eines einfacheren Modells durch die Verringerung der Features zurückgegriffen. Im Rahmen einer Merkmalsauswahl sollen zunächst aussagekräftige Features ermittelt werden. Abbildung 2 zeigt die im Rahmen des Gradient Boosting implizit ermittelten Merkmalswichtigkeiten im Ranking. Hieraus wird deutlich, dass die wichtigsten vier Features bereits ca. 75 % des gesamten Informationsgehaltes aufweisen. Das gleiche Ergebnis liefert die Gegenüberstellung der Mittelwerte für den Cross-Validation Score und den Trainings-Score unter zunehmender Anzahl an Features in Abbildung 3. Das Modell mit dem höchsten mittleren Cross-Validation Score und der geringsten Differenz zwischen Cross-Validation Score und Trainings-Score weist die geringste Überanpassung auf.

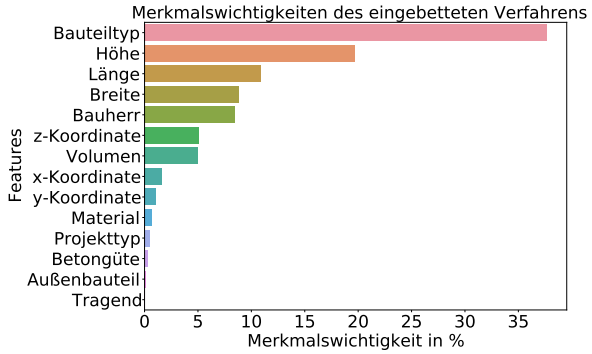

Abbildung 2: Ranking der Features unter Anwendung eines eingebetteten Verfahrens

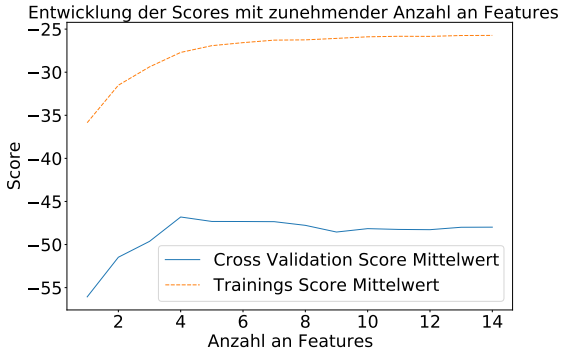

Abbildung 3: Entwicklung des Cross-Validation Score und des Trainings-Score mit zunehmender Anzahl an Features

Im Rahmen einer sich anschließender Hyperparameterabstimmung werden die Hyperparameter Learning-Rate, n-estimators und max-depth mittels Validierungskurven getrennt und mittels Rastersuche kombiniert untersucht. Die abschließende Lernkurve in Abbildung 5 zeigt, dass trotz der geringeren Komplexität des Modells durch die Merkmalsauswahl die Performance geringfügig gesteigert werden konnte. Die Annäherung der Scores zeigt den Lernprozess des Modells. Die Lernkurven schließen jeweils bei einem Wert von 28 bzw. 47 für den MAE ab. Die Annäherung der beiden Kurven in einem so hohen Wertebereich deutet auf eine große Verzerrung und eingeschränkte Generalisierungsfähigkeit des Modells hin. Bei der Ermittlung der Bewehrungsgrade einzelner Bauteile verschiedener Projekte wird deutlich, dass die zum derzeitigen Stand vorliegenden Daten nicht ausreichen um den Bewehrungsgrad eines Bauteils entsprechend genau zu prognostizieren.

Die Auswertung des Bewehrungsgrades zeigt, dass der Bewehrungsgrad vorrangig Werte zwischen 100 und 200 kg/m³ annimmt. Bei einem angenommenen Wert von 150 kg/m³ für den Bewehrungsgrad

eines beispielhaften Bauteils bedeutet ein MAE in Höhe von 45 kg/m³ eine prozentuale Abweichung von 30 % , welche oberhalb der angesetzten 20 % Abweichung von der Gesamtbewehrungsmenge liegt. Die hohen mittleren absoluten Fehler deuten darauf hin, dass zum einen gewisse Informationen, welche für den Bewehrungsgrad entscheidend sind, nicht enthalten sind und zum anderen, dass die Menge an Daten noch nicht ausreichend ist, wodurch der Informationsgehalt vieler Features unter Umständen nicht erfasst werden kann. Dies bewirkt, dass die Lernmodelle nur aus wenigen Features einen Performancezuwachs erzielen. Es fehlen Informationen zu der genauen Beanspruchung der Bauteile in Form von Schnittgrößen, aber auch Belastungen auf die Bauteile oder die Expositionsklassen können vielversprechende Informationsquellen sein. Trotz der geringeren Generalisierungsfähigkeit ist es mit dem ausgearbeiteten Lernmodell möglich die Gesamtbewehrungsmengen von Projekten, welche in den Daten in ausreichender Häufigkeit und Ähnlichkeit vertreten sind, zuverlässig zu prognostizieren. Grund hierfür ist die in der Verallgemeinerungsfähigkeit und im MAE nicht erfasste Streuung des Fehlers in positive und negative Richtung. Demnach kann die Bewehrung eines Bauteils unterschätzt und die des nächsten überschätzt werden. So werden Fehler bei den Bewehrungsgraden einzelner Bauteile bei der Ermittlung der Gesamtbewehrungsmenge wieder ausgeglichen. Dies setzt voraus, dass die Bewehrungsgrade ausgewogen über- und unterschätzt werden und dass das Bauwerk eine hohe Anzahl an Bauteilen besitzt, sodass sich dieser Effekt auch einstellen kann. Zum anderen sind für die Gesamtbewehrungsmenge vor allem die voluminösen Bauteile relevant, da diese mit einer höheren Gewichtung eingehen. Deswegen besitzt der MAE in Bezug auf die Gesamtbewehrungsmenge nur eine bedingte Aussagekraft. Eine Metrik, die den Fehler anhand des Volumens gewichtet wäre in diesem Fall zielführender.

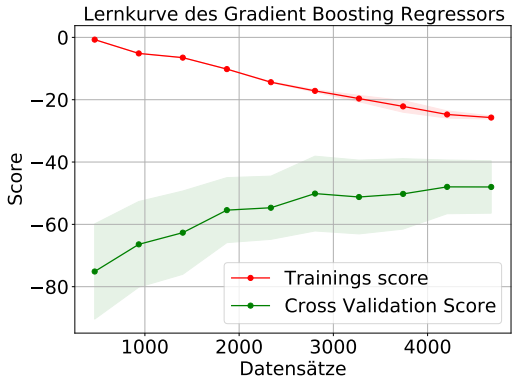

Abbildung 4: Lernkurve unter Verwendung aller Features

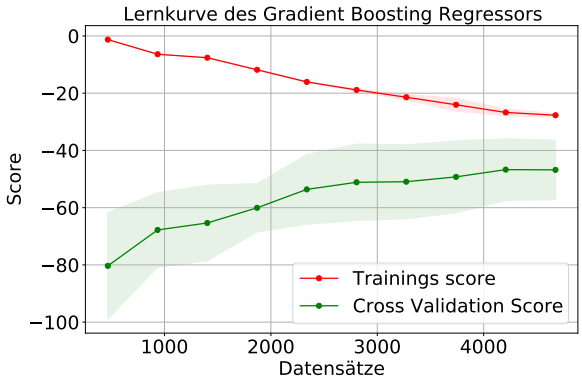

Abbildung 5: Lernkurve nach Feature Selection und Hyperparameterabstimmung

6 Fazit und Ausblick

Die Ergebnisse zeigen, dass die Anwendung des überwachten, maschinellen Lernens zur Ermittlung der Bewehrungsmenge von Stahlbetonhochbauprojekten in der Entwurfsplanung in der Praxis bereits mit der geringen Menge an Daten und Informationen unter Einschränkungen möglich ist und in der Theorie außerdem noch weitere Potentiale birgt. So konnte mit dem entwickelten Lernmodell bei

Wohnungsbauprojekten die Zielvorgabe von einer Abweichung von weniger als 20 % der tatsächlichen Gesamtbewehrungsmenge eingehalten werden. Um eine ausreichende Repräsentativität der Ergebnisse zu gewährleisten ist jedoch eine umfangreichere Validierung der Lernmodelle unabdingbar. Eine Einschränkung ergibt sich aus der zur erfolgreichen Prognose der Gesamtbewehrungsmenge notwendigen Ähnlichkeit des neuen Projektes mit den Projekten, welche Grundlage der Trainingsdaten sind. Drei große Probleme, die sich im Rahmen dieser Arbeit herauskristallisierten, sind die geringe Menge an Daten, deren ungleichmäßige Verteilung und deren für dieses Anwendungsziel nicht vollständiges Informationsprofil. Dies führt zu einer unzureichenden Generalisierungsfähigkeit des entwickelten Lernmodells hinsichtlich des Bewehrungsgrades eines Bauteils. Durch die sich immer weiterverbreitende BIM Planungsweise, kommt es zwangsläufig zu einer weiteren Ansammlung von strukturierten Daten, die genutzt werden können. BIM-Modelle befinden sich zudem in einer ständigen Entwicklung. So wird der Informationsgehalt in den BIM-Modellen mit dieser Entwicklung noch zunehmen und diese können wiederum im überwachten Lernen genutzt werden. Informationen wie die Expositionsklassen, Feuchtigkeitsklassen, Einwirkungen oder die Beanspruchungen der einzelnen Bauteile in Form der Schnittgrößen können einen immensen Mehrwert bieten. Um dies zu erreichen ist es jedoch erforderlich derzeit bestehende Datensilos wie BIM-Daten und Statik-Daten im Rahmen eines ganzheitliches Datenmanagements gezielt zu verknüpfen.

Literatur

[1] HOAI.de, *HOAI 2021: Volltext der aktuellen HOAI online auf HOAI.de*, Okt. 2021. Adresse: https://www.hoai.de/hoai/volltext/hoai-2021/#A14 (besucht am 24. 05. 2022).

[2] C. Hofstadler, *Bauablaufplanung und Logistik im Baubetrieb: Mit 5 Tabellen*. Berlin, Heidelberg und New York: Springer, 2007, ISBN: 3-540-34320-2.

[3] R. Rybicki und F. U. Prietz, *Faustformeln und Faustwerte für Tragwerke im Hochbau: Geschossbauten, Konstruktionen, Hallen*, 6. aktualisierte Auflage. Köln: Reguvis, 2021, ISBN: 978-3-8462-1095-6.

[4] D. Dix, *Kalkulation im Schlüsselfertigbau leicht gemacht: Stahlbedarfsfaktoren für den Hochbau*. Hamburg: Diplomica Verl., 2010, ISBN: 3836696940.

[5] P. Wennker, *Künstliche Intelligenz in der Praxis: Anwendungen in Unternehmen und Branchen: KI wettbewerbs- und zukunftsorientiert einsetzen*. Wiesbaden, Germany und Heidelberg: Springer Gabler, 2020, ISBN: 978-3-658-30479-9. DOI: 10.1007/978-3-658-30480-5.

[6] sdac.tech, *Smart design and construction - SDAC - smart design and construction through Artificial Intelligence*, Feb. 2022. Adresse: https://sdac.tech/ (besucht am 01. 07. 2022).

[7] C. Frías, J. Peña, É. Sánchez und L. Almeida, »BIMBOT-(Artificial intelligence applied to BIM design)«, *EGE-Expresión Gráfica en la Edificación*, S. 45, Juli 2020. DOI: 10.4995/ege.2020.13942.

[8] K. Chang und C. Cheng, »Learning to simulate and design for structural engineering«, *CoRR*, Jg. abs/2003.09103, 2020. arXiv: 2003.09103. Adresse: https://arxiv.org/abs/2003.09103.

KI-basierte Aufnahme sicherheitstechnischer Indikatoren auf freien Strecken von Landstraßen & abschnittsbasierte Integration zur Ableitung von Defiziten

André Hoffmann[1] and Marek Skakuj[2]
[1] Institut für Numerische Methoden und Informatik im Bauwesen, TU Darmstadt, Franziska-Braun-Str. 7, 64287 Darmstadt, Deutschland
[2] HELLER Ingenieurgesellschaft mbH, Otto-Hesse-Straße 19/T9, 64293 Darmstadt, Deutschland
E-mail(s): hoffmann@iib.tu-darmstadt.de, marek.skakuj@heller-ig.com

Abstract: Im Zuge des „Vision Zero“ Ansatzes der Bundesregierung sollen vermehrt präventive Verfahren zur Anwendung kommen, welche die Straße auf Grund von sicherheitsrelevanten indikativen Elementen bewerten. Im vorliegenden Paper soll ein Ansatz gezeigt werden, der es erlaubt auf Grundlage der Streckenbilder der ZEB und der zugehörigen Meta- und Stammdaten zur sicherheitstechnischen Bewertung relevante Größen abschnittsweise integriert bereitzustellen. Die Streckenbilder der ZEB werden hierbei mit Faltungsnetzen zur Erkennung der Fahrstreifenposition und Art, der Position der passiven Schutzeinrichtung, der Vegetation im Seitenraum sowie Verkehrsschildern, welche Geschwindigkeitsgebote sowie Gefahrenschilder umfassen, durchsucht. In mehrstufigen Pipelines werden sicherheitsrelevante Indikatoren und Defizite aus den erkannten physischen Objekten abgeleitet. Zur Demonstration werden die erkannten Defizite an einer Unfallstelle analysiert.

Keywords: Machine Learning, KI, Verkehrssicherheit, Zustandserfassung

1 Einführung

Bei der Zustandserfassung und Bewertung (ZEB) handelt es sich um ein amtlich festgelegtes Verfahren in welchen in Zyklen, öffentliche Straßen befahren werden, um mit visuellen und messtechnischen Methoden Zustandsmerkmale zu erfassen [1]. Ziel ist die Ermittlung des Zustandes und der zugehörigen Unterhaltskosten. Bei den Zustandsmerkmalen handelt es sich um Fahrbahnoberflächenschäden, Längs- und Querunebenheit, Griffigkeit und Straßenentwässerung. Zur Einordung werden außerdem Frontal-, Seiten- und Rückfahrkamerabilder angefertigt. Die Zustandsmerkmale werden abschnittsweise zu Zustandsnoten aggregiert und in Karten sowie Streckenbändern visualisiert, um auf ihrer

Basis strategische Entscheidungen über aufgrund des hohen Materialeinsatzes oftmals kostspielige Erhaltungsmaßnahmen zu treffen. In dieser Arbeit wird dargestellt, wie diese Daten auch für verkehrssicherheitstechnische Auswertungen eingesetzt werden können, um die Verkehrssicherheitsarbeit in Deutschland zu unterstützen. Auf Netzebene existiert zur Bewertung der Verkehrssicherheit in Deutschland die „Empfehlungen für die Sicherheitsanalyse von Straßennetzen (ESN)“ [2]. In diesen Verfahren wird das Sicherheitspotential eines Streckenabschnitts als Differenz der auf in auftretenden Unfallkosten und dem für diesen Streckenabschnitt zu erwartenden Unfallkosten berechnet (Grundunfallkosten). In den USA existiert vergleichbar das Highway Safety Manual [3], welches die Berechnung eines Erwartungswerts für Unfallhäufungen vorsieht, der mit Unfallhäufigkeitsfaktoren an regionale Gegebenheiten angepasst werden kann. Neben diesen auf Unfalldaten angewiesenen (reaktiven) Verfahren, wird in Deutschland an einem proaktiven Verfahren gearbeitet, dem Handbuch für die Bewertung der Verkehrssicherheit von Straßen (HVS) [4]. Mit dem HVS wird es möglich ohne bestehende Unfalldaten anhand von Defziten, welche Abweichungen vom für Deutschland spezifischen richtliniengerechten Ausbau darstellen, in der Verkehrsinfrastruktur eine Bewertung in Form des sogenannten Gefahrengrades vorzunehmen. Im Ausland existiert mit dem Road Assesment Programm (usRAP,EuroRAP, AusRAP usw.) [5] ebenfalls ein Verfahren mit dem die Straßen anhand indikativer Elemente auf Sicherheit untersucht werden können. Diese Stellen allerdings keine Abweichungen von den im jeweiligen Land geltenden Richtlinien dar, sondern beziehen sich lediglich auf das Vorhandensein allgemein gültiger verkehrstechnischer Zusammenhänge (z.B. Anzahl der Fahrstreifen, Vorhandensein von passiver Schutzeinrichtung). Parallel hierzu wurden im Forschungszweig des Visual Computing mit der Weiterentwicklung von Faltungsnetzen entscheidende Fortschritte gemacht, welche es ermöglichen auf Bildern der Straße Objekte und Zusammenhänge zu erkennen und zu segmentieren. In dieser Arbeit soll aufgezeigt werden wie Faltungsnetz basierte Methoden auf die Frontalkamerabilder der ZEB angewendet werden können, um in einen mehrstufigen Verfahren relevante Größen für die sicherheitstechnische Bewertung abzuleiten, welche statistisch analysiert bzw. auf Karten visualisiert werden können, um die Arbeit der Unfallkommissionen und Bestandsauditoren zu unterstützen. Hierzu soll zunächst das Gesamtkonzept und Architektur der Anwendung vorgestellt werden. Danach werden die zu erkennenden Objekte und eingesetzten Netzarchitekturen diskutiert. Das nächste Kapitel widmet sich der Integration und Ableitung der Sicherheitsdefizite. Abschließend werden die Sicherheitsdefizite anhand eines Streckenabschnitts exemplarisch diskutiert.

2 Gesamtkonzept

Der Datengewinnungsprozess basiert auf den Ergebnissen der ZEB und erzeugt aus diesen strukturierte Daten, welche vom Benutzer anhand einer Applikation nach Defiziten durchsucht werden können. Um die Anforderung an den Datengewinnungsprozess zu kennen, muss das Datenmodell in welches die Daten gespeichert werden sollen, bekannt sein. Um das Datenmodell zu generieren, müssen wiederum Anforderungen der Applikation definiert werden.

2.1 Fachliche Anforderungen

Als Ziel der Anwendung werden freie Strecken von Landstraßen definiert. Diese haben den Vorteil, dass sie im Handbuch für die Bewertung der Verkehrssicherheit von Straßen (HVS) [4] behandelt werden und dieses somit als Orientierungspunkt bei fachlichen Fragen dienen kann. Instanzen von Landstraßen sind außerdem auf Grund ihrer niedrigeren Verbindungsfunktion in größerer Anzahl vorhanden als Autobahnen, was es erleichtert Trainingsbeispiele zu generieren. In einer Betrachtung wie sie hier der Fall ist, können nur Defizite untersucht werden, die sich aus den Streckenbildern erfassen lassen und somit statischer Natur sind. Das heißt auch, dass Defizite, die sich aus den unterschiedlichen Fahrtbeziehungen am Knotenpunkt ergeben nicht geprüft werden können, daher wurde der Schwerpunkt auf Defizite gelegt, die sich auf freie Strecken beziehen. Die Defizite werden angelehnt an das HVS gewählt:

- Bäume im kritischen Abstand mit und ohne passive Schutzeinrichtung
- Fahrbahnbreite nicht ausreichend für den Regelquerschnitt
- Radius zu gering für den Regelquerschnitt
- Radienrelation nicht ausreichend für den Regelquerschnitt

2.2 Datenfluss und wesentliche Bausteine

Der Datengewinnungsprozess besteht aus mehreren Typen von Convolutional Neural Networks die auf die Frontalkamerabilder trainiert werden und verschiedene physische Objekte und deren grundlegende Geometrien zurückgeben. Die Objekte werden mit 3D-Informationen aus den Tiefenschätzungsnetz „Monodepth2“ [6] angereichert. Aus den verorteten Objekten werden kombiniert und zusammen mit den Stammdaten der Straße aus den Länderstraßendatenbanken, in mehreren Prozessen Indikatorgrößen und aus diesen schließlich Defizite abgeleitet. Diese Defizite werden anschließend zur Validierung auf einer Karte visualisiert. In den Folgekapiteln werden zunächst die zu erkennenden Objekte und darauf basierend die gewählten Netzarchitekturen vorgestellt. Danach wird die prozessuale Verarbeitung zu Indikatoren und schließlich zu Defiziten beschrieben und wie diese gespeichert werden.

3 Faltungsnetze zur Erkennung der Objekte

Die Auswahl der Netze zur Erkennung der physischen Objekte orientiert sich hauptsächlich an der Form in der das Ergebnis vom Netz bereitgestellt werden soll und an der Beschaffenheit des Objektes auf den Bildern. Auch die Einfachheit des Labelings spielt für die Annotation des eigenen Trainingsdatensatzes eine wichtige Rolle. Es wurden vier Arten von grundlegenden Formen festgestellt:

3.1 Polylinien

Die folgenden Objekte werden als Polylinien erkannt:

Fahrbahnmarkierungen kommen in Fahrbahnmitte sowie seitlich als Fahrbahnbegrenzung vor. In ihrer Form unterscheiden sie sich in gestrichelte, durchgezogene Fahrstreifen und bei niedrigen Entwurfsklasse vor allem bei Ortsverbindungen in nicht markierte Fahrbahnbegrenzung. Mittlere Fahrstreifen kommen außerdem bei Querschnitten der Entwurfsklasse 1 und 2 auch mehrfach vor, wenn eine Überholspur angeordnet ist. In den Metadaten der genutzten Straßeninformationsbank (SIB) [7], zeigt sich, dass dies sehr selten der Fall ist. Mehrstreifig sind die Landstraßen im Datensatz meist nur innerorts oder in der Nähe von Knotenpunkten, welche nicht Teil der der Betrachtung sind. Die große Mehrheit der Landstraßen gehört zu Entwurfsklasse 3 und 4, so dass diese im Fokus der Analyse stehen.

Abbildung 1: Darstellung der durch die KI erkannten Elemente in der Visualisierungsanwendung

Baumlinien: Bäume gelten als „nicht verformbare punktuelle Einzelhindernisse“ nach RPS2009 [8] und sollten sofern sie nicht den kritischen Abstand einhalten bei Neubauten entfernt werden. Bäume kommen allerdings auf Grund ihrer Beschaffenheit auf äußerst vielfältige Weise auf den Kameraufnahmen der Zustandserfassung vor. Gerade bei dichter Vegetation ist es nicht möglich einzelne Bäume auszumachen. Daher werden Bäume zusammen mit dichter Vegetation anhand ihres Aufsatzpunktes am Boden gelabelt. Diese wird in dieser Arbeit als Baumlinie bezeichnet.

Passive Schutzeinrichtung: Passive Schutzeinrichtung (PSE) kommt in verschiedenen Ausprägungen vor. Laut RPS2009 [8] ist diese je nach Gefährdungsstufe in unterschiedlichen Leistungsklassen anzuordnen. Die Leistungsklasse ist aber nach rein äußeren Kriterien nicht zu unterscheiden, so dass letztlich nur in passive Schutzeinrichtung links und rechts der Fahrbahn unterschieden wird. Als Netzarchitektur wurde für diese Art von Objekten Resa (Recurrent Feature-Shift Aggregator,[9]) verwendet. RESA wendet auf das durch einen Encoder kreierte Feature-Map Merkmalsverschiebungsoperationen in 4 Richtungen an, was es ermöglichen soll auf jeden Punkt Informationen von allen Orten des Feature Maps einzubeziehen. Hierdurch sollen beispielsweise auch verdeckte Fahrspuren erkannt werden können, auf welche in anderen Teilen des Bildes aber Anhaltspunkte zu finden sind. RESA wurde in erster Linie für Fahrstreifenerkennung entwickelt, wobei die Klassifizierung der Ground-Truth-Fahrstreifen bei der Originalimplementierung aufgrund der Struktur der vorhandenen Benchmarkdatensätze anhand der Fahrstreifenwinkel erfolgt. Neben der Segmentierung im Decoder wird außerdem eine zusätzliche Klassifizierung vorgenommen (Exists-Head), der vorhersagt ob ein Fahrstreifentyp auf dem Bild vorhanden ist. Im Rahmen dieser Arbeit wurden andere Klassen, anhand der individuellen Merkmalsauprägungen definiert, die für die Sicherheitsbetrachtung notwendig sind. Diese gliedern sich nach je nach Position (rechts, links, Mitte, Mitte-rechts, Mitte-links) und Form (gestrichelt, durchgezogen, natürliche Begrenzung) in 12 Klassen. Für die Fahrstreifen (12 Klassen),

passive Schutzeinrichtung und die Baumlinien (je in zwei Klassen: links und rechts) wurden jeweils eigene Netze trainiert.

3.2 Begrenzungsrechteck mit mit Schlüsselpunkten (Keypoints)

Als Begrenzungsrechteck mit Schlüsselpunkten werden die folgenden Objekte erkannt:
Einzelne Baumstämme: Es werden einzelne Bäume erkannt, welche nicht in einer Vegetation eingebunden sind. Diese sind zum Zwecke der Eindeutigkeit maximal zwei Bäume deren Aufsatzpunkte im unteren Bildbereich liegen. Sind drei Bäume oder mehr Vegetation zu erkennen, werden diese als Baumlinie erfasst. Der Begrenzungsrahmen (Bounding Box) wird um den Baumstamm gezogen und der Aufsatzpunkt auf dem Boden und der oberste Punkt des Stammes als Schlüsselpunkte markiert (siehe Abbildung 1).
Pfosten: Es werden Pfosten von Schildern und Straßenbeleuchtung erkannt, welche laut RPS2009 [8] als unverformbare oder auch verformbare punktuelle Einzelhindernisse gelten. Als Schlüsselpunkte wird wie bei den Baumstämmen der untere Aufsatzpunkt auf den Boden und der oberste erkennbare Punkt des Pfostens definiert.

Für die Ermittlung der Schlüsselpunkte wird ein adaptiertes Mask-RCNN verwendet [10]. Mask-RCNN basiert selbst auf einer Erweiterung des Faster-RCNN [11], welches aus dem Bild zunächst ein Feature Map generiert und aus diesem verschiedene Regions of Interest (Region Proposal Network). Diese werden gepoolt und klassifiziert sowie die zugehörigen Begrenzungsrahmen berechnet. Mask RCNN generiert aus dem gepoolten Layer zusätzlich neben der Klassifizierung noch mit einem FCN Segmentationsmasken. Beim Keypoint-RCNN wird für jeden Schlüsselpunkt (Keypoint) einer dieser Segmentationsmasken erstellt. Das Netz wurde in der ursprünglichen Anwendung zur Schätzung menschlicher Posen verwendet.

3.3 Begrenzungsrechteck (BoundingBox)

Verkehrszeichen werden mit Begrenzungsrechtecken umrandet.
Geschwindigkeitsbegrenzende Verkehrszeichen: Geschwindigkeitsgebote und Ortstafeln werden zur Bestimmung der zulässigen Geschwindigkeit erkannt, welche in den Planungsrichtlinien zur Bestimmung von Grenzwerten dienen. Außerdem gilt innerorts die Richtlinie für die Anlage von Stadtstraßen, welche hier nicht geprüft wird. Die betroffenen Abschnitte können so aussortiert werden.
Warnzeichen: Gefahrenzeichen sowie Teile der Verkehrseinrichtung wie Baken und Richtungspfeile werden ebenfalls erkannt, um zu prüfen, ob diese als Hinweis auf mögliche Gefahrenstellen bereits eingesetzt werden.

Dieser Prozess lässt sich grundsätzlich in zwei verschiedene Schritte unterteilen. Zunächst wurde ein Modell trainiert, welches die Schilder in 10 Oberklassen unterteilt. Diese Oberklassen haben ähnliche Eigenschaften, wie zum Beispiel alle runden Verkehrsschilder mit einer roten Umrandung. Als Modell wurde das Faster R-CNN ResNet101 [11] genutzt und mit den eigenen Trainingsdaten trainiert. Im Anschluss wurde das Modell auf die Streckenbilder angewendet und dabei die Bildkoordinaten der Begrenzungsrahmen und die Klassenbezeichnung in der Datenbank gespeichert. Um

eine noch bessere Eingrenzung vornehmen zu können, wurde im Anschluss für einzeln Oberklassen Klassifizierungsmodelle entwickelt.Trotz relativ guter Ergebnisse, wurde ,auch im Hinblick für die spätere Nutzung für andere sicherheitstechnische Anwendungen, zusätzlich eine Applikation entwickelt, welche ermöglicht, die finale Entscheidung von einem Menschen zu verifizieren und die Ergebnisse des Machine Learning Prozesses als Vorschläge zu übernehmen.

4 Datenbank, Softwarearchitektur und Prozessbeschreibung

Zentral ist die Tabelle „Messung“, welche auf den Rasterrohdaten der ZEB basiert. Die Rasterrohdaten beinhalten alle 10 m der Strecke einen Messpunkt relevanten Messdaten, welcher nach ASB (Anweisung Straßeninformationsbank, [7]) sowie zusätzlich mit GPS-Koordinaten positioniert ist. Zusätzlich finden sich in den Rasterrohdaten die Bildpfade der aufgenommenen Bilder der Messfahrzeuge. In der internen Tabelle „Messung“ werden Positionierung sowie die Bildpfade aus den Rohdaten der Messkampagne in 10m-Abschnitten gespeichert. Hinzu kommen außerdem Trassierungselemente, deren Grundtyp (Bogen oder Gerade), Radius und Länge auf Basis des in der ZEB aufgenommenen Krümmungswerte bestimmt wurde. Anschließend wurde die Relationstrassierung der einzelnen Elemente zueinander berechnet und elementweise zugordnet, ob diese im guten und zu vermeidenden oder brauchbaren Bereich liegt. Nachdem der Erkennungsprozess durchgeführt wurde, werden die erkannten Zusammenhänge in der Datenbank normalisiert gespeichert. Begrenzungsrahmen und Polylinien werden jeweils dem Messpunkt zugeordnet, auf dessen Frontalkamerabild sie erkannt wurden. Die Unterscheidung der einzelnen Objekte erfolgt durch ein Klassenattribut. Die zugehörigen Punkte (Polylinienpunkte, Schlüsselpunkte und Punkte des Begrenzungsrahmens) werden in der Tabelle Punkt gespeichert. Über das Attribut Sequence wird definiert, welche Rolle der jeweilige Punkt für das Objekt spielt. Um die erkannten Zusammenhänge miteinander kombinieren und vergleichen zu können, werden sie als Eigenschaft eines Messpunkts (10-Abschnitts) abgebildet. Dies erfordert in Teilen eine Denormalisierung der erkannten Zusammenhänge. Passive Schutzeinrichtung wird statt als Polylinie in zwei Attributen „passive Schutzeinrichtung rechts vorhanden“ und „links vorhanden“ gespeichert. Außerdem wird jedem Messpunkt, die Eigenschaften des Trassierungselements auf dem sich dieser befindet, zugordnet.

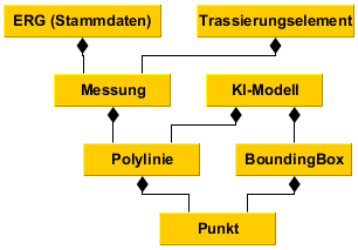

Abbildung 2: Normalisiertes Model zur Speicherung der Eingangsdaten

Die erkannten Schilder werden in Eigenschaften wie „Geschwindigkeitsbeschränkung“ und „Ortsdurchfahrt“ umgewandelt, auf den Messpunkten, auf denen diese gelten. Außerdem werden aus den Baumlinien und einzelnen Bäumen und den äußeren Fahrbahnrändern links und rechts die minimalen Abstände sowie die Fahrbahnbreite mittels der Geometriebibliothek pythonOCC [12] berechnet. Zusätzlich wird der Regelquerschnitt aus den Stammdaten und den vorhandenen Fahrbahnmarkierungen bestimmt und ebenfalls auf den Messpunkt bezogen abgespeichert. Aus den so gespeicherten Messpunkt bezogenen Indikatoren können nun im letzten Schritt mit separaten Routinen Defizite abgeleitet werden. Diese werden je Defizittyp mit etwas anderen Eigenschaften gespeichert. Es wird in Defizite, welche die kritische Distanz nicht einhalten, Defizite, in denen die Trassierung nicht richtlinienkonform ist, und Defizite, in denen die Fahrbahnbreite nicht dem zugordneten Regelquerschnitt entspricht, unterschieden.

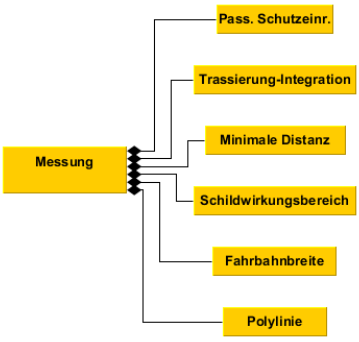

Abbildung 3: Denormalisiertes Indikatorenmodell

5 Visualisierung und demonstrative Analyse

Aus den abgeleiteten Indikatoren werden mit Routinen, welche die Regeln aus der Richtlinie anwenden, automatisiert Defizite abgeleitet. Anhand zugeordneter Regelquerschnitte lassen sich Plangeschwindigkeiten und Richtwerte entnehmen und die Indikatoren mithilfe der HVS [4] und der betreffenden Richtlinien prüfen. Das Verfahren wurde an einer Landesstraße, die weitestgehend ortsverbindenden Charakter hatte, getestet, kann aber auch auf jeden anderen Landstraßenabschnitt der von der ZEB erhoben wurde, angewendet werden. Zur demonstrativen Analyse wird eine Stelle auf der Landstraße betrachtet, an der im Februar 2020 ein Motoradunfall bei Tag und trockener Straße mit tödlichen Ausgang passierte (schwarzes Kreuz auf Abbildung 4).

Abbildung 4: Visualisierung der Defizite

Fahrbahnbreitenbezogene Defizite: Der zugeordnete Regelquerschnitt für den Abschnitt ist RQ11.5, entspricht also Entwurfsklasse 3. Allerdings ist die Straße vermutlich nicht nach der Richtlinie für die Anlage von Landstraßen (RAL, [13]), sondern nach einem älteren Regelwerk trassiert. Aufgrund des hohen Anteils von Abschnitten zwischen 6.5 bis 6 m Fahrbahnbreite könnte dies RQ 9.5 aus der "Richtlinien für die Anlage von Straßen - Querschnitt"(RAS-Q, [14])) sein. Wie in der vorliegenden Entwurfsversion der HVS vorgesehen, wurde dieser Bestandsquerschnitt mit den Regeln für RQ11.5 geprüft, was zwangsläufig zu einer hohen Anzahl an Defiziten führt, da diese eine 1m größere Fahrbahnbreite vorsieht. Farblich unterschieden sind in der Analyse die Schwere des Defizits in absteigender Sortierung (rot, orange, blau in Abbildung 4). Hierbei zeigt sich, dass in der Kurve in Unfallnähe eine deutliche Verengung der Fahrbahn stattfindet. Etwa knapp unter 6m, was auch unter

der Regelbreite von 6 m des RQ9.5 aus der alten Richtlinie liegt. Der Unfall findet in einem Bereich statt in der sich die Fahrbahn wieder etwas aufweitet.
Kritischer-Abstandsbezogene Defizite: Der Unfall findet am Anfang eines Waldabschnitts statt. Der Mindestabstand sollte in Ortsverbindungsstraßen mindestens 4.5 m betragen. Mit der zulässigen Geschwindigkeit von 80 - 100 km / h eigentlich sogar 7.5 m. Der kritische Abstand rechts der Fahrbahn ist durch eine Baumreihe nicht eingehalten. Aufgrund dessen ist passive Schutzeinrichtung verbaut. Hier wird das Defizit „Gefahrenstelle am äußeren Fahrbahnrand innerhalb des kritischen Abstands mit Schutzeinrichtung"über einen längeren Abschnitt klassifiziert (dunkelgrüne Baum-Icons). Stahlschutzplanken sind für gewöhnlich auf PKW-Fahrer optimiert, was zur Folge hat, dass die Verletzungsschwere bei verunfallten Motoradfahrer häufig sehr hoch ist [15].
Trassierungselementbezogene Defizite; Der Mindestradius der Kurve vor der Unfallstelle ist für den angesetzten Regelquerschnitt deutlich unterschritten (rosa eingezeichnetes Trassierungselement in Abbildung 4) und liegt bei etwa 136 m. Auch die Relationstrassierung zum vorherigen Geradenabschnitt liegt entsprechend im zu vermeidenden Bereich (blau gestrichelt eingezeichnet).
Eine Geschwindigkeitsbegrenzung liegt nicht vor, auch Gefahrenzeichenschilder sind nicht vorhanden. Diese könnten, falls es zu einer Häufung kommt, eine relativ günstige Maßnahme sein, um die Gefährlichkeit der Unfallstelle zu senken.

6 Fazit

In der vorgestellten Arbeit wurde ein Ansatz gezeigt, mit welchem Defizite anhand der bestehenden Daten der ZEB automatisiert abgeleitet werden können. Hierfür wurden Netzarchitekturen zur Erfassung von Fahrstreifentyp und -position, passiver Schutzeinrichtung, des Baumbestands sowie relevanter Verkehrsschilder trainiert. In einem zweiten Schritt wurden Routinen kreiert um aus den mittels der Netze erfassten Zusammenhänge und Stammdaten der ZEB Indikatoren wie den Regelquerschnitt, den Minimalabstand eines Baums zur Fahrbahn und die Fahrbahnbreite abzuleiten. Für diese Indikatoren wurden außerdem Klassifizierungsroutinen geschrieben um aus ihrer Kombination Verstöße zur geltenden Richtlinie abzuleiten. Zu beachten ist, dass bei der Schätzung der Tiefenkoordinate vortrainierte Netze (monodepth2, [6]) eingesetzt wurden, da bei der ZEB weder Lidarscans noch stereoskope Aufnahmen angefertigt werden. Ein systematischer Fehler kann daher nicht ausgeschlossen werden, mit passender Skalierung können jedoch für bestimmte Aufgabenstellungen zumindest im Nahbereich plausible Ergebnisse generiert werden. Würden in Zukunft einige Messfahrzeuge mit der notwendigen Technik ausgerüstet werden, könnte das Netz auch auf die ZEB antrainiert werden und die Genauigkeit voraussichtlich nochmal deutlich verbessern. Auch andere Defizite, die sich auf Haltsichtweiten oder die Länge von Überholabschnitten beziehen sind denkbar. So könnte langfristig ein Werkzeug geschaffen werden, welches die Verkehrssicherheitsarbeit in Deutschland sowohl präventiv als auch reaktiv unterstützen kann.

Literatur

[1] Forschungsgesellschaft für Straßen- und Verkehrswesen Arbeitsgruppe Sonderaufgaben, *Zusätzliche technische Vertragsbedingungen und Richtlinien zur Zustandserfassung und -bewertung von Straßen ZTV ZEB-StB*, Ausg. 2006. Köln: FGSV-Verl., 2007, ISBN: 9783939715030.

[2] Forschungsgesellschaft für Straßen- und Verkehrswesen - Arbeitsgruppe Verkehrsführung und Verkehrssicherheit, *Empfehlungen für die Sicherheitsanalyse von Straßennetzen : ESN*, Köln, 2003.

[3] National Research Council (U.S.) and American Association of State Highway and Transportation Officials and National Cooperative Highway Research Program, Hrsg., *Highway safety manual*, 1st ed. Washington, D.C: American Association of State Highway and Transportation Officials, 2010, OCLC: ocn645094631, ISBN: 9781560514770.

[4] Arbeitsgruppe Straßenentwurf - Arbeitsausschuss: Verkehrssicherheitsbewertung von Straßen, »Entwurfsversion: HVS - Handbuch für die Bewertung der Verkehrssicherheit von Straßen«, 4. Nov. 2019.

[5] The International Road Assessment Programme (iRAP), »iRAP Methodology fact sheets«. Adresse: https://irap.org/methodology/ (besucht am 17. 05. 2022).

[6] C. Godard, O. M. Aodha und G. J. Brostow, »Digging Into Self-Supervised Monocular Depth Estimation«, *CoRR*, Jg. abs/1806.01260, 2018. arXiv: 1806.01260. Adresse: http://arxiv.org/abs/1806.01260.

[7] Projektgruppe „ASB“ der Dienstbesprechung „IT-Koordinierung im Straßenwesen“, »ASB - Anweisung Straßeninformationsbank Teilsystem Netzdaten«, Bundesministerium für Verkehr, Bau und Stadtentwicklung - Abteilung Straßenbau, Straßenverkehr, Anweisung Straßeninformationsbank, 9. März 2011. Adresse: https://itzeb.heller-ig.de/files/asb-netzdaten.pdf.

[8] Forschungsgesellschaft für Straßen- und Verkehrswesen, Hrsg., *Richtlinien für passiven Schutz an Straßen durch Fahrzeug-Rückhaltesysteme: RPS*, ger, Ausg. März 2009, Ser. FGSV R1 343. Köln: FGSV, 2009, ISBN: 978-3-939715-74-0.

[9] T. Zheng, H. Fang, Y. Zhang u. a., »RESA: Recurrent Feature-Shift Aggregator for Lane Detection«, *CoRR*, Jg. abs/2008.13719, 2020. arXiv: 2008.13719. Adresse: https://arxiv.org/abs/2008.13719.

[10] K. He, G. Gkioxari, P. Dollár und R. B. Girshick, »Mask R-CNN«, *CoRR*, Jg. abs/1703.06870, 2017. arXiv: 1703.06870. Adresse: http://arxiv.org/abs/1703.06870.

[11] S. Ren, K. He, R. B. Girshick und J. Sun, »Faster R-CNN: Towards Real-Time Object Detection with Region Proposal Networks«, *CoRR*, Jg. abs/1506.01497, 2015. arXiv: 1506.01497. Adresse: http://arxiv.org/abs/1506.01497.

[12] T. Paviot, *pythonOCC, 3D CAD/CAE/PLM development framework for the Python programming language, PythonOCC – 3D CAD Python.* Adresse: https://github.com/tpaviot/pythonocc (besucht am 17. 05. 2022).

[13] Forschungsgesellschaft für Straßen- und Verkehrswesen, *Richtlinien für die Anlage von Landstraßen RAL*, G. Hartkopf, Hrsg., Ser. FGSV 201. Köln: FGVS-Verl, 2013, ISBN: 978-3-86446-039-5.

[14] Forschungsgesellschaft für Straßen- und Verkehrswesen - Arbeitsgruppe Straßenentwurf, *Richtlinien für die Anlage von Straßen. Teil: Querschnitte ; RAS-Q 96*. 1996, ISBN: 978-3-7812-1470-5.

[15] R. Klöckner, *Anprallversuche an motorradfahrerfreundlichen Schutzeinrichtungen: Bericht zum Forschungsprojekt F 1100.6406008*, ger, Ser. Berichte der Bundesanstalt für Straßenwesen V, Verkehrstechnik 193. Bremerhaven: Wirtschaftsverl. NW, Verl. für Neue Wiss, 2010, ISBN: 978-3-86918-002-1.

Potentials of Symbolic AI Planning for Construction

Shermin Sherkat[1], Thomas Wortmann[1] and Andreas Wortmann[2]
[1]Institute for Computational Design and Construction,Chair for Computing in Architecture, University of Stuttgart,Keplerstrasse 11, 70174 Stuttgart, Deutschland
[2]Institute for Control Engineering of Machine Tools and Manufacturing Units, University of Stuttgart,Keplerstrasse 11, 70174 Stuttgart, Deutschland
E-mail(s): shermin.sherkat@icd.uni-stuttgart.de, thomas.wortmann@icd.uni-stuttgart.de, andreas.wortmann@isw.uni-stuttgart.de

Abstract: AI planning aims to automate the reasoning process that underlies the plan formulation to achieve a particular goal for a particular problem. Research in this field has focused on symbolic methods -which represent knowledge with human readable symbols- to efficiently and systematically produce plans, i.e., sequences of actions to be performed, from well-defined problem statements. Despite advances in leveraging AI for construction planning and scheduling, most construction projects still adopt fully manual work templates. We outline the current state, challenges, and potentials of using symbolic AI in construction process planning. We first discuss the challenges in construction process planning. Then, we summarize potential applications of symbolic AI planning methods in the construction industry providing a resource for both practitioners and researchers to familiarize themselves with the potential of these powerful AI methods.

Keywords: Model-based planning, Construction industry, motion planning, TAMP, Task planning

1 Introduction

Today, artificial intelligence (AI) is frequently linked with machine learning methods, such as deep learning, that leverages neural networks. Traditionally, there have always been two main paradigms of AI: symbolic vs. subsymbolic, model-based vs. function-based, or knowledge-driven vs. data-driven [1]. While advances in the availability of data training, data transmission, and data processing have given rise to the resurgence of data-driven AI methods, which were considered being of little use in the “AI winter” of the 1980s, symbolic AI methods enable a plethora of successful applications based on structured knowledge, such as expert systems, path planners, or production planning. Despite not being in the spotlight currently, symbolic AI has been with us all the time.

AI planning is an abstract, explicit reasoning process that selects and organizes sequences of actions based on their anticipated outcomes. This reasoning seeks to achieve predetermined goals as efficiently as possible. Automated planning is an AI subdomain that studies this reasoning process computationally [2]. We believe that automated planning methods, particularly model-based planning (or so called symbolic AI planning), can facilitate construction planning.

In model-based planning, the controller that selects the next action to be performed is derived automatically from models of the actions, states, and goals defined in a declarative language like the Planning Domain Definition Language (PDDL) [3]. Our aim is to provide insights for researchers who want to use this technique in construction process planning.

Several challenges have hindered the scalability and widespread use of automated planning systems in construction planning [4]. Construction planning is consequently still mostly done manually, which results in inefficient plans and arguably contributes to construction's large environmental impact [5]. Model-based planning can address challenges related to knowledge formalization, inflexible work templates, and the disconnected nature of planning and scheduling. Towards leveraging model-based planning in construction, the contributions of this paper are:

1. Summarizing model-based planning methods and their corresponding environmental characteristics;
2. Reviewing selected applications of model-based planning in fields other than construction; and
3. Discussing the potential application of these planning methods in construction.

Our key insights are twofold: First, complex problems in the construction industry require a hybrid of model-based planning methods, and these problems all need the probabilistic method. Second, for the problem of robotic assembly, integrating task and motion planning methods is the most promising approach, while other problems can be modeled and solved with task planning methods.

We focus more on task planning methods in this paper and do not discuss motion planning methods in detail. In the remainder, Section 2 discusses construction planning and related automation challenges. Section 3 introduces the methods of planning, and Section 4 discusses the use of these methods in other fields. Finally, Section 5 outlines potential use-cases of each method for construction planning challenges.

2 Planning in Construction

Planning is required for many activities of construction processes, such as allocating labor, equipment, and material for efficient and economical operations. Sarker, Egbelu, Liao, *et al.* [6] categorize these activities into 10 categories, out of which model-based planning can potentially be applied to six: (1) delivery process of ready mixed concrete (RMC) trucks, (2) resource allocation and leveling (to reduce peak requirements and resource fluctuation), (3) inspection of partially completed work at the end of one activity and before the start of the next known as buffer stocks (modeling the link between processes), (4) planning for linear projects such as railroads and pipelines, (5) time and

cost estimation, and (6) controlling the cost escalation in big infrastructure projects [6]. Additionally, model-based planning can support automated assembly (cf. Table 1). Several methods and systems

Table 1: This table shows construction industry planning categories, their scope and application

Planning categories	Scope	Application
Scheduling and dispatching	Dispatching space	RMC trucks
Resource allocation and leveling	All projects	Equipment. manpower balancing
Buffer stocks	Project sites, Procurement	Work in progress, work flow reduction, cycle time
Linear projects	Highway and road construction	Schedululing, traverse operations, cost estimation
Time and cost estimation	All projects	Risk management, quality assurance, intellectual property
Infrastructure	Public project, bridge and highways construction	Cost escalation factor
Automated assembly	Project sites, prefabrication	Task and motion planning

have been developed so far to automate planning processes. However, construction planning is done mostly manually because (C1) flexible knowledge formalization is missing for storing construction models and templates for sequencing algorithms, (C2) current automated scheduling methods are dependent on manually formed and maintained work templates, (C3) research on automated planning and scheduling is decoupled, (C4) existing automated planning systems are only partly validated in real-life construction projects, and (C5) automated learning methods are needed to learn construction knowledge from existing records without extensive human input [4]. Model-based planning, as illustrated in the following sections, has the potential to address C1-C3.

3 Planning Methods

Model-based planning for creating the sequence of actions to be performed to reach a specific goal consists of two main parts: (1) the domain models that define the states, goals, and actions, specified in a planning language; and (2) the algorithms that use the models to generate the plan [4]. A planner then inputs the domain models and derives a sequence of actions required for reaching the goal state. Thus, given an initial state (e.g., concrete hollow core slabs on the ground) and a goal state (e.g., concrete hollow core slabs in their position on the roof) of a problem, planners will use various search and reasoning techniques to find a sequence of actions leading from the initial state to the goal state.

Depending on the problem environment, search and reasoning techniques differ. For planning in construction, classical planning, temporal and numerical planning, probabilistic planning, and hierarchical task networks appear to be promising techniques, which can be used together (hybrid planning) to address more complex problems. Table 2 defines important characteristics of the planning environment. Based on the environment characteristics we defined in Table 2, we now define planning methods.

Classical planning is the problem of planning in deterministic, fully observable, and discrete environments [7]. While classical planning answers what to do and in which order, **temporal planning** answers when an action takes place and how long it takes for planning in a continuous environment [7]. The difference between temporal and **numerical planning** is that in temporal planning, the only continuous variable is time and all other variables are discrete [8]. However, continuous variables

Table 2: This table shows the the definitions of environmental characteristics [7]

Task environment characteristics		Definition
Observability	Fully observable	The sensors detect all environmental aspects that are relevant to the choice of action.
	Partially observable	The sensors are noisy and inaccurate or parts of the state are missing from the sensor data.
	Unobservable	There is no sensor.
State transition	Deterministic	The next state of the environment is fully determined by the current state and the action executed
	Stochastic	Actions are characterized by their possible (not deterministic) outcomes.
Time and perception	Discrete	The state, time and actions are used as discrete variables.
	Continuous	The state, time and actions are used as continuous variables.

are allowed other than time in numerical planning, but it is insufficient for defining high dimensional geometrical problems [8].

Probabilistic planning is planning in partially observable, stochastic environments [7]. Markov Decision Process (MDP) planning is used when the actions have effects that can only be predicted probabilistically, but the state of the problem is always observable [3]. Partially Observable Markov Decision Process (POMDP) planning problem is used for problems where the actions have stochastic effects, but the state cannot be fully observed [3].

Hierarchical Task Networks (HTNs) are methods for solving planning problems that consist of abstract tasks and their methods (decomposition). Therefore, instead of going through all possible actions in each state, the methods decompose high-level relevant tasks to build a task network containing both compound and primitive tasks (actions) [9]. This approach can make the large problems more manageable.

The methods mentioned above are widely used for solving task planning problems. We also briefly discuss the problem of motion planning as it is relevant to construction industry challenges: The challenge of **Motion planning** is finding a feasible trajectory in space and time [2]. It includes (1) finding a path in an environment for moving a mobile system from the start position to the goal position and (2) the control law along the path considering the mobile system's dynamic limitations (speed, kinematics, and acceleration). Motion planning requires a geometric CAD model of the environment with the obstacles and free space; Methods of this planning problem deal with high dimensional geometry in a continuous environment [2]. Table 3 shows a summary of the mentioned planning methods and their main environmental characteristics.

Table 3: This table shows the main characteristic of each planning method

Planning methods		Environmental characteristics		
		Observability	State transition	Time and perception
Classical planning		Observable	Deterministic	Discrete
Numeric and temporal planning		-	-	Continuous
Probabilistic planning	MDP	Observable	Non deterministic	-
	POMDP	Partially observable		
	Conformant	Unobservable		
Motion planning methods		-	-	Continuous

4 Applications of Model-Based Planning

4.1 Classical Planning

Classical planning has applications including planning military logistics [10], and RoboCup Logistics League (RCLL) [8]. However, to use classical planning in non-deterministic and partially observable real-world problems, abstraction and hierarchy both in activities and in states have been used [8]. In robotics, a classical planner is rarely used to control a robot's motors directly. Instead, they usually assume the robot can perform a set of tasks (tasks defined with classical planning methods). Then, these tasks could be implemented in a lower-level probabilistic process [11], in custom rule-based systems [12], or in other ways to control the robot's motors. In the RCLL scenario for example, the classical planner does not need to know about the continuous coordinates of the robot and only plans the discrete move actions between the different machines [8].

4.2 Temporal and Numeric Planning

Robots could use temporal planning to (1) meet a deadline (e.g., complete a task before 6 PM), (2) meet a time window (e.g., the charging station is only operating between 2 and 4 PM), or (3) coordinate concurrent activities. Combinations of numeric and temporal planning allow modeling numeric changes over time, which is useful for resource management (e.g., the battery level) [8]. But, the duration of actions being executed by robots can only be observed and not controlled directly because many external factors will affect these durations. To handle this, robots need to determine when to dispatch each action for execution and to understand when the deviation of observed durations from those in the model has invalidated the plan [8].

4.3 Probabilistic Planning/ Planning Under Uncertainty

MDPs and POMDPs have been used for optimizing dam management in hydroelectric power plants because, for example, a valve can get stuck and not respond correctly to a signal from the controller (stochastic actions), errors in the flow measurement in pipes are common (uncertainty in the state), or the level in a steam reservoir is a variable that cannot be observed directly (partial observability) [13]. But probabilistic planning requires a precise representation of the possible states and actions, which leads to exponential growth of the problem space and limits their use for real-world problems. In dam management, the challenge of state and action exponential growth has been addressed through factored representations, which uses Bayesian networks [13]–[15]. Another challenge with using MDP is that they become difficult to solve for large problems with hundreds of state variables. In this case, abstraction or decomposition strategies might help [16].

4.4 Motion Planning

Free-space motion is the most basic motion planning problem, in which the agent must just move across space without colliding with anything [17]. Multimodal motion planning extends the problem

Table 4: This table shows potential planning methods for each of the construction process categories.

	Construction planning categories	Planning methods				
		Classical	Temporal and Numeric	Probabilistic	Hierarchical task network	Motion planning methods
1	Scheduling and dispatching of RMC trucks	×	×	×	-	-
2	Resources allocation and leveling	-	×	×	-	-
3	Impact of buffers in construction processes	-	×	×	×	-
4	Scheduling linear projects	-	×	×	×	-
5	Time, cost and quality	-	×	×	-	-
6	Large infrastructure projects .	-	×	×	×	-
7	Robotic assembly	×	-	×	×	×

space to include changing the state of other objects in the world [17], [18]. However, for a robot to act fully autonomously, planning needs to be in a hybrid environment that contains both discrete and continuous actions and variables. For example, if the problem is packing some boxes into a defined region, we need to model both discrete (e.g., move, pick, boxes) and continuous (e.g., robot trajectory, box poses) variables and actions [19]. To solve this, research has devised fully integrated task and motion planning tools, such as PDDLStream [19].

5 Potential Uses of Model-Based Planning in Construction

Model-based planning can be applied to construction process planning categories and challenges mentioned in Section 2 . However, construction processes are non-deterministic and large; thus, we should solve them by combining several planning methods. For instance, scheduling and dispatching of RMC trucks can be modeled as a hybrid of (1) classical planning for finding the shortest path to the construction sites, (2) temporal and numeric planning for dispatching hours, costs, and revenues, (3) probabilistic for considering delays, accidents and other things that can interrupt the delivery process. Table 4 shows the potential methods for the rest of the construction planning categories.

As shown in Table 4, probabilistic planning is a part of all the construction processes since they are rarely deterministic. The plan should consider all the possibilities that might happen after performing an action. However, this is not possible in real world construction problems and requires other measures as mentioned in Section 4.3.

Temporal and numeric planning can automate schedule planning and schedule optimization in construction projects. For example, costs, labor, material and time are linear continuous variables that can be planned and scheduled automatically using temporal and numerical planning methods (Table 4).

Classical planning is used for planning parts of the process that include discrete objects. It can be used to sequence and allocate the tasks in a construction process, since the tasks are discrete variables.

Motion planning is concerned with geometry. So, the kinematic limits of the robots and their trajectory and path planning in the construction site is done by motion planning. For robotic assembly of building parts, integrating task and motion planning methods looks promising as it includes both discrete and continuous actions and variables. For example, the building components are discrete variables and the location of them are continuous variables.

Additionally, we can use abstraction and hierarchy (HTN) for modeling larger problem domains, as shown in the examples in Section 4.

Model-based planning also has the potential to address the challenges In Section 2 : Formal representation (C1): each method of planning provides the essential language requirements for formally representing the problem. Inflexibility of knowledge base (C2): once the model is properly built for a problem, it can solve any instance of that problem automatically. Also, using probabilistic planning methods can increase the flexibility of the knowledge base. Decoupled nature of planning and scheduling (C3): planning and scheduling are merged in temporal and numerical planning.

5.1 Conclusion

Model-based AI planning uses symbols to model the problem and then logic to solve them. Recent reviews on automated planning in construction suggest that formal representation, the rigidity of process templates, and the decoupled nature of planning and scheduling are among the reasons that hinder the use of existing automated planning systems [4]. Based on these insights, we conclude that different methods for task planning, e.g., classical, temporal, probabilistic, and motion planning have different advantages, limitations, and applications. Classical planning can be used for parts of the problems that are discrete, like finding the shortest path in a delivery process. Temporal planning can be used for processes that include resources and scheduling. Probabilistic planning is a part of all construction processes. These methods should be used together as construction processes are complex and cannot be modeled with a single planning method. Finally, a hybrid of task and motion planning methods has the potential for automating robotic assembly in construction. Discussing the languages for modeling these methods and planners that solve them using different algorithms and heuristics, and learning methods are beyond the scope of this paper, but are discussed in [2]–[4], [7], [20].

Acknowledgements

Financial support was provided by Artificial Intelligence Software Academy (AISA), University of Stuttgart.

References

[1] P. Hitzler and M. K. Sarker, editors, *Neuro-symbolic artificial intelligence: the state of the art*, ser. Frontiers in artificial intelligence and applications / FAIA 342. Washington: IOS Press, 2022.

[2] M. Ghallab, D. S. Nau, and P. Traverso, *Automated planning: theory and practice*. Amsterdam ; Boston: Elsevier/Morgan Kaufmann, 2004.

[3] H. Geffner and B. Bonet, *A concise introduction to models and methods for automated planning*, eng, ser. Synthesis lectures on artificial intelligence and machine learning 22. San Rafael: Morgan & Claypool Publishers, 2013.

[4] F. Amer, H. Y. Koh, and M. Golparvar-Fard, “Automated Methods and Systems for Construction Planning and Scheduling: Critical Review of Three Decades of Research”, en, *Journal of Construction Engineering and Management*, vol. 147, no. 7, (ASCE)CO.1943–7862.0002093, 03 121 002, Jul. 2021.

[5] S. O. Abioye, L. O. Oyedele, L. Akanbi, *et al.*, “Artificial intelligence in the construction industry: A review of present status, opportunities and future challenges”, *Journal of Building Engineering*, vol. 44, 2021.

[6] B. R. Sarker, P. J. Egbelu, T. W. Liao, and J. Yu, “Planning and design models for construction industry: A critical survey”, en, *Automation in Construction*, vol. 22, pp. 123–134, Mar. 2012.

[7] S. J. Russell, P. Norvig, and E. Davis, *Artificial intelligence: a modern approach*, 3rd ed, ser. Prentice Hall series in artificial intelligence. Upper Saddle River: Prentice Hall, 2010.

[8] E. Karpas and D. Magazzeni, “Automated Planning for Robotics”, en, *Annual Review of Control, Robotics, and Autonomous Systems*, vol. 3, no. 1, pp. 417–439, May 2020.

[9] D. Holler, G. Behnke, P. Bercher, and S. Biundo, “Language Classification of Hierarchical Planning Problems”, in *ECAI*, Prague, Czech Republic, 2014, pp. 447–452.

[10] S. S. Chouhan and R. Niyogi, “Multi-agent planning with quantitative capability”, in *2016 International Conference on Advances in Computing, Communications and Informatics (ICACCI)*, Jaipur, India: IEEE, Sep. 2016, pp. 602–606.

[11] G. Konidaris, L. P. Kaelbling, and T. Lozano-Perez, “From Skills to Symbols: Learning Symbolic Representations for Abstract High-Level Planning”, *Journal of Artificial Intelligence Research*, vol. 61, pp. 215–289, Jan. 2018.

[12] T. Niemueller, T. Hofmann, and G. Lakemeyer, “CLIPS-based Execution for PDDL Planners”, in *Proceedings of the 28th International Conference on Automated Planning and Scheduling (ICAPS), Workshop on Integrated Planning, Acting, and Execution (IntEx)*, Delft, The Netherlands, 2018.

[13] A. Reyes, L. E. Sucar, P. H. Ibargüengoytia, and E. F. Morales, “Planning Under Uncertainty Applications in Power Plants Using Factored Markov Decision Processes”, en, *Energies*, vol. 13, no. 9, May 2020, ISSN: 1996-1073.

[14] C. Boutilier, R. Dearden, and M. Goldszmidt, “Stochastic dynamic programming with factored representations”, en, *Artificial Intelligence*, vol. 121, no. 1-2, pp. 49–107, Aug. 2000.

[15] A. Darwiche and M. Goldszmidt, “Action Networks: A Framework for Reasoning about Actions and Change under Uncertainty”, en, in *Uncertainty Proceedings 1994*, Elsevier, 1994, pp. 136–144.

[16] A. Reyes, P. Ibargüengoytia, L. E. Sucar, and E. Morales, “Abstraction and Refinement for Solving Markov Decision Processes. In Workshop on Probabilistic Graphical Models”, in *Citeseer*, Prague, Czech Republic, 2006, pp. 263–270.

[17] C. R. Garrett, R. Chitnis, R. Holladay, *et al.*, “Integrated Task and Motion Planning”, en, *Annual Review of Control, Robotics, and Autonomous Systems*, vol. 4, no. 1, pp. 265–293, May 2021.

[18] K. Hauser and V. Ng-Thow-Hing, “Randomized multi-modal motion planning for a humanoid robot manipulation task”, en, *The International Journal of Robotics Research*, vol. 30, no. 6, pp. 678–698, May 2011.

[19] C. R. Garrett, T. Lozano-Pérez, and L. P. Kaelbling, “PDDLStream: Integrating Symbolic Planners and Blackbox Samplers via Optimistic Adaptive Planning”, *arXiv:1802.08705 [cs]*, Mar. 2020.

[20] P. Haslum, editor, *An Introduction to the Planning Domain Definition Language*, eng, ser. Synthesis Lectures on Artificial Intelligence and Machine Learning 42. S.l.: Morgan et Claypool Publishers, 2019.

Mixture-of-Experts-Ensemble Meta-Learning for Physics-Informed Neural Networks

Rafael Bischof[1] and Michael A. Kraus[2]
[1]Swiss Data Science Center, Turnerstrasse 1, 8092 Zürich, Switzerland
[2]Design++ and Chair of Concrete Structures and Bridge Design (IBK), ETH Zürich, Stefano-Franscini-Platz 5, 8093 Zürich, Switzerland
E-mail(s): rafael.bischof@sdsc.ethz.ch, kraus@ibk.baug.ethz.ch

Abstract: Partial Differential Equations (PDEs) arise in natural and engineering sciences to model reality and allow for numerical assessment of these phenomena. Classical numerical solutions for PDEs rely on discretisations such as e.g. the finite or spectral element method (FEM/SEM). Physics Informed Neural Networks (PINN) leverage physical laws by including PDE together with a respective set of boundary and initial conditions (BC / IC) as penalty terms into their loss function during training without the need for discretisation. However, as the computational domain or the nonlinearity of the PDE becomes more complex, finding PDE solutions via FEM/SEM as well as PINNs becomes hard. Mixture of Experts (MoE) is a probabilistic model, consisting of local experts weighted by a gating network. As in ensemble methods, MoE involves decomposing predictive modeling tasks into sub-tasks, i.e. training an expert model on partitions of the input space, and devising a gating model that learns to weight the experts' predictions conditioned on the input. In this work, we combine the two methods to form Physics Informed Mixture of Neural Network Experts (PIMNNE) / Mixture of Experts Physics Informed Neural Networks (MoE-PINNs) and investigate the learning and predictive capabilities by the example of a 2-dimensional Poisson PDE over a L-shaped domain with homogeneous Dirichlet BC. Our simulation studies show, that all MoE-PINNs setups approximate the SEM reference solution to a satisfactory high degree. A hyperparameter study revealed that an increase in the number of PINN experts reduces the approximation error significantly even if regularised aggressively for sparsity. A second interesting finding is that a resolute regularisation - effectively driving weak learners importance towards zero - is to be preferred over a uniform penalty. We also found the most popularly used *tanh* activation function for PINNs being consistently discarded by the gating network, while PINNs with *sine* activations provided an additional boost of performance. Our proposed Moe-PINNs in the future serve as differentiable computational performance predictors for computational mechanics or fluid dynamics applications in design and verification of structures.

Keywords: Physics-Informed Machine Learning, Multi-Objective Optimisation (MOO), Ensemble Methods, Computational Mechanics

1 Introduction and Related Work

During the design and verification of engineering structures, PDEs are employed to describe and model the mechanical or fluid behavior in order to allow for a computational assessment, design and verification. Solving partial differential equations (PDEs), which arise from various first-order principles in natural and engineering sciences, by using neural networks was first introduced by Lagaris et al. [1] and revived in 2017 by Raissi et al. [2], who coined the term Physics-Informed Neural Networks (PINNs). By leveraging physical laws and the power of automatic differentiation, readily implemented in all major deep learning libraries, they require just a few lines of code to be implemented and trained. Further boosted by industry scale software packages like "Modulus" by NVIDIA [3], PINNs have so far been successfully applied to various linear and nonlinear PDEs from e.g. computational mechanics , fluid dynamics [2] and more. Often however, a number of pathologies have been observed at training time, impeding proper training and ultimately leading to unsatisfactory solutions. Addressing these pathologies in PINNs is an active area of research and a number of extensions have recently been proposed, such as building specialised architectures that favor backpropagation [4], or improving the network initialisation by resorting to meta learning [5].

Analogously to major established numerical solution methods such as the finite element method (FEM), which split (i.e. discretise) the domain prior to optimisation, cPINNS or XPINNs [6] apply different networks to slightly overlapping partitions of the domain in a divide and conquer fashion. While having several advantages over vanilla PINNs, such as larger representation capabilities and the possibility of distributed computing, selecting the optimal number of networks to distribute over the domain and defining the boundaries between partitions are sensitive hyperparameters that require considerable labour to tune. Instead, Stiller et al. proposed GatedPINNs [7], a framework leveraging multiple networks as an ensemble and an additional learner acting as the gate, which appoints the various models to partitions of the domain. Such frameworks have been successfully applied in different fields of ML and are known as Mixtures of Experts (MoE) [8]. It allows the individual learners to specialise on distinct subsets of the data, while also providing the possibility to average the results of several experts in challenging areas of the input space [9]. MoE have been of particular interest in multitask learning problems, as devising different portions of the model for different tasks while keeping some shared layers constitutes an effective way of reducing the bias-variance trade-off. PINNs are similar to multitask learning problems in that they have to optimise multiple different terms representing the governing equation as well as one or more IC and/or BC.

2 Contribution and Methods

We introduce a number of extensions to the original formulation of GatedPINNs and demonstrate their effectiveness on a new benchmark for ensembles of PINNs. We will hereafter be referring to GatedPINNs including our extensions as MoE-PINNs.

- We add a regularisation term to the loss function, which in a data-driven fashion incentives the model to utilise as few PINNs as possible.
- We show that this regularisation can act as an automated and differentiable architecture search by initialising a large bag of PINNs with varying depth, width and activation functions, and letting the gating network select the most suitable subset of models at training time.
- We apply MoE-PINNs to a new benchmark for ensembles of PINNs, the Poisson equation on a L-shaped domain (as investigated initially in [6], used as validation reference here).

2.1 Physics-Informed Neural Networks (PINNs)

Consider the following abstract parameterised and nonlinear PDE problem:

$$\begin{aligned} \text{PDE} &: \mathcal{F}\left(\hat{\mathbf{u}}, \partial_t\hat{\mathbf{u}}, \partial_x\hat{\mathbf{u}}, \cdots; \mu\right) = 0, \quad \mathbf{x} \in \Omega, t \in [0, T] \\ \text{B.C.} &: \mathcal{B}\left(\hat{\mathbf{u}}, \partial_x\hat{\mathbf{u}}, \partial_x^2\hat{\mathbf{u}}, \cdots\right) = 0, \quad \mathbf{x} \in \Gamma \\ \text{I.C.} &: \mathcal{C}\left(\hat{\mathbf{u}}, \partial_t\hat{\mathbf{u}}, \partial_t^2\hat{\mathbf{u}}, \cdots\right) = 0, \quad t \in \Upsilon \end{aligned} \tag{1}$$

where $\mathbf{x} \in \mathbb{R}^d$ is the spatial coordinate and t is the time; $\mathcal{F}$ denotes the residual of the PDE, containing the differential operators (i.e. $\partial_{\mathbf{x}}\hat{\mathbf{u}}, \partial_t\hat{\mathbf{u}}, ...$); $\mu = [\mu_1, \mu_2, ...]$ are the PDE parameters; $\hat{\mathbf{u}}(\mathbf{x}, t)$ is the solution of the PDE with initial condition $\mathcal{C}$ and boundary condition $\mathcal{B}$ (which can be Dirichlet, Neumann or mixed); Ω, Γ and Υ represent the spatial domain resp. boundaries. In order to find the unknown function $\hat{\mathbf{u}}(\mathbf{x}, t)$, satisfying the residual $\mathcal{F}$ as well as the boundary- and initial conditions, $\mathcal{B}$ and $\mathcal{C}$, Raissi et al. [2] proposed to use a neural network $U(\mathbf{x}, t; \theta)$ as solution to the nonlinear PDE problem of eq. 1, and train it to optimally approximate the conditions $\mathcal{F} = 0$, $\mathcal{B} = 0$ and $\mathcal{C} = 0$. This is achieved by taking the necessary derivatives of U through automatic differentiation (AD), inserting these expressions into $\mathcal{F}$, $\mathcal{B}$ and $\mathcal{C}$, applying the mean squared error and training the network as a scalarised multi-objective optimisation, where the several terms are aggregated using weights [10].

2.2 Ensemble Learners and Mixture-of-Experts

Mixture of Experts (MoE) is an ensemble learning technique implementing a training of experts on subtasks (e.g. a particular data region) of a predictive modeling problem [11]. The MoE model works in a four-step fashion: (i) division of a task into subtasks, e.g. by decomposition of the input space, (ii) develop an expert for each subtask, (iii) use a gating model to decide which expert to use, and (iv) pool expert outputs and gating model output to make a prediction. The subtasks may or may not overlap, and experts from similar or related subproblems may be able to contribute to the examples that are technically outside of their expertise. The MoE regressor is defined as

$$g(x) = \sum_{i}^{m} P(i|\mathbf{x}, \theta_{\mathbf{p}}) f(\mathbf{x}, \theta_{\mathbf{i}}) \tag{2}$$

with a local expert regressor $f(\mathbf{x}, \theta_i)$ and associated model parameters θ_i of expert i and a gating function P conditioned on the input $\mathbf{x}$ as well as its parameters θ_p delivering the probability of association $P(i|x, \theta_p)$ between input and expert i (i.e. the degree to which the expert contributes to the total output).

3 Mixture of Experts of Physics Informed Neural Networks (MoE-PINNs)

Employing PINNs as expert models to assemble the PDE solution and defining $\mathbf{x} = (\mathbf{x}, t)$, with $\mathbf{x}$ and t being the spacial and / or time variables, it follows that $f(\mathbf{x}, \theta_i) = U(\mathbf{x}, t; \theta_i)$ (cf. Fig. 1). As the gating network represents the conditional probability $P(i|\mathbf{x}, \theta_i)$ of datum $\mathbf{x}$ given by expert m_i, a proper gate is formulated via the *softmax* function:

$$\lambda(\mathbf{x})_i = \frac{\exp(P(i|\mathbf{x}, \theta_i))}{\sum_{j=1}^{m} \exp(P(j|\mathbf{x}, \theta_j))} \tag{3}$$

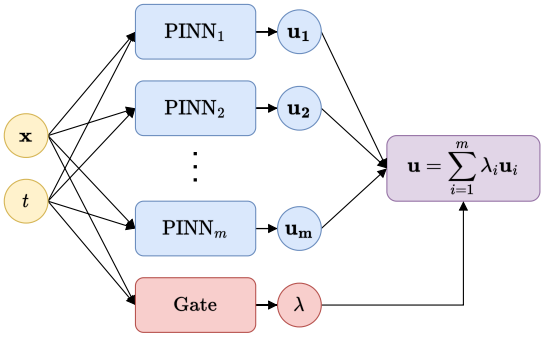

Figure 1: Mixture-of-Experts PINN.

where $\lambda(\mathbf{x})_i$ is called "importance" of expert i.

As previously established, the number of experts in the ensemble m constitutes an additional, sensitive hyperparameter. In order to reduce the laborious process of hyperparameter-tuning, we introduce a sparsity inducing regularisation to act as data-driven selection of the amount of experts m.

$$\mathcal{L}_{sp} = \left| \frac{1}{|B|} \sum_{i}^{m} \sum_{\mathbf{x} \in B} \lambda_i(\mathbf{x}) \right|^p \tag{4}$$

where B is a batch of collocation points (x, t) and p is a hyperparameter. We are particularly interested in selecting $0 < p \leq 1$, as these values yield a regularisation term that penalises small values more than larger ones, and which will thus lead to more sparsity in the importances across experts.

4 Results: Poisson's Equation on L-shaped Domain

The Poisson equation is a second-order, elliptic partial differential equation and has many applications in natural or engineering sciences, e.g. the elastostatic problem of a rod under a torsion load, the Helmholtz equation in dynamically excited continua without bending stiffness or the equilibrium displacement of a stretched membrane subjected to a distributed force. Given the brevity of this paper, we investigate the solution efficiency and quality of the MoE-PINNs approach for solving the Poisson's problem, defined over a 2-dimensional L-shaped domain Ω with homogeneous Dirichlet boundary conditions on Γ:

$$\begin{aligned} -\Delta u(x, y) &= 1, \quad (x, y) \in \Omega = [-1, 1]^2 \setminus [0, 1]^2 \\ u(x, y) &= 0, \quad (x, y) \in \Gamma \end{aligned} \tag{5}$$

The training data for MoE-PINNs is sampled at the collocations points within the domain Ω as $\{x_i, \mathcal{F}(x_i)\}_{i=1}^{N_\Omega=683}$ and on the boundary $\{x_{\Gamma,i}, \mathcal{B}(x_{\Gamma,i})\}_{i=1}^{N_\Gamma=341}$.

Table 1: Performance of MoE-PINNs with different configurations and *tanh* activation function. MSE u denotes the mean squared error between the prediction and the reference solution computed using the spectral element method (SEM).

# of experts m	Depth	Width	Parameters	Order p	MSE u	MSE u GatedPINN
1	3	128	33'537	none	$8.32 \cdot 10^{-5}$	
1	3	256	132'609	none	$8.73 \cdot 10^{-5}$	
3	3	128	105'164	none	$9.42 \cdot 10^{-5}$	$9.06 \cdot 10^{-4}$
3	3	128	105'164	0.25	$5.93 \cdot 10^{-5}$	
3	3	128	105'164	0.5	$8.27 \cdot 10^{-5}$	
3	3	128	105'164	2	$1.08 \cdot 10^{-4}$	
4	3	128	138'767	none	$7.78 \cdot 10^{-5}$	$1.38 \cdot 10^{-3}$
4	3	128	138'767	0.25	$6.38 \cdot 10^{-5}$	
4	3	128	138'767	0.5	$6.89 \cdot 10^{-5}$	
4	3	128	138'767	2	$7.69 \cdot 10^{-5}$	
5	3	128	172'370	none	$7.70 \cdot 10^{-5}$	$1.71 \cdot 10^{-3}$
5	3	128	172'370	0.25	$8.28 \cdot 10^{-5}$	
5	3	128	172'370	0.5	$7.75 \cdot 10^{-5}$	
5	3	128	172'370	2	$8.56 \cdot 10^{-5}$	

For ease of interpretation of the results, we manually varied the values of only a selection of the most important hyperparameters. More specifically, we first compared ensembles containing $m \in \{1, 3, 4, 5\}$ experts, each with a depth of 3 layers, a width of 128 nodes each and the hyperbolic tangent as activation function. In a second step, the experiments involving the automated architecture search were conducted on a more diverse set of architectures. We initialised the PINN experts in the ensemble with the activation functions *tanh*, *sigmoid*, *sine*, *softplus* or *swish*, varied the depth between 1 and 4 layers and selected the width from the set 32, 64, 128, 256. Since the experiments were all conducted on the Poisson PDE with L-shaped domain, we kept the hyperparameters of the gating network fixed at depth 2, width 64 and used the hyperbolic tangent as activation function. In addition to the losses from the PINNs and the gating NN, a penalisation of the number of experts is added by setting a sparsity order p. The contributions of the terms in the objective function are balanced using ReLoBRaLo [10]. Furthermore, we initialised the learning rate of the Adam optimiser at 0.001 and decreased it by a multiplicative factor of 0.1 whenever the optimisation stopped making progress for over 3'000 optimisation steps and finally used early stopping in the event of 9'000 steps without improvement, followed by an additional 15'000 iterations of L-BFGS. The validation data (ground truth $\bar{u}$) are taken from [12] and were obtained using the spectral element method (SEM). All computations in the scope of this study were performed on a NVIDIA A5000 GPU. Table 1 summarises the performances of MoE-PINNs with different configurations and compares them to GatedPINNs with similar configurations. Note that the largest improvement over the baseline GatedPINNs stems from replacing the *ReLU*

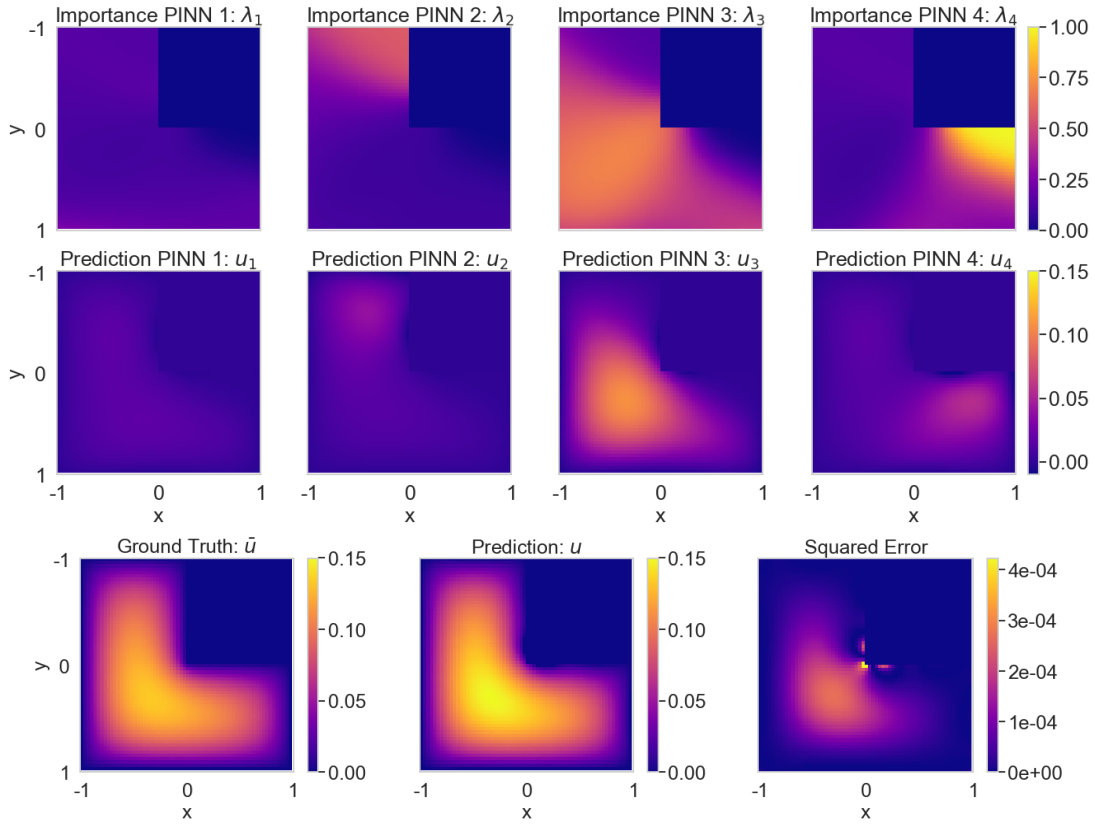

Figure 2: Results for a MoE-PINN containing 4 experts with depth 3, width 128, *tanh* activation function and sparsity order p = 0.5. Top row: distribution and magnitude of the importances for each PINN in the ensemble. Center row: output of each individual PINN. Bottom row: ground truth and prediction of the entire ensemble.

activation function in the gate with the infinitely, continuously differentiable function *tanh*. Finally, the results for the automated and differentiable architecture search with MoE-PINNs for different activation functions and varying number of experts is presented in Fig. 3.

5 Discussion and Conclusions

In general, we can show that all MoE-PINNs setups approximate the reference solution to a satisfactory degree. It can be observed that an ensemble of three learners noticeably improves the performance over the baseline model with a comparable number of parameters. However, the accuracy deteriorates when increasing the number of experts beyond 3. Thus, we conjecture that the sparsity regularisation is not enough for the MoE-PINNs to automatically tend towards the optimal number of three experts and dropping any additional networks in the ensemble. However, note that choosing the sparsity regularisation p = 0.5 results in a lower error than the less aggressive p = 2 across all conducted experiments. This indicates that a resolute regularisation, which effectively drives weak learners towards zero importance, is to be preferred over a more uniform division of the domain. Future research will therefore evolve around model pruning, where experts falling below a certain threshold of

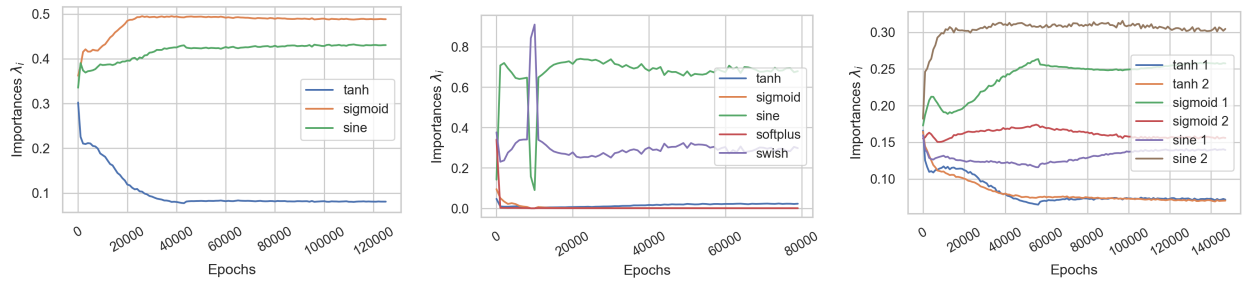

Figure 3: Evolution of the importances λ_i averaged over the entire batch of random collocation points per expert PINN with different activation functions with a total number of experts equal to the number of lines in each plot.

importance are removed from the ensemble and the model subsequently fine-tuned solely with the remaining experts.

Fig. 2 illustrates the results of a MoE-PINN with four equivalent experts. It is noticeable that the gating network opted for almost completely dropping one expert under the sparsity regularisation, and divided the domain symmetrically amongst the remaining PINNs by assigning one dominant expert to each of the three quadrants.

When inspecting the importances in ensembles of very diverse experts, i.e. consisting of a variable number of layers and nodes, as well as different activation functions, it was surprising to observe that the gating consistently discarded the networks with *tanh* activations (c.f. Fig. 3), as the *tanh* is one of the most common choices in the literature of PINNs. On the other hand, MoE-PINNs containing the *sine* activation performed exceedingly well compared to the case where a single PINN was initialised with this same activation function. There have been several attempts at making use of the *sine* function due to its well-behaved derivatives, but it has so far not been able to depose *tanh* or *swish* as the most popular choices. The observations in Figure 3 suggest that an ensemble of networks with *sine* activations may provide this function with an additional boost of performance. Finally, the notion of a linear combination of *sine* waves ties in nicely with the popular signal decomposition as used for example in the Fourier Transform.

Future research is concerned with inspection of performance, efficiency, robustness and scalability of MoE-PINNs to other PDE families arising in civil engineering.

Acknowledgements

The authors would like to thankfully acknowledge the facilities of Design++ at ETH Zürich and the funding through ETH Foundation grant No. 2020-HS-388 (provided by Kollbrunner/Rodio) as well as the SDSC Project "Domain-Aware AI-augmented Design of Bridges (DAAAD Bridges)".

References

[1] I. E. Lagaris, A. Likas, and D. I. Fotiadis, “Artificial neural networks for solving ordinary and partial differential equations”, *IEEE transactions on neural networks*, vol. 9, no. 5, pp. 987–1000, 1998.

[2] M. Raissi, P. Perdikaris, and G. E. Karniadakis, “Physics Informed Deep Learning (Part II): Data-driven Discovery of Nonlinear Partial Differential Equations”, *arXiv*, 2017.

[3] *Nvidia modulus*, 2022. [Online]. Available: https://developer.nvidia.com/modulus.

[4] S. Wang, Y. Teng, and P. Perdikaris, “Understanding and mitigating gradient pathologies in physics-informed neural networks”, *arXiv e-prints*, arXiv:2001.04536, arXiv:2001.04536, Jan. 2020. arXiv: 2001.04536 [cs.LG].

[5] X. Liu, X. Zhang, W. Peng, W. Zhou, and W. Yao, “A novel meta-learning initialization method for physics-informed neural networks”, *arXiv preprint arXiv:2107.10991*, 2021.

[6] A. Jagtap and G. Karniadakis, “Extended physics-informed neural networks (xpinns): A generalized space-time domain decomposition based deep learning framework for nonlinear partial differential equations”, *Communications in Computational Physics*, vol. 28, pp. 2002–2041, Nov. 2020.

[7] P. Stiller, F. Bethke, M. Böhme, *et al.*, “Large-scale Neural Solvers for Partial Differential Equations”, *arXiv e-prints*, arXiv:2009.03730, arXiv:2009.03730, Sep. 2020. arXiv: 2009.03730 [cs.LG].

[8] R. Jacobs, M. Jordan, S. Nowlan, and G. Hinton, “Adaptive mixture of local expert”, *Neural Computation*, vol. 3, pp. 78–88, Feb. 1991.

[9] S. Masoudnia and R. Ebrahimpour, “Mixture of experts: A literature survey”, *Artificial Intelligence Review*, vol. 42, no. 2, pp. 275–293, 2014.

[10] R. Bischof and M. Kraus, “Multi-Objective Loss Balancing for Physics-Informed Deep Learning”, *arXiv*, Oct. 2021.

[11] C. Zhang and Y. Ma, *Ensemble machine learning: methods and applications*. Springer, 2012.

[12] L. Lu, X. Meng, Z. Mao, and G. E. Karniadakis, “DeepXDE: A deep learning library for solving differential equations”, *arXiv e-prints*, arXiv:1907.04502, arXiv:1907.04502, Jul. 2019. arXiv: 1907.04502 [cs.LG].

Teil IX

Industry Foundation Classes & BIM Collaboration Format

IFC2TSO – Algorithmic processing, complexity reduction, and transfer of information regarding technical systems from IFC to TSO

Nicolas Pauen[1], Jérôme Frisch[1] and Christoph van Treeck[1]
[1]Institute of Energy Efficiency and Sustainable Building - E3D, RWTH Aachen University, Mathieustraße 30, 52074 Aachen, Germany
E-mail(s): pauen@e3d.rwth-aachen.de

Abstract: Technical systems in the Architecture, Engineering, Construction and Operations (AECO) industry are complex interconnected structures that are interdependent with each other and with spatial entities. Building Information Modeling (BIM) makes it possible to represent these systems using structured, digital information in machine-readable representations. However, not all hierarchical, topological, and functional aspects of technical systems can be represented in current data models and linked with information on further domains. Therefore, ontologies such as the TUBES System Ontology (TSO), which are based on Semantic Web Technologies (SWT), offer representations of building service systems and the possibility to link information web-based on data level. To improve the application of TSO in particular and knowledge representations based on SWT in general and, thus, to create a concrete added value in practice, appropriate tools have to be designed or the concepts have to be integrated into existing software applications. This contribution proposes a workflow for algorithmic processing, topological complexity reduction, and transfer of the information regarding technical systems from Industry Foundation Classes (IFC) models to TSO. The process has a modular structure consisting of three individual process steps IFC2GRAPH, GRAPH, and GRAPH2TSO, which can be used independently and, thus, also for review processes and quality assurance of technical systems in BIM models. The proposed workflow is implemented and validated using two application examples.

Keywords: BIM, IFC, Building Service Systems, Linked Data, TUBES System Ontology

1 Introduction

In recent years, the use of Semantic Web Technologies (SWT) in the Architecture, Engineering, Construction and Operations (AECO) industry has increased significantly [1]. For this purpose, different ontologies, such as the Building Topology Ontology (BOT) [2], Semantic Sensor Network

(SSN)/ Sensor, Observation, Sample, and Actuator (SOSA) ontology [3], Smart Applications Reference (SAREF) ontology [4], and the BRICK Schema [5] have been developed, covering various use cases. Another recent development is the TUBES System Ontology (TSO) [6], which aims to explicitly define interconnected technical systems in the AECO industry, their hierarchical structure, structural and functional relationships, and links to spatial entities. As such, TSO supports the effort to represent linkable information in a future semantic web of building data. To improve the application of TSO in particular and knowledge representations based on SWT in general and, thus, to create a concrete added value in practice, appropriate tools have to be designed or the concepts have to be integrated into existing software applications. Efforts such as the transformation of Industry Foundation Classes (IFC) into the Web Ontology Language (OWL) [7] and the Linked Building Data Converter [8] offers the possibility to transfer and represent data from IFC files. But the quality of the data cannot be checked nor can the information be enriched to represent additional concepts of building service systems which are not included in IFC.
Therefore, this work proposes a workflow for algorithmic processing, topological complexity reduction, and transfer of information regarding technical systems from IFC models to TSO which enhances the work presented in [9]. The process has a modular structure consisting of three individual process steps IFC2GRAPH, GRAPH, and GRAPH2TSO, which can be used independently and, thus, also for review processes and quality assurance of technical systems in BIM models. Each process step focuses on a different aspect of technical systems. In IFC2GRAPH, topological information is considered and missing semantic links can be enriched based on the position of the components. GRAPH focuses on hierarchical information and the complexity reduction of topological data. GRAPH2TSO focuses on the functional information and dependencies between technical systems and spatial entities that can be enriched based on spatial representations. The results of each process step can also be exported as a BIM Collaboration Format (BCF) files to allow verification in the authoring software. The workflow is implemented as a Command Line Interface application based on Python 3.7.12 and validated using the fictitious DigitalHub [10] and a real-world project.

2 IFC2TSO

The workflow of the IFC2TSO process and the modular process steps IFC2GRAPH, GRAPH and GRAPH2TSO are visualized in figure 1 and explained in the following sections.

2.1 IFC2GRAPH

In the IFC2GRAPH process step, information regarding building service systems contained in one or multiple IFC4 models is analyzed, enriched and converted into graphs. The focus of the enrichment is on topological information. Therefore, all elements with a subclass of *IfcDistributionElement* and *IfcBuildingElementProxies* are considered. Their classes, predefined types, systems and topological connections through *IfcDistributionPorts* are analysed and parsed into a directed graph. Each node in the graph represents an element and each edge represents a topological connection. To enrich further connections and revise modeling errors, the absolute positions of these *IfcDistributionPorts*

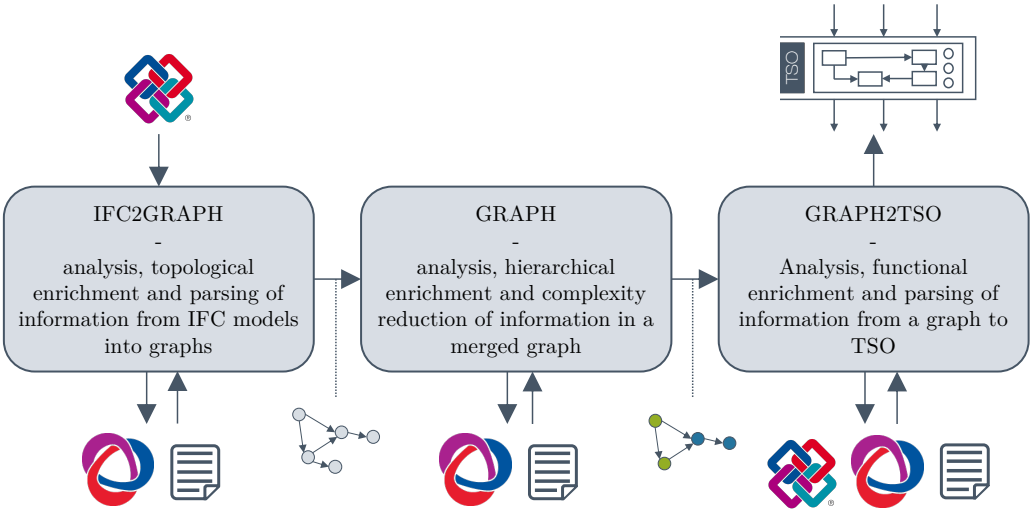

Figure 1: Schematic visualization of the IFC2TSO process

are calculated using a recursive algorithm and organized in a R-tree. R-trees are multidimensional, dynamic index structures, which allow efficient queries based on the location of the objects. To find possible matches for open ports, which have no connection assigned, the constructed R-tree can be queried. Hereby, ports within defined boundaries, which have no topological neighbor and the same *PredefinedType* are considered. The default boundary is 50 mm, but can be customized by the user. If these conditions apply to multiple ports, the closest port in the three-dimensional Euclidean space is selected and the connection is stored in an array. The results of the enrichment can be exported as BIM Collaboration Format (BCF) files, which enable a correction of possible errors in the original authoring software. Additionally, based on the enriched connections, further edges can be added to the graph.

2.2 GRAPH

In the GRAPH process step, the resulting graphs are merged and the contained information is enriched by a hierarchical structure and reduced in its topological complexity. During merging, the user can explicitly define further edges between components of different IFC models. Based on given IFC systems, classification of components and their topological structure, system aggregations on different levels of hierarchy are enriched. For the top level integrated systems, the merged graph is examined for connectivity. For each weakly connected subgraph with a size of at least R, which can be assigned by the user to clear up interfering artifacts, an integrated system is created. Next, the contained functional systems and their classification are determined for each integrated system. Therefore, the IFC systems and component classifications contained in the weakly connected graph are analyzed using regular expressions. If all IFC systems and components can be unambiguously assigned to a classification of functional systems presented in https://w3id.org/tso, the assumption is made that the integrated system consists only of one functional system of the analyzed classification. Thus, the definition as an integrated system is discarded. If more than one differently classified functional system exists in the weakly connected system, the boundaries of the functional systems are defined

based on the given IFC systems and enriched accordingly. This hierarchical structure can be further enriched based on explicit input of the user in the form of a JSON file to take complex structures and detailed subdivisions into consideration.
For the reduction of complexity and memory requirement, the topological complexity of the graph is reduced while maintaining the same topological information content. It is assumed, that active elements, such as sensors, valves, and energy converters, have a higher topological value than passive components, such as pipes, ducts, or corresponding fittings. The topological value of each node is calculated based on its classification and the number of its neighbors. If the number of neighbors is less than three and the classification of the component is a subclass of *IfcFlowSegment* or *IfcFlowFitting*, the node is considered irrelevant and is removed from the graph along with the connected edges. Based on this, a new edge is added that connects the neighbors of the removed node. All edges have the attribute *node_ids* assigned, in which the GUIDs of the reduced nodes are stored. This process of aggregation is performed iteratively until the number of nodes before and after an iteration does not change anymore.

2.3 GRAPH2TSO

In the GRAPH2TSO process step, the functional information contained in the graph is analyzed, enriched and transferred to TSO. The focus of the enrichment is on functional concepts and the relation to spatial entities. To enrich the correct flow direction and the transferred matter, energy or data, additional user input is needed. Based on explicit input, search algorithms, such as depth-first search, are used to evaluate different system topologies in an efficient and scalable way.
Additionally, spatial entities, which are included in a given IFC4 model can be analysed and their relationships to technical system can be enriched. All spatial entities as subclasses of *IfcSpatialElement*, are transferred while taking their hierarchical subdivision into consideration. In addition, their geometric representations are transformed into a triangulated tessellation. Based on the position of the components, which were calculated in the IFC2GRAPH process step and stored as parameters in the graph, the location of the components in these spatial entities can be enriched by calculating the *signed distance* to the triangulated tessellations. Moreover, based on the element classification and the enriched classification of upper hierarchical systems, it is determined whether a spatial entity is served by the component. This can be extended by explicit user specifications. The distinction of IFC models according to spatial concepts and technical systems is necessary, as not in every building service systems model are corresponding spatial entities. Often, these are only represented in the architecture model and, thus, the semantic relations between the spatial entities and the technical systems are not explicitly given.

3 Implementation

An implementation of the IFC2TSO process is published at https://github.com/RWTH-E3D/IFC2TSO and licensed using the MIT License. In addition, an Anaconda environment basend on python 3.7.12 with the libraries used to run the process is given. These are among others ifcopenshell 0.6.0 for

parsing the IFC models, lxml 4.6.1 for designing the XML based BCF files, NetworkX 2.5 for handling the graphs, Rtree 0.9.7 for setting up and querying r-trees, trimesh 3.10.2 for spatial dependency analysis, and rdflib 6.1.1 for conception and serialization of the knowledge representation. If the specified libraries are no longer available in the above given versions, it is possible that adjustments have to be made to the program code to ensure functionality. Optional parameters can be used to adjust the functionality of the IFC2TSO process. A subset of possible parameters is given in table 1.

Table 1: Subset of optional parameters to customize the functionality of the IFC2TSO process

Parameter	**Description**
-bcf_pm	Export of possible topological connections as compressed BCF files at the path of the model.
-ce {L}	Automated extension of the graph with directed edges, based on the possible topological connections with the maximum allowed distance of L in mm.
-cr	Reduction of the topological complexity of the merged graph.
-add_fc {JSON}	Enrichment of functional concepts, such as flow of matter, energy, and data, sources and sinks, contained in the JSON file at the given path.
-add_spatial {IFC}	Transfer of spatial concepts contained in the IFC model at the given path and the enriched dependencies to technical systems.
-ifcowl	Extension of the A-Box with classifications of components based on IFCowl.

4 Validation

The validation of the IFC2TSO process is shown based on the fictitious DigitalHub project [10] and a real-world project. Due to the page limit, the focus is set on the IFC2GRAPH process step and the enrichment of spatial relationships. The figures are created using BIMcollab ZOOM and the resulting BCF files from the IFC2TSO process. The validation was run on a MacBook Pro with 16 GB RAM and an Intel i7 dual core with 3.3 GHz.

Table 2 summarizes the results of the parsing and enrichment of topological information from IFC models to graphs. It is shown, that all elements, which have the correct class and at least one port assigned, can be exported and added as nodes. Moreover, all existing topological connections can be exported as edges. The amount of exported edges is sometimes higher than half of the amount of connected ports, since some ports have an assigned bidirectional flow, which results in two inverse directed edges. This is shown for the enrichment of additional edges based on the spatial position of the ports as well. The results of the enrichment were validated by implementing visual checks of the resulting BCF files. Two examples of enriched connections are presented in figure 2.

Table 2: Results of the parsing and enrichment of topological information in the process step IFC2GRAPH

Model	**MR** [MB]	**CwP**	**Ports**	**open Ports**	**Nodes**	**Edges**	**eE**	**RT** [s]
DH-HC	25.9	1,795	3,760	14	1,795	1,901	0	8.9
DH-V	15.0	1,310	2,656	36	1,310	1,341	0	7.4
DH-S	23.0	911	2,079	33	911	1,284	2	6.3
RWP-HC	682.0	31,607	65,385	7,103	31,607	39,724	4,116	132.1
RWP-V	191.8	12,418	24,892	186	12,418	12,710	50	60.9
RWP-S	575.2	17,024	35,181	2,951	17,024	23,719	1,618	145.1

MR = Memory Requirement, CwP = Components with Ports, eE = enriched Edges, RT = Runtime,
DH = DigitalHub, RWP = Real-World Project, HC = Heating & Cooling, V = Ventilation, S = Sanitary

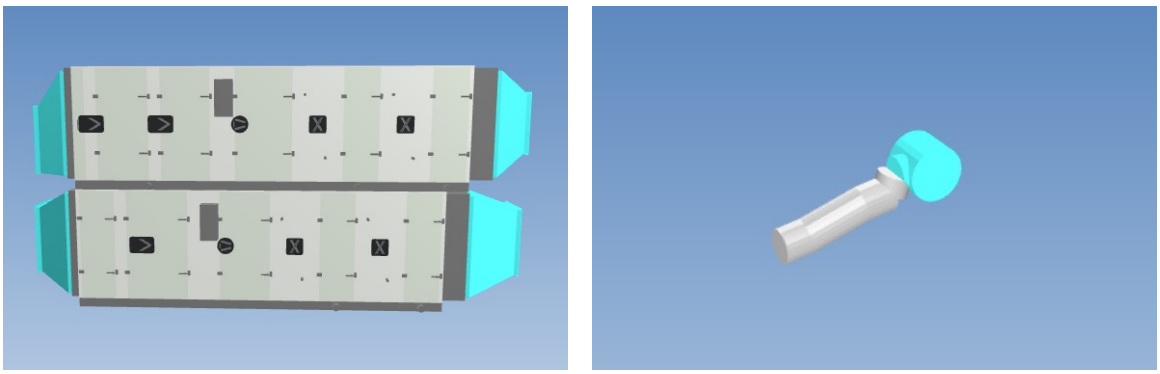

Figure 2: Visualization of components and their enriched topological connections in the ventilation model of the real-world project in BIMcollab ZOOM

The results for the enrichment of spatial concepts are given in table 3. It is shown, that all *IfcSpatialElements*, which are included in the given IFC model, could be parsed into the knowledge representation. Moreover, 2,412 spatial relationships could be enriched for the DigitalHub. This is less than the existing amount of components, since some of those are located outside of the building or in between walls. The components with an enriched relationship to a given spatial entity of the DigitalHub project and the real-world project are visualized in figure 3.

Table 3: Results of the enrichment of spatial concepts in the process step GRAPH2TSO

Model	**IfcSE**	**Spatial Instances**	**Spatial Relationships**	**MR** [MB]	**RT** [s]
DigitalHub-ARC	69	69	2,412	7.8	29.4
RWP-ARC	265	265	59,757	112.6	1412.4

IfcSE = IfcSpatialElements, RT = Runtime, MR = Memory Requirements, RWP = Real-World Project

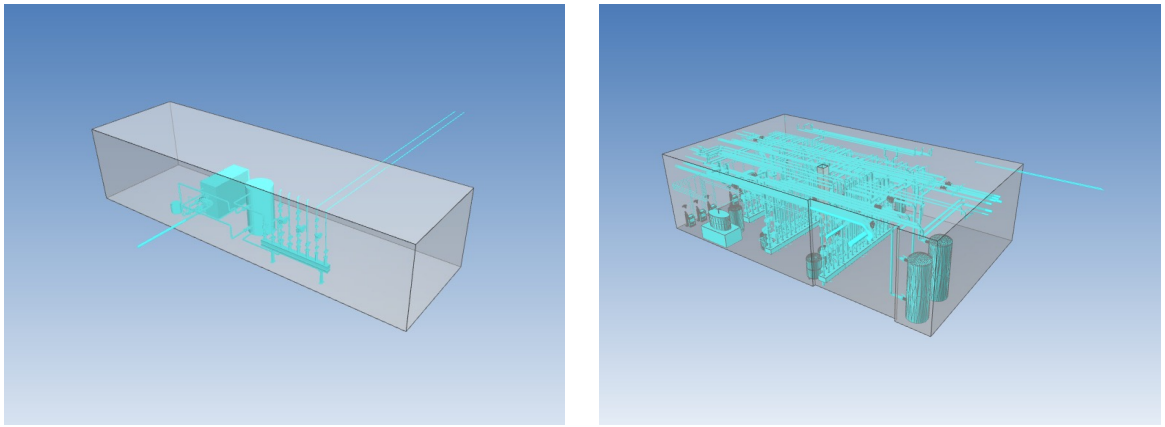

Figure 3: Visualization of components with an enriched relationship to the shown spatial entities of the DigitalHub (left) and the real-world project (right) in BIMcollab ZOOM

5 Conclusion

This contribution presents the modular IFC2TSO process for algorithmic processing, topological complexity reduction, and transfer of information regarding technical systems from IFC to TSO. IFC2TSO consists of three process steps IFC2GRAPH, GRAPH, and GRAPH2TSO, each of which can be used independently for applications such as model checking, quality control of BIM models, or for parsing data to other ontologies. Several optional parameters have been considered, allowing the user to customize the functionality. It has been shown that all relevant topological information inside the IFC models of the application examples could be successfully analyzed and parsed into a graph and subsequently into a knowledge representation. In addition, components that are not correctly connected are exported as BCF files, which enables the analysis and resolving of modelling errors in the original authoring software. Automatic enrichment of the connections is also possible, but not persistent, since the native model is not corrected. The integration of a graphical user interface is a possible field of further research. This could be implemented either by using an open tool, such as IFC.js, or by integrating the process into an existing software application, such as Autodesk REVIT. The user would thus have the opportunity to use algorithms for information enrichment of matter, energy, and data, among others, through direct interaction with the components, as well as receive direct feedback on the potential results of the enrichment. This would make the process more robust and could guarantee continuous use of the enriched data.

Acknowledgements

The research within the project EnergyTWIN leading to these results has received funding from the German Ministry for Economic Affairs and Climate Action (BMWK) under grant agreement no. 03EN1026A.

References

[1] P. Pauwels, S. Zhang, and Y.-C. Lee, “Semantic web technologies in AEC industry: A literature overview”, *Automation in Construction*, vol. 73, pp. 145–165, 2017.

[2] M. H. Rasmussen, M. Lefrancois, G. F. Schneider, and P. Pauwels, “BOT: The Building Topology Ontology of the W3C Linked Building Data Group”, *Semantic Web – Interoperability, Usability, Applicability*, 2020. DOI: https://doi.org/10.3233/SW-200385.

[3] A. Haller, K. Janowicz, S. J. D. Cox, *et al.*, “The modular SSN ontology: A joint W3C and OGC standard specifying the semantics of sensors, observations, sampling, and actuation”, *Semantic Web*, vol. 10, pp. 9–32, 2018. DOI: https://doi.org/10.3233/SW-180320.

[4] L. Daniele, F. den Hartog, and J. Roes, “Created in Close Interaction with the Industry: The Smart Appliances REFerence (SAREF) Ontology”, in *Formal Ontologies Meet Industry*, Springer International Publishing, 2015, pp. 100–112. DOI: https://doi.org/10.1007/978-3-319-21545-7_9.

[5] B. Balaji, A. Bhattacharya, G. Fierro, *et al.*, “Brick: Metadata schema for portable smart building applications”, *Applied Energy*, vol. 226, pp. 1273–1292, 2018. DOI: https://doi.org/10.1016/j.apenergy.2018.02.091.

[6] N. Pauen, D. Schlütter, J. Frisch, and C. van Treeck, “TUBES System Ontology: Digitalization of building service systems”, in *Proceedings of the 9th Linked Data in Architecture and Construction Workshop*, M. Poveda-Villalon, A. Roxin, K. McGlinn, and P. Pauwels, editors, 2021.

[7] J. Beetz, J. van Leeuwen, and B. de Vries, “IfcOWL: A case of transforming EXPRESS schemas into ontologies”, *Artificial Intelligence for Engineering Design, Analysis and Manufacturing*, vol. 23, no. 1, pp. 89–101, Dec. 2008. DOI: 10.1017/s0890060409000122.

[8] M. Bonduel, J. Oraskari, P. Pauwels, M. Vergauwen, and R. Klein, “The IFC to Linked Building Data Converter - Current Status”, in *Proceedings of the 6th Linked Data in Architecture and Construction Workshop*, 2018.

[9] N. Pauen, D. Schlütter, J. Siwiecki, J. Frisch, and C. van Treeck, “Integrated representation of building service systems: Topology extraction and TUBES ontology”, *Bauphysik*, vol. 42, no. 6, pp. 299–305, 2020. DOI: https://doi.org/10.1002/bapi.202000027.

[10] N. Pauen, L. Unruh, D. Schlütter, J. Siwiecki, J. Frisch, and C. van Treeck, “Technical Report: IFC Modell DigitalHub”, Tech. Rep., 2020. DOI: https://doi.org/10.18154/RWTH-2020-11683.

B-Spline Surfaces in IFC: Implementing an Open-Source Viewer

Christoph Kaiser[1], Štefan Jaud[2] and Jonas Schlenger[1]
[1]Chair for Computational Modelling and Simulation, Technical University of Munich, Arcisstraße 21, 80333 Munich, Germany
[2]The Hard Code GmbH, Moorenweis, Germany
E-mail(s): chr.kaiser@tum.de, stefan.jaud@outlook.com, jonas.schlenger@tum.de

Abstract: On the one hand, modern architecture, engineering, and construction (AEC) design often use free-form (curved) surfaces. The best-fitting general-purpose formal geometry description is a B-spline or non-uniform rational B-splines (NURBS) surface. However, in order to inspect such implicitly defined surfaces, a viewer constitutes an essential tool. On the other hand, the exchange format Industry Foundation Classes (IFC) is getting increasingly used in the building information modeling (BIM) processes. The IFC standard supports advanced boundary representations (BReps), which can contain B-spline or NURBS surfaces. There is a lack of IFC viewers which correctly visualize such geometries, especially among open-source solutions. We present an extension to the open-source software TUM OpenInfraPlatform (OIP) to fill this gap. We test the quality of our implementation with all officially available example files. Moreover, we devised additional examples which indicate an explicit improvement in comparison to other open-source viewers.

Keywords: B-spline surface, NURBS surface, Industry Foundation Classes (IFC), open-source viewer

1 Introduction

Modern architecture, engineering, and construction (AEC) design often use free-form (curved) surfaces. B-spline and non-uniform rational B-splines (NURBS) surfaces present the best-fitting general-purpose formal geometry description of such geometric representations in storage as well as in expressiveness. The implicit representation allows an infinite smooth surface evaluation for analysis and visualization. To inspect this implicitly defined geometry, a viewer constitutes an essential tool. However, many popular viewers support neither B-spline nor NURBS surfaces. Because of this deficiency, these advanced surfaces often have to be triangulated during the export process from the design software. During this step, the advantages of the implicit geometry description get lost, e.g. the ability for an easy modification and the small size of the exchange file [1].

The file format Industry Foundation Classes (IFC) is getting increasingly popular for AEC data exchange. It supports such complex surfaces with specialized entities [1]. However, not many IFC viewers support B-spline surfaces and even less the NURBS surfaces, especially in the field of open-source software. Thus, IFC exchanges often refrain from using these advanced surface definitions, e.g. both Coordination View and Reference View exclude these specialized entities. We fill this lack of readily available viewers with our solution. This paper serves as a guide to other (open-source) implementors to ensure unambiguous interpretation of advanced surface geometries across the industry.

The paper is structured as follows. The state-of-the-art is described in Section 2. We summarize the concepts of B-spline and NURBS surfaces and explain the corresponding parts of the IFC data model in Section 3. After that, Section 4 presents TUM OpenInfraPlatform (OIP) and describes how B-spline and NURBS surfaces are implemented. Additionally, it addresses the topological properties the computed geometry must fulfill. The validation of our implementation with multiple examples is shown in Section 5. Finally, Section 6 formulates a conclusion and lists remaining future work.

2 State of the Art

We selected 14 open-source and proprietary software solutions available, both online and desktop programs. For each software, we tested the visualization of B-spline and NURBS surfaces. The former is tested with the official example files *basin-advanced-brep* (basin) and *cube-advanced-brep* (cube) provided by buildingSMART International Ltd. [2]. The latter is tested with our own example file containing a NURBS surface, as described in 5 [3]. Table 1 shows the results of the selected IFC viewers. We denote the test as passed if the geometry is correctly shown. An error message, program crash, or a mere false visualization constitute a fail.

Not many IFC viewers support B-spline surfaces and even less the NURBS surfaces. Except for the proprietary viewer of BIMcollab, all viewers fail to visualize the NURBS correctly. Furthermore, most viewers treat the NURBS surface like an ordinary B-spline surface, resulting in incorrect geometry, as depicted in Figure 1. For users who do not know how the surface should look, this mishandling remains unnoticed and constitutes a false impression of correctness.

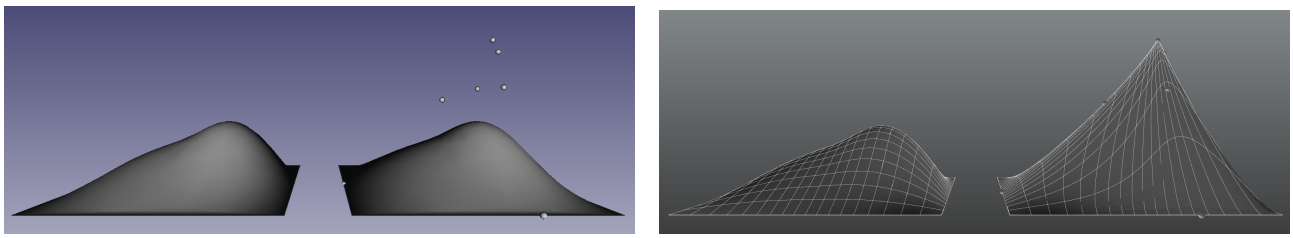

Figure 1: An example data set with a B-spline surface on the left and a NURBS surface on the right, both visualized in FreeCAD (left) and OIP (right).

Table 1: Test results of different IFC viewers for B-spline surface visualization. The viewers are grouped in open-source and proprietary software, as well as online and offline viewers. We have used the most recent software version available to the authors at the time of writing. The test results include B-spline surfaces and NURBS surfaces.

viewer	OIP[1]	FreeCAD[2]	IfcOpenShell[3]	IFC.js[4]	IFC Query[5]	xBIM[6]	BIMcollab[7]	BIMvision[8]	FZK Viewer[9]	Open IFC Viewer[10]	wikiifc[11]	Aspose Viewer[12]	Autodesk Viewer[13]	GOAT viewer[14]
open source	✓	✓	✓	✓	✓	✓	✗	✗	✗	✗	✗	✗	✗	✗
online viewer	✗	✗	✓	✓	✗	✗	✗	✗	✗	✗	✓	✓	✓	✓
B-spline surface	✓	✓	✓	✗	✗	✗	✓	✗	✗	✗	✓	✗	✗	✗
NURBS surface	✓	✗	✗	✗	✗	✗	✓	✗	✗	✗	✗	✗	✗	✗

[1] Jaud, Hecht, Schlenger, *et al.* [4] [2] by opensourceBIM. URL: www.freecadweb.org
[3] *IfcOpenShell* [5] [4] URL: https://ifcjs.github.io/web-ifc-viewer/example/index
[5] by Bauhaus University Weimar. URL: www.ifcquery.com [6] Lockley, Benghi, and Černý [6]
[7] BIMcollab ZOOM. URL: https://www.bimcollab.com
[8] by Datacomp IT Sp. z o.o. URL: https://bimvision.eu/
[9] by Karlsruhe Institute of Technology (KIT). URL: https://www.iai.kit.edu/1302.php
[10] by OpenDesign alliance. URL: https://openifcviewer.com/ [11] URL: https://wikiifc.com/
[12] by Aspose Pty Ltd. URL: https://products.aspose.app/cad/viewer [13] by Autodesk, Inc. URL: https://viewer.autodesk.com/ [14] by VISOPLAN GmbH. URL: https://www.ifcviewer.de/

3 Fundamentals

3.1 B-Spline Surfaces and Non-uniform Rational B-splines Surfaces

In order to visualize the implicit geometry, the actual surface geometry in three-dimensional (3D) space needs to be evaluated. Rogers [7] defines the geometry of B-spline surfaces as:

$$Q(u,v) = \sum_{i=1}^{n+1} \sum_{j=1}^{m+1} P_{i,j} \cdot N_{i,k}(u) \cdot M_{j,l}(v) \,, \tag{1}$$

based on a rectangular grid of control points $P_{i,j} = [x_{i,j}\ y_{i,j}\ z_{i,j}]^T$ in the 3D space. k and l are the order of the normalized basis functions, with u and v representing the current parameter position within the knot vectors X and Y. The basis functions (also called shape functions) $N_{i,k}$ and $M_{j,l}$ are defined with piecewise polynomials according to the Cox-De Boor Algorithm as:

$$N_{i,k}(u) = \frac{(u - x_i) \cdot N_{i,k-1}(u)}{x_{i+k-1} - x_i} + \frac{(x_{i+k} - u) \cdot N_{i+1,k-1}(u)}{x_{i+k} - x_{i+1}} \quad \text{with convention } \frac{0}{0} = 0, \text{ and} \tag{2a}$$

$$N_{i,1}(u) = \begin{cases} 1 \text{ , if } x_i \leq u < x_{i+1} \\ 0 \text{ , otherwise.} \end{cases} \tag{2b}$$

The equations 2a and 2b can be applied correspondingly for $M_{j,l}$ with the variables v and y instead of u and x. The polynomial degree of the basis functions N and M are derived as $k-1$ and $l-1$, respectively. NURBS surfaces are defined similarly as:

$$Q(u,v) = \left(\sum_{i=1}^{n+1} \sum_{j=1}^{m+1} h_{i,j} \cdot P_{i,j} \cdot N_{i,k}(u) \cdot M_{j,l}(v) \right) \left(\sum_{i=1}^{n+1} \sum_{j=1}^{m+1} h_{i,j} \cdot N_{i,k}(u) \cdot M_{j,l}(v) \right)^{-1}, \tag{3}$$

with each control point $P_{i,j}$ having a corresponding weight $h_{i,j}$. This determines the influence the corresponding control point has on the surface's geometry, i.e. a high weight value results in a surface closer to the corresponding control point.

3.2 Industry Foundation Classes

IFC is a vendor-neutral data schema that enables the exchange of digital building models throughout the entire lifecycle of a building. The number of software products which support IFC and the range of possible use cases rise rapidly [1]. The International Organization for Standardization (ISO) standardizes the current release of IFC 4.0 in ISO 16739-1:2018 [8].

IFC distinguishes between semantic and geometric descriptions [1]. While the semantic descriptions are not of interest for this study, we focus on a few concepts from the geometric descriptions as presented in Figure 2. IFCADVANCEDBREP allows representing volumes with curved surfaces. The IFCCLOSEDSHELL points to one or several instances of the type IFCFACE, e.g. each side of a cube could be one surface part described by an individual IFCFACE instance. IFCADVANCEDFACE is a subtype of IFCFACESURFACE and inherits its attributes accordingly. Both are subtypes of IFCFACE. IFCADVANCEDFACE has no additional attributes but adds limitations to the allowed attribute types. The actual surface geometry needs to be described by an IFCSURFACE, e.g. by an IFCBSPLINESURFACE-WITHKNOTS or IFCRATIONALBSPLINESURFACEWITHKNOTS that describe a B-spline surface and a NURBS surface, respectively. An IFCFACEOUTERBOUND describes the topology of a boundary loop, which can limit the extent of the surface. [1], [9]

4 Process and Implementation

4.1 TUM OpenInfraPlatform

OIP is an open-source application for viewing and analyzing building information modeling (BIM) models. To achieve this, OIP allows to read, visualize, navigate, and handle IFC and point cloud data

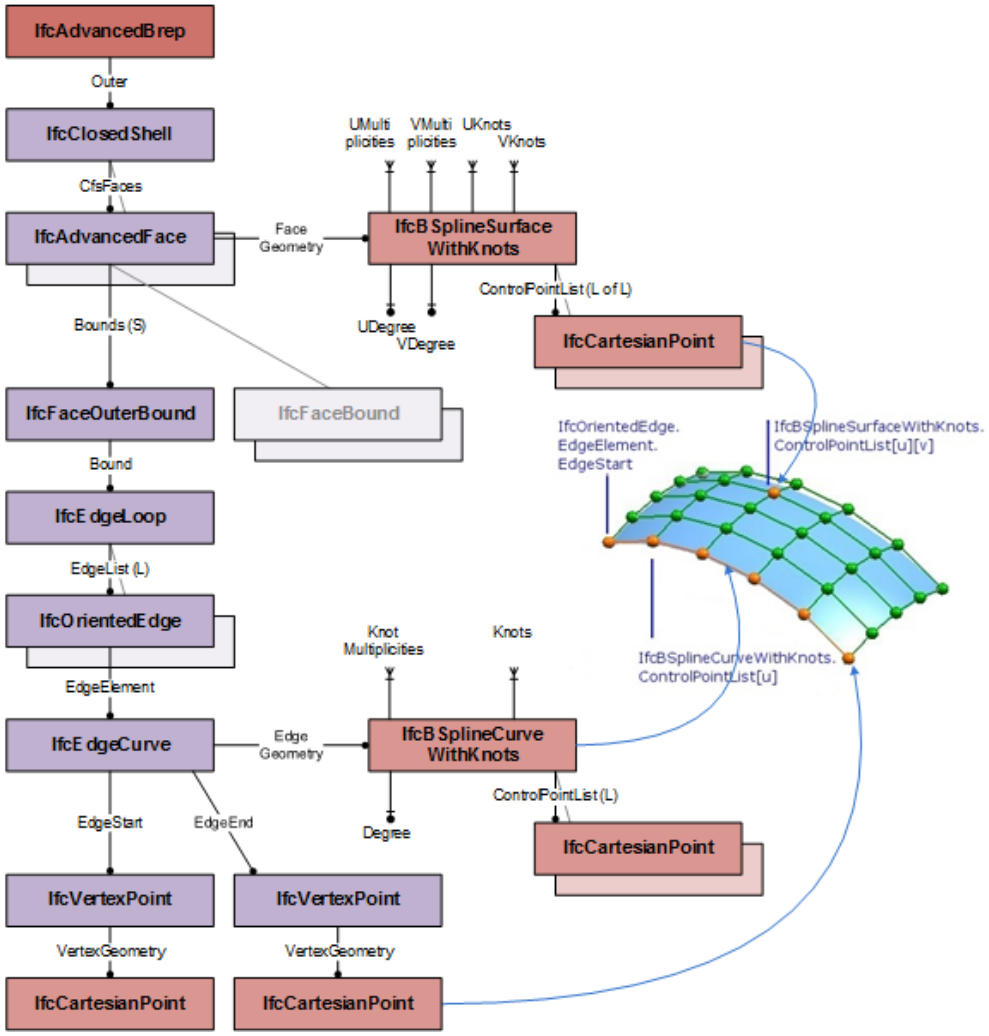

Figure 2: Topological (violet) and geometrical (red) entities orchestrate an IFCADVANCEDBREP with B-spline surfaces as parts of its geometrical description [9].

(PCD). Furthermore, both can be compared by simultaneous loading and overlapping. OIP provides a prototypical playground for developers, in which features and functionalities can be changed, added, or removed as required. One mentionable feature is the support of IFC candidate versions beyond the current release version IFC 4.0. [4]

The software is separated into the parts early-binding generator, graphical user interface (GUI), core components, and additional plugin modules. The core component is written in the programming language C++. Its main task is converting geometric descriptions from IFC to a triangulated geometry, represented in the geometry kernel carve. [10]

4.2 Implementation

In OIP, the core component mirrors the hierarchical IFC structure, as mentioned in Subsection 3.2. There are converter functions for each abstract supertype, which hand over the input parameters depending on their subtype. For example, the IFCADVANCEDBREP provides the attribute outer closed

shell, which is handed over to the corresponding converter function. After that, each part of the object's surface is converted individually. Algorithm 1 describes the processing of a vector of IFCFACEs in more detail, which takes its inheritance structure into account. The entity IFCFACE can be of the subtype IFCFACESURFACE, which in turn can be of the subtype IFCADVANCEDFACE. As mentioned in Subsection 3.2, if the limitations of an IFCADVANCEDFACE are fulfilled, the instance can be treated the same as an IFCFACESURFACE.

Listing 1: Decision tree of IfcFace.

```
Input: ifcFaces
Output: itemData
function convertIfcFaceList
  initialize triangulatedGeometry
  foreach ifcFace in ifcFaces
    if ifcFace is IfcFaceSurface
      ifcFaceSurface ← ifcFace as IfcFaceSurface
      if ifcFaceSurface is IfcAdvancedFace
        ifcAdvancedFace ← ifcFaceSurface as IfcAdvancedFace
        if ifcAdvancedFace has valid attributes
          call computeIfcFaceSurface(ifcAdvancedFace, triangulatedGeometry)
        end if
      else
        call computeIfcFaceSurface(ifcFaceSurface, triangulatedGeometry)
      end if
    else
      call computeIfcFace(ifcFace, triangulatedGeometry)
    end if
  end foreach
  add triangulatedGeometry to itemData
end function
```

The function `computeIfcFaceSurface` calculates the surface geometry depending on its type. Since the geometry can be larger than the boundary loop, it must be trimmed accordingly. One specialized function is `convertIfcBSplineSurface`, which converts instances of the abstract supertype IFCBSPLINESURFACE according to its inheritance structure similar to the algorithm above. The IFCBSPLINESURFACE can be of the subtype IFCBSPLINESURFACEWITHKNOTS. The entity IFCBSPLINESURFACEWITHKNOTS can be of the subtype IFCRATIONALBSPLINESURFACEWITHKNOTS. According to the type, the function loads the attributes from the IFC entity and hands them over to the corresponding compute function, which is independent of the IFC instances. The equations 1 and 3 are used to calculate the actual geometry of the surface in 3D space, according to the algorithms by Rogers [7]. As mentioned in Subsections 3.2, each surface part of the entire object surface is represented in one IFC entity and converted individually. As a final step, these single surfaces are merged into one topological connected polyhedron and coincident vertices are removed to achieve the requirements of an IFCADVANCEDBREP.

5 Results

5.1 Examples

The presented implementation in OIP visualizes advanced boundary representations (BReps) with B-Spline surfaces and NURBS surfaces described in an IFC file. buildingSMART International Ltd. [2] provides the official examples basin and cube, which use B-Spline surfaces. Figures 3 and 5 show the officially provided screenshots of the examples. In comparison, figures 4 and 6 show the corresponding visualizations in OIP.

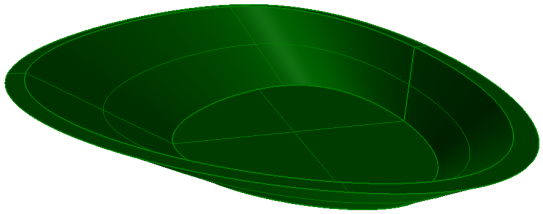

Figure 3: Example *basin advanced brep* [2].

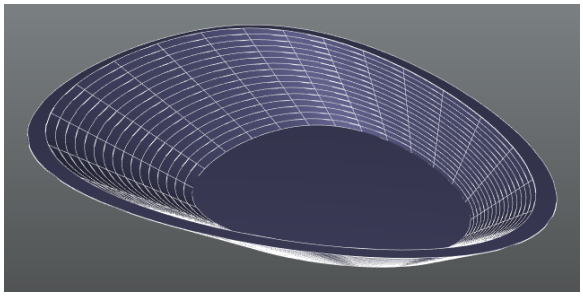

Figure 4: Example *basin advanced brep* visualized in OIP.

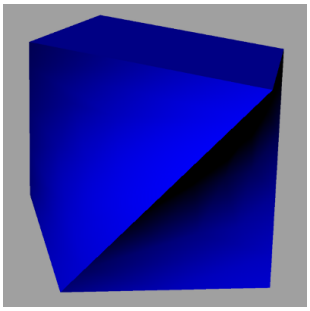

Figure 5: Example *cube advanced Brep* [2].

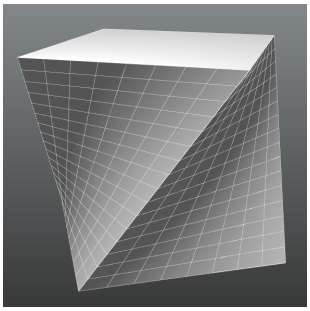

Figure 6: Example *cube advanced Brep* visualized in OIP.

buildingSMART International (bSI) does not provide an official example that includes a NURBS surface. For this reason, we developed the example *rational-BSpline-surface-with-knots* by ourselves to test our solution. The IFC file is available on the OIP GitHub repository [3]. Figure 1 of OIP visualizes the result, which shows a B-spline surface on the left and a NURBS surface on the right. Both geometries are generated with an identical control point grid. By definition, the B-spline surface uses equal weights of the value one at all control points. In contrast, this NURBS surface uses a weight value of 50 at the control point with the increased z coordinate.

5.2 Validation

The IFC documentation provides only a few screenshots and no analytically calculated points for verification. Therefore, checking by eye is the first approach for validation. Comparing Figures 3 and 4

of the example basin, as well as Figures 5 and 6 of the example cube, the geometries of the official screenshots and the visualizations in OIP seem equal. This is the first indication of the correctness of our geometry computation.

Figure 1 of OIP compares a B-spline surface with a NURBS surface. The single increased weight value of the NURBS surface leads to the noticeable peak of the geometry. For further verification of our implementation, we added small markers (spheres with radius = 0.05) in the IFC file (see Figure 1), which highlight a few points on the NURBS surface. The coordinates of these markers are calculated separately from OIP with MATLAB and visually verified with the NURBS surface generator of the 3D creation suite Blender. The center of all spheres lies directly on the visualized surface, which further confirms the correctness of the computed NURBS surface. The shown markers have the following coordinates:

$Q(0.0, 1.0) = (5.0, 2.0, 0.0)$	$Q(0.5, 1.0) = (6.974, 2.0, 1.690)$	$Q(1.5, 1.0) = (7.988, 2.0, 2.887)$
$Q(1.9, 1.0) = (8.098, 2.0, 2.652)$	$Q(2.0, 1.0) = (9.0, 2.0, 0.0)$	$Q(1.5, 0.0) = (7.8123, 0.0, 0.0)$
$Q(1.5, 0.2) = (7.925, 1.421, 1.925)$	$Q(1.5, 1.8) = (7.925, 2.579, 1.925)$	$Q(1.5, 2.0) = (7.813, 4.0, 0.0)$

All three examples demonstrate the ability of OIP to visualize B-spline surfaces and NURBS surfaces. Moreover, they provide validation within the scope of available reference and test data.

6 Conclusions

As discussed, the calculation and visualization of advanced BReps with B-spline surfaces and NURBS surfaces in OIP is more refined in comparison to other free viewers. However, as OIP is a development playground, the IFC standard is not supported fully. For example, not all subtypes of IFCSURFACE have been implemented yet, thus BReps using these subtypes in the attribute face surface could not be visualized. Additionally, the boundary loop trimming that was mentioned above is still to be implemented. The current implementation requires the face surface to fit into the boundary loop, which is the case for all officially provided examples. Applying a suitable trimming algorithm is the next step to improve the variety of possible advanced BReps visualized in OIP. Furthermore, this step eases the support of the pending subtypes mentioned in this section. To further verify the correctness of the visualization, a more automated and quantitative verification process will be developed in the future.

In conclusion, it has been shown that the OIP can overcome common shortcomings of existing free IFC viewers in regards to the visualization of advanced BReps with B-spline surfaces and NURBS surfaces. The OIP open-source project offers excellent transparency to guide other software providers in implementing B-spline and NURBS surfaces. Furthermore, an additional IFC example file has been created that helps software users to assess an IFC viewer's correctness visually.

References

[1] A. Borrmann, M. König, C. Koch, and J. Beetz, *Building Information Modeling: Technologische Grundlagen und industrielle Praxis*, 2nd ed. Springer, 2021.

[2] buildingSMART International Ltd., *IFC 4 - Examples*, Accessed: 2022-03-12, 2020. [Online]. Available: https://standards.buildingsmart.org/IFC/RELEASE/IFC4/ADD2_TC1/HTML/link/annex-e.htm.

[3] TUM OpenInfraPlatform, *Rational-bspline-surface-with-knots marks.ifc*, Accessed: 2022-07-10, 2022. [Online]. Available: https://github.com/tumcms/Open-Infra-Platform/blob/development/testdata/IFC4ExampleFiles/rational-bspline-surface-with-knots%20marker.ifc.

[4] Š. Jaud, H. Hecht, J. Schlenger, and J. Amann, "TUM Open Infra Platform: an open source package for simultaneous viewing and analysis of digital models in the civil engineering domain", *Journal of Open Source Software*, vol. 7, no. 72, p. 3061, 2022. DOI: 10.21105/joss.03061. [Online]. Available: https://doi.org/10.21105/joss.03061.

[5] *Ifcopenshell*, Accessed: 2022-05-16, 2021. [Online]. Available: https://ifcopenshell.github.io/docs/.

[6] S. Lockley, C. Benghi, and M. Černý, "Xbim.essentials: A library for interoperable building information applications", *Journal of Open Source Software*, vol. 2, no. 20, p. 473, 2017. DOI: 10.21105/joss.00473. [Online]. Available: https://doi.org/10.21105/joss.00473.

[7] D. F. Rogers, *An introduction to NURBS: with historical perspective*. Morgan Kaufmann Publishers Inc, 2001.

[8] ISO, "Industry Foundation Classes (IFC) for data sharing in the construction and facility management industries – Part 1: Data schema", International Organization for Standardization, Geneva, CH, Standard, Nov. 2018.

[9] buildingSMART International Ltd., *IFC 4 - IfcAdvancedBrep*, Accessed: 2022-03-12, 2020. [Online]. Available: https://standards.buildingsmart.org/IFC/RELEASE/IFC4/ADD2_TC1/HTML/link/ifcadvancedbrep.htm.

[10] H. Hecht and Š. Jaud, "Tum openinfraplatform: The open-source bim visualisation software", in *Proceedings of the 31st Forum Bauinformatik*, Berlin, Germany, 2019. [Online]. Available: https://publications.cms.bgu.tum.de/2019_Hecht_Jaud_FBI.pdf.

BCFViewer – BIM Collaboration Format tool development

F. Lourenzi and A. Geiger

[1] Karlsruhe Institute for Technology, Hermann-von-Helmholtz-Platz 1 76344 Eggenstein-Leopoldshafen

fernanda.lourenziv@gmail.com

Abstract: Building Information Modelling (BIM) is the foundation of a digital workflow between different fields in the architecture and construction industry. It establishes a method that integrates multidisciplinary data to create a digital twin of a building throughout its lifecycle, going from its initial planning and construction phases to the final execution. With the BIM Collaboration Format (BCF), buildingSMART provides a standard for the cross-application communication within an openBIM process. Therefore, the data can be exchanged and opened by different programs without the additional need to exchange the entire model. As part of an internship semester, a stand-alone application is being developed for managing BCF files. The BCFViewer, as the application is called, is designed to read data in the BCF standard and shows its content without losing information. New data including issues, comments and images can be created and saved. In addition, it is possible to share the data with project partners via integrated email notification. The resulting files can be read by other software applications for BCF management. The viewer is a stand-alone tool just for BCF management, as it does not interpret IFC files. That means an interactive view of the object is not possible. In the present paper the development as well as the functionality of this stand-alone software tool is described. The plan for additional complementary features is discussed and how it was designed as a module for the software tool FZKViewer. Finally, it is shown which features the application offers compared to similar tools.

Keywords: BIM, BIM Collaboration Format, Tool Development, BCF Viewer, BCF

1 Introduction

BIM is undeniably important to projects nowadays in a variety of fields in the AEC industry. It can help to see through details in the whole process of multidisciplinary work. Workflow methodologies are however essential to this and sometimes what the team needs for communication is rather a reference to the data-model containing the required information than the big-scale project. BIM Collaboration Format (BCF) comes in handy for this, as it is an open file format that raises issues efficiently while avoiding heavy file exchange [1].

Today it is possible to find BIM software with tools or complementary modules that support BCF files. What is required most of the time is to have said programs to be able to visualize the issues or information. With stand-alone BCF applications, it is possible to easily view those files when the goal is only to have knowledge of it or make a couple of notes on its content.

This paper intends to show a free stand-alone application for BCF management which has been implemented as part of an internship semester for a bachelor civil engineering course. It was initially conceived in order to complement some of the missing features of the FZKViewer tool. The application covers the basic needs for an easy reading and writing of a BCF file and focuses on sharing its content between interested people.

1.1 BIM Collaboration Format

The BIM Collaboration Format (BCF) was developed by BuildingSMART as an international open standard that allows different BIM applications to communicate modal-based issues improving the IFC-based process. BCF bases the model workflow in three stages: Define (what is the issue?), specify (what is the original problem that caused it?) and delegate (what is your suggestion and to whom are you assigning the action?) [1].

BCF was meant for a better communication over issues, and that’s why most of the BIM Softwares offer BCF coordination through collision detection or model checking tools. It can also be used to exchange information, expectations, comments or remarks on the project. The data can be shared in two formats: XML, where the information is written in XML files exported to a ZIP container; or the BCF API [2], where the information can be exchanged via a webserver based on cloud synchronisation.

1.2 BCF Structure

When passed through the XML-format, the basic content of a BCF file includes the issue itself with comments and references of spoken objects (possible through its Global Unique ID in IFC). It is possible to add a Status-information, making it easier to track the development when discussed by multiple users, along with a viewpoint or screenshot of the situation in the application where the issue was created [3].

The structure of the BCF Version 2.1 is a ZIP file (Figure 1) containing one folder for each *topic* and XML-files defining the extension (extensions.xml) and the details (project.bcfp) of a project, the documents (documents.xml) in it as well as a XML file with the information of the BCF schema used (bcf.version). The name of the issue folder is the GUID of the topic and must be written in all-lowercase. Inside the folder are the following files [4]:

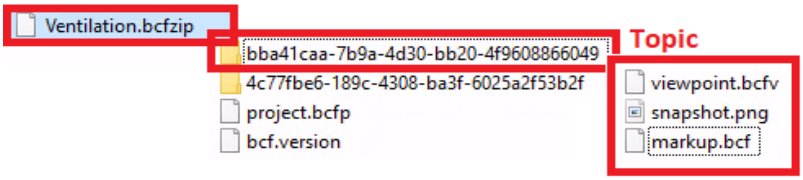

Figure 1: BCF ZIP file

- markup.bcf - an XML following the markup.xsd schema with text information about the topic. The information is separated into the nodes *Header, Topic, Comment and Viewpoints.* The *Header* contains attributes about the IFC file from where the issues are from. The *Topic* contain attributes to identify it (*GUID*), the *TopicType* and *TopicStatus.* The last two includes a predefined list to help cathegorize the topic. Besides that, the *Topic* contain several elements such as *Title*, *CreationDate* and *CreationAuthor* (obligatory); and *Priority*, *Labels*, *Description*, etc. (optional). The *Comment* node contains comments related to the *topic*. Each one has an unique identifier as attribute and may refer it to a *viewpoint*.

- Viewpoint files - an XML conforming the visinfo.xsd schema with information of components related to the topic, camera settings, and possible markup and clipping information.

- Snapshot files - PNG or JPG related to the object

2 BCF Software Tools

In some cases, BCF is used not only for reporting issues. The direct and simple structure is easy to implement and also very useful when it comes to documentation. There is a study, for example, that evaluates the methodology for image-documentation in the early phases of existing buiding through a BCF API, using different search parameters for image localization [5]. Keeping the simple specification in mind, BCF was also thought to be expanded to attend to the demands of task management in the building industry [6], by creating a data schema architecture that supports the

requirements such as topic definition, users involved or dates. Through the viewpoints components in the BCF parameters, which ar able to show data-model relationships, it is also easy to spatialize information. For example, the damage mapping on-site for a later conversion to the BCF parameters is a cost-effective and simple solution for small and medium enterprises to make damage documentation and facilitate their workflows with a better accessibility to the provided data [7].

There are many tools available for the managing of BCF files that can assist the workflow and provide help in the desired domain. Some are integrated with BIM software or are modules that help with the Issue handling, which means that in most cases a license or purchase is required to see or edit the BCF. Even though the BCF standard is intended to be software independent, it is sometimes necessary for a casual viewer to go through this process and own one of these programs just to visualize the project issues or, as stated earlier, documentation. Software tools just for BCF viewing with different functions are available on the market. However, only a few of them are free. The BCFViewer as a freeware will be an additional option to fill this role of software-independent BCF viewer and/or editor. Later, a few more options for free stand-alones will be presented.

3 BCFViewer

The BCFViewer is a Windows desktop application able to read and create BCF files.The implementation of the tool was developed with Microsoft Visual Studio. The C++ programming language and Microsoft Foundation Classes (MFC) were utilized for this purpose. MFC is a library that wraps parts of the Windows API in C++ classes, including functions that allow them to use a standard application framework.

The goal of the tool was initially to be a built-in module for an IFC visualization Software, the FZKViewer. The FZKViewer was able to create BCF files through a model checking when errors were identified. The Issues were created automatically when selected with the information from the checking tool with no editing possibilities. For a more detailed issue handling with more freedom, a new module with some complementary features were desired. With the BCFViewer, now it was possible to create not only its own issues, but also new remarks or requests and send it to someone. There is also the possibility to add several comments and/or snapshots to each topic.

3.1 Features

The BCFViewer as a stand-alone tool is just for the viewing and creation of BCF and does not interpret IFC files. The goal is an easy and fast way of viewing and editing topics without the need of a BIM Software. That means that an interactive view of a viewpoint object is not possible.

In the main dialog (Figure 2), there is the possibility to open BCF files and view its content. There is a list of topics and a window containing information about the selected topic, comments and, if

available, a snapshot for the selected comment. It is possible to create and/or edit topics or comments and, if so desired, upload images to each comment.

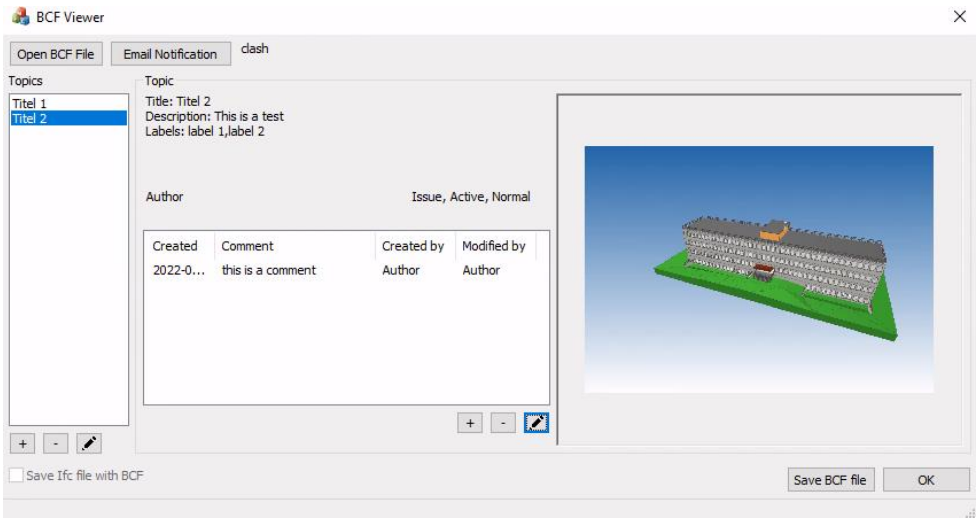

Figure 2: BCFViewer features

Each time a change is made in BCF it is possible to send a notification to any person. In each topic or comment dialog there is a notification section (Figure 3) where you can select who should be sent an email to and a checkbox that defines if the BCF file should be sent as an attachment or not. Since the BCF file has not been saved yet, a temporary file of the current state will be created if the checkbox is activated. The selected people will receive an email with the most important details about the changed topic and the attachment, which can be loaded and visualized either in the BCFViewer or any other program that supports BCF.

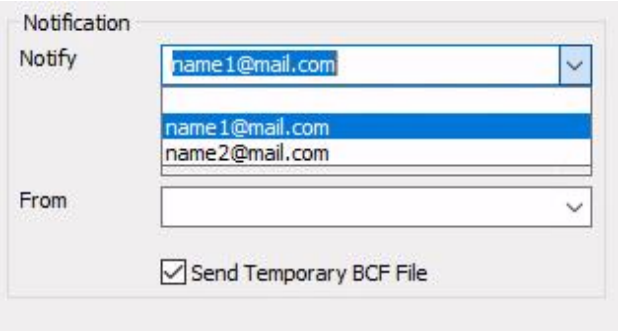

Figure 3: BCFViewer Notification

BCFViewer offers the functionality to save regular contacts to which the user wants to send notifications. The list can be edited in a separate dialog (Figure 3). When the list is saved, an external XML file is created, which is read each time the tool is initialized.

3.2 Future implementation plans

The next step for the BCF viewer would be the editing of the Snapshots images, where drawings on the pictures could be made, and the possibility of adding attachments to each topic. These attachments can be any kind of document that contributes to the understanding of the topic, illustrates it or adds something that was mentioned in the comments. For example, this could be a PDF or an XML file.

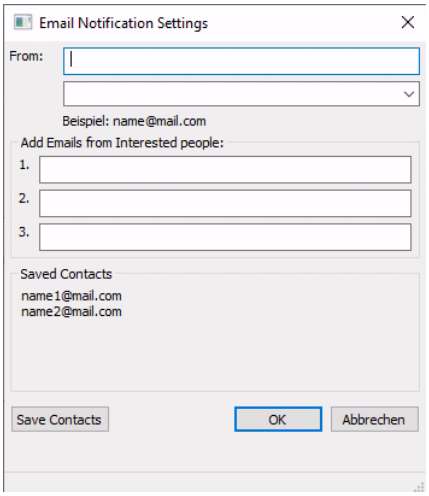

Figure 4: Notification Settings

It is planned for further functions to be implemented to complement the module for the FZKViewer, such as the ability to save the IFC project with the BCF zip file, take screenshots of the current viewpoint, and save a viewpoint file with the appropriate components.

3.3 Comparison with similar tools

There are a number of similar free tools for managing BCF data, and here BCFViewer is compared to three of them: the free version of BIMCollab ZOOM [8], a tool for model viewing and BIM validation that is fully integrated with problem management workflows; BCFier [9], a set of plugins and apps (modules) that handle BCF and integrate directly with BIM tools; and Sloth [10], an online BCF report generator.

BIMCollab ZOOM works with version 2.1 of BCF and creates files with the extension ".bcf". It is possible to add or edit different snapshots and viewpoints and upload IFC files. When dealing with older BCF versions, where just one snapshot per topic was allowed, there is no possibility of replacing it. BIMCollab has a cloud support where it is possible to log in and have an overview of the issues and send notifications. It is not possible to get a local copy of the BCF file once the user is

logged. With the BCFViewer the notifications are sent offline. That means that an account for the app is not necessary.

BCFier is currently composed of Autodesk Revit 2015 and 2016 add-ins and stand-alone Windows Viewer. It creates files with the extension ".bcfzip" and allows the user to have more than one BCF report at the same time. When adding a new view from BCFier Viewer no viewpoint will be added in the view therefore it will not contain 3D information.

The Sloth web-app offers a way to upload a BCF file and see the resulting report in your browser, showing the main information in your issue, along with the first screenshot. Sloth has the feature to export your report to Word or Excel format. It uses basic Styles in Microsoft Word to highlight titles and dates.

Table 1: BCF tool comparison

	BCFViewer	BIM Collab ZOOM	BCFier	Sloth
IFC viewer as Stand-alone	No	Yes	No	No
Read BCF files	Yes	Yes	Yes	Yes
Edit BCF files	Yes	Yes	Yes	No
Upload snapshots	Yes	Yes	Yes	No
Edit Image from Snapshot	No	Yes	Yes	No
Send notification	Yes (offline)	Yes (through cloud)	No	No
Report export	No	No	No	Yes

4 Conclusion

In this paper, the development of a new tool for collaborating with BCF data is presented and it is shown how this tool can be used in a BIM workflow. The features are shown and compared to other similar tools. The BCFViewer provides reading and edition of BCF data, but the lack of an IFC viewer, that is, a lack of 3D graphical representation, can make it difficult to visualize some of the issues listed in the file. Although if the goal is a quick and easy file manager, BCFViewer provides the basic necessities and allows a way to exchange content via Email notifications without further work. It has a simple, self-explanatory user interface and it's more convenient to use than an integrated module within more complex BIM software. There are still some steps to be taken in the devepment of the

BCFViewer, such as the plan for new implementations as attachments of files to the BCF or editing of the Snapshot image. The IFC interaction integration for the FZKViewer is also in development, so it will be possible for example to save the object components in the viewpoint file or take screenshots. The implementations should however be made without sacrificing the premise of simplicity so that in the end a complete yet user-friendly tool is offered that enhances the workflow.

References

[1] BuildingSMART International. Available: https://www.buildingsmart.org/standards/bsi-standards/bim-collaboration-format-bcf/. [Accessed March. 15, 2022].

[2] Github, “buidingSMART/ BCF Rest API” [Online]. Available: https://github.com/BuildingSMART/BCF-API/. [Accessed 3 September, 2021].

[3] K. Linhard, R. Steinmann, “BIM-collaboration processes – from fuzziness to practical implementation”, *in eWork and eBusiness in Architecture, Engineering and Construction: ECPPM*, Vienna, Austria, 2014.

[4] Github,”buildingSMART/ BCF-XML/ Documentation” [Online]. Available: https://github.com/buildingSMART/BCF-XML/tree/release_3_0/Documentation/. [Accessed 3 September, 2021].

[5] O. Schulz, J. Beetz, “Image-documentation of existing buildings using a server-based BIM Collaboration Format workflow”, August 2021. [Online], Available: https://www.researchgate.net/. [Accessed March 23, 2022].

[6] N. Treldal, H. Parsianfar, J. Karlshoj, “Using BCF as a mediator for task management in building design”, Proceedings of the International RILEM Conference Materials, Systems and Structures in Civil Engineering, Denmark, August 2016.

[7] O. Schulz, “Spatialization of damage to buildings using a BIM collaboration Format approach,” September 2021. [Online], Available: https://www.researchgate.net/. [Accessed March 23, 2022].

[8] BIMcollab [Online]. Available: https://www.bimcollab.com/. [Accessed 20 September, 2021].

[9] BCFier [Online]. Available: http://bcfier.com/. [Accessed 23 March, 2022].

[10] Sloth [Online]. Available: https://www.bim42.com/2017/07/sloth/. [Accessed 25 March, 2022].

[11] L. van Berlo, T. Krijnen, “Using the BIM Collaboration Format in a server based workflow”, presented at 12th International Conference on Design and Decision Support Systems in Architecture and Urban Planning, DDSS 2014.

Teil X

Point Clouds

From Point Cloud to as-built BIM: automated Detection of Openings in existing Buildings

Ziyuan Chen[1]
[1]Technische Universität Darmstadt, Karolinenpl. 5, 64289 Darmstadt, Germany
E-mail(s): ziyuanchen89@gmail.com

Abstract: Nowadays, point clouds acquired from laser scanning have become one of the main sources for building modeling. The generation of as-built BIM models for existing buildings brings benefits for building energy analyze and information management. However, the acquired point clouds may contain unwanted elements placed in rooms, which results in clutters and occlusions in the extracted wall structures. Thus, how to extract the correct information of openings from the occluded walls is a challenging task for the indoor modeling. This paper proposes a methodology to detect the information of openings, such as windows and doors, from occluded walls and generate the BIM components automatically. To extract the features of openings, the gradient based maximum likelihood algorithm with shape grammar is used. The corresponding BIM component can be generated using the scripts created by visual programming language. The proposed approach is evaluated with a case study and the obtained results are discussed. The paper concludes with a summary and an outlook of future investigation directions.

Keywords: Building Information Modeling(BIM), as-built BIM, Point clouds, 3D Reconstruction, Automation

1 Introduction

With the more frequent and practical use of Building Information Management (BIM) model in built environment, generating building models from existing buildings is getting more attentions nowadays. The major information sources for BIM modeling of existing buildings are point clouds acquired by laser scanners. However, many methods focus on extracting wall structures (without openings) from point clouds. Fewer attentions are paid to the reconstruction of openings on the wall structures in the BIM model, which is important and worth investigating. For example, in the research of energy consumption analyze of existing buildings, the positions of windows and doors play an important role in the energy consumption simulation. However, the acquired point clouds may contain unwanted elements placed in rooms, which can result in clutters and occlusions in the extracted wall structures.

Thus, how to extract the correct information about openings from the occluded walls is a challenging task for the indoor modeling.

The state-of-the-art researches working on openings' extraction are based on neural networks. However, neural networks have two main drawbacks. First, the pre-training needs a huge amount of training examples (point clouds), which may not be easy to get. Second, the performance of neural network degenerates easily on noisy and low-quality point clouds.

To address these two problems, we propose a novel method based on maximum likelihood estimation to precisely detect the information about openings (such as windows and doors) from occluded walls and then generate the BIM components automatically by using visual programming language Dynamo. We made three main contributions in our proposed method, namely:

1. We extract the information directly from the raw input point cloud without using enormous amount of training examples like neural networks,
2. Our method performs reasonably good on low-quality point clouds,
3. We can achieve effectively and highly precise automatically modelling by combining Python, Dynamo and Revit.

This paper is composed of five chapters, including this introductory chapter. At first, a literature review of the development of scan to BIM methods in aspect of structure segmentation as well as information extraction of openings. Chapter three begins by laying out the developed methodology for processing of point cloud and semi-automatically generating of openings in BIM model. We show the use case and results in the fourth chapter. The last section provides a summary and future researches.

2 Literature Review

Comparing with point cloud data, BIM has the ability to provide not only a 3D geometry model of the building components, but also a comprehensive set of semantic information. [1] The research of [2] also identified that the integration of point cloud with BIM is one of the hot topics after analyzing the research trends between 2007 and 2020.

Many researches have studied on reconstruction of building interiors and exteriors using laser scanner. Tang [3] have reviewed the overall process of creating as-built BIMs. Recently, Xu [4] also provided a thorough review of the state-of-the-art acquisition and processing techniques for building reconstruction using point clouds. The core operations include geometric modelling, object recognition, and object relationship modelling. The most common used method of planar surface detection is Hough transform[5], [6] or RANSAC algorithm [7], [8], and with the development of artificial intelligence, machine learning methods. However, using RANSAC may cause so called 'bad-segmentation' problems. The reason is that points constituting the maximum consensus may be derived from different objects, according to Previtali's research[9]. Macher with the group did a series of researches on

how to transform the building structure from a point cloud model into BIM model semi-automatically. [10]–[12] The process proposed in [10] included plane segmentation, point classification and BIM model reconstruction. Instead of using the RANSAC algorithm, a more precise algorithm with the same sampling strategy was used for plane segmentation. After that, the points were classified into different objects. To create the BIM model, the extracted structures were firstly transformed into .obj format and then created an IFC file using the FreeCAD software. The same method of creating BIM model with IFC file was also used in Thomson's research [7]. Various attempts have auch been implemented to detect the openings from the wall structures.[12]–[14] However, the developed methods by using energy function and radiometric information need high-quality data. To better overcome the problem with cluttered and occulated environment, Muraet.al combined the operation process both in 3D space and in 2D projection[6]. The basic room detection was performed in the 2D projection, while the patch detection and the occlusion-based pruning and the final fitting were performed in 3D space. The process costs more time while increasing the accuracy. The developed method by combining histogram and shape grammar approach[15].The work showed an approach to generate building elements in a hierarchical structure by using shape grammar approach. The Approach consists of 6 rules, which can also analyze and extract the topological relation such as containment, adjacency, and connectivity. With the rapid development of artificial intelligence, many machine learning technologies can be used for scan to BIM. Bassier et al. [16] presented a method using random forests to identify and classify of structural elements automatically, which showed a good performance in feature labeling in different buildings. Similarly, Sahebdivani et al. [17] used the PointNet deep learning network for semantic segmentation in the point cloud data. The PointNet neural network is a novel type of neural network developed in 2017 [18] for object classification and segmentation of 3D point cloud data. Currently, it has been developed to PointNet++[19].

Since using machine learning methods require high quality of data and large amount of training data, this paper attempt to analyze the raw point cloud data even with a high level of clutter without training process. The developed method is implemented by combining maximum likelihood estimator and shape grammar to extract the openings of wall structures even with low quality of data.

3 Methodology

The input data of the methodology is the segmented information as well as the created BIM model of wall structures by using the proposed method from the previous work [20]. Figure 1 shows the overview of the method. To extract the potential positions of openings apart from clutters or occlusions, we implement the gradient based maximum likelihood algorithm on the point clouds firstly. After that, we use the shape grammar rules to get the geometrical information about each opening from the potential positions. Then, the corresponding BIM components can be generated using the scripts created by visual programming language Dynamo automatically.

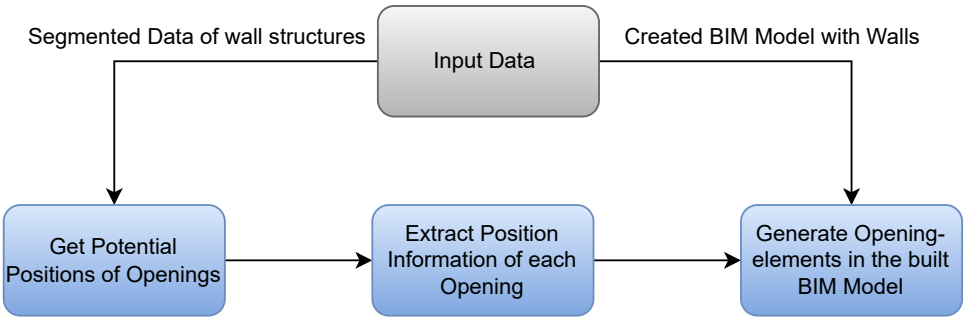

Figure 1: Overview of the developed Methodology

3.1 Using gradient maximum likelihood to detect the potential positions of openings

The potential positions of openings can be detected by using gradient-based maximum likelihood. Algorithm2 shows the workflow. Using Maximum likelihood estimation with histogram has been proven as a convincing method for wall segmentation of the point cloud [20]. It can also be extended to extract the information of openings. Different from the data distribution of wall structures, which has a significantly dense distribution at each potential position, the data distribution of each opening changes significantly at the start and end point. Therefore, we can use gradient-base maximum likelihood estimation with histogram to get the potential positions of openings. The start and end point can be identified by the calculated value by checking whether it is positive or negative.

Algorithm 2 Get Potential Positions with Gradient-based Maximum Likelihood

Require: Point cloud of each wall elements $Wall_i$, $i = 0 \cdots N$

```
n ← 0
while n ≤ N do
    Implement Histogram in corresponded axes of wall_n: xy and z;
    Get the positions and count values: P_axis, C_axis ;
    Calculate gradient-based count values: g_Ci = (C_i+1 − C_i)/mean(C);
    Select Index with Maximum Likelihood: Idx_axis = Where (|g_Ci| > mean(g_Ci) );
    Get Positions with selected Indexes: P_Saxis = P_axis[Idx_axis];
    i = 0;
    for i ≤ len(P_Saxis) do
        if P_Saxis[i] < 0 then
            i+= 1
        else if P_Saxis[i + 1] > 0 then
            i += 1
        else
            export P_Saxis[i]
        end if
    end for
end while
```

3.2 Using Shape Grammar to get the information of openings.

It is critical to get the extracted information of each opening only with the information of potential positions. Since the combination possibilities of different coordinates are more than one. As figure 2 shows, with two pairs of potential positions in z-axis and in x-axis, there are already 4 possibilities of combinations. To classify whether the potential position is an opening, the shape grammar is implemented. In Tran's research [15], there is a formulated grammar rule for die classification, which can be reformulated to do the windows and doors classification. The Rule is formulated as equation 1. With the calculated value, we can get the geometrical information about each opening, the openings can then be classified as window or door based on the positions in z-axis.

$$R_{class} : A \rightarrow A[type] : cond, \qquad I_{PoF} = n/A \tag{1}$$

with the variables are:

I_{PoF} Index for Point of Face

n Number of points that fall into the surface A

A The area of the evaluated place

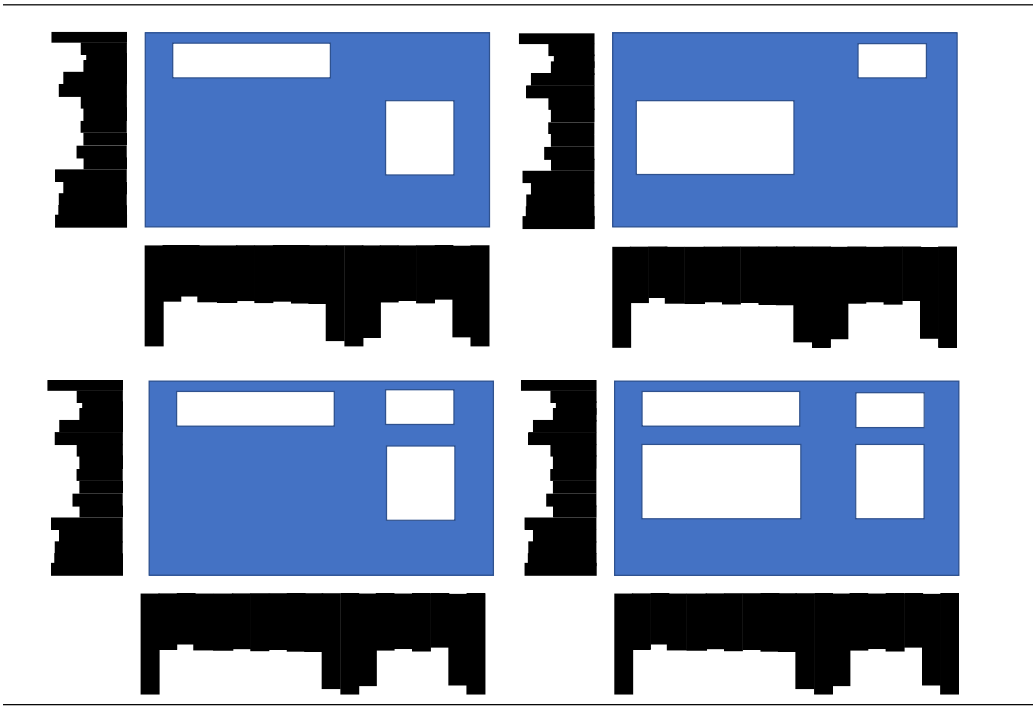

Figure 2: Possible combinations of openings based on the same distribution.

3.3 BIM Model generation of openings

The BIM model (including the opening elements) is created based on the extracted information. The input data in this step is the build wall model in Revit. Instead of creating the elements manually, a more efficient method is implemented for modeling, which is parametric design with Dynamo visual programming for Revit.

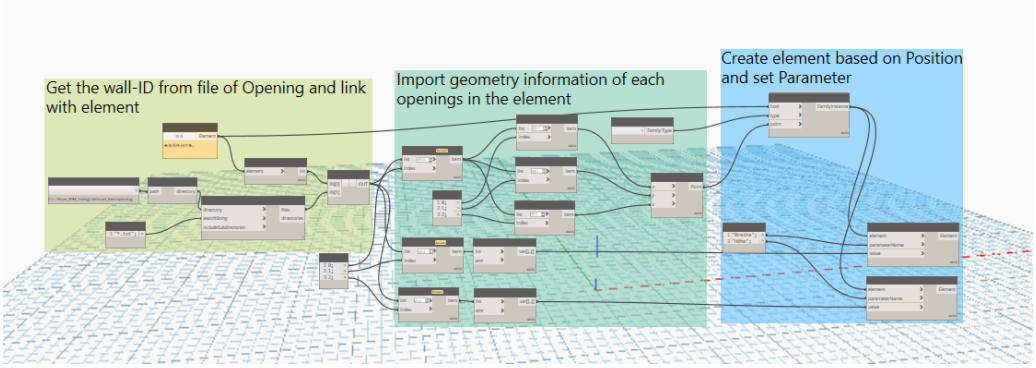

Figure 3: An illustration of a Dynamo diagram

Figure 3 demonstrates the model (with openings) generation process. The extracted opening information is imported into dynamo at the beginning. The opening of corresponded wall element is linked by the ID number of the wall element. Finally, a Revit opening element is created based on the geometry and the element type. Since the process of each can be created using the same processing method, a more automated and efficient way is implemented in this step. Instead of filling the required information separately, a python script with a loop function is written in dynamo to create all opening elements automatically.

4 Case Study and Results

One of the data set provided from ISPRS Benchmark on Indoor Modelling is used to evaluate the performance of the developed method. The ISPRS Benchmark [21] provides a public benchmark data set including six point clouds to enable performance evaluation and bench marking of indoor modelling methods. Since the point cloud of Fire Brigade contains 9 rooms on the same level, 10 doors and 53 windows with a high level of clutter, it is a challenging task to test the performance of our methodology. Figure 5 shows the reconstructed windows and doors in the BIM model. Since the detection of openings from point clouds is no longer the process of segmentation, it is critical to evaluate the process with precision and recall. Totally, 55 windows and 8 doors are extracted with the proposed method, which means 2 doors were classified as windows.

5 Conclusion and Outlook

In this paper, we propose a novel algorithm to address the two main problems of automatic building modelling, namely: 1. precisely extract the information by using the raw inputs, 2.efficiently modelling

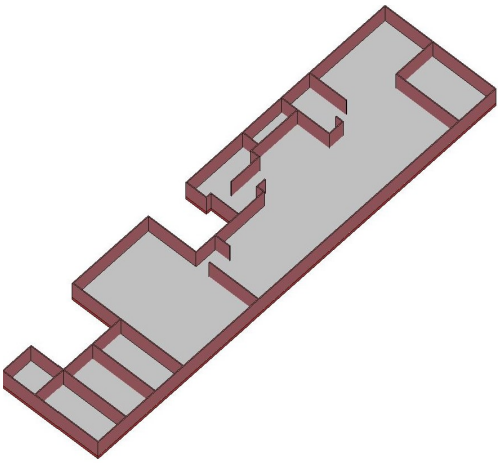

Figure 4: Reconstructed Wall Structures

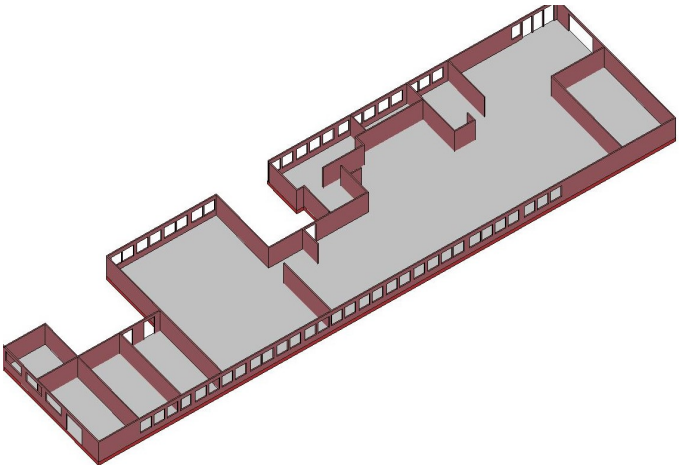

Figure 5: Reconstructed Openings in the BIM Model

based on the extracted information. By formalizing the raw inputs as a model represented by math equations, We rely on the maximum likelihood estimator to extract the parameters of the windows and door structure based on the gradient map of the acquired information. To the best of the authors' knowledge, this is the first work which directly handles the raw input point clouds, which doesn't rely on deep neural network or the generated pictures from the point cloud. The case study results show the preciseness and robustness of this proposed method. In summary, Our methods can deal with raw inputs without training data and also have no requirements of the point cloud quality. It can have a reasonably good performance on low-quality point cloud. The whole modeling process is automatic.

For the future work, combining the already well-trained neural network with our proposed method is an interesting way to go, in which we can make use of individual strengths by combining them. Another interesting point is using the generated model to perform the energy consumption prediction. Last but not least, the provided results of benchmark data set by [22] was measured only for wall elements. To evaluate the results of opening reconstruction process, the completeness, correctness and accuracy also need to be implemented to the opening detection.

References

[1] A. Borrmann, M. König, C. Koch, and J. Beetz, *Building Information Modeling: Technologische Grundlagen und industrielle Praxis*. Springer-Verlag, 2015.

[2] S. A. Adekunle, C. Aigbavboa, and O. A. Ejohwomu, "SCAN TO BIM: A systematic literature review network analysis", *IOP Conference Series: Materials Science and Engineering*, vol. 1218, no. 1, p. 012 057, Jan. 2022. DOI: 10.1088/1757-899x/1218/1/012057. [Online]. Available: https://doi.org/10.1088/1757-899x/1218/1/012057.

[3] P. Tang, D. Huber, B. Akinci, R. Lipman, and A. Lytle, "Automatic reconstruction of as-built building information models from laser-scanned point clouds: A review of related techniques",

Automation in Construction, vol. 19, no. 7, pp. 829–843, 2010, ISSN: 09265805. DOI: 10.1016/j.autcon.2010.06.007. [Online]. Available: http://dx.doi.org/10.1016/j.autcon.2010.06.007.

[4] Y. Xu and U. Stilla, "Toward Building and Civil Infrastructure Reconstruction from Point Clouds: A Review on Data and Key Techniques", *IEEE Journal of Selected Topics in Applied Earth Observations and Remote Sensing*, vol. 14, no. X, pp. 2857–2885, 2021, ISSN: 21511535. DOI: 10.1109/JSTARS.2021.3060568.

[5] A. Adan and D. Huber, "3D reconstruction of interior wall surfaces under occlusion and clutter", *Proceedings - 2011 International Conference on 3D Imaging, Modeling, Processing, Visualization and Transmission, 3DIMPVT 2011*, no. December 2016, pp. 275–281, 2011. DOI: 10.1109/3DIMPVT.2011.42.

[6] C. Mura, O. Mattausch, A. Jaspe Villanueva, E. Gobbetti, and R. Pajarola, "Automatic room detection and reconstruction in cluttered indoor environments with complex room layouts", *Computers and Graphics (Pergamon)*, vol. 44, no. 1, pp. 20–32, 2014, ISSN: 00978493. DOI: 10.1016/j.cag.2014.07.005.

[7] C. Thomson and J. Boehm, "Automatic geometry generation from point clouds for BIM", *Remote Sensing*, vol. 7, no. 9, pp. 11 753–11 775, 2015, ISSN: 20724292. DOI: 10.3390/rs70911753.

[8] I. Anagnostopoulos, V. Pătrăucean, I. Brilakis, and P. Vela, "Detection of walls, floors, and ceilings in point cloud data", in *Construction Research Congress 2016*, 2016, pp. 2302–2311.

[9] M. Previtali, L. Barazzetti, R. Brumana, and M. Scaioni, "Towards automatic indoor reconstruction of cluttered building rooms from point clouds", *ISPRS Annals of the Photogrammetry, Remote Sensing and Spatial Information Sciences*, vol. 2, no. 5, pp. 281–288, 2014, ISSN: 21949050. DOI: 10.5194/isprsannals-II-5-281-2014.

[10] H. Macher, T. Landes, and P. Grussenmeyer, "From point clouds to building information models: 3d semi-automatic reconstruction of indoors of existing buildings", *Applied Sciences*, vol. 7, no. 10, p. 1030, 2017.

[11] H. Macher, P. Grussenmeyer, T. Landes, G. Halin, C. Chevrier, and O. Huyghe, "Photogrammetric recording and reconstruction of town scale models – the case of the plan-relief of strasbourg", *The International Archives of the Photogrammetry, Remote Sensing and Spatial Information Sciences*, vol. XLII-2/W5, pp. 489–495, 2017. DOI: 10.5194/isprs-archives-XLII-2-W5-489-2017.

[12] H. Macher, T. Landes, P. Grussenmeyer, and E. Alby, "Semi-automatic segmentation and modelling from point clouds towards historical building information modelling", Nov. 2014, ISBN: 978-3-319-13694-3. DOI: 10.1007/978-3-319-13695-0_11.

[13] H. Macher, T. Landes, and P. Grussenmeyer, "Automation of thermal point clouds analysis for the extraction of windows and thermal bridges of building facades", *ISPRS - International Archives of the Photogrammetry, Remote Sensing and Spatial Information Sciences*, vol. XLIII-B2-2020, pp. 287–292, Aug. 2020. DOI: 10.5194/isprs-archives-XLIII-B2-2020-287-2020.

[14] H. Macher, L. Roy, and T. Landes, “Automation of windows detection from geometric and radiometric information of point clouds in a scan-to-BIM process”, in *XXIV ISPRS Congress (2021 edition), 5-9 juillet 2021, Nice (en ligne)*, vol. XLIII-B2-2021, Nice, France, Jul. 2021. DOI: 10.5194/isprs-archives-XLIII-B2-2021-193-2021. [Online]. Available: https://hal.archives-ouvertes.fr/hal-03402839.

[15] H. Tran, K. Khoshelham, A. Kealy, and L. Diaz-Vilarino, “Shape grammar approach to 3d modeling of indoor environments using point clouds”, *Journal of Computing in Civil Engineering*, vol. 33, p. 04 018 055, 1 2019, ISSN: 0887-3801. DOI: 10.1061/(asce)cp.1943-5487.0000800.

[16] M. Bassier, B. Van Genechten, and M. Vergauwen, “Classification of sensor independent point cloud data of building objects using random forests”, *Journal of Building Engineering*, vol. 21, pp. 468–477, 2019.

[17] S. Sahebdivani, H. Arefi, and M. Maboudi, “Deep learning based classification of color point cloud for 3d reconstruction of interior elements of buildings”, in *2020 International Conference on Machine Vision and Image Processing (MVIP)*, IEEE, 2020, pp. 1–6.

[18] C. R. Qi, H. Su, K. Mo, and L. J. Guibas, “Pointnet: Deep learning on point sets for 3d classification and segmentation”, in *Proceedings of the IEEE conference on computer vision and pattern recognition*, 2017, pp. 652–660.

[19] C. R. Qi, L. Yi, H. Su, and L. J. Guibas, “Pointnet++: Deep hierarchical feature learning on point sets in a metric space”, *Advances in neural information processing systems*, vol. 30, 2017.

[20] Z. Chen and S. Gentes, “From point cloud to as-built bim: Semi-automated wall reconstruction for dismantling of nuclear power plants”,

[21] K. Khoshelham, L. Diaz Vilarino, M. Peter, Z. Kang, and D. Acharya, “The isprs benchmark on indoor modelling”, *The International Archives of the Photogrammetry, Remote Sensing and Spatial Information Sciences*, vol. XLII-2/W7, pp. 367–372, 2017. DOI: 10.5194/isprs-archives-XLII-2-W7-367-2017.

[22] K. Khoshelham, H. Tran, L. Diaz-Vilarino, M. Peter, Z. Kang, and D. Acharya, “An evaluation framework for benchmarking indoor modelling methods”, *The International Archives of the Photogrammetry, Remote Sensing and Spatial Information Sciences*, vol. XLII-4, pp. 297–302, 2018. DOI: 10.5194/isprs-archives-XLII-4-297-2018.

Implementierung des Internet of Things (IoT) auf Basis von Radio-Frequency Identification (RFID) in das Building Information Modeling (BIM)

Abduaziz Juraboev[1,2]

[1]Fachbereich Bauwesen an der Technischen Hochschule Mittelhessen, [2]5D Institut GmbH

E-Mail: Abduaziz.Juraboev@bau.thm.de

Abstract: Die digitale Transformation im Bauwesen ist im permanenten Fortschritt begriffen. Ein wichtiges Instrument in diesem Zusammenhang stellt die kooperative Arbeitsmethodik Building Information Modeling (BIM) dar. Hierbei können durch objektorientierte, dreidimensionale, digitale Bauwerksmodelle jederzeit ganzheitlich projektrelevante Informationen auf den aktuellen Planungsstand gebracht werden. Zudem können diverse Werkzeuge, Sensoren und Apps für die Nutzung während der Planung, des Bauens und des Betriebs in zahlreichen Anwendungsgebieten eingesetzt werden. Im Mittelpunkt steht dabei immer der Mensch. Der folgende Beitrag beschäftigt sich mit der Einbindung von Sender-Empfänger-Systemen (RFID) und dem Internet of Things (IoT) in digitale Gebäudemodelle (BIM), womit die Verknüpfung von digitalen Bauwerksmodellen mit realen Bauelementen hergestellt wird. Der Fokus der Untersuchung liegt dabei auf einem wichtigen Anwendungsfall in diesem Zusammhang: „Entwicklung eines barrierefreien digitalen Leitsystems für Blinde und Sehbehinderte auf Basis von RFID&BIM“. Die physische Realisierung des Blindenleitsystems erfolgt über ein RFID-System, das aus RFID-Tags und einem elektronischen Blindenstock besteht, in den eine RFID-Sende- und Leseantenne integriert ist. Die passiven RFID-Tags werden in textile und mineralische Bauelemente am Boden integriert. Die in den RFID-Tags enthaltenen Informationen werden durch das Lesegerät am Blindenstock ausgelesen und auf Basis des BIM-Modells weiterverarbeitet. Die BIM-Modelle enthalten sämtliche Bauwerksinformationen in Form von Attributen, die mit Hilfe einer App an die Nutzer übermittelt werden. Insbesondere werden durch die Verknüpfung der RFID-Tags mit BIM-Daten zur Navigation erforderliche Informationen weitergegeben. Über eine App und akustische Elemente wie Audiospuren wird der Nutzer zu seinem gewünschten Zielort geleitet. Weiterhin können Umgebungsinformationen zum aktuellen Standort, z.B. zu Gegenständen wie Feuerlöscher, Hindernisse oder Räumlichkeiten etc., übermittelt werden. Gebäude und Städte werden somit auch akustisch erlebbar.

Keywords: Building Information Modelling (BIM), elektronisches Blindenleitsystem, modellbasierte Ortungs- und Navigationssystem, UHF Radio Frequency Identification (RFID), mobile App

1 Einleitung

Ein wichtiger Baustein der Inklusion sehgeschädigter und mobilitätseingeschränkter Menschen für die Teilhabe an gesellschaftlichen und beruflichen Aktivitäten ist die eigenständige Mobilität und Informationsbeschaffung. In Deutschland gab es laut statischem Bundesamt 2019 ca. 600.000 blinde und sehgeschädigte Menschen. Laut einer Hochrechnung auf Basis der Daten der WHO wird von 1,2 Mio. blinden und sehgeschädigten Menschen in Deutschland ausgegangen [1]. Die Zahl der sehbehinderten Personen ist viermal so hoch wie die Zahl blinder Personen. Einer von drei Senioren über 65 ist von Sehkraftverlust betroffen, dies entspricht 90 % der sehbehinderten Personen [2].

Blinde und sehgeschädigte Menschen orientieren sich im Allgemeinen mit Hilfe eines Blindenstocks in ihrer Umgebung, mit welchem sie Hindernisse erkennen. Sie orientieren sich im öffentlichen Bereich mit Hilfe taktiler Bodenindikatoren, sofern diese vorhanden sind. Im Bereich der taktilen Bodenplatten sind Aufmerksamkeitsfelder vorhanden, mit deren Hilfe sich blinde und sehgeschädigte Personen auch in komplexeren Umgebungsbereichen orientieren können. Weitere taktile Orientierungsmöglichkeiten für sehbehinderte Personen bieten in Brailleschrift gehaltene Schilder, z.B. Tür- und Handlaufschilder. Auch akustische Signale, wie bei Ampelanlagen oder an Bushaltestellen kommen in der Praxis häufig zum Einsatz [3]. Die genannten Leitsysteme haben allerdings den Nachteil, dass sie

- sehgeschädigte Personen nur leiten, keine genaueren Umgebungsinformationen liefern,
- im Indoor-Bereich relativ selten verbaut werden,
- in Notsituationen ungeeignet sind, wenn es z.B. darum geht, im Brandfall sehgeschädigte Personen schnell und zielsicher aus Gebäuden zu führen.

Besonders problematisch wird die Orientierung für sehgeschädigte Menschen in fremden Umgebungen (Straße, Gebäude) aufgrund der Ungenauigkeit der bereits vorhandenen Systeme. Ein Betroffener, der sich in der unbekannten Umgebung befindet, hat es schwer sich zurechtzufinden, da die Informationen über die vorher beschriebenen taktilen Hilfsmittel begrenzt sind. Die Nutzbarkeit von Gebäuden, insbesondere solchen mit komplexen Aufbauten ist für Menschen mit Beeinträchtigung, aber auch für Menschen ohne Einschränkungen, dadurch limitiert, dass eine Navigation innerhalb des Gebäudes ohne fremde Hilfe nur schwer möglich oder sehr mühsam ist. In Notfällen kann dies gravierende Folgen haben. Vor diesem Hintergrund gibt es im Sinne des barrierefreien Bauens dringenden Entwicklungsbedarf [4]. Um eine verbesserte Navigation zu ermöglichen, kommen elektronische Blindenleitsysteme zum Einsatz. Für die Entwicklung eines elektronischen, zentimetergenauen Blindennavigationssystems eignen sich z.B. RFID-Systeme. Durch Verknüpfung von elektronischen Blindenleitsystemen mit digitalen Bauwerksmodellen (BIM) wird eine präzise Navigation von blinden und sehbehinderten Personen im Innenbereich beliebiger Bauwerke möglich, ähnlich wie bei der Navigation über google maps im Außenbereich.

Ziel von Untersuchungen an der Technischen Hochschule Mittelhessen (THM) war es, ein zentimetergenaues Innen- und Außennavigationssystem für blinde und sehgeschädigte Menschen durch den kombinierten Einsatz innovativer Technologienkomponenten (Building Information Modeling (BIM), Radio Frequency Identification (RFID), Internet of Things (IoT) und cloud-basierter mobiler Anwendungen (App)) zu entwickeln (Abbildung 1). Durch die Zusammenführung der einzelnen Bausteine (Technologien und Methoden) auf dem jeweils neuesten Stand der Technik wird ein ganzheitliches System geschaffen, das dem Benutzer ermöglicht, sich präziser in unbekannter Umgebung zu bewegen und auditive Informationen aus den Bauteilen zu empfangen. Die RFID-Systeme werden bereits heute aufgrund ihrer einfachen Architektur und ihrer vielseitigen Erfassungsbereiche in vielen Branchen und bei groß angelegten IoT-Anwendungen eingesetzt. Es wurden passive RFID-Transponder im Ultrahochfrequenzbereich (865-928 MHz) verwendet. Sie sind batterielos, haben eine lange Lebensdauer, sind klein und kostengünstig [5], [6]. In Abbildung 1 ist das kombinierte RFID- & BIM-gestütze Blindenleitsystem in veranschaulichter Form dargestellt.

Abbildung 1: RFID- & BIM-Modell-gestütztes, präzises Indoor-& Outdoornavigationssystem auf Basis von Bauelementen

Im Rahmen der Untersuchungen wurden das o.g. Blindenleitsystem durch die Einbindung des RFID-Systems in die BIM-Planung mit Hilfe geeigneter Softwareprodukte auf Basis des openBIM-Ansatzes weiterentwickelt, um eine optimierte Navigation im Innenbereich zu ermöglichen. In diesem Beitrag wird die Implementierung der RFID-gestützten Blindenleitsysteme in die BIM-Planung vorgestellt. Grundlage für den Datenaustausch ist der openBIM-Standard Industry Foundation Classes (IFC), ein offener, herstellerneutraler, internationaler Standard nach ISO 16739-1:2018, [7].

2 Grundlagen und Stand der Technik

Das elektronische Blindenleitsystem, das im Rahmen der Untersuchungen in diesem Projekt entwickelt wurde, beruht auf dem kombinierten Einsatz folgender drei Technologienkomponenten: Building Information Modeling (BIM), Internet of Things (IoT) / Radio Frequency Identification (RFID), cloud-basierter mobiler Anwendungen (App) zur Navigation.

Building Information Modeling bezeichnet eine Arbeitsmethodik, bei der auf Grundlage eines digitalen, dreidimensionalen Gebäudemodells alle für den gesamten Lebenszyklus relevanten Daten und Informationen eines Bauwerks erfasst, verwaltet und verarbeitet werden [8]. Diese Informationen werden transparent unter den Beteiligten ausgetauscht und für die weitere Bearbeitung zur Verfügung gestellt. Die erfassten Daten und Informationen werden sowohl für die Planung und die Ausführung als auch für den Betrieb und Rückbau des Bauwerks genutzt [9], [10]. Ein BIM-Bauwerksmodell stellt in der digitalen Welt den digitalen Zwilling zum realem Bauwerk dar und kann durch die Integration von RFID-Tags in unterschiedlichen Bauteilen im realen Bauwerk (z.B. in textile- oder mineralische- Bodenbeläge) mit diesem verknüpft werden. Die Verknüpfung von BIM-Daten mit den physischen Bauwerken auf Basis von RFID, Sensoren und/oder weiteren drahtlosen IoT-Technologien in einer Multi-Plattform-Applikation ermöglicht die Nutzung und Nachverfolgung einzelner Bauwerksobjekte. Einer der vielfältigen Anwendungsbereiche ist die Einbindung eines Real Time Locating Systems (RTLS) in die BIM-Planung.

RTLS [11] werden zur automatischen Bestimmung und Verfolgung des Standorts von Objekten oder Personen in Echtzeit eingesetzt. RTLS kann z. B. zur Verfolgung von Paletten in Lagern, zur Lokalisierung medizinischer Geräte in einer Klinik oder zur Verfolgung von Personen zu Sicherheitszwecken eingesetzt werden. Zu den gängigsten Ortungstechnologien neben GPS gehören Wi-Fi, Bluetooth Low Energy (BLE) Beacon, Ultrabreitband (UWB) sowie die drahtlosen RFID-Sender-Empfängersysteme. Die heute auf dem Markt befindlichen GPS-Systeme eignen sich im Allgemeinen aufgrund der relativ ungenauen Positionsbestimmung für die Fußgängernavigation sehbehinderter Menschen im Innenbereich nicht [12], da im Innenbereich eine sehr hohe Dichte an Aufmerksamkeitsfeldern im Vergleich zum Außenbereich notwendig ist. Betrachtet man z.B. einen Korridor in einem Verwaltungsgebäude mit mehreren Büroeingängen, Treppen und Aufzügen auf beiden Seiten, würde dies zu einem Bereich von vielen sehr nahe beieinander liegenden Feldern (teilweise < 1 m) führen. Es müssen zielgerichtet Räume, Gänge, Feuerlöscher, Defibrillatoren, Schalter etc. ohne größere Suchaktionen gefunden werden können. Ein geeignetes Positionierungssystem muss hierbei eine sehr hohe Genauigkeit besitzen, damit keine falschen Felder erkannt werden.

RFID ist eine Technologie für Sender-Empfängersysteme, mit deren Hilfe ein automatisches und berührungsloses Identifizieren und Lokalisieren von Objekten mithilfe von Radiowellen möglich ist [5]. Während mithilfe von RFID die Gegenstände eindeutig identifiziert werden können, bietet die IoT

darüber hinaus die Möglichkeit über das Internet bzw. andere Kommunikationsnetze Daten mit anderen Geräten und Systemen mithilfe von Soft- und Hardware auszutauschen.

Die Web-Anwendung ist die stabile und bewährte weltweite universelle Laufzeitumgebung. Heute unterstützt das Web eine vielfältige und ständig wachsende Anzahl an Anwendungen von traditionellen mobilen Desktop-Anwendungen bis hin zu progressiven Web-Apps und IoT-Geräten. Die in diesem Projekt entwickelte Prototyp-App beruht auf den open-source Webtechnologien HTML, CSS, JavaScript und kann in einer Cloud-Plattform hochgefahren werden. Dazu zählen u.a. Heroku, Azure, Digital Ocean.

3 Untersuchungen

3.1 Überblick und Workflow

Ein Überblick & Workflow bzgl. der durchgeführten Untersuchungen ist in

Abbildung 2 dargestellt.

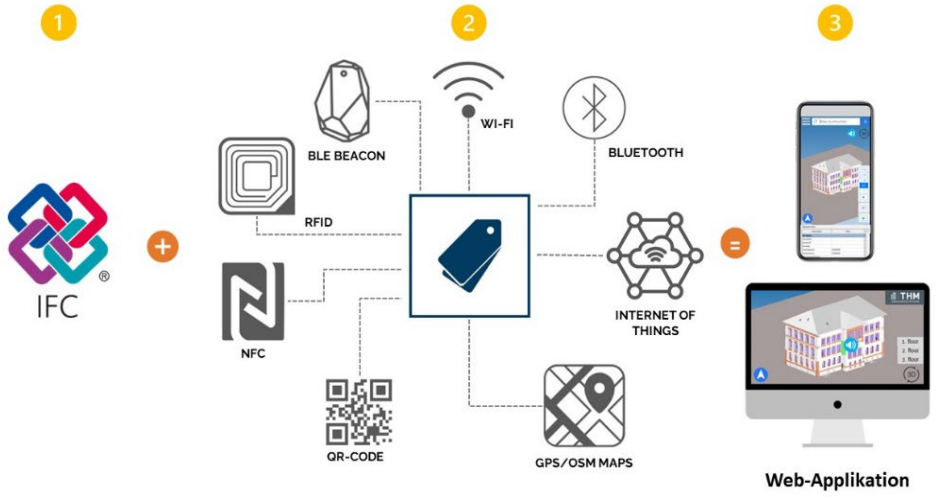

Abbildung 2: Workflow zur Integration von RTLS- und IoT-Technologien in digitale Bauwerks-Informations-Modellen und physische Bauelementen

1. BIM-Modelle werden zur Planung von Navigationspfaden mit sämtlichen Informationen in Form von Attributen definiert. Da RFID-Elemente in der aktuellen Ausgabe des IFC-Standards noch nicht abgebildet sind [13], werden sie in diesem Projekt in das bestehende IFC-Dateiformat durch Verwendung von Proxy-Elementen *(IfcBuildingElementProxy)* und Eigenschaftssätzen *(Property sets)* integriert [14]. Die Seriennummern von RFID-Tags (UID) werden in Revit als Attribute definiert und in das *.ifc*-Dateiformat exportiert. Dadurch wird die Verknüpfung des physischen Objekts mit dem virtuellen BIM-Modell über die im Rahmen des Projektes entwickelte App ermöglicht.

2. Die passiven RFID-Tags wurden in unterschiedliche Baustoffe (Betonplatten, Pflastersteine und Teppichfliesen) an wichtigen Orten (Ein- und Ausgang, Kreuzungen, Abzweigungen) in taktile Aufmerksamkeitsfelder (Point of Interests) eingebracht. Die Untersuchungen zeigten, dass die optimale Empfangsreichweite für die Entwicklung eines lückenlosen RFID-gestützten Navigationssystems durch das Scannen mit dem elektronischen Blindenstock bei max. 15 cm beträgt. Daher wurde in jeden taktilen Bodenindikator jeweils 1 Stück passiver RFID-Tag verbaut. Es wurden unterschiedliche RFID-Tags in die Untersuchung einbezogen und deren Verlegeanordnung (z.B. kreuzförmig, linienförmig) variiert mit dem Ziel die Empfangsreichweite des RFID-Systems zu optimieren. Das im Blindenstock integrierte RFID-Lesegerät kann beim Scannen der Tags mit Hilfe der Bluetooth-Funktion mit der entwickelten App gekoppelt werden. Die physischen realen Bauwerksobjekte werden durch die App mit den virtuellen digitalen Bauwerksmodellen und -daten (BIM) beim Scannen der RFID-Tags verknüpft.

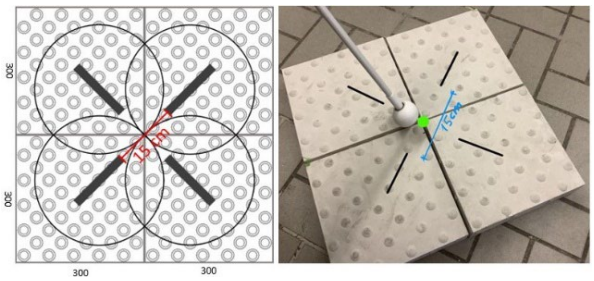

Abbildung 3: Einbringung von passiven RFID tags in die taktilen Bodenindikatoren

3. Eine mobile Web-App für Smartphones wurde als Multi-Plattform-Lösung implementiert, die mit Hilfe von Bluetooth und Wi-Fi mit dem elektronischen Blindenstock gekoppelt wird. Beim Scannen eines RFID-Tags werden die Audio-Informationen abgespielt, die in der gemeinsamen Datenumgebung (CDE) in den BIM-Modellen abgelegt wurden.

3.2 Architektur des entwickelten Systems

Peripheriegeräte: Hierzu gehören das RFID-System incl. dem Blindenlangstock (1) mit integrierter Lese- und Sende-Einheit sowie die Middleware. In den Bodenbelag wurden passive RFID-Transponder (2) jeweils in 15 cm Abständen (Außenkante Tag) eingebracht.

Frontend und Backend: Sobald der Blindenstock ein oder mehrere RFID-Tags ausgelesen hat, wird die Seriennummer an die entwickelte App (3) über eine Bluetooth-Verbindung weitergeleitet. Die hybride App ermöglicht es einerseits dem Planer und Betreiber BIM-Modelle jederzeit zu prüfen und anzupassen und andererseits dem Nutzer alle notwendigen Bauwerksinformationen abzurufen und sich präzise navigieren zu lassen. Zum Laden, Anzeigen und Bearbeiten von open-source IFC-Modellen wurde Ifc.JS [15], eine JavaScript BIM-Toolkit (4) verwendet. Damit können die BIM-Modell-gestützen Daten in jedem Browser zur Verfügung gestellt werden. Die Seriennummern der RFID-Tags mit den entsprechenden Raumpositionen (Koordinaten) sind in BIM als Objekte und Attribute eingetragen (5) und werden beim Scannen des Tags aus dem Modell extrahiert. Daraufhin wird eine Audio-Datei abgespielt. In der Datenbank MongoDB und dem Cloud-Speicher Digital Ocean (6) werden die IFC-Modelle gespeichert und dem Nutzer zur Verfügung gestellt. Das BIM-Modell (5) wurde mit der Software Revit erstellt und als IFC-Datei exportiert.

Die Architektur des entwickelten Blindenleitsystems wird in Abbildung 4 beschrieben.

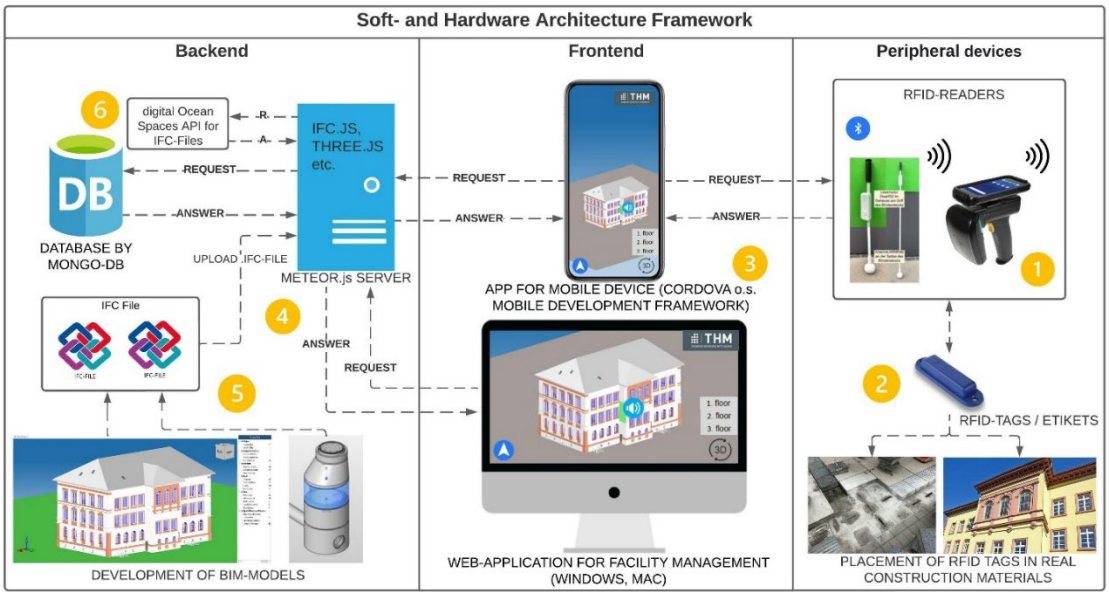

Abbildung 4: Die Architektur von RFID- und drahtlosen IoT-Technologien in BIM für die Entwicklung einer Multi-Plattform-Applikation für verschiedene Anwendungsgebiete

Die im Rahmen dieses Projektes entwickelte Prototyp-App „openNaviBIM“ kann unter dem Link https://opennavibim.herokuapp.com/ abgerufen werden und ist in der Weiterentwicklung.

4 Ergebnise und Ausblick

Die Implementierung des IoT auf Basis von RFID in das digitale Bauwerksmodell liefert einen Beitrag zur barrierefreien Planung und zur präzisen Orientierung in der Umgebung. Zusätzlich schafft sie einen Mehrwert beim Zusammenwirken von Menschen, Werkzeugen und Prozessen in der langen Betriebs- und Nutzungsphase der Bauwerke für die Öffentlichkeit. Die taktilen Blindenleitsysteme sind bereits heute etabliert [3]. Ein audio-basiertes Blindenleitsystem auf Basis von BIM, IoT und RFID ist ein ganzheitlicher Ansatz, um die Bauwerkselemente mit den zugeordneten Informationen der Tags zu kennzeichnen und diese für den Planungsprozess und für eine präzise Navigation zu nutzen. Des Weiteren stellt BIM die Metadaten zur Verfügung, die zur Etablierung eines Leitsystems in Bauwerken notwendig sind. Um die reale Welt mit den digitalen Bauwerksmodellen auf Basis von BIM verknüpfen zu können, wurden RFID und drahtlose IoT-Technologien eingesetzt.

Die Untersuchungen haben gezeigt, dass physische Bauwerksobjekte mit BIM-Modellen und RFID-Systemen verknüpft werden können. Für die akustische und visuelle Darstellungen aller wichtigen Bauwerksinformationen steht die entwickelte App zur Verfügung. Auf dieser Grundlage können sehbehinderte Personen präzise durch ein Gebäude geleitet werden.

Die Verknüpfung digitaler Modelle mit realen Bauobjekten kann für weitere innovative Anwendungen einen Mehrwert darstellen, beispielhaft seien die modellbasierte Ortungs- und Instandhaltung von Objekten oder die Unterstützung von Managementprozessen und Logistik genannt.

Literatur

[1] Deutscher Blinden- und Sehbehindertenverband e.V: DBSV-Stellungnahme zum Regierungsentwurf eines Gesetzes zur Modernisierung des Personenbeförderungsrechts (PBefG) - Deutscher Blinden- und Sehbehindertenverband e.V, 2021. https://www.dbsv.org/stellungnahme/PBefG-RegE.html, abgerufen am: 29.10.2021

[2] European Blind Union: Facts and figures about Blindness and partial sight, 2021. https://www.euroblind.org/about-blindness-and-partial-sight/facts-and-figures, abgerufen am: 05.12.2021

[3] nullbarriere: DIN 32984 - Bodenindikatoren im öffentlichen Raum, 2021. https://nullbarriere.de/din32984.htm, abgerufen am: 26.12.2021

[4] Bundesministerium für Verkehr u. Bau und Stadtentwicklung: Bewertungssystem Nachhaltiges Bauen (BNB) Büro- und Verwaltungsgebäude. 3.2.1 Barrierefreiheit, 2015. https://www.bnb-nachhaltigesbauen.de/fileadmin/steckbriefe/verwaltungsgebaeude/neubau/v_2015/BNB_BN2015_321.pdf, abgerufen am: 26.12.2021

[5] Finkenzeller, K.: RFID-Handbuch. Grundlagen und praktische Anwendungen von Transpondern, kontaktlosen Chipkarten und NFC. München: Hanser 2015

[6] Schatz, G.: Active Vs. Passive RFID For Location Tracking, 2022. https://www.link-labs.com/blog/active-vs-passive-rfid, abgerufen am: 24.01.2022

[7] ISO 16739-1:2018 16739-1:2018:2021-12. *ISO 16739-1:2018. Industry Foundation Classes (IFC) for data sharing in the construction and facility management industries — Part 1: Data schema*. https://www.iso.org/standard/70303.html, abgerufen am: 23.12.2021

[8] Jens Minnert, Joaquin Diaz, Christian Baier: Einführung in die statische Berechnung von Bauwerken. WIT. Köln: Reguvis 2020

[9] Bundesministerium für Verkehr und Digitale Infrastruktur: Handreichungen BIM4INFRA2020. Grundlagen und BIM-Gesamtprozess, 2019. https://bim4infra.de/wp-content/uploads/2019/07/BIM4INFRA2020_AP4_Teil1.pdf, abgerufen am: 29.12.2021

[10] Borrmann, A., König, M., Koch, C. u. Beetz, J.: Building Information Modeling. Technologische Grundlagen und industrielle Praxis. Wiesbaden: Springer Fachmedien Wiesbaden 2021

[11] RFID JOURNAL: The Differences Between RFID and RTLS, 2017. https://www.rfidjournal.com/the-differences-between-rfid-and-rtls, abgerufen am: 05.01.2022

[12] Elektronik Kompendium: GPS - Global Positioning System, 2022. https://www.elektronik-kompendium.de/sites/kom/1201071.htm, abgerufen am: 24.01.2022

[13] buildingSMART International Ltd.: 7 Domain specific data schemas of IFC. IfcSensor, 2022. https://standards.buildingsmart.org/IFC/RELEASE/IFC4/ADD2_TC1/HTML/, abgerufen am: 10.02.2022

[14] Motamedi, A., Soltani, M. M., Setayeshgar, S. u. Hammad, A.: Extending IFC to incorporate information of RFID tags attached to building elements. Advanced Engineering Informatics 30 (2016) 1, S. 39–53

[15] Perdigao, B.: A new browser IFC viewer is released in IFC.js. OSArch (2020)

Enriching Point Features to Improve Semantic Segmentation of Point Clouds

Yuandong Pan[1,2], M. Saeed Mafipour[1] and Mansour Mehranfar[1]
[1]Chair of Computational Modeling and Simulation, Technical University of Munich, Arcisstrasse 21, 80333 Munich, Germany
[2]Institute for Advanced Study, Technical University of Munich, Lichtenbergstrasse 2a, 85748 Munich, Germany
E-mail(s): yuandong.pan@tum.de, m.saeed.mafipour@tum.de, mansour.mehranfar@tum.de

Abstract: Recent advances in capturing technologies have resulted in the fast capturing process of existing assets with high measurement accuracy. The resulting point cloud data (PCD) can be processed and used for the digital twinning of existing facilities. Point cloud segmentation is a critical step, and it has been continuously improved by 3D deep learning approaches, which require point features as input and predict labels as output. In this paper, apart from those features from raw data such as spatial information (x-, y-, z-coordinates) and colour information (RGB values), we propose a set of new point features which considers points' local neighbouring information and the global information in the entire point cloud. We compute new point features in two different facilities (building and bridge) and evaluate the performance of two different networks with and without new features as input. The results show that the proposed feature enrichment can improve point cloud segmentation as well as digital twinning of assets.

Keywords: Semantic Segmentation, Digital Twins, Deep Learning, Point Cloud Data

1 Introduction

In the architecture, engineering, and construction (AEC) industry, digital methods have revealed tremendous applications in facilitating the operation and maintenance process of structures. In this domain, building information modeling (BIM) has been able to provide descriptive models to support structures through their life cycle. A building information model contains the geometry and corresponding data to represent the design and construction activities. As one of the recent advances in AEC, BIM has been used not only in the as-designed phase of the structure but also in as-built and as-is phases. In recent decades, there have been concerted research efforts to create and optimize BIM in the as-designed phase of structures. However, the lack of descriptive and digital methods in the as-built and as-is phases is still tangible.

As-built and as-is models correspond to the descriptive representation of existing assets from their post-construction phases. These models are utilized for monitoring and evaluation of the structure as well as its maintenance and operation. Recently, the concepts of as-built and as-is have been extended to digital twin (DT). In the domain of BIM, a DT can be defined as a geometric-semantic replica that represents the current status of the structure. DT of a structure inherits all the features of an as-is model and also demonstrates the interaction of humans with the structure. A DT can be updated in regular intervals depending on the type of the product. These intervals can be longer in the case of structures, as the physical features of the asset change gradually. The modeling process of an as-is or DT is generally started from the 3D model reconstruction of the existing structure. This model is then enriched with the information collected from the construction site. These models are generally created from the point cloud data (PCD) captured by laser scanning or photogrammetry. Semantic segmentation is an essential step in processing PCD and creating as-built, as-is, or DT models. Through semantic segmentation, the entire PCD is separated into the point clusters demonstrating the desired elements (classes). The point cloud of elements can then be used to create the 3D model of the structure. Semantic segmentation has two significant advantages: 1) the modeling process is simplified from the entire PCD to the cloud of elements, and 2) the element type of the segmented clouds is recognized. In the current practice, the semantic segmentation process of assets is performed manually, which is labor-intensive and error-prone. Recently, there have been efforts to automate the semantic segmentation process of PCD captured from buildings and bridges. Especially with the help of deep learning, the results of point cloud segmentation have been improved a lot. Apart from designing the new architecture of neural networks, point features also have a significant impact on the result.

This paper is organised as follows. Section 2 discussed some related research in point cloud segmentation by deep learning. The proposed feature design is introduced in Section 3. Results and discussions are shown in Section 4. In Section 5, we summarise the output and discuss potential future work.

2 Related research

Deep learning approaches have been widely applied to predict unknown information based on input features in the dataset. In general, predicting unknown labels from input features is the classification problem in deep learning [1]. When processing point cloud, we usually use the term segmentation. But it can also be seen as a classification problem for each point in the point cloud. Many networks are designed to adapt to both classification problems and segmentation problems in one architecture framework.

As point clouds are usually unstructured data, some deep learning approaches requires a pre-processing step. By voxelisation, the unstructured point cloud data are converted to voxel structure. In [2], 3D Convolutional Neural networks (CNNs) are applied to solve a binary classification problem. A more general network with 3D CNN architecture, VoxNet [3] is proposed to detect classes of objects

for 3D point cloud data. A volumetric grid that can represent the spatial occupancy is calculated first and then applied to 3D CNNs. However, some original information from the raw point cloud could be lost in the voxelisation process.

Many networks try to work with points directly. One architecture named PointNet, proposed in [4], is the pioneer in this field. It takes point clouds as input directly and outputs labels for the entire input (classification task) or labels for each point (segmentation task). The novel design of PointNet considers each point (x-, y-, z-coordinate) independently at the first stage. Apart from the three spatial coordinates values (x,y,z), it can also use additional features like colours, normals, etc. An improved network based on PointNet considering spatial information of point sets proposed by the same author is called PointNet++ [5]. In PointNet++, points are grouped into overlapping local regions by their distance. Then local features are extracted by extracting fine geometric structures from small neighbour regions. These local features are then grouped together into larger units and processed to make relative higher-level features. Many more advanced networks are proposed to improve the prediction performance. In [6], a module that learns spatial contextual features from the point cloud is implemented and embedded in an encoder-decoder architecture. In [7], the local information of points is extracted, and the distinctness of the points from multiple resolutions is considered to achieve semantic segmentation. In recent years, the transformer architecture [8], originated from natural language processing (NLP), is applied in point cloud segmentation, such as [9], [10], and [11]. These networks prove the transformer architecture is very powerful in 3D deep learning.

With regard to processing point cloud in built environment, [12] employed a heuristic top-down approach to detect the bridge elements in the point cloud of concrete bridges. [13] elaborated a hybrid image-based-geometric point cloud segmentation method to extract features from images and train a multilayer perceptron (MLP). [14] applied a density-based heuristic algorithm to detect elements in the point cloud of bridges. As a geometric approach, [15] added contextual features of points to improve the accuracy of PointNet, and deep graph-convolutional neural network (DGCNN) [16]. [17] introduced a heuristic algorithm based on the existing connection rules in the point cloud of steel bridges for semantic segmentation. [18] defined a local descriptor to calculate the local features of points for semantic segmentation of bridges through a geometric method. In [19], the authors design a network for the Scan-to-BIM process to segment the structural, architectural, and mechanical components.

3 Proposed Method

Depending on device that used to collect point clouds, point features available in the point clouds can be differentiated. The basic features that usually exist in most of the point clouds are 3D coordinates (x,y,z) and colour values (r,g,b). In this section, seven more features are calculated from the point clouds and the input feature vector is enriched from the 6 original features to 13 features.

3.1 Features representing local information

The components of normal vectors in 3D are the first three values that are added to the feature vector. Basically, the normal of a point can to be estimated from the surrounding neighbouring points by estimating the normal of a plane tangent to the surface. normal vector of points can be a valuable property that differentiates various points easily. For example, the normal of a point on the vertical wall is horizontal while this normal vector is vertical on the horizontal floor points. Since estimated normals can only represent the neighbouring geometric information of points, more features that include other information are considered.

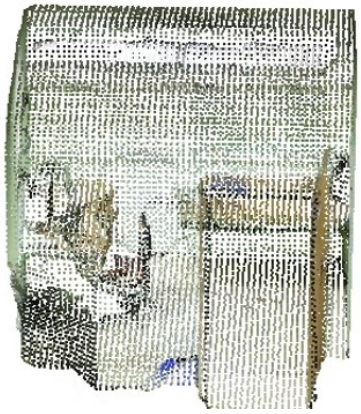

Figure 1: Original point cloud of room

Figure 2: Colour field for number of neighbouring points

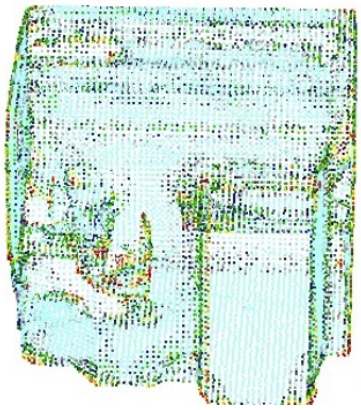

Figure 3: Colour field for mean shift

The number of neighbouring points within a given radius of a point can also differentiate some points. For those point located in dense region (for example room corner), their value would be higher than others. The colour-coded scalar field for the number of neighbouring points is shown in Figure 2, in which the neighbouring number for red points is larger. Another local feature that we use is the mean shift of a point. We compute the centroid of a point's neighbouring points within a radius first and then compute the distance between the centroid and the point. The colour-coded scalar field for the mean shift value is shown in Figure 3. We can see the value for those points on edges is usually larger.

3.2 Features representing density after projection

Apart from the features incorporating the local information of points, two more features representing the density of points after projection are added. The first one, called the 2D density, is the number of neighboring points after projection. This feature is calculated after projection of all points onto the XY plane and computing the number of neighbours within a circle with a predefined radius. The colour-coded scalar field for this value is shown in Figure 4. As we can see, this value is larger for those points on the vertical plane (yellow/red points) while smaller on the horizontal plane (blue points). This value shows the distribution of all points in the point cloud on the XY plane.

Similarly, for the second density-based feature, all the points are projected onto the z-axis and the number of neighbours within a range on the axis is computed. The colour-coded scalar field for this

value is shown in Figure 5. As we can see, this value is larger for those points on the horizontal plane (yellow/red points) while smaller on the vertical plane (blue points).

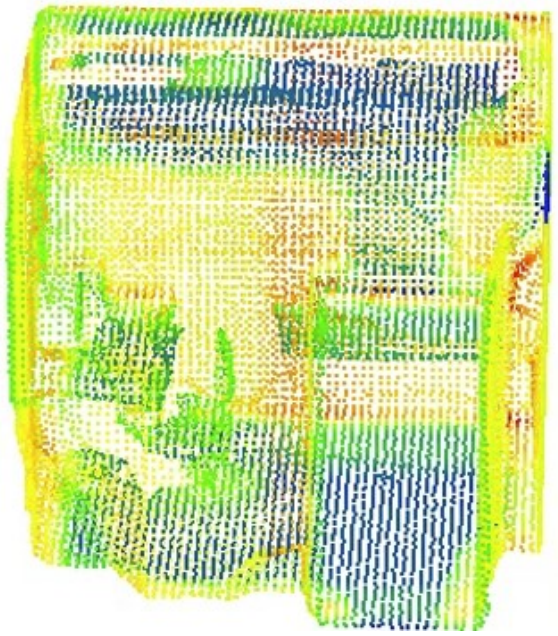

Figure 4: Colour field for number of neighbours in XY plane

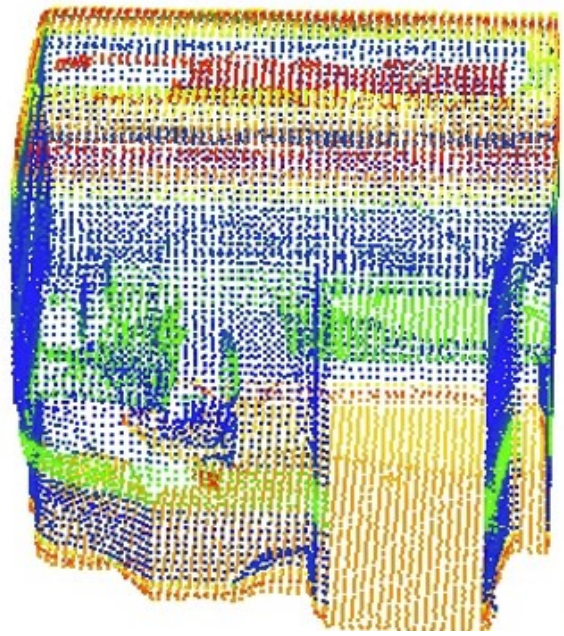

Figure 5: Colour field for number of neighbours in vertical direction

4 Experiment and Result

The designed features are extracted for two datasets including the S3DIS dataset [20] which is the point cloud dataset of large scale indoor environment, and a birdge dataset that contains 10 bridges [12]. Also, the performance of enriching features are evaluated in two networks (Pointnet++ [5] and RandLA-Net [21]).

Test results of RandLA-Net [21] on the bridge dataset are shown in Figure 6 to Figure 9. It can be seen that the prediction with feature enrichment is closer to the ground truth. This can be also seen in the Table 1, where Intersection over Union (IoU), as a statistical indicator, is higher for the dataset with feature enrichment. It is obvious that the results of all classes are improved by enriching features of points.

Figure 6: Original point cloud of bridge

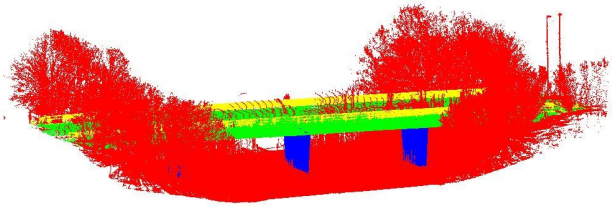

Figure 7: Semantic ground truth for bridge

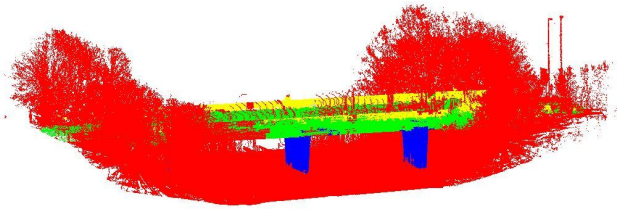

Figure 8: Prediction result without feature enrichment

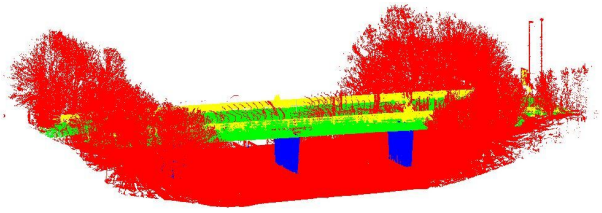

Figure 9: Prediction result with feature enrichment

Table 1: Prediction result with/without feature enrichment in bridge dataset (IoU:%)

	mIoU	Deck	Pier	Railing	Background
without	74.4	77.6	78.5	48.4	93.0
with	87.8	93.6	88.3	72.7	96.7

In the dataset of indoor environments, Pointnet++ [5] is trained and evaluated based on IoU as well. The quantitative evaluation result is shown in Table 2. It can be seen that the results of most classes of structural elements such as ceiling, floor, wall, and column are improved. However, the prediction accuracy for some classes such as sofa (from 42.2% to 26.6%) and bookcase (from 59.8% to 56.2%) decreases.

The potential reason is that most of the structural elements in buildings and bridges are either horizontal or vertical. Horizontal elements such as slabs or decks generally provide the required surfaces for sustaining and transferring the applying live loads to the structure. Vertical elements such as columns or piers on the other side convey the dead and live loads of the structure to the ground. The newly added features can represent the information of vertical and horizontal planes. However, they cannot illustrate geometric information of furniture points which are not horizontal or vertical. Hence, the newly added information makes the model more confused in distinguishing those points.

Table 2: Prediction result with/without feature enrichment in building dataset (IoU:%)

	mIoU	Ceiling	Floor	Wall	Beam	Column	Window	Door	Table	Chair	Sofa	Bookcase	Board	Clutter
without	52.7	86.0	96.2	70.3	0	4.2	37.2	26.8	66.2	71.4	42.2	59.8	47.1	40.2
with	54.7	88.8	96.4	74.4	1.1	15.4	38.2	26.6	67.2	78.8	26.6	56.2	45.6	38.8

5 Conclusion

The paper presents a new feature enrichment design for semantic segmentation of point cloud data. The results of testing two different network architectures on the dataset of two different facilities shows that feature enrichment can improve the performance of the deep learning models. In addition, the results show higher improvement in the prediction accuracy of the bridge dataset than that of the building dataset. It seems that there are two potential reasons behind that. Firstly, the class number in the bridge dataset is smaller, and this makes the segmentation relatively easier. Secondly, the occlusion in the bridge point cloud is not as much as that in the building where lots of furniture exists.

Despite improvements in the prediction accuracy of deep learning models, the impact of each feature on the performance of the model is still unclear.

In the future, more features are added and tested separately for improving the performance of 3D deep learning models. Also more hand-crafted features are explicitly designed for the models.

References

[1] I. Goodfellow, Y. Bengio, and A. Courville, *Deep learning*. MIT press, 2016.

[2] D. Prokhorov, "A convolutional learning system for object classification in 3-d lidar data", *Trans. Neur. Netw.*, vol. 21, no. 5, pp. 858–863, May 2010, ISSN: 1045-9227. DOI: 10.1109/TNN.2010.2044802. [Online]. Available: http://dx.doi.org/10.1109/TNN.2010.2044802.

[3] D. Maturana and S. Scherer, "Voxnet: A 3d convolutional neural network for real-time object recognition", in *Ieee/rsj International Conference on Intelligent Robots and Systems*, 2015, pp. 922–928.

[4] C. R. Qi, H. Su, K. Mo, and L. J. Guibas, "Pointnet: Deep learning on point sets for 3d classification and segmentation", *arXiv preprint arXiv:1612.00593*, 2016.

[5] C. R. Qi, L. Yi, H. Su, and L. J. Guibas, "Pointnet++: Deep hierarchical feature learning on point sets in a metric space", *arXiv preprint arXiv:1706.02413*, 2017.

[6] S. Fan, Q. Dong, F. Zhu, Y. Lv, P. Ye, and F.-Y. Wang, "Scf-net: Learning spatial contextual features for large-scale point cloud segmentation", in *Proceedings of the IEEE/CVF Conference on Computer Vision and Pattern Recognition*, 2021, pp. 14 504–14 513.

[7] S. Qiu, S. Anwar, and N. Barnes, "Semantic segmentation for real point cloud scenes via bilateral augmentation and adaptive fusion", in *Proceedings of the IEEE/CVF Conference on Computer Vision and Pattern Recognition (CVPR)*, 2021, pp. 1757–1767.

[8] A. Vaswani, N. Shazeer, N. Parmar, *et al.*, "Attention is all you need", *Advances in neural information processing systems*, vol. 30, 2017.

[9] M.-H. Guo, J.-X. Cai, Z.-N. Liu, T.-J. Mu, R. R. Martin, and S.-M. Hu, "Pct: Point cloud transformer", *Computational Visual Media*, vol. 7, no. 2, pp. 187–199, 2021.

[10] H. Zhao, L. Jiang, J. Jia, P. H. Torr, and V. Koltun, "Point transformer", in *Proceedings of the IEEE/CVF International Conference on Computer Vision*, 2021, pp. 16 259–16 268.

[11] N. Engel, V. Belagiannis, and K. Dietmayer, "Point transformer", *IEEE Access*, vol. 9, pp. 134 826–134 840, 2021.

[12] R. Lu, I. Brilakis, and C. R. Middleton, "Detection of structural components in point clouds of existing rc bridges", *Computer-Aided Civil and Infrastructure Engineering*, vol. 34, no. 3, pp. 191–212, 2019, ISSN: 1093-9687. DOI: http://dx.doi.org/10.1111/mice.12407.

[13] F. Hu, J. Zhao, Y. Huang, and H. Li, “Structure-aware 3d reconstruction for cable-stayed bridges: A learning-based method”, *Computer-Aided Civil and Infrastructure Engineering*, vol. 36, no. 1, pp. 89–108, 2021, ISSN: 1093-9687.

[14] G. Qin, Y. Zhou, K. Hu, D. Han, and C. Ying, “Automated reconstruction of parametric bim for bridge based on terrestrial laser scanning data”, *Advances in Civil Engineering*, vol. 2021, p. 8 899 323, 2021, ISSN: 1687-8086. DOI: https://doi.org/10.1155/2021/8899323.

[15] J. S. Lee, J. Park, and Y.-M. Ryu, “Semantic segmentation of bridge components based on hierarchical point cloud model”, *Automation in Construction*, vol. 130, p. 103 847, 2021, ISSN: 0926-5805.

[16] Y. Wang, Y. Sun, Z. Liu, S. E. Sarma, M. M. Bronstein, and J. M. Solomon, “Dynamic graph cnn for learning on point clouds”, *ACM Transactions on Graphics (TOG)*, vol. 38, pp. 1–12, 2019.

[17] Y. Yan and J. F. Hajjar, “Automated extraction of structural elements in steel girder bridges from laser point clouds”, *Automation in Construction*, vol. 125, p. 103 582, 2021, ISSN: 0926-5805.

[18] T. Xia, J. Yang, and L. Chen, “Automated semantic segmentation of bridge point cloud based on local descriptor and machine learning”, *Automation in Construction*, vol. 133, p. 103 992, 2022, ISSN: 0926-5805.

[19] Y. Perez-Perez, M. Golparvar-Fard, and K. El-Rayes, “Scan2bim-net: Deep learning method for segmentation of point clouds for scan-to-bim”, *Journal of Construction Engineering and Management*, vol. 147, no. 9, p. 04 021 107, 2021.

[20] I. Armeni, O. Sener, A. R. Zamir, *et al.*, “3d semantic parsing of large-scale indoor spaces”, in *Proceedings of the IEEE International Conference on Computer Vision and Pattern Recognition*, 2016.

[21] Q. Hu, B. Yang, L. Xie, *et al.*, “Randla-net: Efficient semantic segmentation of large-scale point clouds”, *Proceedings of the IEEE Conference on Computer Vision and Pattern Recognition*, 2020.

Semantic Segmentation of Real and Synthetic Point Cloud Data for Digital Twinning of Bridges

M. Saeed Mafipour[1], Cagatay Alici[1], S. Saadat Shakeel[1] and Affan Kalkavan[1]
[1]Chair of Computational Modeling and Simulation, Technical University of Munich, Arcisstraße 21, 80333 Munich, Germany
E-mail(s): m.saeed.mafipour@tum.de, cagatay.alici@tum.de, saadat.shakeel@tum.de, affan.kalkavan@tum.de

Abstract: Digital twins (DT) can decrease the maintenance costs of bridges through a 3D geometric-semantic model representing the current status of the structure. The 3D model of a DT is generally created from point cloud data (PCD) captured by laser scanning or photogrammetry. Semantic segmentation is an essential step in processing PCD and 3D bridge modeling. Deep learning models are efficient tools to automate semantic segmentation. These models, however, need a large dataset for training which is challenging to achieve for bridges. This paper proposes an approach to generate synthetic PCD of bridges for training deep learning models. The parametric model of bridges is created, and their synthetic PCD is simulated. This dataset is then added to the real dataset of bridges for training a deep learning model. The paper results show that the synthetic PCD can be used for data augmentation and improving the performance of deep learning models.

Keywords: Digital Twins, Point Cloud Data, Semantic Segmentation, Synthetic, Deep Learning

1 Introduction

Bridges, as critical structures, require maintenance during their service life. Recent ASCE report card [1] shows that the number of deficient bridges is increasing as the rate of deterioration is higher than rehabilitation and replacement. Despite the feasibility of the conventional methods for evaluation and condition assessment of bridges, they are loosely and only partially supported by digital methods. Digitization of existing bridges can support the inspection and maintenance process of the structure and decrease the applying costs to a large extent.

The concept of digital twin (DT), originated from the industry [2], is concerned with providing the digital counterpart of a system or object. In the domain of building information modeling (BIM), a digital twin represents the digital replica of an existing structure [3]. This 3D model can incorporate all the collected information from the construction site. This information can include the current geometry of the structure, cracks and their location on the body of the structure. In comparison with a building

information model, a DT is largely concerned with the as-performed and as-is phases of the structure [4]. Also, it illustrates the interaction of humans with the structure and can be updated in specific intervals. In bridges, these intervals might be longer as the physical features of the asset vary gradually [5]. A digital twin is generally created from the point cloud data (PCD) resulting from terrestrial and aerial capturing methods. Laser scanning and photogrammetry are two common methods that can capture existing assets with high measurement accuracy [6], [7]. Compared to a visual inspection, these methods are faster and less labor-intensive. To create the DT model of a bridge, its PCD needs to be processed. Semantic segmentation is an essential step in processing PCD. Through semantic segmentation, the entire PCD of the bridge is divided to clusters representing the point cloud of elements. In the current practice, this step is conducted manually that in turn, increases the costs of digital twinning to a large extent. To benefit from the advantages of a DT, semantic segmentation is required to be automated or at least semi-automated.

2 Related research

Recently, there have been efforts to automate the point cloud segmentation of bridges. The proposed methods can be divided to heuristic algorithms and deep learning models. In what follows, some of these methods are reviewed.

Lu, Brilakis, and Middleton [8] detected elements in the point cloud of concrete bridges by a heuristic algorithm following the relative distance of points in the point clusters of elements. Hu, Zhao, Huang, *et al.* [9] used a multi-view convolutional neural network (CNN) to extract features from photogrammetry and linked it with a multi-layer perceptron (MLP) to segment the point cloud of bridges. Lee, Park, and Ryu [10] added contextual features by kd-tree and K-nearest neighbors (KNN) to PointNet [11] and deep graph-convolutional neural network (DGCNN) [12] and improved the performance of the models. Yan and Hajjar [13] segmented the point cloud of steel bridges by a heuristic algorithm based on the connection rules that generally exist in the bridges. Truong-Hong and Lindenbergh [14] proposed a heuristic algorithm to segment elements in the point cloud of bridges by a voxel growing algorithm. Xia, Yang, and Chen [15] calculated a local feature descriptor for classifying points in the PCD of bridges.

3 Overview of the paper

Heuristic algorithms are capable of labeling the input PCD of bridges without training. These algorithms, however, are mostly limited to presumptions and conditions that might not be satisfied in all bridges. On the other side, deep learning models are highly generic and can learn the features of points. These models, however, need a large dataset for training. Despite the recent advances in technologies such as laser scanning and photogrammetry, the capturing process of existing bridges is still challenging and time-consuming. Also, deep models generally need more than a few samples of PCD for training. The main objective of this paper is to provide a workflow for simulation of bridges and generating their PCD. For this purpose, the 3D models of bridges are created in a BIM-authoring system. These models are then used as input in Helios++ [16] to generate their PCD. RGB channels are also added

by interpolating the points of the real PCD. First, the model is trained only by using real PCD. Next, to evaluate the augmentation impact of synthetic data, the model is trained with both real and synthetic PCD. Finally, the statistical metrics obtained from the models with and without augmentation are compared.

4 Synthetic point cloud data

Synthetic PCD of bridges can be created and used to augment the dataset for training the deep learning models. Generating synthetic PCD requires modeling and simulating the existing bridges along with the capturing process by scanning tools. In what follows the required steps to create synthetic PCD are described.

4.1 Parametric modeling

Parametric modeling is a computer-aided design (CAD) approach for creating dynamic models. As a result of parametric modeling, the model of bridges achieves the capability of reshaping as the value of parameters change. To generate the synthetic PCD of bridges, the parametric model of bridges is created on Revit [17] using a plugin named SOFiSTiK Bridge Modeler [18]. To provide more realistic bridge models, the dimension of structural elements are considered following the structural drawings of actual bridges. Each part of the bridge, including the surrounding background, is designed to resemble the real PCD of bridges. The dimensions of the components, number of spans, and the shape of elements are varied to increase the diversity of the parametric models. Trees with dense vegetation are also modeled around the structure, as shown in Figure 1.

4.2 Simulation

To create the PCD of the modeled bridges, the laser scanning process of actual bridges is simulated by Helios++ [16]. In this software, tripods are placed around the structure to ensure the full coverage of the models, as shown in Figure 1. The scanning process of the bridge models is conducted by rotating optics with 120Hz scanning frequency, 5000Hz pulse frequency, 180° scanning angle, and 10 head rotate per sec/deg.

To automate the annotation process of the synthetic PCD, the 3D model of each structural element, including piers, railings, deck, and background, is scanned separately. This process results in the exact labeling of synthetic PCD; however, some regions that cannot be generally captured in real bridges are scanned as well. To simulate occlusion that generally exist in the PCD of real bridges, these regions are cropped out and deleted. To add RGB channels to the synthetic PCD, the elements of real PCD are selected and aligned with the corresponding elements of the synthetic PCD. Next, the RGB channels are interpolated from the real data to the synthetic data, as shown in Figure 1.

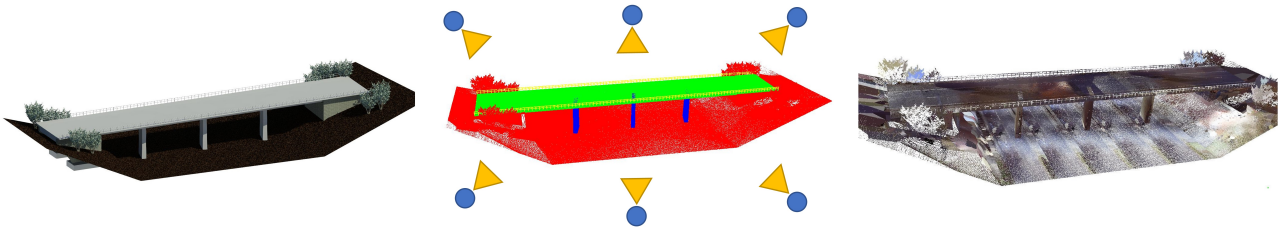

Figure 1: Creating synthetic PCD: parametric modeling (left); laser scanning of the bridge model (middle); resulting synthetic PCD (right).

5 Semantic segmentation

semantic segmentation of PCD can be defined as the labeling process of the data at a point level. Through semantic segmentation, the entire PCD is summarized to segments that show the element of interest in bridges. In this section, details of the deep learning model for processing points and the dataset are mentioned.

5.1 Deep learning model

As a deep learning model capable of processing points, RandLA-Net [19] is utilized for semantic segmentation. This model can process and learn features of large-scale point clouds. It applies random sampling in subsequent layers of the network to reduce the number of points. Simultaneously, to prevent the loss of key features through sampling, a local feature aggregation module is proposed to progressively increase the receptive field for each point. This module contains a local spatial encoding (LocSE) and an attentive pooling block, as shown in Figure 2. LocSE computes the neighboring points of each point by K-nearest neighbors (KNN) and sends the relative Euclidean distance of the point to its neighbors to a multi-layer perceptron (MLP). Next, the resulting features are concatenated with the input features of the point. In the attentive pooling unit, these features are aggregated through a weighted sum. The weights (scores) of the operation are obtained from a shared MLP to emphasize the more important features. Finally, every two feature aggregation modules are stacked to expand the receptive field of the point.

5.2 Dataset

The bridge PCD of Cambridge [8] is used for training and testing the deep learning model. This *Real* dataset contains 10 samples of reinforced concrete bridges captured by laser scanning. Following section 4, 10 samples of synthetic PCD is also created for bridges. Next, the synthetic data is added to the dataset of real bridges to provide an *Augmented* dataset containing 20 bridges in total. Figure 3 depicts two typical samples of the real and synthetic PCD, respectively.

5.3 Hyperparameters

The model is trained for semantic segmentation of four classes, namely: piers, deck, railings, and background. The hyperparameters of RandLA-Net are tuned through a trial and error process, and the parameters with the best validation accuracy are selected. The model is trained for 512 epochs with a batch size of two. The input channel of the network is considered 6, representing *X, Y, Z* and *R, G, B*. The number of 16 neighbors is selected for the KNN search block of the model. Also, 6 neurons are used in the attentive pooling block of the network.

6 Results

To evaluate the impact of the synthetic data on the results, the model is trained on two datasets and tested on the same samples of the real bridges. The first dataset is the PCD of the real bridges containing 10 samples, and the next one is the PCD of the real bridges combined with 10 samples of the synthetic PCD. The validation is performed on only the real samples of the bridges using leave one out cross validation (LOOCV) method. In every iteration, a real PCD is left out for testing, and the training process is conducted on the other remaining samples. The test results of the models are reported by the mean intersection over union (MIoU) and mean accuracy (MAcc) over classes. These statistical indices are calculated from the confusion matrix of the predicted labels in validation or testing phases. Table 1 shows the results of the model on each test sample of the real PCD. As can be seen, the results have improved for some of the test samples. Averaging the results over all the test samples illustrates that augmentation has increased MIoU by 5.2% and MAcc by 3.1%.

Considering the prediction results over each test sample, a noticeable change is observed in the accuracy of Bridge 02 and Bridge 08 where MIoU has increased more than 20% after synthetic data augmentation. One reason for such improvement could be due to the slight horizontal curvature of these bridges. Adding synthetic samples with horizontal curvature has resulted in a more generic dataset for the model to learn the features of curve bridges. Figure 4 visually depicts the prediction

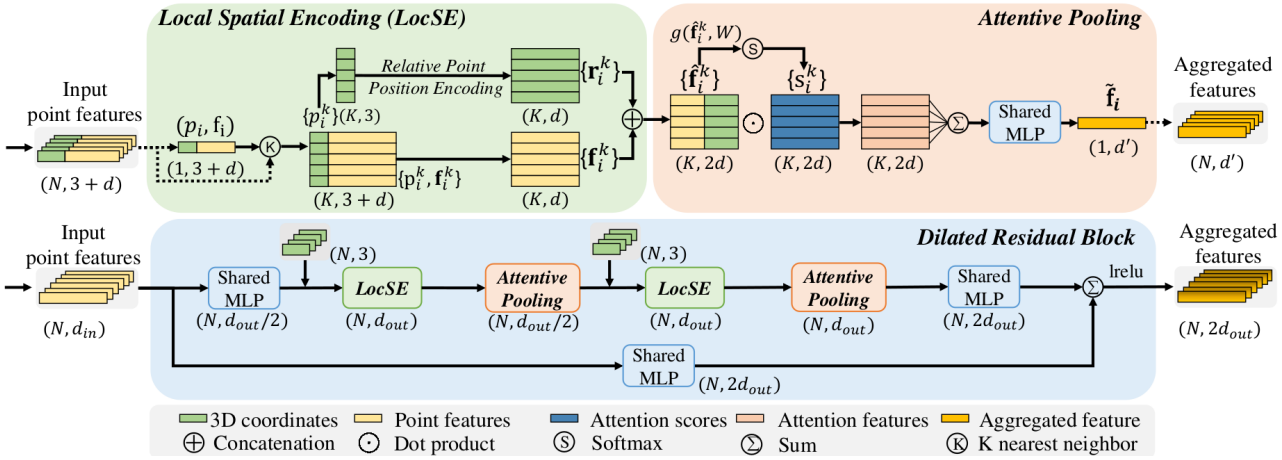

Figure 2: Architecture of RandLA-Net [19].

Figure 3: Two typical point clouds of each dataset: real samples [8] (left); synthetic samples (right).

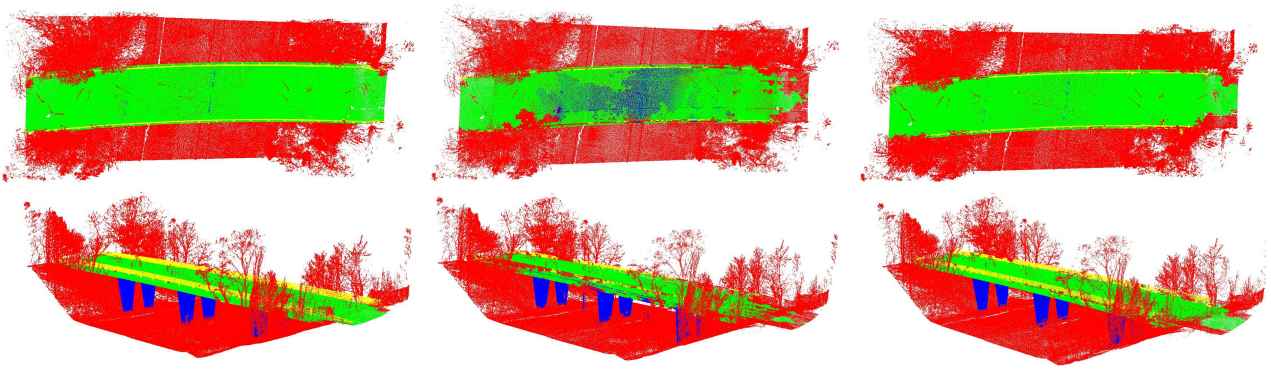

Figure 4: Prediction results of the model: ground truth (left), training on real PCD (middle), training on augmented data (right). Class labels: railings (yellow), background (red), deck (green), piers (blue).

Table 1: The results of semantic segmentation of the real and augmented PCD (%)

Test Sample	MAcc Real	MAcc Aug	ΔMAcc	MIoU Real	MIoU Aug	ΔMIoU
Bridge 01	86.7	84.2	-2.9	81.2	79.6	-2.0
Bridge 02	82.2	90.4	10.0	71.1	88.0	23.8
Bridge 03	97.0	95.7	-1.3	92.7	91.5	-1.3
Bridge 04	93.2	95.9	2.9	89.9	92.2	2.6
Bridge 05	96.4	98.0	1.7	92.6	95.5	3.1
Bridge 06	95.6	98.2	2.7	87.3	89.0	2.0
Bridge 07	93.7	92.2	-1.6	76.0	72.5	-4.6
Bridge 08	78.1	93.8	20.1	70.6	90.5	28.2
Bridge 09	94.1	94.0	-0.1	89.8	89.2	-0.7
Bridge 10	85.0	84.8	-0.2	76.2	76.6	0.5
Average	90.2	92.7	3.1	82.7	86.5	5.2

results of the model on Bridge 08. As can be seen, data augmentation has improved the prediction accuracy of the model especially in regions where the piers and railings are connected to the deck.

7 Conclusion

Semantic segmentation is an essential step in the 3D modeling of bridges and creating digital twins. Despite the recent advances in technologies such as laser scanning and photogrammetry, the scanning process of real bridges is still labor-intensive and costly. Deep learning models have recently shown successful performance in automating the labeling process of PCD. These models, however, need a large dataset for training which is hard to achieve for bridges. This paper proposed an approach to

generate synthetic PCD of bridges for data augmentation. Parametric models of real bridges were created, and their PCD was simulated. This synthetic dataset was combined with the dataset of real bridges and used for training a deep learning model. Training on the real and augmented datasets demonstrated that data augmentation by synthetic PCD improves the accuracy of the models. On average, the MIoU of the deep model in predicting the labels of real PCD increased by 5.2%. This improvement shows the feasibility of using synthetic PCD for augmentation. However, the factors affecting the results are still unclear. To provide more accurate point clouds for data augmentation and training deep learning models, these factors need to be investigated in the future.

References

[1] ASCE, "Asce's 2021 infrastructure report card", American Society of Civil Engineers, Report, 2021.

[2] E. Negri, L. Fumagalli, and M. Macchi, "A review of the roles of digital twin in cps-based production systems", *Procedia Manufacturing*, vol. 11, pp. 939–948, 2017, ISSN: 2351-9789.

[3] F. Collins, M. Mafipour, F. Noichl, Y. Pan, and M. Vega, "Towards applicable scan-to-bim and scan-to-floorplan: An end-to-end experiment", in *Proc. of the 32th Forum Bauinformatik*, 2021.

[4] Y. Pan, A. Borrmann, H.-G. Mayer, *et al.*, "Built environment digital twinning", Technical University of Munich, Report, 2019.

[5] M. S. Mafipour, S. Vilgertshofer, and A. Borrmann, "Deriving digital twin models of existing bridges from point cloud data using parametric models and metaheuristic algorithms", in *Proc. of the EG-ICE Conference 2021*, 2021.

[6] Z. Zhu, S. German, and I. Brilakis, "Detection of large-scale concrete columns for automated bridge inspection", *Automation in construction*, vol. 19, no. 8, pp. 1047–1055, 2010, ISSN: 0926-5805. DOI: http://dx.doi.org/10.1016/j.autcon.2010.07.016.

[7] Z. Zhu, S. German, and I. Brilakis, "Visual retrieval of concrete crack properties for automated post-earthquake structural safety evaluation", *Automation in Construction*, vol. 20, no. 7, pp. 874–883, 2011, ISSN: 0926-5805. DOI: http://dx.doi.org/10.1016/j.autcon.2011.03.004.

[8] R. Lu, I. Brilakis, and C. R. Middleton, "Detection of structural components in point clouds of existing rc bridges", *Computer-Aided Civil and Infrastructure Engineering*, vol. 34, no. 3, pp. 191–212, 2019, ISSN: 1093-9687. DOI: http://dx.doi.org/10.1111/mice.12407.

[9] F. Hu, J. Zhao, Y. Huang, and H. Li, "Structure-aware 3d reconstruction for cable-stayed bridges: A learning-based method", *Computer-Aided Civil and Infrastructure Engineering*, vol. 36, no. 1, pp. 89–108, 2021, ISSN: 1093-9687.

[10] J. S. Lee, J. Park, and Y.-M. Ryu, "Semantic segmentation of bridge components based on hierarchical point cloud model", *Automation in Construction*, vol. 130, p. 103 847, 2021, ISSN: 0926-5805.

[11] C. R. Qi, H. Su, K. Mo, and L. J. Guibas, “Pointnet: Deep learning on point sets for 3d classification and segmentation”, in *Proceedings of the IEEE conference on computer vision and pattern recognition*, 2017, pp. 652–660.

[12] Y. Wang, Y. Sun, Z. Liu, S. E. Sarma, M. M. Bronstein, and J. M. Solomon, “Dynamic graph cnn for learning on point clouds”, *ACM Transactions on Graphics (TOG)*, vol. 38, pp. 1–12, 2019.

[13] Y. Yan and J. F. Hajjar, “Automated extraction of structural elements in steel girder bridges from laser point clouds”, *Automation in Construction*, vol. 125, p. 103 582, 2021, ISSN: 0926-5805.

[14] L. Truong-Hong and R. Lindenbergh, “Automatically extracting surfaces of reinforced concrete bridges from terrestrial laser scanning point clouds”, *Automation in Construction*, vol. 135, p. 104 127, 2022, ISSN: 0926-5805.

[15] T. Xia, J. Yang, and L. Chen, “Automated semantic segmentation of bridge point cloud based on local descriptor and machine learning”, *Automation in Construction*, vol. 133, p. 103 992, 2022, ISSN: 0926-5805.

[16] L. Winiwarter, A. M. E. Pena, H. Weiser, *et al.*, “Virtual laser scanning with helios++: A novel take on ray tracing-based simulation of topographic full-waveform 3d laser scanning”, *Remote Sensing of Environment*, vol. 269, p. 112 772, 2022.

[17] Autodesk, *Revit*, version 2021. [Online]. Available: https://www.autodesk.com/products/revit/overview.

[18] SOFiSTiK, *Sofistik bridge + infrastucture modeler*, version 2021. [Online]. Available: https://www.sofistik.com/products/bim-cad/bridge-infrastructure-modeler.

[19] Q. Hu, B. Yang, L. Xie, *et al.*, “Randla-net: Efficient semantic segmentation of large-scale point clouds”, in *Proceedings of the IEEE/CVF Conference on Computer Vision and Pattern Recognition*, 2020, pp. 11 108–11 117.

An investigation into the impact of the Scan-to-BIM method on the design and construction of technical building services

Nijanthan Mohan[1], Michelle Ulbrich[1], Stefanie Bongard[1] and Rolf Gross[1]

Smart Building Engineering, Department of Civil Engineering, Aachen University of Applied Sciences, Bayernallee 9, 52066 Aachen, Germany

Abstract: The evolution of computers and information technology led to a digital revolution in the Architecture, Engineering and Construction (AEC) industry, which gave rise to the Building Information Modelling (BIM) technique. BIM is a process that generates and manages digital representations of buildings in terms of both physical and functional characteristics. Scan-to-BIM is a method for creating a 3D-building model based on point cloud data taken by a laser scan, which can be used for the different BIM-compliant design and construction processes. In this context, this research paper aims to investigate the impact of the Scan-to-BIM method on operations in the design and construction of Heating, Ventilation and Air Conditioning (HVAC) systems. To achieve this, a market study was made on the predominately used 3D laser scanners and point cloud processing software in Germany. For the processes in the design phase of HVAC systems, energy analysis of existing buildings involving heat load calculation according to DIN EN 12831 standard and energy balance according to DIN V 18599 standard was selected, analysed and evaluated. The software tool liNear from the liNear company for construction design and the ETU-Planer from the Hottgenroth AG were used for energy calculations. Adhering to the construction phase, a study was made to analyse the impact of digital twins and point clouds for construction progress inspection in the field of building services.

Keywords: BIM, Laser scanning, Digital twins, Construction progress control

1 Introduction and Aim

The construction industry is lagging in digitisation compared to other sectors. This is due to, on the one hand, the lack of willingness to introduce new planning methods and, on the other hand, the lack of expertise in this area. However, for years, digital tools and working techniques have been developed for the construction industry. One important method for digitising the construction industry is Building Information Modelling (BIM). BIM is a process for integrating information and technology to create a digital representation of a project. BIM brings together data from various sources and evolves in parallell with the actual project through its entire life cycle, including planning, construction, and facility management. It is a way of optimising planning and action in the construction industry and networks the various trades with each other to improve cooperation between the different specialist planners. The path from the drawing board and two-dimensional planning to three-dimensional planning is also inherent in using the BIM method. The digitalisation of essential processes in the entire life cycle of a building, from planning to the construction phase to operation, is intended to optimise processes and increase efficiency [1], [2]. In this context, this paper is aimed to analyse the impact of the scan-to-BIM process on the design and construction of technical building services. The study was commenced with a market study to identify the available hardware for laser scanning and was followed by expert interviews with construction managers in the field of technical building services to get an insight into current practices and expectations of the scan-to-BIM process. With this background, different applications of the method are to be investigated, and their suitability is to be analysed.

2 Scan-to-BIM

Currently, there are four different technical measurement methods used for building surveying.

- Electronic manual measurement, Tacheometry, Laser scanning and Photogrammetry.

The surveying methods can be further divided into point-based, which includes electronic manual measurement and tachometery, and area-based, which includes laser scanning and photogrammetry. In this paper, we consider the laser scanning method. 3D laser scanning is the process of capturing a real-world object or environment to gather information on its shape and appearance (e.g. colour). The collected data can then be used to create the as-built or as-is 3D model). A non-contact and non-destructive technology (Light Detection and Ranging (LIDAR) method) is used to create point cloud data. This point cloud data is used either for inspection or to make the 3D model [3]. With the augmentation of information to the created 3D model, a scan-to-BIM method is completed.

The scan-to-BIM workflow can be simplified into four steps.

1. Project preparation

Goal definition & Evaluation of the Existing Documents

Required Level of Detail (LOD) & Level of Accuracy (LOA)

2. Scan data acquisition

Selecting the scanning device & Scan settings

Execution of the individual scans

Possible pre-registration

3. Registration

Registration into a cloud of measuring points

Clean-up of the data & Export to a suitable format

Documentation of the scan quality

4. Modelling

Import of point cloud data into the modelling software

Modelling of the components

Augmentation with information

Figure 1: Scan-to-BIM workflow

3 Market study and expert interviews

Software and hardware tools are an integral part of BIM implementation, and there is no digitisation without the software program. To adhere to the paper's aim involving laser scanning, a study on the available hardware for laser scanning is also necessary. Hence, this section aims to provide insight into the available hardware/software tools for 3D laser scanning. Table 1 provides the properties of the widely used 3D laser scanner.

To analyse the impact of Scan-to-BIM on building services more closely, seven expert interviews were conducted with employees of leading building services providers in the region of Aachen, Germany. The interviews covered the current workflows of construction progress control and the integration of laser scanning and digital twins. The experts are project managers and construction

managers with comprehensive experience in their respective fields. To obtain a comparable result, all participants were asked the following seven questions in a 15-minutes interview:

- Do you work according to the BIM method in your company?
- Which software is used in your company for planning the building services?
- Do you use a software/ digital tool for construction progress control/ as-built recording?
- Do you have experience in laser scanning?
- How do you currently carry out the construction progress control?
- Where do you see the difficulties/ problems in the current workflow?
- What could improve the workflow, in your opinion?

The summary of the interviews is depicted in figure 2.

Table 1: Technical specifications - 3D laser scanner [9], [10]

	Focus S70	**TX6**	**BLK360**	**RTC360**
Manufacturer	Faro	Trimble	Leica	Leica
Type of scanner	Stationary	Stationary	Stationary	Stationary
Scan speed	1 million pts/sec	500,000 pts/sec	360,000 pts/sec	2 billion pts/sec
Scan rate	3 - 6 min per scan	3 - 6 min per scan	5 - 7 min per scan	2 min per scan
Communication	USB/Wi-Fi	USB/Wi-Fi	Wi-Fi	USB/Wi-Fi
Output format	.pts	.pts, .las	.pts	.pts
Additional device	Inbuilt OS	Trimble tablet or similar	iPad pro	iPad pro
Cost (approx.)	25,000 €	45,000 €	20,000 €	50,000 €

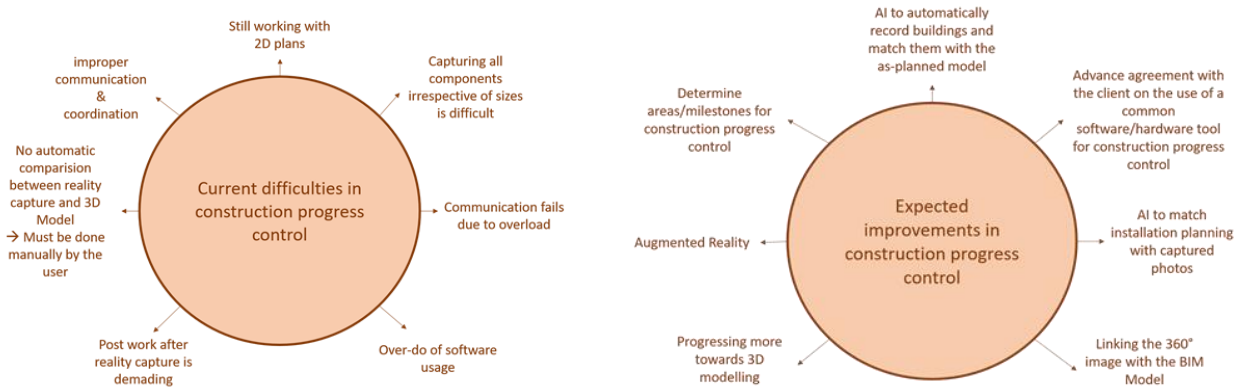

Figure 2: Overview of the results from expert interviews

4 Impact analysis of Scan-to-BIM method on design and construction of technical building services – Case studies

4.1 Scan-to-BIM method for energy analysis of existing buildings (Design phase)

To analyse the suitability of the Scan-to-BIM method for energy analysis, an existing building was captured using the Leica BLK360 laser scanner and processed through the Leica Cyclone Register 360 software to create point cloud data. The point cloud data was then imported into the modelling software - Autodesk Revit and a 3D model was constructed (Figure 3a). Furthermore, the 3D model was augmented with heat transmission information attributes for walls, windows etc., thereby creating a BIM Model.

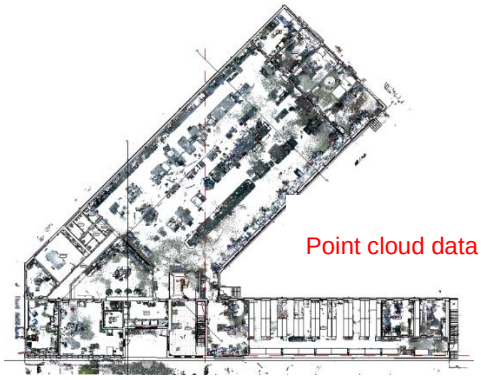

(a)

Heating Load Calculation Results

		liNear	ETU
Gebaudedaten			
Nettogrundfläche	A_{NGF}	1493 m²	1495 m²
Nettovolumen	V_{build}	8058 m³	5350 m³
Hüllfläche	A_{env}	2937 m²	2389 m²
Wärmeverluste			
Transmission	$\sum\Phi_T$	36654 W	40472 W
Lüftung	$\sum\Phi_V$	27631 W	24266 W
Heizlast			
Norm-Heizlast	Φ_{HL}	64285 W	64699 W
spezifisch (Fläche)	φ_{HL}	43 W/m²	43 W/m²

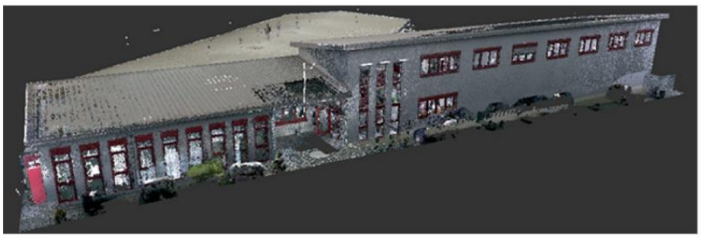

(b)

Energy balance – DIN V 18599

	Gesamt	Heizung	Kühlung	Lüftung	Beleuchtung
Nutzenergie	146026	112107	25367	0	8551
Endenergie	164088	135486	11596	2171	14835
Primärenergie	147006	95522	20873	3908	26703

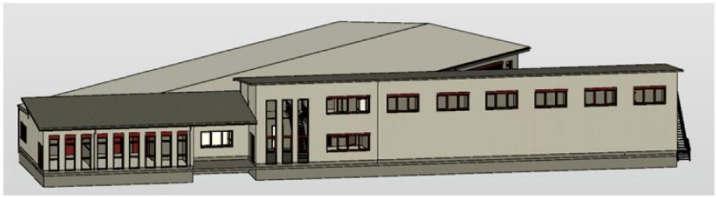

(c)

Figure 3: (a) Point cloud registration from the Cyclone Register software; (b) Heating load calculation according to DIN EN 12831-1 (Left); Point cloud data of the building (Right); (c) Energy Balance calculation according to DIN V 18599 (Left); BIM Model from the Autodesk Revit software (Right)

The created BIM Model is then exported to the liNear software (through Revit Plug-in) and ETU Planer software (as an IFC file), and the heating load calculation according to DIN EN 12831-1 [4] was executed. Furthermore, according to DIN V 18599 [5], energy balance calculations were performed using the ETU Planer software [6], as currently, the liNear software [7] cannot carry out energy balance for non-residential buildings. The results are depicted in figure 3b and 3c.

4.1.1 Result analysis - Scan-to-BIM method for energy analysis of existing buildings

The investigation has shown that the geometrical and non-geometrical data correctness of the model depends on the data format in which the model is available and the software interfaces used by the calculation programs. Due to insufficiently stored information and errors during the geometry export, both software tools had problems with the calculations. The results show that energy calculations in the form of a heating load calculation according to DIN EN 12831 and an energy balance according to DIN V 18599 based on a Scan-to-BIM model are possible provided the model contains all the required information to perform the calculations. The quality of the model significantly influences the quality of the results.

4.2 Scan-to-BIM method for construction progress control and revision documentation (Construction phase)

To analyse the suitability of the Scan-to-BIM method for construction progress control and creation of revision documentation, various existing technical rooms were captured using the Leica BLK360 laser scanner and processed through the Leica Cyclone Register 360 software to create a point cloud data. For construction progress control, the resulted point cloud data was uploaded onto the Dalux field platform [8], and a comparison was made between as-planned and as-built.

The interface from the Dalux program is depicted in figure 4. With the Dalux field application, a field test was conducted at the construction site to investigate the usability for project progress control. The user was able to visualise the as-built and as-planned scenarios together on one screen, and the program provides the possibility to create tasks such as adjusting the model as per the as-build situation or demanding queries on unfinished tasks as tickets. The construction manager could assign these tickets directly to the responsible stakeholder, facilitating transparent communication among the project participants.

Furthermore, the obtained point cloud data was used to create a 3D BIM model (figure 5a). This drafted BIM Model can be handed over directly to facility management as revision documentation and can be developed further as a digital twin. The point cloud model can also be used as a reference for installation planning of new components (renovation purposes) without developing a 3D model, which results in considerable savings in terms of time and effort (figure 5b).

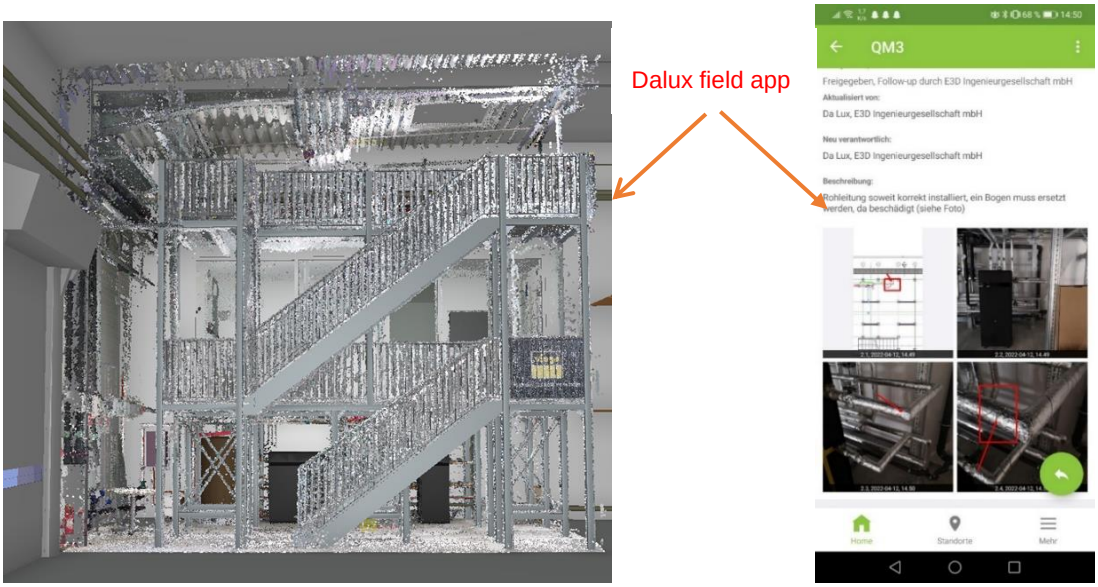

Figure 4: Screenshots from Dalux field applications showing the import of point cloud data

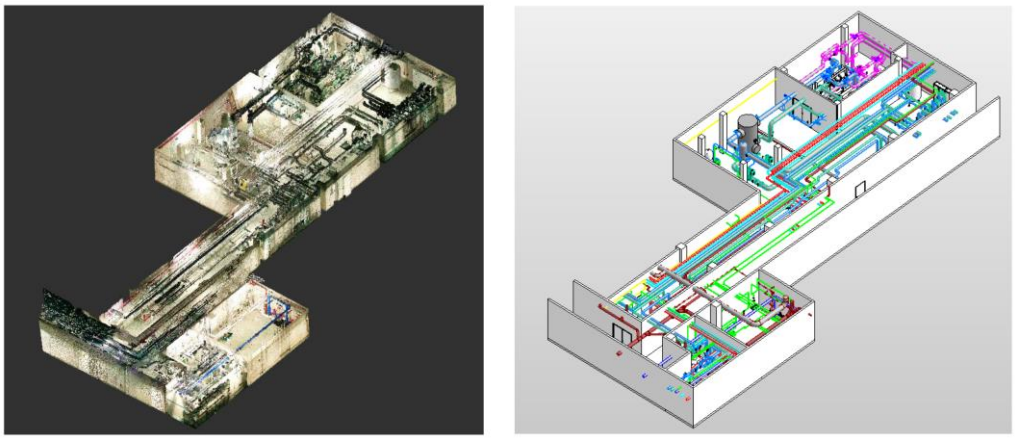

(a)

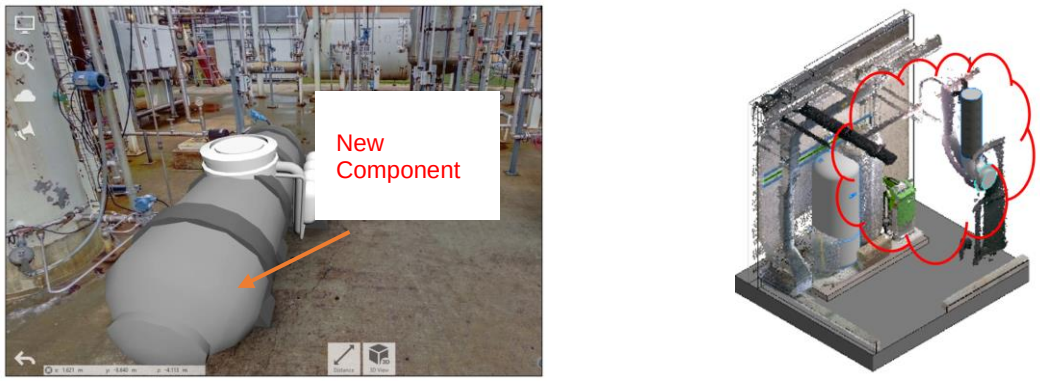

(b)

Figure 5: (a) Creation of 3D model from point cloud data; (b) Planning of new components with point cloud as reference (Left); Comparison of point cloud data with installation model (Right).

5 Conclusion

As with any building data model, the user must ensure the geometrical and non-geometrical quality of the scan-to-BIM models to achieve adequate results for the intended calculations mentioned in section 4.1.1. The scan-to-BIM method proves to be effective in achieving the required geometrical quality in the model, which forms the base for energy simulations. The responsibility for the quality of the non-geometrical attributes lies primarily with the model author. In the construction phase, the scan-to-BIM process proves to be effective in the case of the creation of BIM model / digital twins for facility management and comparison/ adaptation of as-planned models with respect to the as-built scenarios by reducing the time taken and increasing the quality of the output compared to the conventional way of recording. For construction progress control applications, due to the demanding post-processing works of the captured point cloud data, it is not economically efficient to have the construction site captured regularly. Instead, a reality capture with a 3D laser scanner on planned milestones in the construction progress to check for discrepancies would be reasonable. Based on the above case studies, the scan-to-BIM process is beneficial for the user but also has its limitations in terms of demanding post-processing works and costs associated with it. With the ongoing research in the combination of artificial intelligence with laser scanning for the automatic recognition of components, the scan-to-BIM process is set to have a significant positive impact in the field of technical building services.

References

[1] W. A. Hatem, A. M. Abd, N. N. Abbas: “Motivation Factors for Adopting Building Information Modelling (BIM) in Iraq”, Engineering, Technology & Applied Science Research, April 2018.

[2] Q. Wang, J. Guo, K. Kim: “An application oriented scan-to-BIM framework”, Remote sensing, vol. 11, 2019.

[3] J. Blankenbach, “Bauwerksvermessung für BIM in Building Information Modeling - Technologische Grundlagen und industrielle Praxis“, Springer Vieweg. 2015.

[4] “DIN EN 12831-1 - Heizungsanlagen in Gebäuden - Verfahren zur Berechnung der Norm-Heizlast”, Beuth-Verlag GmbH, 2017.

[5] “DIN V18599 - Energetische Bewertung von Gebäude”, Beuth-Verlag GmbH, 2018.

[6] https://www.hottgenroth.de/index.html, access in 05/2022.

[7] https://www.linear.eu/de/home/, access in 05/2022.

[8] https://www.dalux.com/dalux-field/, access in 05/2022.

[9] https://www.faro.com/en/Products/Hardware/Focus-Laser-Scanners, access in 05/2022.

[10] https://leica-geosystems.com/products/laser-scanners/scanners/blk360, access in 05/2022.

Teil XI

Design Support with Artificial Intelligence

Informed Machine Learning Methods for Instance Segmentation of Architectural Floor Plans

Alexander Hakert[1] and Phillip Schönfelder[1]
[1]Department of Civil and Environmental Engineering, Ruhr University Bochum,
Universitätsstraße 150, 44801 Bochum, Germany
E-mail(s): alexander.hakert@rub.de, phillip.schoenfelder@rub.de

Abstract: Architectural floor plans can be a valuable source of information for reconstructing digital models for existing buildings. For instance, room geometry and topology are essential to create building models and therefore need to be extracted from drawings. In case the drawings only exist as raster-image files (e.g., from scanning), engineers have to be assigned the tedious task of converting the pure image data into geometrically rich models. Driven by advances in deep learning-based image processing methods and the need to automate the extraction of floor plan geometry, earlier studies subjected floor plan images to semantic segmentation and instance segmentation. This research focuses on potential improvements to these approaches, primarily motivated by informed machine learning (IML) concepts. In this regard, expert knowledge is integrated to accelerate the training process and improve inference performance. A baseline Mask R-CNN model is trained on an open-source dataset and is compared to models enhanced with IML techniques. Among others, the effects of (1) a neighboring pixel loss, (2) a weighted cross-entropy loss, and (3) human preprocessing are investigated. Finally, the most promising techniques are combined to train a model which outperforms the baseline by 10.1% in the average precision score. In general, all of the proposed IML techniques improve segmentation results and can be considered in the development of future methods for segmenting floor plan images.

Keywords: BIM, Deep Learning, Informed Machine Learning, Instance Segmentation, Floor Plan

1 Introduction

The idea of building information modeling (BIM) [1] includes the development and maintenance of a digital building model which contains geometric and semantic information about a given structure. While BIM models for new buildings may be created during planning, models are rarely available for existing buildings. Therefore, in order to ensure efficient planning of maintenance, extension or deconstruction tasks, the necessary building documentation files must be collected, and the contained information must be manually assembled to form a digital model. An important type of raw data is

2D drawings, e.g., the floor plans of buildings, which are usually available as raster graphics from scanning paper drawings. Individual elements, such as walls, doors or rooms, must be segmented in the raster graphics and converted to a vector graphic in order to be transformed into BIM model elements with correct geometry.

Various methods have already been developed to automatically extract information from drawings: For the task of segmenting floor plan images, more and more data-driven approaches using convolutional neural networks (CNN) are applied in the automated creation of BIM models. Dodge et al. [2] test different architectures of fully convolutional network for the segmentation task and obtain state-of-the-art accuracies in the segmentation of walls. Liu et al. [3] use a CNN as part of a pipeline for vectorizing raster graphics. The CNN segments and detects connection points of walls, which are combined into vectorized walls in further steps. Also, Surikov et al. [4] use multiple machine learning approaches to vectorize floor plan images: A UNet model is used to efficiently segment walls and a Faster R-CNN model is used to detect windows and doors. Jang et al. [5] use a version of the DeepLab architecture to segment walls, which are then vectorized in further steps along with doors. Kim et al. [6] present a solution to the problem of analyzing floor plans of different size and complexity. They divide the floor plans into segments of fixed size and use a CNN for element detection. The authors of [7] also deal with complex floor plans by presenting a method that converts floor plans of different drawing styles to a unified format using an adversarial network and then vectorizes them using a junction extraction method. While many of the methods use segmentation and vectorization of walls to identify rooms, in other models rooms are directly segmented by CNNs: For instance, Kalervo et al. [8] present a method that segments and vectorizes floor plans using a multi-task CNN. Ramasamy et al. [9] use a Cascade Mask R-CNN in combination with a keypoint CNN to improve detection results.Chen et al. [10] also use a Mask R-CNN to segment rooms. They then perform a coordinate descent on each room, which eventually results in a vector graphics version of the floor plan, i.e. geometries are described by fundamental primitives. Recent approaches show promising results in the automatic conversion of raster-image floor plans to vector graphics. However, the precise segmentation of floor plan drawings remains a challenge due to the diversity in complexity and style of actual floor plans.

The concept of IML describes the integration of external knowledge into the machine learning pipeline. The knowledge can originate from different sources and may be integrated into the pipeline in various ways. Potentially, these techniques may lead to shorter training time, i.e. faster convergence, and better inference performance, without altering or expanding the training dataset. This makes it possible to train better models, given the same data, with only some tweaks to the training process, the model architecture, or the preprocessing. For more information, the reader is referred to [11], which defines a taxonomy on the topic and provides many examples for the use of IML.

This study focuses on the aspect of instance segmentation and the influence of IML methods on the performance of the chosen model. It proposes possible enhancements to the automated segmentation of floor plan drawings by inducing expert knowledge into the training process via four informed machine learning (IML) techniques: (1) a pixel neighborhood loss, (2), a weighted loss function to account for an uneven distribution of elements, (3) manual preprocessing of floor plan drawings, and (4) prior knowledge about topological relationships of elements. To test the effect of the IML approaches, a baseline Mask R-CNN model [12] is trained and tested on images taken from a publicly available

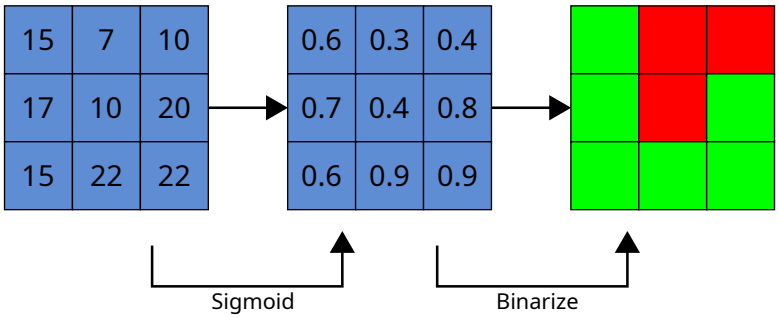

Figure 1: Procedure for determining a pixel weight for the neighbor loss.

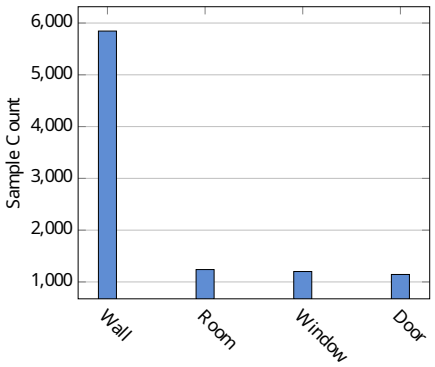

Figure 2: Number of samples per class in the CVC-FP dataset [13].

dataset. The performance scores of the baseline model and the IML models are compared to quantify the effects of the IML techniques. The presented methods can be used to develop future floor plan segmentation methods, contributing to the automated creation of BIM models. The paper is organized as follows: The used IML techniques are described in Section 2 and the performance of the accordingly modified models is evaluated in Section 3. Section 4 concludes the study and addresses possible future studies.

2 Methodology

2.1 Pixel Neighborhood

The concept of pixel neighborhood is introduced to take the connections of neighboring pixels of the floor plan image into account. In most cases, rooms have a large, simple polygon shape and are bounded by walls and other elements in straight lines. Therefore, irregularities (i.e., deviations from rectangular or similar geometries) can be considered unlikely and, thus, neighboring pixels are usually expected to belong to the same class. In order to incorporate this piece of external knowledge in the training process, Yuan and Xu [14] introduce a *neighbor loss*, which is used as a replacement for the Mask loss in this work. The idea of neighbor loss is to weight the individual pixels depending on their neighborhood when determining the binary cross entropy loss. In the first step, a sigmoid function is applied to all logits, normalizing the values to a range between 0 and 1. Then, the individual pixel values are binarized with a threshold of 0.5. The weight w_i of each pixel i is finally determined by the number of differently classified neighboring pixels and multiplied by a factor K, i.e.,

$$w_i = \max\left(1, K\left|\sum_{j\in 3\times 3} D_j M_j\right|\right), \quad \text{with } D = \begin{pmatrix} -1 & -1 & -1 \\ -1 & 8 & -1 \\ -1 & -1 & -1 \end{pmatrix}, \tag{1}$$

where M is the binarized neighborhood mask and D is a constant matrix to count the neighbors different to the pixel. The process is repeated for each pixel of the Mask R-CNN's output mask of size $m \times m$. The resulting weight matrix W of the pixels is then incorporated into the mask loss

$$L_{mask}(t, y, W) = -\frac{1}{m^2} \sum_{i \in m \times m} W_i * (t_i * \log(\varphi(y_i)) + (1 - t_i) * \log(1 - \varphi(y_i))), \tag{2}$$

where t is the ground truth mask, y is the output from the mask branch, and φ is the sigmoid function. The factor K is a hyperparameter and, thus, may be optimized with respect to the resulting model performance. Within this study, it is set to K = 10, inspired by [14].

2.2 Class Weights

This approach addresses the distribution of class occurrences within the dataset. In this study, the CVC-FP dataset [13] is used for all experiments. The wall class strongly dominates the dataset, amounting to five times as many samples as the other classes. This imbalance can cause the model to develop a tendency towards neglecting rooms, windows, and doors, while showing satisfactory performance for wall objects. As a remedy, the loss of the class branch L_{cls} is adjusted so that it accounts for the different number of samples per class. In the training process, the number of samples per class in the ground truth of each image is counted. Then, as described by Shrivastava [15], the weights for each class are determined by

$$w_c = \frac{1}{\sqrt{n_c}}, \tag{3}$$

where w_c is the weight for class c and n_c is the number of samples of that class in a given image. The *weighted loss* L_{cls} for each region of interest (RoI) is then determined by

$$L_{cls}(p, w, k) = -w_k * \log p_k, \tag{4}$$

where p is the probability distribution of classes at the output of the class branch, w is the weight vector determined by equation 3, and k is the ground truth class of the RoI.

2.3 Manual Preprocessing

As a further approach, it is investigated how the pre-processing of floor plan images by a user affects the model's performance. Floor plan images often measure up to several thousand pixels in height and width. If these images are then scaled to a size of 512×512 pixels to be fed into the model for segmentation, floor plan elements such as walls, doors, or windows may become too small to be detected and segmented. To avoid this information loss during scaling, the floor plan images are preprocessed by the expert user. The scanned images usually contain not only the actual floor plan, but also additional information, such as title blocks, descriptions, tables, or simply whitespace. Since this information is not needed for the task at hand, it can be removed by the user by simply cropping

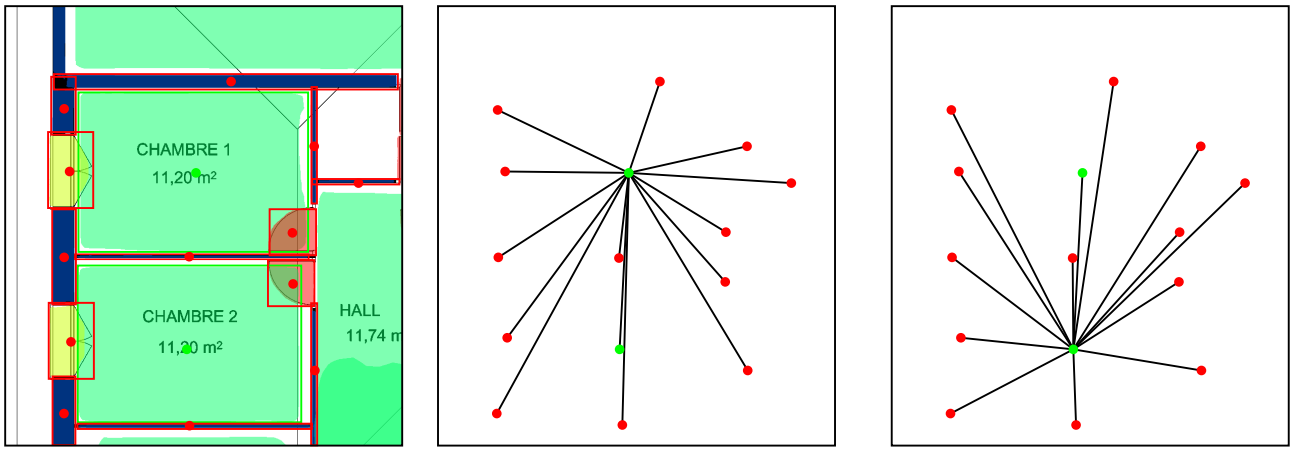

Figure 3: Visualization of $L_{neighborhood}$ computation. a) display of segmented objects with bounding boxes, b) and c) distances from room 1 and 2, respectively, to other objects.

the floor plan out of the scanned image. In this work, for the training process of the Mask R-CNN, the user's pre-processing is simulated by automatically cropping the ground plan of the images of the dataset used. To do this, the ground truth segmentation map of the images is used to cut out the floor plans with a random distance of 50 to 150 pixels from the outermost elements.

2.4 Class Neighborhood

Floor plans exhibit various topological relationships between the depicted elements. For example, doors and windows are connected to walls, and rooms are enclosed by several walls. It follows that two rooms are typically separated by elements that do not belong to the room class. To incorporate this structural relationship into the Mask R-CNN training process, an additional *class neighborhood loss* function is proposed for the model. During training, the model computes bounding boxes and class predictions for all the RoIs of an image. The predicted positions and classes are then used for the loss computation. Figure 3 shows an example of the steps to determine the loss. First, the class for each RoI is predicted. Second, the respective bounding box centers are determined. Finally, the Euclidean distances between the center points of all detected room objects are determined and sorted in ascending order according to the distance to the room object under consideration. The C nearest neighbors of each room object determine the loss. The hyperparameter C is set to 10. For the loss, the number of rooms in the immediate vicinity of the room under consideration is counted. The process is repeated for all detected rooms of the image. The counted room neighbors are summed up and then averaged over the number of considered rooms. The loss $L_{neighborhood}$ is thus determined by

$$L_{neighborhood}(E, C) = \frac{1}{|E|} \sum_{e \in E} C_k, \tag{5}$$

where E is the set of detected room elements of the image and C_k is the number of rooms among the 10 nearest neighbor objects of room e.

3 Results

For the experiments in this work, the CVC-FP dataset [13] is used to train and to test the Mask R-CNN models. The dataset consists of 122 scanned floor plans with different sizes, images qualities and drawing styles, which are annotated with object segmentation masks. In particular, it contains 5845 walls, 1239 rooms, 1201 windows, and 1144 doors. The image sizes in the dataset range from 1098 $\times$ 905 pixels to 7,383 $\times$ 5,671 pixels. For all experiments, 102 images of the dataset are used for training, 10 images are used for validation, and 10 images are used for testing. Three consecutive experiments are performed using a publicly available Mask R-CNN implementation [16]. First, it is investigated how the described IML approaches affect the instance segmentation performance of the Mask R-CNN. For this purpose, they are compared to a baseline version of the model. In a second experiment, multiple approaches are applied simultaneously to investigate which combination of approaches can further improve the model. Finally, the performance of the Mask R-CNN is increased through a longer training process.

To test the effect of the IML approaches on the performance of Mask R-CNN, the baseline model is modified according to each technique. For the first two experiments, the respective models are trained for 50 epochs with a learning rate of 0.001, using 100 RoIs for each image. The model is initialized by taking the weights of a model pre-trained on the COCO dataset. For the last experiment, the models are trained for 150 epochs with a lower learning rate of 0.0001. Table 1 shows the results of the evaluation of each experiment. The authors choose the metrics AP_{50} with the IoU threshold 0.5 as a measure for detection accuracy, AP with IoU thresholds 0.5–0.95 in steps of 0.05 for potential comparison with other methods, and AP_{tight} with IoU threshold 0.75–0.95 as a metric for accurate segmentations. It is noted that all methods improve the basic model in certain aspects. The most notable improvement is observed when using user-based preprocessing of the floor plan images. The best result is achieved by combining pixel neighborhood and preprocessing, resulting in an AP_{50} score of 76.2%. Figure 5 shows the validation performance of each model during the longer training process. The use of the pixel neighborhood has the highest impact on the AP_{tight}, presumably, due to the generation of more regularly shaped masks. Figure 4 shows exemplary segmentations of a floor plan with the baseline model and a model with all presented IML techniques combined. The latter achieves a segmentation performance of 46.7% AP and 75.9% AP50, exceeding the baseline model performance by 9.9% and 10.4%, respectively.

4 Conclusion

In this work, expert knowledge in the form of four different IML approaches is integrated into the training process of a Mask R-CNN, for instance segmentation of floor plan images. The used methods include three different loss functions and the preprocessing of floor plan images. It is evident that the integration of expert knowledge has a strong positive effect on the model's performance. Combining methods improves the AP_{50} and AP_{tight} scores up to 16.3% and 52.9% AP_{tight}, respectively, relative to the baseline model. For better performance, the methods can be optimized and extended in future

Table 1: Test results of the baseline model and the modified versions in percent. Bold values indicate the best performance scores among the tested models, given a fixed number of training epochs. The most promising model configurations are trained for 150 epochs.

	E = 50				E = 150			
IML approach	AP	AP_{tight}	AP_{50}	mIoU	AP	AP_{tight}	AP_{50}	mIoU
Original	28.6	11.6	51.1	36.7	36.8	15.7	65.5	55.4
Neighbor	29.3	13.3	50.6	38.9	-	-	-	-
Weights	29.9	12.1	54.5	41.9	-	-	-	-
Crop	32.0	12.7	58.1	44.3	42.9	19.2	74.1	58.0
ClsNeighbor	29.0	11.5	53.8	39.7	-	-	-	-
Neighbor+Weights	29.3	12.6	51.5	37.5	-	-	-	-
Neighbor+Crop	35.3	16.4	61.2	47.2	**46.9**	**24.0**	**76.2**	**61.4**
Weights+Crop	36.0	**16.6**	61.4	44.1	43.3	19.6	75.0	59.7
ClsNeighbor+Crop	**36.7**	16.5	**63.7**	**48.0**	44.4	21.7	74.0	59.5
All	36.3	16.2	63.3	47.5	46.7	23.4	75.9	58.3

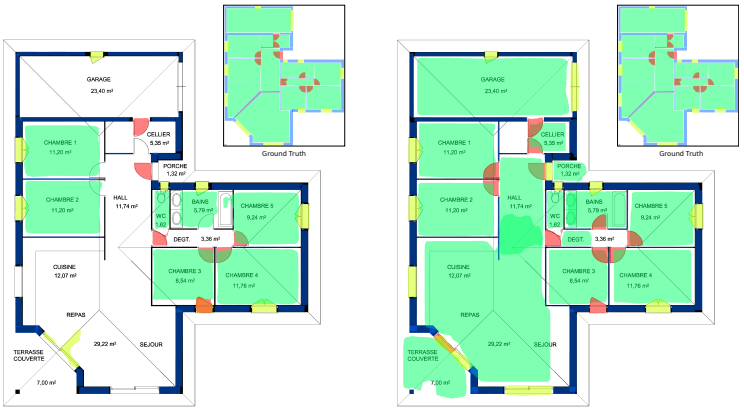

Figure 4: Example segmentations with the original model on the left and the combination of all approaches on the right. Floor plan image taken from the CVC-FP dataset [13].

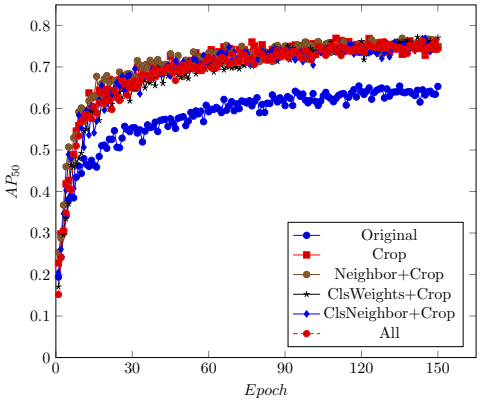

Figure 5: The models' AP_{50} scores on the validation set during the training of the different models.

works. The presented approaches to integrate expert knowledge show great potential and should be considered for the development of new floor plan segmentation methods.

Acknowledgements

This research is conducted as part of the BIMKIT project, funded by the German Federal Ministry for Economic Affairs and Climate Action.

References

[1] A. Borrmann, M. König, C. Koch, and J. Beetz, editors, *Building Information Modeling: Technology Foundations and Industry Practice*. 2018. DOI: 10.1007/978-3-319-92862-3.

[2] S. Dodge, J. Xu, and B. Stenger, “Parsing floor plan images”, in *15th Int. Conf. on Machine Vision Appl.*, 2017, pp. 358–361. DOI: 10.23919/MVA.2017.7986875.

[3] C. Liu, P. Kohli, J. Wu, and Y. Furukawa, “Raster-to-vector: Revisiting floorplan transformation”, in *IEEE Int. Conf. on Comput. Vision*, 2017, pp. 2214–2222. DOI: 10.1109/ICCV.2017.241.

[4] I. Y. Surikov, M. A. Nakhatovich, S. Y. Belyaev, and D. A. Savchuk, “Floor plan recognition and vectorization using combination UNet, Faster-RCNN, statistical component analysis and Ramer-Douglas-Peucker”, in *Int. Conf. on Comput. Sci., Commun. and Security*, vol. 1235, 2020, pp. 16–28. DOI: 10.1007/978-981-15-6648-6_2.

[5] H. Jang, K. Yu, and J. Yang, “Indoor reconstruction from floorplan images with a deep learning approach”, *Int. J. of Geo-Information*, vol. 9, p. 65, 2020. DOI: 10.3390/ijgi9020065.

[6] H. Kim, S. Kim, and K. Yu, “Automatic extraction of indoor spatial information from floor plan image”, *Int. J. of Geo-Information*, vol. 10, p. 828, 2021. DOI: 10.3390/ijgi10120828.

[7] S. Kim, S. Park, H. Kim, and K. Yu, “Deep floor plan analysis for complicated drawings based on style transfer”, *J. of Comput. in Civil Eng.*, p. 04 020 066, 2021. DOI: 10.1061/(ASCE)CP.1943-5487.0000942.

[8] A. Kalervo, J. Ylioinas, M. Häikiö, A. Karhu, and J. Kannala, “Cubicasa5k: A dataset and an improved multi-task model for floorplan image analysis”, pp. 28–40, 2019. DOI: 10.1007/978-3-030-20205-7_3.

[9] A. Ramasamy Arunkumar, S. Mohan, and J. Kumar, “Segmentation of spatial and geometric information from floorplans using CNN model”, *Turkish J. of Comput. and Math. Edu.*, vol. 12, pp. 1909–1920, 2021. DOI: 10.17762/turcomat.v12i9.3620.

[10] J. Chen, C. Liu, J. Wu, and Y. Furukawa, “Floor-SP: Inverse cad for floorplans by sequential room-wise shortest path”, in *IEEE/CVF Int. Conf. on Comput. Vision*, 2019, pp. 2661–2670. DOI: 10.1109/ICCV.2019.00275.

[11] L. von Rueden, S. Mayer, K. Beckh, *et al.*, “Informed machine learning - a taxonomy and survey of integrating prior knowledge into learning systems”, *IEEE Trans. on Knowl. and Data Eng.*, pp. 1–1, 2021. DOI: 10.1109/TKDE.2021.3079836.

[12] K. He, G. Gkioxari, P. Dollár, and R. Girshick, “Mask R-CNN”, in *IEEE Int. Conf. on Comput. Vision*, 2017, pp. 2980–2988. DOI: 10.1109/ICCV.2017.322.

[13] L.-P. de las Heras, O. R. Terrades, S. Robles, and G. Sánchez, “CVC-FP and SGT: A new database for structural floor plan analysis and its groundtruthing tool”, *Int. J. on Document Anal. and Recognition*, vol. 18, pp. 15–30, 2015. DOI: 10.1007/s10032-014-0236-5.

[14] W. Yuan and W. Xu, “NeighborLoss: A loss function considering spatial correlation for semantic segmentation of remote sensing image”, *IEEE Access*, vol. 9, pp. 75 641–75 649, 2021. DOI: 10.1109/ACCESS.2021.3082076.

[15] I. Shrivastava, *Handling class imbalance by introducing sample weighting in the loss function*, 2020. [Online]. Available: https://medium.com/gumgum-tech/handling-class-imbalance-by-introducing-sample-weighting-in-the-loss-function-3bdebd8203b4 (visited on 04/05/2022).

[16] A. Kelly, *Mask r-cnn for object detection and instance segmentation on keras and tensorflow*, https://github.com/akTwelve/Mask_RCNN, 2020.

Methoden zur KI-basierten Autovervollständigung von frühen Grundrissentwürfen: Methodologie und Integration in ein bestehendes Framework

V. Eisenstadt[1,2], J. Bielski[3], C. Langenhan[3], B. Mete[3], K.-D. Althoff[1,2] and A. Dengel[1]
[1]Deutsches Forschungszentrum für Künstliche Intelligenz (DFKI), Deutschland
[2]Universität Hildesheim, Institut für Informatik, Deutschland
[3]Technische Universität München, Dept. Architektur, Deutschland
E-mail(s): viktor.eisenstadt@dfki.de

Abstract: Der Prozess des Entwerfens in der Architektur verbindet die Kreativität des Designers mit gesetzlichen Regularien sowie den spezifischen Einschränkungen und Vorgaben des Bauprojektes. Der Entwurfsprozess ist somit eine geeignete Domäne für die Unterstützung durch den Computer, welcher die Aufgabe eines Assistenten übernimmt und das Projekt getreu der Vorgaben ko-kreativ begleitet. Die Methoden der Künstlichen Intelligenz (KI), insbesondere Deep Learning, haben in der letzten Zeit große Fortschritte gemacht, in der Unterstützung des Entwurfsprozesses in der Architektur spielen sie zur Zeit jedoch noch eine untergeordnete Rolle. Ein möglicher Einsatz der KI-Techniken im Entwurfsprozess von der Architektur ist die automatische Vervollständigung der Grundrisse in den frühen Entwurfsphasen. Die von der KI generierten Vorschläge für die nächsten Entwurfsschritte basieren dabei auf vorhandenen konsistenten semantischen Daten und tragen so zu mehr Präzision sowie Effizienz im Entwurfsprozess bei. Wir präsentieren eine Methodologie für eine solche Autovervollständigung und beschreiben wie sie in ein bestehendes verteiltes KI-basiertes Framework integriert wird und wie die generierten Vorschläge dem Nutzer erklärt werden.

Keywords: Frühe Entwurfsphasen, Raumkonfiguration, Autovervollständigung, Deep Learning

1 Einführung

In den letzten Dekaden verzeichnet Künstliche Intelligenz (KI) einen kontinuierlichen Zuwachs an neuen Methoden und Techniken. Insbesondere Deep Learning (DL) erfreut sich einer stetig wachsenden Anwendung. Neueste Entwicklungen wie Generative Adversarial Nets [1] oder GPT-3 (Generative Pre-trained Transformer) [2] werden als wichtige Fortschritte der aktuellen KI-Forschung betrachtet.

In der Architektur ist die Anwendung der genannten KI-Methoden jedoch noch nicht etabliert. Die Forschungsprojekte *metis-I* und *metis-II*, gefördert durch Deutsche Forschungsgemeinschaft (DFG),

untersuchen das Potential der KI-Methoden für die frühen Phasen des Entwurfsprozesses in der Architektur. Angefangen mit der fallbasierten Suche nach ähnlichen Entwürfen, wurden die Forschungsaktivitäten mit den Methoden zur synthetischen Generierung von hochwertigen Entwürfen fortgesetzt. Aktuell beschäftigen sich die Projekte mit der Autovervollständigung von graphbasierten Raumkonfigurationen mithilfe von DL, um die frühen Designphasen in der Architektur effizienter und ressourcenschonender zu gestalten und damit die allgemeine Qualität des frühen Entwurfs zu erhöhen [3]. Die Effizienz und die Ergebnisqualität der frühen Designentscheidungen beeinflussen den weiteren Verlauf des Entwurfsprozesses [4, S. 10]. Es ist also von besonderer Bedeutung auf die Methoden zu setzen, die in der Lage sind große Datenmengen effizient und zuverlässig zu verarbeiten und die Ergebnisse der vorherigen Aktionen für die nächsten Handlungsempfehlungen (und die möglichen Alternativen) zu berücksichtigen. Deep Learning hat sich dabei als eine geeignete Grundlage bewiesen, bspw. bei der Autokorrektur der Sätze auf dem Smartphone oder Früherkennung der Börsentrends.

In diesem Beitrag stellen wir eine Methodologie der DL-basierten Autovervollständigung von frühen Grundrissentwürfen vor, mit einem besonderen Fokus auf dem Zusammenspiel der beteiligten Algorithmen und Datenstrukturen. Zum Einsatz kommen die Methoden wie die künstlichen Neuronalen Netze, Clustering, Link Prediction und Multiagentensysteme. Ein besonderer Schwerpunkt ist das (selbst-)erklärende Handeln des Systems, welches mithilfe der Anwendung von eXplainable AI (XAI) erreicht werden soll. Die Methodologie wird dabei als ein ganzheitlicher Prozess gesehen, der die Architekten sowohl auf der Suche nach den nächsten Designentscheidungen begleiten soll als auch in der Lage ist den aktuellen Status des Entwurfs zu ermitteln, um fehlende Elemente oder Korrekturen für die aktuelle Entwurfsaufgabe vorzuschlagen. Die Vorschläge zur Vervollständigung basieren dabei auf den Erfahrungen des aktuellen Nutzers (Personalisierung), aber auch auf den Aufzeichnungen der Entwurfsprozesse anderer Architekten und den Referenz-Entwürfen bereits gebauter Projekte. Abgeschlossen wird der Beitrag mit einem Ausblick auf die weiteren Perspektiven der Methodologie.

2 Grundlagen der Methodologie

Die Grundlagen der KI-basierten Vervollständigung der frühen Grundrissentwürfe können grob in die technischen Voraussetzungen sowie die Rahmenbedingungen innerhalb des Entwurfsprozesses unterteilt werden. Technisch sind vor allem die richtige Repräsentation der Semantik der Grundrissdaten sowie die passenden Methoden der KI notwendig. Der Einsatzrahmen dieser KI-Methoden ist die frühe Entwurfsphase, in der die einflussreichen Designentscheidungen getroffen werden (s. Kap. 1).

Gekennzeichnet ist die frühe Entwurfsphase vor allem durch die Vielfalt der (vagen) Ideen, die sowohl intern als auch extern diskutiert und evaluiert werden [4, S. 24]. Kommuniziert werden diese frühen Ideen in der Regel mithilfe von Skizzen, die eine Auswahl an Variationen des Konzeptes repräsentieren und so einen Ideenraum schaffen, der den weiteren Verlauf des Bauprojektes maßgeblich mitbestimmt. Laseau [5] betrachtet die Visualisierung der Ideen mithilfe von Skizzen als optimalen Kommunikationsweg. HOAI (Honorarordnung für Architekten und Ingenieure) und AIA (American Institute of Architects) schätzen den Anteil der frühen Entwurfsphase auf ca. 30% der gesamten Entwurfszeit.

Während der frühen Entwurfsphase entstehen die Ideen im Wesentlichen mithilfe von Inspirationen durch die Inspektion der Referenzobjekte in Form von Abbildungen/3D-Modellen oder durch persönliche Besuche von Objekten [6, S. 143ff]. Digitale Methoden können die Suche nach Inspirationen beschleunigen und wurden im Forschungsprojekt *metis-I* untersucht. Eine weitere Möglichkeit der Unterstützung der frühen Ideenfindung durch den Computer ist die Erarbeitung einer oder mehrerer Alternativen zur Fortsetzung des Entwurfsprozesses basierend auf den Erfahrungen des Entwerfenden und anderer Architekten. KI-Methoden der Autovervollständigung erhalten oder erhöhen dabei die Qualität des Entwurfs, reduzieren den Arbeitsstress und beschleunigen die Entscheidungsfindung. Dies erhöht ebenfalls die Nachhaltigkeit durch Reduzierung von Bauschutt [7].

Die KI-kompatible Repräsentation des frühen Grundrisses erfolgt über die Interpretation der Semantik der Skizze als Graph in dem die Knoten für die Räume stehen (bspw. *Living*, *Working*, *Sleeping*) und die Kanten die Verbindungen zwischen den Räumen (bspw. *Door*, *Passage*) repräsentieren. Der Graph wird dabei als *Raumkonfiguration* bezeichnet (s. Abb. 1). Während für die Suche nach ähnlichen Referenzen der Graph selbst oder seine attribut-wert-basierte Repräsentation ausreichen, erfordert der Einsatz von Deep Learning andere Repräsentationsformen. Im Forschungsprojekt *metis-II* wurde zu diesem Zweck die tensor-basierte Repräsentation „Relation Map“ [8] entwickelt, die die Semantik der Raumkonfiguration in Form von One-Hot-Vektoren, numerischen Codes oder Texte darstellt. Dabei wird jeweils eine mehrdimensionale Matrix angelegt, die in dieser Form von den bekannten Deep-Learning-Softwarebibliotheken TensorFlow oder PyTorch interpretiert werden kann.

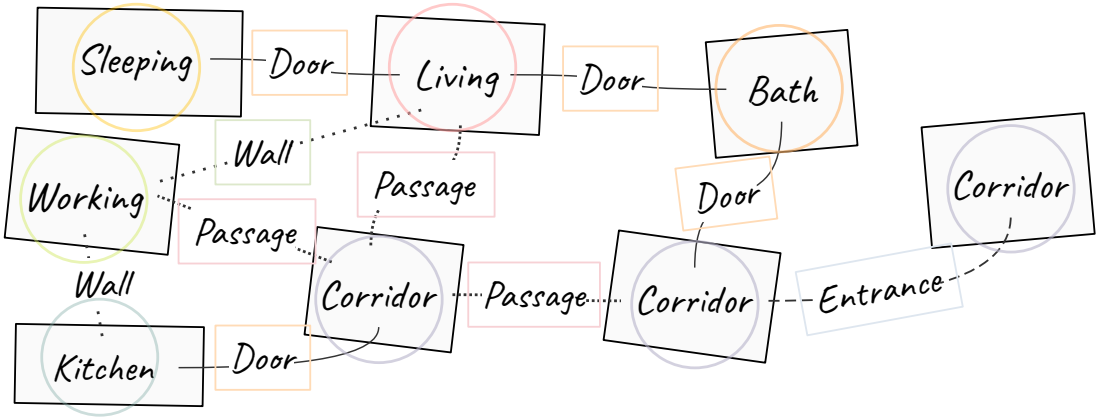

Abbildung 1: Grundrissskizze interpretiert als Graph (Raumkonfiguration).

Ferner können die Daten des Entwurfsprozesses als eine Folge von ausgeführten Entwurfsschritten während der Skizzierung eines frühen Grundrisses repräsentiert werden. Diese können entweder als konkrete Aktionen (bspw. Raum oder Verbindung hinzufügen/entfernen) in einer Sequenz aufgezeichnet oder über die Angaben zur Position/Druckstärke/Zeitstempel des digitalen Stifts ermittelt werden. Beide Formen wurden bereits im Rahmen des Projektes *metis-II* in spezifischen Tools implementiert und evaluiert. Erforderlich sind solche Daten unter anderem für die Erkennung der Phase in der sich der aktuelle Nutzer befindet. Im Projekt *metis-II* wird dabei auf die Erweiterung des Modells ASE [9] gesetzt, das zwischen den einzelnen Phasen *Analysis*, *Synthesis* und *Evaluation* unterscheidet.

3 Methodologie der Autovervollständigung

In diesem Kapitel wird die Methodologie der Autovervollständigung von Raumkonfigurationen vorgestellt. Basierend auf der Gesamtübersicht (s. Abb. 2) werden nachfolgend die detaillierten Beschreibungen der KI-Algorithmen, der Datenstrukturen und der Erklärungskomponente präsentiert.

3.1 KI-Algorithmen & Datenstrukturen

Insgesamt werden bei der Methodologie zwei Ansätze verfolgt. Beide setzen auf eine überwiegend sequentielle Ausführung der beteiligten Methoden zur Generierung von einer oder mehreren Alternativen zur Fortsetzung des frühen Entwurfsprozesses, basierend auf dem aktuellen Stand des Entwurfs. Der aktuelle Stand (s. Abb. 2, oben) setzt sich zusammen aus den oben genannten Datenstrukturen Graph (Raumkonfiguration) sowie Textsequenz (bisherige Entwurfsschritte). Diese werden dann für den jeweiligen Ansatz als initiale Anfrage genutzt und im weiteren Verlauf modifiziert.

3.1.1 Ansatz 1: ASE-Phase + Intention + Entwurfsschritt

Im ersten Schritt des ersten Ansatzes (s. Abb. 2, links) wird die aktuelle ASE-Phase des Nutzers ermittelt indem die Teilsequenz der bisherigen Entwurfsschritte von einem rekurrenten neuronalen Netz (engl.: recurrent neural network, RNN) ausgewertet wird. Die ASE-Phase beschreibt im wesentlichen die aktuelle Aktivität des Entwerfenden während der frühen Entwurfsphase gemäß dem ASE-Modell. Das RNN ist in der Lage sich an die Folge und Abhängigkeiten zwischen den Einträgen (hier: Entwurfsschritten) in einer Sequenz zu erinnern und ist daher die passende Wahl für diesen Ansatz. Als Ergebnis gibt das RNN die aktuelle Phase des Entwurfs zurück, basierend auf den Weiterentwicklungen des ASE-Modells (s. Kap. 2) durch Laseau [5] und Barelkowski [10]. Bspw. können die Phasen *Analysis-Understanding* (Festlegen der Entwurfsziele), *Synthesis-Discovery* (Lösungsfindung in einer der Entwurfsalternativen), oder *Evaluation* (Vergleich/Selektion der Lösungen) erkannt werden.

Ist die ASE-Phase erkannt, geht es mit dem zweiten Schritt weiter in dem die aktuelle Intention des Entwerfenden erkannt wird. Dies geschieht mithilfe eines weiteren RNNs auf Basis der Entwurfsschritte und der zuvor ermittelten ASE-Phase. Die Intention präzisiert dabei das aktuelle Vorhaben des Architekten, geteilt in Aspekte *wie* und *was* [9]. Bspw. können die Intentionen wie „requesting information“, „exploring different direction“ oder „modifying/adding/deleting solution“ erkannt werden.

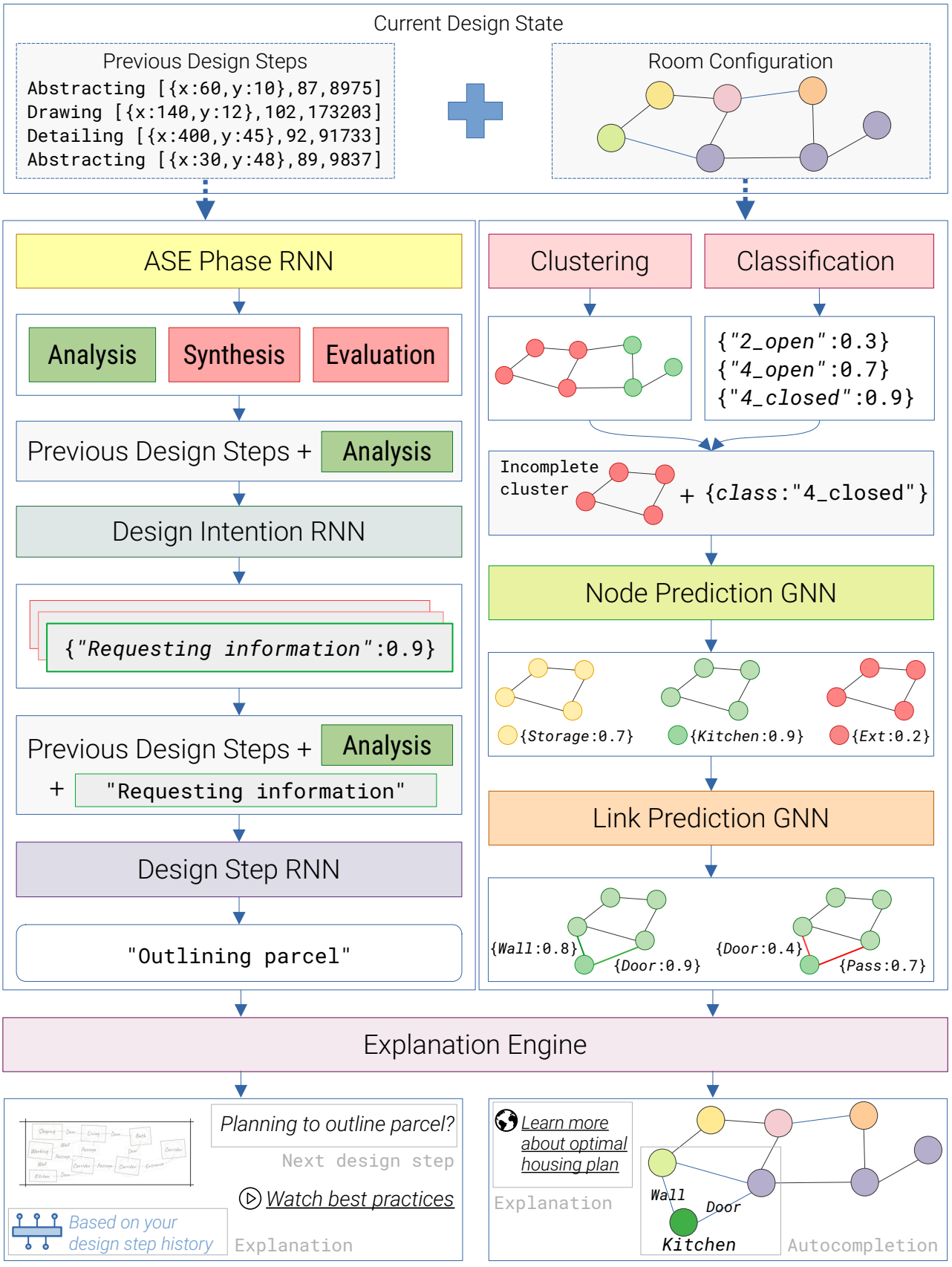

Abbildung 2: KI-Ansätze zur Autovervollständigung von Raumkonfigurationen und Entwurfsschritten.

Die ermittelte Intention wird dann der nächsten Anfrage hinzugefügt, ebenso die Entwurfsschritte und die Entwurfsphase. Mithilfe eines dritten RNNs wird dann diese gesamte Sequenz analysiert um den nächsten Entwurfsschritt vorzuschlagen. Dieser beschreibt die konkrete Aktion des Skizzierens in der frühen Entwurfsphase, bspw. „starting new sketch“, „outlining parcel“ oder „abstracting with bubble diagrams“. Dieser Teilschritt schließt zunächst den ersten Ansatz der Methodologie ab.

3.1.2 Ansatz 2: Autovervollständigung der Raumkonfiguration

Im zweiten Ansatz der KI-Methodologie werden Vorschläge zur Komplettierung der aktuellen Raumkonfiguration erarbeitet (s. Abb. 2, rechts). Angefangen wird mit den folgenden parallelen Teilschritten:

- *Clustering*: Hierbei wird die Raumkonfiguration in die Teilkonfigurationen (Cluster) aufgeteilt, bspw. mit dem Verfahren nach Girvan und Newman [11]. Dabei werden sog. problematische bzw. im architektonischen Sinne unvollständige Cluster ermittelt.
- *Klassifikation*: In diesem Teilschritt wird die Wohnbauklasse der Raumkonfiguration, repräsentiert als „Relation Map“(s. Kap 2), mithilfe eines Convolutional Neural Networks ermittelt. Die Klasse besteht aus der Anzahl der Wohnräume (bspw. 2 oder 3) und der Angabe, ob das Wohnzimmer mit der Küche durch eine Passage verbunden („Wohnküche“) ist oder nicht („open“ oder „closed“).

Die Kombination aus der Wohnbauklasse und den nicht vollständigen Clustern wird dann als Anfrage an ein Graph Neural Network (GNN) benutzt, welches die Räume vorschlagen soll, die für die Verbindungen im Cluster und die Wohnbauklasse typisch sind. GNNs sind ein spezieller Subtyp von neuronalen Netzen, der direkt mit dem Graphen arbeiten kann, anstatt den Umweg über Konvertierung in eine andere Repräsentation (Feature-Vektor, 3D-Matrix) zu nehmen. Alternativ kann hier auch ein Verfahren aus dem Bereich *Fallbasiertes Schließen* (engl: case-based reasoning, CBR) verwendet werden, welches ähnliche Cluster in einer Datenbank durchsucht und die Raumdifferenzen auflistet.

Nachdem die Räume der Autovervollständigung hinzugefügt wurden, werden mit dem ebenfalls GNN-basierten Verfahren *Link Prediction* [12] die Verbindungen zwischen den fehlenden bzw. vorgeschlagenen und den bereits existierenden Räumen im Cluster gesucht. Link Prediction versucht dabei alle möglichen Verbindungen zu prüfen um dann diejenigen mit der höchsten Wahrscheinlichkeit der Autovervollständigung hinzuzufügen. Mit dem kombinierten Vorschlag, bestehend aus neuen Räumen und Verbindungen endet zunächst der zweite Ansatz der Methodologie.

3.2 Erklärbarkeit

Für die vorläufigen Ergebnisse beider Ansätze der Methodologie wird dann das XAI-Verfahren angewandt, welches diese Ergebnisse um visuelle und/oder textuelle Komponenten ergänzt, die der Zielgruppe der Anwender gegenüber die vorgeschlagenen Lösungen nachvollziehbar machen sollen. XAI steht für *eXplainable AI* (erklärbare künstliche Intelligenz) und ist ein Forschungsbereich der KI in dem die Methoden zur menschenlesbaren Erklärung von Verhalten von intelligenten Systemen erarbeitet und angewandt werden [13]. Mögliche Ansätze die für die Erklärung von Autovervollständigungen

in Frage kommen können sind die Erklärungsmuster (engl.: explanation patterns) nach Cassens und Kofod-Petersen [14], die bereits im Rahmen der Forschungsprojekte *metis* für die Rechtfertigung, Relevanzanalyse, und den Transparenzbericht zur fallbasierten Suche nach ähnlichen Referenzen angewandt wurden. Ein weiter Ansatz ist das XAI-Framework nach Wang et al. [15], das kontrastive (warum), transfaktische (wie) oder kontrafaktische (was wäre wenn) Erklärungen generiert.

Das endgültige Ergebnis beider Ansätze zur automatischen Vervollständigung von frühen Grundrissen ist dann die Kombination aus den Ergebnissen, die von den KI-Ansätzen erzielt wurden und den dazugehörigen Erklärungen, visualisiert für die Ausgabe in einer Benutzeroberfläche (s. Abb 2, unten).

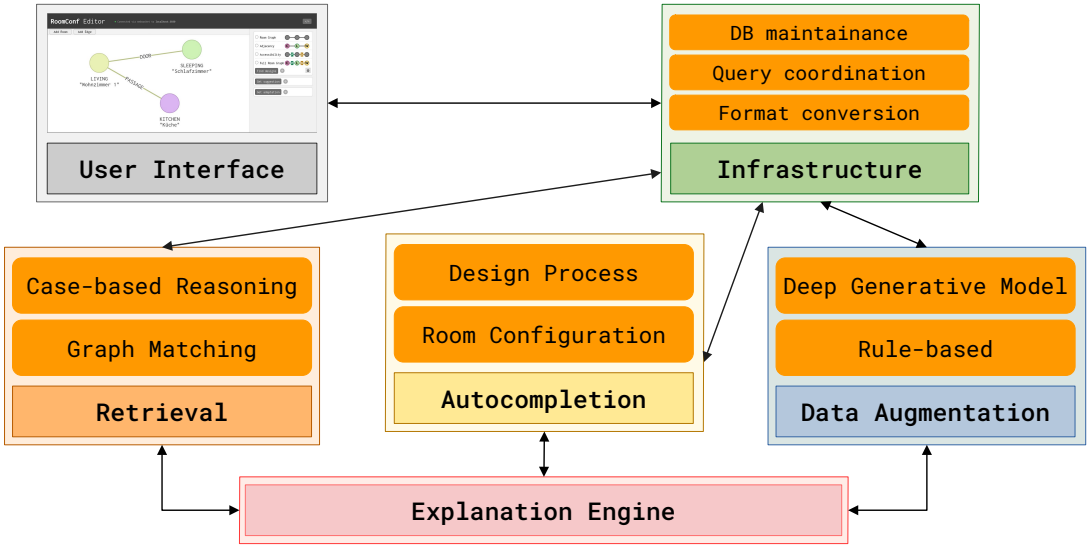

Abbildung 3: Framework *MetisCBR* mit Integration der Autovervollständigung.

4 Integration in das Framework & Evaluation

Die Ansätze zur Autovervollständigung werden dann, so wie bereits die XAI-Komponente und die Benutzeroberfläche, in das Framework *MetisCBR* zur Unterstützung der frühen Entwurfsphase in der Architektur integriert. Zum Framework gehören außerdem die bereits erwähnte Retrieval-Komponente zur Suche nach ähnlichen Referenzen sowie die Methoden zur KI-basierten Generierung von architektonisch konsistenten Grundrissdaten zum Training von Deep-Learning-Modellen. Der Grundaufbau des Frameworks setzt auf eine verteilte agentenbasierte Software-Architektur (Multiagentensystem), die während der Forschungsaktivitäten für die Projekte *metis* entwickelt wurde. Die Integration der Ansätze zur Autovervollständigung in *MetisCBR* (s. Abb. 3) erweitert das Framework um eine weitere Methode zur Unterstützung des frühen Entwurfs und macht es zu einem Referenz-Tool der Projekte *metis*, mit dem der Einsatz der KI in der Architektur weiter erforscht und evaluiert werden kann.

Die initialen Evaluationen der Integration der Methodologie bestätigen die Eignung der RNNs für die Erkennung der ASE-Entwurfsphase bzw. GNNs für Link Prediction, beide erreichen Werte von über 90% Richtigkeit. Die Implementierung der Methodologie wird mit einer Gesamtevaluation abgeschlossen.

Literatur

[1] I. Goodfellow, J. Pouget-Abadie, M. Mirza u. a., »Generative adversarial nets«, *NeurIPS*, 2014.

[2] T. Brown, B. Mann, N. Ryder u. a., »Language models are few-shot learners«, *NeurIPS*, 2020.

[3] V. Eisenstadt, J. Bielski, B. Mete, C. Langenhan, K.-D. Althoff und A. Dengel, »Autocompletion of Floor Plans for the Early Design Phase in Architecture: Foundations, Existing Methods, and Research Outlook«, in *CAADRIA 2022 Proceedings*, 2022, S. 323–332.

[4] D. Aliakseyeu, »A computer support tool for the early stages of architectural design«, English, Diss., Industrial Engineering und Innovation Sciences, 2003, ISBN: 90-386-1598-1.

[5] P. Laseau, *Graphic Thinking for Architects and Designers*. Wiley, 2000, ISBN: 9780471352921.

[6] K. Richter, *Augmenting Designers' Memory: Case-based Reasoning in Architecture*. Logos-Verlag, 2011, ISBN: 9783832527334.

[7] M. H. Haeusler, A. Butler, N. Gardner, S. Sepasgozar und S. Pan, »Wasted... Again-Or how to understand waste as a data problem and aiming to address the reduction of waste as a computational challenge«, in *CAADRIA 2021 Proceedings*, Bd. 1, 2021, S. 371–380.

[8] V. Eisenstadt, H. Arora, C. Ziegler u. a., »Exploring optimal ways to represent topological and spatial features of building designs in deep learning methods and applications for architecture«, in *CAADRIA 2021 Proceedings*, Bd. 1, 2021, S. 191–200.

[9] B. Lawson, *How Designers Think: The Design Process Demystified*, Ser. How Designers Think: The Design Process Demystified. Elsevier/Architectural, 2006, ISBN: 9780750660778.

[10] R. Barelkowski, »Learning design from knowing less. On approaches to architectural design process«, in *Knowing (by) Designing*, 1st. LUCA KU Leuven, 2013, Kap. 8.1, S. 517–526.

[11] M. Girvan und M. E. Newman, »Community structure in social and biological networks«, *Proceedings of the national academy of sciences*, Jg. 99, Nr. 12, S. 7821–7826, 2002.

[12] M. Zhang und Y. Chen, »Link prediction based on graph neural networks«, *NeurIPS*, 2018.

[13] W. Samek, G. Montavon, A. Vedaldi, L. Hansen und K. Müller, *Explainable AI: Interpreting, Explaining and Visualizing Deep Learning*, Ser. LNCS. Springer, 2019, ISBN: 978-3-030-28954-6.

[14] J. Cassens und A. Kofod-Petersen, »Designing Explanation Aware Systems: The Quest for Explanation Patterns.«, in *ExaCt*, 2007, S. 20–27.

[15] D. Wang, Q. Yang, A. Abdul und B. Y. Lim, »Designing theory-driven user-centric explainable AI«, in *Proceedings of the 2019 CHI conference on human factors in computing systems*, 2019.

Formal knowledge as a basis for BIM-based design decision support in additive manufacturing

Chao Li [1] and Frank Petzold [1]

[1]Chair of Architectural Informatics, Technical University of Munich, Arcisstraße 21, 80333 Munich, Germany

E-Mails: chao1.li@tum.de, petzold@tum.de

Abstract: Emerging Additive Manufacturing in Construction (AMC) technologies provide efficient use of material and multi-function integration for novel architectural design. Coined by the synergy of multi-disciplinary activities incorporating computational design, mechanical engineering, material science, and so forth, AMC has drawn noticeable attention in architecture, engineering, and construction (AEC) industries and remarkable academic efforts. To integrate AM into the well-established Building Information Modeling (BIM) methodology, an essential step is to provide design decision support driven by a formal knowledge base to assist architects and engineers in choosing appropriate AM methods. The purpose of this paper is to introduce the basics of AMC knowledge formalization to support decision-making on appropriate AM methods in the early design stages.

Keywords: BIM, data modeling in construction, design support, AMC

1 Introduction

The construction industry consumes critical amounts of the world's materials and energy while generating construction waste and greenhouse gases that seriously impact the environment. Under the trends of urbanization and population increase, it is urgent to rethink conventional construction approaches to transition towards sustainability in the construction and built world. Recent advancement in AMC has presented advantages, including extended freedom of design, sound mechanical performance, and integration of multiple functions [1][2][3]. To realize AM's capabilities in AEC, Labonnote et al. [4] identified a demanding shift in the architectural design paradigm, a holistic design process incorporating material science and engineering, and more rational designs in compliance with existing regulations. For years, Building Information Modeling (BIM) has been deemed an enabler for digital transformation in the AEC domain. The work of [5] proposes BIM as a methodology

for digital planning and data interoperability for AMC. More specifically, based on the object-oriented modeling language of EXPRESS, the Industry Foundation Classes (IFC) data model covers plenty of essential aspects in the construction sector, thus contributing to the data interoperability across heterogenous software from design to construction. Accordingly, the potential of using the IFC schema for fabricating BIM-based design with AM technologies has been demonstrated [6]. Collaborative activities involving different participants, including architects, stakeholders, engineers, etc., can be federated by the common data environment (CDE), information exchange management, and cooperative data management [7].

Although BIM provides a framework for boarding AM technologies in AEC, the challenges raised by Labonnote et al. [4] remain unsolved, primarily due to the missing AMC knowledge and the readily used evaluation tools during the design stages. As such, participating architects and engineers could not answer the questions of: “should AM technologies be applied for current design” and “what are the suitable AM methods for it”. It is known that rational decisions to these questions during early design stages are critical to avoid costly adaptations in the developed design and in-field construction phases. Li and Petzold [8] have proposed a methodology of integrating AM into BIM in the early design stages through decision support of choosing suitable AM methods. On top of that, this paper elaborates on the preliminary procedures to formalize AMC knowledge using OWL 2 DL and SWRL rules, meanwhile proposing a future alignment with the ontological version of IFC to bring AMC knowledge into the BIM model.

2 Background and Related Work

2.1 Overview of AMC

The versatility of AMC methods is mainly reflected in the innovations of processes, materials, and machinery use. Regarding 3D concrete printing (3DCP), Buswell et al. [9] classified the AM processes as particle-bed binding, material extrusion, and material jetting. In addition to concrete, more sustainable construction materials such as earth and wood have also been applied; however, using such materials could require printing of larger components to meet the exact load requirements or restrict the presence environment due to limited durability. Regarding machine systems, particle-bed binding processes generally use gantry systems mounting special-designed nozzles with jetting or spraying mechanisms. In contrast, material extrusion processes often leverage novel machinery solutions for mobility, near-nozzle mixing, and extended degree of freedom (DOF). Using manipulators with high DOF relaxes the slicing orientation from the horizontal and potentially increases geometry freedom of design but imposes complex trajectory planning tasks and careful coordination with feedstock’s fresh state properties. Furthermore, printing processes should be planned on-site or off-site depending on AMC methods’ environmental requirements, machine systems' workspace, and transport regulations. For off-site fabrication, large building components must be manufactured in

smaller sizes and milled to the proper profile, then assembled on site. Layer-wise printed building components are inherently weaker in flexural loads. To overcome this deficiency, different reinforcement strategies have been applied in 3DCP to enhance the inter-layer binding of printed components [10]. Another critical research field in AMC is integrating multiple functions with rational inner design to save material and energy consumption and advocating the adoption of AMC for sustainability [11].

2.2 Knowledge Formalization and Semantic Web Technologies

In Artificial Intelligence, formal knowledge representation is a top-down methodology of encoding explicit knowledge in symbolic, machine-interpretable formalisms such as semantic networks, logic, rules, etc. Domain knowledge can then be formalized as ontology, representing experts' understanding of particular professions with cognitive bias. Constituents of an ontological knowledge base formalized with expressive description logic (DL) are, in principle, interdepending concepts (TBox), roles (RBox), and assertions regarding individuals' concepts and role connections (ABox). Accordingly, the World Wide Web Consortium (W3C) has recommended a set of languages for ontology modeling (OWL 2), querying (SPARQL), validation (SHACL), etc. To embody Horn-like rules in the knowledge base, SWRL and nominal schemas are often applied to complement the expressivity limit of OWL 2 while keeping decidability.

The ontology representation of the IFC standard termed ifcOWL is constructed from the translation of EXPRESS expressions using the DL dialect of OWL2 (OWL2 DL). It is in the same status as EXPRESS and XSD schemas of IFC. Pauwels, Zhang, and Lee [12] summarized three expectancies when applying Semantic Web technologies in AEC: *data interoperability*, *linking across domains*, and *logical inference and proofs*. Respectively, collaboration using ABox of ifcOWL-complied knowledge base unsurprisingly enables *data interoperability* through the unified technology stack in terms of serialization, modeling, querying, etc. *Cross-domain data linking* can be triggered by the alignment of domain ontologies and their accessibility in the web environment. *Logical inference and proofs* considerably demand the co-existence of a full-fledged knowledge base and tailored reasoner with proper reasoning capability.

3 BIM-based DDSS for AMC

The gap between BIM-based design and the AMC knowledge base can be bridged by consolidating BIM information retrieval, manufacturing feature extraction, and reasoning of the AMC method's conformity. As illustrated in Figure 1, the fundamental elements of AMC are formalized in modular ontologies and linked at an application level as the AMC knowledge base. The captured AMC knowledge is a triple store by its ABox and the basis of an intelligent agent by its TBox and RBox: when coupled with a dedicated inference engine, new information will be derived regarding existing facts in the knowledge base. The proposed DDSS queries the building components' information from

BIM-based design through a specific API, extracts the geometry and semantic features important to manufacturing processes, accesses the AMC knowledge base, and then makes use of an embedded inference engine to reason material, building space, regional rules and manufacturability conformities w.r.t. different AMC methods. Decisions of appropriate AM method(s) would be supported by visual and textual explanations. Afterwards, the DDSS will enrich both geometric and semantic information of the BIM-based design.

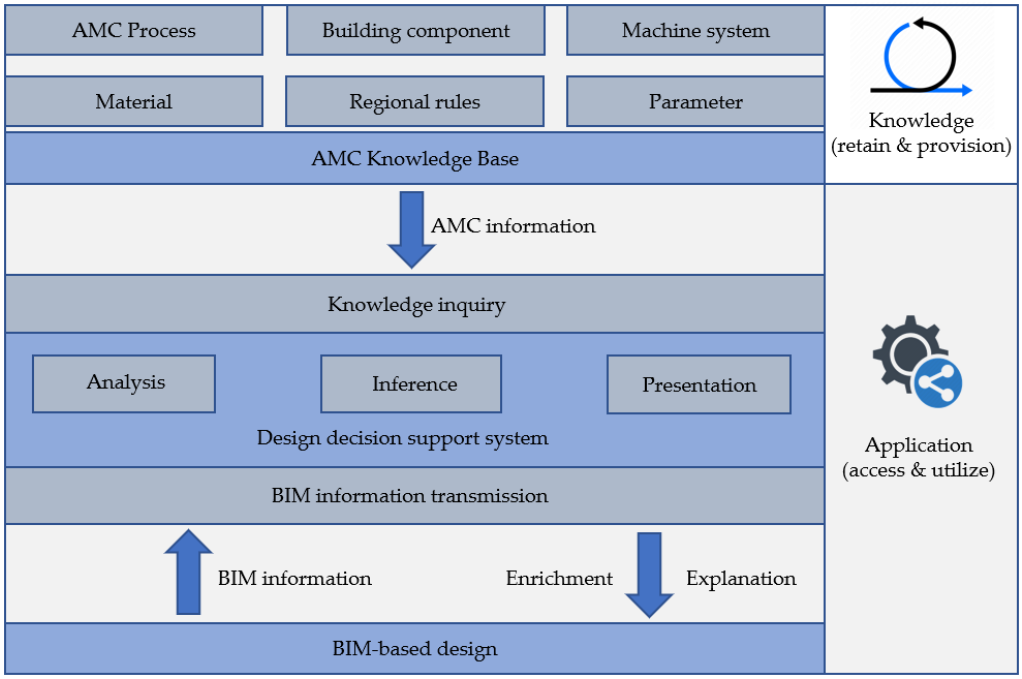

Figure 1: Structure of the DDSS for AMC

4 Formalize AMC Knowledge Base for Design Decision Support

Essential activities for most ontology-development methodologies comprise *specification*, *knowledge acquisition*, *conceptualization*, *formalization*, and *validation* [13][14]. Due to AMC's ever-increasing implementations and complex nature, domain experts' knowledge might be incomplete or inaccurately comprehended by ontology engineers during knowledge acquisition. Therefore, it is reasonable to follow the development life cycle of *evolving prototypes* [14]. After each involved activity, if the ontology does satisfy the required evaluation criteria, the previous activity should be repeated to improve the prototype. Furthermore, knowledge acquisition should be performed throughout the whole life cycle to improve the quality of the ontologies. During the course of conceptualization, working on taxonomies of different concepts and grouping them into modules consequently draws an activity of ontology reuse.

4.1 Strategy of Ontology Alignment

In manufacturing, AM techniques have long been deployed. Many studies put efforts into formalizing AM-specific ontologies, especially for manufacturability analysis of designed parts [15]. Due to the distinctive nature of AMC, reuse of these ontologies requires significant adaptions, at least for concept definition and application scenarios. Process type material jetting is defined by ASTM as an "*additive manufacturing process in which droplets of feedstock material are selectively deposited*" and specified by curing or bonding using UV light, chemical reaction, etc. [16]. In the scope of 3DCP, it is informally described as "*where layers are sprayed, using compressed air, one after another*" and is often referred to as the Shotcrete process [17]. Moreover, the semantic information from the BIM model must be provided for meaningful manufacturability assertion, e.g., an overhang feature of 90 degrees has been detected from a wall panel without knowing that this overhang belongs to the opening assigned to a window element, and placement of window frame is one of the integrated tasks for the printing process. It would be falsely stated that no AMC method can print such a wall panel.

As it to the AEC domain, it is unsurprising that existing ontologies rarely embody the AMC-specific knowledge that most practitioners do not yet recognize. The ifcOWL ontology is prioritised due to its remarkable coverage of domain entities, ISO-standard affinity, and potential to facilitate semantic enrichment in a BIM model after decision-making. Admittedly, transcription of EXPRESS to OWL 2 DL for knowledge representation is debatable as EXPRESS is used for information modeling regarding data structure and integrity, while OWL 2 DL is a computational fragment of first-order logic to model human knowledge. Further, the Semantic Web is built upon the open-world-assumption that incompleteness of knowledge is common and permissible. Sanfilippo et al. pointed out that the ifcOWL requires fundamental analysis and further clarifications as a qualifiable domain ontology for practical application [18]. We, therefore, start from a bottom-up and task-driven approach to formalize AMC ontologies and approach to soft reuse and extension of the ifcOWL. As such, it is possible to pertain to both the knowledge embodiment and seamless information flow after decision-making. Knowledge transition from the open-world AMC knowledge base to the closed-world BIM model is out of the scope for this work but would be enabled by a validation process using SHACL.

4.2 AMC Ontology Development

The *specification* process identifies the use of the ontology and its interested domain of discourse. First, we clarify that the AMC ontology is an application-level ontology to choose suitable AM methods. It is not a domain or fundamental ontology consisting of semantically sound definitions of basic terms - in fact, creating computational ontologies for manufacturing processes could require more expressive logic than DL. The ontology should comprise concepts and relationships regarding operational *resources*, *product* categories, descriptive AMC *processes*, etc. A set of competency questions (CQs) should be answered, for instance:

CQ_example: what is the maximum overhang degree printable by each AMC method?

Knowledge acquisition activities, according to Mendonça et al. [13], involve extraction, elicitation, validation and refinement. Based upon it, we first studied AMC-related bibliography to extract technical terms of AMC processes, then drafted an informal questionnaire as the protocol of semi-structured interviews. During interviews, experts in different AMC methods were requested to elaborate and guide the completion of the questionnaire. Experts could also complement and review the critical technical aspects, depending on their subjective willingness to participation. Overall, the filled questionnaire and relevant bibliography become the basis of the conceptualization process. *Conceptualization* phase figures out required concepts for AMC and clarifies their relations. *Process*, *product* and *resource* are indispensable for the entire manufacturing domain; it is, therefore, necessary to classify and relate AMC processes (*process*), building components (*product*), material (resource) and machine systems (*resource*). Further, identified boundary conditions, e.g., manufacturing feature constraints, machine systems' workspace and printed specimens' mechanical properties, should be conceptualized and indicated by corresponding *parameter*s. *Formalization* is meant to transform the concepts and relations in a quasi-formal model. Considering the prior determination of knowledge representation language (OWL2), in this phase, we practically implemented a primary AMC ontology as a basis for upcoming refinement prescribed in the aforementioned *evolving prototype life cycle*. *The validation* phase demonstrates the competency of the ontology regarding CQs raised in the specification process. Due to the limit of length, here we only proof the exemplified CQ in one SPARQL query: as the prefixes' names indicate, *amc_method* refers to the knowledge of AM methods where information about machine systems (*amc_ms*), material (*amc_material*), building components (*buildingcomponent*) and parameters (*amc_parameter*) are aggregated.

Sample query for competency validation

```
1  SELECT ?Method ?overhangDegreeVal
2        WHERE {
3        ?Method amc_method:overhangFeatureBoundaryCondition
4              [amc_method:upperBoundOverhangFeatureParam
5              [amc_parameter:overhangFeatureAngle
6              [express:hasDouble ?overhangDegreeVal ]]]. }
```

Method	overhangDegreeVal
AMC_Method:Method_Shotcrete_TRR277	"30.0"^^xsd:double
AMC_Method:Method_OrientedLacePressing_TRR277	"45.0"^^xsd:double
AMC_Method:Method_SelectivePasteInstrusion_TRR277	"90.0"^^xsd:double
AMC_Method:Method_SelectiveCementActivation_TRR277	"90.0"^^xsd:double

Figure 2: Query result for the sample CQ. Visualized in GraphDB.

As it to manufacturability assertion, SWRL rules were applied to link manufacturing features' values to corresponding boundary conditions of AMC methods. Through R1, the manufacturing features are able to be determined by methods' boundary conditions. Accordingly, Figure 2 illustrates the inference of an unprintable overhang.

```
        greaterThan(?featureValue, ?upperBound),
         relatingProcess(?upperBound, ?method),
          assertedByMethod(?feature, ?method),                    R1
hasManufacturabilityAssertion(?feature, ?assertion) →
 hasAssertionEnum(?assertion, IS_NOT_MANUFACTURABLE)
```

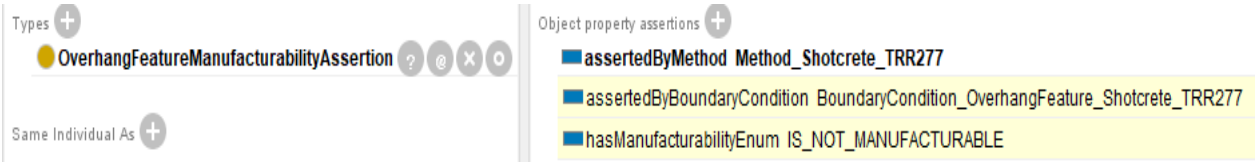

Figure 3: Overhang feature manufacturability assertion for Shotcrete method

5 Conclusion

This paper briefly introduces the structure of the DDSS and the development life cycle for the AMC knowledge base. As proof of concept, the use of the SWRL rule has been demonstrated to assert the manufacturability of the overhang feature. Alignment with the ifcOWL remains unsolved, but future work would investigate the extension of reused ifcOWL terms within the AMC knowledge base's TBox. Use cases could be ifcProxy for industrial robotics, ifcTaskType for AMC process types, etc. The type-occurrence pattern would be further analyzed for proper description of AMC planning in the overall supply chain.

Acknowledgements

This research was supported by the Deutsche Forschungsgemeinschaft (DFG, German Research Foundation) – Projektnummer 414265976 – TRR 277 Additive Manufacturing in Construction.

References

[1] “3D Printing.” https://d-shape.com/3d-printing/ (accessed Apr. 03, 2022).

[2] H. Kloft et al., “Influence of process parameters on the interlayer bond strength of concrete elements additive manufactured by Shotcrete 3D Printing (SC3DP),” Cem. Concr. Res., vol. 134, 2020.

[3] C. Gosselin, R. Duballet, P. Roux, N. Gaudillière, J. Dirrenberger, and P. Morel, “Large-scale 3D printing of ultra-high performance concrete - a new processing route for architects and builders,” Mater. Des., vol. 100, pp. 102–109, 2016

[4] N. Labonnote, A. Rønnquist, B. Manum, and P. Rüther, “Additive construction: State-of-the-art, challenges and opportunities,” Autom. Constr., vol. 72, pp. 347–366, 2016

[5] A. Paolini, S. Kollmannsberger, and E. Rank, “Additive manufacturing in construction: A review on processes, applications, and digital planning methods,” Addit. Manuf., vol. 30, no. October, p. 100894, 2019

[6] O. Davtalab, A. Kazemian, and B. Khoshnevis, “Perspectives on a BIM-integrated software platform for robotic construction through Contour Crafting,” Autom. Constr., vol. 89, no. January, pp. 13–23, 2018

[7] Building Information Modeling : Technology Foundations and Industry Practice, edited by André Borrmann, et al., Springer International Publishing AG, 2018

[8] C. Li and F. Petzold, “Integrating Digital Design and Additive Manufacturing Through BIM-Based Digital Support,” Proceedings of the 26th CAADRIA, 2021, vol. 1, pp. 263–270.

[9] R. A. Buswell et al., “A process classification framework for defining and describing Digital Fabrication with Concrete,” Cem. Concr. Res., vol. 134, no. December 2019, 2020

[10] N. Freund, I. Dressler, and D. Lowke, Studying the Bond Properties of Vertical Integrated Short Reinforcement in the Shotcrete 3D Printing Process, vol. 28. Springer International Publishing, 2020.

[11] G. Dielemans, D. Briels, F. Jaugstetter, K. Henke, and K. Dörfler, “Additive Manufacturing of Thermally Enhanced Lightweight Concrete Wall Elements with Closed Cellular Structures,” J. Facade Des. Eng., vol. 9, no. 1, pp. 59–72, 2021

[12] P. Pauwels, S. Zhang, and Y. C. Lee, “Semantic web technologies in AEC industry: A literature overview,” Autom. Constr., vol. 73, pp. 145–165, 2017

[13] F. M. Mendonça, K. C. Coelho, A. Q. Andrade, and M. B. Almeida, “Knowledge acquisition in the construction of ontologies: A case study in the domain of hematology,” CEUR Workshop Proc., vol. 897, pp. 2–6, 2012.

[14] H. S. Pinto and J. P. Martins, “Ontologies: How can They be Built?,” Knowl. Inf. Syst., vol. 6, no. 4, pp. 441–464, 2004

[15] M. Mayerhofer, W. Lepuschitz, T. Hoebert, M. Merdan, M. Schwentenwein, and T. I. Strasser, “Knowledge-Driven Manufacturability Analysis for Additive Manufacturing,” IEEE Open J. Ind. Electron. Soc., vol. 2, no. March, pp. 207–223, 2021

[16] ISO/ASTM, “INTERNATIONAL STANDARD ISO / ASTM 52900 Additive manufacturing — General principles — Terminology,” Int. Organ. Stand., vol. 5, no. I, pp. 1–26, 2015

[17] F. Dietrich, “Development of a Shotcrete 3D-Printing (SC3DP) Technology for Additive Manufacturing of Reinforced Freeform Concrete Structures,” pp. 1–12.

[18] E. M. Sanfilippo, W. Terkaj, and S. Borgo, “Ontological modeling of manufacturing resources,” Appl. Ontol., vol. 16, no. 1, pp. 87–109, 2021

Multi-view fusion of technical drawings for a conceptual 3D reconstruction using deep-learning

Andrea Carrara[1]
[1]Lehrstuhl für Computergestützte Modellierung und Simulation, TU München, Arcisstr. 21, 80333 München, Deutschland
E-mail(s): andrea.carrara@tum.de

Abstract: Technical drawings, often in the form of floor plans, are required to design, define, and execute a building project. Still, it is becoming increasingly common to develop 3D models of the building defined in floor plans since it allows to perform simulations, spot structural flaws, and easily visualize the final result. The modeling task is not automatic; it requires less time and effort if the drawings are in a vector format, but often it is the case that the floor plan is rasterized, which means that the drawing is transformed into an image from the vector format in which it was produced, all the semantic information contained in the drawing are lost in the pixel transformation. Retrieving the lost semantic information frequently involves professionals in reconstructing the floor layout; it is time-consuming and prone to errors. Automatically generating models from floor plans is an in-depth researched topic. Although various researchers have addressed the topic, most studies' complexity remains low, focusing on parsing pre-processed or simplified datasets far from the actual floor plans used in the construction industry. The difficulty of creating adequate datasets partially explains this, annotating floor plans requires a significant amount of time, and the drawings are often copyrighted. The central lack in the research is creating a building 3D model based only on the main view, not considering cross-sections and the annotations of the measurements. Those are all essential information in the actual floor plans used in the construction industry that is always omitted in research. The task of automatically creating a realistic 3D model from multiple view floor plans is a novel research topic that has the potential to broaden the field of floor plan analysis. This research aims to identify a research gap and present two conceptual AI-based pipelines for completing this novel task for raster and vector data.

Keywords: Artificial Intelligence, Design Automation, Graph Neural Network, Multi-Source Linking

1 Introduction

A technical drawing, also known as an engineering drawing, is a thorough, accurate diagram or plan explaining how an object works or is built. Engineers, electricians, and contractors use these drawings as guidelines while constructing or repairing products and buildings. Therefore, technical drawings are a standard tool shared among engineering fields to convey knowledge using a common graphical language; they bridge communication between the designers and the producers.
Technical drawings are required to design, define, and execute a building project. Many types of architectural drawings are used in the construction process; each type represents specific details of the building. The floor plan, for example, shows the layout of the rooms and the placement of doors and windows; floor plans are a special kind of top view in which the roof is removed to show the rooms' disposition offering the wall layout. It is one of the most important tools to represent knowledge in building, especially in residential construction projects. In contrast, cross-section drawings show a vertical cut of the building providing vertical information about the building.
Complex projects contain many technical drawings to represent all the particles of the building or infrastructure in the finest detail. Professional architects and engineers create the drawings.
Combining the information from all the data from different sources is necessary to have the best comprehension of the project.
Traditionally all the drawings were designed and drawn on paper. Still, recently with the development of technology, with the introduction of computer-aided design (CAD) software, the standard for technical drawings changed from paper to computer-based drawings: the digitalization of the process allows to improve the accuracy of the drawing, reducing the time and errors. Consequently, the state-of-the-art practice in the construction industry is to design drawings in digital form with a CAD system and create 3D semantically rich BIM models to perform checks, simulations, and evaluations. This is straightforward in creating a new building, but it is necessary to deal with drawings on paper when the project is about an already existing building.
In this scenario, the conventional technique is to have experts reconstruct the drawings in digital form based on the paper version. It is time-consuming, error-prone, and has a large margin of automation potential.
Automatically generating models from floor plans is an in-depth researched topic. Initially, this was primarily accomplished with heuristic-based systems, but with the advancement of artificial intelligence, learning-based systems have taken over, outperforming prior methods. This is because, while floor plans have a standard fundamental structure depicting doors, walls, and windows in the case of buildings, the representation design of these elements might vary between projects.
This paper aims to highlight the research gap in technical analysis and define the problem statement. Two data pipelines based on the neural network are presented. The systems are designed to solve the problem of the most common representations of floor plans: raster and vector format.

2 Related Work

Former methods utilize heuristic-based methods derived from domain knowledge to extract the information from the floor plans and classic computer vision methods such as Hough Transformation to detect lines. Hough Transformation is a feature extraction technique used in computer vision. The HT transforms a difficult global detection task in image space into a more straightforward local peak detection problem in parameter space [1].
In “A System to Detect Rooms in Architectural Floor Plan Images” [2] a system to detect rooms in architectural floor plan images is described, they base their approach on the Hough Transformation, but they try to overcome the drawbacks by applying it on the result of image vectorization.
In Automatic reconstruction of 3D building models from scanned 2D floor plans [3], Lucile Gimenez et al. tackle the problem of constructing 3D building models from 2D plans using a topological approach. They start with a pre-processing phase of binarization and noise cleaning from the scanned plans. Subsequently, a separation of the input image in the text image containing textual information and the geometry image containing geometry elements like lines and arcs is performed.
More recently, many data-driven approaches were proposed for architectural elements detection and room classification of floor plans. Dodge et al. provide a technique for analyzing floor plan images utilizing object identification, semantic wall segmentation, and OCR (Optical Character Recognition) in "Parsing Floor Plan Images" [4]. They use a fully connected network for wall segmentation and Faster R-CNN to detect windows and doors.
Liu et al. in “Raster-to-Vector: Revisiting Floorplan Transformation” [5] focus on the vectorization of raster floor plan images with a learning-based approach but maintain an aspect of rule-based in the process by implementing an integer programming mechanism that refines the primitives extracted from the deep learning network.
Kim et al. use a style transfer technique to automatically deal with the diverse architectural styles and construct a simplified form of the floor plan image in "Application of Style Transfer in the Vectorization Process of Floorplans" [6]. The integrated format for the style transfer is a simplified geometrical representation of walls and openings. The network attempts to learn the representation of the standard simplified geometries in the floor plan, ignoring the details intrinsic to the type of plan.
Kalervo et al. in “CubiCasa5K: A Dataset and an Improved Multi-Task Model for Floor plan Image Analysis” [7] released a new dataset for automatic parsing of floor plan images containing 5000 floor plans annotated by experts. The authors present a multi-task network based on an encoder-decoder system to address the vectorization problem of the novel dataset.
In "FloorPlanCAD: A Large-Scale CAD Drawing Dataset for Panoptic Symbol Spotting" [8] Fan et al. present a new dataset it includes 15000 floor plans ranging from residential to commercial structures. The paper’s primary strategy is to use Graph Neural Networks to analyze vector data. Hence the graph must be constructed from the CAD drawings. They combine graph convolution based on the message passing mechanism with Faster R-CNN for the instance symbol spotting tasks.

3 Multi view technical drawing analysis and automatic data linking

3.1 Problem definition

The elements in different floor plans are represented differently depending on the perspective; the goal is to automatically link the items in multiple formats to acquire the most information for representation. The requirement originates from the large number of technical drawings used to depict engineering projects; the analytical focus is frequently on a single element, but examining the entirety of perspectives allows a deeper examination of the entire project. In the case of technical drawings, the process differs depending on the input source; two primary forms of representation are usually used: raster data constituted of pixels and vector data. For each type of input, one pipeline is provided, noting commonalities, advantages, and limitations.

3.2 Raster Data analysis

Raster data is a pixel representation; each pixel has a value that represents the pixel's color. The typical workflow for this type of data includes pre-processing the drawing, binarizing the colors, and cleaning the picture of noise. This approach frequently enhances the results of the pipeline's subsequent stages, allowing the learning algorithm to perform better.

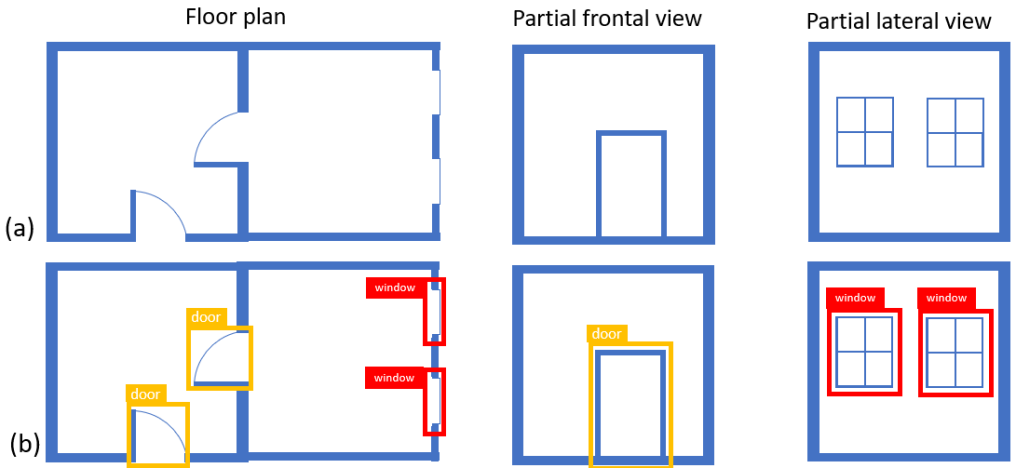

Figure 1: Object detection on multi view in technical drawings

The next stage in the processing is the detection of single elements based on the kind of view of the artwork. The floor plan needs to detect the walls and architectural components such as windows and doors from the top perspective; similarly, this categorization may be extended to other viewpoints of the structure.
For the raster data, two techniques are possible: semantic segmentation for walls and object detection on architectural parts or an entire object detection strategy. The goal of wall detection as a semantic segmentation task is to distinguish between pixels of walls and pixels of the background. Binary classification is performed on all pixels in the image, allowing for a general approach to any wall and shape because the neural network learns based on the proximity of pixels, and no geometrical

function is used to fit the pixels. The deep learning model used in this assignment is often U-net or any autoencoder with skip connections, with input data in the same format as output data. Convolutional layers take features from the original input learning to represent it in dense space,. In contrast, deconvolutional recover information from the dense space to rebuild the original input or a detection mask defined in the dataset. In the case of the U-net design, certain skip connections are given to enhance the reconstruction loss when information is sent from the convolution layer to the deconvolution layer of the same dimension. The process of recognizing windows and doors on the picture is handled by region proposal networks like YOLO [9] or Fast R CNN [10].

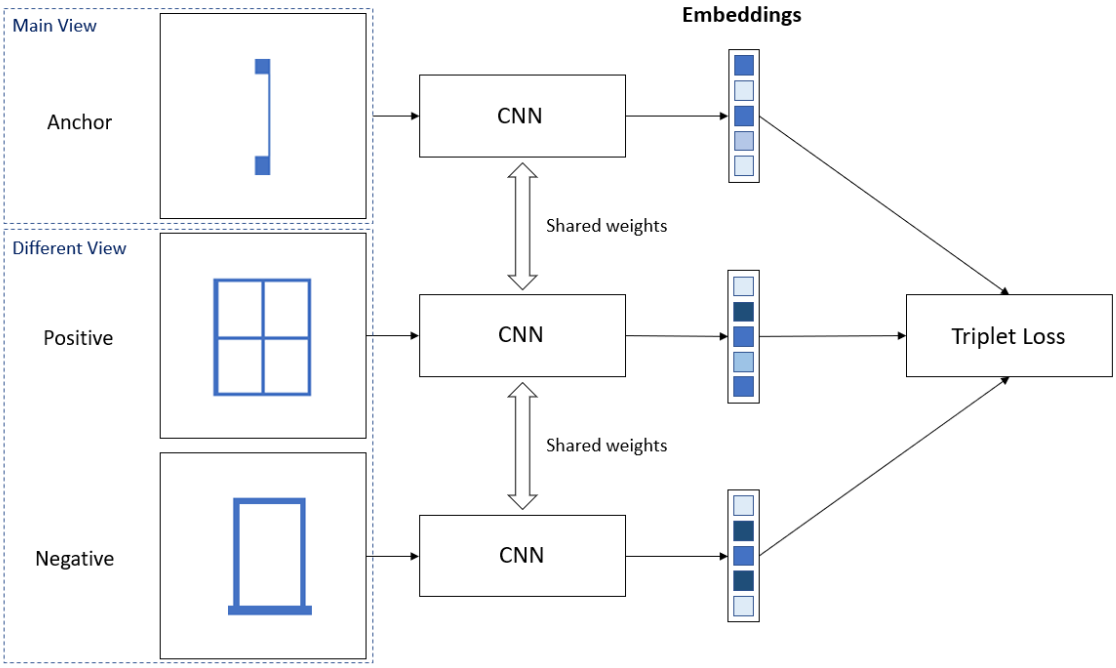

Figure 2: The triplet loss from multi view technical drawings

The alternative is to treat each element in the drawing as an element and perform object detection on the entire image, which means that either all of the walls are segmented and detected, or the distinction occurs at junctions. When the junctions are detected, the walls are connected to the points in a manner similar to graphs. This technique allows for the formation of a singular neural network, but the system loses the ability to analyse any type of wall shape.
The connecting between drawings is expressed as a similarity problem. The suggested method is based on triplet loss [11], which creates a differentiable loss function to compute image similarity. The fundamental concept is to use a Convolutional Neural Network with shared weights to transform an anchor, a positive and a negative picture into an embedding space, and then compute the distance between them automatically based on the training phase. The reference picture is the anchor, the positive image is another image that is equal to the anchor but in another view, and a negative image is a different object in another view. The triplet loss minimizes the distance to the positive while maximizing the distance to the negative. When performed on multiple instances the distances are

fine-tuned to express optimally the similarities in a multidimensional space.
Finally, the goal is to have objects from various perspectives that are near the same embedding space. Combining the triplet loss in semantic/object recognition in a multi-task learning approach might enable the training of an end-to-end neural network that identifies and automatically combines walls, windows, and doors, learning the relations between entities in the floor plan and different views.

3.3 Vector data analysis

Vector data is more popular in current drawing systems than raster data since the information is stored in line segments specified by mathematical functions rather than pixels. The various aspects of the design are frequently represented in distinct layers in CAD systems that can reflect the semantic value; however, this is not enforced by any standard and so it is not always viable to extract semantic information from it.
The vector data may be transformed into a graph format, where nodes represent vector segments and edges are constructed based on geometrical elements in the drawing (connectivity, parallelism, incidence of lines).

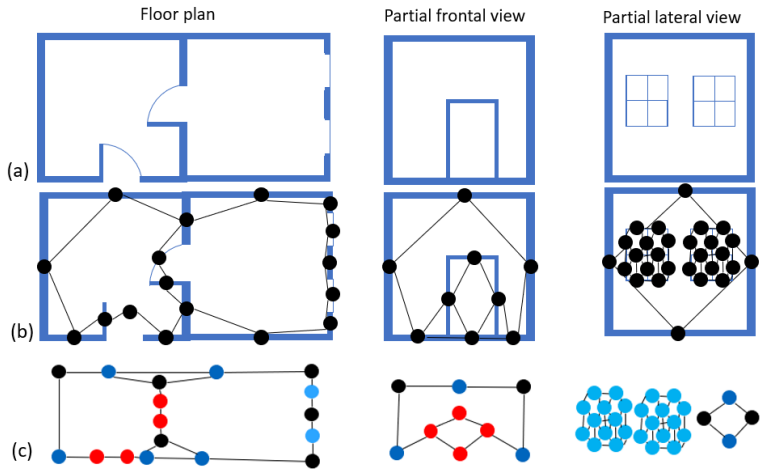

Figure 3: Subfigure (a) shows the input multi view technical drawings. Subfigure (b) depicts the transformation of vector data into the graph based on proximity and the subfigure (c) shows the node classification done by Graph Neural Network

The aggregate function combines information from nearby nodes and produces a message, while the update function combines the target node's embedding with the message to update the target node's new latent embedding vector.
In the update function, a set of weights W is introduced to enhance the embeddings by backpropagation of the loss function, and a nonlinear function is applied to the update function. These aggregate and update layers are stacked similarly to CNN convolutional layers, allowing the algorithm to learn longer node and edge relationships.
A graph connection problem can be used to define the multi-view connectivity job. The graph is built as a one-to-one translation of segments into graphs, and the node classification seeks to forecast each line into a class made up of distinct nodes. Following the initial classification, it is feasible to cluster

close nodes with the same label into a higher conceptual representation of the floor plan. Aggregating the nodes again, it is possible to obtain a representation of the layout in rooms and, if possible, the whole floor plan representation.
This enables the transformation of each graphic into a knowledge tree that begins with a single node and provides a more detailed representation of the architectural entities at each level. The drawings are connected at various levels, and a neural network may be trained to learn the graph's adjacency matrix, learning to automatically link components across drawings based on graph inter connectivity.

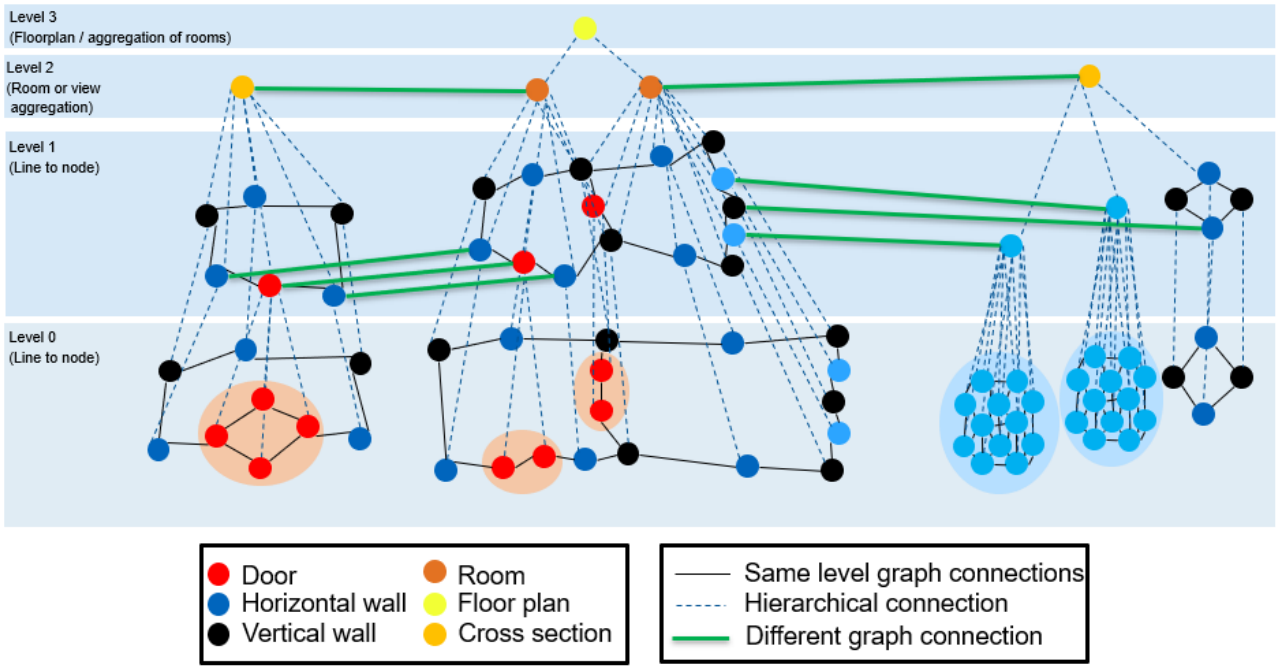

Figure 4: Hierarchical representation of technical drawings and multi view linking problem definition

This technique has possible implementation difficulties since it is hard to incorporate all of the tasks into a single network because the objective is constituted of node and edge classification. Also, it is important to specify or implement the hierarchy heuristic in the network. In any case, the suggested method has the capacity to accurately describe a technical drawing's hierarchical knowledge and link elements in a multi-view input.

4 Final Remarks

The report identifies a research gap in the field of technical drawing information extraction. To address this novel task, two data-driven techniques are offered; the approaches are theoretical due to the lack of available datasets for this sort of work. The emphasis is on data connectivity; nevertheless, transforming different perspectives in the 3D representation remains an open task.

References

[1] J. Illingworth and J. Kittler, “A survey of the hough transform”, *Computer vision, graphics, and image processing*, vol. 44, no. 1, pp. 87–116, 1988.

[2] S. Macé, E. Valveny, H. Locteau, and S. Tabbone, “A system to detect rooms in architectural floor plan images”, 2010, pp. 167–174, ISBN: 9781605587738. DOI: 10.1145/1815330.1815352.

[3] “Automatic reconstruction of 3d building models from scanned 2d floor plans”, *Automation in Construction*, vol. 63, pp. 48–56, Mar. 2016, ISSN: 09265805. DOI: 10.1016/j.autcon.2015.12.008.

[4] “Parsing floor plan images”, 2017.

[5] C. Liu, J. Wu, P. Kohli, and Y. Furukawa, “Raster-to-vector: Revisiting floorplan transformation”, vol. 2017-October, 2017. DOI: 10.1109/ICCV.2017.241.

[6] “Application of style transfer in the vectorization process of floorplans”, vol. 114, Aug. 2018, ISBN: 9783959770835. DOI: 10.4230/LIPIcs.GIScience.2018.39.

[7] A. Kalervo, J. Ylioinas, M. Häikiö, A. Karhu, and J. Kannala, “Cubicasa5k: A dataset and an improved multi-task model for floorplan image analysis”, vol. 11482 LNCS, 2019. DOI: 10.1007/978-3-030-20205-7_3.

[8] Z. Fan, †. L. Zhu, H. Li, *et al.*, “Floorplancad: A large-scale cad drawing dataset for panoptic symbol spotting”. [Online]. Available: https://floorplancad.github.io/..

[9] J. Redmon, S. Divvala, R. Girshick, and A. Farhadi, *You only look once: Unified, real-time object detection*, 2015. DOI: 10.48550/ARXIV.1506.02640. [Online]. Available: https://arxiv.org/abs/1506.02640.

[10] R. Girshick, *Fast r-cnn*, 2015. DOI: 10.48550/ARXIV.1504.08083. [Online]. Available: https://arxiv.org/abs/1504.08083.

[11] E. Hoffer and N. Ailon, *Deep metric learning using triplet network*, 2014. DOI: 10.48550/ARXIV.1412.6622. [Online]. Available: https://arxiv.org/abs/1412.6622.

The Morphological Echo of Architects Concept for a Conversational Artificial Intelligence to Support Architects during the Early Design Stages

Jessica Bielski[1], Viktor Eisenstadt[2,3], Christoph Langenhan[1] and Burak Mete[1]
[1]Technical University of Munich, Arcisstr. 25, 80333 Munich, GER
[2]German Research Center for Artificial Intelligence, Trippstadter Str. 122, 67663 Kaiserslautern, GER
[3]University of Hildesheim, Universitätsplatz 1, 31141 Hildesheim, GER
E-mail(s): jessica.bielski@tum.de, viktor.eisenstadt@dfki.de, langenhan@tum.de, burak.mete@tum.de

Abstract: *Communication* is considered an essential aspect of a successful architectural design process. Sketching plays an important role as a tool of *Communication*, while supporting the design development. Using Artificial Intelligence (AI) methods for auto-completion, accelerating and improving work, the metis projects pursue a conversational intelligent design assistant suggesting further *design steps*. Similar to human conversations, the system aims to understand the architect to provide comprehensible suggestions with coherent and appropriate explanations in the user's language at the correct time for improved Human-System-Interaction (HSI), User Experience (UX) and ultimately the effectiveness of the application. We plan to investigate explainability (XAI) and its temporal aspects to eventually generate these individually and automatically in real time.

Keywords: XAI, Explainability, Artificial Intelligence, Design Decision Support, Sequencing

1 Introduction

Communication is considered an essential part throughout all design phases of a successful architectural design process, differentiated into external communication (e.g. public participation), communication within the team, and internal communication (architect's inner dialogue) [1], [2]. Hand-drawings inhabit a special role by clearly illustrating ideas, providing tangibility. Sketching supports the designing by instantly depicting the implications of design decisions. The sketch is both tool and language of *Communication*, as well as a catalyst of the design selection process for further design development [3]. Therefore, sketching is an intuitive interaction method for Computer-Aided

Architectural Design (CAAD) naturally integrating into the design process [4]. Derived from Artificial Intelligence (AI) methods of auto-completion to solve tasks faster and more efficiently, the metis projects pursue the development of an intelligent design assistant. It suggests further *design steps* for the floor plan design during the early design stages, inspired by the 'Architecture Machine' of Negroponte [5]. The system aims to enter the architect's inner dialogue as a conversational partner by suggesting possible solutions. Similar to human conversations, the system needs to understand the user to provide comprehensible suggestions with complementary explanations in the same language at the appropriate time. These explanations are essential for enabling mutual understanding, promoting Human-System-Interaction (HSI), Human-Data-Interaction (HDI), User Experience (UX) and ultimately the effectiveness of the application through explainability as an eXplainable Artificial Intelligence (XAI).

In the following, we will present our approach for determining the appropriate timing of each design step accompanied with explanations and their respective visualisations, by deducing *when which information* is suitable to support the user's understanding of the individual suggestion. Thus, we will describe the current state of research for both current technology and literature, describe three phases of our approach, based on the previously developed and implemented methods within the metis projects accompanied by an extensive further literature review, and finally, discuss possible obstacles and other applications within the research projects.

2 Current State of Research

2.1 Artificial Intelligence and Explainability

Within the past few decades, AI methods have been applied in various capacities and varieties in different industries, research and even daily life (e.g. weather forecast). However, their use within the architecture, engineering and construction (AEC) industry is rather rare. Following the adoption of Case-Based Reasoning (CBR) as Case Based Design (CBD) in the 1990s, contemporary AI approaches focus on optimisation during later stages of the construction process from Building Information Modelling (BIM) information formalising the final building, e.g. financial, temporal and performance [6]. None of these approaches deal with the complex designs of the early design stages, which are often vague and incomplete because of a non-standardised design process, ill-defined design problems and hand-drawn sketching as a best practice for ideation. Nevertheless, the impact of the design decisions of the early stages are significant on the overall design and sustainability of the construction process and building itself. Vice versa, the later the stages fatal flaws and issues are detected, the more difficult it becomes to remedy these shortcomings and change the design [3], [7]. Thus, the early design stages are a good time for supporting the architectural design decision making to enable faster and more efficient designing while increasing architectural quality [7].

While the decisions of the first AI systems were easily understandable for the human user, much more complex contemporary models like Deep Learning (DL), including Recurrent Neural Networks (RNNs), resulted in the lost connection of the comprehension between the system's output and the internal system operations for the output – the *black box* problem. To remedy these shortcomings,

transparency is used to externalise the internal mechanisms in a comprehensible way for the human user [8], based on principles of HCI, adopted for HSI and HDI. Current RNN-related XAI research can be divided into explainability based on the data learned by the RNN models (e.g. feature relevance methods) or based on the modifications of the RNN architecture outputting insight on the decision (e.g. local explanations) [8]. Both types use post-hoc explainability by re-formatting RNN model data into human interpretable information through different techniques (e.g. visualisations, text, explanation by example). These explanations can be generated by *hybrid transparent* and *black box* methods for creating transparent design methods, which are enhanced in different ways (e.g. constituting data, replacing output) with more interpretable models (e.g. CBR) to create explainable outputs for the user.

Wang, Yang, Abdul, *et al.* [9] shift the perspective of XAI from the system implementation to the theoretical necessities of explainability for the user, based on User-Centred Design (UCD). They propose a conceptual framework and adaptation steps for theory-driven designing of explainability for a specific target group (see Figure 1). The framework is based on the human dual process model of reasoning, where explanation goals, and inherent inquiry and reasoning, as well as possible errors and weaknesses of heuristic System 1 and analytical System 2, inform XAI strategies to support the user in the decision making process. Wang, Yang, Abdul, *et al.* [9] describe the following steps for adapting the framework, tested in a case study for medical diagnoses: clarify the user's reasoning goals and possible biases for the respective applications through a literature review, ethnography, and/or participatory design, deduce appropriate explanation ways for reaching the reasoning goals and/or mitigating cognitive biases using the pathways of the framework, and integrate the explainable intelligent system facilities to create an explainable user interface.

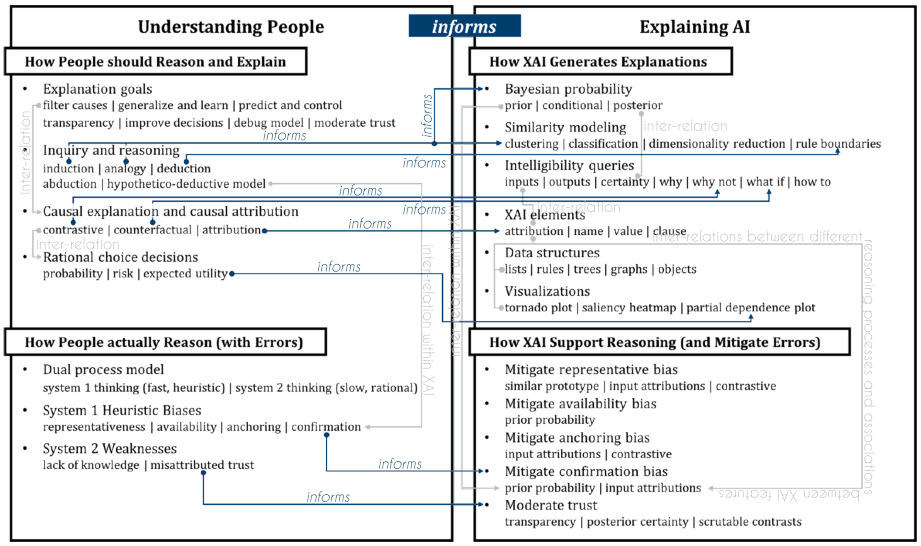

Figure 1: Framework for human reasoning informing XAI techniques [Adapted from 9, p. 4]

2.2 Design Process Protocolling and Sequencing

Design protocolling is a concept for tracking the architectural design process, which can be applied to the sketch process of architects and designers [1], [2]. It is based on the premise of mental design

activities being evident through sketching and consequently, sketch protocol studies. Lawson [10] summarises two methods of segmenting the design process: *temporal* and *relational*. He recommends *relational* protocolling by clustering connected sketching activities in a sensible way. Design protocol studies are commonly divided into 'Thinking aloud' studies and retrospective (reporting) studies. Even though both protocol study types suffer from an artificial setting within a limited work environment, Lawson [10] and Suwa and Tversky [11] identify the retrospective protocol study as superior by providing a more genuine and less distorted design and sketching process. Further, the latter [11] suggest video recording the sketching to support the participant during the retrospective reporting, providing visual cues to avoid selective recall and post-hoc realisation. Sketch protocol studies results are interpreted, whereat only qualitative data is available through approaches of established literature known to the authors. Even though every design process is truly unique because of the problems, tools, stakeholders, and designers, Lawson [10] sees the potential for receiving reproducible results through sketch protocol studies in the manner of the natural science paradigm.

Different attempts at sequencing the architectural design process have been made. The nine service phases by the German 'Honorarordnung für Architekten und Ingenieure' (HOAI; eng.: Fee Structure for Architects and Engineers), and its equivalent of seven phases by the American Institute of Architects (AIA) describe the period from client brief to constructed building, which Lawson [10] calls the 'primary design problem'. However, he defines the *design problem* itself simply as a problem solved through designing. Thus, the architectural design process consists of a multitude of individual design problems to be adhered to and solved [10]. Consequently, Lawson [10] introduces the following order-less 'design activities' for solving a singular *design problem* with an overarching *Communication* for the process: *Analysis*, *Synthesis* and *Evaluation*, the *ASE* model. Laseau [2] further differentiates the *Synthesis* into *Exploration* and *Discovery*. Barelkowski [12] uses knowledge management to further separate the *Analysis* into *Knowing* and *Understanding*, resulting in the *Evaluation* as the final selection, as well as a tool for creating more information in the form of *Evaluation - (informing) Knowing*. Further, Lawson [10] segments the design process through 'design events' in sketches, whereas he deems the 'intention behind' more important to identify the mental activity. Thus, we formulate the following three *relationally* clustering categories for temporal sequences of the architectural design process: *design steps* as the finest clustering method, followed by *design intentions*, and further *design phases*.

3 Approach

In order to truly design and implement a conversational intelligent design assistant that is able to assimilate to the architect's inherent idiosyncrasies, it is necessary for the system to distinguish what *design steps* the architects takes with what *design intention*. The system aims to enter the internal dialogue of the architect and their sketch to suggest appropriate further *design steps*, as well as predict possible biases and weaknesses during the architect's design decision making process. Through an interdisciplinary approach at the interface of AI and architecture, we utilise methods of computer science, design theory and Human-Computer-Interaction (HCI) to ultimately be able to predict and thus, suggest further *design steps* through creating a closed AI pipeline, which constantly re-informs

and improves itself [13]. In order to design and implement timed explainability into the existing DL pipeline of the metis project, we formulate the following research questions for architects designing through hand-drawn sketching during the early design stages:

1. When is what kind of information relevant for the user to make design decisions?
2. When are what explanation techniques needed to answer to the relevant information? When are what explanation visualisations necessary to be dominantly visible?
3. How can we implement our explainability methods, including the newly explored temporal aspect, into our existing DL pipeline?

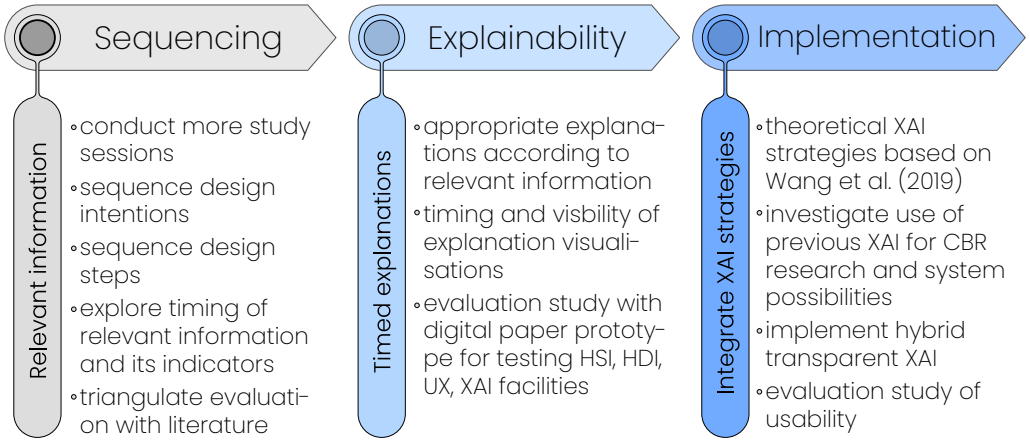

Figure 2: Approach divided by phases answering the three research questions and work steps.

We propose the following approach for answering these research questions on the backdrop of the already conducted research, incorporating their findings, results and evaluations, as illustrated in Figure 2 with three phases: Sequencing, Explainability, and Implementation. We use our successful prediction approach for sequential learning of *design phases* of a refined *ASE* model with six design phases (see Section 2.2) with an overarching *Communication*, based on sketch protocol data [14], quantified through manually assigning sequences within our open-source tool [15], within an Long Short-Term Memory (LSTM) model [16], for further investigating the segmentation of the design process (i.e. *design intention*, followed by *design steps*) by testing the appropriation and robustness of our current LSTM model. Thus, the sketch protocol study needs to be extended with new sequencing labels, while more sessions are continuously conducted to gain more training data. Using this information, we aim to explore *when what information* is relevant to the architect through *design intentions* and how these requests of different information is visible through the sketch and sketching process as *design steps*. We aim to further triangulate, derived from social sciences, these findings through a further literature research, for example Darke [17], Schön and Wiggins [18] and Rezaei [19].

Afterwards, we explore the appropriate explanations for the previously determined relevant information considering their timing, based on the framework of Wang, Yang, Abdul, *et al.* [9] (see Figure1 in Subsection 2.1) and their recommended steps for adaptation. Thus, we explore the temporal aspect of the individual explanations according to their request by the architect. Based on the

necessary explanation techniques according to the architectural design process, we determine *when what explanations* need to be visible to the architect through what representation, e.g. *explanation visualisation* and/or *text*. This includes *when what kind* of interaction methods need to be presented to the user to provide *scrutinising methods* for correcting or improving feature values, and ultimately the suggestions. Through *transparency and scrutability* of the system, we plan to extend the conversational properties of an intelligent design assistant, entering the architect's internal dialogue with the sketch, by providing options for feedback to the system. In order to evaluate the findings in terms of HSI, HDI, UX and XAI, we plan to conduct a case study utilising a digital paper prototype with working architects, based on these findings [14]. Implemented as a high-fidelity clickdummy, incorporating timed explainability, we are enabled to observe the interaction and UX of the study participants.

Even though no XAI facilities are implemented in the latest AI system of the metis projects, explanation modules have been integrated in previous CBR models for retrieval of spatial configurations during the early design stages, based on the 'semantic fingerprint' [20] as a search pattern. They generate textual explanations using Natural Language Generation (NLG) [21] through case-based agents, explanation ontology, and explanation patterns as its foundational components for *transparency*, *traceability*, *relevance* and *justification* After exploring the theoretical XAI strategies proposed by Wang, Yang, Abdul, *et al.* [9] for implementing the explanation strategies to either support the design decision making process or to mitigate possible biases of architects, we investigate the possibilities and mechanisms of our system in order to determine *how we can* implement the theoretical and previous findings combined with our successful explainability for CBR. Thus, we aim to create a *hybrid transparent* system capable of producing the explanations interpretable for the user [8]. Finally, the explainability under the backdrop of its temporal aspect will be implemented into our existing DL pipeline, which will be evaluated through a case study by domain experts - architects.

4 Discussion

Creating explainability for an intelligent design assistant supporting architects through assimilating to the inherent idiosyncrasies, bears great potential to provide actual conversational properties. Based on previous experiences, we will need to take appropriate measures to be able to react to the expected limited data volume produced from the different studies of the proposed approach. Nevertheless, if the process and the implementation of our approach can be validated, it creates potential for formalising a transferable framework for explainability with temporal aspects. Further, the findings of the timing of explainability can be re-used within the metis projects for determining phases of deep concentration to minimise distraction on the user interface on a whole for the truly rewarding *Discovery* of ideas and solutions, maximising the feeling of ownership over the design and satisfaction. Meanwhile, the feedback acquired through the *scrutability* features of the system will provide us with valuable information to improve the intelligent design assistant. Ultimately, the results and findings of the proposed research are promising for creating an intelligent design assistant, which is in a constant conversation with the architect to externalise the internal dialogue for supporting the design decision making process using the silent language of architects, sketches.

Acknowledgements

We want to thank the DFG for funding the metis projects and the participants of the mentioned studies.

References

[1] B. Lawson, *How Designers Think, Fourth Edition: The Design Process Demystified*, 4th. Taylor & Francis Ltd, Jan. 2005.

[2] P. Laseau, *Graphic thinking for architects and designers*, 3rd. Wiley, 2000.

[3] B. Buxton, *Sketching User Experiences: Getting the Design Right and the Right Design*, 1st. Morgan Kaufmann, 2007.

[4] P. Leclercq and R. Juchmes, "The absent interface in design engineering", *Artificial Intelligence for Engineering Design, Analysis and Manufacturing*, vol. 16, pp. 219–227, 2002.

[5] N. Negroponte, *The Architecture Machine: Toward a More Human Environment*. The MIT Press, Jan. 1973.

[6] S. O. Abioye, L. O. Oyedele, L. Akanbi, *et al.*, "Artificial intelligence in the construction industry: A review of present status, opportunities and future challenges", *Journal of Building Engineering*, vol. 44, p. 103 299, 2021.

[7] T. Harputlugil, A. T. Gultekin, M. M. Prins, and Y. I. Topcu, "Architectural design quality assessment based on analytic hierarchy process: A case study", *Metu Journal of The Faculty of Architecture*, vol. 31, pp. 139–161, 2014. DOI: 10.4305.

[8] A. Barredo Arrieta, N. Díaz-Rodríguez, J. Del Ser, *et al.*, "Explainable artificial intelligence (xai): Concepts, taxonomies, opportunities and challenges toward responsible ai", *Information Fusion*, vol. 58, pp. 82–115, 2020.

[9] D. Wang, Q. Yang, A. Abdul, and B. Y. Lim, "Designing theory-driven user-centric explainable ai", ser. CHI '19, Glasgow, Scotland Uk: Association for Computing Machinery, 2019, pp. 1–15.

[10] B. Lawson, *What Designers Know*, 1st. Oxford: Elsevier/Architectural Press, 2004.

[11] M. Suwa and B. Tversky, "What do architects and students perceive in their design sketches? a protocol analysis", *Design Studies*, vol. 18, no. 4, pp. 385–403, 1997.

[12] R. Barelkowski, "Learning design from knowing less. on approaches to architectural design process", in *Knowing (by) Designing*, J. Verbeke and B. Pak, editors, 1st. LUCA Sint Lucas School of Architecture Ghent-Brussels KU Leuven Faculty of Architecture, Jan. 2013, ch. 8.1, pp. 517–526.

[13] J. Bielski, B. Mete, V. Eisenstadt, *et al.*, "Chasing the white rabbit – a case study of predicting design phases of architects by training a deep neural network with sketch recognition through a digital drawing board", in *ICCC*, [Preprint], Pinhal de Marrocos: Association for Computational Creativity, Jun. 2022.

[14] J. Bielski, C. Langenhan, C. Ziegler, V. Eisenstadt, A. Dengel, and K.-D. Althoff, “Quantifying the intangible - a tool for retrospective protocol studies of sketching during the early conceptual de-sign of architecture”, in *CAADRIA*, vol. 1, Hong Kong: Association for Computer-Aided Architectural Design Research in Asia, Apr. 2022, pp. 403–411.

[15] C. Ziegler, *Sketch protocol analyser*, version 1.2, [Computer Software], Sep. 2021. [Online]. Available: https://github.com/KSD-research-group/sketch-protocol-analyser.

[16] B. Mete, J. Bielski, V. Eisenstadt, C. Langenhan, F. Petzold, and K.-D. Althoff, “Predicting semantic building information (bim) with recurrent neural networks”, in *ECPPM*, [Accepted], Trondheim, Norway: European Association of Product and Process Modelling, Sep. 2022.

[17] J. Darke, “The primary generator and the design process”, *Design Studies*, vol. 1, no. 1, pp. 36–44, 1979.

[18] D. A. Schön and G. E. Wiggins, “Kinds of seeing and their functions in designing”, *Design Studies*, vol. 13, pp. 135–156, 1992.

[19] M. Rezaei, *Reviewing Design Process Theories: Discourses in Architecture, Urban Design and Planning Theories*, ser. SpringerBriefs in Architectural Design and Technology. Springer, 2020.

[20] C. Langenhan, “Datenmanagement in der architektur”, Dissertation, Technical University of Munich, Munich, 2017.

[21] V. Eisenstadt, C. Espinoza-Stapelfeld, A. Mikyas, and K.-D. Althoff, “Explainable distributed case-based support systems: Patterns for enhancement and validation of design recommendations”, in *ICCBR*, M. T. Cox, P. Funk, and S. Begum, editors, Cham: Springer International Publishing, 2018, pp. 78–94.

$NTAB_0$: Design Priors for AI-Augmented Generative Design of Network Tied-Arch-Bridges

Sophia V. Kuhn[1], Rafael Bischof[2], Georgios Klonaris[1], Walter Kaufmann[1] and Michael A. Kraus[1]
[1]Chair of Concrete Structures and Bridge Design, ETH Zurich, Stefano-Franscini-Platz 5, 8093 Zurich, Switzerland
[2]Swiss Data Science Center, Turnerstrasse 1, 8092 Zürich, Switzerland
E-mail(s): {sophia.kuhn,kraus}@ibk.baug.ethz.ch

Abstract: Projects in the Architecture, Engineering and Construction (AEC) industry inherit a great complexity due to a tremendous amount of design parameters, multiple objectives, and many involved stakeholders. Especially in the conceptual design stage of bridges, an in-detail analysis of many performance attributes for each design alternative is time-consuming and infeasible under the current approaches. In the industry today, therefore the initial design solution predominantly depends on the expertise of the involved team. In contrast to the status quo, this paper introduces the novel concept of bridge design prior models to predict the layout and structural properties of bridges as the (near-optimal) starting point for Generative Design. The concept of design prior models for bridges is demonstrated on network tied-arch bridges (NTAB). $NTAB_0$ is calibrated upon a curated database consisting of existing real-world NTABs and captures numeric, semantic, and topological relations between bridge properties such as materials, cross-sections or bracing systems. First, a clustering analysis is performed by applying the k-Prototype and DBSCAN algorithms. In the second step, a predictive model is trained using a gradient-boosted decision tree algorithm. A subsequent study evaluates the suitability of the algorithms to serve as sensible design priors. We found that the AI prior model $NTAB_0$ is able to suggest meaningful design parameters, assisting the designing team with an informed initial bridge design for further design space exploration and optimisation. It enables designers to make more informed decisions towards optimised bridge structures at an early design stage. The application of the AI prior model shows great potential to improve future construction projects by providing easy and fast access to the information saved in the existing structures of today.

Keywords: Conceptual Structural Design, Machine Learning, Design Automation, Algorithms

1 Introduction

In current Architecture, Engineering and Construction (AEC) practice, the conceptual design phase is often disconnected from performance evaluations of the structure with respect to safety, functionality, cost, material impacts, and the construction processes. However, this phase is most influential for a building project. Today, the initial design is mainly based on the prior knowledge of (i) the designing team, and (ii) the manual analysis of a few similar reference projects. This design practice results in lengthy and costly processes with numerous manual translations, detailing, and reiterations of rigid design models between early-stage designers and engineers or contractors of later planning stages.

Built bridge structures however represent the final result of detailed investigations during a bridge project, in which the expertise of civil engineers was applied. This fact motivates the derivation of a method for data collection and automated analysis as well as calibration of quantitative prior design models to be used in conceptual design phases. Specifically, this paper proposes to (i) start free-access and open databases on structural properties of bridges, and (ii) use modern Machine Learning (ML) algorithms for data mining and calibration of predictive prior models upon these databases to speed up early phase design and/or validate the design process choices. This idea is investigated within the *Bridge Genome Project*, cf. Fig. 1, for different bridge types. The prior models and their insights are interpreted as the "genome" of how bridges have been planned and built. The workflow and results for calibrating a design prior model upon a repository are presented for the case of network tied-arch bridges (NTAB), described by a parameter set $\theta_B \in R^d$, leading to the $NTAB_0$ prior.

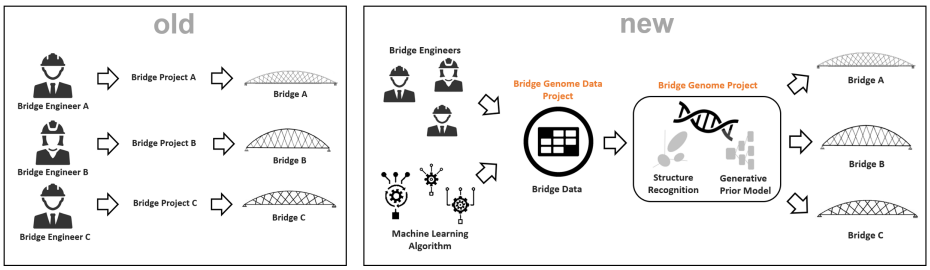

Figure 1: The Bridge Genome Project

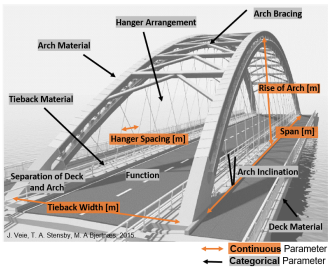

Figure 2: Bridge properties

2 Background and Related Literature

Bayesian methods are an alternative approach to traditional statistical analysis. They are employed widely for analysing and interpreting data or training Artificial Intelligence (AI) models in many fields, including data and computer science as well as civil engineering [1]. The Bayesian method computes a posterior probability about a problem based on observed data (likelihood) and prior knowledge using Bayes' theorem, cf. Sec. 3. Prior information is obtained from the results of previous experiments, simulations, domain theory, and expert assessments [2]. Data-driven learning (i.e. learning from data repositories or sets) through Machine and Deep Learning allows for new discriminative and generative models to be employed to the design task. Discriminative models learn to solve a learning task (e.g. classification, regression, clustering, dimensionality reduction) where for a new input the

respective output is provided. Applying a Bayes view, a discriminative model strictly learns the posterior probabilities of the output given an input [2]. In our present work, the inferred discriminative models serve as prior models for the design task. Here the posterior probabilities of the design output for a given input (i.e. a specific bridge construction project situation) are augmented by the informative prior.

The potential of repositories, evolutionary algorithms, and parametric tools as drivers for design actions was explored for performance-based shading device design for office buildings by [3]. [4] is one of the few studies on bridge simulation data mining as an approach to extract knowledge and decision rules from a database of pre-computed models (design variants) containing simulation results. However, the greatest current hurdle for data mining employing AI in the AEC sector is the lack of systematized, free-accessible databases to learn from the successes and failures of past engineering projects. The potentials and pitfalls of data mining in the AEC sector are addressed in [5].

3 Methods

The formal capturing and quantitative incorporation of domain-knowledge in the form of priors distributions of data about a design problem works within the Bayesian framework: $\mathcal{P}(\mathcal{D}|\mathcal{M}(\theta))$, where $\mathcal{P}$ denotes a probability distribution, $\mathcal{D}$ is the data set and $\mathcal{M}(\theta)$ the parametric model with design parameters $\theta \in \mathrm{R}^{\mathrm{d}}$ respectively. Instead of employing Bayesian model averaging, we suggest to a-priori select a model $\mathcal{M}^*(\theta)$, and subsequently the observed data set is a manifestation of that model drawn according to the probability $\mathcal{P}(\mathcal{D}|\mathcal{M}^*(\theta))$. The goal of the ML algorithms then is to estimate $\mathcal{P}(\mathcal{M}^*(\theta))$. This paper applies the described approach to NTABs for calibrating the NTAB_0 prior.

3.1 Database of Network Tied-Arch Bridges (NTABs)

In the AEC Industry, the systematic documentation of structural data (such as cross-sections, material grades, bracing system types, etc.) of completed projects is currently still insufficient due to the absence of public repositories. To nevertheless have a basis for creating a prior model for bridge design, a data set was curated, which is publicly available via [6]. The database is structured in a table containing mixed-data-type properties including functionality, geometrical, and material parameters of 203 NTABs. Fig. 2 shows the important bridge features together with a distinction of the categorical resp. continuous data types. As the curated data set exhibits missing values, two pre-processing methods are followed to gain a complete data set: for the first data set, the data is filtered for complete rows (bridges). For the second, the missing values are filled utilizing a k-NN algorithm [7]. k-NN estimates missing data by computing a weighted average over the k nearest neighbors in the data set based on the euclidean distance between non-missing entries. We empirically found k = 3 to yield a good compromise between consistency and diversity in the data set.

NTABs belong to the class of (tied-)arch bridges and have been first introduced by Per Tveit in the 1950s [8]. Arches are highly efficient structures due to their ability to carry loads by compression in the case that the thrust line lies within its cross-section [9]. The horizontal forces carried by the arch

are short-circuited through the deck in tension. The structure typically includes two arch ribs to which the vertical loads acting on the deck are suspended by inclined and intersecting hangers.

3.2 Machine Learning (ML) Algorithms

Our approach suggests to (i) identify structure (i.e. similarity groups) within the bridge data using clustering algorithms, and (ii) train a discriminative ML model for predicting suitable bridge parameters.

The cluster analysis is applied to the filtered data set. As the NTAB data set carries mixed data types, the k-Prototype algorithm as implemented in [10] is applied. The k-Prototype algorithm combines the well-known k-means algorithm [11] with the k-modes algorithm [12], to handle mixed data types of continuous and categorical data. To enable the identification of well separated clusters in all dimensions the equal contribution of all properties to the clustering process is achieved by (i) individually standardizing each property column to zero mean and unit variance, and (ii) by iteratively choosing a relative importance weight γ so that an even contribution of both the continuous and categorical properties is observed within the loss function of the k-prototype algorithm. Furthermore, the clustering is conducted 100 times in parallel with a new 'Cao' initialisation each time. The number of clusters k is chosen according to the 'elbow method'. In order to test the stability of the clusters induced via distance-metrics by the k-prototype algorithm, the Density-Based Spatial Clustering of Applications with Noise (DBSCAN) [13] algorithm is used to provide a clustering of the data by fitting probability distributions. However, the results are not shown within this paper.

The second step is to calibrate mixed-data-type ML algorithms upon the NTAB data set as a discriminative design prior for predicting structural bridge properties for a specific project. This means, that starting from a set of fixed design parameters $\theta_{B_1} \in R^{d_1}$, the algorithm generates meaningful suggestions for the remaining parameters $\theta_{B_2} \in R^{d-d_1}$ in a specific order, taking into account all the previous predictions that have been made. For the data set at hand, a decision tree approach is chosen as these algorithms are capable of solving both classification as well as regression tasks, which is necessary due to the mixed-type nature of the data set. Specifically, we calibrate a CatBoost [14] algorithm to the bridge data set as in a pre-study it outperformed other existing state-of-the-art implementations of gradient boosted decision trees (such as XGBoost) in terms of accuracy. This is in accordance with literature, where CatBoost was found especially efficient and accurate if categorical features are present and play an important role [15]. The model is trained on 85% of the bridges from the second imputed NTAB data set. The residual 15% of samples are used to test model performance. A stratified train-test splitting method was applied. For the regression head, `CatBoostRegressors` [14] are fitted to the training data using the *Root Mean Squared Error* (RMSE) loss function with an evaluation via the RMSE on the test data set. For the classification head, `CatBoostClassifiers` [14] are calibrated to the training set using the *Logloss* function for binary categorical properties and the *MultiClass* loss function for categorical properties with more than two categories (i.e. classes). Model evaluation was also conducted on the test data by calculating the accuracy and balanced accuracy. For both algorithm heads, hyper-parameter tuning was performed using grid search.

4 Results

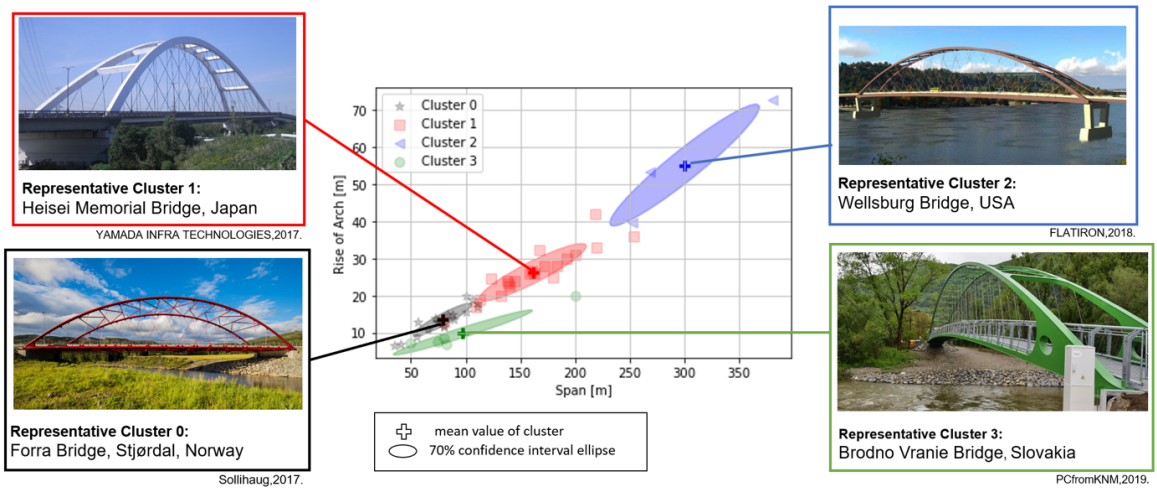

Figure 3: 2D cut scatter plot of the multi-dimensional clusters with a representative bridge for each

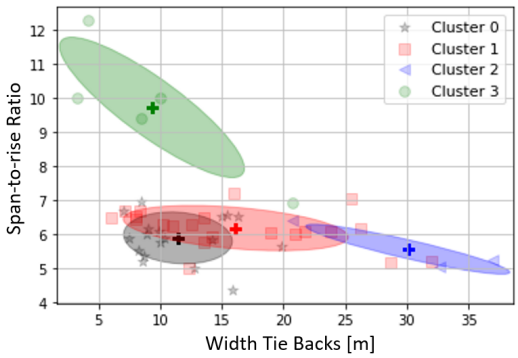

Figure 4: 2D scatter plot of the multi-dimensional clusters (+: Mean value of cluster; 70% confidence interval ellipse)

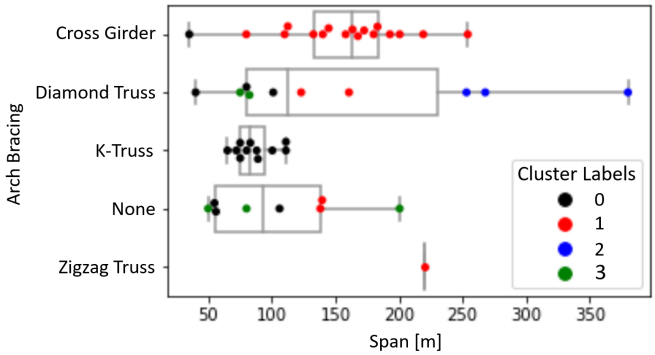

Figure 5: 2D swarm plot of the four multi-dimensional clusters identified with the k-Prototype algorithm (25%- and 75%-quantile Boxplot limits)

For the clustering analysis a reasonable number of clusters for the k-Prototype algorithm is established upon the resulting cost degradation with increasing number of clusters k, which shows a slope change ("elbow") at k = 4 for multiple γ-values. A suitable γ was found to be 4. The four multi-dimensional clusters found in the bridge data set by the k-Prototype algorithm are visualised in Figs. 3, 4, and 5. A good separation between the clusters is visible in all dimensions, where we show as an example the distributions for span to rise, width-tie-back to span-to-rise ratio, and span to arch-bracing. These are to be interpreted as 2D-cuts of the multi-dimensional cluster.

The achieved performance of the trained ML model w.r.t. individual parameter predictions are summarized in Table 1. Initially, we assume the parameters *span, tie back width* and *bridge function* as fixed. The remaining parameters are predicted in series by the ML model. For the classification heads, a high predictive performance was achieved for all parameters on the training set. On the evaluation set an accuracy of above 77% was achieved for all parameters, but a decreased balanced accuracy for

Table 1: Prediction performances of the regression - classification models of the $NTAB_0$ prior model

	On Training Set		On Evaluation Set	
Classification:	Accuracy	Balanced Accuracy	Accuracy	Balanced Accuracy
1. Separation Deck-Arch Structure	0.87	0.87	0.84	0.85
2. Arch Material	1.00	1.00	0.97	0.67
3. Tieback Material	0.97	0.68	0.81	0.52
4. Deck Material	0.92	0.82	0.94	0.89
Regression:	RMSE		RMSE	
5. Rise of Arch	5.81 m		15.58 m	
6. Hanger Spacing	1.2 m		16.7 m	
Classification:	Accuracy	Balanced Accuracy	Accuracy	Balanced Accuracy
7. Hanger Arrangement	0.99	0.98	0.84	0.46
8. Arch Inclination	0.89	0.89	0.94	0.94
9. Arch Bracing	0.95	0.91	0.77	0.53

arch and tieback material, hanger arrangement and arch bracing is visible. The regression models are performing well on the training set, but exhibit a substantially increased RMSE on the evaluation set.

5 Discussion

The k-Prototype appropriately solved the pattern recognition task given the difficulty of the mixed data types present. Four clusters, distinctly well-separated in all dimensions, were found, which proves the equal contribution of all bridge features (both continuous and categorical) during the clustering process. Comparing the probability distributions of the individual features within the clusters reveals interesting relations: The identified bridge clusters are clearly separated w.r.t the span, indicating strong similarities in all bridge properties for the span ranges of the clusters (Fig. 3). Another dominant distinction is the span-to-rise ratio, separating mostly pedestrian bridges from the road and rail bridges (Fig. 4). Fig. 5 displays the cross girder as the most frequently used arch bracing type, mostly used for medium-span NTABs. In addition, engineers in the past have found K-truss bracings beneficial for short-span NTABs and diamond truss bracings effective for long-span NTABs. These detected distinct patterns indicate a good chance for calibrating discriminative ML prediction models for bridge features.

Evaluation of the trained discriminative model showed that gradient boosted decision trees are suitable to capture the dependencies of all bridge parameters in the training set. A reduced balanced accuracy compared to the unbalanced accuracy is identified on the evaluation data set for the classification of some of the bridge parameters. The reason here is the strong imbalance of classes present in the data set, leading to a more performant ML classifier for the dominant classes. Improving the performance by employing skew-insensitive metrics such as DKM and Hellinger distance as splitting criteria in the construction of the decision tree [16] is omitted given the small size of the bridge data set. The limited performance of the regression algorithm on the evaluation data is a result of overfitting, which is often detected for small data sets. Another probable reason is that the available features are insufficient to find a generalised relationship. While the performance evaluation proves that the ML model provides suitable recommendations based on past bridge projects, we can also compare the recommendations to research findings on NTABs. For an input parameter vector falling in the medium-span cluster (red in Fig. 5) the model recommends a span-to-rise ratio of 6.4, which matches literature recommendations

of 5.8 to 6.67 [17]. For the same example, the model advocates the cross girder due to its frequent use, while [18] identifies it to be the least cost-efficient arch bracing type. This reveals a limitation of the the presented method. It does not evaluate weather the underlying data of existing bridges is compliant with current design standards or good engineering practice w.r.t. efficiency, durability, etc.. Hence, the method can adopt systematic mistakes from past bridge projects due to its data-driven nature. Additionally, The cluster analysis and prior model calibration were performed on a small data set of 203 bridges and can therefore not claim to be entirely representative of all the already built NTABs worldwide. Consequently, gathering a larger data set of NTABs is initiated for future investigations. While the approach was applied to NTABs in the present work, the implemented framework is directly applicable to further data sets of other frequently built structure types.

6 Conclusions

Today, the conceptual bridge design remains disconnected from performance evaluations of later stages and therefore dictated by the prior knowledge of the involved experts, leading to a lengthy and costly design process characterized by many iterations. We provide a two-stage method of clustering a data set of structural bridge information and subsequent building discriminative regression resp. classification models as informative design prior. The performed k-Prototype cluster analysis detected design patterns for NTABs in the form of 4 distinct clusters. The identified structure enabled to draw useful conclusions about sensible bridge parameter choices, which can be checked for plausibility by bridge engineering experts yet also inform about hidden design patterns. The discriminative gradient boosted decision tree algorithms serve as a powerful prior model for predicting sensible parameters for a new bridge project situation based on existing bridge construction projects. The two-stage prior modelling approach is found especially useful for detecting multi-dimensional dependencies between the bridge features, which are not easily identifiable by conventional methods. Identified limitations are the risk of adopting mistakes from the past and the limited availability of data in the AEC sector.

Acknowledgements

The authors would like to thankfully acknowledge the facilities of Design++ at ETH Zürich and the funding through ETH Foundation grant No. 2020-HS-388 (provided by Kollbrunner/Rodio).

References

[1] M. A. Kraus, “Machine learning techniques for the material parameter identification of laminated glass in the intact and post-fracture state”, 2019.

[2] C. M. Bishop, *Pattern Recognition and Machine Learning*. Springer, 2016.

[3] B. Ercan and S. T. Elias-Ozkan, “Performance-based parametric design explorations: A method for generating appropriate building components”, *Design Studies*, vol. 38, pp. 33–53, 2015.

[4] S. Burrows, B. Stein, J. Frochte, D. Wiesner, and K. Müller, “Simulation data mining for supporting bridge design”, in *Proceedings of the Ninth Australasian Data Mining Conference-Volume 121*, Citeseer, 2011, pp. 163–170.

[5] V. Ahmed, Z. Aziz, A. Tezel, and Z. Riaz, “Challenges and drivers for data mining in the aec sector”, *Engineering, Construction and Architectural Management*, 2018.

[6] A. Müller, S. Kuhn, and M. Kraus, *Scientific machine learning for structural engineering repository*, 2022. [Online]. Available: https://sciml4structeng.github.io/Repository, (accessed: 07.07.2022).

[7] G. Batista and M.-C. Monard, “A study of k-nearest neighbour as an imputation method.”, vol. 30, Jan. 2002, pp. 251–260.

[8] P. Tveit, “Considerations for design of network arches”, *Journal of Structural Engineering*, vol. 113, no. 10, pp. 2189–2207, Oct. 1, 1987, Publisher: American Society of Civil Engineers.

[9] W. Kaufmann, *Lecture Notes: Arch Bridges*, 2021.

[10] N. de Vos. “Kmodes”. (2021), [Online]. Available: https://datasolut.com/wiki/clusteranalyse/. (accessed: 10.04.2021).

[11] E. W. Forgy, “Cluster analysis of multivariate data : Efficiency versus interpretability of classifications”, *Biometrics*, vol. 21, pp. 768–769, 1965.

[12] Z. Huang, “Extensions to the k-means algorithm for clustering large data sets with categorical values”, *Data Mining and Knowledge Discovery*, pp. 283–304, 1998.

[13] Andrewngai, “Understanding dbscan algorithm and implementation from scratch”, *Towards Data Science*, 2020.

[14] Y. LLC, *Catboost*, 2019. [Online]. Available: https://github.com/catboost/catboost.

[15] A. Jha. “CatBoost – A new game of Machine Learning”. (2020), [Online]. Available: https://affine.ai/catboost-a-new-game-of-machine-learning/. (accessed: 27.06.2021).

[16] W. Daelemans and B. Goethals and K.Morik (Eds.), *Machine Learning and Knowledge Discovery in Databases - ECML PKDD 2008, Part I*. Springer Berlin Heidelberg, 2008, pp. 241–256.

[17] P. Tveit, “Systematic Thesis on Network Arches”, Adger University, 2014.

[18] F. Schanack, “Network arch bridges”, Ph.D. dissertation, University of Cantabria, 2008.